frontiers | Research Topics

Rising stars in hydrothermal vents and cold seeps 2021

Edited by
Brett J. Baker and S. Emil Ruff

Published in
Frontiers in Microbiology

ISSN 1664-8714
ISBN 978-2-8325-3755-8
DOI 10.3389/978-2-8325-3755-8

About Frontiers

Frontiers is more than just an open access publisher of scholarly articles: it is a pioneering approach to the world of academia, radically improving the way scholarly research is managed. The grand vision of Frontiers is a world where all people have an equal opportunity to seek, share and generate knowledge. Frontiers provides immediate and permanent online open access to all its publications, but this alone is not enough to realize our grand goals.

Frontiers journal series

The Frontiers journal series is a multi-tier and interdisciplinary set of open-access, online journals, promising a paradigm shift from the current review, selection and dissemination processes in academic publishing. All Frontiers journals are driven by researchers for researchers; therefore, they constitute a service to the scholarly community. At the same time, the *Frontiers journal series* operates on a revolutionary invention, the tiered publishing system, initially addressing specific communities of scholars, and gradually climbing up to broader public understanding, thus serving the interests of the lay society, too.

Dedication to quality

Each Frontiers article is a landmark of the highest quality, thanks to genuinely collaborative interactions between authors and review editors, who include some of the world's best academicians. Research must be certified by peers before entering a stream of knowledge that may eventually reach the public - and shape society; therefore, Frontiers only applies the most rigorous and unbiased reviews. Frontiers revolutionizes research publishing by freely delivering the most outstanding research, evaluated with no bias from both the academic and social point of view. By applying the most advanced information technologies, Frontiers is catapulting scholarly publishing into a new generation.

What are Frontiers Research Topics?

Frontiers Research Topics are very popular trademarks of the *Frontiers journals series*: they are collections of at least ten articles, all centered on a particular subject. With their unique mix of varied contributions from Original Research to Review Articles, Frontiers Research Topics unify the most influential researchers, the latest key findings and historical advances in a hot research area.

Find out more on how to host your own Frontiers Research Topic or contribute to one as an author by contacting the Frontiers editorial office: frontiersin.org/about/contact

Rising stars in hydrothermal vents and cold seeps: 2021

Topic editors

Brett J. Baker — The University of Texas at Austin, United States

S. Emil Ruff — Marine Biological Laboratory (MBL), United States

Citation

Baker, B. J., Ruff, S. E., eds. (2023). *Rising stars in hydrothermal vents and cold seeps: 2021*. Lausanne: Frontiers Media SA. doi: 10.3389/978-2-8325-3755-8

Table of contents

05 Editorial: Rising stars in hydrothermal vents and cold seeps: 2021
S. Emil Ruff and Brett J. Baker

07 Microbial Community Response to Polysaccharide Amendment in Anoxic Hydrothermal Sediments of the Guaymas Basin
Viola Krukenberg, Nicholas J. Reichart, Rachel L. Spietz and Roland Hatzenpichler

18 Comparative Analysis of Intestinal Microflora Between Two Developmental Stages of *Rimicaris kairei*, a Hydrothermal Shrimp From the Central Indian Ridge
Li Qi, Chun-Ang Lian, Fang-Chao Zhu, Mengke Shi and Li-Sheng He

29 Activity of Ancillary Heterotrophic Community Members in Anaerobic Methane-Oxidizing Cultures
Qing-Zeng Zhu, Gunter Wegener, Kai-Uwe Hinrichs and Marcus Elvert

41 Deep-branching ANME-1c archaea grow at the upper temperature limit of anaerobic oxidation of methane
David Benito Merino, Hanna Zehnle, Andreas Teske and Gunter Wegener

57 Microbial ecology of a shallow alkaline hydrothermal vent: Strýtan Hydrothermal Field, Eyjafördur, northern Iceland
Katrina I. Twing, L. M. Ward, Zachary K. Kane, Alexa Sanders, Roy Edward Price, H. Lizethe Pendleton, Donato Giovannelli, William J. Brazelton and Shawn E. McGlynn

71 Microbial diversity gradients in the geothermal mud volcano underlying the hypersaline Urania Basin
Cassandre Sara Lazar, Frauke Schmidt, Marcus Elvert, Verena B. Heuer, Kai-Uwe Hinrichs and Andreas P. Teske

89 Structure and metabolic potential of the prokaryotic communities from the hydrothermal system of Paleochori Bay, Milos, Greece
Sven Le Moine Bauer, Guang-Sin Lu, Steven Goulaouic, Valentine Puzenat, Anders Schouw, Thibaut Barreyre, Vera Pawlowsky-Glahn, Juan José Egozcue, Jean-Emmanuel Martelat, Javier Escartin, Jan P. Amend, Paraskevi Nomikou, Othonas Vlasopoulos, Paraskevi Polymenakou and Steffen Leth Jørgensen

109 Carbon metabolism and biogeography of candidate phylum "*Candidatus* Bipolaricaulota" in geothermal environments of Biga Peninsula, Turkey
Ömer K. Coskun, Gonzalo V. Gomez-Saez, Murat Beren, Dogacan Ozcan, Hakan Hosgormez, Florian Einsiedl and William D. Orsi

121 Mapping the microbial diversity associated with different geochemical regimes in the shallow-water hydrothermal vents of the Aeolian archipelago, Italy
Bernardo Barosa, Alessandra Ferrillo, Matteo Selci, Marco Giardina, Alessia Bastianoni, Monica Correggia, Luciano di Iorio, Giulia Bernardi, Martina Cascone, Rosaria Capuozzo, Michele Intoccia, Roy Price, Costantino Vetriani, Angelina Cordone and Donato Giovannelli

frontiers | Frontiers in Microbiology

TYPE Editorial
PUBLISHED 06 October 2023
DOI 10.3389/fmicb.2023.1297372

OPEN ACCESS

EDITED AND REVIEWED BY
Andreas Teske,
University of North Carolina at Chapel Hill, United States

*CORRESPONDENCE
S. Emil Ruff
✉ eruff@mbl.edu
Brett J. Baker
✉ brett_baker@utexas.edu

RECEIVED 20 September 2023
ACCEPTED 26 September 2023
PUBLISHED 06 October 2023

CITATION
Ruff SE and Baker BJ (2023) Editorial: Rising stars in hydrothermal vents and cold seeps: 2021. *Front. Microbiol.* 14:1297372. doi: 10.3389/fmicb.2023.1297372

Editorial: Rising stars in hydrothermal vents and cold seeps: 2021

S. Emil Ruff[1,2]* and Brett J. Baker[3,4]*

[1]The Marine Biological Laboratory, Ecosystems Center, Woods Hole, MA, United States, [2]The Marine Biological Laboratory, Josephine Bay Paul Center for Comparative Molecular Biology and Evolution, Woods Hole, MA, United States, [3]Department of Integrative Biology, University of Texas at Austin, Austin, TX, United States, [4]Department of Marine Science, University of Texas at Austin, Austin, TX, United States

KEYWORDS

sediment biogeochemistry, chemosynthesis, microbial symbioses, microbiome, extreme environment

Editorial on the Research Topic
Rising stars in hydrothermal vents and cold seeps: 2021

Research in the ecology and biogeochemistry of hydrothermal vents and methane seeps are driven—just like all science—by the hard work of early career scientists. To highlight recent work and invaluable contributions of young scholars we wanted to specifically focus on this demographic group in this Research Topic. Thus, the first authors of all nine articles featured here are graduate students, postdocs, and assistant professors at the beginning of their career and almost all senior authors are early- or mid-career principal investigators. The articles featured here span a broad range of environments around the world, from the deep sea, via shallow marine regions to laboratory cultures, using a broad range of methods from biogeochemical measurements to multi-omics.

This Research Topic includes studies on deep-sea hydrothermal vents and cold seeps. These environments remain fruitful for exploring microbial diversity, as they are difficult to access and require costly sampling vessels. As a result surveys of diversity are still an active area of research. In this topic we had two publications that harnessed rRNA-based studies. In Lazar et al. the authors examined microbial diversity in a geothermal mud volcano underlying the hypersaline Urania Basin, which is off the coast of Crete in the Mediterranean Sea. This study revealed distinct shifts in community structures between brines, muds, and sediments samples. They also found a predominance of spore-forming bacteria likely sourced from deep fluids to the volcanoes. These types of ecosystems are a window into the subsurface. Qi et al. compared the intestinal communities of hydrothermal shrimp (*Rimicaris exoculata*) in the central Indian Ridge, and found distinctions in community structures between juvenile and adults. Juveniles mainly harbored Deferribacterota, while in adults Campilobacterota dominated the intestines.

This Research Topic also comprises studies investigating shallow hydrothermal vent ecosystems. In contrast to deep-sea ecosystems these shallow systems have a direct impact on the food webs and biogeochemistry of coastal and surface environments. The Mediterranean and North Atlantic shallow vents that were studied here are thus located in marine areas that are under more anthropogenic influence, but also easier to access than vents in the deep sea. The coastal hydrothermal vent field of Paleochori Bay, off the island of Milos, Greece, is an example of an ecosystem that has been extensively studied and is used as a model ecosystem for processes that occur at less accessible deep-sea vents. Le Moine Bauer et al. carried out a

survey of the microbial communities across eight different hydrothermal habitats and used select metabolic marker genes to investigate major biogeochemical processes. They found that microbial diversity and composition are best explained by the thermal gradients, with archaea dominating the highest temperature regimes. Barosa et al. carried out a similar study yet investigated shallow hydrothermal vent ecosystems in the Aeolian Archipelago, Italy. These vent sites comprised highly diverse communities, potentially driven by light and chemical gradients, and were also shaped by the distinct geochemical regimes.

In contrast to the slightly acidic (Barosa et al.) and strongly acidic vents (Le Moine Bauer et al.) in the Mediterranean, the vents off Iceland studied by Twing et al. were alkaline. The communities of these vents were fundamentally different from most marine hydrothermal ecosystems, they comprised hardly any archaea and resembled those of terrestrial hot springs. One of the lineages typical for terrestrial systems was the phylum Bipolaricaulota (aka Acetothermia or OP1). This phylum was also the focus of the work reported by Coskun et al.. The extreme physicochemical conditions at hydrothermal ecosystems often select for communities of low complexity that are dominated by few lineages of highly specialized microorganisms. Coskun et al. studied such natural "enrichment cultures" in terrestrial hydrothermal springs on the Biga Peninsula, Turkey. The team characterized the metabolic capabilities of two major Bipolaricaulota lineages, an autotrophic lineage thriving in low salinity springs and a heterotrophic lineage abundant at high salinity.

Field studies of diversity, distribution, and biogeochemistry have, and will continue to, advance our understanding of the microbial world. However, linking microbial activity and diversity remains at the forefront of discovery in microbial ecology. The growing toolbox to investigate microbial physiology without culturing includes bioorthogonal non-canonical amino-acid tagging (BONCAT). In Krukenberg et al. the authors couple this approach with fluorescence-activated cell sorting (FACS) to determine the which members of the Guaymas Basin (Gulf of California) hydrothermal sediments are involved in polysaccharide degradation (specifically cellulose, chitin, laminarin, and starch). Another powerful approach to understanding physiological activity and interactions in microbial consortia is to obtain enrichments of mixed communities. This is what was employed by Zhu et al. and Benito Merino et al. to understand methane-oxidizing communities. These studies revealed that lineages commonly associated with these communities including Bathyarchaeota, Lokiarchaeota, and Thermoplasmatales are involved in breakdown of organic compounds (Zhu et al.). Benito Merino et al. obtained thermophilic methane-oxidizing enrichments of ANME-1c archaea and their sulfate-reducing syntrophs (Thermodesulfovibrio spp) from Gulf of California hydrothermal sediments, thus extending the thermal range of anaerobic methane oxidation toward 70°C.

The studies in this Research Topic covered a broad range of hydrothermal environments, deep and shallow, marine and terrestrial, natural and artificial. To characterize and understand the diversity, metabolic capabilities, and ecological niches of vent- and seep-associated microbial communities the researchers used a broad array of culture dependent and independent methods. Despite their different approaches, all studies show that a comprehensive understanding of an ecosystem can only be achieved by combining physicochemical and microbiological analyses. Furthermore, the studies are a reminder that we still know so little about these ecosystems that every survey and investigation of these communities represents a substantial and valuable gain in knowledge.

Author contributions

SER: Conceptualization, Project administration, Writing—original draft. BB: Conceptualization, Project administration, Writing—original draft.

Funding

The author(s) declare financial support was received for the research, authorship, and/or publication of this article. This work was supported by a grant from the Simons Foundation (824763, SER).

Conflict of interest

The authors declare that the research was conducted in the absence of any commercial or financial relationships that could be construed as a potential conflict of interest.

Publisher's note

frontiers in Microbiology

ORIGINAL RESEARCH
published: 10 December 2021
doi: 10.3389/fmicb.2021.763971

Microbial Community Response to Polysaccharide Amendment in Anoxic Hydrothermal Sediments of the Guaymas Basin

Viola Krukenberg[1,2,3*†], *Nicholas J. Reichart*[1,2,3†], *Rachel L. Spietz*[1,2,3†] *and Roland Hatzenpichler*[1,2,3,4*†]

[1] Department of Chemistry and Biochemistry, Montana State University, Bozeman, MT, United States, [2] Thermal Biology Institute, Montana State University, Bozeman, MT, United States, [3] Center for Biofilm Engineering, Montana State University, Bozeman, MT, United States, [4] Department of Microbiology and Cell Biology, Montana State University, Bozeman, MT, United States

OPEN ACCESS

Edited by:
Jesse G. Dillon,
California State University, Long Beach, United States

Reviewed by:
Mark Alexander Lever,
ETH Zürich, Switzerland
Petra Pjevac,
University of Vienna, Austria

***Correspondence:**
Viola Krukenberg
viola.krukenberg@montana.edu
Roland Hatzenpichler
roland.hatzenpichler@montana.edu

†ORCID:
Viola Krukenberg
orcid.org/0000-0001-8369-8114
Nicholas J. Reichart
orcid.org/0000-0002-3901-2039
Rachel L. Spietz
orcid.org/0000-0001-5277-0734
Roland Hatzenpichler
orcid.org/0000-0002-5489-3444

Specialty section:
This article was submitted to Extreme Microbiology, a section of the journal Frontiers in Microbiology

Received: 24 August 2021
Accepted: 09 November 2021
Published: 10 December 2021

Citation:
Krukenberg V, Reichart NJ, Spietz RL and Hatzenpichler R (2021) Microbial Community Response to Polysaccharide Amendment in Anoxic Hydrothermal Sediments of the Guaymas Basin. Front. Microbiol. 12:763971. doi: 10.3389/fmicb.2021.763971

Organic-rich, hydrothermal sediments of the Guaymas Basin are inhabited by diverse microbial communities including many uncultured lineages with unknown metabolic potential. Here we investigated the short-term effect of polysaccharide amendment on a sediment microbial community to identify taxa involved in the initial stage of macromolecule degradation. We incubated anoxic sediment with cellulose, chitin, laminarin, and starch and analyzed the total and active microbial communities using bioorthogonal non-canonical amino acid tagging (BONCAT) combined with fluorescence-activated cell sorting (FACS) and 16S rRNA gene amplicon sequencing. Our results show a response of an initially minor but diverse population of *Clostridia* particularly after amendment with the lower molecular weight polymers starch and laminarin. Thus, *Clostridia* may readily become key contributors to the heterotrophic community in Guaymas Basin sediments when substrate availability and temperature range permit their metabolic activity and growth, which expands our appreciation of the potential diversity and niche differentiation of heterotrophs in hydrothermally influenced sediments. BONCAT-FACS, although challenging in its application to complex samples, detected metabolic responses prior to growth and thus can provide complementary insight into a microbial community's metabolic potential and succession pattern. As a primary application of BONCAT-FACS on a diverse deep-sea sediment community, our study highlights important considerations and demonstrates inherent limitations associated with this experimental approach.

Keywords: metabolic activity, heterotrophic community, microbial ecology, substrate analog probing, bioorthogonal non-canonical amino acid tagging, fluorescence-activated cell sorting

INTRODUCTION

Hydrothermal vent fields provide areas of high biodiversity and primary productivity within a predominantly oligotrophic sea. In the Guaymas Basin, Gulf of California, active seafloor spreading and high sedimentation rates result in a unique system of hydrothermal vents within sediments with up to 4% organic matter content (Calvert, 1966; De la Lanza-Espino and Soto, 1999). Fresh organic

matter derived from high phytoplankton productivity in surface waters and terrestrial runoff, is introduced into sediments while hydrothermal pyrolysis transforms and remobilizes buried organic matter, creating hydrocarbons and low molecular weight compounds that are mobilized via hydrothermal circulation (Calvert, 1966; Von Damm et al., 1985; De la Lanza-Espino and Soto, 1999). The wide range of available organic and inorganic substrates sustains a metabolically versatile anaerobic microbial community including heterotrophs and chemolithoautotrophs, and populations that typically occur only in geographically distant hydrothermal vents, cold seeps and organic-rich sediments (Teske et al., 2016, 2021). Recent metagenomic surveys detected many previously unknown and uncultured lineages and indicated that much of the metabolic diversity of the microbial community remains to be discovered (Dombrowski et al., 2017, 2018; Baker et al., 2021).

Revealing the metabolism of uncultured microbes and their function in the environment remains a challenge and frequently relies on combinatorial approaches to link taxonomic identity with metabolic activity on a single cell level. Stable isotope probing combined with fluorescence *in situ* hybridization and nanoscale secondary ion mass spectrometry or Raman microspectroscopy allows tracking incorporation of growth substrates into biomass of individual taxonomically identified cells (Huang et al., 2007, 2009; Dekas and Orphan, 2011; Berry et al., 2015; Musat et al., 2016). While powerful, this approach relies on isotope-labeled substrates that are not generally available for experimental testing, especially in the case of complex compound classes. Substrate analog probing is a promising but comparatively new alternative to stable isotope probing (Hatzenpichler et al., 2020). Currently, the most widely used substrate analog probing approach in microbial ecology is bioorthogonal non-canonical amino acid tagging (BONCAT) in combination with fluorescence-activated cell sorting (FACS). BONCAT-FACS can be combined with 16S rRNA gene amplicon sequencing or metagenomics to assess the anabolically active fraction of a microbial community. BONCAT uses a non-canonical amino acid, such as *L*-homopropargylglycine (HPG), that is incorporated into newly synthesized proteins by methionyl-tRNA synthetase, and that can be fluorescently detected via azide-alkyne click chemistry (Kiick et al., 2002; Hatzenpichler et al., 2014). Subsequently, FACS enables the separation of translationally active (BONCAT positive) cells for taxonomic identification via gene sequencing. BONCAT-FACS was recently applied on environmental and human microbiome samples to reveal anabolically active community members and to test responses in metabolic activity upon substrate amendments (Hatzenpichler et al., 2016; Couradeau et al., 2019; Reichart et al., 2020; Riva et al., 2020; Valentini et al., 2020; Marlow et al., 2021; Taguer et al., 2021). Here, we applied this approach to investigate the microbial community involved in anaerobic polysaccharide mineralization in Guaymas Basin sediments.

Guaymas Basin sediments contain a variety of organic macromolecules (lipids, proteins, DNA and polysaccharides) (De la Lanza-Espino and Soto, 1999; Teske et al., 2002; Zheng et al., 2021) and harbor a diverse heterotrophic community with the genetic potential to degrade a wide range of these compounds (Dombrowski et al., 2018; Baker et al., 2021; Perez Castro et al., 2021). Polysaccharides are abundant in the ocean and are commonly introduced into sediments from surface waters or terrestrial runoffs or are produced from decaying biomass. We focused on testing the potential for anaerobic microbial degradation of four polymers: cellulose, chitin, laminarin, and starch, which serve to represent marine and terrestrial polysaccharides of differing complexity that are introduced into Guaymas Basin sediments due to very high sedimentation rates and terrestrial input (Calvert, 1966; De la Lanza-Espino and Soto, 1999). Laminarin and starch are storage polysaccharides found in marine macroalgae, phytoplankton and microbial cells, while the structural carbohydrates cellulose and chitin are components of fibers and exoskeletons (Arnosti et al., 2021). The utilization of polysaccharides relies on extracellular carbohydrate-activating enzymes (CAZymes) for the initial cleavage and uptake through membrane transporters prior to intracellular degradation. Substrate-specific CAZymes such as for starch (alpha-amylase) or cellulose (glycoside hydrolase) are synthesized by specialized functional guilds while the produced oligo- and monosaccharides or intermediates of their degradation provide substrates for other metabolically diverse community members. Here, we exposed anoxic hydrothermal sediments to polysaccharides for a short time period and analyzed shifts in the overall community and active community via BONCAT-FACS combined with 16S rRNA gene amplicon sequencing providing complementary insight into primary responders and response succession.

MATERIALS AND METHODS

Sample Collection and Material Selection

Hydrothermally heated sediments were collected with push cores in the Marker 14 hydrothermal area in the Guaymas Basin, Gulf of California, Mexico during R/V *Atlantis* research cruise AT42-05 (November 2018) with the submersible *Alvin* (Dive 4998; 2011 m; 27.0079° N, 111.4072° W). *In situ* temperature profiles were recorded using *Alvin's* heat flow probe adjacent to the sampled sediment cores every 10 cm down to a depth of 50 cm. Two of the retrieved sediment cores (11 and 12; **Supplementary Figure 1**) were sectioned into three horizons: (H1) upper horizon 0–10 cm (excluding bacterial mats), 4–33°C; (H2) middle horizon 10–20 cm, 33–74°C; (H3) lower horizon, 20–30 cm, 74–110°C (**Supplementary Table 1**). Replicate horizons from both cores were combined into glass bottles, degassed with N_2, and stored under N_2 headspace at 4°C until further processing (February 2020).

As fresh organic matter is frequently introduced into surface sediments from the overlaying water column, sediments of the upper horizon were selected for mesocosm experiments testing the microbial community's potential to utilize complex carbon polymers. Furthermore, due to the steep temperature gradient and elevated temperatures in the lower horizons, cell numbers rapidly decreased with sediment depth. Initial cell extraction tests showed that sufficient cells needed for the BONCAT-FACS approach could only be recovered from the upper sediment

horizon. This highlights that selection and preliminary evaluation of the starting material is crucial in designing experiments for BONCAT-FACS.

Mesocosm Setup

Mesocosms were prepared in an anoxic glove box under $N_2/CO_2/H_2$ (90%/5%/5%) atmosphere. Sediment of the top horizon (H1) was diluted (1:5) with anoxic artificial seawater (Widdel and Bak, 1992). During experiment set up the slurry was homogenized by constant stirring using a magnetic plate and stir bar. To preserve material for DNA extraction, three aliquots (1 mL each) were centrifuged 10 min at 16,000 × *g*, supernatant was decanted, and pellets were frozen at −80°C until further processing. To set up mesocosms, the remaining slurry was distributed in aliquots of 30 mL into 156 mL sterile serum vials using sterile serological plastic pipettes. All vials were sealed with a butyl rubber stopper and aluminum crimp. The headspace was degassed with N_2/CO_2 (90%/10%) at 100 kPa for 5 min to remove H_2 introduced during set up inside the glove box and the final headspace was set to 200 kPa. The vials were placed at 33°C, which conforms with the upper *in situ* temperature measured in the sediment horizon, for 16 h to allow the microbial community to adapt to the incubation temperature after long-term storage at 4°C. After this preincubation, the following treatments were set up, each in triplicate: (1) no substrate amendment, or amendment with (2) cellulose, (3) chitin, (4) laminarin, or (5) starch. Substrates were added from sterile anoxic stock solutions to final concentrations of 0.01% w/v. The amino acid analog *L*-homopropargylglycine (HPG; Click Chemistry Tools, Scottsdale, AZ) was added to all treatments from an anoxic stock solution to a final concentration of 100 μM. Controls were prepared without HPG and without substrate amendment. Incubation was continued at 33°C and subsamples were collected after two (T1) and five (T2) days from each mesocosm using a syringe and needle. Subsamples (1 mL each) were preserved for DNA extraction by centrifugation (10 min at 16,000 × *g*), supernatant removal, and storage at −80°C. Replicate subsamples (2.5 mL each) were preserved for cell extraction by transfer into sterile 10% Glycerol Tris/EDTA (GlyTE) solution and storage at −80°C.

DNA and Cell Extraction

DNA was extracted from sediment pellets (see above) using the FastDNA Spin Kit for Soil (MP Biomedicals, Irvine, CA) following the manufacturer's guidelines. Blank DNA extractions were performed as a negative control. DNA extracts were quantified using the Qubit high sensitivity assay (Invitrogen, Carlsbad, CA) and were stored at −20°C.

Cells were extracted from duplicate 2.5 mL aliquots preserved in GlyTE (see above). For this, samples were thawed at 4°C, amended with 7.5 mL of sterile 1× phosphate buffered saline (PBS; filter-sterilized (0.2 μm pore size) and UV treated for 16 h) containing Tween 20 at a final concentration of 0.02% and vortexed for 10 min at speed 8 (approx. 2000 rpm, Vortex-Genie2, Scientific Industries, Inc., Bohemia, NY, United States) to detach cells from particles. Blank extractions using 1 × PBS were processed in parallel to assess contamination introduced during the extraction process. A density gradient separation was performed by carefully adding an equal volume (10 mL) of Nycodenz solution (60%) underneath the sample using a sterile serological pipette and centrifugation at 14,000 × *g* for 45 min. Following centrifugation, avoiding any sediment particles in the lower phase, the upper phase and interphase containing the cells were transferred to a new tube prefilled with 20 mL 1 × PBS. To collect cells, the sample was centrifuged 10 min at 16,000 × *g*, supernatant was carefully removed, and the cell pellet resuspended in the remaining liquid (approx. 1 mL). Subsequently, the sample was transferred to a 1.5 mL tube and cells were concentrated by centrifugation for 10 min at 18,000 × *g*, supernatant removal, and resuspension in 50 μL of 1 × PBS. The cell suspensions from duplicate extractions were combined and immediately further processed for FACS.

Click Reaction, Fluorescence-Activated Cell Sorting and Cell Lysis

Cell extracts were subjected to click reaction as previously described (Hatzenpichler and Orphan, 2015; Reichart et al., 2020). For this, 200 μL of click reaction solution were added to and mixed with the cell extract by pipetting up and down. The cell click reaction mixture was comprised of 5 mM aminoguanidine hydrochloride (Sigma-Aldrich, St. Louis, MO), 5 mM sodium *L*-ascorbate (Sigma-Aldrich, St. Louis, MO), 100 μM copper sulfate pentahydrate (Sigma Aldrich), 500 μM THPTA (Click Chemistry Tools, Scottsdale, AZ) and 4 μM Cy5 picolyl-azide dye (Click Chemistry Tools, Scottsdale, AZ), and was incubated for 40 min in the dark at room temperature. Subsequently, the click reaction solution was removed from the cells by three cycles of centrifugation at 18,000 × *g* for 5 min, aspiration of the supernatant by pipette, and resuspension of the cell pellet in 1 mL of 1 × PBS. To remove any remaining larger particles prior to cell sorting, a slow centrifugation was performed at 500 × *g* for 5 min, followed by passage of the supernatant through a 35 μm pore size filter cap (BD-falcon cell strainer cap, Corning, Corning, NY, United States). A subsample (50 μL) of the final cell suspension (filtrate) was transferred to a new tube and was stored at 4°C until further processing. This subsample represents the total extractable cells in our experiment. Fluorescence signal intensity and density of labeled cells was checked by epifluorescence microscopy (Leica DM4B microscope).

Cell sorting was performed using a Sony SH800S FACS (Sony Biotechnology, San Jose, CA) equipped with a 70 μm chip, set to detect Cy5 dye on the red channel (excitation 638 nm) and operated with 1 × PBS (sterilized as described above) as sheath fluid. Sorting gates were established as previously described (Reichart et al., 2020). Briefly, two gates were drawn based on forward and back scatter to exclude any larger particles and background noise; the third gate was drawn based on forward scatter and Cy5 fluorescence intensity to capture BONCAT positive cells (i.e., the fluorescent, translationally active cell fraction). Cell extracts from control incubations without HPG (no BONCAT signal) were used to delineate the gates for BONCAT positive and BONCAT negative cells. Each sample was sorted for a maximum of 250,000 fluorescent events from

the BONCAT positive (active) fraction or until the volume was exhausted (**Supplementary Figure 2**). Sorted cells were stored at 4°C for up to 8 h until further processing.

Cells in the sorted and extractable cell fractions were lysed for DNA recovery as previously described (Reichart et al., 2020). In short, cells were centrifuged at 18,000 × *g* for 5 min followed by supernatant removal and pellet resuspension in 20 μL of nuclease-free water. Cell suspensions were transferred into 96-well plates, sealed with adhesive sterile aluminum foil and subjected to three cycles of freezing (−80°C, 10 min) and thawing (99°C, 10 min) with a short centrifugation prior to each freezing step. Lysed cell extracts were stored at −80°C until further processing.

16S rRNA Gene Amplification and Sequencing

Amplification of bacterial and archaeal 16S rRNA genes was performed following the Earth Microbiome protocol (Thompson et al., 2017) using revised primers 515F (5′-GTGYCAGCMGCCGCGGTAA-3′) (Parada et al., 2016) and 806R (5′-GGACTACNVGGGTWTCTAAT-3′) (Apprill et al., 2015) with DNA templates recovered from either (1) sediment samples using a DNA extraction kit or (2) cell suspensions of extractable and sorted fractions using freeze/thaw cycles (described above). Polymerase chain reaction (PCR) was performed in a final volume of either (1) 25 μL consisting of 5 μL template from extraction kits (1 ng DNA/μL), 10 μL Invitrogen Platinum Taq II 2X Master Mix, 0.5 μL (0.2 μM) of each primer, and 9 μL nuclease-free water or (2) 50 μL consisting of 20 μL template from freeze/thaw extractions, 20 μL Invitrogen Platinum Taq II 2X Master Mix, 1 μL (0.2 μM) of each primer, and 8 μL nuclease-free water. The thermocycler conditions were: 94°C for 3 min followed by 28 cycles of 94°C for 45 sec, 50°C for 60 sec, and 72°C for 90 sec, followed by a final elongation step at 72°C for 10 min. PCR on sorted and extractable cell fractions from T1 was performed with two additional cycles (for a total of 30 cycles) due to lower cell recovery. A negative control using nuclease-free water as template was included in each PCR set to determine PCR contamination. PCR products were checked for the expected length on a 1% agarose gel and subsequently were purified using AMPure XP beads (Beckman Coulter, Brea, CA, United States) following the manufacturer's protocol with a final elution volume of 40 μL nuclease-free water. To prepare amplicons for Illumina sequencing, Illumina dual index barcode and sequencing adapters were attached in a second PCR reaction. This PCR was performed in a final volume of 25 μL containing 5 μL of purified amplicons, 12.5 μL Invitrogen Platinum Taq II 2X Master Mix, 2.5 μL (0.25 μM) of each primer (i5 and i7), and 2.5 μL nuclease-free water. The PCR conditions were as follows: 95°C for 3 min followed by 8 cycles of 95°C for 30 sec, 55°C for 30 sec, and 72°C for 30 sec, followed by a final elongation step at 72°C for 5 min. PCR products were purified using AMPure XP beads as described above and were quantified in triplicate reactions using the Quant-iT Picogreen dsDNA Assay (Invitrogen) on a Biotek Synergy H1 Hybrid microplate reader following the manufacturer's guidelines. Purified amplicons from all samples were pooled at 10 ng DNA each, and the pooled library was quantified with the Qubit high sensitivity assay (Invitrogen, Carlsbad, CA, United States). Purification, quality assessment and sequencing of pooled libraries was performed at the Molecular Research Core Facility at Idaho State University (Pocatello, ID) using Illumina's MiSeq chemistry for 2 × 250 bp paired end reads. Sequences are deposited at NCBI's GenBank under BioProject PRJNA748056.

Bioinformatics Data Analyses

Amplicon data were processed using QIIME 2 version 2020.2 (Bolyen et al., 2019). In short, primer sequences were removed from demultiplexed reads using *cutadapt* (Martin, 2011) with an error rate of 0.12. Reads were truncated to 145 bp and subsequently filtered, denoised and merged in DADA2 with default settings (Callahan et al., 2016). The resulting 16S rRNA gene amplicon sequence variants (ASVs) were taxonomically classified with the *sklearn* method and the SILVA 132 database (Quast et al., 2013). Contaminating ASVs were removed using the R package *decontam* with the prevalence model at a threshold of 0.6 followed by manual inspection and further curation considering multiple controls included in the dataset (i.e., PCR negative controls, DNA extraction blanks, sheath fluid controls) (**Supplementary Figure 3**). Samples with less than 10,000 reads were excluded and ASVs with less than 0.001% relative sequence abundance across all samples were removed prior to further analysis. Diversity metrics were calculated on the level of ASVs in the R package *Phyloseq* (McMurdie and Holmes, 2013). ANOVA-like differential gene expression analysis was conducted in the R package *Aldex2* (Fernandes et al., 2013, 2014) between no amendment control and each substrate treatment on the level of ASVs. Adjusted *p*-values <0.05 were considered for calling differential abundance of ASVs (**Supplementary Table 2**).

RESULTS AND DISCUSSION

Sampling Site Description and Experimental Strategy

Sediment for mesocosm experiments was recovered from the Marker 14 site in the Guaymas Basin, an area with strong hydrothermal influence (**Supplementary Figure 1**). The sediments were covered with orange *Beggiatoa* mats, and were characterized by steep temperature gradients reaching 115°C at 35 cm depth (**Supplementary Table 1**). Further, sulfide and ammonia concentrations ranged between 2–4 mM and 2–6 mM, respectively, and sulfate concentrations decreased with depth (Ramírez et al., 2021). Previously recorded *in situ* microprofiles from the same area showed rapid oxygen depletion in the upper two sediment millimeters, with occasional deeper oxygen traces due to hydrothermal circulation (Teske et al., 2016).

In mesocosm experiments we exposed sediments of the upper horizon to polysaccharides of differing complexity for a limited time period (2 and 5 days) to identify populations involved in the initial polysaccharide activation and utilization under anoxic conditions. While substrate-specific enrichments

select for specialized communities over time, they may not reveal the community members first responding to a substrate. As metabolic activity precedes growth, tracking the active community members via BONCAT-FACS after short-term exposure to a substrate can provide complementary insight into the primary degraders and degradation succession. To identify substrate-specific responses we compared the active and total communities in substrate amended mesocosms to controls without amendments. Notably, the studied sediments are naturally rich in organic and inorganic compounds that support microbial metabolism. We analyzed the microbial community composition in three fractions obtained by (1) DNA extraction, (2) cell extraction, and (3) cell sorting, which are considered representative of (1) the total DNA extractable community, (2) the total cell extractable community, and (3) the translationally active, cell extractable community. As the DNA extractable (1) vs cell extractable (2, 3) fractions result from different extraction processes an unbiased representation of the *in situ* community cannot be provided. Furthermore, assessment of the active fraction is affected by limitations associated with BONCAT and FACS. Finally, primer-based PCR amplification and sequencing introduce additional biases; thus, all relative sequence abundance data is limited in its representation of community composition.

Diversity and Composition of the Total and Active Communities

Alpha diversity indices showed a decrease in diversity from the extractable DNA to the cell extractable fraction consistent for both timepoints analyzed (**Figure 1A** and **Supplementary Figure 4**). However, alpha diversity was lowest in the fraction recovered after cell sorting, representing only the subset of taxa that have been active in a mesocosm. Generally, the alpha diversity measure of the total community decreased with incubation time, indicating a selective enrichment of taxa within days. Interestingly, a slightly reversed trend was observed in the active community, suggesting more taxa became active over time. Community structure as displayed by principal component analysis showed overall separation by fraction (DNA extract, cell extract, cell sort) (**Figure 1B**). Within each fraction samples tended to cluster by timepoint. A few notably different samples included replicates amended with starch at day 5, especially in the DNA extract and cell sort fractions, one replicate amended with cellulose at day 2 in the cell extract fraction and one replicate amended with chitin at day 5 in the cell sort fraction (**Figure 1C**).

Based on relative sequence abundance the inoculum sediment was largely composed of Deltaproteobacteria (17%), Campylobacteria (15%), JS1 (14%), Gammaproteobacteria (8%), Bacteroidia (8%), Anaerolineae (5%), and Methanomicrobia (4%) (**Figure 2**). A similar, bacteria-dominated community has previously been described for Marker 14 surface sediments (Ramírez et al., 2021). The community in mesocosms recovered in the DNA extract fraction after 2 and 5 days of incubation overall showed similar composition as the inoculum sediment. Most prominent was an increase in relative proportion of Clostridia in mesocosms amended with starch (1 replicate at day 2, all replicates at day 5). Clostridia were detected initially in low abundance in the inoculum, and may have been present as endospores. In our experiments we exposed sediments to elevated temperatures after long-term cold storage, which possibly caused spore germination upon favorable temperatures followed by activity and rapid growth upon substrate availability. The microbial community might experience similar conditions in their natural environment, where, due to the high dynamics in hydrothermal activity, sediment temperatures fluctuate over time and space. For example, over a distance of a few centimeters sediment temperature often ranges from 50–100°C to 4°C (Teske et al., 2016). The cell extractable community was mostly dominated by JS1 (Atribacteria) after 2 and 5 days, except for in starch amended mesocosms where Clostridia prevailed after 5 days. The active community (cell sort fraction) at day 2 was dominated by Clostridia under starch amendment and Thermotogae under all other treatments, and generally shifted towards an Atribacteria (JS1) and Firmicutes (Clostridia and Negativicutes) dominated community at day 5. Notably, while Clostridia were prominent in incubations amended with the low complexity polysaccharides starch and laminarin, Negativicutes were prevalent in replicates without amendment or with cellulose amended.

Altogether, we observed a strong contrast between the microbial community recovered via DNA extraction and cell extraction. A lower alpha diversity index in cell extracts compared to DNA extracts indicates a preferential recovery of taxa in cell extraction procedures. Cell extractions are potentially biased and cell recovery is a frequent challenge, in particular for complex sample types such as organic carbon-rich hydrothermal sediments, which likely explains the observed differences in community structure (Morono et al., 2013; Doud and Woyke, 2017; Hatzenpichler et al., 2020). Improved cell separation techniques might lead to different observations than reported here; however, a comparison of cell extraction procedures was outside the scope of our study, which was limited by the amount of available sediment material. Further, a size selection (35 μm filtration) prior to FACS, necessary to avoid clogging of the sample line, impeded the detection of larger cell aggregates and possibly other morphologies such as long filaments in the active fraction.

Besides possible biases introduced during cell extract preparation, extracellular DNA, only represented in the DNA extract may contribute to discrepancies in community composition (Couradeau et al., 2019). Deep-sea sediments are known to contain extracellular DNA, which is also considered an important macromolecular carbon source for the heterotrophic microbial community including in Guaymas Basin sediments (Jørgensen and Jacobsen, 1996; Dell'Anno and Danovaro, 2005; Corinaldesi et al., 2007; Perez Castro et al., 2021), but the effect of extracellular DNA on microbial diversity surveys is disputed and not well established (Lever et al., 2015; Carini et al., 2016; Ramírez et al., 2018; Torti et al., 2018).

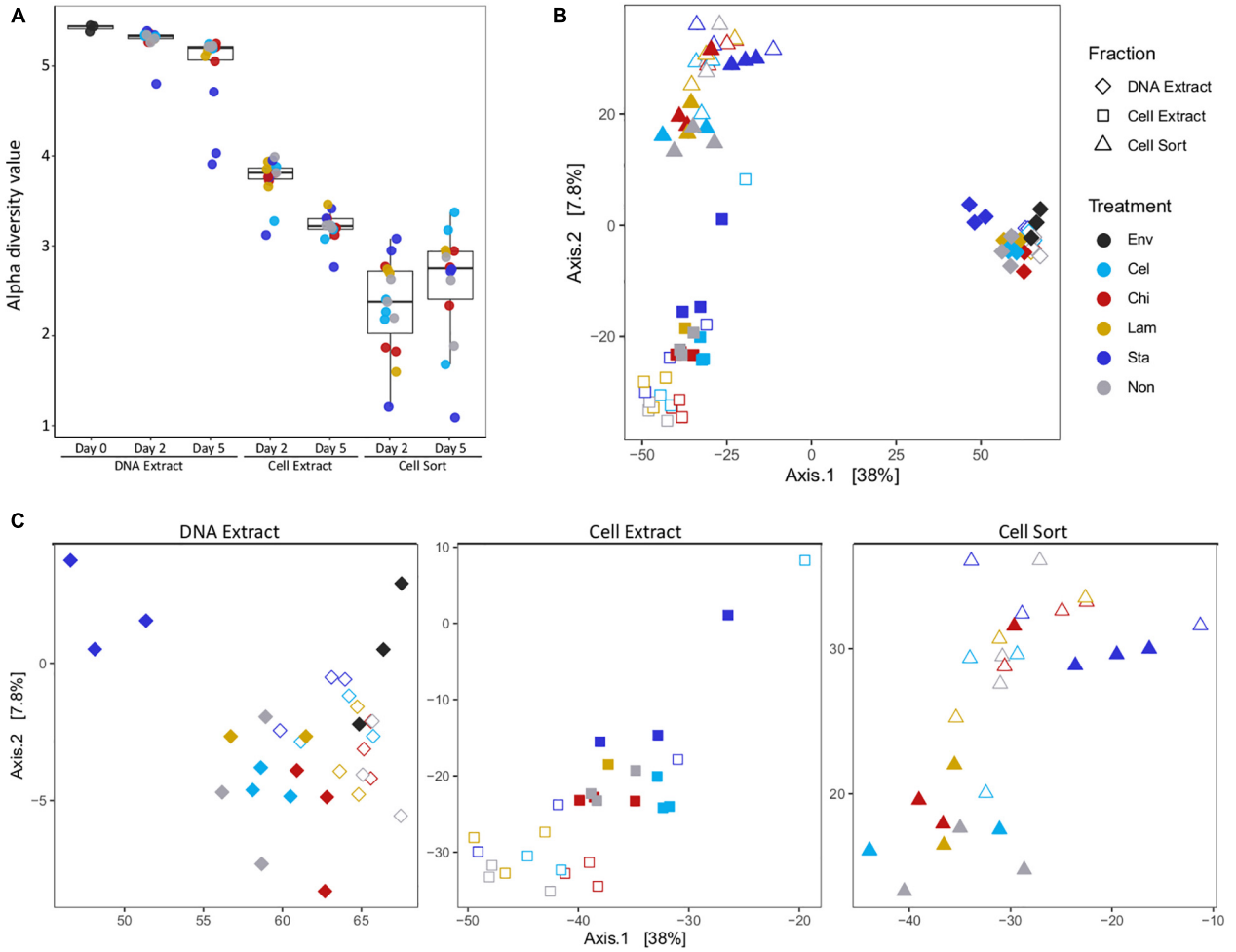

FIGURE 1 | Alpha and beta diversity. Alpha diversity (Shannon index) decreased between fractions and timepoints **(A)**. Principal coordinate analysis showing differences in beta diversity between samples of all fractions **(B)** and each fraction separately **(C)**. Env: environmental sample (inoculum), Cel: cellulose, Chi: chitin, Lam: laminarin, Sta: starch, Non: no amendment. For each treatment filled symbols show day 2 and open symbols day 5.

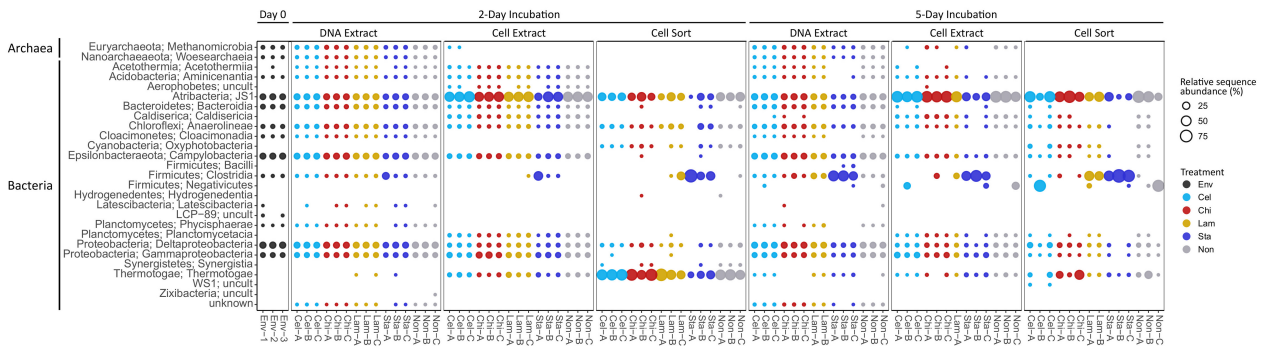

FIGURE 2 | Community composition on class level showing relative sequence abundance (%) for taxa occurring with >1% in at least one sample. Env: environmental sample (inoculum), Cel: cellulose, Chi: chitin, Lam: laminarin, Sta: starch, Non: no amendment.

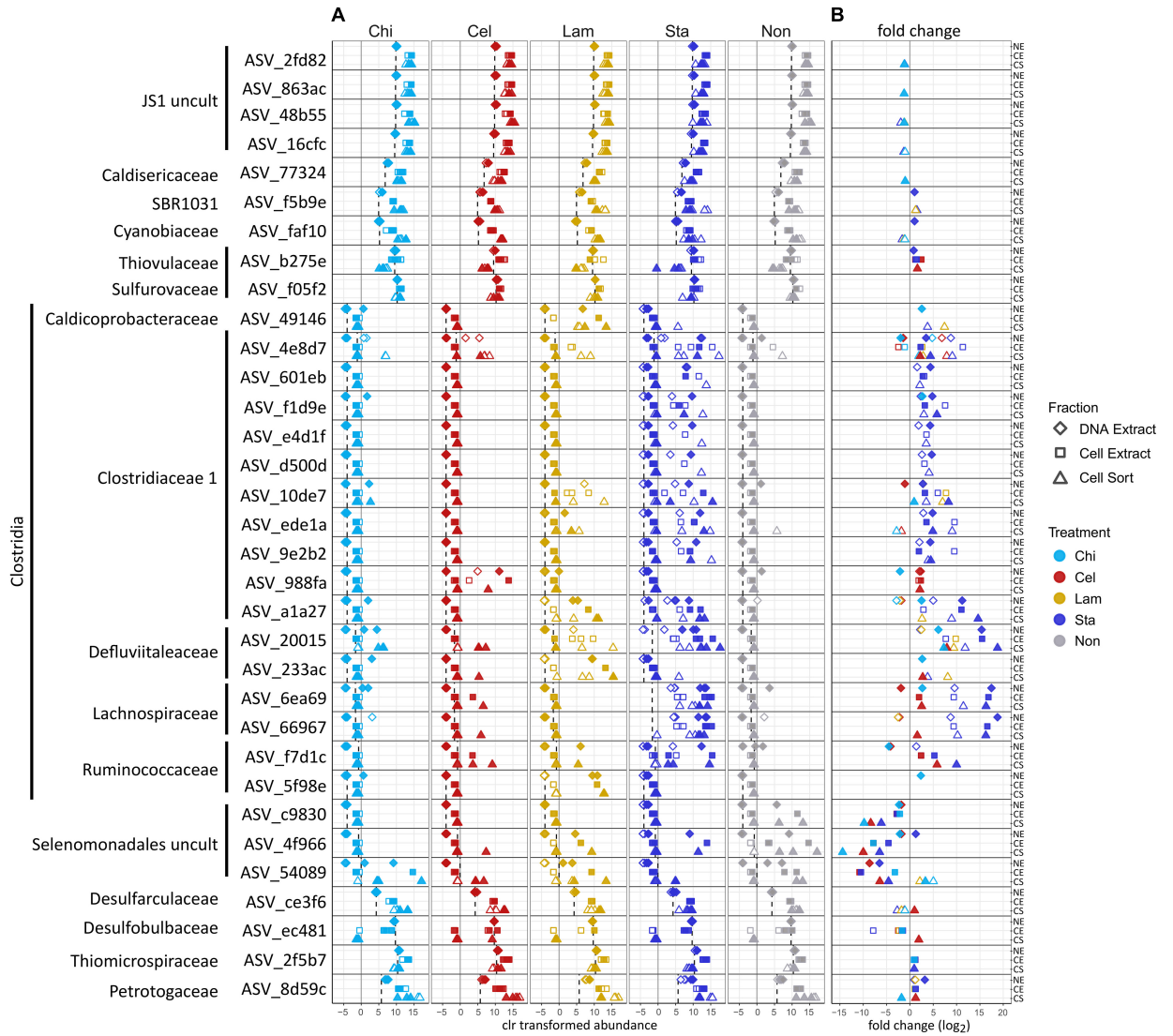

FIGURE 3 | Effect of polysaccharide amendment on abundant ASVs (i.e., occurring with >3% relative sequence abundance in at least one sample). Center log ratio (clr) transformed abundance of ASVs **(A)**. Note that clr values indicate abundance of an ASV as relative to the mean abundance of all ASVs in a sample with positive clr values indicating abundance greater than the mean abundance. Dashed line: mean clr transformed abundance of an ASV in the environmental sample (inoculum, day 0). Log_2 fold changes >1 between no amendment and each substrate treatment for each ASV **(B)**. Gray line represents a fold change of 0 (i.e., no difference between no amendment and substrate amendment). No data are available for Lam at day 5 as replicate C was lost and analysis relied on triplicate samples. Diamonds: DNA extract, squares: cell extract, triangles: cell sort, open symbols: day 2, filled symbols: day 5. Cel: cellulose, Chi: chitin, Lam: laminarin, Sta: starch, Non: no amendment.

Effect of Substrate Amendment on Abundant Populations

To further characterize the community members responding to polysaccharide amendment, we analyzed the frequency of abundant ASVs (>3% relative sequence abundance in at least one sample) across fractions and treatments (**Figure 3A**) and tested the effect of substrate amendment by comparing the differential abundance of individual ASVs between no amendment and each substrate treatment (**Figure 3B**). Notably, low number of replicates and variation between replicates limited the statistical significance of our differential abundance analysis, although large fold changes were observed (**Supplementary Table 2**). We identified 33 abundant ASVs, which together represented a large proportion of the microbial community, encompassing a relative sequence abundance of 31% in the environmental sample and up to 97% in the active community of mesocosms, which often was dominated by only a few ASVs (**Supplementary Table 2**). Most of the abundant ASVs (17) affiliated with Clostridia representing six families: *Clostridiaceae* 1 (10 ASVs), *Defluviitaleaceae* (2 ASVs), *Lachnospiraceae* (2 ASVs), *Ruminococcaceae* (2 ASVs), and *Caldicoprobacteraceae* (1 ASV). All Clostridia-affiliated ASVs were initially detected in low abundance in the inoculum

sediment but generally increased in proportions in the total and active community in mesocosms. Amendment with the more accessible storage polymers starch and laminarin resulted in the fasted and strongest response observed for several ASVs. In particular ASVs affiliated with the *Defluviitaleaceae* (2) and *Lachnospiraceae* (2) showed high fold changes (**Figure 3B**) upon starch amendment. *Defluviitaleaceae*-affiliated ASV_20015 was detected at elevated frequency in the active fraction of substrate amended incubations but not unamended controls, showing a broad response to all polysaccharides with the highest detected fold change and highest relative sequence abundance (80%) in response to starch amendment (**Figure 3B** and **Supplementary Table 2**). While many ASVs affiliated with the *Clostridiaceae* 1 occurred mostly in laminarin and starch amended incubations, ASV_4e8d7 was detected at elevated proportion in the active fraction under all treatments including unamended controls (**Figure 3A**); activity and growth, however, were stimulated by substrate availability (**Figure 3B**). This indicates that some members of the *Clostridiaceae* 1 family may utilize the substrates available in the inoculum, as Guaymas Basin sediments are naturally rich in organic and inorganic compounds (Calvert, 1966; Von Damm et al., 1985; De la Lanza-Espino and Soto, 1999). The response to chitin and cellulose amendment was generally less pronounced and limited to a few Clostridia ASVs. This suggests longer response times for these more complex structural polymers, which would be better captured with extended incubation times. ASV_988fa (*Clostridiaceae* 1) specifically responded only to chitin amendment (**Figure 3B**), suggesting specialized degradation capacities in members of this lineage. Besides Clostridia, other Firmicutes-affiliated ASVs belonging to an uncultured Selenomonadales clade showed strong increase in proportions, most notably in the no amendment control, and thus, no strong substrate specific response was detected.

Other abundant ASVs were affiliated to Atribacteria (JS1) (4 ASVs) which showed high initial proportions in the inoculum but little variation in mesocosms. ASVs affiliating with *Petrotogaceae* (1), SBR1031 clade (Anaerolineae) (1), *Desulfarculaceae* (1) and *Cyanobiaceae* (1) increased in the active fraction across all treatments after 2 days relative to their proportion in the inoculum. This indicates that their initial activity likely resulted from utilization of substrates supplied with the sediment and was promoted by the switch to elevated incubation temperatures but was not sustained possibly due to substrate limitation. Notably, Thermotogae were detected with the highest relative sequence abundance in the active fraction of most mesocosms after 2 days (**Figure 2**) but the abundant Thermotogae-affiliated ASV (ASV_8d59c) did not show a strong substrate specific response. However, Thermotogae are widespread in marine hydrothermal sediments and some members have recently been implicated in polysaccharide degradation in Guaymas Basin sediments (Perez Castro et al., 2021). In contrast, ASVs affiliated with *Thiomicrospiraceae* (1), *Thiovulaceae* (1), *Sulfurovaceae* (1) and *Desulfobulbaceae* (1), while abundant in the inoculum, decreased in proportion in the active fraction, suggesting that these organisms initially did not benefit from selected incubation conditions. However, their activity may be promoted once intermediates of polysaccharide degradation are available, possibly requiring incubation times longer than performed here. For example, production of H_2 during polysaccharide degradation as previously observed in anoxic Guaymas Basin sediments, may favor the activity and growth of sulfate reducers (Perez Castro et al., 2021).

Overall, an increase in proportion of Clostridia-affiliated ASVs in mesocosms was observed in all fractions, and was often detected in the cell sorted fraction (day 2) prior to the DNA extractable fraction (day 5), which shows that BONCAT-FACS can reveal changes in metabolic activity before changes in cell abundance (i.e., cell division) occur. In contrast, an analysis of the DNA extractable community detects responding taxa only after DNA replication and cell division have occurred. However, both approaches produce compositional sequence data and do not provide insight into relative cell abundances.

Potential Implications for Polysaccharide Degradation in Hydrothermal Sediments

During a relatively short incubation time, the Guaymas Basin sediment microbial community showed activity and growth when supplied with polysaccharides, indicative of the capacity to quickly (within days) synthesize the enzymatic machinery necessary to metabolize preferably low complexity storage polymers. Notably, Clostridia showed the most prominent response to substrate amendment (**Figure 3B**) and were frequently detected with increased proportions in all treatments but were low in abundance in the initial sediments (**Figures 2**, **3A**) as previously observed (Perez Castro et al., 2021). In the sediments used for our experiment dormant Clostridia endospores likely endured long-term cold (4°C) storage and germinated upon exposure to elevated temperatures (33°C) prior to substrate addition. Previously, the germination of thermophilic, endospore-forming bacteria including Firmicutes and their activity in organic matter mineralization have been demonstrated when cold marine sediments were exposed to elevated temperatures (Isaksen et al., 1994; Hubert et al., 2009, 2010). Our results also suggest that while temperature may induce germination the magnitude of activity and growth likely depends on the availability of suitable substrates as a stronger response was observed in polysaccharide amended incubations compared to unamended controls. Future BONCAT-FACS experiments testing the effect of polysaccharide amendment on freshly recovered sediments (i.e., no long-term cold storage) over a range of temperatures including at 4°C would provide extended insights into the populations active in the environment under different temperature regimes.

Altogether, in sediments exposed to hydrothermal activity such as in Guaymas Basin temperature induced germination of Clostridia spores may frequently occur resulting in these organisms becoming active and important in community function as primary polymer degraders for as long as temperature regimes permit their metabolism. This suggests that a flexible lifestyle between metabolic activity and dormancy is an effective strategy for long-term survival in environments with extreme and fluctuating physicochemical conditions. Thus, in hydrothermally influenced sediments temporal and spatial fluctuations in

temperature and substrate availability will constrain metabolic activity and growth resulting in dynamic microbial communities.

CONCLUSION

Our study investigated the effect of polysaccharide addition on the total and active microbial communities in anoxic hydrothermal sediments. We identified a diverse, yet initially minor population of Clostridia rapidly responding with activity and growth to the availability of primarily low complexity polymers, starch and laminarin. Clostridia likely persisted in the sediments as spores during long-term cold storage and their germination in mesocosms was initiated by a switch to elevated temperatures. This indicates that in environments with fluctuating physicochemical regimes and diverse community assemblies, such as in Guaymas Basin sediments, taxa that are low in abundance or possibly dormant, including spore-forming Clostridia, may frequently assume important functions in a heterotrophic community. Consequently, time resolved correlative analysis of community composition and physicochemical parameters together with experimental investigations into metabolic activity are imperative to identify environmentally relevant taxa and assess community function.

Our study evaluated the application of BONCAT-FACS to trace metabolic responses in a hydrothermal deep-sea sediment community and highlighted the prominent challenges associated with this method when applied to a unique sample type. The outcomes will inform experimental design for future studies on the *in situ* activity and functional role of uncultured taxa in Guaymas Basin and other deep-sea sediments. In particular, cell recovery from the organic-rich sediment matrix and high diversity of the microbial community limited the comparability between DNA and cell extractable fractions and subsequently the encompassing detection of active taxa. Further, the detection of a selective effect of substrate amendment was initially limited (day 2) possibly due to the naturally high organic matter content of Guaymas Basin sediments and was more pronounced after prolonged incubation (day 5), suggesting that time of substrate exposure is critical (Calvert, 1966; Von Damm et al., 1985; De la Lanza-Espino and Soto, 1999; Zheng et al., 2021). The statistical power of our analysis was qualified by a combination of low replication and high variability between triplicates, potentially due to a preferential response of minor populations in individual replicates. Thus, cell recovery difficulties together with high cell quantity requirements and elevated replication demand challenge both applicability and throughput of BONCAT-FACS, especially when available sample material is limited. However, upon careful optimization and integration into combinatorial approaches, BONCAT-FACS expands available methods with prospect for wider implementation in microbial ecology research.

DATA AVAILABILITY STATEMENT

The datasets presented in this study can be found in online repositories. The names of the repository/repositories and accession number(s) can be found in the article/**Supplementary Material**.

AUTHOR CONTRIBUTIONS

VK and RH designed this study. VK performed experiments and data analysis. VK, RS, and NR developed fluorescence-activated cell sorting protocols. VK wrote the manuscript which was edited by all authors.

FUNDING

This study was funded by U.S. National Science Foundation award MCB-1817428 to RH. Sampling in Guaymas Basin was supported by the National Science Foundation (BIO-OCE 1357238).

ACKNOWLEDGMENTS

We thank chief scientist Andreas Teske, the scientific party, the crew members of R/V *Atlantis*, and the pilots of DSV *Alvin* of research expedition AT42-05 (2018). The acquisition of a FACS was made possible through a grant by the Gordon and Betty Moore Foundation (GBMF5999) to RH. We thank Andreas Teske for critically reading the manuscript draft.

SUPPLEMENTARY MATERIAL

The Supplementary Material for this article can be found online at: https://www.frontiersin.org/articles/10.3389/fmicb.2021.763971/full#supplementary-material

REFERENCES

Apprill, A., Mcnally, S., Parsons, R., and Weber, L. (2015). Minor revision to V4 region SSU rRNA 806R gene primer greatly increases detection of SAR11 bacterioplankton. *Aquat. Microb. Ecol.* 75, 129–137.

Arnosti, C., Wietz, M., Brinkhoff, T., Hehemann, J., Probandt, D., Zeugner, L., et al. (2021). The biogeochemistry of marine polysaccharides: sources, inventories, and bacterial drivers of the carbohydrate cycle. *Ann. Rev. Mar. Sci.* 13, 81–108. doi: 10.1146/annurev-marine-032020-012810

Baker, B. J., Appler, K. E., and Gong, X. (2021). New microbial biodiversity in marine sediments. *Ann. Rev. Mar. Sci.* 13, 161–175. doi: 10.1146/annurev-marine-032020-014552

Berry, D., Mader, E., Lee, T. K., Woebken, D., Wang, Y., Zhu, D., et al. (2015). Tracking heavy water (D2O) incorporation for identifying and sorting active microbial cells. *Proc. Natl. Acad. Sci.* 112, E194–E203. doi: 10.1073/pnas.1420406112

Bolyen, E., Rideout, J., Dillon, M., Bokulich, N., Abnet, C., Al-Ghalith, G., et al. (2019). Reproducible, interactive, scalable and extensible microbiome data science using QIIME 2. *Nat. Biotechnol.* 37, 852–857.

Callahan, B., McMurdie, P., Rosen, M., Han, A., Johnson, A., Holmes, S., et al. (2016). DADA2: High-resolution sample inference from Illumina amplicon data. *Nat. Methods* 13, 581–583.

Calvert, S. E. (1966). Origin of diatom-rich, varved sediments from the Gulf of California. *J. Geol.* 74, 546–565.

Carini, P., Marsden, P., Leff, J., Morgan, E., Strickland, M., and Fierer, N. (2016). Relic DNA is abundant in soil and obscures estimates of soil microbial diversity. *Nat. Microbiol.* 2:16242. doi: 10.1038/nmicrobiol.2016.242

Corinaldesi, C., Dell'Anno, A., and Danovaro, R. (2007). Early diagenesis and trophic role of extracellular DNA in different benthic ecosystems. *Limnol. Ocean* 52, 1710–1717. doi: 10.4319/lo.2007.52.4.1710

Couradeau, E., Sasse, J., Goudeau, D., Nath, N., Hazen, T. C., Bowen, B. P., et al. (2019). Probing the active fraction of soil microbiomes using BONCAT-FACS. *Nat. Commun.* 10:2770. doi: 10.1038/s41467-019-10542-0

De la Lanza-Espino, G., and Soto, L. A. (1999). Sedimentary geochemistry of hydrothermal vents in Guaymas Basin, Gulf of California, Mexico. *Appl. Geochem.* 14, 499–510. doi: 10.1016/s0883-2927(98)00064-x

Dekas, A., and Orphan, V. (2011). Identification of diazotrophic microorganisms in marine sediment via fluorescence *in situ* hybridization coupled to nanoscale secondary ion mass spectrometry (FISH-NanoSIMS). *Methods Enzym.* 486, 281–305. doi: 10.1016/B978-0-12-381294-0.00012-2

Dell'Anno, A., and Danovaro, R. (2005). Extracellular DNA plays a key role in deep-sea ecosystem functioning. *Science* 30:2179. doi: 10.1126/science.1117475

Dombrowski, N., Seitz, K. W., Teske, A. P., and Baker, B. J. (2017). Genomic insights into potential interdependencies in microbial hydrocarbon and nutrient cycling in hydrothermal sediments. *Microbiome* 5:106. doi: 10.1186/s40168-017-0322-2

Dombrowski, N., Teske, A., and Baker, B. (2018). Expansive microbial metabolic versatility and biodiversity in dynamic Guaymas Basin hydrothermal sediments. *Nat. Commun.* 9:4999. doi: 10.1038/s41467-018-07418-0

Doud, D. F. R., and Woyke, T. (2017). Novel approaches in function-driven single-cell genomics. *FEMS Microbiol. Rev.* 41, 538–548. doi: 10.1093/femsre/fux009

Fernandes, A., Macklaim, J., Linn, T., Reid, G., and Gloor, G. (2013). ANOVA-like differential gene expression analysis of single-organism and meta-RNA-seq. *PLoS One* 8:e67019. doi: 10.1371/journal.pone.0067019

Fernandes, D. A., Reid, J., Macklaim, M. J., McMurrough, T., Edgell, D. R., and Gloor, B. G. (2014). Unifying the analysis of high-throughput sequencing datasets: characterizing RNA-seq, 16S rRNA gene sequencing and selective growth experiments by compositional data analysis. *Microbiome* 2:15. doi: 10.1186/2049-2618-2-15

Hatzenpichler, R., and Orphan, V. (2015). "Detection of protein-synthesizing microorganisms in the environment via bioorthogonal noncanonical amino acid tagging (BONCAT)" in *Hydrocarbon and Lipid Microbiology Protocols*. ed. T. McGenity (Berlin: Springer). 145–157. doi: 10.1007/8623_2015_61

Hatzenpichler, R., Connon, S. A., Goudeau, D., Malmstrom, R. R., Woyke, T., and Orphan, V. J. (2016). Visualizing *in situ* translational activity for identifying and sorting slow-growing archaeal-bacterial consortia. *Proc. Natl. Acad. Sci.* 113, E4069–E4078. doi: 10.1073/pnas.1603757113

Hatzenpichler, R., Krukenberg, V., Spietz, R. L., and Jay, Z. J. (2020). Next-generation physiology approaches to study microbiome function at single cell level. *Nat. Rev. Microbiol.* 18, 241–245. doi: 10.1038/s41579-020-0323-1

Hatzenpichler, R., Scheller, S., Tavormina, P. L., Babin, B. M., Tirrell, D. A., and Orphan, V. J. (2014). *In situ* visualization of newly synthesized proteins in environmental microbes using amino acid tagging and click chemistry. *Environ. Microbiol.* 16, 2568–2590. doi: 10.1111/1462-2920.12436

Huang, W. E., Ward, A. D., and Whiteley, A. S. (2009). Raman tweezers sorting of single microbial cells. *Environ. Microbiol. Rep.* 1, 44–49. doi: 10.1111/j.1758-2229.2008.00002.x

Huang, W., Stoecker, K., Griffiths, R., Newbold, L., Daims, H., Whiteley, A., et al. (2007). Raman-FISH: combining stable-isotope Raman spectroscopy and fluorescence *in situ* hybridization for the single cell analysis of identity and function. *Environ. Microbiol.* 9, 1878–1889. doi: 10.1111/j.1462-2920.2007.01352.x

Hubert, C., Arnosti, C., Brüchert, V., Alexander, L., Verona, V., and Jørgensen, B. B. (2010). Thermophilic anaerobes in Arctic marine sediments induced to mineralize complex organic matter at high temperature. *Environ. Microbiol.* 12, 1089–1104. doi: 10.1111/j.1462-2920.2010.02161.x

Hubert, C., Loy, A., Nickel, M., Arnosti, C., Baranyi, C., Brüchert, V., et al. (2009). A constant flux of diverse thermophilic bacteria into the cold arctic seabed. *Science* 325, 1541–1544. doi: 10.1126/science.1174012

Isaksen, M. F., Bak, F., and Jørgensen, B. B. (1994). Thermophilic sulfate-reducing bacteria in cold marine sediment. *FEMS Microbiol. Ecol.* 1, 1–8. doi: 10.1111/j.1574-6941.1994.tb00084.x

Jørgensen, N. O. G., and Jacobsen, C. S. (1996). Bacterial uptake and utilization of dissolved DNA. *Aquat. Microb. Ecol.* 11, 263–270. doi: 10.3354/ame011263

Kiick, K., Saxon, E., Tirrell, D., and Bertozzi, C. (2002). Incorporation of azides into recombinant proteins for chemoselective modification by the Staudinger ligation. *Proc. Natl. Acad. Sci. U. S. A.* 99, 19–24. doi: 10.1073/pnas.012583299

Lever, M. A., Torti, A., Eickenbusch, P., Michaud, A. B., Šantl-Temkiv, T., and Jørgensen, B. B. (2015). A modular method for the extraction of DNA and RNA, and the separation of DNA pools from diverse environmental sample types. *Front. Microbiol.* 6:476. doi: 10.3389/fmicb.2015.00476

Marlow, J., Spietz, R., Kim, K.-Y., Ellisman, M., Girguis, P., and Hatzenpichler, R. (2021). Spatially-resolved correlative microscopy and microbial identification reveals dynamic depth- and mineral- dependent anabolic activity in salt marsh sediment. *Environ. Microbiol.* 23, 4756–4777. doi: 10.1111/1462-2920.15667

Martin, M. (2011). Cutadapt removes adapter sequences from high-throughput sequencing reads. *EMBnet J.* 17, 10–12. doi: 10.1089/cmb.2017.0096

McMurdie, P. J., and Holmes, S. (2013). phyloseq: an R package for reproducible interactive 884 analysis and graphics of microbiome census data. *PLoS One* 8:e61217. doi: 10.1371/journal.pone.0061217

Morono, Y., Terada, T., Kallmeyer, J., and Inagaki, F. (2013). An improved cell separation technique for marine subsurface sediments: Applications for high-throughput analysis using flow cytometry and cell sorting. *Environ. Microbiol.* 15, 2841–2849. doi: 10.1111/1462-2920.12153

Musat, N., Musat, F., Weber, P., and Pett-Ridge, J. (2016). Tracking microbial interactions with NanoSIMS. *Curr. Oin. Biotechnol.* 41, 114–121. doi: 10.1016/j.copbio.2016.06.007

Parada, A., Needham, D., and Fuhrman, J. (2016). Every base matters: assessing small subunit rRNA primers for marine microbiomes with mock communities, time series and global field samples. *Environ. Microbiol.* 18, 1403–1414. doi: 10.1111/1462-2920.13023

Perez Castro, S., Borton, M. A., Regan, K., de Angelis, I. H., Wrighton, K. C., Teske, A. P., et al. (2021). Degradation of biological macromolecules supports uncultured microbial populations in Guaymas Basin hydrothermal sediments. *ISME J.* doi: 10.1038/s41396-021-01026-5 [Epub online ahead of print].

Quast, C., Pruesse, E., Yilmaz, P., Gerken, J., Schweer, T., Gloeckner, F. O., et al. (2013). The SILVA ribosomal RNA gene database project: improved data processing and web-based tools. *Nucleic Acids Res.* 41, 590–596. doi: 10.1093/nar/gks1219

Ramírez, G. A., Jørgensen, S. L., Zhao, R., and D'Hondt, S. (2018). Minimal influence of extracellular DNA on molecular surveys of marine sedimentary communities. *Front. Microbiol.* 9:2969. doi: 10.3389/fmicb.2018.02969

Ramírez, G. A., Mara, P., Sehein, T., Wegener, G., Chambers, R. C., Joye, S. B., et al. (2021). Environmental factos shaping bacterial, archaeal and fungal community structure in hydrothermal sediments of Guaymas Basin, Gulf of California. *PLoS One* 16:e0256321. doi: 10.1371/journal.pone.0256321

Reichart, N. J., Jay, Z. J., Hatzenpichler, R., Krukenberg, V., Parker, A. E., and Spietz, R. L. (2020). Activity-based cell sorting reveals responses of uncultured archaea and bacteria to substrate amendment. *ISME J.* 14, 2851–2861. doi: 10.1038/s41396-020-00749-1

Riva, A., Kolimár, D., Spittler, A., Wisgrill, L., Herbold, C., Abrankó, L., et al. (2020). Conversion of rutin, a prevalent dietary flavonol, by the human gut microbiota. *Front. Microbiol.* 11:585428. doi: 10.3389/fmicb.2020.585428

Taguer, M., Shapiro, B. J., and Maurice, C. F. (2021). Translational activity is uncoupled from nucleic acid content in bacterial cells of the human gut microbiota. *Gut. Microbes* 13:1. doi: 10.1080/19490976.2021.1903289

Teske, A., de Beer, D., McKay, L., Tivey, M. K., Biddle, J. F., Hoer, D., et al. (2016). The Guaymas Basin hiking guide to hydrothermal mounds, chimneys and microbial mats: complex seafloor expressions of subsurface hydrothermal circulation. *Front. Microbiol.* 7:75. doi: 10.3389/fmicb.2016.00075

Teske, A., Hinrichs, K., Edgcomb, V., Gomez, D. V., Kysela, D., Sylva, S. P., et al. (2002). Microbial diversity of hydrothermal sediments in the Guaymas Basin: Evidence for anaerobic methanotrophic communities. *Appl. Environ. Microbiol.* 68, 1994–2007. doi: 10.1128/AEM.68.4.1994-2007.2002

Teske, A., Wegener, G., Chanton, J. P., White, D., MacGregor, B. J., Hoer, D., et al. (2021). Microbial communities under distinct thermal and geochemical regimes in axial and off-axis sediments of Guaymas Basin. *Front. Microbiol.* 12:633649. doi: 10.3389/fmicb.2021.633649

Thompson, L., Sanders, J., McDonald, D., Amir, A., Ladau, J., Locey, K., et al. (2017). A communal catalogue reveals Earth's multiscale microbial diversity. *Nature* 551, 457–463. doi: 10.1038/nature24621

Torti, A., Jørgensen, B. B., and Lever, M. A. (2018). Preservation of microbial DNA in marine sediments: insights from extracellular DNA pools. *Environ. Microbiol.* 20, 4526–4542. doi: 10.1111/1462-2920.14401

Valentini, T., Lucas, S., Binder, K., Cameron, L., Motl, J., Dunitz, J., et al. (2020). Bioorthogonal non-canonical amino acid tagging reveals translationally active subpopulations of the cystic fibrosis lung microbiota. *Nat. Commun.* 11:2287. doi: 10.1038/s41467-020-16163-2

Von Damm, K. L., Edmond, J. M., Measures, C. I., and Grant, B. (1985). Chemistry of submarine hydrothermal solutions at Guaymas Basin, Gulf of California. *Geochim. Cosmochim. Acta* 49, 2221–2237. doi: 10.1016/0016-7037(85)90223-6

Widdel, F., and Bak, F. (1992). "Gram-negative mesophilic sulfate-reducing bacteria," in *The Prokaryotes, 2nd edn.,* eds A. Balows, H. G. Trüper, M. Dworkin, W. Harder, K.-H. Schleifer (New York, NY: Springer), 3352–3378.

Zheng, Q., Lin, W., Wang, Y., Li, Y., He, C., Shen, Y., et al. (2021). Highly enriched N-containing organic molecules of *Synechococcus* lysates and their rapid transformation by heterotrophic bacteria. *Limnol. Ocean* 66, 335–348. doi: 10.1002/lno.11608

Conflict of Interest: The authors declare that the research was conducted in the absence of any commercial or financial relationships that could be construed as a potential conflict of interest.

Publisher's Note: All claims expressed in this article are solely those of the authors and do not necessarily represent those of their affiliated organizations, or those of the publisher, the editors and the reviewers. Any product that may be evaluated in this article, or claim that may be made by its manufacturer, is not guaranteed or endorsed by the publisher.

frontiers in Microbiology

ORIGINAL RESEARCH
published: 15 February 2022
doi: 10.3389/fmicb.2021.802888

Comparative Analysis of Intestinal Microflora Between Two Developmental Stages of *Rimicaris kairei*, a Hydrothermal Shrimp From the Central Indian Ridge

*Li Qi[1,2], Chun-Ang Lian[1], Fang-Chao Zhu[1,3], Mengke Shi[1,2] and Li-Sheng He[1]**

[1] Institute of Deep-Sea Science and Engineering, Chinese Academy of Sciences, Sanya, China, [2] College of Earth Sciences, University of Chinese Academy of Sciences, Beijing, China, [3] Key Laboratory of Tropical Marine Ecosystem and Bioresource, Fourth Institute of Oceanography, Ministry of Natural Resources, Beihai, China

OPEN ACCESS

Edited by:
S. Emil Ruff, Marine Biological Laboratory (MBL), United States

Reviewed by:
Girish Beedessee, University of Cambridge, United Kingdom
Tongtong Li, Zhejiang University of Technology, China

***Correspondence:**
Li-Sheng He
he-lisheng@idsse.ac.cn

Specialty section:
This article was submitted to Extreme Microbiology, a section of the journal Frontiers in Microbiology

Received: *27 October 2021*
Accepted: *28 December 2021*
Published: *15 February 2022*

Citation:
Qi L, Lian C-A, Zhu F-C, Shi M and He L-S (2022) Comparative Analysis of Intestinal Microflora Between Two Developmental Stages of Rimicaris kairei, a Hydrothermal Shrimp From the Central Indian Ridge. Front. Microbiol. 12:802888. doi: 10.3389/fmicb.2021.802888

Despite extreme physical and chemical characteristics, deep-sea hydrothermal vents provide a place for fauna survival and reproduction. The symbiotic relationship of chemotrophic microorganisms has been investigated in the gill of *Rimicaris exoculata*, which are endemic to the hydrothermal vents of the Mid-Atlantic Ridge. However, only a few studies have examined intestinal symbiosis. Here, we studied the intestinal fauna in juvenile and adult *Rimicaris kairei*, another species in the *Rimicaris* genus that was originally discovered at the Kairei and Edmond hydrothermal vent fields in the Central Indian Ridge. The results showed that there were significant differences between juvenile and adult gut microbiota in terms of species richness, diversity, and evenness. The values of Chao1, observed species, and ASV rarefaction curves indicated almost four times the number of species in adults compared to juveniles. In juveniles, the most abundant phylum was Deferribacterota, at 80%, while in adults, Campilobacterota was the most abundant, at 49%. Beta diversity showed that the intestinal communities of juveniles and adults were clearly classified into two clusters based on the evaluations of Bray–Curtis and weighted UniFrac distance matrices. *Deferribacteraceae* and *Sulfurovum* were the main featured bacteria contributing to the difference. Moreover, functional prediction for all of the intestinal microbiota showed that the pathways related to ansamycin synthesis, branched-chain amino acid biosynthesis, lipid metabolism, and cell motility appeared highly abundant in juveniles. However, for adults, the most abundant pathways were those of sulfur transfer, carbohydrate, and biotin metabolism. Taken together, these results indicated large differences in intestinal microbial composition and potential functions between juvenile and adult vent shrimp (*R. kairei*), which may be related to their physiological needs at different stages of development.

Keywords: intestine microflora, hydrothermal vent, *Rimicaris kairei*, *Deferribacteraceae*, *Sulfurovum*

INTRODUCTION

Deep-sea hydrothermal vents are distributed along mid-ocean ridges and are characterized by high temperatures and environments that are sulfide- and iron-rich, with a low pH (White et al., 2006; Möller et al., 2017). Despite the hostile environment, a large number of microorganisms and macroorganisms can be found in the hydrothermal area. The shrimp *Rimicaris exoculata* is one of the dominant macroorganisms in the hydrothermal vents of the Mid-Atlantic Ridge (MAR) and can reach densities of up to 3,000 individuals per square meter in the mixing zone of hydrothermal fluid and the surrounding cold, oxygenated seawater (Gebruk et al., 2000).

In deep-sea hydrothermal vents, symbiosis between macroorganisms and chemoautotrophic microorganisms is a common phenomenon (Goffredi et al., 2004; Goffredi, 2010; Watsuji et al., 2015; Hinzke et al., 2019). *R. exoculata* has been reported to coexist with branchiostegite chemoautotrophic microorganisms (Zbinden et al., 2008; Petersen et al., 2010; Hügler et al., 2011; Guri et al., 2012; Jan et al., 2014). Microbial symbionts benefit from the relatively stable habitat at the interface between electron donors and receptors for energy metabolism and provide organic carbon in return to their hosts. In contrast, only a few studies have been focused on the intestinal microflora of macroorganisms in hydrothermal vents, although intestinal microflora play important roles in diverse physiological events, such as nutrient absorption and immune protection, in almost all vertebrates and invertebrates outside vents (Dick, 2019). Van Dover et al. (1988) found that metallic sulfide crystals filled the stomach and gut of hydrothermal shrimp in the MAR. At the time, it was thought that they ate the sulfur compounds around the chimneys for nutrition. The presence of microorganisms in the gut of *R. exoculata* from the MAR was first observed by transmission electron microscopy in 2003; subsequent 16S rRNA analysis identified them as mainly Epsilonproteobacteria, Entomoplasmatales, and Deferribacterota (Zbinden and Cambon-Bonavita, 2003). Later, Durand et al. (2010) found that long-term starvation changed the dominant gut microflora of *R. exoculata*, supporting the hypothesis that a symbiotic relationship existed between *R. exoculata* and its gut epibionts. Durand et al. (2015) further defined the main lineage of resident gut epibionts at five hydrothermal vent locations and analyzed the relationship between the gut microbial communities and the different geographical locations. Apremont et al. (2018) reported the distribution, morphology, and phylogeny of microbial communities associated with the gut and gill of *Rimicaris chacei* in the MAR. The results showed that ε- and γ-proteobacteria were mainly found in the cephalothorax and digestive tract, and that Deferribacterota and Mollicutes were mainly found in the digestive tract. The microbial proliferation was explored during embryonic development of *R. exoculata* and increased with aged eggs (Methou et al., 2019).

Rimicaris kairei was discovered at the Kairei and Edmond fields in 2002, near the Rodriguez Triple Junction, Central Indian Ridge, Indian Ocean, at depths of 2,415–3,320 m (Watabe and Hashimoto, 2002). In this study, we comparatively characterized the gut microbial community of two developmental stages of the vent shrimp *R. kairei*, which further shed light on features of the intestinal microbiome in hydrothermal zones and provided basic information for functional analysis of the intestinal flora.

MATERIALS AND METHODS

Sample Collection and Identification

The shrimps were collected at two hydrothermal vent fields on the Central Indian Ridge, Edmond (69.59667°E, 23.87782°N; 3,281 m depth) and Kairei (70.04010°E, 25.32048°N; 2,421 m depth), during the cruises on February 2019 by the research ship "Tan Suo Yi Hao." All shrimps were obtained using the suction sampler from a manned submersible ("Shen Hai Yong Shi"). Once onboard, specimens were immediately frozen at −80°C or stored in 75% ethanol at −20°C.

According to body length, these shrimps were divided into two groups, defined as juveniles (<4 cm in length), and adults (>6 cm in length) (Jiang et al., 2020). Ten individuals of juvenile and ten individuals of adult were randomly selected from the two hydrothermalvents. Species of these shrimp were identified based on cytochrome *c* oxidase subunit I (*COI*). We identified the species as *R. kairei* (**Supplementary Figure 1**), based on the similarity of the *COI* sequence and the phylogenetic tree constructed through MEGA-X (64-bit) (Kumar et al., 2018) and Neighbor-Joining using Tamura 3-parameter model, with 1,000 bootstrap replications.

DNA Extraction and Sequencing

The leg muscle (for *COI* sequence) and whole gut samples were isolated under sterile conditions. The gut before the fourth body segment is the foregut, while the rest constitute the hindgut (Zbinden and Cambon-Bonavita, 2003; Durand et al., 2010). DNA was extracted from each sample with the Power Soil DNA isolation kit (Qiagen, Hilden, Germany) following the manufacturer's instructions. The V3–V4 region of 16S rRNA was amplified from the extracted DNA using the bacterial universal primers 341F: 5′-CCTAYGGGRBGCASCAG-3′ and 806R: 5′-GGACTACHVGGGTWTCTAAT-3 (Gonnella et al., 2016). Amplifications were performed on a Gene Amps PCR System 9700 (PE Applied Biosystems, Foster City, CA, United States) with the following program: 98°C for 30 s; 98°C for 15 s, 58°C for 15 s, and 72°C for 15 s, for a total of 30 cycles, followed by 72°C for 1 min. DNA was amplified in a 50 μl reaction composed of 25 μl Phusion High-Fidelity PCR Master Mix with HF Buffer, 3 μl DMSO, 0.3 μM of each primer, 50 ng DNA template, and nuclease-free water. The PCR products were purified with an AxyPrep DNA Gel Extraction Kit (Axygen, Union City, CA, United States) and quantified by Qubit fluorometric quantitation (Life Technologies, Carlsbad, CA, United States). Paired-end sequencing was performed on a NovaSeq PE-250 (Illumina) platform of GuHe Bioinformatics Technology (Hangzhou, China).

Taxonomic Classification, Diversity Analysis, and Statistical Analysis

The V3–V4 sequences of 16S rRNA from a total of 40 samples were deposited in an SRA (Sequence Read Archive) database under accession numbers SRR16293710–SRR16293749. The datasets of microbiota from the vent environment were downloaded from SRA compared with the intestinal microbiota of *R. kairei*. Relative information on the vent environmental samples is summarized in **Supplementary Table 1**.

Analysis of the V3–V4 sequence was conducted with QIIME2 v2021.8 along with the built-in plugins (Bolyen et al., 2019). First, adapters at both ends of the sequences were removed using the q2-cutadapt plugin after demultiplex. Then, DADA2 (v1.16) (Callahan et al., 2016) was used for sequence trimming, denoising, and dereplication. Chimera sequences were also filtered. Paired reads were merged with a minimum length of 12 bp overlap. The ASV table was filtered out by q2-filter-feature after removing the ASVs with frequencies less than 5. Taxonomic classification was processed using the q2-classify-sklearn algorithm, and the SILVA (V.138) database was used as a reference with a threshold of 0.8. Annotations were obtained after removing contamination using the q2-feature-table plugin and visualized by the q2-taxa-barplot plugin. The ASVs annotated as mitochondria, chloroplasts, or eukaryotes were also removed.

Alpha diversities (Faith_phylogenetic diversity, Pielou's evenness, observed_species, Chao1, Shannon and Simpson indices) and beta diversities (Bray–Curtis, weighted UniFrac, and unweighted UniFrac) were estimated using q2-diversity after normalization to 16,714 sequences per sample according to the minimum number of sequences in the samples. Kruskal–Wallis rank-sum tests were used to detect significant differences in alpha diversity. Beta diversities were visualized using non-metric multidimensional scaling (NMDS) and principal coordinate analysis (PCoA) plots. ANOSIM (analysis of similarities) was used to analyze the similarities of the microbial community compositions of the two groups.

Identification of Featured Microbes

To identify the discriminative microbes of juvenile and adult groups, two methods were used: Random Forest and STAMP (v2.1.3). Random Forest is a machine learning classification algorithm that creates predictions by parallel learning of multiple tree predictors built randomly and trained on different subsets of data (Breiman, 2001). The ASV table with abundance was divided into 80:20 for training and testing. The 'randomForest' package in R 4.0.3 was used to classify the training data, specify juvenile and adult groups as classification variables, and calculate the importance of each ASV feature by assigning 'importance = TRUE'. The out-of-bag (oob) error estimate of the error rate was 4%. Next, the test dataset and the key characteristic bacteria were predicted based on the value of mean decrease accuracy. According to the 'confusionMatrix' and 'multiclass.roc' functions, the accuracy of the confusion matrix was 93.33%, the balanced accuracy was 95%, and the area under the curve (AUC) value was 0.98. Finally, the 20 microbes with the highest mean decrease accuracy were selected and visualized by bar plots and heatmaps, using the 'ggplot2' package. Two-sided Welch's tests with 95% confidence intervals were used in STAMP v2.1.3 and corrected by Benjamini–Hochberg FDR multiple tests (Parks et al., 2014; Li et al., 2021). The shared microbes resulting from the aforementioned approaches were selected and considered as featured microbes that discriminated juvenile and adult groups.

Analysis of Potential Functions

The Phylogenetic Investigation of Communities by Reconstruction of Unobserved States (PICRUSt) 2.0 pipeline was used to predict the potential functions of the bacterial communities based on 16S rRNA sequences (Douglas et al., 2020). Sequences used in the PICRUSt analysis were first clustered into ASVs, with a similarity threshold of 0.99 in QIIME2 v2021.8 and using the Greengenes database (version 13.5) as a reference for clustering. The Kyoto Encyclopedia of Genes and Genomes (KEGG) annotation was performed by the KEGG Automatic Annotation Server (KAAS) with a bidirectional best-hit method and the representative genome set of prokaryotes. According to the KEGG database, KO level 3 was displayed within the KEGG pathway hierarchy. Kruskal–Wallis rank-sum test was used to evaluate the significance. Pearson correlations were used to estimate the relationship between metabolic pathways and featured bacteria. The plot was constructed using ggplots2 in R (v.4.0.3).

RESULTS

Compositions of the Microbial Communities

The rarefactions for these studied samples were saturated and are displayed in **Supplementary Figure 2**. We obtained 1,280,230 raw sequences from the 40 samples, ranging from 16,714 to 40,375 per sample. After cleaning, a total of 1,265,852 high-quality reads were generated, with an average of 31,646 reads per sample. A total of 1,412 unique ASVs were identified and included in all downstream analyses. These ASVs were classified into 29 phyla and 340 genera.

The top 5 phyla in the juvenile group included Deferribacterota, Bacteroidetes, Firmicutes, Proteobacteria, and Campilobacterota, accounting for almost 100% of the total ASVs, and the predominant phylum was Deferribacterota, accounting for approximately 80% (**Figure 1A**). In the adult group, the most dominant phylum was Campilobacterota, with approximately 50% of the total ASVs. Deferribacterota, which accounted for approximately 80% of the total ASVs in juveniles, accounted for the second-largest proportion in adults, at 20%. The proportions of Bacteroidetes and Firmicutes in the juvenile and adult groups were similar, close to 10%. However, proteobacteria varied greatly between the adult and juvenile groups, occupying approximately about 8% in the adult group and only 0.5% in the juvenile group (**Figure 1B**). A total of 340 genera were identified, but there were only 44 genera with an abundance of more than 1% (**Supplementary Figure 3**). In juveniles, the largest group was *Deferribacteraceae*, accounting for 80% ± 16% (mean ± SD), followed by *Flavobacteriaceae*,

which accounted for 8% ± 7%. In adults, the top genus was *Sulfurovum*, accounting for 40% ± 20%. The second one was *Deferribacteraceae*, which accounted for 17% ± 17%. Among these 44 genera, 34 showed significant differences in abundance between the whole gut bacteria of the two developmental groups, according to Wilcoxon rank-sum tests (**Supplementary Table 2**). Among these different genera, only *Deferribacteraceae* and *Tyzzerella* were more enriched in juveniles, while the other 32 genera were more enriched in adults. The genera with the greatest difference were *Deferribacteraceae* (juvenile vs. adult: 80% vs. 17%), and *Sulfurovum* (juvenile vs. adult: 2% vs. 40%) (**Supplementary Figure 4**).

Structural Characteristics of the Intestinal Microbial Communities

Species richness, diversity, and evenness were compared between the juvenile and adult groups. The results showed that the indices examined in this study were significantly higher in adults than in juveniles, indicating that the adult gut microbial community had more species, more diversity, and more evenness (**Figure 2**). For Chao1 and Observed species index, the adult group was more than four times higher than the juvenile group, which was consistent with the ASVs by rarefaction curves (**Supplementary Figure 2**). And for other indices, the adult group appeared at least two times of juveniles (**Figure 2**). The beta diversity analysis clearly revealed two clusters of juvenile and adult gut microbial communities (**Figure 3**). The adult gut microbial community was dispersed in the NMDS (non-metric multidimensional scaling) analysis (**Figure 3A**). Significant differences between the two bacterial communities were identified by the analysis of similarities (ANOSIM) based on Bray–Curtis distance (ANOSIM statistic R: 0.972, $p = 0.001$). In the PCoA, principal coordinate 1(PCo1) explained 79.1% of the variance (**Figure 3B**), R was 0.938 and $p = 0.001$ in ANOSIM analysis, indicating a significant difference between the juvenile and adult groups. In addition, the gut microbial community exhibited low richness, diversity, and evenness compared to the environmental samples (**Supplementary Figures 5A–F**). According to the beta diversity analysis, the gut community was clearly distinct from environmental samples but had a relatively high dispersion (ANOSIM: R = 0.485, $p = 0.001$) (**Supplementary Figure 5G**).

Featured Gut Microbes in Juveniles and Adults

To identify the featured microbes that differed between the juvenile and adult gut microbial communities, a random forest model was constructed. The top 20 genera with the highest variable importance are shown in **Figure 4**. Among these genera, only one (classified as *Deferribacteraceae*) was more abundant in juveniles than in adults; the other 19 genera were lower in juveniles. The top five most featured microbes included *Sulfurovum*, *Deferribacteraceae*, *Mycoplasmataceae*, *Maritinminonas*, and *Entomoplasmatales*_type_III. *Sulfurovum*, the top-ranking microbe, had a mean decrease accuracy (MDA) value of approximately 8 and showed high abundance in all adult samples. *Deferribacteraceae*, the second-ranking microbe, had an MDA value of 7 and the highest abundance in all juvenile samples, but was almost absent in most of the adult samples. The MDA values of *Mycoplasmataceae*, *Maritinminonas*, and *Entomoplasmatales*_type_III ranged from 6 to 5. In the STAMP analysis, 13 genera were filtered out (**Supplementary Figure 6**), 10 of which were shared with random forest analysis.

Potential Functions of Gut Microbiota

Based on 16S rRNA, 45 pathways, each with more than 1% abundance, were predicted by PICRUSt2; of these, 39 pathways were significantly different between the juvenile and adult groups. These pathways were primarily concerned with metabolism, cell processes, genetic information processing, and environmental information processing. Most of the pathways displayed a higher abundance in juveniles, except pathways for glycolysis; the citrate cycle; the sulfur relay system; metabolism of glycine, serine, threonine, pyruvate, biotin, cysteine, methionine, and selenocompound; folate biosynthesis; and the bacterial secretion system, which were more abundant in adults. The biosynthesis of ansamycins and the cell motility pathway were enriched in the juvenile group. In addition, the pathways related to lipid metabolism and essential amino acid synthesis were also higher in juveniles (**Figure 5**). Correlation analysis was performed between 10 featured microbes and the pathways with significant differences between juveniles and adults. The results revealed that *Deferribacteraceae*, the featured bacteria in juveniles, was negatively correlated with the other nine featured microbes in adults in most of the different pathways (**Supplementary Figure 7**).

DISCUSSION

Community Structures of Gut Microbiota Differed Between Juveniles and Adults

The assemblage of a resident microbial community is important for animal development. By investigating the gut microbial communities of juvenile and adult hydrothermal vent shrimp, we found that developmental stage is an important factor affecting the intestinal flora of *R. kairei*. This study showed that the adult gut microbial community had higher index values of species richness, diversity, and evenness than juveniles. This phenomenon has also been reported in other animals. In Malaysian mahseer (*Tor tambroides*), the gut microbiota showed higher diversity in the larval, juvenile, and adult stages than that in fingerling and yearling stages by a culturable approach (Mohd Nosi et al., 2018). The community structure of *Triatoma rubrofasciata* gut microbiota also appeared to be affected by aging, with increased species richness and evenness in aged individuals (Hu et al., 2020). This phenomenon applies not only to marine animals and insects but also to humans. Researchers have reported that healthy adults have significantly higher diversity of their gut microbiomes than young children in the United States (Ringel-Kulka et al., 2013). Similarly, a detailed comparison of the intestinal microbiota of 1-year-old infants and 4-year-old children in China revealed that the species

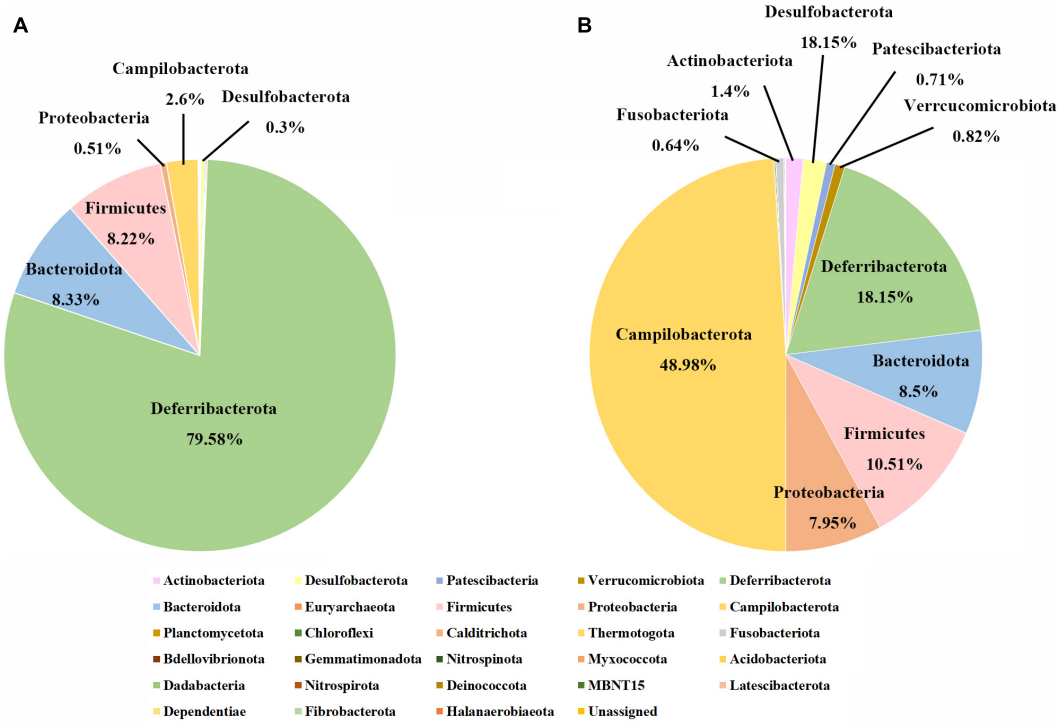

FIGURE 1 | Gut microbial compositions of juvenile and adult samples at the phylum level. **(A)** The phylum level in the juvenile group; **(B)** the phylum level in the adult group.

richness, evenness, and diversity of the intestinal microbiota were significantly lower in the 1-year-olds (Guo et al., 2020). These aging effects not only occur in gut microbiota but also in other parts of the symbiotic microbiota. A study reported that the surface flora structure of *R. exoculata* embryos changed during development. The species diversity and evenness of the bacterial assemblages on egg and pleopod surfaces were higher in the late stage than in the early and middle stages (Methou et al., 2019). There are several possible explanations as to why aged gut flora are richer and more diverse. First, with aging, intestinal cells not only increase in number but also become more increasingly complex in morphology and physiological functions. The diverse intestinal cells and diverse intestinal microenvironment affect the growth and composition of attached microorganisms (Bergh, 1995). Stephens et al. (2016) reported that the morphological changes of intestinal cells during development may be the main driver of changes in the intestinal microbiome, investigating 135 zebrafish intestinal microbial communities from developmental periods given the same diet and environmental conditions (Stephens et al., 2016). Second, adult individuals tend to have more complex diets and living conditions than juveniles, resulting in changes in intestinal microbial diversity. Jin et al. (2021) evaluated the effects of dietary changes, habitat changes, and lifestyle shifts on the gut microbiota of giant pandas with high-throughput sequencing and genome-resolved metagenomics. The results showed that high-fiber diets significantly increased the species diversity and decreased the richness of gut bacterial communities (Jin et al., 2021). Third, the habitat can also greatly affect bacterial communities. Although it is currently unclear whether the habitats of *R. kairei* adults and juveniles are the same, it has been suggested that hydrothermal shrimp may migrate from a few 100 m above the hydrothermal vents to the area around the chimneys, according to the isotopic trace of carbon found in *R. exoculata* (Methou et al., 2020). External environmental conditions can certainly affect diet. In the alpha diversity results of this study, Chao 1 indicated that species richness exhibited the greatest difference between juveniles and adults, with an almost fourfold change. Species diversity and evenness differed between these developmental stages. The changes in intestinal microflora community indicated that their role changes between developmental stages of *R. kairei*.

Potential Functions of Gut Microbiota in Juvenile and Adult Shrimp

According to the PICRUST results, many metabolic pathways exhibited differences between adult and juvenile *R. kairei*. Although ansamycin biosynthesis was the most abundant metabolic pathway in both juvenile and adult groups, the relative abundance of ansamycin synthesis pathways in juvenile compared to other pathways was almost 1.5-fold that in adults. Carbon metabolic and sulfur transfer pathways were substantially more abundant in the adult group. These results indicate that the gut microbiota of juvenile individuals includes more antibacterial functions to protect their hosts from the invasion of pathogenic

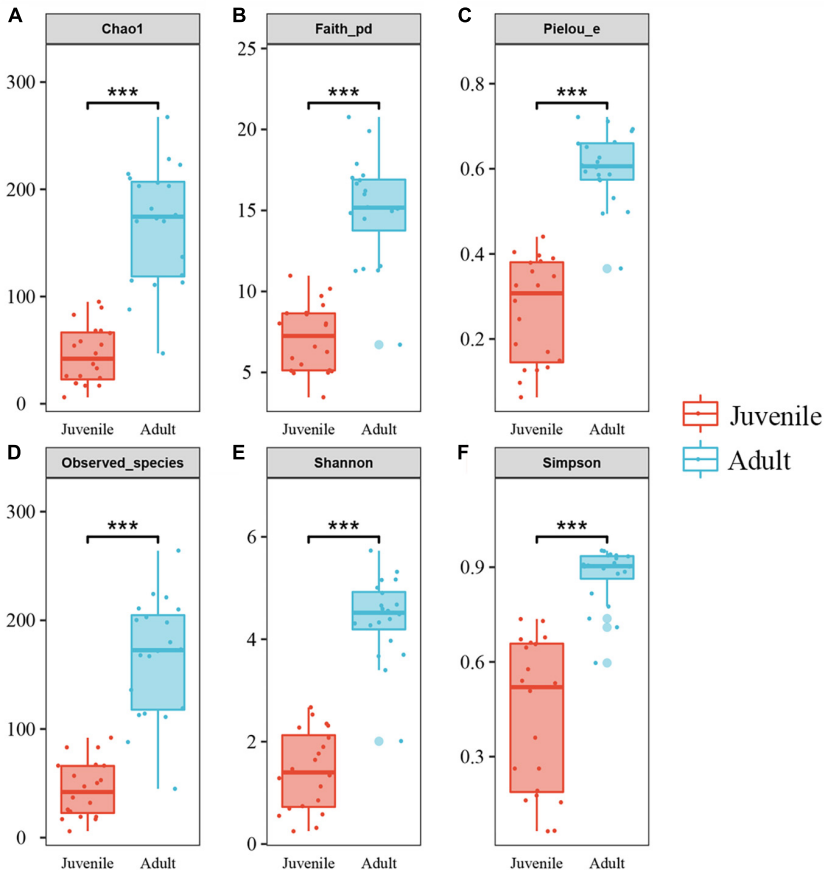

FIGURE 2 | Alpha diversities of gut microbiota in the two developmental stages of *R. kairei*. **(A–F)**: Chao1, Faith_phylogenetic diversity, Pielou's evenness, observed_species, Shannon and Simpson indices are displayed in the box plots (Non-parametric Kruskal–Wallis tests, ***$p < 0.001$). The middle lines in the boxes indicate the median. The upper and lower lines of the box indicate the upper and lower quartiles, respectively. The scattered dots represent the values of each sample. The larger dots represent outliers.

bacteria, while the gut microbiota of adults is more related to energy metabolism.

The most featured bacterial group in the guts of juveniles was *Deferribacteraceae*, which was also a main lineage found in the gut of other vent shrimp (Durand et al., 2010; Apremont et al., 2018). The functions of the phylum Deferribacterota have received less attention, perhaps because most of them are uncultivable. The most studied genus is *Deferribacter*, which inhabits deep and shallow seas and includes four species: *Deferribacter thermophilus*, *Deferribacter desulfuricans*, *Deferribacter abyssi*, and *Deferribacter autotrophicus*. Of these, *D. desulfuricans* and *D. autotrophicus* are the only two species with an available complete genome and whose possible metabolic pathways have been reported. The novel anaerobic heterotrophic bacterium *D. desulfuricans* SSM1 was isolated from a deep-sea hydrothermal vent chimney at the Suiyo Seamount of the Izu-Bonin Arc, Japan (Takai et al., 2003). Genomic annotation and comparison revealed that many of its genes were similar to sulfur-reducing or sulfate-reducing bacteria in the phylum Deltaproteobacteria. Analysis of metabolic pathways revealed that the bacterium was capable of using a variety of organic acids, such as formate, acetate, and pyruvate, as carbon sources. This genome also encodes chemoreceptors, chemotaxis-like systems, and signal transduction machinery, suggesting that the bacterium possesses versatile energy metabolism for surviving its extreme environments (Takaki et al., 2010). In contrast, *D. autotrophicus* is a thermophilic chemolithoautotrophic anaerobe that is capable of CO_2 fixation by the roTCA cycle and that couples the oxidation process of CO with nitrate reduction using anaerobic [Ni, Fe]-containing CO dehydrogenase, the first carbon monoxide oxidation process identified in the phylum Deferribacterota (Slobodkin et al., 2019). A Nap-type complex encoding nitrate reduction was also identified, which may be involved in Fe(III) reduction. Deferribacteraceae, along with Muribaculaceae and Lachnospiraceae, was also the dominant family present in mouse intestines and was associated with cofactor, vitamin, and amino acid metabolism (Chung et al., 2020). Another study reported that the relative abundance of *Deferribacter* spp. and *Spirochaetes* spp. in the gut microbial community of horses increased after 160 h of dietary treatment with moxidectin (Daniels et al., 2020). Taken together, it is hypothesized that *Deferribacteraceae* in the

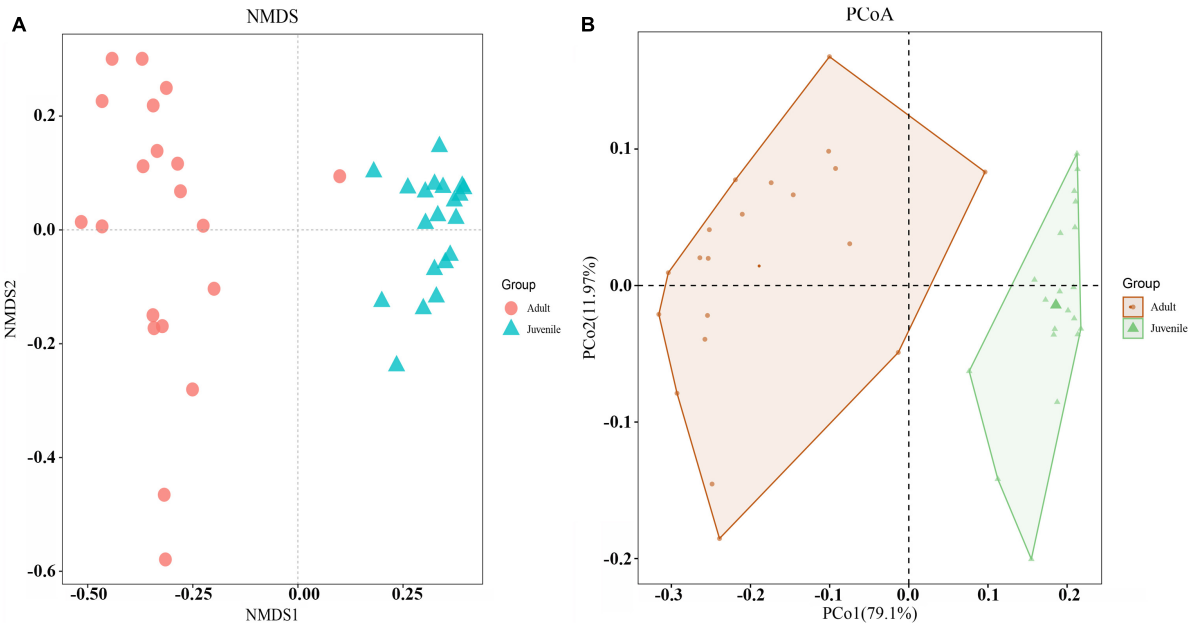

FIGURE 3 | Beta diversities of the two gut microbial communities. **(A)** NMDS was calculated by Bray–Curtis distance for juvenile and adult shrimp (stress = 0.07). Red dots indicate adult samples. Green triangles indicate juvenile samples. **(B)** PCoA indicated the similarity of microbiota composition and the phylogenetic distance between the two groups based on the weighted UniFrac algorithm. Component axes indicate the degree of variance.

FIGURE 4 | Random forest analysis was performed between the two different developmental stages of *R. kairei*. The bar plot shows the influence of the top 20 bacteria based on the accuracy of the random forest model. The heatmap shows the bacteria with normalized abundance in the two different groups. Cam, Campilobacterota; Def, Deferribacterota; Fir, Firmicutes; Bac, Bacteroidetes; Pro, Proteobacteria; Ver, Verrucomicrobia; Act, Actinobacteria; Pat, Patescibacteria. F, foregut; H, hindgut. * indicates the shared bacteria with STAMP.

juvenile gut may be important for host health and adaptation to extreme environments.

The genus *Sulfurovum* belongs to the family *Sulfurovaceae*. Most strains of this genus grow chemolithoautotrophically using sulfur as an energy source. Representatives of this genus include *Sulfurovum lithotrophicum* (Inagaki et al., 2004), *Sulfurovum riftiae* (Giovannelli et al., 2016), *Sulfurovum* sp. (Nakagawa et al., 2007), *Sulfurovum aggregans* (Mino et al., 2014), *Sulfurovum denitrificans* (Mori et al., 2018), and *Sulfurovum indicum* (Xie et al., 2019). Most of them are from lithological samples, except *S. riftiae*, which was isolated from the hydrothermal tubeworms. Among them, only *S. lithotrophicum* and *S. denitrificans* can use oxygen as the electron acceptor; the others can use nitrate, sulfur, or thiosulfate as the electron acceptor. All of these species mainly use hydrogen, sulfur, or thiosulfate as the electron donors. As an environmental bacterium, *Sulfurovum* sp. NBC37-1 utilized

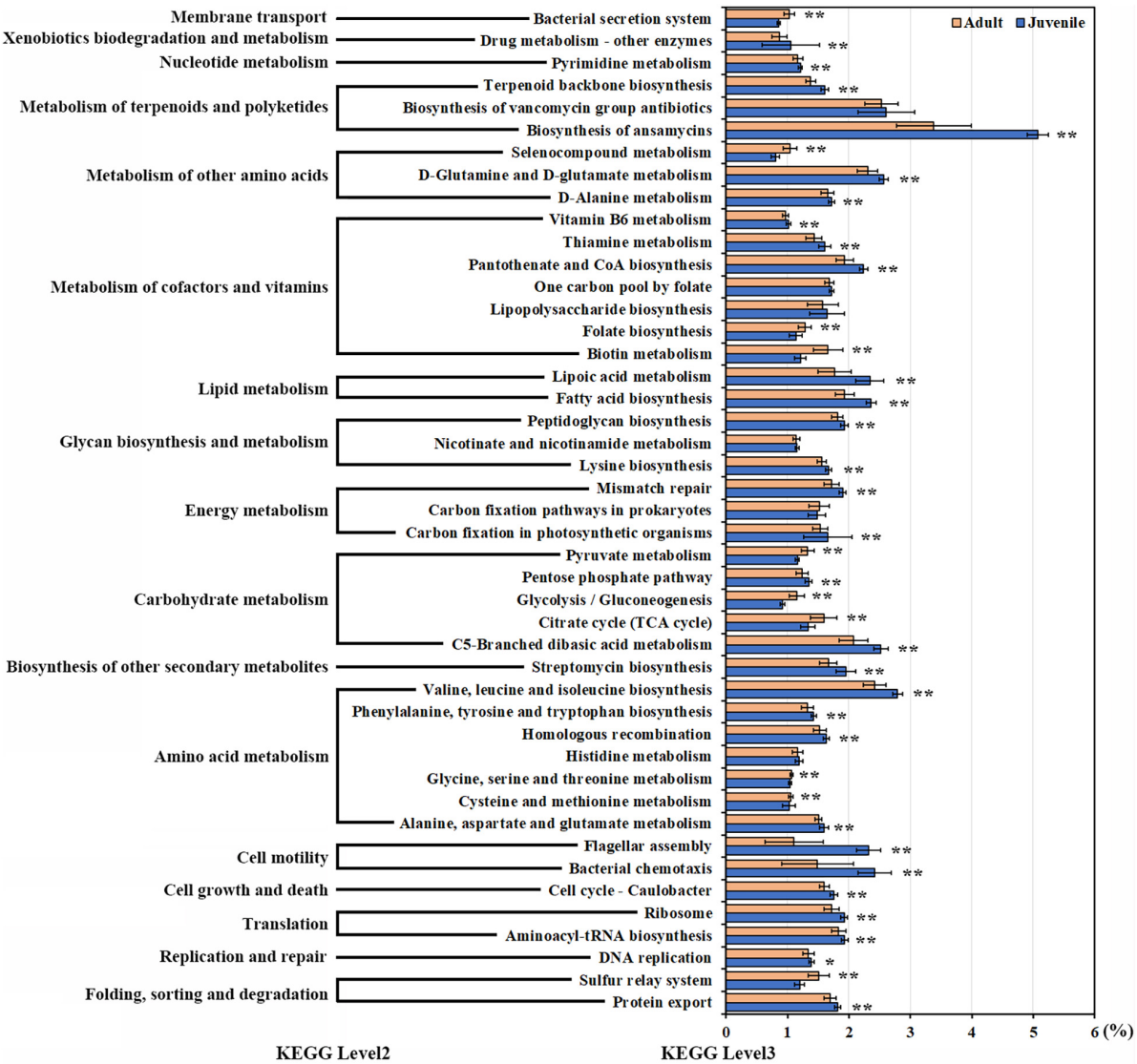

FIGURE 5 | The pathways with significant differences between juveniles and adults. Pathways with more than 1% abundance were included in this differential analysis. The diverse pathways are displayed on the *y*-axis. Relative abundances are displayed on the *x*-axis. Orange bars indicate adult samples. Blue bars indicate juvenile samples. Asterisks indicate a significant difference. (Non-parametric Kruskal–Wallis tests, $^{*}p < 0.05$, $^{**}p < 0.01$).

hydrogen-oxidizing sulfur respiration and thiosulfate-oxidizing nitrate/oxygen respiration for sulfur-related energy metabolism (Nakagawa et al., 2007; Lösekann et al., 2008). *Sulfurovum* sp. NBC37-1 can use elemental sulfur as both electron acceptor and donor, which allows this class of microorganisms to adapt to both highly reduced hydrothermal and oxygen-rich environments (Yamamoto et al., 2010). *S. riftiae* is an anaerobic, nitrate-reducing, sulfur- and thiosulfate-oxidizing bacterium, which uses CO_2 as the only carbon source and nitrate as the only terminal electron acceptor (Giovannelli et al., 2016). A recent metagenomic study on the hydrothermal vent shrimp *R. exoculata* revealed that the reductive tricarboxylic acid (rTCA) and Calvin–Benson–Bassham (CBB) cycles were used for carbon fixation by two filamentous epibionts belonging to Campylobacteria and Gammaproteobacteria, respectively. These epibionts could couple the oxidation of reduced sulfur compounds or molecular hydrogen to oxygen or nitrate reduction (Jan et al., 2014). *Sulfurovum* was the most abundant genus in the adult guts of *R. kairei*. At present, the understanding of the intestinal flora of hydrothermal shrimp is unclear. *Sulfurovum* lineage exists in both gill and intestinal tract besides environments; some researchers speculated that the bacteria in the intestinal tract may belong to the transient community retained by permanent feeding (Zbinden and Cambon-Bonavita, 2020). A recent study on the symbiosis of gills in five different hosts in a hydrothermal environment found that *Sulfurovum* is an opportunistic combination with weak host selectivity (Lee et al., 2021). In the guts of *R. kairei*, there is more than 100 ASVs in the

genus *Sulfurovum* and the top 10 ASVs in abundance accounted for 88.7%. None of the 10 ASVs was assigned as a known species with cutoff of 0.8. Guts provide an anaerobic or hypoxic environment. Strains in *Sulfurovum* are facultative anaerobes or anaerobes. Moreover, metallic sulfide crystals filled the stomach and gut of hydrothermal shrimp (Van Dover et al., 1988; Zbinden and Cambon-Bonavita, 2003). All of these suggest that it is possible for *Sulfurovum* to grow in guts, even as symbionts, and to be involved in sulfur cycle and other functions.

Possible Horizontal Transmission of Gut Microbiota in *R. kairei*

Like all other arthropods, *R. exoculata* undergoes molts, which regularly eliminate the bacterial community that has settled on the cuticle (Corbari et al., 2008). In contrast, the gut has no cuticle layer, and therefore, the gut surface does not renew during molting. The symbionts of this area were therefore supposedly maintained throughout the lifecycle of the animal following their acquisition (Durand et al., 2010). Regarding life history, isotopic data have been used to argue that *R. exoculata* has a long planktotrophic larval dispersal stage before it settles on hydrothermal vents and transitions to the chemosynthetic feeding pattern of juveniles (Gebruk et al., 2000). Lipids and stable carbon isotope analyses of *R. exoculata* indicated that these animals possess a high level of polyunsaturated fatty acids, which can be mobilized to enable growth and maturation of the vent shrimp at a suitable site (Pond et al., 2000). Previous studies have shown that *R. exoculata* harbors two symbioses: epibiotic communities located at branchiostegites, including a wide diversity of Epsilon-, Gamma-, Alpha-, Beta-, Delta-, Zetaproteobacteria, and Bacteroidetes (Zbinden et al., 2008; Petersen et al., 2010; Hügler et al., 2011; Guri et al., 2012; Jan et al., 2014; Cambon-Bonavita et al., 2021), and bacterial communities colonized in guts, which are composed of Deferribacteres, Mollicutes, Campylobacteria, and, to a lesser extent, Gammaproteobacteria (Zbinden and Cambon-Bonavita, 2003; Durand et al., 2010, 2015). These results are consistent with the intestinal microflora of *R. kairei* from the CIR in this study, which is also mainly composed of Deferribacteres, Mollicutes, and Campylobacteria. However, Bacteroidetes was the major phylum in the guts of *R. kairei* from the CIR, but that was not reported in the guts of *R. exoculata* from MAR. Tyzzerella, belonging to the Lachnospiraceae family, in a relatively high proportion in the juvenile group, was not reported in the guts of *R. exoculata* from MAR. All of these suggest that though *R. kairei* and *R. exoculata* belong to hydrothermal shrimp, the microorganism community in their guts appeared different. And the different composition may be affected by geographical environment, species, and others. Although the same species, gut microbial community still showed difference to some extent, indicating the importance of the environmental factor. Cowart et al. (2017) analyzed the communities in three MAR hydrothermal vents across two organs (digestive tract and stomach), three molting colors (white, red, and black), and three life stages (egg, juvenile, and adult) using cluster network analysis. The results showed that the OTUs of Epsilonproteobacteria were geographically segregated, and proposed a combination of transmission modes including environmental selection and vertical inheritance for the symbiont of hydrothermal shrimp *R. exoculata* (Cowart et al., 2017). In the current study, of the 44 genera with abundances above 1%, 36 genera showed significant differences in abundance across the whole gut microbiota between the two groups. These 36 significantly different genera occupied approximately 90 and 80% of the total composition in juveniles and adults, respectively. Taken together with the diversity and discriminative flora analysis, this indicates that there may be horizontal transmission in the gut microbiota of *R. kairei*. Whether there is vertical propagation is uncertain and would require more information related to embryos.

CONCLUSION

There were significant differences in the gut microflora structure, such as species richness, diversity, and evenness, between juvenile and adult *R. kairei*. These results suggest that the presence of gut microbial variation across two developmental stages could be an adaptation strategy for both symbionts and hosts in extreme environments.

DATA AVAILABILITY STATEMENT

The datasets presented in this study can be found in online repositories. The names of the repository/repositories and accession number(s) can be found in the article/**Supplementary Material**.

AUTHOR CONTRIBUTIONS

LQ and L-SH conceived and designed the experiments and wrote the manuscript with input from all other authors. LQ, C-AL, F-CZ, and MS performed the experiments and analyzed the data. L-SH directed and supervised all of the research. All authors contributed to the article and approved the submitted version.

FUNDING

This study was supported by the National Key R&D Program of China (2018YFC0309804); the General projects of National Natural Science Foundation of China (42176125); and the Major Scientific and Technological Projects of Hainan Province (ZDKJ2019011).

SUPPLEMENTARY MATERIAL

The Supplementary Material for this article can be found online at: https://www.frontiersin.org/articles/10.3389/fmicb.2021.802888/full#supplementary-material

REFERENCES

Apremont, V., Cambon-Bonavita, M. A., Cueff-Gauchard, V., François, D., Pradillon, F., Corbari, L., et al. (2018). Gill chamber and gut microbial communities of the hydrothermal shrimp *Rimicaris chacei* Williams and Rona 1986: a possible symbiosis. *PLoS One* 13:e0206084. doi: 10.1371/journal.pone.0206084

Bergh, Ø (1995). Bacteria associated with early life stages of halibut, *Hippoglossus hippoglossus* L., inhibit growth of a pathogenic *Vibrio* sp. *J. Fish Dis.* 18, 31–40. doi: 10.1111/j.1365-2761.1995.tb01263.x

Bolyen, E., Rideout, J. R., Dillon, M. R., Bokulich, N. A., Abnet, C. C., Al-Ghalith, G. A., et al. (2019). Author correction: reproducible, interactive, scalable and extensible microbiome data science using QIIME 2. *Nat. Biotechnol.* 37:1091. doi: 10.1038/s41587-019-0252-6

Breiman, L. (2001). Random forests. *Mach. Learn.* 45, 5–32. doi: 10.1023/A:1010933404324

Callahan, B. J., McMurdie, P. J., Rosen, M. J., Han, A. W., Johnson, A. J., and Holmes, S. P. (2016). DADA2: high-resolution sample inference from Illumina amplicon data. *Nat. Methods* 13, 581–583. doi: 10.1038/nmeth.3869

Cambon-Bonavita, M. A., Aubé, J., Cueff-Gauchard, V., and Reveillaud, J. (2021). Niche partitioning in the *Rimicaris exoculata* holobiont: the case of the first symbiotic Zeta*proteobacteria*. *Microbiome* 9:87. doi: 10.1186/s40168-021-01045-6

Chung, Y. W., Gwak, H. J., Moon, S., Rho, M., and Ryu, J. H. (2020). Functional dynamics of bacterial species in the mouse gut microbiome revealed by metagenomic and metatranscriptomic analyses. *PLoS One* 15:e0227886. doi: 10.1371/journal.pone.0227886

Corbari, L., Zbinden, M., Cambon-Bonavita, M., Gaill, F., and Compère, P. (2008). Bacterial symbionts and mineral deposits in the branchial chamber of the hydrothermal vent shrimp *Rimicaris exoculata*: relationship to moult cycle. *Aquat. Biol.* 1, 225–238. doi: 10.3354/ab00024

Cowart, D. A., Durand, L., Cambon-Bonavita, M. A., and Arnaud-Haond, S. (2017). Investigation of bacterial communities within the digestive organs of the hydrothermal vent shrimp *Rimicaris exoculata* provide insights into holobiont geographic clustering. *PLoS One* 12:e0172543. doi: 10.1371/journal.pone.0172543

Daniels, S. P., Leng, J., Swann, J. R., and Proudman, C. J. (2020). Bugs and drugs: a systems biology approach to characterising the effect of moxidectin on the horse's faecal microbiome. *Anim. Microb.* 2:38. doi: 10.1186/s42523-020-00056-2

Dick, G. J. (2019). The microbiomes of deep-sea hydrothermal vents: distributed globally, shaped locally. *Nat. Rev. Microbiol.* 17, 271–283. doi: 10.1038/s41579-019-0160-2

Douglas, G. M., Maffei, V. J., Zaneveld, J. R., Yurgel, S. N., Brown, J. R., Taylor, C. M., et al. (2020). PICRUSt2 for prediction of metagenome functions. *Nat. Biotechnol.* 38, 685–688. doi: 10.1038/s41587-020-0548-6

Durand, L., Roumagnac, M., Cueff-Gauchard, V., Jan, C., Guri, M., Tessier, C., et al. (2015). Biogeographical distribution of *Rimicaris exoculata* resident gut epibiont communities along the Mid-atlantic Ridge hydrothermal vent sites. *FEMS Microbiol. Ecol.* 91:fiv101. doi: 10.1093/femsec/fiv101

Durand, L., Zbinden, M., Cueff-Gauchard, V., Duperron, S., Roussel, E. G., Shillito, B., et al. (2010). Microbial diversity associated with the hydrothermal shrimp *Rimicaris exoculata* gut and occurrence of a resident microbial community. *FEMS Microbiol. Ecol.* 71, 291–303. doi: 10.1111/j.1574-6941.2009.00806.x

Gebruk, A. V., Southward, E. C., Kennedy, H., and Southward, A. J. (2000). Food sources, behaviour, and distribution of hydrothermal vent shrimps at the mid-atlantic ridge. *J. Mar. Biol. Assoc. U. K.* 80, 485–499. doi: 10.1017/S0025315400002186

Giovannelli, D., Chung, M., Staley, J., Starovoytov, V., Le Bris, N., and Vetriani, C. (2016). *Sulfurovum riftiae* sp. nov., a mesophilic, thiosulfate-oxidizing, nitrate-reducing chemolithoautotrophic epsilonproteobacterium isolated from the tube of the deep-sea hydrothermal vent polychaete *Riftia pachyptila*. *Int. J. Syst. Evol. Microbiol.* 66, 2697–2701. doi: 10.1099/ijsem.0.001106

Goffredi, S. K. (2010). Indigenous ectosymbiotic bacteria associated with diverse hydrothermal vent invertebrates. *Environ. Microbiol. Rep.* 2, 479–488. doi: 10.1111/j.1758-2229.2010.00136.x

Goffredi, S. K., Warén, A., Orphan, V. J., Van Dover, C. L., and Vrijenhoek, R. C. (2004). Novel forms of structural integration between microbes and a hydrothermal vent gastropod from the Indian Ocean. *Appl. Environ. Microbiol.* 70, 3082–3090. doi: 10.1128/aem.70.5.3082-3090.2004

Gonnella, G., Böhnke, S., Indenbirken, D., Garbe-Schönberg, D., Seifert, R., Mertens, C., et al. (2016). Endemic hydrothermal vent species identified in the open ocean seed bank. *Nat. Microbiol.* 1:16086. doi: 10.1038/nmicrobiol.2016.86

Guo, M., Miao, M., Wang, Y., Duan, M., Yang, F., Chen, Y., et al. (2020). Developmental differences in the intestinal microbiota of Chinese 1-year-old infants and 4-year-old children. *Sci. Rep.* 10, 19470–19470. doi: 10.1038/s41598-020-76591-4

Guri, M., Durand, L., Cueff-Gauchard, V., Zbinden, M., Crassous, P., Shillito, B., et al. (2012). Acquisition of epibiotic bacteria along the life cycle of the hydrothermal shrimp *Rimicaris exoculata*. *ISME J.* 6, 597–609. doi: 10.1038/ismej.2011.133

Hinzke, T., Kleiner, M., Breusing, C., Felbeck, H., Häsler, R., Sievert, S. M., et al. (2019). Host-Microbe interactions in the chemosynthetic *Riftia pachyptila* symbiosis. *mBio* 10:e02243-19. doi: 10.1128/mBio.02243-19

Hu, Y., Xie, H., Gao, M., Huang, P., Zhou, H., Ma, Y., et al. (2020). Dynamic of composition and diversity of gut microbiota in *Triatoma rubrofasciata* in different developmental stages and environmental conditions. *Front. Cell Infect. Microbiol.* 10:587708. doi: 10.3389/fcimb.2020.587708

Hügler, M., Petersen, J. M., Dubilier, N., Imhoff, J. F., and Sievert, S. M. (2011). Pathways of carbon and energy metabolism of the epibiotic community associated with the deep-sea hydrothermal vent shrimp *Rimicaris exoculata*. *PLoS One* 6:e16018. doi: 10.1371/journal.pone.0016018

Inagaki, F., Takai, K., Nealson, K. H., and Horikoshi, K. (2004). *Sulfurovum lithotrophicum* gen. nov., sp. nov., a novel sulfur-oxidizing chemolithoautotroph within the epsilon-*Proteobacteria* isolated from okinawa trough hydrothermal sediments. *Int. J. Syst. Evol. Microbiol.* 54(Pt 5), 1477–1482. doi: 10.1099/ijs.0.03042-0

Jan, C., Petersen, J. M., Werner, J., Teeling, H., Huang, S., Glöckner, F. O., et al. (2014). The gill chamber epibiosis of deep-sea shrimp *Rimicaris exoculata*: an in-depth metagenomic investigation and discovery of Zeta*proteobacteria*. *Environ. Microbiol.* 16, 2723–2738. doi: 10.1111/1462-2920.12406

Jiang, L., Liu, X., Dong, C., Huang, Z., Cambon-Bonavita, M. A., Alain, K., et al. (2020). "*Candidatus Desulfobulbus* rimicarensis," an uncultivated Delta*proteobacteria*l epibiont from the deep-sea hydrothermal vent shrimp *Rimicaris exoculata*. *Appl. Environ. Microbiol.* 86:e02549-19. doi: 10.1128/aem.02549-19

Jin, L., Huang, Y., Yang, S., Wu, D., Li, C., Deng, W., et al. (2021). Diet, habitat environment and lifestyle conversion affect the gut microbiomes of giant pandas. *Sci. Total Environ.* 770:145316. doi: 10.1016/j.scitotenv.2021.145316

Kumar, S., Stecher, G., Li, M., Knyaz, C., and Tamura, K. (2018). MEGA X: molecular evolutionary genetics analysis across computing platforms. *Mol. Biol. Evol.* 35, 1547–1549. doi: 10.1093/molbev/msy096

Lee, W. K., Juniper, S. K., Perez, M., Ju, S. J., and Kim, S. J. (2021). Diversity and characterization of bacterial communities of five co-occurring species at a hydrothermal vent on the Tonga Arc. *Ecol. Evol.* 11, 4481–4493. doi: 10.1002/ece3.7343

Li, W. L., Dong, X., Lu, R., Zhou, Y. L., Zheng, P. F., Feng, D., et al. (2021). Microbial ecology of sulfur cycling near the sulfate-methane transition of deep-sea cold seep sediments. *Environ. Microbiol.* 23, 6844–6858. doi: 10.1111/1462-2920.15796

Lösekann, T., Robador, A., Niemann, H., Knittel, K., Boetius, A., and Dubilier, N. (2008). Endosymbioses between bacteria and deep-sea siboglinid tubeworms from an arctic cold seep (Haakon Mosby Mud Volcano, Barents Sea). *Environ. Microbiol.* 10, 3237–3254. doi: 10.1111/j.1462-2920.2008.01712.x

Methou, P., Hernández-Ávila, I., Aube, J., Cueff-Gauchard, V., Gayet, N., Amand, L., et al. (2019). Is it first the egg or the shrimp? – Diversity and variation in microbial communities colonizing broods of the vent shrimp *Rimicaris exoculata* during embryonic development. *Front. Microbiol.* 10:808. doi: 10.3389/fmicb.2019.00808

Methou, P., Michel, L. N., Segonzac, M., Cambon-Bonavita, M.-A., and Pradillon, F. (2020). Integrative taxonomy revisits the ontogeny and trophic niches of *Rimicaris* vent shrimps. *R. Soc. Open Sci.* 7:200837. doi: 10.1098/rsos.200837

Mino, S., Kudo, H., Arai, T., Sawabe, T., Takai, K., and Nakagawa, S. (2014). *Sulfurovum aggregans* sp. nov., a hydrogen-oxidizing, thiosulfate-reducing chemolithoautotroph within the Epsilon*proteobacteria* isolated from a deep-sea hydrothermal vent chimney, and an emended description of the genus *Sulfurovum*. *Int. J. Syst. Evol. Microbiol.* 64(Pt 9), 3195–3201. doi: 10.1099/ijs.0.065094-0

Mohd Nosi, M. Z., Syed Jamil Fadaak, S. N. E., Muhammad, M. D. D., and Iehata, S. (2018). Assessment of gut microbiota in different developmental stages of malaysian mahseer (Tor tambroides). *Aquacul. Res.* 49, 2977–2987. doi: 10.1111/are.13757

Möller, F. M., Kriegel, F., Kieß, M., Sojo, V., and Braun, D. (2017). Steep pH gradients and directed colloid transport in a microfluidic alkaline hydrothermal pore. *Angew. Chem.* 56, 2340–2344. doi: 10.1002/anie.201610781

Mori, K., Yamaguchi, K., and Hanada, S. (2018). *Sulfurovum denitrificans* sp. nov., an obligately chemolithoautotrophic sulfur-oxidizing epsilonproteobacterium isolated from a hydrothermal field. *Int. J. Syst. Evol. Microbiol.* 68, 2183–2187. doi: 10.1099/ijsem.0.002803

Nakagawa, S., Takaki, Y., Shimamura, S., Reysenbach, A. L., Takai, K., and Horikoshi, K. (2007). Deep-sea vent epsilon-*proteobacteria*l genomes provide insights into emergence of pathogens. *Proc. Natl. Acad. Sci. U.S.A.* 104, 12146–12150. doi: 10.1073/pnas.0700687104

Parks, D. H., Tyson, G. W., Hugenholtz, P., and Beiko, R. G. (2014). STAMP: statistical analysis of taxonomic and functional profiles. *Bioinformatics* 30, 3123–3124. doi: 10.1093/bioinformatics/btu494

Petersen, J. M., Ramette, A., Lott, C., Cambon-Bonavita, M. A., Zbinden, M., and Dubilier, N. (2010). Dual symbiosis of the vent shrimp *Rimicaris exoculata* with filamentous gamma- and epsilon*proteobacteria* at four mid-atlantic ridge hydrothermal vent fields. *Environ. Microbiol.* 12, 2204–2218. doi: 10.1111/j.1462-2920.2009.02129.x

Pond, D., Gebruk, A., Southward, E., Southward, A., Fallick, A. E., Bell, M. V., et al. (2000). Unusual fatty acid composition of storage lipids in the bresilioid shrimp *Rimicaris exoculata* couples the photic zone with MAR hydrothermal vent sites. *Mar. Ecol. Prog. Ser.* 198, 171–179. doi: 10.3354/meps198171

Ringel-Kulka, T., Cheng, J., Ringel, Y., Salojärvi, J., Carroll, I., Palva, A., et al. (2013). Intestinal microbiota in healthy U.S. young children and adults–a high throughput microarray analysis. *PLoS One* 8:e64315. doi: 10.1371/journal.pone.0064315

Slobodkin, A., Slobodkina, G., Allioux, M., Alain, K., Jebbar, M., Shadrin, V., et al. (2019). Genomic insights into the carbon and energy metabolism of a thermophilic deep-sea bacterium *Deferribacter autotrophicus* revealed new metabolic traits in the phylum deferribacteres. *Genes* 10:849. doi: 10.3390/genes10110849

Stephens, W. Z., Burns, A. R., Stagaman, K., Wong, S., Rawls, J. F., Guillemin, K., et al. (2016). The composition of the zebrafish intestinal microbial community varies across development. *ISME J.* 10, 644–654. doi: 10.1038/ismej.2015.140

Takai, K., Kobayashi, H., Nealson, K. H., and Horikoshi, K. (2003). *Deferribacter desulfuricans* sp. nov., a novel sulfur-, nitrate- and arsenate-reducing thermophile isolated from a deep-sea hydrothermal vent. *Int. J. Syst. Evol. Microbiol.* 53(Pt 3), 839–846. doi: 10.1099/ijs.0.02479-0

Takaki, Y., Shimamura, S., Nakagawa, S., Fukuhara, Y., Horikawa, H., Ankai, A., et al. (2010). Bacterial lifestyle in a deep-sea hydrothermal vent chimney revealed by the genome sequence of the thermophilic bacterium *Deferribacter desulfuricans* SSM1. *DNA Res.* 17, 123–137. doi: 10.1093/dnares/dsq005

Van Dover, C. L., Fry, B., Grassle, J. F., Humphris, S., and Rona, P. A. (1988). Feeding biology of the shrimp *Rimicaris exoculata* at hydrothermal vents on the mid-atlantic ridge. *Mar. Biol.* 98, 209–216. doi: 10.1007/BF00391196

Watabe, H., and Hashimoto, J. (2002). A new species of the genus *Rimicaris* (Alvinocarididae: *Caridea*: Decapoda) from the active hydrothermal vent field, "Kairei Field," on the Central Indian Ridge, the Indian Ocean. *Zool. Sci.* 19, 1167–1174. doi: 10.2108/zsj.19.1167

Watsuji, T. O., Yamamoto, A., Motoki, K., Ueda, K., Hada, E., Takaki, Y., et al. (2015). Molecular evidence of digestion and absorption of epibiotic bacterial community by deep-sea crab Shinkaia crosnieri. *Isme J.* 9, 821–831. doi: 10.1038/ismej.2014.178

White, S. N., Dunk, R. M., Peltzer, E. T., Freeman, J. J., and Brewer, P. G. (2006). In situ Raman analyses of deep-sea hydrothermal and cold seep systems (Gorda Ridge and Hydrate Ridge). *Geochem. Geophys. Geosyst.* 7:Q05023. doi: 10.1029/2005GC001204

Xie, S., Wang, S., Li, D., Shao, Z., Lai, Q., Wang, Y., et al. (2019). *Sulfurovum indicum* sp. nov., a novel hydrogen- and sulfur-oxidizing chemolithoautotroph isolated from a deep-sea hydrothermal plume in the Northwestern Indian Ocean. *Int. J. Syst. Evol. Microbiol.* 71:004748. doi: 10.1099/ijsem.0.004748

Yamamoto, M., Nakagawa, S., Shimamura, S., Takai, K., and Horikoshi, K. (2010). Molecular characterization of inorganic sulfur-compound metabolism in the deep-sea epsilonproteobacterium *Sulfurovum* sp. NBC37-1. *Environ. Microbiol.* 12, 1144–1153. doi: 10.1111/j.1462-2920.2010.02155.x

Zbinden, M., and Cambon-Bonavita, M. A. (2003). Occurrence of deferribacterales and entomoplasmatales in the deep-sea Alvinocarid shrimp *Rimicaris exoculata* gut. *FEMS Microbiol. Ecol.* 46, 23–30. doi: 10.1016/s0168-6496(03)00176-4

Zbinden, M., and Cambon-Bonavita, M. A. (2020). *Rimicaris exoculata*: biology and ecology of a shrimp from deep-sea hydrothermal vents associated with ectosymbiotic bacteria. *Mar. Ecol.Prog. Ser.* 652, 187–222. doi: 10.3354/meps13467

Zbinden, M., Shillito, B., Le Bris, N., de Villardi de Montlaur, C., Roussel, E., Guyot, F., et al. (2008). New insigths on the metabolic diversity among the epibiotic microbial communitiy of the hydrothermal shrimp *Rimicaris exoculata*. *J. Exp. Mar. Biol. Ecol.* 359, 131–140. doi: 10.1016/j.jembe.2008.03.009

Conflict of Interest: The authors declare that the research was conducted in the absence of any commercial or financial relationships that could be construed as a potential conflict of interest.

Publisher's Note: All claims expressed in this article are solely those of the authors and do not necessarily represent those of their affiliated organizations, or those of the publisher, the editors and the reviewers. Any product that may be evaluated in this article, or claim that may be made by its manufacturer, is not guaranteed or endorsed by the publisher.

frontiers | Frontiers in Microbiology

ORIGINAL RESEARCH
published: 02 June 2022
doi: 10.3389/fmicb.2022.912299

Activity of Ancillary Heterotrophic Community Members in Anaerobic Methane-Oxidizing Cultures

Qing-Zeng Zhu[1], Gunter Wegener[1,2], Kai-Uwe Hinrichs[1,3] and Marcus Elvert[1,3]*

[1] MARUM – Center for Marine Environmental Sciences, University of Bremen, Bremen, Germany, [2] Max Planck Institute for Marine Microbiology, Bremen, Germany, [3] Faculty of Geosciences, University of Bremen, Bremen, Germany

Consortia of anaerobic methanotrophic archaea (ANME) and sulfate-reducing bacteria mediate the anaerobic oxidation of methane (AOM) in marine sediments. However, even sediment-free cultures contain a substantial number of additional microorganisms not directly related to AOM. To track the heterotrophic activity of these community members and their possible relationship with AOM, we amended meso- (37°C) and thermophilic (50°C) AOM cultures (dominated by ANME-1 archaea and their partner bacteria of the Seep-SRB2 clade or *Candidatus* Desulfofervidus auxilii) with L-leucine-3-^{13}C (^{13}C-leu). Various microbial lipids incorporated the labeled carbon from this amino acid, independent of the presence of methane as an energy source, specifically bacterial fatty acids, such as *iso* and *anteiso*-branched $C_{15:0}$ and $C_{17:0}$, as well as unsaturated $C_{18:1\omega9}$ and $C_{18:1\omega7}$. In natural methane-rich environments, these bacterial fatty acids are strongly ^{13}C-depleted. We, therefore, suggest that those fatty acids are produced by ancillary bacteria that grow on ^{13}C-depleted necromass or cell exudates/lysates of the AOM core communities. Candidates that likely benefit from AOM biomass are heterotrophic bacterial members of the Spirochetes and Anaerolineae—known to produce abundant branched fatty acids and present in all the AOM enrichment cultures. For archaeal lipids, we observed minor ^{13}C-incorporation, but still suggesting some ^{13}C-leu anabolism. Based on their relatively high abundance in the culture, the most probable archaeal candidates are Bathyarchaeota, Thermoplasmatales, and Lokiarchaeota. The identified heterotrophic bacterial and archaeal ancillary members are likely key players in organic carbon recycling in anoxic marine sediments.

Keywords: anaerobic oxidation of methane, archaea, bacteria, heterotrophy, stable isotope probing, lipid biomarkers

OPEN ACCESS

Edited by:
S. Emil Ruff, Marine Biological Laboratory (MBL), United States

Reviewed by:
Susma Bhattarai, IHE Delft Institute for Water Education, Netherlands
Axel Schippers, Federal Institute for Geosciences and Natural Resources, Germany

****Correspondence:***
Qing-Zeng Zhu
qzzhu@marum.de

Specialty section:
This article was submitted to Extreme Microbiology, a section of the journal Frontiers in Microbiology

Received: *04 April 2022*
Accepted: *02 May 2022*
Published: *02 June 2022*

Citation:
Zhu Q-Z, Wegener G, Hinrichs K-U and Elvert M (2022) Activity of Ancillary Heterotrophic Community Members in Anaerobic Methane-Oxidizing Cultures. Front. Microbiol. 13:912299. doi: 10.3389/fmicb.2022.912299

INTRODUCTION

Methane is the most abundant hydrocarbon in marine sediments. The emission of methane from sediments into the water column and eventually the atmosphere is attenuated by the anaerobic oxidation of methane (AOM), which is performed by anaerobic methane-oxidizing archaea (ANME) and sulfate-reducing bacteria consortia (SRB) (Hinrichs et al., 1999; Boetius et al., 2000; Reeburgh, 2007; Wegener et al., 2016). The ANMEs completely oxidize methane to carbon dioxide, and their partner bacteria use the reducing equivalents produced in this reaction for sulfate reduction (Orphan et al., 2001). This exchange likely involves direct electron transfer mediated by cytochromes and nanowires

(McGlynn et al., 2015; Wegener et al., 2015). ANME archaea are found in three clades known as ANME-1, ANME-2, and ANME-3 (Orphan et al., 2002; Niemann et al., 2006). Psychro- and mesophilic ANMEs form a consortium with SRB of the *Desulfosarcina/Desulfococcus* (DSS), classified as Seep-SRB1, or *Desulfobulbus* group (Boetius et al., 2000; Michaelis et al., 2002; Niemann et al., 2006). The thermophilic ANME-1 archaea form a consortium with *Candidatus* Desulfofervidus auxilii (Ca. D. auxilii) in heated sediments (e.g., Guaymas Basin). In contrast to SRBs in the psychro- and mesophilic consortia, *Ca.* D. auxilii has been isolated using molecular hydrogen as an alternative electron donor (Krukenberg et al., 2016).

ANMEs are characterized by diagnostic lipid biomarker patterns. ANME-1 archaea predominantly synthesize glycerol dialkyl glycerol tetraethers (GDGTs) as opposed to ANME-2 and ANME-3 that produce archaeol-based diethers, predominantly hydroxyarchaeol (Blumenberg et al., 2004; Rossel et al., 2008, 2011). Nonetheless, a thermophilic ANME-1 AOM enrichment from the Guaymas Basin revealed a substantial quantity of archaeol lipids in comparison to GDGTs, especially in the active growth phase (Kellermann et al., 2016; Wegener et al., 2016). The corresponding lipid patterns of SRB partners determined from AOM environments and cultures are more diverse and taxonomically only partly distinctive (e.g., Hinrichs et al., 2000; Elvert et al., 2003, 2005; Blumenberg et al., 2004; Niemann and Elvert, 2008). It has been shown that bacterial fatty acids (FAs) from environments dominated by ANME-2 include large proportions of $C_{16:1\omega5c}$ and cyclopropane (cy)-$C_{17:0\omega5,6}$ (Elvert et al., 2003; Blumenberg et al., 2004), while those dominated by ANME-1 predominantly produce *ai*-$C_{15:0}$ (Blumenberg et al., 2004; Elvert et al., 2005). All of the aforementioned archaeal or bacterial lipids show strong ^{13}C-depletions with $\delta^{13}C$ values of –70‰ and lower, which are assumed to be caused by the distinctively low $\delta^{13}C$ values of methane (e.g., Hinrichs et al., 1999; Thiel et al., 1999; Pancost et al., 2001; Orphan et al., 2002; Elvert et al., 2003; Blumenberg et al., 2004).

Multiple stable isotope probing (SIP) experiments indicate that ANMEs and their direct SRB partners predominantly assimilate inorganic carbon (Wegener et al., 2008; Kellermann et al., 2012). Specifically, ANME-1 was classified as a methane-oxidizing chemoorganoautotroph (Kellermann et al., 2012). Here, we used long-term meso- and thermophilic AOM enrichment cultures obtained from hydrocarbon-rich heated sediments in the Guaymas Basin. The mesophilic culture grown at 37°C (AOM37) is dominated by ANME-1 and Seep-SRB2; the thermophilic culture maintained at 50°C (AOM50) is dominated by ANME-1 and *Ca.* D. auxilii (Krukenberg et al., 2016; Wegener et al., 2016). Although maintained for 5 years with methane as the sole energy source, these cultures contain substantial numbers of additional bacteria and archaea (Wegener et al., 2016). The functions and carbon sources of these ancillary microbes and their relationship with the AOM consortia remain largely unknown. Kellermann et al. (2012) suggested that these uncultured microbes may be heterotrophs, which likely feed on labile organic compounds, such as acetate or protein-like dissolved organic carbon detected in the pore waters of AOM environments (Heuer et al., 2006; Yoshinaga et al., 2015; Yang et al., 2020; Hu et al., 2021; Pérez Castro et al., 2021).

Leucine is one of the most abundant amino acids produced by microorganisms and, if released into the environment, becomes a carbon, nitrogen, and energy source (Kirchman et al., 1985). Because leucine metabolism was found to be particularly essential during starvation conditions (Harwood and Canale-Parola, 1981; Mårdén et al., 1987), it is ideal for tracking heterotrophic activity in slow-growing enrichment cultures, such as AOM consortia. To explore the activity of these heterotrophic community members and their signaling lipids in AOM environments, we incubated active Guaymas Basin AOM enrichment cultures with ^{13}C-leu, a particular precursor for iso-branched FAs (cf. Aepfler et al., 2019), which are abundant in natural ANME-1 systems. Additionally, we used the same cultures devoid of methane to suppress the activity of AOM consortia members and to track the utilization of leucine for lipid biosynthesis by non-AOM microbes. Based on our ^{13}C-leu incubation and published microbial community data on the same cultures (Wegener et al., 2016; Krukenberg et al., 2018), we were able to trace ancillary heterotrophic bacteria and archaea in AOM enrichment cultures, detected by strong ^{13}C-enrichments of diagnostic FAs but only minor for archaeal lipids, highlighting the identification of branched fatty acids as indicators of bacterial heterotrophy.

MATERIALS AND METHODS

Anaerobic Oxidation of Methane Cultures

The production and maintenance of the sediment-free AOM cultures from the Guaymas Basin were performed as described before (Wegener et al., 2016; Laso-Pérez et al., 2018). In brief, both AOM37 and AOM50 were incubated with marine sulfate reducer medium supplemented with trace amounts of vitamins (Widdel and Bak, 1992) under a CH_4:CO_2 atmosphere (2.5 atm; 90:10) at temperatures of 37°C and 50°C, respectively. The initial concentration of sulfate was 28 mM. The carbon isotopic composition of methane used was −35‰ (Wegener et al., 2021), and sulfide concentrations were measured as described before (Cord-Ruwisch, 1985). When sulfide concentrations exceeded 15 mM, microbial biomass was transferred into a fresh medium. Under these conditions, the AOM37 and AOM50 cultures show doubling times of 69 and 55 days, respectively (Holler et al., 2011). The sulfate reducer *Ca.* D. auxilii was isolated from AOM50 with hydrogen as the sole electron donor and sulfate as an electron acceptor. It is chemolithoautotrophic and grows at temperatures between 50 and 70°C, and has a doubling time of 4–6 days (Krukenberg et al., 2016).

Experimental Setup

For all experiments with the AOM cultures, the culture medium was exchanged, and cultures were equally distributed in 156 ml cultivation bottles. In the case of *Ca.* D. auxilii, new dilutions were prepared (5 ml of active culture for inoculation). ^{13}C-leu was dissolved in Milli-Q water and sterilized by filtration

TABLE 1 | Overview of incubation experiments.

Enrichment/culture	$\delta^{13}C_{DIC}$ at T_0	Incubation time (days)	Experiment 1	Experiment 2 negative control	Experiment 3 positive control	Experiment 4
			+ CH_4 + ^{13}C-leu	+ CH_4	+ ^{13}C-leu	+ H_2 + ^{13}C-leu
AOM37	−14.9	0–28*	2	2	2	
AOM50	−25.8	28	2	2	2	
Ca. D. auxilii	−17.5	40				2

*CH_4 is provided as an energy source in AOM37 and AOM50, while Ca. D. auxilii uses hydrogen (H_2) as an energy source. *AOM37 was incubated for 0, 0.5, 3, 7, 14, and 28 days, and both biomass and medium in each bottle were harvested to track ^{13}C-incorporation into membrane lipids. The numbers indicate the number of bottles used for each experiment.*

(Minisart High Flow, PES, 28 mm, 0.1 μm, sterile). The AOM37 and AOM50 cultures were amended with 100 μM of sterilized ^{13}C-leu and incubated under different experimental conditions for 28 days (**Table 1**): experiment 1 with CH_4 and ^{13}C-leu to track characteristic lipid production by microbial community members involved in leucine metabolism during active AOM; experiment 2 with CH_4 and without ^{13}C-leu as a negative control; experiment 3 with ^{13}C-leu and without CH_4 as a positive control to specifically track ancillary community members and identify their lipids by suppressing the activity of AOM consortia. Through these three experiments, we were able to target ancillary microbial communities existing in the current AOM cultures and constrain their potential heterotrophic capabilities. In contrast, experiment 4 utilized the autotrophic *Ca.* D. auxilii culture and was likewise amended with 100 μM of sterilized ^{13}C-leu. This experiment lasted for 40 days, and it thoroughly tested whether the partner bacterium *Ca.* D. auxilii can metabolize ^{13}C-leu and constrain its lipid pattern. A ^{13}C-leu concentration of 100 μM was chosen to ensure a sufficient supply of substrate and to maximize the potential to observe various pathways of leucine metabolism during prolonged incubation, even though the concentration is higher than existing leucine data from estuarine pore water (up to 3 μM, Henrichs and Farrington, 1979).

Determination of Sulfide Concentration and Isotopic Composition of Dissolved Inorganic Carbon

Sulfide concentrations were used to monitor the growth of AOM consortia and *Ca.* D. auxilii. The medium subsampling of AOM37 for sulfide concentrations analysis was at 0, 0.5, 3, 7, 14, 21, and 28 days; AOM50 medium subsampling was at 0, 7, 21, and 28 days; and *Ca.* D. auxilii medium subsampling was at 0 and 40 days. The subsampling for the measurements of the carbon isotopic composition of dissolved inorganic carbon ($\delta^{13}C_{DIC}$) was performed on the same days to constrain the leucine mineralization (Aepfler et al., 2019). In brief, 1 ml of the sample was taken by syringe from the incubation serum bottles and filtered through a 0.2 μm filter (Minisart regenerated cellulose syringe filter, 15 mm) to remove cells and other particles. Finally, samples were acidified with 100 μl phosphoric acid overnight in an Exetainer vial pre-purged with CO_2-free air before isotopic analysis. All samples were measured with a Thermo Scientific Delta Ray isotope ratio infrared spectrometer with an analytical error of ±1‰, which is obtained by repeated measurement of the laboratory CO_2 reference gas (n = 8). All isotopic values are reported in the delta notation as δ^{13}C relative to the Vienna PeeDee Belemnite (VPDB) standard.

Lipid Extraction, Identification, Quantification, and Isotopic Analysis

Due to potential contamination, we avoided subsampling for lipid analysis from the same bottle as used for sulfide concentration and $\delta^{13}C_{DIC}$ determination by obtaining biomass from replicate samples. Cell pellets from these incubations were extracted wet using a modified Bligh and Dyer protocol (Sturt et al., 2004). Before extraction, 1 μg of 1,2-diheneicosanoyl-*sn*-glycero-3-phosphocholine and 2-methyloctadecanoic acid were added as internal standards. Polar lipid-derived fatty acids (PLFAs) in the total lipid extract (TLE) were converted to fatty acid methyl esters (FAMEs) using saponification with KOH/MeOH and derivatization with BF_3/MeOH (Elvert et al., 2003). Archaeal intact polar lipids (IPLs) in the TLE were separated from the apolar core lipids (CLs) using preparative liquid chromatography (Meador et al., 2015), followed by ether cleavage of both fractions with BBr_3 in dichloromethane and reduction of the resulting alkyl bromides with superhydride to form isoprenoid hydrocarbons (Jahn et al., 2004). The hydrocarbon products were purified by silica gel column chromatography using 4 ml of hexane as an eluent. Both FAMEs and isoprenoid hydrocarbons were measured by gas chromatography coupled to flame ionization detection (GC-FID, Thermo Finnigan Trace GC) for quantification and gas chromatography-mass spectrometry (GC-MS, Trace GC coupled to Trace MS, both from Thermo Finnigan) for structural identification using the protocols described by Aepfler et al. (2019). Using the same GC conditions, lipid δ^{13}C values were determined by GC-isotope ratio-MS (Thermo Finnigan Trace GC coupled to a Thermo Scientific Delta V Plus) connected *via* a GC IsoLink interface and are reported relative to VPDB. The precision of a lab FA standard (2-methyloctadecanoic acid, n = 3) was greater than 0.7‰, while the deviations of duplicate isotopic measurement of sample FAs were between ± 1‰ and ± 100‰ (for PLFAs with label uptake of > 1,000‰).

The incorporation of ^{13}C-leu into bacterial lipids expressed as a percentage of ^{13}C incorporation was calculated as the product of excess ^{13}C and the amount of FA carbon based on

the quantification *via* GC-FID. Excess ^{13}C is derived from the difference between the fractional abundance (F) of ^{13}C in FAs after 28 days relative to T_0 with $F = {}^{13}C/({}^{13}C + {}^{12}C) = R/(R + 1)$ and R being derived from the measured $\delta^{13}C$ values as $R = (\delta^{13}C/1{,}000 + 1) \times R_{VPDB}$.

RESULTS

Contents and $\delta^{13}C$ Values of Microbial Lipids in the Original Cultures

The FA distribution in the original AOM37 culture mainly consisted of $C_{18:1\omega7}$ (37%), $C_{16:0}$ (24%), and $C_{18:0}$ (21%) (**Figure 1A**). Branched-chain FAs accounted for 7% of the total. The AOM50 culture was dominated by $C_{16:0}$ and $C_{18\cdot0}$ with a content of 46 and 28%, respectively. Branched-chain FAs accounted for 12%. The original *Ca.* D. auxilii culture had a FA pattern similar to AOM50, with $C_{16:0}$ (40%) and $C_{18:0}$ (52%) as the dominant FAs. Branched-chain FAs were below the detection limit in the *Ca.* D. auxilii culture. For archaea, we reported the relative content of phytane (Phy) and the three biphytanes (BP0, BP1, and BP2) derived from archaeols and GDGTs, respectively (**Figure 1B**). The content of Phy in AOM 37 was 23%, higher than that in AOM50 (10%). BPs had similar content in AOM37, with BP1 being highest at 30%. At the higher incubation temperature in AOM50, the BP pattern strongly shifted to BP2 (64%).

In AOM37, the $\delta^{13}C$ values of monounsaturated FAs ranged from −55 to −68‰ except $C_{18:1\omega9}$ with a $\delta^{13}C$ value of −29‰. Saturated $C_{14:0}$, $C_{16:0}$, and $C_{18:0}$ FAs had less negative $\delta^{13}C$ values between −25 and −38‰ (**Figure 1C**). The branched-chain FAs were more ^{13}C-depleted, with $\delta^{13}C$ values ranging from −46 to −61‰. FAs in AOM50 are generally less depleted in ^{13}C than AOM37 and showed $\delta^{13}C$ values between −25 and −45‰, with the most negative $\delta^{13}C$ values found for the branched-chain FAs $iC_{16:0}$ and $aiC_{17:0}$. Different carbon fixation pathways of the respective partner bacterium may cause the difference in $\delta^{13}C$ values of FAs in AOM37 and AOM50. The Seep-SRB-2 partner fixes carbon *via* the Wood-Ljungdahl pathway with a fractionation up to 36‰ (Preuß et al., 1989; Krukenberg et al., 2018), whereas *Ca.* D. auxilii uses the rTCA pathway with a lower carbon isotope fractionation of up to 12‰ (Wirsen et al., 2002; Suzuki et al., 2005; Krukenberg et al., 2016). The $\delta^{13}C$ values of FAs in the culture of *Ca.* D. auxilii were even more positive, ranging between −21 and −28‰. $\delta^{13}C$ values of TLE-derived Phy and BPs in the AOM37 and AOM50 were similar and around −70‰ (**Figure 1D**).

Temporal Development of Sulfide Production and $\delta^{13}C_{DIC}$ Values During Incubation

Sulfide concentrations (HS^-) were measured to monitor the metabolic activity of the microorganisms involved in AOM and of *Ca.* D. auxilii (**Figure 2A**). In AOM37 and AOM50 cultures without CH_4 (experiment 3), HS^- concentrations remained stable, indicating a lack of methane-dependent sulfate reduction. When CH_4 was provided (experiments 1 and 2), HS^- increased gradually from 2.8 to 15.5 mM ($\Delta HS^- = 12.7$ mM) for AOM37 and from 2.2 to 24.7 mM ($\Delta HS^- = 22.5$ mM) for AOM50 within 28 days of incubation. There was no substantial difference between incubations with and without ^{13}C-leu addition, indicating that leucine did not affect sulfate reduction. For *Ca.* D. auxilii, HS^- increased from 2.7 to 26.1 mM ($\Delta HS^- = 23.4$ mM) after 40 days of incubation with hydrogen and ^{13}C-leu (experiment 4).

We also measured the development of $\delta^{13}C_{DIC}$ values as an indicator of microbial oxidation of ^{13}C-leu (**Figure 2B**). In AOM37 and AOM50 incubated with CH_4 (experiment 2), $\delta^{13}C_{DIC}$ values decreased from −15 to −20‰ ($\Delta\delta^{13}C_{DIC} = -5$‰) and −26 to −34‰ ($\Delta\delta^{13}C_{DIC} = -8$‰), respectively, after 28 days of incubation caused by the oxidation of CH_4. When both CH_4 and ^{13}C-leu were supplied for 28 days (experiment 1), the $\delta^{13}C_{DIC}$ value increased from −15 to +51‰ ($\Delta\delta^{13}C_{DIC} = 66$‰) in AOM37 and from −26 to +118‰ ($\Delta\delta^{13}C_{DIC} = 144$‰) in AOM50. If only ^{13}C-leu was provided (experiment 3), $\delta^{13}C_{DIC}$ increased slightly more from −15 to +68‰ ($\Delta\delta^{13}C_{DIC} = 83$‰) and from −26 to +125‰ ($\Delta\delta^{13}C_{DIC} = 151$‰) in AOM37 and AOM50, respectively. The slight offset in $\Delta\delta^{13}C_{DIC}$ values between experiments 1 and 3 results from the dilution of the DIC signal with DIC derived from the oxidation of unlabeled CH_4 with a $\delta^{13}C$ value of −35‰ in the former experiment. The continuous increase of $\delta^{13}C_{DIC}$ values suggested a replete supply of ^{13}C-leu during the whole incubation process. During incubation of *Ca.* D. auxilii, the addition of ^{13}C-leu (experiment 4) did not alter the $\delta^{13}C_{DIC}$ values.

Alteration of ^{13}C Values of Microbial Lipids in ^{13}C-Leu Treatments

The lipid compositions of cultures that received ^{13}C-leu were similar to those of the original cultures, suggesting that the overall community was stable during the incubations (**Figure 1A** and **Supplementary Table 1**), which did not cover a full doubling time. However, the ^{13}C-leu additions in experiments 1 and 3 strongly altered the isotopic compositions of bacterial FAs (**Figure 3** and **Supplementary Table 1**). In the AOM37 experiment, the ^{13}C-leu addition already resulted in the increase of $\delta^{13}C$ values by up to 260‰ relative to T_0 ($\Delta\delta^{13}C = \delta^{13}C_T - \delta^{13}C_{T0}$) in iso-branched FAs $iC_{15:0}$ and $iC_{17:0}$ after 0.5 days. After 28 days of incubation, the anteiso-branched $aiC_{15:0}$ incorporated most of the ^{13}C ($\delta^{13}C = 2{,}800$‰), while $iC_{15:0}$ showed a lower value of 2,100‰. In the AOM50 incubation, ^{13}C-incorporation was even more pronounced, and $\delta^{13}C$ values reached up to 6,400‰ for $iC_{15:0}$ and $iC_{17:0}$ after 28 days. Next to the branched FAs, the monounsaturated FA $C_{18:1\omega9}$ was highly labeled in the AOM37 incubation with a $\delta^{13}C$ value of 2,200‰, which was not the case in AOM50. In both AOM37 and AOM50 enrichment cultures, carbon-numbered saturated FAs were at least ^{13}C-labeled. Their $\delta^{13}C$ values remained lower than those of the DIC, suggesting that the autotrophic partner bacteria mostly synthesize these lipids (**Figure 2B**). Overall, the $\delta^{13}C$ values of FAs during incubation without CH_4 (experiment 3) show a similar ^{13}C-labeling strength to those in the incubation with CH_4 (experiment 1, **Supplementary Table 1**), indicating

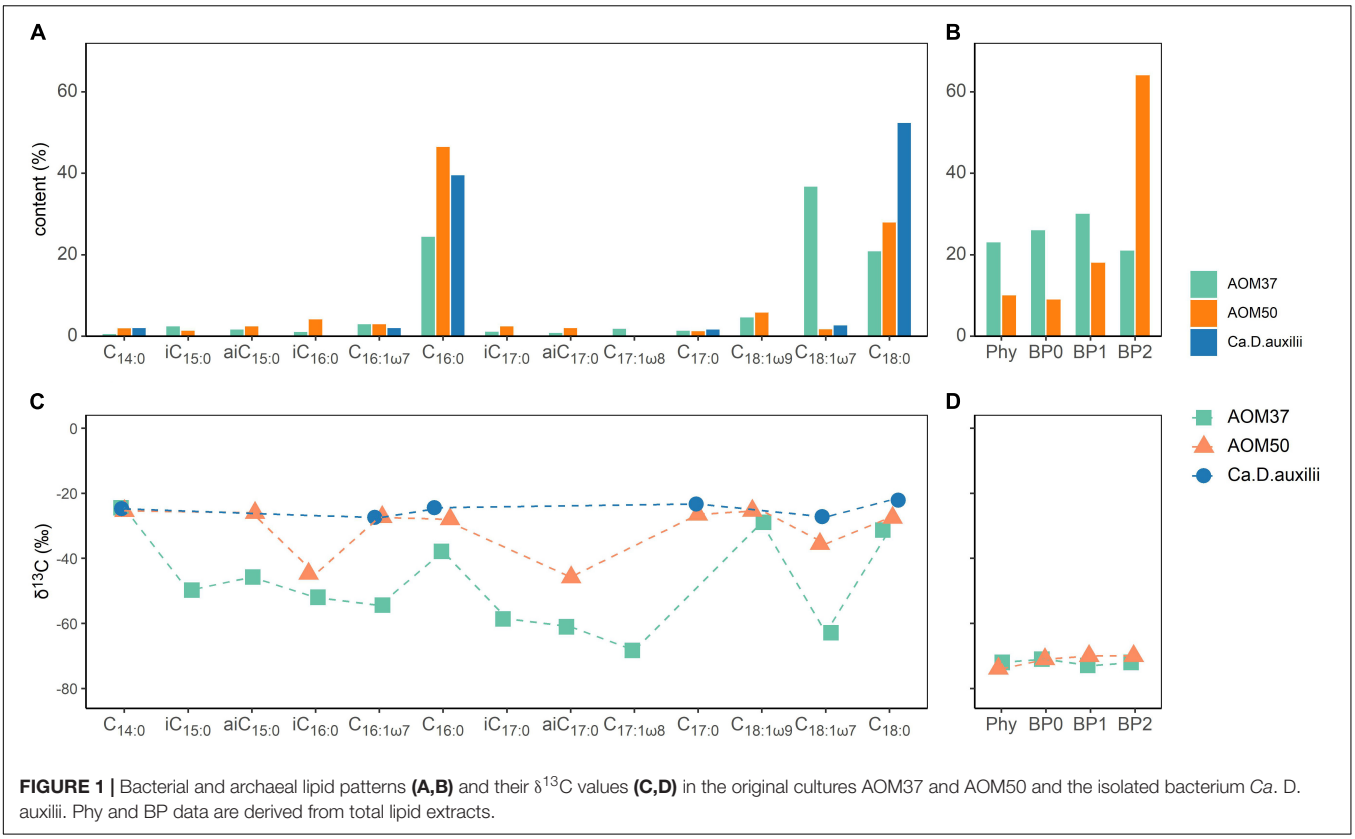

FIGURE 1 | Bacterial and archaeal lipid patterns **(A,B)** and their $\delta^{13}C$ values **(C,D)** in the original cultures AOM37 and AOM50 and the isolated bacterium *Ca*. D. auxilii. Phy and BP data are derived from total lipid extracts.

that the incorporation of ^{13}C-leu is independent of AOM activity. In contrast, the 40-day incubation with ^{13}C-leu did not affect the lipid isotopic composition of the isolated autotrophic SRB partner *Ca*. D. auxilii (**Supplementary Table 1**), confirming its autotrophic lifestyle.

We calculated the relative FA ^{13}C-incorporation pattern of the heterotrophic bacterial community members of both AOM enrichment cultures (**Figure 4**) based on the FA content (**Figure 1A**) and respective $\delta^{13}C$ values (**Supplementary Table 1**) after 28 days. In AOM37, the strongest ^{13}C-incorporation is observed for the monounsaturated FAs $C_{18:1\omega9}$ (30.0%) and $C_{18:1\omega7}$ (20.6%), followed by $iC_{15:0}$ (16.8%), $aiC_{15:0}$ (13.3%), and $iC_{17:0}$ (7.5%). In AOM50, we observed the highest ^{13}C-incorporation in FAs $iC_{15:0}$ (39.6%) and $iC_{17:0}$ (31.2%), followed by $iC_{16:0}$ (9.0%), while even-numbered FAs ($C_{16:0}$ and $C_{18:0}$) show much less ^{13}C-incorporation, despite, as a sum, being the dominant fatty acids in all incubations (**Figure 1**). These results are independent of whether CH_4 was supplied to the enrichment cultures or not (**Figure 4**).

Changes in $\delta^{13}C$ values relative to T_0 of CL and IPL derived Phy and BPs in treatments with ^{13}C-leu of AOM37 and AOM50 are shown in **Figure 5**. For all data on archaeal lipid-derived isoprenoid hydrocarbons, we refer to **Supplementary Table 2**. In both ^{13}C-leu experiments, the ^{13}C-incorporation into Phy and BPs was lower after 28 days (maximum $\delta^{13}C$ value of 118‰ in IPL-Phy). These values are in the range of the corresponding ^{13}C-label transfer into DIC ($\delta^{13}C_{DIC}$ values up to 151‰; **Figure 2**). However, the ^{13}C-incorporation was independent of AOM activity. Throughout the experiments, BPs incorporated less ^{13}C than Phy, regardless of whether they were being retrieved from the CL or IPL fractions. In particular, BP0, which is mostly derived from the GDGT caldarchaeol, had a $\delta^{13}C$ value up to 16‰ higher in the ^{13}C-leu-treated AOM37 and AOM50 culture than in the original cultures, independent of the addition of CH_4 (experiments 1 and 3 compared to experiment 2). The CL-derived BP1 and BP2, AOM37, and AOM50 did not incorporate the ^{13}C-label from ^{13}C-leu (**Supplementary Table 2**). In contrast, CL- and IPL-derived Phy increased by up to 113‰ with CH_4 (experiment 1) and up to 118‰ without CH_4 (experiment 3) in AOM37 after 28 days. These values are specifically higher than $\delta^{13}C_{DIC}$ values, which increased by 66‰. For the AOM50 culture, minute amounts of IPL-derived Phy and BPs obtained after ether cleavage prevented isotope analyses.

DISCUSSION

Ancillary Microorganisms Grow on Leucine

In the AOM enrichment cultures, sulfide production quantitatively depends on CH_4 as an energy source. The turnover of ^{13}C-leu, as observed by changes in $\delta^{13}C_{DIC}$ values, had no measurable effect on sulfide production (**Figure 2A**) and occurred independent of the supply of CH_4, indicating that leucine was predominantly metabolized by ancillary microbes not involved in AOM. This is in line with constant $\delta^{13}C_{DIC}$

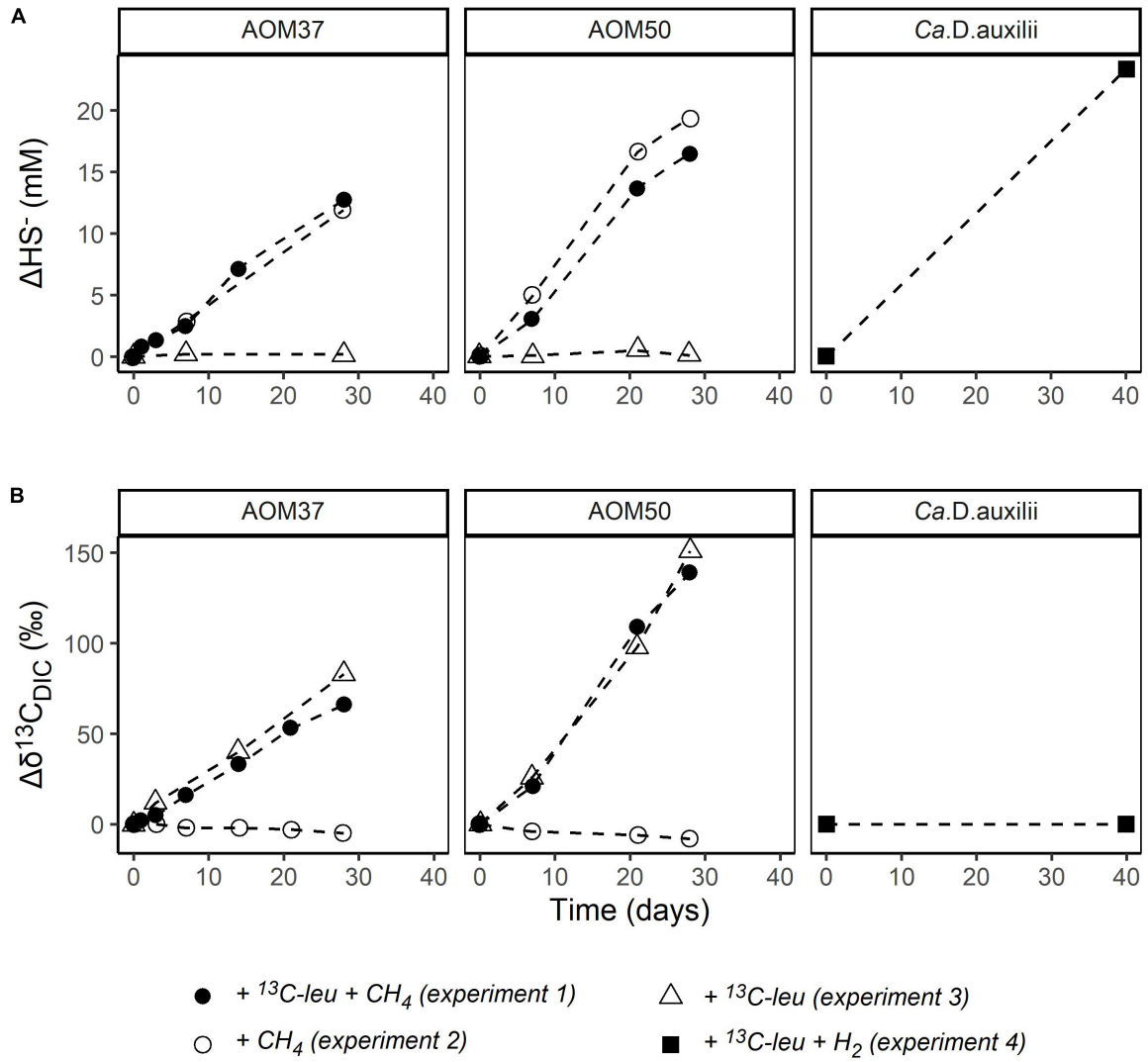

FIGURE 2 | Development of ΔHS^- (mM, **A**) and $\Delta\delta^{13}C_{DIC}$ (‰, **B**) relative to T_0 in the incubation experiments with the AOM37 and AOM50 cultures over 28 days and the *Ca.* D. auxilii culture over 40 days.

values during the 40-day *Ca.* D. auxilii incubation (**Figure 2B**), providing concrete evidence that *Ca.* D. auxilii does not utilize leucine.

The microbial degradation and assimilation of leucine proceeds in diverse reactions. Leucine is deaminated and decarboxylated, resulting in isovaleryl-CoA, which can be used as a primer for odd-numbered iso-series FAs in bacteria, such as $iC_{15:0}$ and $iC_{17:0}$ (Kaneda, 1977; Aepfler et al., 2019). In addition, isovaleryl-CoA can be transformed *via* acetoacetate into acetyl-CoA (Yamauchi, 2010; Díaz-Pérez et al., 2016). Acetyl-CoA can either be completely oxidized or used for the synthesis of biomolecules, including the generation of bacterial FAs during elongation *via* malonyl-CoA or isoprenoid ether lipids in the case of halophilic archaea (Harwood and Canale-Parola, 1981; Yamada et al., 2006). Our experiments demonstrated the incorporation of ^{13}C-leu into selected branched FAs, such as $iC_{15:0}$ and $iC_{17:0}$, independent of CH_4 supply (**Figure 4**). Additionally, we observed a substantial ^{13}C-incorporation into aiC_{15} and aiC_{17}, which is explained by the production of a 2-methylbutyric acid intermediate during leucine catabolism under starvation conditions (Ganesan et al., 2006; Díaz-Pérez et al., 2016). This leads to the formation of 2-methylbutyryl-CoA, which serves as a primer molecule for the synthesis of anteiso FAs. Similarly, the interconversion of leucine and valine gives rise to isobutyryl-CoA (Monticello and Costilow, 1982), which serves as a primer of even-numbered iso-branched FAs, such as iC_{16}. The high labeling of these fatty acids suggests that abundant heterotrophic bacteria not involved in sulfate-dependent AOM, such as Spirochetes or Anaerolineae (**Supplementary Table 3**), are generally active and likely to thrive on free amino acids or other protein-like organic matter (Hu et al., 2021). These carbon pools are highly

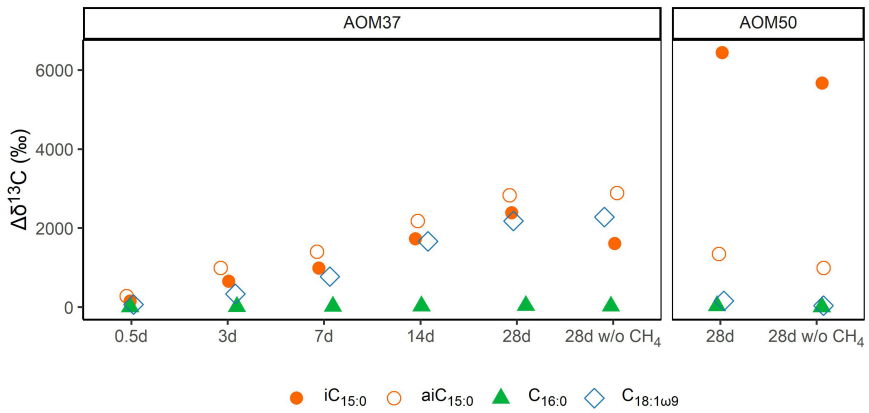

FIGURE 3 | Development of $\delta^{13}C$ values (in ‰ relative to T_0) of bacterial FAs during ^{13}C-leu incubation of AOM37 and AOM50 with and without (w/o) CH_4 over 28 days (experiments 1 and 3, respectively).

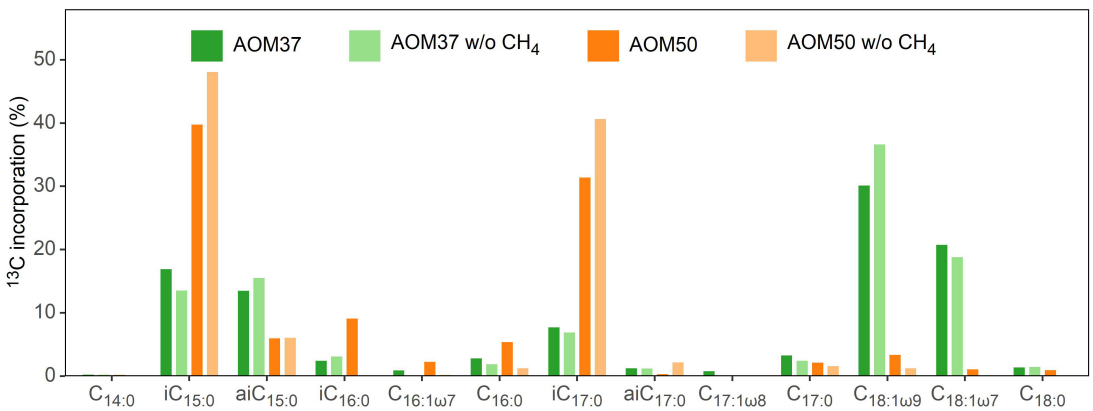

FIGURE 4 | Pattern of ^{13}C-incorporation into bacterial FAs in the AOM37 and AOM50 cultures during ^{13}C-leu incubation with and without (w/o) CH_4 after 28 days (experiments 1 and 3, respectively).

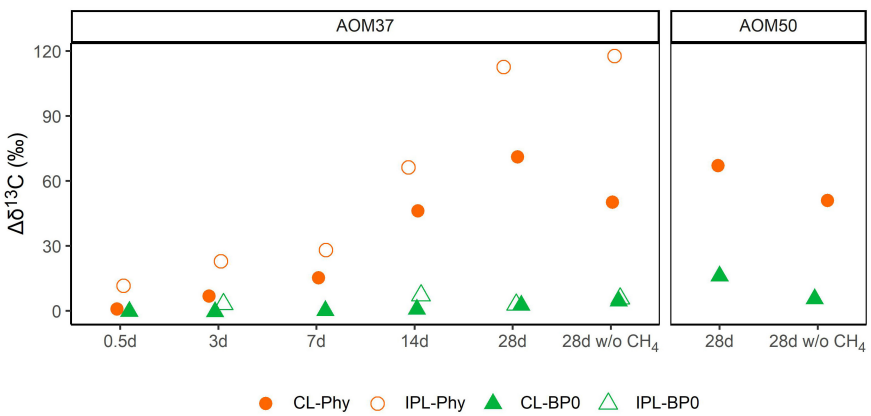

FIGURE 5 | Development of $\delta^{13}C$ values (in ‰ relative to T_0) of archaeal lipid-derived isoprenoid hydrocarbons during ^{13}C-leu incubation of AOM37 and AOM50 cultures with and without (w/o) CH_4 over 28 days (experiments 1 and 3, respectively). In the AOM50 culture, the amounts of IPL-Phy and IPL-BP0 were too low to obtain $\delta^{13}C$ values.

^{13}C-depleted if derived from the biomass of AOM consortia in natural environments (Takano et al., 2018; Hu et al., 2021).

The partner bacterium *Ca.* D. auxilii neither incorporate ^{13}C-leu into its dominant FAs $C_{16:0}$ and $C_{18:0}$, nor into any other FAs (**Supplementary Table 1**). The incorporation of ^{13}C-leu differs between the meso- and thermophilic AOM enrichment cultures at 37°C and 50°C, respectively (**Figures 3**, **4**). Compared to AOM37, AOM50 tends to channel more ^{13}C from leucine into iso-branched than anteiso-branched FAs (AOM50, iso:anteiso = 92:8; AOM37, iso:anteiso = 63:37). Moreover, in AOM37, we observe a predominant ^{13}C-incorporation into straight-chain FAs $C_{18:1\omega9}$ and $C_{18:1\omega7}$. These straight-chain FAs are likely synthesized by downstream ^{13}C-leu products, such as acetate, and are probably derived from ancillary heterotrophic bacterial community members in AOM37 but not in AOM50, such as Spirochetes (**Supplementary Table 3**).

In the incubation of AOM37 and AOM50 with ^{13}C-leu, Phy and BPs (derived from archaeal di- and tetraether lipids, respectively) incorporated much less ^{13}C than bacterial FAs (**Figures 3**, **5**). In the AOM37 culture, IPL-derived Phy provided a 47‰ stronger change in its δ^{13}C value ($\Delta\delta^{13}$C = 113‰, **Figure 5**) than the corresponding DIC ($\Delta\delta^{13}$C = 66‰, **Figure 2**) after 28 days. This divergence suggests that archaeal IPLs are not solely biosynthesized *via* DIC assimilation in AOM37 (**Supplementary Figure 1**). Eventually, possible carbon substrates are leucine or, more likely, secondary metabolites, such as acetate, which is released during leucine catabolism of heterotrophic bacteria (Aepfler et al., 2019). Unfortunately, we could not examine this relationship in AOM50 due to very few isoprenoid hydrocarbons obtained after ether cleavage. In the ^{13}C-leu incubations of our study, the relative ^{13}C-enrichment of BPs was negligible compared to Phy but reached up to 16‰ for CL-derived BP0 in AOM50. Based on our short-time incubation, this is in agreement with former labeling experiments of ANME-1 dominated Guaymas Basin sediments using $^{13}C_{DIC}$ and D_2O, which revealed an initial production of diether lipids that are later transformed into tetraether lipids (Kellermann et al., 2016). The observed isotopic evidence of the enhanced formation of ^{13}C-enriched archaeal lipids over time suggests that some archaea participated in the leucine metabolism or the assimilation of metabolic intermediates. Nonetheless, their role in amino acid mineralization seems to be less important than heterotrophic bacterial community members due to their low ^{13}C-label incorporation.

Minor Bacterial and Archaeal Community Members Thrive on Anaerobic Oxidation of Methane Necromass

Methane-rich sediments contain a large number of AOM consortia and diverse host archaeal and bacterial communities, with a substantial proportion of heterotrophic microorganisms (Biddle et al., 2006; Ruff et al., 2015; Dombrowski et al., 2018; Pérez Castro et al., 2021). These heterotrophs coexist with AOM consortia in natural environments and enrichment cultures, even after many years of maintenance (Wegener et al., 2016). Prior microbial composition analysis of the Guaymas Basin AOM cultures revealed that ANME-1 archaea and their partners dominate AOM37 and AOM50 (Seep-SRB2 and *Ca.* D. auxilii, Holler et al., 2011; Wegener et al., 2015, 2016). Ancillary microbial communities, identified by amplified 16S rRNA gene sequences of the AOM37 and the AOM50 culture (Wegener et al., 2016) and 16S rRNA genes recruited from the metagenomes of the AOM37 and the AOM60 culture (**Supplementary Table 3**; Krukenberg et al., 2018), are presumably unrelated to AOM. These include Anaerolineaceae and Spirochetes, and Candidate divisions JS1, WS3, and KB, many of which are known to be heterotrophs. Anaerolineae, which occupy up to 3.7% of the Guaymas Basin cultures (**Supplementary Table 3**), are strictly anaerobic heterotrophs and thrive on carbohydrates and amino acids (Rosenkranz et al., 2013; Liang et al., 2016). The cultured strains of this group produce mainly iso- and anteiso-C_{15} and C_{17} FAs (Yamada et al., 2006). Spirochetes similarly thrive on the degradation of carbohydrates and proteins (Paster, 2010; Dong et al., 2018) and are abundant in anoxic hydrocarbon-rich habitats (Dong et al., 2018). The AOM37 culture contains up to 5% Spirochetes, whereas these heterotrophs are absent in the AOM50 culture (**Supplementary Table 3**). Spirochetes primarily synthesize branched fatty acids, but some also produce substantial amounts of $C_{18:1\omega9}$ and $C_{18:1\omega7}$ (Livermore and Johnson, 1974; Vishnuvardhan Reddy et al., 2013). Hence, in the AOM37 culture, the substantial ^{13}C-incorporation into branched fatty acids and $C_{18:1\omega9}$ and $C_{18:1\omega7}$ FAs is most likely due to the Spirochetes activity (**Figure 4**). The production of the latter can be attributed to the prolonged transformation and oxidation of isovaleryl-CoA in the tricarboxylic acid cycle, leading to acetyl-CoA and thus the production of even-numbered FAs (Aepfler et al., 2019).

In natural AOM environments, there is circumstantial evidence for the presence of heterotrophic bacteria because of the abundance of branched FAs. Originally, different FA patterns have been described as originating from environments dominated by either ANME-1 or -2 but showing the presence of the same SRB partner (Blumenberg et al., 2004; Elvert et al., 2005; Niemann and Elvert, 2008). ANME-1 dominated AOM systems are related to lower methane flux and are dominated by *ai*$C_{15:0}$ as well as other branched-chain FAs (Stadnitskaia et al., 2008), while ANME-2 dominated systems are indicated by the presence of monounsaturated $C_{16:1\omega5}$ and cy$C_{17:0\omega5,6}$ FAs at sites with high methane flux intensity (Elvert et al., 2003). Taking the results of our study into account, we suggest that the different FA patterns, particularly the larger amounts of branched and partly unsaturated fatty acids, originate from the activity of heterotrophic bacteria inhabiting the vicinity of AOM consortia. These heterotrophic bacteria effectively utilize available amino acids, such as valine, leucine, or isoleucine, which are derived from ^{13}C-depleted proteins from AOM consortia necromass or AOM cell exudates/lysates, such as

amino acids and acetate (Middelboe and Jørgensen, 2006; Takano et al., 2018; Yang et al., 2020; Hu et al., 2021). Thus, if amino acid-based carbon is available, especially under energy- and nutrient-limited conditions in ANME-1 dominated settings, bacterial heterotrophs will produce more branched FAs. Under natural conditions, such branched FAs become even more negative in $\delta^{13}C$ values than FAs derived from the autotrophic SRB partner in AOM consortia (Elvert et al., 2005). Moreover, the activity of such heterotrophic bacteria may explain the difficulty of detecting AOM biomarkers in the sulfate methane transition zone (SMTZ) or their disappearance below the current SMTZ (Niemann et al., 2005; Biddle et al., 2006; Zhu et al., 2021) because AOM biomass is more labile and accessible to these degraders than recalcitrant background organic matter. As a result, they actively reshape different carbon pools and contribute to biogeochemical carbon cycling in anoxic marine sediments.

In addition, both AOM enrichment cultures contain archaea with potential heterotrophic metabolisms, including the members of the Bathyarchaeota, Thermoplasmatales, and Lokiarchaeota (**Supplementary Table 3**; Wegener et al., 2016; Krukenberg et al., 2018). All these three archaeal groups encode protein catabolism or have been cultured on proteinaceous substrates (Imachi et al., 2020; Yin et al., 2022). The metabolic activity of these microbes in the AOM37 culture is supported by the methane-independent incorporation of ^{13}C-leu into IPL-derived Phy (**Figure 5**). Bathyarchaeota—formerly known as the Miscellaneous Crenarchaeotal Group (MCG)—are widespread in anoxic sediments. Based on their genomes, some Bathyarchaeota may be protein-degrading heterotrophs with acetyl-CoA centralized pathways for energy conservation (Lloyd et al., 2013). In the AOM50 culture, Bathyarchaeota, which accounts for approximately 10% of all cells (**Supplementary Table 3**), may be responsible for the trace incorporation of ^{13}C into the CL-derived BP0 during the incubation (**Figure 5**). Another candidate for ^{13}C-label incorporation from leucine is Thermoplasmatales, which occupy up to 4.9% of the total population in the Guaymas Basin cultures (**Supplementary Table 3**). The members of the Thermoplasmatales have been cultured with yeast extract as their carbon and energy sources (Itoh et al., 2007). They, therefore, may also be candidates for using leucine or its metabolized derivatives in the AOM enrichments. Lokiarchaeota, the third potential group, accounted for 0.4% of the whole population. Lokiarchaeota were only recently isolated and able to degrade amino acids *via* syntrophy, and they are likely to produce both archaeol and GDGTs as lipid membrane constituents (Imachi et al., 2020), which would be consistent with our study here. In summary, the low ^{13}C labeling of archaeal lipids indicates that ancillary archaea play a small role in leucine turnover. However, given the widespread distribution of archaea and their postulated advantage over bacteria under conditions of severe energy stress, an archaeal contribution to the utilization of AOM-derived (dissolved) organic matter in the methane-laden sediments has to be taken into account (Biddle et al., 2006; Kubo et al., 2012; Yoshinaga et al., 2015).

CONCLUSION

Meso- and thermophilic AOM cultures from the Guaymas Basin were incubated with position-specifically labeled ^{13}C-leu to investigate heterotrophic lipid formation by ancillary community members. Most of the ^{13}C from leucine was incorporated into branched-chain and unsaturated FAs of heterotrophic bacteria, such as Anaerolineae or Spirochetes. No ^{13}C-leu incorporation into FAs was observed for the cultured *Ca. D. auxilii* SRB representative, confirming that this partner bacterium is an autotroph. Combining our results with former environmental information of FA patterns of different AOM consortia indicates that bacterial heterotrophs thrive on ^{13}C-depleted AOM necromass or cell exudates/lysates in the form of amino acids in the marine environment, addressing the frequently observed strong decline of AOM biomass and lipid biomarkers below current SMTZs. In addition, archaeol-based IPLs and some tetraether CLs showed minor methane-independent assimilation of ^{13}C, suggesting that ancillary, potentially heterotrophic archaea, such as Bathyarchaeota, Thermoplasmatales, and Lokiarchaeota, are active. All these taxa are minor community members in our enrichment cultures but commonly appear in subsurface sediments and can thus be specialists for the recycling of necromass in anoxic hydrocarbon-rich habitats. The AOM cultures, with their limited microbial diversity, appear to be a promising source of materials for confirming the function of these mostly uncultured microorganisms through targeted cultivation.

DATA AVAILABILITY STATEMENT

The original contributions presented in this study are included in the article/**Supplementary Material**, further inquiries can be directed to the corresponding author/s.

AUTHOR CONTRIBUTIONS

ME and Q-ZZ designed the research. Q-ZZ and GW performed the experiment. Q-ZZ analyzed the lipid data. Q-ZZ, ME, GW, and K-UH contributed to the discussion of the results and wrote the manuscript. All authors contributed to the article and approved the submitted version.

FUNDING

This study was funded by the Deutsche Forschungsgemeinschaft (DFG) through the Gottfried Wilhelm Leibniz Prize awarded to K-UH (Hi 616-14-1) and DFG under Germany's Excellence Initiative/Strategy through the Clusters of Excellence EXC 309 "The Ocean in the Earth System" (project no. 49926684) and EXC

2077 "The Ocean Floor – Earth's Uncharted Interface" (project no. 390741601). Q-ZZ was sponsored by the China Scholarship Council (CSC) and Bremen International Graduate School for Marine Sciences (GLOMAR).

ACKNOWLEDGMENTS

We are grateful to Susanne Menger for assisting in the cultivation and Heidi Taubner for her help in measuring $\delta^{13}C$ values of DIC. We are also thankful to Xavier Prieto and Jenny Wendt for their support in instrument maintenance. We also thank the editor SE and the reviewers SB and AS for their feedback on improving the manuscript.

SUPPLEMENTARY MATERIAL

The Supplementary Material for this article can be found online at: https://www.frontiersin.org/articles/10.3389/fmicb.2022.912299/full#supplementary-material

REFERENCES

Aepfler, R. F., Bühring, S. I., and Elvert, M. (2019). Substrate characteristic bacterial fatty acid production based on amino acid assimilation and transformation in marine sediments. *FEMS Microbiol. Ecol.* 95:fiz131. doi: 10.1093/femsec/fiz131

Biddle, J. F., Lipp, J. S., Lever, M. A., Lloyd, K. G., Sørensen, K. B., Anderson, R., et al. (2006). Heterotrophic archaea dominate sedimentary subsurface ecosystems off Peru. *PNAS* 103, 3846–3851. doi: 10.1073/pnas.0600035103

Blumenberg, M., Seifert, R., Reitner, J., Pape, T., and Michaelis, W. (2004). Membrane lipid patterns typify distinct anaerobic methanotrophic consortia. *PNAS* 101, 11111–11116. doi: 10.1073/pnas.0401188101

Boetius, A., Ravenschlag, K., Schubert, C. J., Rickert, D., Widdel, F., Gieseke, A., et al. (2000). A marine microbial consortium apparently mediating anaerobic oxidation of methane. *Nature* 407, 623–626. doi: 10.1038/35036572

Cord-Ruwisch, R. (1985). A quick method for the determination of dissolved and precipitated sulfides in cultures of sulfate-reducing bacteria. *J. Microbiol. Methods* 4, 33–36. doi: 10.1016/0167-7012(85)90005-3

Díaz-Pérez, A. L., Díaz-Pérez, C., and Campos-García, J. (2016). Bacterial l -leucine catabolism as a source of secondary metabolites. *Rev. Environ. Sci. Biotechnol.* 15, 1–29. doi: 10.1007/s11157-015-9385-3

Dombrowski, N., Teske, A. P., and Baker, B. J. (2018). Expansive microbial metabolic versatility and biodiversity in dynamic Guaymas Basin hydrothermal sediments. *Nat. Commun.* 9:4999. doi: 10.1038/s41467-018-07418-0

Dong, X., Greening, C., Brüls, T., Conrad, R., Guo, K., Blaskowski, S., et al. (2018). Fermentative Spirochaetes mediate necromass recycling in anoxic hydrocarbon-contaminated habitats. *ISME J.* 12, 2039–2050. doi: 10.1038/s41396-018-0148-3

Elvert, M., Boetius, A., Knittel, K., and Jørgensen, B. B. (2003). Characterization of specific membrane fatty acids as chemotaxonomic markers for sulfate-reducing bacteria involved in anaerobic oxidation of methane. *Geomicrobiol. J.* 20, 403–419. doi: 10.1080/01490450303894

Elvert, M., Hopmans, E. C., Treude, T., Boetius, A., and Suess, E. (2005). Spatial variations of methanotrophic consortia at cold methane seeps: implications from a high-resolution molecular and isotopic approach. *Geobiology* 3, 195–209. doi: 10.1111/j.1472-4669.2005.00051.x

Ganesan, B., Dobrowolsk, P., and Weimer, B. C. (2006). Identification of the leucine-to-2-methylbutyric acid catabolic pathway of *Lactococcus lactis*. *Appl. Environ. Microbiol.* 72, 4264–4273. doi: 10.1128/AEM.00448-06

Harwood, C. S., and Canale-Parola, E. (1981). Branched-chain amino acid fermentation by a marine spirochete: strategy for starvation survival. *J. Bacteriol.* 148, 109–116. doi: 10.1128/jb.148.1.109-116.1981

Henrichs, S. M., and Farrington, J. W. (1979). Amino acids in interstitial waters of marine sediments. *Nature* 279, 319–322. doi: 10.1038/279319a0

Heuer, V., Elvert, M., Tille, S., Krummen, M., Mollar, X. P., Hmelo, L. R., et al. (2006). Online δ13C analysis of volatile fatty acids in sediment/porewater systems by liquid chromatography-isotope ratio mass spectrometry. *Limnol. Oceanogr-Meth.* 4, 346–357.

Hinrichs, K.-U., Hayes, J. M., Sylva, S. P., Brewer, P. G., and DeLong, E. F. (1999). Methane-consuming archaebacteria in marine sediments. *Nature* 398, 802–805. doi: 10.1038/19751

Hinrichs, K.-U., Summons, R. E., Orphan, V., Sylva, S. P., and Hayes, J. M. (2000). Molecular and isotopic analysis of anaerobic methane-oxidizing communities in marine sediments. *Org. Geochem.* 31, 1685–1701. doi: 10.1016/S0146-6380(00)00106-6

Holler, T., Widdel, F., Knittel, K., Amann, R., Kellermann, M. Y., Hinrichs, K.-U., et al. (2011). Thermophilic anaerobic oxidation of methane by marine microbial consortia. *ISME J.* 5, 1946–1956. doi: 10.1038/ismej.2011.77

Hu, T., Luo, M., Xu, Y., Gong, S., and Chen, D. (2021). Production of labile protein-like dissolved organic carbon associated with anaerobic methane oxidization in the haima cold seeps, south china sea. *Front. Microbiol.* 8:1841. doi: 10.3389/fmars.2021.797084

Imachi, H., Nobu, M. K., Nakahara, N., Morono, Y., Ogawara, M., Takaki, Y., et al. (2020). Isolation of an archaeon at the prokaryote–eukaryote interface. *Nature* 577, 519–525. doi: 10.1038/s41586-019-1916-6

Itoh, T., Yoshikawa, N., and Takashina, T. (2007). Thermogymnomonas acidicola gen. nov., sp. nov., a novel thermoacidophilic, cell wall-less archaeon in the order thermoplasmatales, isolated from a solfataric soil in Hakone, Japan. *Int. J. Syst. Evol. Microbiol.* 57, 2557–2561. doi: 10.1099/ijs.0.65203-0

Jahn, U., Summons, R., Sturt, H., Grosjean, E., and Huber, H. (2004). Composition of the lipids of *Nanoarchaeum Equitans* and their origin from its host *Ignicoccus* sp. strain KIN4/I. *Arch. Microbiol.* 182, 404–413. doi: 10.1007/s00203-004-0725-x

Kaneda, T. (1977). Fatty acids of the genus *Bacillus*: an example of branched-chain preference. *Bacteriol. Rev.* 41, 391–418. doi: 10.1128/br.41.2.391-418.1977

Kellermann, M. Y., Wegener, G., Elvert, M., Yoshinaga, M. Y., Lin, Y.-S., Holler, T., et al. (2012). Autotrophy as a predominant mode of carbon fixation in anaerobic methane-oxidizing microbial communities. *PNAS* 109, 19321–19326. doi: 10.1073/pnas.1208795109

Kellermann, M. Y., Yoshinaga, M. Y., Wegener, G., Krukenberg, V., and Hinrichs, K.-U. (2016). Tracing the production and fate of individual archaeal intact polar lipids using stable isotope probing. *Org. Geochem.* 95, 13–20. doi: 10.1016/j.orggeochem.2016.02.004

Kirchman, D., K'nees, E., and Hodson, R. (1985). Leucine incorporation and its potential as a measure of protein synthesis by bacteria in natural aquatic systems. *Appl. Environ. Microbiol.* 49, 599–607. doi: 10.1128/aem.49.3.599-607.1985

Krukenberg, V., Harding, K., Richter, M., Glöckner, F. O., Gruber-Vodicka, H. R., Adam, B., et al. (2016). Candidatus desulfofervidus auxilii, a hydrogenotrophic sulfate-reducing bacterium involved in the thermophilic anaerobic oxidation of methane. *Environ. Microbiol.* 18, 3073–3091. doi: 10.1111/1462-2920.13283

Krukenberg, V., Riedel, D., Gruber-Vodicka, H. R., Buttigieg, P. L., Tegetmeyer, H. E., Boetius, A., et al. (2018). Gene expression and ultrastructure of meso- and thermophilic methanotrophic consortia. *Environ. Microbiol.* 20, 1651–1666. doi: 10.1111/1462-2920.14077

Kubo, K., Lloyd, K. G., Biddle, F. J., Amann, R., Teske, A., and Knittel, K. (2012). Archaea of the miscellaneous crenarchaeotal group are abundant, diverse and widespread in marine sediments. *ISME J.* 6, 1949–1965. doi: 10.1038/ismej.2012.37

Laso-Pérez, R., Krukenberg, V., Musat, F., and Wegener, G. (2018). Establishing anaerobic hydrocarbon-degrading enrichment cultures of microorganisms under strictly anoxic conditions. *Nat. Protoc.* 13, 1310–1330. doi: 10.1038/nprot.2018.030

Liang, B., Wang, L.-Y., Zhou, Z., Mbadinga, S. M., Zhou, L., Liu, J.-F., et al. (2016). High frequency of Thermodesulfovibrio spp. and Anaerolineaceae in

association with *Methanoculleus* spp. in a long-term incubation of n-alkanes-degrading methanogenic enrichment culture. *Front. Microbiol.* 7:1431. doi: 10.3389/fmicb.2016.01431

Livermore, B. P., and Johnson, R. C. (1974). Lipids of the *Spirochaeta*les: comparison of the lipids of several members of the genera *Spirochaeta*, *Treponema*, and *Leptospira*. *J. Bacteriol.* 120, 1268–1273.

Lloyd, K. G., Schreiber, L., Petersen, D. G., Kjeldsen, K. U., Lever, M. A., Steen, A. D., et al. (2013). Predominant archaea in marine sediments degrade detrital proteins. *Nature* 496, 215–218.doi: 10.1038/nature12033

Mårdén, P., Nyström, T., and Kjelleberg, S. (1987). Uptake of leucine by a marine Gram-negative heterotrophic bacterium during exposure to starvation conditions. *FEMS Microbiol. Ecol.* 3, 233–241. doi: 10.1111/j.1574-6968.1987.tb02361.x

McGlynn, S. E., Chadwick, G. L., Kempes, C. P., and Orphan, V. J. (2015). Single cell activity reveals direct electron transfer in methanotrophic consortia. *Nature* 526, 531–535. doi: 10.1038/nature15512

Meador, T. B., Bowles, M., Lazar, C. S., Zhu, C., Teske, A., and Hinrichs, K.-U. (2015). The archaeal lipidome in estuarine sediment dominated by members of the miscellaneous crenarchaeotal group. *Environ. Microbiol.* 17, 2441–2458. doi: 10.1111/1462-2920.12716

Michaelis, W., Seifert, R., Nauhaus, K., Treude, T., Thiel, V., Blumenberg, M., et al. (2002). Microbial reefs in the Black Sea fueled by anaerobic oxidation of methane. *Science* 297, 1013–1015. doi: 10.1126/science.1072502

Middelboe, M., and Jørgensen, N. O. G. (2006). Viral lysis of bacteria: an important source of dissolved amino acids and cell wall compounds. *J. Mar. Biol. Assoc. U. K.* 86, 605–612. doi: 10.1017/S0025315406013518

Monticello, D. J., and Costilow, R. N. (1982). Interconversion of valine and leucine by *Clostridium sporogenes*. *J. Bacteriol.* 152, 946–949. doi: 10.1128/jb.152.2.946-949.1982

Niemann, H., and Elvert, M. (2008). Diagnostic lipid biomarker and stable carbon isotope signatures of microbial communities mediating the anaerobic oxidation of methane with sulphate. *Org. Geochem.* 39, 1668–1677. doi: 10.1016/j.orggeochem.2007.11.003

Niemann, H., Elvert, M., Hovland, M., Orcutt, B., Judd, A., Suck, I., et al. (2005). Methane emission and consumption at a North Sea gas seep (Tommeliten area). *Biogeosciences* 2, 335–351. doi: 10.5194/bg-2-335-2005

Niemann, H., Lösekann, T., de Beer, D., Elvert, M., Nadalig, T., Knittel, K., et al. (2006). Novel microbial communities of the Haakon Mosby mud volcano and their role as a methane sink. *Nature* 443, 854–858. doi: 10.1038/nature05227

Orphan, V. J., House, C. H., Hinrichs, K.-U., McKeegan, K. D., and DeLong, E. F. (2001). Methane-consuming archaea revealed by directly coupled isotopic and phylogenetic analysis. *Science* 293, 484–487. doi: 10.1126/science.1061338

Orphan, V. J., House, C. H., Hinrichs, K.-U., McKeegan, K. D., and DeLong, E. F. (2002). Multiple archaeal groups mediate methane oxidation in anoxic cold seep sediments. *PNAS* 99, 7663–7668. doi: 10.1073/pnas.072210299

Pancost, R. D., Hopmans, E. C., and Sinninghe Damsté, J. S. (2001). Archaeal lipids in Mediterranean cold seeps: molecular proxies for anaerobic methane oxidation. *Geochim. Cosmochim. Acta* 65, 1611–1627. doi: 10.1016/S0016-7037(00)00562-7

Paster, B. J. (2010). "Phylum XV. Spirochaetes Garrity and Holt 2001," in *Bergey's Manual$of Systematic Bacteriology: Volume Four The Bacteroidetes, Spirochaetes, Tenericutes (Mollicutes), Acidobacteria, Fibrobacteres, Fusobacteria, Dictyoglomi, Gemmatimonadetes, Lentisphaerae, Verrucomicrobia, Chlamydiae, and Planctomycetes*, eds N. R. Krieg, J. T. Staley, D. R. Brown, B. P. Hedlund, B. J. Paster, N. L. Ward, et al. (New York, NY: Springer), 471–566. doi: 10.1007/978-0-387-68572-4_4

Pérez Castro, S., Borton, M. A., Regan, K., Hrabe de Angelis, I., Wrighton, K. C., Teske, A. P., et al. (2021). Degradation of biological macromolecules supports uncultured microbial populations in Guaymas Basin hydrothermal sediments. *ISME J* 15, 1–18. doi: 10.1038/s41396-021-01026-5

Preuß, A., Schauder, R., Fuchs, G., and Stichler, W. (1989). Carbon isotope fractionation by autotrophic bacteria with three different C02 fixation pathways. *Z. Naturforsch. C* 44, 397–402. doi: 10.1515/znc-1989-5-610

Reeburgh, W. S. (2007). Oceanic methane biogeochemistry. *Chem. Rev.* 107, 486–513. doi: 10.1021/cr050362v

Rosenkranz, F., Cabrol, L., Carballa, M., Donoso-Bravo, A., Cruz, L., Ruiz-Filippi, G., et al. (2013). Relationship between phenol degradation efficiency and microbial community structure in an anaerobic SBR. *Water Res.* 47, 6739–6749. doi: 10.1016/j.watres.2013.09.004

Rossel, P. E., Elvert, M., Ramette, A., Boetius, A., and Hinrichs, K.-U. (2011). Factors controlling the distribution of anaerobic methanotrophic communities in marine environments: evidence from intact polar membrane lipids. *Geochim. Cosmochim. Acta* 75, 164–184. doi: 10.1016/j.gca.2010.09.031

Rossel, P. E., Lipp, J. S., Fredricks, H. F., Arnds, J., Boetius, A., Elvert, M., et al. (2008). Intact polar lipids of anaerobic methanotrophic archaea and associated bacteria. *Org. Geochem.* 39, 992–999. doi: 10.1016/j.orggeochem.2008.02.021

Ruff, S. E., Biddle, J. F., Teske, A. P., Knittel, K., Boetius, A., and Ramette, A. (2015). Global dispersion and local diversification of the methane seep microbiome. *PNAS* 112, 4015–4020. doi: 10.1073/pnas.1421865112

Stadnitskaia, A., Ivanov, M. K., and Sinninghe Damsté, J. S. (2008). Application of lipid biomarkers to detect sources of organic matter in mud volcano deposits and post-eruptional methanotrophic processes in the Gulf of Cadiz. *NE Atlantic. Mar. Geol.* 255, 1–14. doi: 10.1016/j.margeo.2007.11.006

Sturt, H. F., Summons, R. E., Smith, K., Elvert, M., and Hinrichs, K.-U. (2004). Intact polar membrane lipids in prokaryotes and sediments deciphered by high-performance liquid chromatography/electrospray ionization multistage mass spectrometry—new biomarkers for biogeochemistry and microbial ecology. *Rapid Commun. Mass Spectrom* 18, 617–628. doi: 10.1002/rcm.1378

Suzuki, Y., Sasaki, T., Suzuki, M., Nogi, Y., Miwa, T., Takai, K., et al. (2005). Novel chemoautotrophic endosymbiosis between a member of the Epsilonproteobacteria and the hydrothermal-vent Gastropod Alviniconcha aff. hessleri (Gastropoda: Provannidae) from the Indian Ocean. *Appl. Environ. Microbiol.* 71, 5440–5450. doi: 10.1128/AEM.71.9.5440-5450.2005

Takano, Y., Chikaraishi, Y., Imachi, H., Miyairi, Y., Ogawa, N. O., Kaneko, M., et al. (2018). Insight into anaerobic methanotrophy from 13C/12C- amino acids and 14C/12C-ANME cells in seafloor microbial ecology. *Sci. Rep.* 8:14070. doi: 10.1038/s41598-018-31004-5

Thiel, V., Peckmann, J., Seifert, R., Wehrung, P., Reitner, J., and Michaelis, W. (1999). Highly isotopically depleted isoprenoids: molecular markers for ancient methane venting. *Geochim. Cosmochim. Acta* 63, 3959–3966. doi: 10.1016/S0016-7037(99)00177-5

Vishnuvardhan Reddy, S., Aspana, S., Tushar, D. L., Sasikala, Ch, and Ramana, Ch (2013). *Spirochaeta* sphaeroplastigenens sp. nov., a halo-alkaliphilic, obligately anaerobic spirochaete isolated from soda lake Lonar. *Int. J. Syst. Evol. Microbiol.* 63, 2223–2228. doi: 10.1099/ijs.0.046292-0

Wegener, G., Gropp, J., Taubner, H., Halevy, I., and Elvert, M. (2021). Sulfate-dependent reversibility of intracellular reactions explains the opposing isotope effects in the anaerobic oxidation of methane. *Sci. Adv.* 7:eabe4939. doi: 10.1126/sciadv.abe4939

Wegener, G., Krukenberg, V., Riedel, D., Tegetmeyer, H. E., and Boetius, A. (2015). Intercellular wiring enables electron transfer between methanotrophic archaea and bacteria. *Nature* 526, 587–590. doi: 10.1038/nature15733

Wegener, G., Krukenberg, V., Ruff, S. E., Kellermann, M. Y., and Knittel, K. (2016). Metabolic capabilities of microorganisms involved in and associated with the anaerobic oxidation of methane. *Front. Microbiol.* 7:46. doi: 10.3389/fmicb.2016.00046

Wegener, G., Niemann, H., Elvert, M., Hinrichs, K.-U., and Boetius, A. (2008). Assimilation of methane and inorganic carbon by microbial communities mediating the anaerobic oxidation of methane. *Environ. Microbiol.* 10, 2287–2298. doi: 10.1111/j.1462-2920.2008.01653.x

Widdel, F., and Bak, F. (1992). "Gram-Negative Mesophilic Sulfate-Reducing Bacteria," in *The Prokaryotes: A Handbook on the Biology of Bacteria: Ecophysiology, Isolation, Identification, Applications*, eds A. Balows, H. G. Trüper, M. Dworkin, W. Harder, and K.-H. Schleifer (New York, NY: Springer), 3352–3378. doi: 10.1007/978-1-4757-2191-1_21

Wirsen, C. O., Sievert, S. M., Cavanaugh, C. M., Molyneaux, S. J., Ahmad, A., Taylor, L. T., et al. (2002). Characterization of an autotrophic sulfide-oxidizing marine *Arcobacter* sp. that produces filamentous sulfur. *Appl. Environ. Microbiol.* 68, 316–325. doi: 10.1128/AEM.68.1.316-325.2002

Yamada, T., Sekiguchi, Y., Hanada, S., Imachi, H., Ohashi, A., Harada, H., et al. (2006). *Anaerolinea thermolimosa* sp. nov., *Levilinea saccharolytica* gen. nov., sp. nov. and Leptolinea tardivitalis gen. nov., sp. nov., novel filamentous anaerobes, and description of the new classes *Anaerolineae* classis nov. and

Caldilineae classis nov. in the bacterial phylum Chloroflexi. *Int. J. Syst. Evol. Microbiol.* 56, 1331–1340. doi: 10.1099/ijs.0.64169-0

Yamauchi, N. (2010). The pathway of leucine to mevalonate in halophilic archaea: efficient incorporation of leucine into isoprenoidal lipid with the involvement of isovaleryl-coa dehydrogenase in *Halobacterium salinarum*. *Biosci. Biotechnol. Biochem.* 74, 443–446. doi: 10.1271/bbb.90814

Yang, S., Lv, Y., Liu, X., Wang, Y., Fan, Q., Yang, Z., et al. (2020). Genomic and enzymatic evidence of acetogenesis by anaerobic methanotrophic archaea. *Nat. Commun.* 11:3941. doi: 10.1038/s41467-020-17860-8

Yin, X., Zhou, G., Cai, M., Zhu, Q.-Z., Richter-Heitmann, T., Aromokeye, D. A., et al. (2022). Catabolic protein degradation in marine sediments confined to distinct archaea. *ISME J.* 1–10. doi: 10.1038/s41396-022-01210-1

Yoshinaga, M. Y., Lazar, C. S., Elvert, M., Lin, Y.-S., Zhu, C., Heuer, V. B., et al. (2015). Possible roles of uncultured archaea in carbon cycling in methane-seep sediments. *Geochim. Cosmochim. Acta* 164, 35–52. doi: 10.1016/j.gca.2015.05.003

Zhu, Q.-Z., Elvert, M., Meador, T. B., Becker, K. W., Heuer, V. B., and Hinrichs, K.-U. (2021). Stable carbon isotopic compositions of archaeal lipids constrain terrestrial, planktonic, and benthic sources in marine sediments. *Geochim. Cosmochim. Acta* 307, 319–337. doi: 10.1016/j.gca.2021.04.037

Conflict of Interest: The authors declare that the research was conducted in the absence of any commercial or financial relationships that could be construed as a potential conflict of interest.

The handling editor SE declared a past co-authorship with one of the authors, GW.

Publisher's Note: All claims expressed in this article are solely those of the authors and do not necessarily represent those of their affiliated organizations, or those of the publisher, the editors and the reviewers. Any product that may be evaluated in this article, or claim that may be made by its manufacturer, is not guaranteed or endorsed by the publisher.

frontiers | Frontiers in Microbiology

TYPE Original Research
PUBLISHED 23 September 2022
DOI 10.3389/fmicb.2022.988871

OPEN ACCESS

EDITED BY
S. Emil Ruff,
Marine Biological Laboratory (MBL),
United States

REVIEWED BY
Maxim Rubin-Blum,
Israel Oceanographic and Limnological Research (IOLR), Israel
Xiyang Dong,
Third Institute of Oceanography of the Ministry of Natural Resources, China

*CORRESPONDENCE
David Benito Merino
dbenito@mpi-bremen.de
Gunter Wegener
gwegener@mpi-bremen.de

SPECIALTY SECTION
This article was submitted to Extreme Microbiology, a section of the journal Frontiers in Microbiology

RECEIVED 07 July 2022
ACCEPTED 15 August 2022
PUBLISHED 23 September 2022

CITATION
Benito Merino D, Zehnle H, Teske A and Wegener G (2022) Deep-branching ANME-1c archaea grow at the upper temperature limit of anaerobic oxidation of methane.
Front. Microbiol. 13:988871.
doi: 10.3389/fmicb.2022.988871

Deep-branching ANME-1c archaea grow at the upper temperature limit of anaerobic oxidation of methane

David Benito Merino[1,2]*, Hanna Zehnle[1,2,3], Andreas Teske[4] and Gunter Wegener[1,3]*

[1]Max Planck Institute for Marine Microbiology, Bremen, Germany, [2]Faculty of Geosciences, University of Bremen, Bremen, Germany, [3]MARUM, Center for Marine Environmental Sciences, University of Bremen, Bremen, Germany, [4]Department of Earth, Marine and Environmental Sciences, University of North Carolina at Chapel Hill, Chapel Hill, NC, United States

In seafloor sediments, the anaerobic oxidation of methane (AOM) consumes most of the methane formed in anoxic layers, preventing this greenhouse gas from reaching the water column and finally the atmosphere. AOM is performed by syntrophic consortia of specific anaerobic methane-oxidizing archaea (ANME) and sulfate-reducing bacteria (SRB). Cultures with diverse AOM partners exist at temperatures between 12°C and 60°C. Here, from hydrothermally heated sediments of the Guaymas Basin, we cultured deep-branching ANME-1c that grow in syntrophic consortia with *Thermodesulfobacteria* at 70°C. Like all ANME, ANME-1c oxidize methane using the methanogenesis pathway in reverse. As an uncommon feature, ANME-1c encode a nickel-iron hydrogenase. This hydrogenase has low expression during AOM and the partner *Thermodesulfobacteria* lack hydrogen-consuming hydrogenases. Therefore, it is unlikely that the partners exchange hydrogen during AOM. ANME-1c also does not consume hydrogen for methane formation, disputing a recent hypothesis on facultative methanogenesis. We hypothesize that the ANME-1c hydrogenase might have been present in the common ancestor of ANME-1 but lost its central metabolic function in ANME-1c archaea. For potential direct interspecies electron transfer (DIET), both partners encode and express genes coding for extracellular appendages and multiheme cytochromes. *Thermodesulfobacteria* encode and express an extracellular pentaheme cytochrome with high similarity to cytochromes of other syntrophic sulfate-reducing partner bacteria. ANME-1c might associate specifically to *Thermodesulfobacteria,* but their co-occurrence is so far only documented for heated sediments of the Gulf of California. However, in the deep seafloor, sulfate–methane interphases appear at temperatures up to 80°C, suggesting these as potential habitats for the partnership of ANME-1c and *Thermodesulfobacteria*.

KEYWORDS

anaerobic oxidation of methane, ANME-1, archaea, deep sea, hydrothermal vents

Introduction

In anoxic deep-sea sediments, the greenhouse gas methane is produced abiotically by thermocatalytic decay of buried organic matter or biotically by methanogens (Whiticar, 1999). Anaerobic oxidation of methane (AOM) mitigates the flux of methane to the water column and eventually to the atmosphere by consuming 90% of the methane produced in the deep sediments (Hinrichs and Boetius, 2002; Reeburgh, 2007; Regnier et al., 2011). In marine sediments, AOM primarily couples to sulfate reduction in a 1:1 stoichiometry:

$$CH_4 + SO_4^{2-} \rightarrow HS^- + HCO_3^- + H_2O. \quad (1)$$

AOM is mediated by anaerobic methanotrophic archaea (ANME) that oxidize methane to CO_2 by reversing the methanogenesis pathway (Hallam et al., 2004; Meyerdierks et al., 2010; Wang et al., 2013). ANME do not encode respiratory pathways, but they pass the reducing equivalents liberated during AOM to sulfate-reducing partner bacteria (SRB), forming characteristic consortia (Boetius et al., 2000; Michaelis et al., 2002; Orphan et al., 2002; McGlynn et al., 2015; Wegener et al., 2015). The nature of this syntrophic association and the mechanisms involved in the transfer of reducing equivalents from ANME toward SRB are not completely resolved at the molecular level. Originally, it was proposed that the archaeal partners produce molecular hydrogen that is consumed by the bacterial partners (Hoehler et al., 1994). However, most ANME do not code for hydrogenases (Chadwick et al., 2022). Previous studies support the hypothesis of direct interspecies electron transfer (DIET) involving multiheme cytochromes and pilus proteins (Meyerdierks et al., 2010; McGlynn et al., 2015; Wegener et al., 2015). The partner SRBs use the AOM-derived electrons for anaerobic respiration with sulfate as final electron acceptor (Boetius et al., 2000; Wegener et al., 2015; Laso-Pérez et al., 2016). The limited energy yield of sulfate-dependent AOM [equation (1), $\Delta G^{\circ\prime} = -16.67\,kJ\,mol^{-1}$ at standard conditions and $\Delta G = -20$ to $-40\,kJ\,mol^{-1}$ in marine AOM habitats] needs to be shared between ANME and their syntrophic partner SRB (Thauer, 2011).

ANME inhabit a variety of marine habitats including cold seeps (Boetius et al., 2000; Orphan et al., 2001), mud volcanoes (Niemann et al., 2006), gas hydrates (Lanoil et al., 2001; Orcutt et al., 2004), hydrothermal vents (Inagaki et al., 2006; Biddle et al., 2012) and deep subsurface sediments (Roussel et al., 2008). ANME are polyphyletic and fall into three distinct phylogenetic groups (ANME-1, ANME-2, and ANME-3). ANME-3 often dominate AOM at mud volcanoes, where they form consortia with *Desulfobulbus*-related bacteria (Niemann et al., 2006; Lösekann et al., 2007). Cultivation attempts of ANME-3 have not been successful so far. ANME-2 are globally distributed in a variety of benthic habitats and are typically found associated with *Desulfosarcina*/*Desulfococcus* bacteria (DSS, Seep-SRB1 and Seep-SRB2 clades; Knittel et al., 2003, 2005; Boetius and Knittel, 2010). ANME-2 are dominant at cold seeps with high methane fluxes and temperatures below 20°C (Knittel et al., 2005). Cultivation attempts at temperatures ≤ 20°C resulted in the enrichment of ANME-2c (Holler et al., 2009; Wegener et al., 2016).

ANME-1 prevail in most deep sulfate–methane transition zones (SMTZs; Ishii et al., 2004; Niemann et al., 2005; Treude et al., 2005), in hydrothermally heated sediments in the Guaymas Basin (Teske et al., 2002; Schouten et al., 2003; Ruff et al., 2015; Dombrowski et al., 2018), and in the Auka vent field, in the Pescadero Basin (Gulf of California; Speth et al., 2022). Meso- and thermo-philic AOM cultures have been obtained from Guaymas Basin sediments at 37°C, 50°C, and 60°C (Holler et al., 2011; Wegener et al., 2016). These cultures consisted of ANME-1a and HotSeep-1 (*Ca.* Desulfofervidus) as partner bacteria. *Ca.* Desulfofervidus sequences are also found *in situ* at these sites (McKay, 2014; Dowell et al., 2016).

Previous short-term incubations revealed AOM activity at temperatures up to 75°C or 85°C, but the microorganisms performing AOM under these conditions were not assessed (Kallmeyer and Boetius, 2004; Holler et al., 2011; Adams et al., 2013). Here, we obtained an active AOM culture at 70°C (AOM70) from Guaymas Basin hydrothermal sediments consisting of a previously uncultured ANME-1 subgroup (Teske et al., 2002) and an apparently obligate syntrophic *Thermodesulfobacterium* partner. We describe their function and interaction based on physiological experiments and molecular data.

Materials and methods

Sediment collection and enrichment culture setup

Sediment push cores from gas-rich hydrothermal vents of the Guaymas Basin (Gulf of California) were collected by the submersible *Alvin* at 2013 m depth during RV *Atlantis* cruise AT42-05 (November 2018). Sediments for this AOM enrichment came from cores 4,991–13 and 4,991–14 in the Cathedral Hill area (27°00.6848′ N, 111° 24.2708′ W) collected on 17 November 2018, in an area covered by dense orange-white *Beggiatoaceae* mats, where temperatures at 50 cm depth reached at least 80°C. On board sediment samples were transferred to glass bottles sealed with butyl rubber stoppers, the headspace was exchanged to argon. Sediments were stored at 4°C until further processing. Sediment slurries were prepared following protocols previously described (Laso-Pérez et al., 2018). Anoxic sediments were mixed with sulfate-reducer medium (Widdel and Bak, 1992) in a 1/10 ratio (v/v) in serum vials sealed with rubber stoppers. The headspace of the serum vials was replaced with 2 atm methane:CO_2 (90:10). The dry weight of the original slurries was $60\,g\,L^{-1}$. The slurries were incubated at 70°C in the dark. Methane-dependent sulfide production was measured with the copper sulfate assay (Cord-Ruwisch, 1985). Incubations with methane-dependent sulfide productions at 70°C are referred to as AOM70 culture.

These cultures were diluted 1/5 with new medium when sulfide levels reached > 10 mM. Cultures were virtually sediment-free after four dilutions.

DNA extraction and long-read sequencing

DNA samples for long-read sequencing were prepared according to previous protocols with few modifications (Zhou et al., 1996; Hahn et al., 2020). In short, 50 ml culture were collected in a Falcon tube and biomass was pelleted by centrifugation at RT (4,000 rpm for 20 min). After removing the supernatant, 800 µl extraction buffer was added (100 mM tris–HCl, 100 mM sodium EDTA, 100 mM sodium phosphate, 1.5 M NaCl, 1% CTAB, pH 8). For physical lysis of cell envelopes, the pellet suspension was frozen twice in liquid nitrogen and thawed in a water bath at 65°C. For enzymatic lysis, 1,000 µl extraction buffer with 60 µl proteinase K (20 mg mL^{-1}) was used at 37°C for 1.5 h with constant shaking. Chemical lysis was done with 300 µl 20% SDS at 65°C for 2 h. Cell debris was pelleted again by centrifugation at RT (13,000 × *g* for 20 min). The clear supernatant was transferred to a new tube and 2 ml of chloroform-isoamyl alcohol (16:1, v:v) were added. The samples were mixed by inverting the tubes and centrifuged at RT (13,000× *g* for 20 min). The aqueous phase was transferred to a new tube and mixed with 0.6 volumes isopropanol. DNA was precipitated overnight at −20°C. After precipitation, DNA was re-dissolved at 65°C in a water bath for 5 min and samples were centrifuged at RT (13,000× *g* for 40 min). Supernatant was removed and the pellet was washed with ice-cold 80% ethanol. Samples were centrifuged at 13,000× *g* for 10 min and the ethanol was removed. Dried pellets were resuspended in 100 µl PCR-grade water. Long-read (>10 kb) genomic DNA was sequenced on a Sequel IIe (Pacific Biosciences) at the Max Planck Genome Centre in Cologne. Read length distributions and abundances are compiled in Supplementary Table 1.

RNA extraction and short-read shotgun sequencing

Triplicates of 30 ml culture were filtered onto 0.2 µl polycarbonate filters under gentle vacuum. Filters were soaked immediately with RNAlater (Invitrogen) preheated at 70°C for 10–15 min. RNAlater was removed by filtration and the filters were stored at −20°C until further processing. For RNA extraction, ¼ of a filter was put into a bead-beating tube (Lysing Matrix E, MPBio) together with 600 µl RNA lysis buffer (Quick-RNA MiniPrep kit, Zymo Research). Tubes were vortexed at maximum speed for 20 min. Biomass was pelleted by centrifugation at RT (10,000× *g* for 5 min). The supernatant was collected and RNA was extracted with the Quick-RNA MiniPrep kit (Zymo Research) including a DNA digestion step with DNase I. Total RNA libraries were sequenced in an Illumina HiSeq2500 machine at the Max Planck Genome Centre (Cologne, Germany). We obtained 4 Mio 2 × 250 bp paired-end reads.

Metagenome and metatranscriptome analysis

Metagenomic long-reads were assembled using Flye v. 2.9 (Kolmogorov et al., 2020). Shotgun metatranscriptomic short reads were quality trimmed using BBduk from the BBtools package v. 38.87[1] with the parameters minlength = 50 mink = 6 hdist = 1 qtrim = r trimq = 20. Metagenomic reads were mapped to the general assembly. Long reads were mapped using minimap2 v. 2.21 (Li, 2018) with default parameters. Open reading frames in metagenomic contigs were predicted with prodigal v. 2.6.3 (Hyatt et al., 2010) and genes were annotated with PFAMs, TIGRFAMs, COGs, KEGGs, and RNAmmer (Kanehisa and Goto, 2000; Haft et al., 2001; Lagesen et al., 2007; Galperin et al., 2015; Mistry et al., 2021). CXXCH motifs in putative multiheme cytochromes were searched with a custom script.[2] Predicted hydrogenase sequences were classified into subgroups with the hydrogenase database (HydDB; Søndergaard et al., 2016). Subcellular localization of heme-containing proteins and hydrogenases was predicted with PSORTb 3.0 (Yu et al., 2010). Metagenomic binning based on differential coverage across metagenomic samples was done with maxbin v 2.2.7 (Wu et al., 2016). Bins were manually refined in anvi'o v. 6 (Eren et al., 2015, 2020) by removing contigs with low coverage from high-coverage bins.

Triplicate metatranscriptomes were mapped to curated bins using bowtie 2 (Langmead and Salzberg, 2012). The rRNA and tRNA gene sequences were removed before calculating gene expression levels. Center-log ratio (CLR) values for relative gene expression were calculated according to the formula:

$$CLR_i = \log_2 \frac{x_i}{L_i \sqrt[n]{x_1 \times x_2 \times \ldots \times x_n}} \quad (2)$$

where x_i are the reads mapped to a specific gene and L_i is the length of the gene in kbp. A 0.5 factor was added to read-mapping values to avoid zero values.

To analyze the similarity of cytochrome-like proteins in ANME-1 and sulfate-reducing bacteria, amino acid sequences from sulfate-reducing partner bacteria genomes were downloaded from NCBI (Krukenberg et al., 2016, 2018). BLAST databases were created from the cytochrome sequences in the reference SRB genomes using makeblastdb (BLAST v. 2.10.1; Altschul et al.,

1 https://sourceforge.net/projects/bbmap/

2 https://github.com/dbenitom/Metagenomics_scripts/blob/main/CXXCH_search_anvio_import.sh

1990). Cytochrome-like proteins in AOM70 cultures were queried against the custom database with BLASTp v 2.5.

Community composition and phylogenetic analyses based on the 16S rRNA gene

16S rRNA genes from long-read metagenomic assemblies were extracted with Metaxa2 (Bengtsson-Palme et al., 2015). Full-length 16S rRNA gene sequences were aligned to the SILVA database release 138.1 using the SINA aligner within the ARB software (Ludwig et al., 2004; Pruesse et al., 2012; Quast et al., 2013). Long reads were mapped against 16S rRNA genes using minimap2 (Li, 2018). Shotgun metatranscriptomic reads were aligned to 16S rRNA gene using bowtie2 (Langmead and Salzberg, 2012). Maximum-likelihood 16S rRNA phylogenetic trees with selected ANME or *Thermodesulfobacteria* sequences were calculated using RAxML with 1,000 bootstraps and a 50% frequency base filter (Stamatakis, 2014).

Phylogenomic and phylogenetic analyses

Archaea and Bacteria genomes were downloaded from public databases (Supplementary Table 3). For ANME-1 phylogenomic analysis, the genomes were annotated with HMMs of 38 conserved archaeal marker genes (Supplementary Table 3; Darling et al., 2014). For *Thermodesulfobacteria*, the genomes were annotated with HMMs of 71 conserved bacterial marker genes (Rinke et al., 2013). The amino acid sequences of each set were aligned and concatenated using MUSCLE (Edgar, 2004). Maximum likelihood phylogenomic trees were calculated with IQTree using the –test option to estimate the best substitution model for each protein in the partition file and using 100 bootstraps (Chernomor et al., 2016; Kalyaanamoorthy et al., 2017; Minh et al., 2020). Reference hydrogenase sequences (Supplementary Table 5) were downloaded from the hydrogenase database (HydDB; Søndergaard et al., 2016). ANME-1 hydrogenases and reference hydrogenases were aligned with muscle (Edgar, 2004). Maximum likelihood phylogenetic trees of the alignment were calculated with IQTree with 100 bootstraps (Chernomor et al., 2016; Kalyaanamoorthy et al., 2017; Minh et al., 2020). Trees were visualized and edited on the Interactive Tree Of Life (iTOL) online server (Letunic and Bork, 2011).

Catalyzed reporter deposition-fluorescent *in situ* hybridization

To prepare catalyzed reporter deposition-fluorescent *in situ* hybridization (CARD-FISH) samples, 5 ml culture were fixed at 1% formaldehyde concentration over night at 4°C. Fixed samples were sonicated (15 s, 30% power, 20% cycle) to detach cells from sediment particles to detach larger aggregates. Samples were then filtered onto 0.2 µm polycarbonate filters and fixed with 0.2% low-melting agarose before CARD-FISH. Samples were stored at −20°C until further processing. CARD-FISH was performed as described previously (Pernthaler et al., 2002). In short, endogenous peroxidases were inactivated with a solution of 0.15% H_2O_2 in methanol for 30 min at RT. Cell walls were permeabilized with lysozyme (Sigma Aldrich, 10 mg mL^{-1} lysozyme in 50 mM EDTA, 100 mM Tris–HCl; 60 min incubation at 37°C), proteinase K (15 µg mL^{-1} proteinase K in 50 mM EDTA, 100 mM Tris–HCl, 500 mM NaCl; 10 min incubation at RT) and HCl (0.1 M HCl; 1 min incubation at RT). Horseradish peroxidase-labeled probes were diluted in hybridization buffer at the adequate formamide concentration for each probe (Supplementary Table 2). Probes were hybridized at 46°C for 2 h. Signal amplification with fluorescent tyramides was done for 45 min at 46°C. For double hybridizations, peroxidases of the prior hybridization step were inactivated by incubating the filter in 0.30% H_2O_2 in methanol for 30 min at RT.

Quantification of methane and hydrogen in AOM cultures

For cultures under AOM conditions, hydrogen formation in the headspace was measured by gas chromatography coupled to reducing compound photometry (RCP, Peak Performer 1 RCP, Peak Laboratories). For cultures under methanogenic conditions, methane formation in the headspace was measured *via* gas chromatography and flame ion detection (GC-FID, Focus GC, Thermo).

Results and discussion

AOM enrichment cultures at 70°C

A slurry produced from hydrothermally-heated sediments from the Guaymas Basin and sulfate-reducer medium was supplemented with a methane:CO_2 headspace and incubated at 70°C. These incubations showed methane-dependent sulfate reduction, as measured by an increase of sulfide in the medium (Figure 1B; Supplementary Figure 1). These incubations produced sulfide 12 to 15 mM sulfide within about 100 days. The slurries were diluted 1/10 (v/v) in fresh SRB medium, and a fresh methane:CO_2 headspace was added and the incubation was proceeded. After four additional incubation and dilution steps, the produced AOM70 cultures were virtually sediment-free, contained microbial aggregates visible with the naked eye and produced approximately. 100 µmol sulfide L^{-1} d^{-1}. To our knowledge, this is the first long-term cultivation of AOM-performing microorganisms above 60°C. The culture showed strongly decreased sulfide production at 60°C. It tolerated a transfer to 75°C, but became inactive at 80°C,

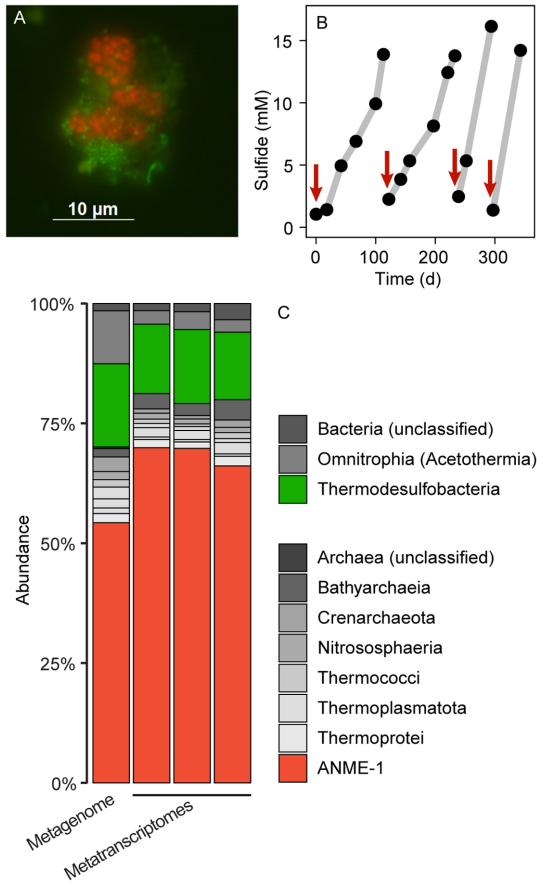

FIGURE 1
Microbial composition and growth of thermophilic AOM cultures. **(A)** CARD-FISH on AOM aggregates with the probes EUB388 I-III (green) and ANME-1-389 (red). Bacteria (green) and archaea (red) form shell-type consortia. **(B)** Methane-dependent sulfide production in AOM cultures. The red arrows indicate when culture medium was replaced. **(C)** 16S rRNA gene relative abundance in long-read metagenomic reads and shotgun metatranscriptomic reads (triplicate metatranscriptomes). The enrichment is dominated by ANME-1 and sulfate reducers of the class Thermodesulfobacteria. Other bacteria and archaea such as Acetothermia and Bathyarchaeia are side community members from original sediment samples.

confirming prior results on the upper-temperature limit of AOM made in short-term incubations with Guaymas Basin sediments (Holler et al., 2011; McKay et al., 2016).

Thermophilic AOM community at 70°C

To resolve the microbial community composition of the AOM70 culture, we obtained a long-read metagenome and triplicate short-read metatranscriptomes. The community consisted mainly of ANME-1 (~50% relative abundance of mapped reads) and *Thermodesulfobacteria* (~20% relative abundance) based on 16S rRNA gene fragments recruited from the metagenome (Figure 1C) that were rare in the original sediment samples

TABLE 1 Metagenome-assembled genomes retrieved from AOM70 enrichment cultures.

	Ca. Thermodesulfobacterium	ANME-1c (*Ca.* Methanophagales)
No. of contigs	4	16
Genome size	1.702 Mbp	1.493 Mbp
L50/N50	2/808,565 bp	5/109,767 bp
GC content	29.0%	47.8%
Completeness*	98.6%	90.8%
Contamination*	<1%	7.89%

*Completeness and contamination were calculated with CheckM.

(Supplementary Figure 2). Metatranscriptomic samples were also dominated by ANME-1 (~70% relative abundance) and *Thermodesulfobacteria* (~15% relative abundance), forming the active AOM community at 70°C. Both the metagenome and metatranscriptome revealed noticeable populations of Bathyarchaeota and Acetothermia (<10% relative abundance of mapped reads). Yet, we were not able to reconstruct MAGs of these organisms; hence, their potential functions are unknown. Previous studies suggest that these organisms ferment or oxidize biomolecules produced by the AOM community (Kellermann et al., 2012; Dombrowski et al., 2017; Hao et al., 2018; Zhu et al., 2022).

After long-read metagenome assembly and binning, we obtained two high-quality MAGs of the two members of the AOM consortium (Table 1). The *Thermodesulfobacterium* MAG has a size of 1.7 Mbp and GC content of 29%. The bin is almost complete (98.6%) and has no contamination based on the presence of 104 bacterial single-copy marker genes (CheckM; Parks et al., 2015). The ANME-1 bin has a size of 1.5 Mbp and a GC content of 47.8%. The bin is 90.8% complete and has contamination of 7.9% based on 149 archaeal marker genes (CheckM; Parks et al., 2015).

We attempted to visualize the enriched ANME-1 using a previously established probe targeting the whole ANME-1 clade (ANME-1-350, Supplementary Table 2; Boetius et al., 2000). *In situ* hybridization with the ANME-1-350 failed, because the probe has two mismatches with the 16S rRNA sequence of the enriched ANME-1. The 16S rRNA gene of this ANME-1 belong to a clade ancestral to all ANME-1a/b, namely ANME-1c (Supplementary Figure 4 and Discussion below; Laso-Pérez et al., 2022). A newly developed ANME-1-389 probe specifically binds to ANME-1c cells. Because the probes available for partner SRB do not target the 16S rRNA sequence of *Thermodesulfobacteria*, we designed three candidate probes to target this clade (Supplementary Table 2). Unfortunately, none of these probes hybridized the 16S rRNA of this organism after various CARD-FISH attempts (Supplementary Table 2). *Thermodesulfobacteria* are likely the partner bacteria of ANME-1c during AOM at 70°C based on the abundance of bacterial cells and their gene content (see Discussion below). Furthermore, all genes coding for dissimilatory sulfate reductase

(*dsr*) in the metagenome belong to the *Thermodesulfobacterium* MAG. Double hybridization with the ANME-1c and the general bacterial probes (Supplementary Table 2) revealed a dominance of "shell-type" aggregates consisting of ANME-1c and partner bacteria (Figure 1A; Supplementary Figure 3). These consortia consist of clumps of ANME-1c cells, surrounded by smaller rod-shaped bacterial cells. These shell-type aggregates differ from the predominantly mixed-type aggregates of moderately thermophilic consortia growing at 50°C–60°C (Holler et al., 2011; Wegener et al., 2015). A shell-type growth morphology is often observed in cold-adapted ANME (Knittel et al., 2005). The reason for the different association types is unknown.

Phylogeny of deep-branching ANME-1c

On the basis of whole genome comparison, the ANME-1 population detected in the AOM70 culture falls into the recently named ANME-1c clade (Figure 2A; Laso-Pérez et al., 2022; Speth et al., 2022).The ANME-1c group is basal to its sister groups ANME-1a and ANME-1b within the order ANME-1 (*Ca.* Methanophagales). The 16S rRNA gene phylogenetic tree supports this phylogenetic placement (Supplementary Figure 4). ANME-1c belong to the class Syntrophoarchaeia with the ANME-1, *Ca.* Syntrophoarchaeales and *Ca.* Alkanophagales. Considering an average nucleotide identity (ANI) of <83% for distinct species and >95% for the same species (Jain et al., 2018) the ANME-1c clade consists of two distinct species clusters (Supplementary Figure 5). The ANME-1c MAG from the AOM70 culture belongs to the cluster of *Ca.* Methanoxibalbensis ujae from Pescadero Basin (Laso-Pérez et al., 2022). ANME-1c 16S rRNA gene sequences have been detected in hydrothermal sediments of the Guaymas Basin and the Juan de Fuca Ridge (Supplementary Figure 4; Teske et al., 2002; Merkel et al., 2013; McKay et al., 2016), and a MAG of the ANME-1c clade (accessions: SAMN09215218, GCA_003661195.1) was derived from Guaymas Basin hydrothermal sediments (Dombrowski et al., 2018). ANME-1c are also present in rock samples from hydrothermal fields in Pescadero Basin (Gulf of California; Speth et al., 2022). The ANME-1c clade was originally named "ANME-1b" by Teske and coworkers to differentiate this lineage from previously described cold-seep ANME-1 (Teske et al., 2002) and later renamed to

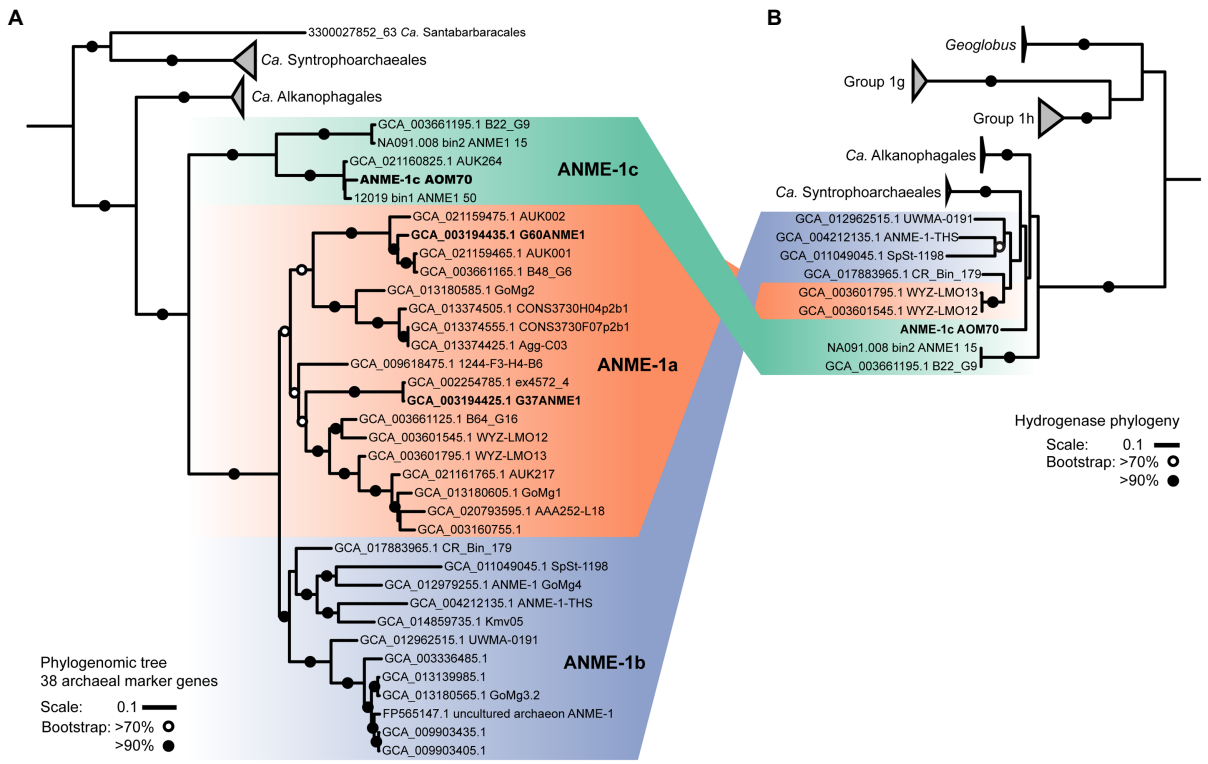

FIGURE 2
ANME-1 phylogenomic tree and hydrogenase phylogeny. **(A)** Phylogeny of ANME-1 order (*Ca.* Methanophagales) with related *Ca.* Alkanophagales, *Ca.* Syntrophoarchaeales, and *Ca.* Santabarbaracales. Maximum likelihood phylogenomic tree based on an alignment of 38 archaeal conserved genes from 55 genomes (Supplementary Table 3). *Geoglobus* sequences were the outgroup to set the tree root (not shown). **(B)** Hydrogenase phylogeny. ANME-1, *Ca.* Alkanophagales and *Ca.* Syntrophoarchaeales hydrogenases are located at the base of groups 1g and 1h of NiFe hydrogenases. A complete hydrogenase tree is shown in Supplementary Figure 11. MAGs from cultured ANME are depicted in bold. Shading in both trees indicates the three subdivisions of the ANME-1: ANME-1c, ANME-1a and ANME-1b. ANME-1 AOM70 is the genome discussed in the main text. Scales indicate nucleotide substitution per site. Bootstrap support is based on 100 iterations above 70% and above 90%.

ANME-1Guaymas because it was predominantly recovered from Guaymas Basin (Biddle et al., 2012; Merkel et al., 2013; Dowell et al., 2016). These sequences originate from sediment cores with sulfate-reducing activity at temperatures between 65°C and 90°C, showing that these archaea are likely all thermophiles (Biddle et al., 2012). Furthermore, the high GC content (>60%) of ANME-1c 16S rRNA genes indicates that these archaea might have temperature optima in the upper range of thermophily above 70°C (Merkel et al., 2013).

Genomic and metabolic features of ANME-1c

ANME-1c codes for a complete methanogenesis pathway including a canonical methane-active Mcr (Figure 3). The *mcr*ABC genes in ANME-1c have the highest expression (CLR > 7) among all genes in the dataset. This high expression of *mcr* confirms previous transcriptomic work in ANME (Haroon et al., 2013; Krukenberg et al., 2018). The activation of methane is the rate-limiting step of AOM, and ANME would promote this reaction by producing large amounts of Mcr (Scheller et al., 2010; Thauer, 2011). Similar to other ANME-1 archaea, ANME-1c does not encode a N^5,N^{10}-methylene-H_4MPT reductase (*mer*). This gene might be substituted by a 5,10-methylenetetrahydrofolate reductase (*met;* Stokke et al., 2012; Krukenberg et al., 2018). The function of this bypass has not been verified yet. All other genes of the methanogenesis pathway show a relatively high expression with CLR values between 0.1 and 3.4 (Supplementary Table 4), supporting a catabolic function of the encoded genes. ANME-1c encodes and expresses the methanogenesis-related membrane-bound complex H^+-translocating F_{420}:quinone oxidoreductase (*fqo*) that catalyzes the transfer of electrons from reduced cofactors to the quinone pool (Pereira et al., 2011). ANME-1c encodes an ATP synthase, which is a common feature in ANME to enable the oxidative phosphorylation of ATP, coupled to the influx of protons. ANME-1c encodes a sulfate adenylyltransferase (*cys*N; low expression, CLR = −0.02) and

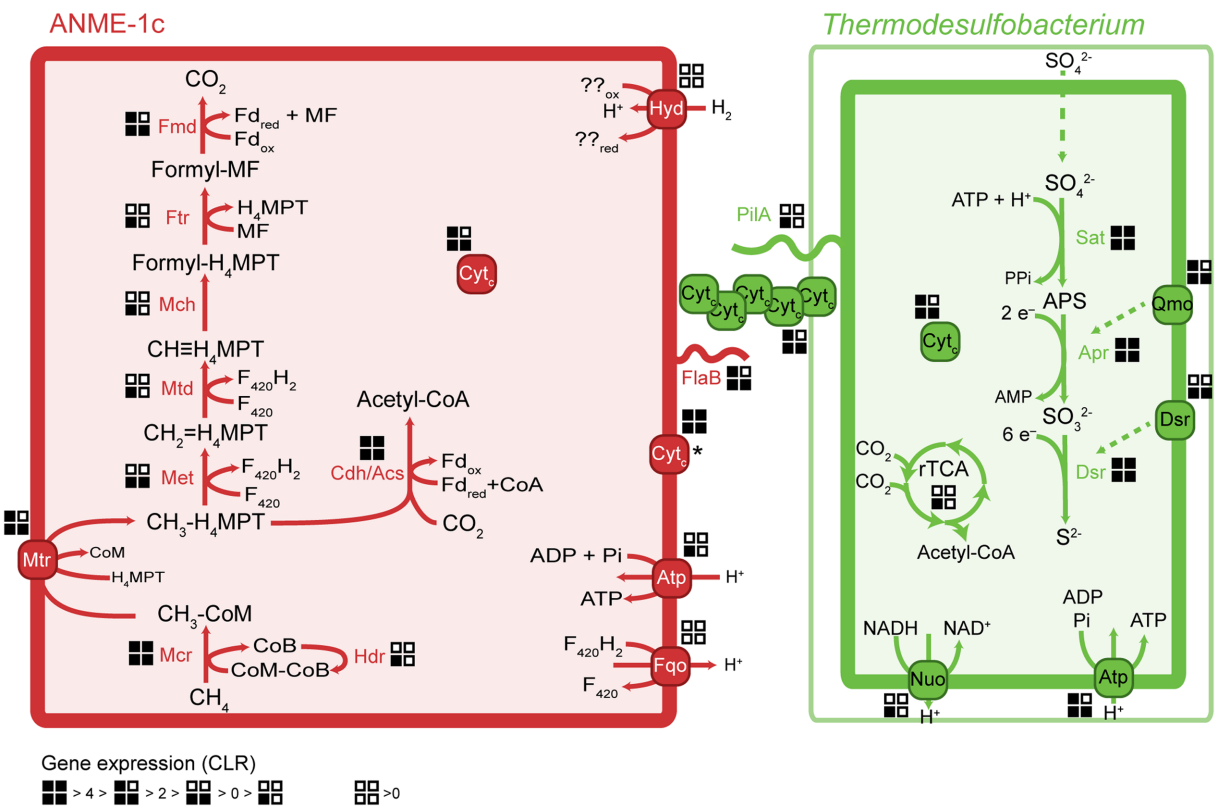

FIGURE 3
Key metabolic pathways in ANME-1c and *Ca.* Thermodesulfobacterium torris and metatranscriptomic expression during AOM. Gene expression values were normalized to centered-log ratios (CLR). A CLR value of 0 represents the mean expression of all genes in a genome. The asterisk next to the ANME-1c cytochrome indicates unknown cell localization. H_4MPT, tetrahydromethanopterin; MF, methanofuran; Fd, ferredoxin; Mcr, methyl-coenzyme M reductase; Mtr, tetrahydromethanopterin S-methyltransferase; Met, 5,10-methylenetetrahydrofolate reductase; Mtd, methylenetetrahydromethanopterin dehydrogenase; Mch, methenyltetrahydromethanopterin cyclohydrolase; Ftr, formylmethanofuran-tetrahydromethanopterin formyltransferase; Fmd, formylmethanofuran dehydrogenase; Cdh/Acs, CO dehydrogenase/acetyl-coenzyme A synthase complex; rTCA, reductive tricarboxylic acid cycle; Sat, sulfate adenylyltransferase; Apr, adenylylsulfate reductase; Dsr, dissimilatory sulfate reductase; Fqo, ferredoxin: quinone oxidoreductase; Atp, ATP synthase; Hyd, hydrogenase; Qmo, quinone-modifying oxidoreductase; Nuo, NADH:ubiquinone oxidoreductase; Cyt_c, multiheme cytochrome *c*-like protein; PilA, bacterial pilus protein; FlaB, archaeal flagellum protein (archaellum).

an adenylylsulfate kinase (*cys*C; high expression, CLR = 2.21) that could be used for assimilatory sulfate metabolism, but it lacks the key genes for dissimilatory sulfate reduction. The ANME-1c MAG lacks a complete nitrogenase operon, suggesting it is incapable of nitrogen fixation. The capability for nitrogen fixation has been shown only in ANME-2 archaea but not in ANME-1 (Dekas et al., 2009, 2015; Orphan et al., 2009; Krukenberg et al., 2018). The nitrogenase subunits *nif*DH detected in ANME-1c and other ANME-1 genomes (Meyerdierks et al., 2010) are likely paralogs of *cfb*CD because they are located in an operon with genes encoding the biosynthetic pathway of coenzyme F_{430} (Zheng et al., 2016; Moore et al., 2017). Coenzyme F_{430} functions as a prosthetic group that binds to the active site of McrA, and is therefore a key molecule for methanogens and methanotrophs (Friedmann et al., 1990; Ermler et al., 1997; Shima et al., 2012).

ANME-1c likely performs autotrophic carbon fixation *via* the carbon monoxide dehydrogenase/acetyl-CoA synthase complex (Cdh/Acs; Kellermann et al., 2012). All the *cdh* transcripts are highly abundant (CLR between 0.4 and 2.0, Supplementary Table 4), supporting the use of this pathway for autotrophy. ANME-1c does not encode other complete carbon fixation pathways. The reductive tricarboxylic acid (rTCA) cycle is incomplete, lacking the key enzyme pyruvate carboxylase. The rTCA cycle genes have relatively low expression (CLR −0.7 to 1.8, Supplementary Table 4). Enzymes of this pathway may play a role in the biosynthesis of cell building blocks (Meyerdierks et al., 2010). Like all ANME-1, ANME-1c contains a β-oxidation pathway. The phylogenetically related multi-carbon alkane oxidizers, *Ca.* Syntrophoarchaeales, *Ca.* Alkanophagales and *Ca.* Santabarbaracales harbor several copies of the β-oxidation genes and use the encoded pathway to split alkane-derived acyl-CoA into acetyl-CoA units (Laso-Pérez et al., 2016; Wang et al., 2021). However, the expression of β-oxidation genes in ANME-1c is relatively low, especially the first two reactions (CLR −0.2 to 0.5, Supplementary Table 4). Furthermore, ANME-1c lacks the electron transfer flavoprotein (*etf*AB) needed to oxidize acyl-CoA to enoyl-CoA. Hence, β-oxidation may not serve a catabolic function in ANME-1c, but play a role in biosynthesis of cell compounds. Wang and colleagues suggested that the ancestor of Syntrophoarchaeia (family including ANME-1, *Ca.* Syntrophoarchaeales and *Ca.* Alkanophagales) activated multi-carbon alkanes with their multi-carbon-alkane specific Mcr (Acrs) forming the corresponding alkyl-CoM as intermediate (Laso-Pérez et al., 2016; Wang et al., 2021). It was proposed that ANME-1 acquired a methane-activating Mcr from methylotrophic methanogens, likely from the clade *Ca.* Methanofastidiosa/*Ca.* Nuwarchaeia, and later lost the *acr* genes (Borrel et al., 2019; Wang et al., 2021).

Phylogeny and environmental distribution of AOM-associated *Thermodesulfobacteria*

We compared the *Thermodesulfobacterium* MAG in AOM70 cultures with the *Thermodesulfobacteria* MAGs from Pescadero Basin and to MAGs retrieved from databases (NCBI and JGI). Our AOM70 *Thermodesulfobacterium* shares >95% ANI with a MAG of a *Thermodesulfobacterium* from Pescadero Basin (Laso-Pérez et al., 2022; Speth et al., 2022; Supplementary Figure 7). Based on 16S rRNA phylogeny (Supplementary Figure 6), the *Thermodesulfobacterium* AOM70 sequences form a cluster with sequences originating from Guaymas Basin and Pescadero Basin hydrothermal seeps (McKay et al., 2016; Lagostina et al., 2021; Pérez Castro et al., 2021; Speth et al., 2022). Several species of *Thermodesulfobacterium* have been isolated from hot springs (Zeikus et al., 1983; Sonne-Hansen and Ahring, 1999; Hamilton-Brehm et al., 2013), petroleum reservoirs (Rozanova and Khudiakova, 1974) and hydrothermal vents (Jeanthon et al., 2002; Moussard et al., 2004). The 16S rRNA gene sequence of our AOM70 *Thermodesulfobacterium* is 96% identical to the closest cultured representative, *Thermodesulfobacterium geofontis*, isolated from Obsidian Pool, Yellowstone National Park (Hamilton-Brehm et al., 2013). Considering an ANI <83% for distinct species and >95% for the same species (Jain et al., 2018) the *Thermodesulfobacteria* MAG from the AOM70 culture metagenome and the Pescadero MAG are a new candidate species in the genus *Thermodesulfobacterium* (Supplementary Figure 8). We propose the taxon name *Candidatus* Thermodesulfobacterium torris (torris "firebrand" referring to the thermophilic lifestyle and the formation of black aggregates in the cultures).

Metabolism of the partner bacteria *Thermodesulfobacteria*

Members of the *Thermodesulfobacteria* family have not been previously reported as partner bacteria in AOM. All *Thermodesulfobacteria* isolates are sulfate-reducing (hyper) thermophiles with growth optima between 65°C and 90°C. They differ in the range of electron donors or carbon sources they use, which include molecular hydrogen, formate, lactate, and pyruvate (Zeikus et al., 1983; Sonne-Hansen and Ahring, 1999; Jeanthon et al., 2002; Moussard et al., 2004). Similar to other members, *Ca.* T. torris encodes a complete dissimilatory sulfate reduction pathway, including sulfate adenylyltransferase (*sat*), adenylylsulfate reductase (*apr*), and dissimilatory sulfite reductase (*dsr*). In *Ca.* T. torris this pathway is highly expressed during AOM (average CLR values between 4.0 and 6.5, Supplementary Table 4). In addition, *Ca.* T. torris contains and expresses the Dsr-associated membrane complex (*dsr*KMOP) which takes up electrons from the periplasmic cytochrome *c* pool to reduce a disulfide bond in the cytoplasmic DsrC (Pereira et al., 2011; Venceslau et al., 2014). The quinone-modifying oxidoreductase (*qmo*ABC) genes are present in an operon together with the Apr genes. In fact, the Qmo membrane complex interacts with Apr through a third unknown protein and channels electrons from the membrane ubiquinones *via* electron confurcation (Ramos et al., 2012). Both the *dsr*KMOP and the *qmo*ABC transcripts have high expression (Supplementary Table 4). Other cytoplasmic enzymes commonly associated with heterodisulfide

reductases, such as the methylviologen reducing hydrogenase (Mvh/Hdr), were not found in the dataset. For energy conservation, *Ca.* T. torris uses a membrane-bound NADH:ubiquinone oxidoreductase (Nuo) and an ATP synthase (Atp). Nuo couples the reduction of NAD^+ by reduced ubiquinones in the cytoplasmic membrane to the translocation of protons to the periplasmic space. The proton gradient generated enables oxidative phosphorylation in the ATP synthase.

The reductive acetyl-CoA pathway (Wood-Ljungdahl pathway) for carbon fixation is incomplete in the genome. *Ca.* T. torris does not encode a formate dehydrogenase (*fdh*) or a carbon monoxide dehydrogenase/acetyl-CoA complex (*cdh*/*acs*), but it encodes the enzymes catalyzing C_1-tetrahydrofolate transformations. These reactions are necessary for several cell processes including nucleic acid biosynthesis (Ducker and Rabinowitz, 2017). Instead, *Ca.* T. torris likely fixes carbon *via* the rTCA cycle. The genome codes for an almost complete rTCA cycle, lacking a succinyl-CoA synthetase. This enzyme is likely substituted by a putative acetyl-CoA synthetase encoded in the genome and highly expressed (CLR = 3.39, locus MW689_000791). Acetyl-CoA synthetases have sequence homology with succinyl-CoA synthetases and are also active toward succinate with reduced affinity (Sánchez et al., 2000). Similarly, the thermophilic partner bacterium *Ca. Desulfofervidus auxilii* and other non-symbiotic thermophilic SRB fix carbon *via* the rTCA cycle (Schauder et al., 1987; Krukenberg et al., 2016). By contrast, meso- and psychrophilic AOM partner bacteria fix carbon using the Wood-Ljungdahl pathway (Skennerton et al., 2017).

We aimed to enrich *Ca.* T. torris by incubating aliquots of the AOM70 culture with H_2, formate, lactate, or pyruvate as electron donors. None of the substrates resulted in immediate sulfide production (Supplementary Figure 9). Pyruvate caused sulfide production after 15 days, which likely indicates the growth of originally rare microorganisms, similar as shown for mesophilic AOM cultures (Zhu et al., 2022). These incubations suggest that *Ca.* T. torris is an obligate syntrophic bacterium that fully depends on the transfer of reducing equivalents in AOM.

Transfer of reducing equivalents between ANME-1c and *Thermodesulfobacteria*

Because ANME have no own respiratory pathways, they need to transfer the reducing equivalents liberated during AOM to their sulfate-reducing partners. Multiple mechanisms have been proposed for syntrophic fermentation, including interspecies hydrogen transfer (Schink, 1997). A canonical syntrophy based on interspecies hydrogen transfer would require membrane-bound hydrogenases in both partners. Notably, the ANME-1c MAGs code for a complete nickel-iron hydrogenase, a feature that is rare in other ANME-1 genomes. The hydrogenase database (HydDB) annotation classifies this hydrogenase within the group 1 g of hydrogenases that are typically found in thermophilic organisms (Brock et al., 1972; Fischer et al., 1983; Huber et al., 2000; Laska et al., 2003). Yet this hydrogenase is only poorly expressed (CLR < −0.3, Supplementary Table 4). In contrast, the *Ca.* T. torris MAG lacks hydrogenases. The addition of molecular hydrogen to the culture did not stimulate sulfide production in the AOM culture, which confirms that *Ca.* T. torris cannot grow on hydrogen. Based on these observations we exclude hydrogen as electron carrier from ANME-1c toward *Ca.* T. torris. Our results confirm thermodynamic models which excluded hydrogen exchange in AOM consortia (Sørensen et al., 2001). Most other AOM partner bacteria such as SeepSRB-1a and SeepSRB2 are also obligate syntrophs and do not encode hydrogenases (Nauhaus et al., 2002; Wegener et al., 2016; Krukenberg et al., 2018). *Ca. D. auxilii*, performs DIET when growing as partner in AOM or short-chain alkane oxidation at 50°C–60°C (Wegener et al., 2015; Laso-Pérez et al., 2016; Krukenberg et al., 2018; Hahn et al., 2020), but it also shows growth on hydrogen (Krukenberg et al., 2016). It has been shown that DIET allows more efficient growth than interspecies hydrogen transfer (Summers et al., 2010).

In AOM and short-chain alkane-oxidizing consortia, cells are densely packed and the intercellular space contains cytochromes and nanowire-like structures (McGlynn et al., 2015; Wegener et al., 2015; Laso-Pérez et al., 2016; Krukenberg et al., 2018). In these mesophilic and thermophilic consortia, both partners express cytochrome and *pil*A genes (Laso-Pérez et al., 2016; Krukenberg et al., 2018). The genes *pil*A (bacterial pilin) in *Ca.* T. torris and *fla*B (archaeal flagellin) in ANME-1c show a high expression in the metatranscriptomes (CLR values of 1.8 and 3.2, respectively, Supplementary Table 4). The archaeal flagellum (archaellum) is highly similar to bacterial type IV pili (Albers and Jarrell, 2015) and might also be involved in electron transfer over longer distances. The conductivity of the archaellum from the methanogen *Methanospirillum hungatei* was demonstrated, yet its possible role in interspecies electron transfer is unclear (Walker et al., 2019). Conductive filaments that enable the transport of electrons across long distances toward extracellular electron acceptors have been widely studied in *Geobacter* (Reguera et al., 2005; Malvankar et al., 2011; Shrestha et al., 2013; Adhikari et al., 2016). Reguera et al. (2005) showed that pilus-deficient *Geobacter* mutants could not transfer electrons to extracellular electron acceptors, suggesting an involvement of pilin proteins in this process (Reguera et al., 2005).

The molecular basis of DIET in sulfate-dependent AOM has been intensively discussed in the past years (McGlynn et al., 2015; Wegener et al., 2015; Chadwick et al., 2022; Yu et al., 2022). McGlynn et al. (2015) proposed a model based on direct interspecies electron transfer *via* multiheme cytochromes for AOM consortia, using evidence from single-cell activities, microscopic observations and genomics (McGlynn et al., 2015). Krukenberg et al. (2018) showed that both partners highly express cytochromes with a low number of heme groups (3–5 heme binding motifs) during thermophilic AOM (Krukenberg et al., 2018). In AOM consortia at 60°C, it was observed that SRB *Ca. Desulfofervidus auxilii* expressed pili genes and that the intercellular space

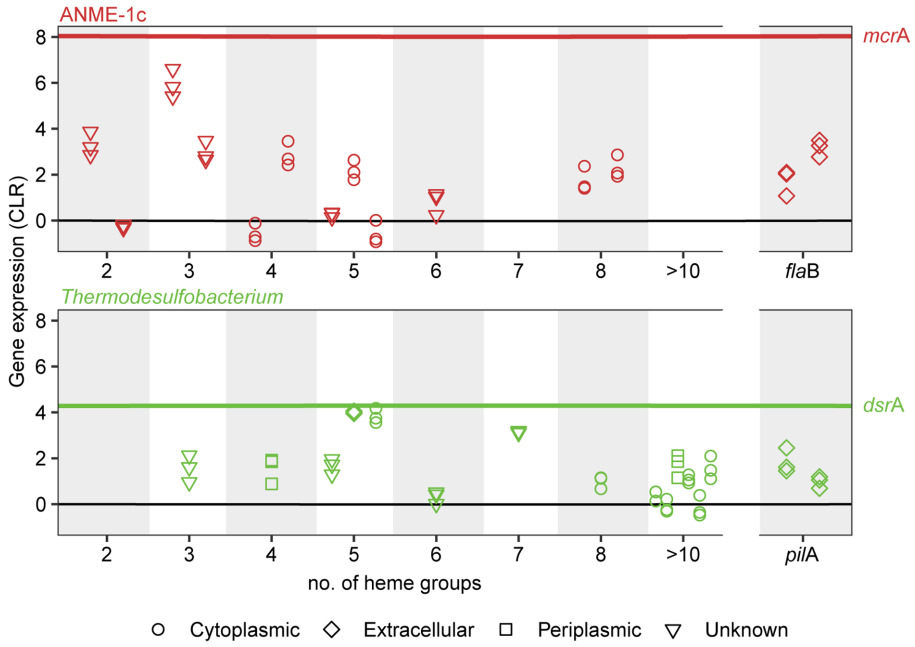

FIGURE 4
Expression and subcellular localization of multiheme cytochromes and cellular appendages in ANME-1c (top) and *Thermodesulfobacterium* (bottom) in AOM70 cultures. Gene expression is noted as centered-log ratio values, with 0 as the mean expression of all genes in each genome. *mcr*A and *dsr*A mean CLR values are displayed as a reference (red and green lines, respectively). Symbols show the predicted subcellular localization of cytochromes (PSORTb). Three symbols in a vertical line correspond to CLR values of a specific locus in triplicate metatranscriptomes.

was filled with nanowire structures similar to syntrophic consortia of *Geobacter* (Wegener et al., 2015). Indeed it was recently shown that the filaments in *Geobacter sulfurreducens* are not formed by pilin proteins (PilA), but rather by stacked OmcS hexaheme cytochromes (Wang et al., 2019). Instead, PilA might be involved in secretion of OmcS cytochromes (Gu et al., 2021). Both ANME-1c and *Ca.* T. torris encode several multiheme cytochromes. ANME-1c codes for several proteins with 2 to 8 heme-binding motifs (Figure 4; Supplementary Table 4). A cytochrome c7 and a protein without annotation, both with 3 heme groups, are among the top expressed genes (CLR values of 5.9 and 2.96, respectively, Supplementary Table 4). However, the predicted subcellular localizations of these putative cytochromes are unknown, as reported by PSORTb. Interestingly, these cytochromes are highly similar to extracellular cytochromes that were highly expressed in ANME-1 during AOM at 60°C (Supplementary Table 4; Krukenberg et al., 2018). *Ca.* T. torris also contains numerous multiheme cytochromes, with up to 26 heme-binding motifs. A cytochrome-like gene with five heme-binding motifs and predicted extracellular localization shows high expression levels similar to the *dsr*A (CLR value of 4.0, Figure 4). This putative pentaheme cytochrome shares high sequence identity (<40% identity) with a *Ca. Desulfofervidus auxilii* OmcS-like protein (Wegener et al., 2015; Krukenberg et al., 2018) (locus tag HS1_000170, Supplementary Figure 10). We hypothesize that the extracellular pentaheme cytochromes from *Ca.* T. torris are likely involved in receiving electrons derived from methane oxidation. ANME-1c cytochromes with undetermined cell localization might also be involved in interspecies electron transfer.

Alternative roles of the membrane-bound hydrogenase in ANME-1c

Some ANME-1c MAGs code for a NiFe membrane-bound hydrogenase, which is an uncommon feature in most ANME genomes (Stokke et al., 2012; Wegener et al., 2015; Krukenberg et al., 2018). This hydrogenase forms a clade with those of *Ca.* Syntrophoarchaeum and *Ca.* Alkanophagales (Figure 2B; Supplementary Figure 11; Laso-Pérez et al., 2016; Wang et al., 2021). In *Ca.* Syntrophoarchaeum, the hydrogenase is highly expressed during anaerobic propane and butane oxidation, albeit its function is also unknown (Laso-Pérez et al., 2016). In contrast, in ANME-1c the NiFe-hydrogenase has low expression (Figure 3; Supplementary Table 4). A recent study described the ANME-1c as an ancestral clade at the base of ANME-1a/1b and as a sister branch of *Ca.* Syntrophoarchaeales (Laso-Pérez et al., 2022). ANME-1c were proposed to be facultative methanogens based

on the encoded hydrogenase and the unclear association with partner bacteria in environmental samples (Laso-Pérez et al., 2022). The capability of ANME-1 to perform methanogenesis has been repeatedly suggested (Seifert et al., 2006; Treude et al., 2007; Orcutt et al., 2008). ANME-1 16S rRNA and *mcr*A genes and transcripts were found in methanogenic sediment horizons at White Oak River estuary and in the sulfate–methane transition zone (Lloyd et al., 2011; Kevorkian et al., 2021). The authors weighted this as an argument for a potential role of ANME-1 in methanogenesis. There is no genomic evidence that ANME-1 from these environment contain hydrogenases, which are required to perform methanogenesis from CO_2, and this question should be addressed in future metagenomic studies. To test whether ANME-1c are capable of methanogenesis, we transferred AOM70 culture aliquots to sulfate-free medium and exchanged the methane in the headspace with an H_2/CO_2 atmosphere. Hydrogen addition did not stimulate production of methane in AOM70 cultures in the course of 4-month incubations (Supplementary Figure 12). According to these results, ANME-1c are incapable of hydrogenotrophic methanogenesis. The habitable zones of the hydrothermally-heated sediments in Guaymas Basin are rich in sulfate due to hydrothermal circulation and seawater advection (Ramírez et al., 2021). This provides additional evidence for ANME-1c being obligate methane oxidizers that depend on syntrophic partnerships with sulfate-reducers. The hydrogenase in ANME-1c might be a remnant from the common ancestor of the *Ca.* Syntrophoarchaeum/*Ca.* Alkanophagales/ANME-1 clade. These ancestral alkanotrophic archaea might have performed interspecies electron transfer based on hydrogen transfer. In the course of evolution that capability was replaced by an apparently more efficient DIET mechanism *via* extracellular multiheme cytochromes (Summers et al., 2010).

Conclusion

Here we cultured a thermophilic AOM consortium at 70°C consisting of methane-oxidizing archaea from the ANME-1c clade with *Thermodesulfobacteria* as sulfate-reducing partner bacteria. Our study bridges the temperature gap between AOM activity previously observed by pore water profiles and tracer experiments, and its *in vitro* demonstration in cultures. ANME-1c is a basal lineage to the ANME-1a/b clade. Interestingly, ANME-1c MAGs encode a hydrogenase operon that is not present in the ANME-1a/b clades. ANME-1c neither produces nor consumes hydrogen. The hydrogenase genes have low expression and this enzyme is likely a remnant of the ancestor of the *Ca.* Syntrophoarchaeia, an organism that was likely a multi-carbon alkane oxidizer. The function of this hydrogenase in ANME-1, but also other members of the Syntrophoarchaeia is unresolved. Based on indirect evidence ANME-1 were repeatedly suggested to be facultative methanogens (Seifert et al., 2006; Treude et al., 2007; Orcutt et al., 2008; Lloyd et al., 2011; Kevorkian et al., 2021). Here, we demonstrated that even ANME-1c that encode a hydrogenase are not able to reverse their metabolism toward net methanogenesis. Cultivation-based approaches should be used to test whether the ANME-1a/b that encode hydrogenases are capable of methanogenesis.

Most likely, ANME and their partners interact *via* DIET. The partner *Thermodesulfobacterium* encodes an extracellular pentaheme c-type cytochrome with high expression. This cytochrome is highly similar to *Ca. Desulfofervidus auxilii* cytochromes that have high expression during AOM at 60°C. This evidence suggests a central role of this pentaheme cytochrome of *Thermodesulfobacteria* in DIET. In addition, multiheme cytochromes and flagella from ANME-1c are highly expressed under AOM conditions. However, the role of these cytochromes with unknown subcellular location in DIET needs further investigation.

Our study provides culture-based evidence for the feasibility of AOM at high-temperature conditions and the versatility and evolutionary diversity of the organisms mediating AOM in marine environments. To our knowledge, this is the first report of syntrophic consortia of ANME and *Thermodesulfobacteria.* ANME-1c and *Ca.* T. torris co-occur in environmental samples from the Guaymas Basin and Pescadero Basin (Gulf of California; Laso-Pérez et al., 2022; Speth et al., 2022). This limited geographical distribution is likely a result of undersampling of heated methane-rich environments. Apart from the rather rare methane-rich hydrothermal vents, consortia of these phylotypes might inhabit deep sulfate–methane interfaces. Indeed, these sulfate–methane interfaces occur at depths up to 150 m below the seafloor and at temperatures of up to 80°C (Teske et al., 2021; Beulig et al., 2022). The question of whether these sulfate–methane interfaces are a habitat for AOM needs to be addressed. Future studies should aim to search for the ANME-1c and *Thermodesulfobacteria* co-occurring in such deep-sea sediments.

Data availability statement

The metagenome-assembled genomes (MAGs) and metagenomic contigs are available on NCBI under BioProject PRJNA805391. Assembled metagenomic contigs are available under BioSample ID SAMN30121676. ANME-1c and Ca. Thermodesulfobacterium torris annotated genomes are available under BioSample IDs SAMN27514932 and SAMN27514933, respectively.

Author contributions

DBM and GW designed the study. GW did sampling on board. AT planned and organized the cruise. DBM and HZ did cultivation experiments. DBM performed laboratory experiments and 'omics analyses and wrote the manuscript with contributions

from all coauthors. All authors contributed to the article and approved the submitted version.

Funding

The study was funded by the Max Planck Society and the DFG under Germany's Excellence Initiative/Strategy through the Clusters of Excellence EXC 2077 "The Ocean Floor—Earth's Uncharted Interface" (project no. 390741601). The Guaymas Basin expedition was supported by the National Science Foundation, Biological Oceanography grant no. 1357238 to AT (Collaborative Research: Microbial Carbon cycling and its interactions with Sulfur and Nitrogen transformations in Guaymas Basin hydrothermal sediments).

Acknowledgments

The authors thank the captain and crew of R/V *Atlantis*, and the *Alvin* group for excellent work during Expedition AT42-05. We thank Susanne Menger for technical support in the laboratory. We also thank Rafael Laso Pérez for providing ANME-1c MAGs from Pescadero Basin.

Conflict of interest

The authors declare that the research was conducted in the absence of any commercial or financial relationships that could be construed as a potential conflict of interest.

The handling editor SER declared past co-authorships with one of the authors GW.

Publisher's note

Supplementary material

The Supplementary material for this article can be found online at: https://www.frontiersin.org/articles/10.3389/fmicb.2022.988871/full#supplementary-material

SUPPLEMENTARY FIGURE 1
Sulfide production in initial sediment slurry and in AOM cultures at 70°C.

SUPPLEMENTARY FIGURE 2
16S rRNA community composition of original sediments.

SUPPLEMENTARY FIGURE 3
CARD-FISH micrographs of AOM the culture at 70°C.

SUPPLEMENTARY FIGURE 4
16S rRNA phylogeny of ANME-1, including ANME-1c.

SUPPLEMENTARY FIGURE 5
Average nucleotide identity of ANME-1c genomes.

SUPPLEMENTARY FIGURE 6
16S rRNA phylogeny of *Thermodesulfobacteria*.

SUPPLEMENTARY FIGURE 7
Phylogenomic tree of *Thermodesulfobacteria*.

SUPPLEMENTARY FIGURE 8
Average nucleotide identity of selected *Thermodesulfobacteria* genomes.

SUPPLEMENTARY FIGURE 9
Sulfide production in incubations with substrates for *Thermodesulfobacteria*.

SUPPLEMENTARY FIGURE 10
Alignment of Ca. Thermodesulfobacterium torris and partner sulfate-reducing bacteria multiheme cytochromes likely involved in interspecies electron transfer.

SUPPLEMENTARY FIGURE 11
NiFe hydrogenase tree including ANME-1 hydrogenases.

SUPPLEMENTARY FIGURE 12
The AOM70 enrichment does not produce methane under methanogenesis conditions.

SUPPLEMENTARY TABLE 1
Abundance and length distribution of PacBio metagenomic long reads.

SUPPLEMENTARY TABLE 2
CARD-FISH probes used in this study.

SUPPLEMENTARY TABLE 3
Genomes and conserved marker genes used for archaeal/bacterial phylogenomic tree calculation.

SUPPLEMENTARY TABLE 4
Annotation and metatranscriptomic expression of main pathways of ANME-1c and Ca. Thermodesulfobacterium torris discussed in the main text.

SUPPLEMENTARY TABLE 5
Reference hydrogenase accession numbers used for hydrogenase phylogenetic tree calculation.

References

Adams, M. M., Hoarfrost, A. L., Bose, A., Joye, S. B., and Girguis, P. R. (2013). Anaerobic oxidation of short-chain alkanes in hydrothermal sediments: potential influences on sulfur cycling and microbial diversity. *Front. Microbiol.* 4:110. doi: 10.3389/fmicb.2013.00110

Adhikari, R. Y., Malvankar, N. S., Tuominen, M. T., and Lovley, D. R. (2016). Conductivity of individual *Geobacter* pili. *RSC Adv.* 6, 8354–8357. doi: 10.1039/C5RA28092C

Albers, S. V., and Jarrell, K. F. (2015). The archaellum: how Archaea swim. *Front. Microbiol.* 6, 1–12. doi: 10.3389/FMICB.2015.00023

Altschul, S. F., Gish, W., Miller, W., Myers, E. W., and Lipman, D. J. (1990). Basic local alignment search tool. *J. Mol. Biol.* 215, 403–410. doi: 10.1016/S0022-2836(05)80360-2

Bengtsson-Palme, J., Hartmann, M., Eriksson, K. M., Pal, C., Thorell, K., Larsson, D. G. J., et al. (2015). Metaxa 2: improved identification and taxonomic classification of small and large subunit rRNA in metagenomic data. *Mol. Ecol. Resour.* 15, 1403–1414. doi: 10.1111/1755-0998.12399

Beulig, F., Schubert, F., Adhikari, R. R., Glombitza, C., Heuer, V. B., Hinrichs, K.-U., et al. (2022). Rapid metabolism fosters microbial survival in the deep, hot subseafloor biosphere. *Nat. Commun.* 131, 1–9. doi: 10.1038/s41467-021-27802-7

Biddle, J. F., Cardman, Z., Mendlovitz, H., Albert, D. B., Lloyd, K. G., Boetius, A., et al. (2012). Anaerobic oxidation of methane at different temperature regimes in Guaymas Basin hydrothermal sediments. *ISME J.* 6, 1018–1031. doi: 10.1038/ismej.2011.164

Boetius, A., and Knittel, K. (2010). "Habitats of anaerobic methane oxidizers," in *Handbook of Hydrocarbon and Lipid Microbiology*. ed. K. N. Timmis (Berlin, Heidelberg: Springer Berlin Heidelberg), 2193–2202.

Boetius, A., Ravenschlag, K., Schubert, C. J., Rickert, D., Widdel, F., Gieseke, A., et al. (2000). A marine microbial consortium apparently mediating anaerobic oxidation of methane. *Nature* 407, 623–626. doi: 10.1038/35036572

Borrel, G., Adam, P. S., McKay, L. J., Chen, L.-X., Sierra-García, I. N., Sieber, C. M. K., et al. (2019). Wide diversity of methane and short-chain alkane metabolisms in uncultured archaea. *Nat. Microbiol.* 4, 603–613. doi: 10.1038/s41564-019-0363-3

Brock, T. D., Brock, K. M., Belly, R. T., and Weiss, R. L. (1972). *Sulfolobus*: A new genus of sulfur-oxidizing bacteria living at low pH and high temperature. *Arch. für Mikrobiol.* 84, 54–68. doi: 10.1007/BF00408082

Chadwick, G. L., Skennerton, C. T., Laso-Pérez, R., Leu, A. O., Speth, D. R., Yu, H., et al. (2022). Comparative genomics reveals electron transfer and syntrophic mechanisms differentiating methanotrophic and methanogenic archaea. *PLoS Biol.* 20:e3001508. doi: 10.1371/journal.pbio.3001508

Chernomor, O., Von Haeseler, A., and Minh, B. Q. (2016). Terrace aware data structure for phylogenomic inference from supermatrices. *Syst. Biol.* 65, 997–1008. doi: 10.1093/SYSBIO/SYW037

Cord-Ruwisch, R. (1985). A quick method for the determination of dissolved and precipitated sulfides in cultures of sulfate-reducing bacteria. *J. Microbiol. Methods* 4, 33–36. doi: 10.1016/0167-7012(85)90005-3

Darling, A. E., Jospin, G., Lowe, E., Matsen, F. A., Bik, H. M., and Eisen, J. A. (2014). Phylo sift: phylogenetic analysis of genomes and metagenomes. *Peer J* 2:e243. doi: 10.7717/peerj.243

Dekas, A. E., Connon, S. A., Chadwick, G. L., Trembath-Reichert, E., and Orphan, V. J. (2015). Activity and interactions of methane seep microorganisms assessed by parallel transcription and FISH-NanoSIMS analyses. *ISME J.* 103, 678–692. doi: 10.1038/ismej.2015.145

Dekas, A. E., Poretsky, R. S., and Orphan, V. J. (2009). Deep-sea archaea fix and share nitrogen in methane-consuming microbial consortia. *Science* 326, 422–426. doi: 10.1126/science.1178223/

Dombrowski, N., Seitz, K. W., Teske, A. P., and Baker, B. J. (2017). Genomic insights into potential interdependencies in microbial hydrocarbon and nutrient cycling in hydrothermal sediments. *Microbiome* 5:106. doi: 10.1186/s40168-017-0322-2

Dombrowski, N., Teske, A. P., and Baker, B. J. (2018). Expansive microbial metabolic versatility and biodiversity in dynamic Guaymas Basin hydrothermal sediments. *Nat. Commun.* 9:4999. doi: 10.1038/s41467-018-07418-0

Dowell, F., Cardman, Z., Dasarathy, S., Kellermann, M. Y., Lipp, J. S., Ruff, S. E., et al. (2016). Microbial communities in methane- and short chain alkane-rich hydrothermal sediments of Guaymas Basin. *Front. Microbiol.* 7:17. doi: 10.3389/fmicb.2016.00017

Ducker, G. S., and Rabinowitz, J. D. (2017). One-carbon metabolism in health and disease. *Cell Metab.* 25, 27–42. doi: 10.1016/J.CMET.2016.08.009

Edgar, R. C. (2004). MUSCLE: A multiple sequence alignment method with reduced time and space complexity. *BMC Bioinformatics* 5, 1–19. doi: 10.1186/1471-2105-5-113/FIGURES/16

Eren, A. M., Esen, Ö. C., Quince, C., Vineis, J. H., Morrison, H. G., Sogin, M. L., et al. (2015). Anvi'o: An advanced analysis and visualization platform for 'omics data. *Peer J* 3:e1319. doi: 10.7717/peerj.1319

Eren, A. M., Kiefl, E., Shaiber, A., Veseli, I., Miller, S. E., Schechter, M. S., et al. (2020). Community-led, integrated, reproducible multi-omics with anvi'o. *Nat. Microbiol.* 61, 3–6. doi: 10.1038/s41564-020-00834-3

Ermler, U., Grabarse, W., Shima, S., Goubeaud, M., and Thauer, R. K. (1997). Crystal structure of methyl-coenzyme M reductase: The key enzyme of biological methane formation. *Science* 278, 1457–1462. doi: 10.1126/science.278.5342.1457

Fischer, F., Zillig, W., Stetter, K. O., and Schreiber, G. (1983). Chemolithoautotrophic metabolism of anaerobic extremely thermophilic archaebacteria. *Nature* 301, 511–513. doi: 10.1038/301511a0

Friedmann, H. C., Klein, A., and Thauer, R. K. (1990). Structure and function of the nickel porphinoid, coenzyme F430 and of its enzyme, methyl coenzyme M reductase. *FEMS Microbiol. Rev.* 7, 339–348. doi: 10.1111/J.1574-6968.1990.TB04934.X

Galperin, M. Y., Makarova, K. S., Wolf, Y. I., and Koonin, E. V. (2015). Expanded microbial genome coverage and improved protein family annotation in the COG database. *Nucleic Acids Res.* 43, D261–D269. doi: 10.1093/NAR/GKU1223

Gu, Y., Srikanth, V., Salazar-Morales, A. I., Jain, R., O'Brien, J. P., Yi, S. M., et al. (2021). Structure of Geobacter pili reveals secretory rather than nanowire behaviour. *Nature* 597, 430–434. doi: 10.1038/s41586-021-03857-w

Haft, D. H., Loftus, B. J., Richardson, D. L., Yang, F., Eisen, J. A., Paulsen, I. T., et al. (2001). TIGRFAMs: A protein family resource for the functional identification of proteins. *Nucleic Acids Res.* 29, 41–43. doi: 10.1093/NAR/29.1.41

Hahn, C. J., Laso-Pérez, R., Vulcano, F., Vaziourakis, K.-M., Stokke, R., Steen, I. H., et al. (2020). "*Candidatus* Ethanoperedens," a thermophilic genus of archaea mediating the anaerobic oxidation of ethane. *MBio* 11. doi: 10.1128/mBio.00600-20

Hallam, S. J., Putnam, N., Preston, C. M., Detter, J. C., Rokhsar, D., Richardson, P. M., et al. (2004). Reverse Methanogenesis: testing the hypothesis with environmental genomics. *Science* 305, 1457–1462. doi: 10.1126/science.1100025

Hamilton-Brehm, S. D., Gibson, R. A., Green, S. J., Hopmans, E. C., Schouten, S., van der Meer, M. T. J., et al. (2013). *Thermodesulfobacterium geofontis* sp. nov., a hyperthermophilic, sulfate-reducing bacterium isolated from obsidian Pool, Yellowstone National Park. *Extremophiles* 17, 251–263. doi: 10.1007/S00792-013-0512-1

Hao, L., McIlroy, S. J., Kirkegaard, R. H., Karst, S. M., Fernando, W. E. Y., Aslan, H., et al. (2018). Novel prosthecate bacteria from the candidate phylum Acetothermia. *ISME J.* 12, 2225–2237. doi: 10.1038/s41396-018-0187-9

Haroon, M. F., Hu, S., Shi, Y., Imelfort, M., Keller, J., Hugenholtz, P., et al. (2013). Anaerobic oxidation of methane coupled to nitrate reduction in a novel archaeal lineage. *Nature* 500, 567–570. doi: 10.1038/nature12375

Hinrichs, K.-U., and Boetius, A. (2002). The anaerobic oxidation of methane: new insights in microbial ecology and biogeochemistry. *Ocean Margin Syst.*, 457–477. doi: 10.1007/978-3-662-05127-6_28

Hoehler, T. M., Alperin, M. J., Albert, D. B., and Martens, C. S. (1994). Field and laboratory studies of methane oxidation in an anoxic marine sediment: Evidence for a methanogen-sulfate reducer consortium. *Global Biogeochem. Cycles* 8, 451–463. doi: 10.1029/94GB01800

Holler, T., Wegener, G., Knittel, K., Boetius, A., Brunner, B., Kuypers, M. M. M., et al. (2009). Substantial $^{13}C/^{12}C$ and D/H fractionation during anaerobic oxidation of methane by marine consortia enriched in vitro. *Environ. Microbiol. Rep.* 1, 370–376. doi: 10.1111/J.1758-2229.2009.00074.X

Holler, T., Widdel, F., Knittel, K., Amann, R., Kellermann, M. Y., Hinrichs, K.-U., et al. (2011). Thermophilic anaerobic oxidation of methane by marine microbial consortia. *ISME J.* 5, 1946–1956. doi: 10.1038/ismej.2011.77

Huber, H., Burggraf, S., Mayer, T., Wyschkony, I., Rachel, R., and Stetter, K. O. (2000). *Ignicoccus* gen. Nov., a novel genus of hyperthermophilic, chemolithoautotrophic Archaea, represented by two new species, *Ignicoccus islandicus* sp nov and *Ignicoccus pacificus* sp nov. and Ignicoccus pacificus sp. nov. *Int. J. Syst. Evol. Microbiol.* 50, 2093–2100. doi: 10.1099/00207713-50-6-2093

Hyatt, D., Chen, G. L., LoCascio, P. F., Land, M. L., Larimer, F. W., and Hauser, L. J. (2010). Prodigal: prokaryotic gene recognition and translation initiation site identification. *BMC Bioinformatics* 11, 1–11. doi: 10.1186/1471-2105-11-119

Inagaki, F., Kuypers, M. M. M., Tsunogai, U., Ishibashi, J. I., Nakamura, K. I., Treude, T., et al. (2006). Microbial community in a sediment-hosted CO_2 lake of the southern Okinawa trough hydrothermal system. *Proc. Natl. Acad. Sci. U. S. A.* 103, 14164–14169. doi: 10.1073/PNAS.0606083103

Ishii, K., Mußmann, M., Mac Gregor, B. J., and Amann, R. (2004). An improved fluorescence *in situ* hybridization protocol for the identification of bacteria and archaea in marine sediments. *FEMS Microbiol. Ecol.* 50, 203–213. doi: 10.1016/J.FEMSEC.2004.06.015

Jain, C., Rodriguez-R, L. M., Phillippy, A. M., Konstantinidis, K. T., and Aluru, S. (2018). High throughput ANI analysis of 90K prokaryotic genomes reveals clear species boundaries. *Nat. Commun.* 91, 1–8. doi: 10.1038/s41467-018-07641-9

Jeanthon, C., L'Haridon, S., Cueff, V., Banta, A., Reysenbach, A.-L., and Prieur, D. (2002). *Thermodesulfobacterium hydrogeniphilum* sp. nov., a thermophilic, chemolithoautotrophic, sulfate-reducing bacterium isolated from a deep-sea hydrothermal vent at Guaymas Basin, and emendation of the genus *Thermodesulfobacterium*. *Int. J. Syst. Evol. Microbiol.* 52, 765–772. doi: 10.1099/00207713-52-3-765

Kallmeyer, J., and Boetius, A. (2004). Effects of temperature and pressure on sulfate reduction and anaerobic oxidation of methane in hydrothermal sediments of Guaymas Basin. *Appl. Environ. Microbiol.* 70, 1231–1233. doi: 10.1128/AEM.70.2.1231-1233.2004

Kalyaanamoorthy, S., Minh, B. Q., Wong, T. K. F., Von Haeseler, A., and Jermiin, L. S. (2017). Model finder: fast model selection for accurate phylogenetic estimates. *Nat. Methods* 14, 587–589. doi: 10.1038/nmeth.4285

Kanehisa, M., and Goto, S. (2000). KEGG: Kyoto encyclopedia of genes and genomes. *Nucleic Acids Res.* 28, 27–30. doi: 10.1093/NAR/28.1.27

Kellermann, M. Y., Wegener, G., Elvert, M., Yoshinaga, M. Y., Lin, Y.-S., Holler, T., et al. (2012). Autotrophy as a predominant mode of carbon fixation in anaerobic methane-oxidizing microbial communities. *Proc. Natl. Acad. Sci.* 109, 19321–19326. doi: 10.1073/pnas.1208795109

Kevorkian, R. T., Callahan, S., Winstead, R., and Lloyd, K. G. (2021). ANME-1 archaea may drive methane accumulation and removal in estuarine sediments. *Environ. Microbiol. Rep.* 13, 185–194. doi: 10.1111/1758-2229.12926

Knittel, K., Boetius, A., Lemke, A., Eilers, H., Lochte, K., Pfannkuche, O., et al. (2003). Activity, distribution, and diversity of sulfate reducers and other bacteria in sediments above gas hydrate (Cascadia margin, Oregon). *Geomicrobiol J.* 20, 269–294. doi: 10.1080/01490450303896

Knittel, K., Lösekann, T., Boetius, A., Kort, R., and Amann, R. (2005). Diversity and distribution of methanotrophic archaea at cold seeps. *Appl. Environ. Microbiol.* 71, 467–479. doi: 10.1128/AEM.71.1.467-479.2005

Kolmogorov, M., Bickhart, D. M., Behsaz, B., Gurevich, A., Rayko, M., Shin, S. B., et al. (2020). Meta Flye: scalable long-read metagenome assembly using repeat graphs. *Nat. Methods* 17, 1103–1110. doi: 10.1038/s41592-020-00971-x

Krukenberg, V., Harding, K., Richter, M., Glöckner, F. O., Gruber-Vodicka, H. R., Adam, B., et al. (2016). *Candidatus* Desulfofervidus auxilii, a hydrogenotrophic sulfate-reducing bacterium involved in the thermophilic anaerobic oxidation of methane. *Environ. Microbiol.* 18, 3073–3091. doi: 10.1111/1462-2920.13283

Krukenberg, V., Riedel, D., Gruber-Vodicka, H. R., Buttigieg, P. L., Tegetmeyer, H. E., Boetius, A., et al. (2018). Gene expression and ultrastructure of meso- and thermophilic methanotrophic consortia. *Environ. Microbiol.* 20, 1651–1666. doi: 10.1111/1462-2920.14077

Lagesen, K., Hallin, P., Rødland, E. A., Stærfeldt, H. H., Rognes, T., and Ussery, D. W. (2007). RNAmmer: consistent and rapid annotation of ribosomal RNA genes. *Nucleic Acids Res.* 35, 3100–3108. doi: 10.1093/NAR/GKM160

Lagostina, L., Frandsen, S., Mac Gregor, B. J., Glombitza, C., Deng, L., Fiskal, A., et al. (2021). Interactions between temperature and energy supply drive microbial communities in hydrothermal sediment. *Commun. Biol.* 41, 4, 1–14. doi: 10.1038/s42003-021-02507-1

Langmead, B., and Salzberg, S. L. (2012). Fast gapped-read alignment with bowtie 2. *Nat. Methods* 94, 357–359. doi: 10.1038/nmeth.1923

Lanoil, B. D., Sassen, R., La Duc, M. T., Sweet, S. T., and Nealson, K. H. (2001). Bacteria and Archaea physically associated with Gulf of Mexico gas hydrates. *Appl. Environ. Microbiol.* 67, 5143–5153. doi: 10.1128/AEM.67.11.5143-5153.2001

Laska, S., Lottspeich, F., and Kletzin, A. (2003). Membrane-bound hydrogenase and sulfur reductase of the hyperthermophilic and acidophilic archaeon *Acidianus ambivalens*. *Microbiology* 149, 2357–2371. doi: 10.1099/MIC.0.26455-0/CITE/REFWORKS

Laso-Pérez, R., Krukenberg, V., Musat, F., and Wegener, G. (2018). Establishing anaerobic hydrocarbon-degrading enrichment cultures of microorganisms under strictly anoxic conditions. *Nat. Publ. Gr.* 13, 1310–1330. doi: 10.1038/nprot.2018.030

Laso-Pérez, R., Wegener, G., Knittel, K., Widdel, F., Harding, K. J., Krukenberg, V., et al. (2016). Thermophilic archaea activate butane via alkyl-coenzyme M formation. *Nature* 539, 396–401. doi: 10.1038/nature20152

Laso-Pérez, R., Wu, F., Crémière, A., Speth, D. R., Magyar, J. S., Krupovic, M., et al. (2022). Evolutionary diversification of methanotrophic *Ca*. Methanophagales (ANME-1) and their expansive virome. bio Rxiv [preprint].

Letunic, I., and Bork, P. (2011). Interactive tree of life v2: online annotation and display of phylogenetic trees made easy. *Nucleic Acids Res.* 39, W475–W478. doi: 10.1093/nar/gkr201

Li, H. (2018). Minimap 2: pairwise alignment for nucleotide sequences. *Bioinformatics* 34, 3094–3100. doi: 10.1093/BIOINFORMATICS/BTY191

Lloyd, K. G., Alperin, M. J., and Teske, A. (2011). Environmental evidence for net methane production and oxidation in putative ANaerobic MEthanotrophic (ANME) archaea. *Environ. Microbiol.* 13, 2548–2564. doi: 10.1111/j.1462-2920.2011.02526.x

Lösekann, T., Knittel, K., Nadalig, T., Fuchs, B., Niemann, H., Boetius, A., et al. (2007). Diversity and abundance of aerobic and anaerobic methane oxidizers at the Haakon Mosby mud volcano, Barents Sea. *Appl. Environ. Microbiol.* 73, 3348–3362. doi: 10.1128/AEM.00016-07

Ludwig, W., Strunk, O., Westram, R., Richter, L., Meier, H., Yadhukumar, A., et al. (2004). ARB: A software environment for sequence data. *Nucleic Acids Res.* 32, 1363–1371. doi: 10.1093/NAR/GKH293

Malvankar, N. S., Vargas, M., Nevin, K. P., Franks, A. E., Leang, C., Kim, B. C., et al. (2011). Tunable metallic-like conductivity in microbial nanowire networks. *Nat. Nanotechnol.* 69, 573–579. doi: 10.1038/nnano.2011.119

McGlynn, S. E., Chadwick, G. L., Kempes, C. P., and Orphan, V. J. (2015). Single cell activity reveals direct electron transfer in methanotrophic consortia. *Nature* 526, 531–535. doi: 10.1038/nature15512

McKay, L. J. (2014). Microbial ecology of a manmade oil spill in the Gulf of Mexico and a natural, hydrothermal oil seep in the Gulf of California. Available at: http://search.proquest.com/docview/1613182914?accountid=14468%5Cnhttp://wx7cf7zp2h.search.serialssolutions.com/?ctx_ver=Z39.88-2004&ctx_enc=info:ofi/enc:UTF-8&rfr_id=info:sid/ProQuest+Dissertations+&+Theses+Global&rft_val_fmt=info:ofi/fmt:kev:mtx:disserta.

McKay, L., Klokman, V. W., Mendlovitz, H. P., Larowe, D. E., Hoer, D. R., Albert, D., et al. (2016). Thermal and geochemical influences on microbial biogeography in the hydrothermal sediments of Guaymas Basin, Gulf of California. *Environ. Microbiol. Rep.* 8, 150–161. doi: 10.1111/1758-2229.12365

Merkel, A. Y., Huber, J. A., Chernyh, N. A., Bonch-Osmolovskaya, E. A., and Lebedinsky, A. V. (2013). Detection of putatively thermophilic anaerobic methanotrophs in diffuse hydrothermal vent fluids. *Appl. Environ. Microbiol.* 79, 915–923. doi: 10.1128/AEM.03034-12

Meyerdierks, A., Kube, M., Kostadinov, I., Teeling, H., Glöckner, F. O., Reinhardt, R., et al. (2010). Metagenome and mRNA expression analyses of anaerobic methanotrophic archaea of the ANME-1 group. *Environ. Microbiol.* 12, 422–439. doi: 10.1111/J.1462-2920.2009.02083.X

Michaelis, W., Seifert, R., Nauhaus, K., Treude, T., Thiel, V., Blumenberg, M., et al. (2002). Microbial reefs in the Black Sea fueled by anaerobic oxidation of methane. *Science* 297, 1013–1015. doi: 10.1126/SCIENCE.1072502

Minh, B. Q., Schmidt, H. A., Chernomor, O., Schrempf, D., Woodhams, M. D., Von Haeseler, A., et al. (2020). IQ-TREE 2: new models and efficient methods for phylogenetic inference in the genomic era. *Mol. Biol. Evol.* 37, 1530–1534. doi: 10.1093/MOLBEV/MSAA015

Mistry, J., Chuguransky, S., Williams, L., Qureshi, M., Salazar, G. A., Sonnhammer, E. L. L., et al. (2021). Pfam: The protein families database in 2021. *Nucleic Acids Res.* 49, D412–D419. doi: 10.1093/NAR/GKAA913

Moore, S. J., Sowa, S. T., Schuchardt, C., Deery, E., Lawrence, A. D., Ramos, J. V., et al. (2017). Elucidation of the biosynthesis of the methane catalyst coenzyme F430. *Nature* 543, 78–82. doi: 10.1038/nature21427

Moussard, H., L'Haridon, S., Tindall, B. J., Banta, A., Schumann, P., Stackebrandt, E., et al. (2004). *Thermodesulfatator indicus* gen. Nov., sp. nov., a novel thermophilic chemolithoautotrophic sulfate-reducing bacterium isolated from the central Indian ridge. *Int. J. Syst. Evol. Microbiol.* 54, 227–233. doi: 10.1099/IJS.0.02669-0

Nauhaus, K., Boetius, A., Krüger, M., and Widdel, F. (2002). *In vitro* demonstration of anaerobic oxidation of methane coupled to sulphate reduction in sediment from a marine gas hydrate area. *Environ. Microbiol.* 4, 296–305. doi: 10.1046/J.1462-2920.2002.00299.X

Niemann, H., Elvert, M., Hovland, M., Orcutt, B., Judd, A., Suck, I., et al. (2005). Methane emission and consumption at a North Sea gas seep (Tommeliten area). *Biogeosciences* 2, 335–351. doi: 10.5194/BG-2-335-2005

Niemann, H., Lösekann, T., De Beer, D., Elvert, M., Nadalig, T., Knittel, K., et al. (2006). Novel microbial communities of the Haakon Mosby mud volcano and their role as a methane sink. *Nature* 443, 854–858. doi: 10.1038/nature05227

Orcutt, B. N., Boetius, A., Lugo, S. K., Mac Donald, I. R., Samarkin, V. A., and Joye, S. B. (2004). Life at the edge of methane ice: microbial cycling of carbon and sulfur in Gulf of Mexico gas hydrates. *Chem. Geol.* 205, 239–251. doi: 10.1016/J.CHEMGEO.2003.12.020

Orcutt, B., Samarkin, V., Boetius, A., and Joye, S. (2008). On the relationship between methane production and oxidation by anaerobic methanotrophic communities from cold seeps of the Gulf of Mexico. *Environ. Microbiol.* 10, 1108–1117. doi: 10.1111/j.1462-2920.2007.01526.x

Orphan, V. J., Hinrichs, K.-U., Ussler, W., Paull, C. K., Taylor, L. T., Sylva, S. P., et al. (2001). Comparative analysis of methane-oxidizing archaea and sulfate-reducing bacteria in anoxic marine sediments. *Appl. Environ. Microbiol.* 67, 1922–1934. doi: 10.1128/AEM.67.4.1922-1934.2001

Orphan, V. J., House, C. H., Hinrichs, K. U., McKeegan, K. D., and DeLong, E. F. (2002). Multiple archaeal groups mediate methane oxidation in anoxic cold seep sediments. *Proc. Natl. Acad. Sci. U. S. A.* 99, 7663–7668. doi: 10.1073/PNAS.072210299/ASSET/06C54137-68B2-457C-8C76-FEA01D3D60DE/ASSETS/GRAPHIC/PQ1122102003.JPEG

Orphan, V. J., Turk, K. A., Green, A. M., and House, C. H. (2009). Patterns of 15N assimilation and growth of methanotrophic ANME-2 archaea and sulfate-reducing bacteria within structured syntrophic consortia revealed by FISH-SIMS. *Environ. Microbiol.* 11, 1777–1791. doi: 10.1111/J.1462-2920.2009.01903.X

Parks, D. H., Imelfort, M., Skennerton, C. T., Hugenholtz, P., and Tyson, G. W. (2015). CheckM: assessing the quality of microbial genomes recovered from isolates, single cells, and metagenomes. *Genome Res.* 25, 1043–1055. doi: 10.1101/gr.186072.114

Pereira, I. A. C., Ramos, A. R., Grein, F., Marques, M. C., da Silva, S. M., and Venceslau, S. S. (2011). A comparative genomic analysis of energy metabolism in sulfate reducing bacteria and archaea. *Front. Microbiol.* 2, 1–22. doi: 10.3389/FMICB.2011.00069

Pérez Castro, S., Borton, M. A., Regan, K., Hrabe de Angelis, I., Wrighton, K. C., Teske, A. P., et al. (2021). Degradation of biological macromolecules supports uncultured microbial populations in Guaymas Basin hydrothermal sediments. *ISME J.* 15, 3480–3497. doi: 10.1038/s41396-021-01026-5

Pernthaler, A., Pernthaler, J., and Amann, R. (2002). Fluorescence in situ hybridization and catalyzed reporter deposition for the identification of marine bacteria. *Appl. Environ. Microbiol.* 68, 3094–3101. doi: 10.1128/AEM.68.6.3094-3101.2002

Pruesse, E., Peplies, J., and Glöckner, F. O. (2012). SINA: accurate high-throughput multiple sequence alignment of ribosomal RNA genes. *Bioinformatics* 28, 1823–1829. doi: 10.1093/BIOINFORMATICS/BTS252

Quast, C., Pruesse, E., Yilmaz, P., Gerken, J., Schweer, T., Yarza, P., et al. (2013). The SILVA ribosomal RNA gene database project: improved data processing and web-based tools. *Nucleic Acids Res.* 41, D590–D596. doi: 10.1093/NAR/GKS1219

Ramírez, G. A., Mara, P., Sehein, T., Wegener, G., Chambers, C. R., Joye, S. B., et al. (2021). Environmental factors shaping bacterial, archaeal and fungal community structure in hydrothermal sediments of Guaymas Basin, Gulf of California. *PLoS One* 16:e0256321. doi: 10.1371/JOURNAL.PONE.0256321

Ramos, A. R., Keller, K. L., Wall, J. D., and Cardoso Pereira, I. A. (2012). The membrane QmoABC complex interacts directly with the dissimilatory adenosine 5′-phosphosulfate reductase in sulfate reducing bacteria. *Front. Microbiol.* 3, 1–10. doi: 10.3389/FMICB.2012.00137

Reeburgh, W. S. (2007). Oceanic methane biogeochemistry. *Chem. Rev.* 107, 486–513. doi: 10.1021/cr050362v

Regnier, P., Dale, A. W., Arndt, S., LaRowe, D. E., Mogollón, J., and Van Cappellen, P. (2011). Quantitative analysis of anaerobic oxidation of methane (AOM) in marine sediments: A modeling perspective. *Earth-Science Rev.* 106, 105–130. doi: 10.1016/J.EARSCIREV.2011.01.002

Reguera, G., McCarthy, K. D., Mehta, T., Nicoll, J. S., Tuominen, M. T., and Lovley, D. R. (2005). Extracellular electron transfer via microbial nanowires. *Nature* 435, 1098–1101. doi: 10.1038/nature03661

Rinke, C., Schwientek, P., Sczyrba, A., Ivanova, N. N., Anderson, I. J., Cheng, J. F., et al. (2013). Insights into the phylogeny and coding potential of microbial dark matter. *Nature* 499, 431–437. doi: 10.1038/nature12352

Roussel, E. G., Bonavita, M. A. C., Querellou, J., Cragg, B. A., Webster, G., Prieur, D., et al. (2008). Extending the sub-sea-floor biosphere. *Science* 320:1046. doi: 10.1126/SCIENCE.1154545

Rozanova, E., and Khudiakova, A. (1974). Novyĭ bessporovyĭ termofil'nyĭ organizm, vosstanavlivaiushchiĭ sul'faty, *Desulfovibrio thermophilus* nov. sp [A new non-spore forming thermophilic organism, reducing sulfates, *Desulfovibrio thermophilus* nov. sp]. *Mikrobiologiia* 43, 1069–1075.

Ruff, S. E., Biddle, J. F., Teske, A. P., Knittel, K., Boetius, A., and Ramette, A. (2015). Global dispersion and local diversification of the methane seep microbiome. *Proc. Natl. Acad. Sci. U. S. A.* 112, 4015–4020. doi: 10.1073/pnas.1421865112

Sánchez, L. B., Galperin, M. Y., and Müller, M. (2000). Acetyl-CoA synthetase from the amitochondriate eukaryote Giardia lamblia belongs to the newly recognized superfamily of acyl-CoA synthetases (nucleoside diphosphate-forming). *J. Biol. Chem.* 275, 5794–5803. doi: 10.1074/JBC.275.8.5794

Schauder, R., Widdel, F., and Fuchs, G. (1987). Carbon assimilation pathways in sulfate-reducing bacteria II. Enzymes of a reductive citric acid cycle in the autotrophic *Desulfobacter hydrogenophilus*. *Arch. Microbiol.* 148, 218–225. doi: 10.1007/BF00414815

Scheller, S., Goenrich, M., Boecher, R., Thauer, R. K., and Jaun, B. (2010). The key nickel enzyme of methanogenesis catalyses the anaerobic oxidation of methane. *Nature* 465, 606–608. doi: 10.1038/nature09015

Schink, B. (1997). Energetics of syntrophic cooperation in methanogenic degradation. *Microbiol. Mol. Biol. Rev.* 61, 262–280. doi: 10.1128/MMBR.61.2.262-280.1997

Schouten, S., Wakeham, S. G., Hopmans, E. C., and Damsté, J. S. S. (2003). Biogeochemical evidence that thermophilic archaea mediate the anaerobic oxidation of methane. *Appl. Environ. Microbiol.* 69, 1680–1686. doi: 10.1128/AEM.69.3.1680-1686.2003

Seifert, R., Nauhaus, K., Blumenberg, M., Krüger, M., and Michaelis, W. (2006). Methane dynamics in a microbial community of the Black Sea traced by stable carbon isotopes in vitro. *Org. Geochem.* 37, 1411–1419. doi: 10.1016/J.ORGGEOCHEM.2006.03.007

Shima, S., Krueger, M., Weinert, T., Demmer, U., Kahnt, J., Thauer, R. K., et al. (2012). Structure of a methyl-coenzyme M reductase from Black Sea mats that oxidize methane anaerobically. *Nature* 481, 98–101. doi: 10.1038/nature10663

Shrestha, P. M., Rotaru, A. E., Summers, Z. M., Shrestha, M., Liu, F., and Lovley, D. R. (2013). Transcriptomic and genetic analysis of direct interspecies electron transfer. *Appl. Environ. Microbiol.* 79, 2397–2404.

Skennerton, C. T., Chourey, K., Iyer, R., Hettich, R. L., Tyson, G. W., and Orphan, V. J. (2017). Methane-fueled Syntrophy through extracellular electron transfer: uncovering the genomic traits conserved within diverse bacterial Partners of Anaerobic Methanotrophic Archaea. *MBio* 8, 1–14. doi: 10.1128/mBio.00530-17

Søndergaard, D., Pedersen, C. N. S., and Greening, C. (2016). HydDB: A web tool for hydrogenase classification and analysis. *Sci. Rep.* 6, 1–8. doi: 10.1038/srep34212

Sonne-Hansen, J., and Ahring, B. K. (1999). *Thermodesulfobacterium hveragerdense* sp. nov., and *Thermodesulfovibrio islandicus* sp. nov., two thermophilic sulfate reducing bacteria isolated from a Icelandic hot spring. *Syst. Appl. Microbiol.* 22, 559–564. doi: 10.1016/S0723-2020(99)80009-5

Sørensen, K. B., Finster, K., and Ramsing, N. B. (2001). Thermodynamic and kinetic requirements in anaerobic methane oxidizing consortia exclude hydrogen, acetate, and methanol as possible electron shuttles. *Microb. Ecol.* 421, 1–10. doi: 10.1007/S002480000083

Speth, D. R., Yu, F. B., Connon, S. A., Lim, S., Magyar, J. S., Peña-Salinas, M. E., et al. (2022). Microbial communities of Auka hydrothermal sediments shed light on vent biogeography and the evolutionary history of thermophily. *ISME J.* 16, 1750–1764. doi: 10.1038/s41396-022-01222-x

Stamatakis, A. (2014). RAxML version 8: A tool for phylogenetic analysis and post-analysis of large phylogenies. *Bioinformatics* 30, 1312–1313. doi: 10.1093/BIOINFORMATICS/BTU033

Stokke, R., Roalkvam, I., Lanzen, A., Haflidason, H., and Steen, I. H. (2012). Integrated metagenomic and metaproteomic analyses of an ANME-1-dominated community in marine cold seep sediments. *Environ. Microbiol.* 14, 1333–1346. doi: 10.1111/J.1462-2920.2012.02716.X

Summers, Z. M., Fogarty, H. E., Leang, C., Franks, A. E., Malvankar, N. S., and Lovley, D. R. (2010). Direct exchange of electrons within aggregates of an evolved syntrophic coculture of anaerobic bacteria. *Science* 330, 1413–1415. doi: 10.1126/science.1196526

Teske, A., Hinrichs, K. U., Edgcomb, V., De Vera Gomez, A., Kysela, D., Sylva, S. P., et al. (2002). Microbial diversity of hydrothermal sediments in the Guaymas Basin: evidence for anaerobic methanotrophic communities. *Appl. Environ. Microbiol.* 68, 1994–2007. doi: 10.1128/AEM.68.4.1994-2007.2002

Teske, A., Lizarralde, D., and Höfig, T. W. (2021). Guaymas Basin tectonics and biosphere. *Proc. Int. Ocean Discov. Progr.* 385. doi: 10.14379/IODP.PROC.385.2021

Thauer, R. K. (2011). Anaerobic oxidation of methane with sulfate: on the reversibility of the reactions that are catalyzed by enzymes also involved in methanogenesis from CO_2. *Curr. Opin. Microbiol.* 14, 292–299. doi: 10.1016/J.MIB.2011.03.003

Treude, T., Krüger, M., Boetius, A., and Jørgensen, B. B. (2005). Environmental control on anaerobic oxidation of methane in the gassy sediments of Eckernförde Bay (German Baltic). *Limnol. Oceanogr.* 50, 1771–1786. doi: 10.4319/LO.2005.50.6.1771

Treude, T., Orphan, V., Knittel, K., Gieseke, A., House, C. H., and Boetius, A. (2007). Consumption of methane and CO 2 by Methanotrophic microbial Mats from gas seeps of the anoxic Black Sea. *Appl. Environ. Microbiol.* 73, 2271–2283. doi: 10.1128/AEM.02685-06

Venceslau, S. S., Stockdreher, Y., Dahl, C., and Pereira, I. A. C. (2014). The "bacterial heterodisulfide," Dsr C is a key protein in dissimilatory sulfur metabolism. *Biochim. Biophys. Acta* 1837, 1148–1164. doi: 10.1016/J.BBABIO.2014.03.007

Walker, D. J. F., Martz, E., Holmes, D. E., Zhou, Z., Nonnenmann, S. S., and Lovley, D. R. (2019). The archaellum of *Methanospirillum hungatei* is electrically conductive. *MBio* 10, 1–16. doi: 10.1128/MBIO.00579-19

Wang, F., Gu, Y., O'Brien, J. P., Yi, S. M., Yalcin, S. E., Srikanth, V., et al. (2019). Structure of microbial nanowires reveals stacked hemes that transport electrons over micrometers. *Cell* 177, 361–369.e10. doi: 10.1016/j.cell.2019.03.029

Wang, Y., Wegener, G., Williams, T. A., Xie, R., Hou, J., Tian, C., et al. (2021). A methylotrophic origin of methanogenesis and early divergence of anaerobic multicarbon alkane metabolism. *Sci. Adv.* 7, 1–12. doi: 10.1126/sciadv.abj1453

Wang, F. P., Zhang, Y., Chen, Y., He, Y., Qi, J., Hinrichs, K. U., et al. (2013). Methanotrophic archaea possessing diverging methane-oxidizing and electron-transporting pathways. *ISME J.* 8, 1069–1078. doi: 10.1038/ismej.2013.212

Wegener, G., Krukenberg, V., Riedel, D., Tegetmeyer, H. E., and Boetius, A. (2015). Intercellular wiring enables electron transfer between methanotrophic archaea and bacteria. *Nature* 526, 587–590. doi: 10.1038/nature15733

Wegener, G., Krukenberg, V., Ruff, S. E., Kellermann, M. Y., and Knittel, K. (2016). Metabolic capabilities of microorganisms involved in and associated with the anaerobic oxidation of methane. *Front. Microbiol.* 7, 1–16. doi: 10.3389/fmicb.2016.00046

Whiticar, M. J. (1999). Carbon and hydrogen isotope systematics of bacterial formation and oxidation of methane. *Chem. Geol.* 161, 291–314. doi: 10.1016/S0009-2541(99)00092-3

Widdel, F., and Bak, F. (1992). Gram-negative mesophilic sulfate-reducing bacteria. *Prokaryotes* 183, 3352–3378. doi: 10.1007/978-1-4757-2191-1_21

Wu, Y.-W., Simmons, B. A., and Singer, S. W. (2016). Max bin 2.0: an automated binning algorithm to recover genomes from multiple metagenomic datasets. *Bioinformatics* 32, 605–607. doi: 10.1093/bioinformatics/btv638

Yu, H., Skennerton, C. T., Chadwick, G. L., Leu, A. O., Aoki, M., Tyson, G. W., et al. (2022). Sulfate differentially stimulates but is not respired by diverse anaerobic methanotrophic archaea. *ISME J.* 16, 168–177. doi: 10.1038/S41396-021-01047-0

Yu, N. Y., Wagner, J. R., Laird, M. R., Melli, G., Rey, S., Lo, R., et al. (2010). PSORTb 3.0: improved protein subcellular localization prediction with refined localization subcategories and predictive capabilities for all prokaryotes. *Bioinformatics* 26, 1608–1615. doi: 10.1093/bioinformatics/btq249

Zeikus, J. G., Dawson, M. A., Thompson, T. E., Ingvorsen, K., and Hatchikian, E. C. (1983). Microbial ecology of volcanic sulphidogenesis: isolation and characterization of *Thermodesulfobacterium commune* gen. Nov. and sp. nov. *Microbiology* 129, 1159–1169. doi: 10.1099/00221287-129-4-1159

Zheng, K., Ngo, P. D., Owens, V. L., Yang, X., and Mansoorabadi, S. O. (2016). The biosynthetic pathway of coenzyme F430 in methanogenic and methanotrophic archaea. *Science* 354, 339–342. doi: 10.1126/science.aag2947

Zhou, J., Bruns, M. A., and Tiedje, J. M. (1996). DNA recovery from soils of diverse composition. *Appl. Environ. Microbiol.* 62, 316–322. doi: 10.1128/aem.62.2.316-322.1996

Zhu, Q.-Z., Wegener, G., Hinrichs, K.-U., and Elvert, M. (2022). Activity of ancillary heterotrophic community members in anaerobic methane-oxidizing cultures. *Front. Microbiol.* 13, 1–12. doi: 10.3389/fmicb.2022.912299

frontiers | Frontiers in Microbiology

TYPE Original Research
PUBLISHED 17 November 2022
DOI 10.3389/fmicb.2022.960335

OPEN ACCESS

EDITED BY
S. Emil Ruff,
Marine Biological Laboratory (MBL),
United States

REVIEWED BY
Emma Bell,
Swiss Federal Institute of Technology
Lausanne, Switzerland
Lauren M. Seyler,
Stockton University, United States

*CORRESPONDENCE
Katrina I. Twing
katrinatwing@weber.edu

SPECIALTY SECTION
This article was submitted to
Extreme Microbiology,
a section of the journal
Frontiers in Microbiology

RECEIVED 02 June 2022
ACCEPTED 05 August 2022
PUBLISHED 17 November 2022

CITATION
Twing KI, Ward LM, Kane ZK, Sanders A, Price RE, Pendleton HL, Giovannelli D, Brazelton WJ and McGlynn SE (2022) Microbial ecology of a shallow alkaline hydrothermal vent: Strýtan Hydrothermal Field, Eyjafördur, northern Iceland.
Front. Microbiol. 13:960335.
doi: 10.3389/fmicb.2022.960335

Microbial ecology of a shallow alkaline hydrothermal vent: Strýtan Hydrothermal Field, Eyjafördur, northern Iceland

Katrina I. Twing[1,2]*, L. M. Ward[3,4], Zachary K. Kane[2], Alexa Sanders[2], Roy Edward Price[5], H. Lizethe Pendleton[1], Donato Giovannelli[3,6], William J. Brazelton[1] and Shawn E. McGlynn[3,7]

[1]School of Biological Sciences, The University of Utah, Salt Lake City, UT, United States, [2]Department of Microbiology, Weber State University, Ogden, UT, United States, [3]Earth-Life Science Institute, Tokyo Institute of Technology, Tokyo, Japan, [4]Department of Geosciences, Smith College, Northampton, MA, United States, [5]School of Marine and Atmospheric Sciences, Stony Brook University, Stony Brook, NY, United States, [6]Department of Biology, University of Naples "Federico II", Naples, Italy, [7]Center for Sustainable Resource Science, RIKEN, Saitama, Japan

Strýtan Hydrothermal Field (SHF) is a submarine system located in Eyjafördur in northern Iceland composed of two main vents: Big Strýtan and Arnarnesstrýtan. The vents are shallow, ranging from 16 to 70 m water depth, and vent high pH (up to 10.2), moderate temperature (T_{max} ~70°C), anoxic, fresh fluids elevated in dissolved silica, with slightly elevated concentrations of hydrogen and methane. In contrast to other alkaline hydrothermal vents, SHF is unique because it is hosted in basalt and therefore the high pH is not created by serpentinization. While previous studies have assessed the geology and geochemistry of this site, the microbial diversity of SHF has not been explored in detail. Here we present a microbial diversity survey of the actively venting fluids and chimneys from Big Strýtan and Arnarnesstrýtan, using 16S rRNA gene amplicon sequencing. Community members from the vent fluids are mostly aerobic heterotrophic bacteria; however, within the chimneys oxic, low oxygen, and anoxic habitats could be distinguished, where taxa putatively capable of acetogenesis, sulfur-cycling, and hydrogen metabolism were observed. Very few archaea were observed in the samples. The inhabitants of SHF are more similar to terrestrial hot spring samples than other marine sites. It has been hypothesized that life on Earth (and elsewhere in the solar system) could have originated in an alkaline hydrothermal system, however all other studied alkaline submarine hydrothermal systems to date are fueled by serpentinization. SHF adds to our understandings of hydrothermal vents in relationship to microbial diversity, evolution, and possibly the origin of life.

KEYWORDS

hydrothermal vent, alkaline, Iceland, microbial diversity, 16S rRNA

Introduction

Alkaline submarine hydrothermal vents have been proposed as potential sites for the origin of life on Earth (and potentially elsewhere in the solar system) because they promote strong proton and redox gradients and facilitate the abiotic synthesis of organic molecules (Russell, 2009; Russell et al., 2010; Price et al., 2017). Specifically, the geochemistry of these systems appears to provide a template for autotrophic metabolic pathways (McCollom and Seewald, 2007; Proskurowski et al., 2008; Hudson et al., 2020), such as the Wood-Ljungdahl pathway shared by methanogens, acetogens, and sulfate-reducers (Martin and Russell, 2007; Adam et al., 2018; Hudson et al., 2020), which may be one of the most ancient metabolic pathways (Ward and Shih, 2019). Previous work on submarine alkaline hydrothermal vents has focused on systems fueled by serpentinization, such as Lost City (Kelley et al., 2005; Lang and Brazelton, 2020; Brazelton et al., 2022), Prony (Monnin et al., 2014; Quéméneur et al., 2014; Postec et al., 2015), and Old City hydrothermal fields (Lecoeuvre et al., 2021). While incredibly valuable, these studies have left many open questions about how opportunities for microbial life may differ in alkaline hydrothermal vents with different geological bases.

Strýtan Hydrothermal Field (SHF), while highly alkaline, is not a serpentinizing system, providing a point of comparison to other alkaline sites. Fresh groundwater is heated, enriched in silica, and brought to high pH before venting into the bottom of the marine Eyjafördur. As the hydrothermal and surrounding marine waters mix, they precipitate magnesium silicate minerals which form chimneys rising up to 55 meters from the seafloor (**Figure 1**) and create steep sodium ion gradients. Harnessing energy as ion gradients across membranes is as universal as the genetic code (Lane and Martin, 2012). As a result, environments with these types of gradients may be important for considering the origin of life (Price et al., 2017); the Na^+ cell membrane pump is crucial for many ancient microbial lineages, including methanogens and acetogens, and is involved in adenosine triphosphate (ATP) synthesis and carbon assimilation in diverse organisms (Lane and Martin, 2012; Branscomb et al., 2017). Although not a focus of this study, it is fascinating to consider an energy source invoked in origin of life theory as possibly being operative in today's microbial communities.

Very little microbiological research has been conducted at SHF. In a study from 2001, researchers exploring vent fluids isolated Aquificales and Korarchaeota from clone libraries (Marteinsson et al., 2001b). However, a full census of microbial diversity at SHF has not been previously conducted. By characterizing the microbial diversity of vent fluids and mineral precipitates at SHF, we can better understand the ability of alkaline hydrothermal systems, and this unique site in particular, to support microbial communities and better constrain their potential roles in the origin of life.

Materials and methods

Sample collection

In August 2017, we performed a 7-day field-sampling campaign to SHF, where scientific SCUBA divers collected actively venting fluids from both Big Strýtan and Arnarnesstrýtan using 30 m of cleaned polypropylene tubing by swimming to the appropriate sampling location and holding the tubing inlet in the actively venting water. On the boat, the tubing was connected to two 12V inline electric galley pumps to pull water from the vent. During sample collection, pH and temperature were monitored to ensure the capture of vent fluids, rather than background seawater. Vent fluid samples for DNA analyses were collected in triple-rinsed 20 L carboys and background seawater samples were collected in sterilized 4 L carboys. A field station laboratory was established in the port dive shop, where collected fluid samples were filtered through 0.22 μm Sterivex cartridge filters (Millipore, MA, United States) using a peristaltic pump and flash-frozen in liquid N_2.

Hydrothermal vent chimney samples from Big Strýtan and Arnarnesstrýtan were collected by scientific divers by breaking off small (~15 cm × 5 cm) pieces into sterile Whirl-pak bags (Nasco, WI, United States). Back in the field-station laboratory, the chimney samples were subsampled into distinct chimney layers (**Supplementary Figures 1**, **2**) using a flame-sterilized scalpel, and these solid samples were immediately frozen in liquid N_2. All frozen filter and chimney samples were shipped back to the University of Utah in dry shippers and stored at −80°C until nucleic acid extraction.

DNA extraction

DNA was extracted from the Sterivex filter cartridges using a lab protocol previously developed for low-biomass alkaline fluid samples (Brazelton et al., 2022). Briefly, cell lysis was performed by alternating freeze/thaw cycles in an alkaline buffer, followed by purification with phenol-chloroform and precipitation with ethanol. Additionally, a laboratory extraction blank (ICEd062, **Supplementary Table 1**), consisting of a new Sterivex filter, was extracted alongside the fluid samples to track any potential laboratory contamination.

DNA was extracted from ~0.5 to 1.0 g of homogenized chimney samples using the MP Biomedical FastDNA Spin kit (CA, United States), per the manufacturer's instructions, with the exception of the use of a Mini-Beadbeater-16 (Biospec Products, OK, United States) in place of the recommended FastPrep Instrument. Technical replicates were pooled, to a total starting mass of 1.5–3.5 g per chimney sample, using an Amicon Ultra-2 Centrifugal Filter Unit with Ultracel-30 membrane (Millipore, Darmstadt, Germany). All DNA samples were purified

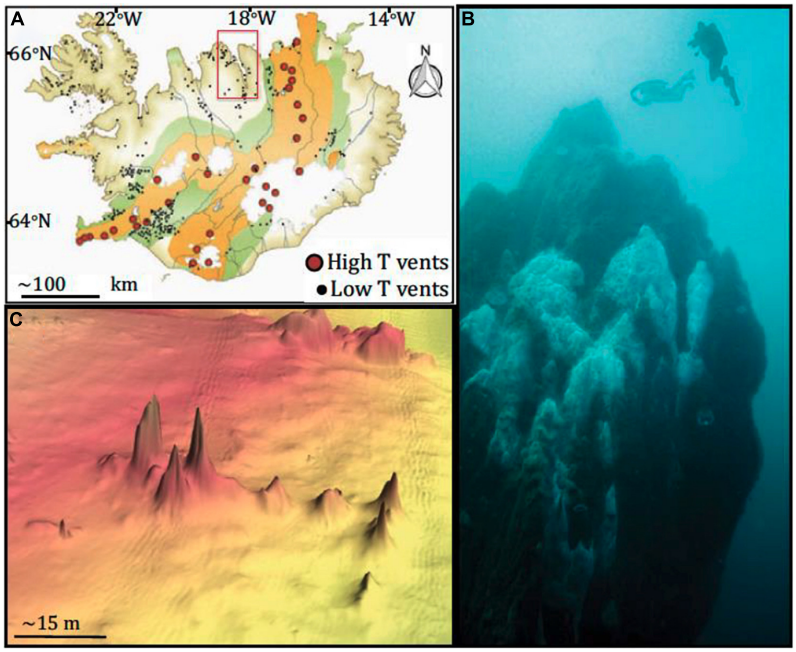

FIGURE 1
Map of sampling site and vents. **(A)** Map of Iceland, highlighting hydrothermal vents. Eyjafjördur, where Big Strýtan and Arnarnesstrýtan are located, is highlighted by the red box; **(B)** photograph of Big Strýtan chimney (courtesy of E. Bogason); **(C)** bathymetric map of Arnarnesstrýtan. Figure from Price et al. (2017). The figure is reprinted with permission under a Creative Commons CC-BY license.

using AMPure XP speedbeads (Rohland and Reich, 2012) and quantified via the Qubit high-sensitivity DNA assay (Invitrogen, CA, United States). A list of all DNA samples included in the study can be found in **Supplementary Table 1**.

16S rRNA sequencing and data analysis

DNA samples were submitted to the Michigan State University Research and Technology Support Facility Genomics Core for sequencing of the V4 region of the 16S rRNA gene on an Illumina MiSeq platform using the universal duel-indexed Illumina fusion primers 515F-806R (Kozich et al., 2013). Amplicon concentrations were normalized and pooled using an Invitrogen SequalPrep DNA Normalization Plate. After library quality control and quantitation, the pool was loaded on an Illumina MiSeq v2 flow cell and sequenced using a standard 500 cycle reagent kit. Base calling was performed by Illumina Real Time Analysis (RTA) software v1.18.54. Output of RTA was demultiplexed and converted to fastq files using Illumina Bcl2fastq v1.8.4.

16S rRNA gene amplicon sequences were processed with cutadapt v. 1.15 (Martin, 2011) and DADA2 v. 1.10.1 (Callahan et al., 2016), including quality trimming and filtering of reads, removal of chimeras, and inference of amplicon sequence variants (ASVs). Taxonomic classification of all ASVs was performed with DADA2 using the SILVA reference alignment (SSURef v138) and taxonomy outline (Pruesse et al., 2012) with the default minimum bootstrap value of 50 for taxonomic assignments (Callahan et al., 2016).

Quality control of sequence data was performed by removing putative contaminant sequences from the dataset. For vent fluid and background seawater samples, which were collected by filtration through Sterivex filters, a laboratory extraction blank (ICEd062; **Supplementary Table 1**) was sequenced and the 73 ASVs detected in that extraction blank were removed from the 8 vent fluid samples and 2 background seawater samples. Chimney samples were extracted via a DNA extraction kit, and 203 ASVs belonging to the genera outlined in Sheik et al. (2018) as putative kit contaminants were removed from the 12 chimney samples. A detailed list of all taxa removed from the dataset can be found in **Supplementary Table 2**. Additionally, any sequences classified to Domain "NA" or "Eukaryota" and all Bacteria classified as "Chloroplast" or "Mitochondria" were removed from the dataset.

After removing potential contaminant sequences, raw counts were converted to proportions to normalize for variations in sequencing depth among samples. The proportional abundances of all 872 unique ASVs among all seawater, vent fluid, and chimney samples were used to calculate the Morisita-Horn community dissimilarity between

each pair of samples. Similar results were obtained with other metrics of dissimilarity (e.g., Bray-Curtis, Sørensen). The multi-dimensional scaling (MDS) plot was generated from a table of ASV proportional abundances across all sample categories (vent fluids, chimneys, and background seawater) using the distance, ordinate, and plot_ordination commands in the R package phyloseq v.1.26.1 (McMurdie and Holmes, 2013). All sequence data is available in the NCBI Sequence Read Archive (SRA) under BioProject PRJNA861241.

Comparison to other high pH vents

We cross-referenced the taxa detected in previous studies of alkaline submarine vents (Quéméneur et al., 2014; Postec et al., 2015; Lecoeuvre et al., 2021; Brazelton et al., 2022) and alkaline hot springs (Reysenbach et al., 1994; Marteinsson et al., 2001a; Blank et al., 2002; Nakagawa and Fukui, 2003; Purcell et al., 2007; Boomer et al., 2009; Meyer-Dombard et al., 2011; Tobler and Benning, 2011; Meyer-Dombard and Amend, 2014; López-López et al., 2015; Martinez et al., 2019) with the abundant (>1% of any sample) taxa detected in this study (**Supplementary Table 3**). For studies conducted with clone-libraries, we included all reported taxa (Reysenbach et al., 1994; Marteinsson et al., 2001a; Blank et al., 2002; Nakagawa and Fukui, 2003; Purcell et al., 2007; Boomer et al., 2009; Meyer-Dombard et al., 2011; Tobler and Benning, 2011; Meyer-Dombard and Amend, 2014; Quéméneur et al., 2014; Postec et al., 2015), while for studies conducted with amplicon and/or metagenomic sequencing, we included taxa representing a relative abundance of >1% of any sample (López-López et al., 2015; Martinez et al., 2019; Lecoeuvre et al., 2021; Brazelton et al., 2022). Similarities between phylum through genus for Archaeon and class through genus for Bacteria were included with the lowest common taxonomic level reported in **Supplementary Table 3**.

Additionally, the only previous microbiological study of SHF was published in 2001 (Marteinsson et al., 2001b) using Sanger sequencing of clone libraries. Given that microbial taxonomy is ever evolving, in order to compare the taxonomy of these previously detected microorganisms to our current data, we classified the sequences reported in Marteinsson et al. (2001a) by searching them against the current (November 2021) NCBI nr database using the BLASTn function (Altschul et al., 1990). Data originally reported in Marteinsson et al. (2001a) and the updated taxonomic assignments can be found in **Supplementary Table 4**.

Aqueous geochemistry

Fluid samples were collected directly from the tubes through which microbial samples were taken. Temperature was measured *in situ* with a Thermo Fisher Scientific temperature probe in an underwater housing constructed at the Max Planck Institute for Marine Microbiology. pH was measured in the field just after surfacing from each dive using a Hanna HALO Bluetooth pH meter with temperature compensation. Samples for major anion concentrations were preserved in the field by 0.2 μm syringe filtered into acid washed HDPE Nalgene® bottles and frozen until analysis. Analyses were performed in the Wehrmann Biogeochemistry Laboratory, School of Marine and Atmospheric Sciences, Stony Brook University using a Metrohm 930 compact ion chromatograph with matrix elimination. Samples for major cation concentrations were preserved in the field by 0.2 μm syringe filtered into acid washed HDPE Nalgene® bottles, acidified to 0.1% acid with ultrapure nitric acid, and frozen until analysis. Analyses were performed in the Black Paleooceanography Laboratory, School of Marine and Atmospheric Sciences, Stony Brook University using a Horiba Ultima 2C inductively coupled plasma–optical emission spectrometer (ICP-OES).

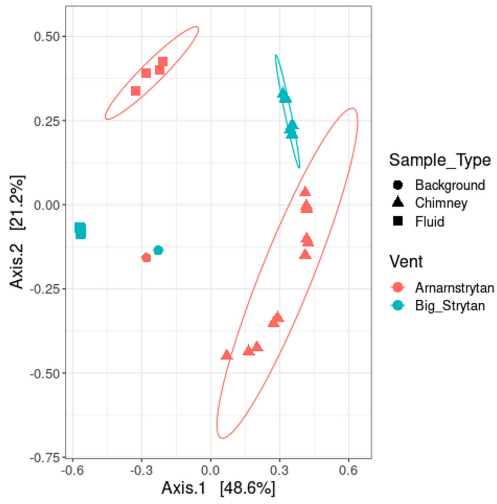

FIGURE 2
Distinct microbial communities between sample types (background seawater, chimney, and vent fluids) and different vents (Big Strýtan, pink; Arnarnesstrýtan, teal). Multi-dimensional scaling plot of community dissimilarity, calculated with the Morisita-Horn dissimilarity index.

Results

Geochemistry of Strýtan Hydrothermal Field

Strýtan Hydrothermal Field is located in Eyjafördur in northern Iceland and consists of two main vent sites: Big Strýtan and Arnarnesstrýtan (**Figure 1**). Each site

TABLE 1 Geochemical parameters measured at Strýtan hydrothermal field.

	Background seawater	Big Strýtan	Arnarnesstrýtan
Date	28 August 2017	31 August 2017	27 August 2017
pH	8.0	10.2	9.4
SO_4 (mM)	27.3	0.1	1.2
H_2S (μM)	n.d.	28.0	10.9
Cl (mM)	530.0	1.3	21.6
Br (μM)	795.3	2.3	36.5
Na (mM)	412.4	4.1	15.2
Ca (mM)	9.9	0.08	0.82
K (mM)	9.12	0.04	0.25
Mg (mM)	49.5	0.1	1.0
Si (mM)	0	1.5	1.3
Fe (μM)	n.d.	1.8	0.32
Sr (μM)	86.0	0.4	3.1

n.d., no data.

consists of several large (up to 55 m tall) chimneys in shallow water (<60 m depth) composed of saponite, a magnesium silicate material with basaltic host rock (Geptner et al., 2002; Price et al., 2017). The chimneys vent pH 10.2 freshwater that is enriched in dissolved silicate and slightly elevated in H_2 (0.1–5.2 μM) and methane (0.5–1.4 μM) (Price et al., 2017). In contrast to other alkaline hydrothermal vents, the Strýtan Hydrothermal Field is hosted in basalt and therefore the high pH is not created by serpentinization but rather a combination of (1) plagioclase hydrolysis, coupled with calcite precipitation, and (2) hydration of Mg in pyroxene and olivine in basalt (Geptner et al., 2002; Price et al., 2017). SHF vent fluids are sourced in groundwater, and the steep sodium ion gradients from the fluids at SHF (from <3 to 468 mM), may be important for understanding processes involved in the origin of life (Lane and Martin, 2012; Price et al., 2017).

Five types of samples were collected during our expedition: (1) vent fluids from Big Strýtan vent, (2) chimney samples from Big Strýtan vent, (3) vent fluids from Arnarnesstrýtan vent, (4) chimney samples from Arnarnesstrýtan vent, and (5) background seawater samples, each of which harbored distinct microbial communities (**Figure 2**). The chimney samples from the two vents, while distinct from one another, were more similar to each other than to any of the fluid samples and all the vent and chimney samples were distinct from the background seawater (**Figure 2**).

The background seawater sample exhibited chemical characteristics typical of seawater (e.g., pH 8, mM concentrations of ions; **Table 1**; Pinet, 2019). The chemistry of the vent fluids from Big Strýtan and Arnarnesstrýtan were similar, with high pH (~10) and generally low in dissolved ions. This is in agreement with previous studies (Marteinsson et al., 2001b; Price et al., 2017). The sample from Arnarnesstrýtan had slightly higher dissolved ions, likely as a result of mixing with seawater, either deeper in the hydrothermal edifice or during sampling. Of particular interest, H_2S and Fe were slightly elevated in the vent fluids relative to seawater. While the relative contributions to the H_2S content of microbial SO_4^{2-} reduction and mobilization from subsurface basalts during water-rock reactions has not been confirmed, the abundance of known dissimilatory sulfate reducing microorganisms in the vent fluids (such as Thermodesulfovibrionales, e.g., Sekiguchi et al., 2008; **Figure 3**) does suggests a role for biological sulfur cycling.

Microbial community of Big Strýtan vent

The microbial communities between background seawater, vent fluids, and chimney material from the Big Strýtan site are distinct (**Figure 3**). Vent fluids from Big Strýtan were dominated by members of the orders Alteromonadales (29.6%), Pseudomonadales (19.1%), Flavobacteriales (14.9%), Saccharimonadales (6.4%), Caulobacterales (6.0%), and Thermodesulfovibrionales (5%; **Figure 3**). Two of the three most abundant ASVs in Big Strýtan vent fluids both belonged to the genus *Pseudoalteromonas* within the class Alteromonadales. The best hit for ASV sq4, which made up 18–21% of the vent fluid community, was *Pseudoalteromonas carrageenovora*, isolated from extremely deep marine sediments from the Challenger Deep (Chen et al., 2021; **Table 2**). ASV sq11, classified as *Pseudoalteromonas* and comprising 5–7% of the vent fluids, had a best hit from a recently formed, circumneutral hydrothermal vent (García-Davis et al., 2021; **Table 2**). There were five ASVs belonging to the Pseudomonadales in Big Strýtan vent fluids (**Supplementary Table 3**). The third most abundant ASV in Big Strýtan vent fluids was sq31 (7.8%), which was classified as *Acinetobacter* sp. and has 100% similarity to a sequence from a subsurface aquifer (**Table 2**; Espín et al., 2020). Two other ASVs belonging to the Pseudomonadales were classified at least the genus level and their best hits were also from hydrothermal vents: ASV sq63 (3.3%) is 100% similar to *Psychrobacter* sp. found at the recently formed vent referenced above (García-Davis et al., 2021) and ASV sq113 (2.2%) is 99.6% similar to *Acinetobacter johnsonii* (unpublished; **Supplementary Table 3**). The two ASVs of *Flavobacterium* spp. had best hits that originated in Arctic sediments (*F. petrolei*, Chaudhary et al., 2019) or volcanic soil samples (*F. degerlachei*, Zeglin et al., 2016; **Supplementary Table 3**). Two ASVs (sq28, sq112) classified as *Thermodesulfovibrio* were close matches to sequences found in terrestrial alkaline hot spring samples

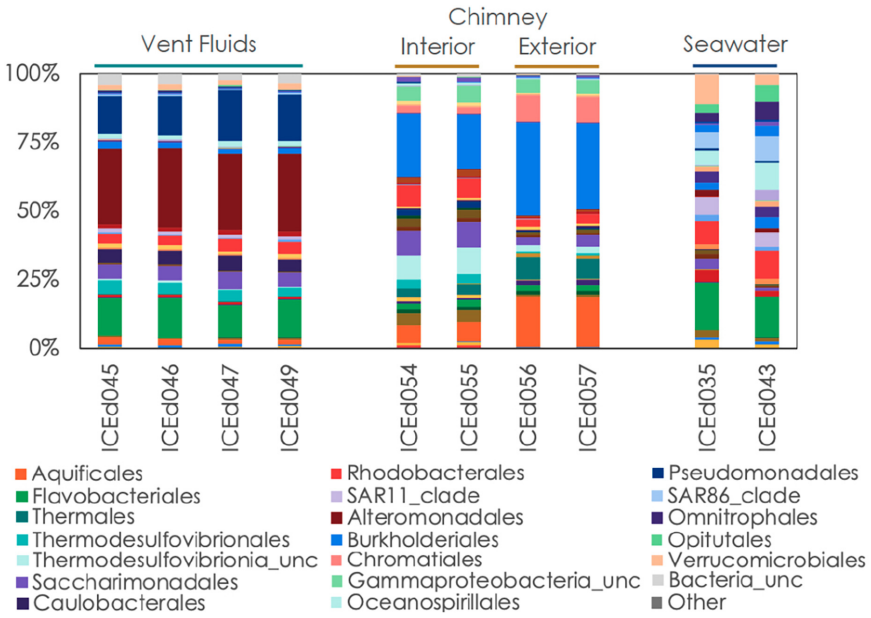

FIGURE 3
Relative abundance of microbial communities in Big Strýtan vent fluids, chimneys, and background seawater at the order level.

TABLE 2 Abundant (>5%) ASVs in big Strýtan vent fluid and chimney samples.

ASV	Best hit			Max abundance (%)			
	% Identity	Environment	Accession number	Fluid	Chimney		Background seawater
					Interior	Exterior	
sq4_Pseudoalteromonas	100	Deep-sea sediments	MW926624[1]	21	0.2	0.01	0.2
sq11_ Pseudoalteromonas	100	Hydrothermal vent	MW826701[2]	7.3	0.1	0.002	0.1
sq31_Acinetobacter	100	Subsurface aquifer	MT941733[3]	7.8	0.08	0	0.01
sq2_Sutterellaceae	99.6	Hot spring	LK936281[4]	0.07	16.6	25.6	0.01
sq3_Thermocrinis	98.8	Hot spring, Iceland	AF361217[5]	0.07	6.3	17.4	0
sq16_Thermodesulfovibrionia	95.7	Hot spring	FJ206245[6]	0	6.7	2.5	0
sq17_Candidatus_Thiobios	99.6	Marine sediments	FM242256[7]	0.03	2.2	9.6	0

[1]Chen et al. (2021). [2]García-Davis et al. (2021). [3]Espín et al. (2020). [4]Anda et al. (2014). [5]Marteinsson et al. (2001b). [6]Boomer et al. (2009). [7]Païssé et al. (2010).

from Iceland (Marteinsson et al., 2001a). While the orders Saccharimonadales and Caulobacterales made up 6.4 and 6.0% of the vent fluids, respectively (Figure 3), no individual ASV belonging to these orders was >1% of any sample.

We subsampled a piece of chimney from Big Strýtan into interior and exterior sections for microbial analyses (Supplementary Figure 1). The interior of the Big Strýtan chimney samples, which were in direct contact with actively venting fluids, were dominated by members of the Burkholderiales (22.1%), Thermodesulfovibrionales (9.1%), Saccharimonadales (8.9%), Rhodobacteriales (7.4%), and Aquificales (6.8%) (Figure 3). The exterior of the chimney samples, which were in contact with surrounding seawater, were dominated by Burkholderiales (33.4%), Aquificales (18.2%), and Chromatiales (9.7%) (Figure 3). The most abundant ASV was sq2_Sutterellaceae (Burkholderiales), which accounted for 16.6% of the inner layers and 25.6% of the outer layers of the chimney (Table 2) and had a best hit match from a circumneutral hot spring in Hungary (Anda et al., 2014). ASV sq3, identified as *Thermocrinis albus* (Aquificales) and first isolated from Hvergerthi in Iceland (Eder and Huber, 2002), was 6.3% and 17.4% of the interior and exterior of Big Strýtan chimney samples, respectively. ASV sq16 was classified to the class Thermodesulfovibrionia and was only 95.7% similar to the best hit match in the NCBI SRA database, which was a sequence from an alkaline spring at Yellowstone National Park

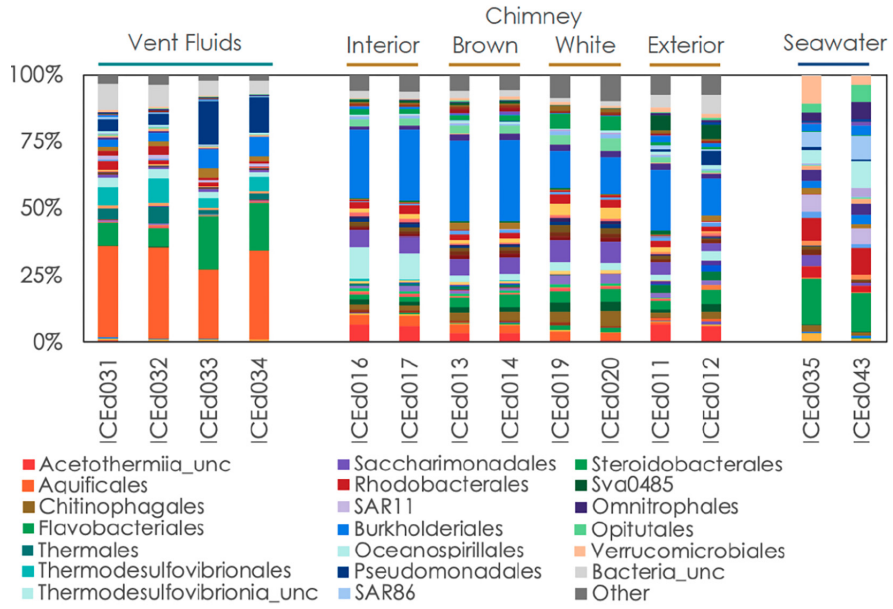

FIGURE 4
Relative abundance of microbial communities in Arnarnesstrýtan vent fluids, chimneys, and seawater at the order level.

(Boomer et al., 2009; **Table 2**). Finally, ASV sq17, comprising 9.6% of the exterior chimney, was classified as Candidatus *Thiobios* (Chromatiales) and had a best hit to a sequence from marine sediments (**Table 2**).

The background seawater samples, which were collected on two separate dives (**Supplementary Table 1**) shared marked similarities in their community composition and were dominated by members of the Flavobacteriales (17.4%), Rhodobacterales (10.4%), Verrucomicrobiales (10.7%), Oceanospirillales (10.3%), SAR86 (9.5%), Opitutales (6.6%), Omnitrophales (6.6%), and SAR11 (6.5%) (**Figures 3**, **4**). It is important to note that the genera within these orders were distinct from members found in the vent or chimney samples (**Supplementary Table 3**).

Microbial community of Arnarnesstrýtan vent

Even at the order level of taxonomy, distinct communities were observed in Arnarnesstrýtan vent fluids, chimney samples, and background seawater (**Figure 4**). Vent fluids from Arnarnesstrýtan were dominated by members of the orders Aquificales (33.9%), Flavobacteriales (19.5%), Pseudomonadales (16.3%), Thermodesulfovibrionales (9%), Burkholderiales (7.5%), and Thermales (6.4%), as well as a significant proportion of unclassified Bacteria (9.7%) (**Figure 4**). There were six ASVs belonging to the Aquificales, two of which were "uncultured" *Thermocrinis* sp. and four classified as *Thermocrinis albus* (**Table 3**). The best hits of all six sequences were from previous studies conducted in alkaline Icelandic hot springs (Marteinsson et al., 2001a; Wirth et al., 2010; Tobler and Benning, 2011), though not specifically at SHF. Three ASVs of *Flavobacterium* spp. all had best hits that originated in Arctic sediments (*F. petrolei*, Chaudhary et al., 2019) or thawing permafrost samples (*F. psychrolimnae*, Aszalós et al., 2020 and *F. degerlachei*, Zeglin et al., 2016) (**Table 3** and **Supplementary Table 3**). *Pseudomonas extremaustralis* (sq55) was also detected in Arnarnesstrýtan vent fluids and has previously been observed in other alkaline hot springs (**Table 3**; Wang and Pecoraro, 2021). Furthermore, this ASV (Sq55_Pseduomonas) was not detected in background seawater samples. There were two ASVs of *Thermodesulfovibrio* (sq28, sq60), both of which were previously detected in alkaline hot springs in Iceland (Marteinsson et al., 2001a; **Supplementary Table 3**). ASV sq14 was classified as *Thermus islandicus* and was 100% similar to the type strain, isolated from a hot spring in southern Iceland (Bjornsdottir et al., 2009).

The Arnarnesstrýtan chimney exhibited distinct color zones and was subsampled to assess the microbial diversity of each zone independently (**Supplementary Figure 2**). The interior-most zone (gray) was in direct contact with venting fluids and expected to be a more anoxic environment than the exterior-most zone (yellow), which was in direct contact with the surrounding seawater (**Supplementary Figure 2**). The interior Arnarnesstrýtan chimney samples were dominated by members of the Burkholderiales (25.9%),

Thermodesulfovibrionia (11.6%), Acetothermiia (6.5%), and Saccharimonadales (5.8%) (Figure 4). Meanwhile, the exterior Arnarnesstrýtan chimney samples were dominated by Burkholderiales (13.7%), Acetothermiia (6.5%), Sva0485 (5.4%), and Pseudomonadales (5.0%) (Figure 4). Similar to the vent fluids, there was a significant proportion of unclassified Bacteria (7%) found in Arnarnesstrýtan chimney samples (Figure 4). Five ASVs from the class Burkholderiales were detected in the chimney samples. The most abundant was ASV sq2_Sutterellaceae, which accounted for 10–20% of the inner layers and 2–3% of the outer layers of the chimney (Table 3). ASV sq66 was identified as *Hydrogenophaga* and was abundant in the exterior layers (white, yellow; Supplementary Table 3). ASV sq7_Hydrogenophilaceae was detected at high abundance (4–7%) in all layers of the chimney sample (Table 3). *Thermodesulfovibrio* spp. were detected in Arnarnesstrýtan vent fluids and in the inner most chimney sample there were three ASVs of unclassified Thermodesulfovibrionia (same Class) that accounted for 7–10% of the replicate samples (Figure 4 and Table 3). Two of those ASVs (sq16, sq134) had sequence similarity of 95% with their closest BLAST hits, both of which were from an alkaline hot spring in Yellowstone National Park (Boomer et al., 2009; Supplementary Table 3). There were two ASVs identified as uncultured Acetothermiia. ASV sq32 was most abundant (4.5%) in the interior layer, while ASV sq41, the closest BLAST hit of which is also from alkaline vents in Iceland (Tobler and Benning, 2011), was abundant (5.9%) in the exterior layer of the chimney (Table 3 and Supplementary Table 3). Finally, an ASV classified as Sva0485 (phylum) was 6% of the exterior (yellow) layer and found in other studies looking at microbialite formation (Table 3; Corman et al., 2016; Couradeau et al., 2017). While the orders Saccharimonadales and Pseudomonadales made up 5.8 and 5.0% of the chimney samples, respectively (Figure 4), no individual ASV belonging to these orders was >1% of any sample. Only one ASV belonging to the domain Archaea accounted for >1% of any sample in the study. This was ASV sq175_Candidatus *Nitrosopumilus*, present in exterior Arnarnesstrýtan chimneys (Supplementary Table 3).

Discussion

Microbial ecology of Strýtan Hydrothermal Field

The vent fluids from both Big Strýtan and Arnarnesstrýtan contain an abundance of *Flavobacterium*, *Pseudoalteromonas*, *Psychrobacter*, *Acinetobacter*, and *Pseudomonas* species (Tables 2, 3 and Supplementary Table 3). Type strain members of these genera are all aerobic, heterotrophic bacteria (Akagawa-Matsushita et al., 1992; Bozal et al., 2003; Van Trappen et al., 2004, 2005; Chaudhary et al., 2019), with the exception of *Pseudomonas extremaustralis*, which is capable of nitrate-reduction (López et al., 2009, 2017). Interestingly, almost all of the species detected exclusively in vent fluids are also found in Arctic and Antarctic samples (Bozal et al., 2003; Van Trappen et al., 2004, 2005; López et al., 2009; Chaudhary et al., 2019). None of these ASVs were detected in background seawater samples, so it is unlikely that the

TABLE 3 Abundant (>5%) in Arnarnesstrýtan vent fluid and chimney samples.

ASV	Best hit			Max abundance (%)			
	% Identity	Environment	Accession number	Fluid	Chimney		Background seawater
					Interior	Exterior	
sq3_Thermocrinis	98.8	Hot spring, Iceland	AF361217[1]	7.9	0.2	0.8	0
sq15_Thermocrinis	99.6	Hot spring, Iceland	GU233821[2]	8.9	0.007	0.009	0
sq20_Thermocrinis	99.2	Hot spring, Iceland	AF361217[1]	8.7	0.007	0.006	0
sq14_Thermus	100	Hot spring, Iceland	NR_116442[3]	6.3	0.3	0	0
sq18_Flavobacterium	100	Arctic sediment	NR_169457[4]	12.5	0	0	0.02
sq55_Pseudomonas	100	Alkaline hot spring	MZ497311[5]	5.4	0	0	0
sq2_Sutterellaceae	99.6	Hot spring	LK936281[6]	0.6	24.0	2.5	0.01
sq7_Hydrogenophilaceae	100	Microbialites	JQ766812[7]	0	6.7	8.0	0
sq13_Thermodesulfovibrionia	99.2	Hot spring	LC422496[8]	0.002	7.9	0.1	0
sq39_Rhodocyclaceae	99.6	Deep gold mine	EF205275[9]	0.004	1.6	9.6	0
sq41_Acetothermiia	100	Hot spring, Iceland	GU233848[2]	0.3	1.8	5.9	0
sq69_Sva0485	99.2	Microbialites	KP589170[10]	0	0.8	6.1	0

[1] Marteinsson et al. (2001b). [2] Tobler and Benning (2011). [3] Bjornsdottir et al. (2009). [4] Chaudhary et al. (2019). [5] Wang and Pecoraro (2021). [6] Anda et al. (2014). [7] Couradeau et al. (2017). [8] Shiraishi et al. (2019). [9] Onstott et al. (2009). [10] Corman et al. (2016).

samples were "contaminated" by seawater. Instead, the vent fluid samples from Big Strýtan and Arnarnesstrýtan represent a mixing zone within the chimney, where deeply sourced hydrothermal fluids, enriched in H_2, CH_4, and H_2S, come into contact with oxygenated seawater, creating a niche habitat for aerobic to microaerophilic organisms capable of H_2 and H_2S-oxidation.

Two ASVs were abundant in both vent fluids from Arnarnesstrýtan and exterior chimney samples from Big Strýtan, but not detected in the other samples. These belonged to *Thermus islandicus* (sq14) and *Thermocrinis albus* (sq3; **Tables 2**, **3** and **Supplementary Table 3**). Additional ASVs of *Thermocrinis albus* (sq15, sq20) were detected only in Arnarnesstrýtan vent fluids (**Supplementary Table 3**). The best hit matches for these four ASVs all originally come from alkaline geothermal vents in Iceland (Marteinsson et al., 2001a; Tobler and Benning, 2011). *Thermus islandicus* is a microaerophilic, mixotrophic, sulfur-oxidizer, originally isolated from a pH 6 hot spring in southern Iceland (Bjornsdottir et al., 2009). *Thermocrinis albus* belongs to the phylum Aquificota and is a microaerophilic chemolithoautotroph that uses the reverse-TCA cycle and is able to utilize H_2, S^0, and thiosulfate as electron donors (Eder and Huber, 2002; Hügler et al., 2007; Wirth et al., 2010). These microaerophilic, sulfur-oxidizing organisms, are likely inhabiting an oxic/anoxic mixing zone within Arnarnesstrýtan fluids and a low-oxygen cavity within the exterior of the Big Strýtan chimney. The chemistry of the fluids suggest that seawater was entrained slightly more for Arnarnesstrýtan compared to Big Strýtan. It is possible that this occurred prior to sampling, deeper within the chimney edifice. If true, then the entire edifice might have elevated O_2 concentrations from seawater, which would help explain the presence of more aerobic metabolisms in Arnarnesstrýtan fluids compared to Big Strýtan.

Taxa with putatively diverse metabolisms were detected within the chimney samples from both vents. Interior chimney samples from both Big Strýtan and Arnarnesstrýtan had an abundance of Thermodesulfovibrionia (sq13, sq16, sq84, sq110, sq117, and sq134) and Sutterellaceae (sq2, sq38, sq78, sq87, sq92, and sq146; **Tables 2**, **3** and **Supplementary Table 3**). Members of both these groups are anaerobes and Thermodesulfovibrionia are capable of nitrate- and sulfate-reduction (Morotomi, 2014; Arshad et al., 2017; Umezawa et al., 2021). The exterior chimney samples from both vents contained Acetothermia (sq41; **Table 3** and **Supplementary Table 3**), a phylum that is also referred to OP1 and Bipolaricaulota in the literature. Genomes of Acetothermia contain the complete Wood-Ljungdahl pathway, allowing for potential acetogenesis in these samples (Youssef et al., 2019). Various taxa putatively capable of carbon-fixation *via* the Calvin-Bassam-Benson cycle were detected in exterior samples from Big Strýtan (Ca. *Thiobios*) and Arnarnesstrýtan (Hydrogenophilaceae, *Hydrogenophaga*) chimney (**Tables 2**, **3** and **Supplementary Table 3**; Willems et al., 1989; Rinke et al., 2009; Orlygsson and Kristjansson, 2014). The apparent transition from Wood-Ljungdahl dominated autotrophy in interior samples to CBB-driven carbon fixation in the exterior may reflect the different sensitivities of these pathways to O_2 concentration (e.g., Berg, 2011) across the chimney/seawater boundary. Additionally, the sulfate-reducing Ca. *Desulforudis* (sq149) was detected in exterior Arnarnesstrýtan chimney samples (Chivian et al., 2008). This organism has previously been shown to be capable of carbon fixation *via* the O_2-sensitive Wood-Ljungdahl pathway (Karnachuk et al., 2019), suggesting low-oxygen conditions extended into at least some distal regions of the chimney interior. Interestingly, no phototrophic bacteria were detected, even in exterior chimney samples, despite the shallow water depth.

TABLE 4 Comparison of geology and geochemistry of submarine alkaline vents.

	Strýtan HF[1]	Prony HF[2,3]	Lost City HF[4]	Old city HF[5]
pH	10.2	10.6	11	7.88–8.18
Temp (C)	70	40	90	Not reported
(H_2)	0.30–5.19 μM	6.4 mM	1–15 mM	Not reported
(CH_4)	0.46–1.41 μM	8.0 mM	1–2 mM	Not reported
Water depth (m)	20–60	16–47	700–900	3,100
Host rock	Basalt	Ultramafic	Ultramafic	Ultramafic
Water source	Meteoric	Meteoric	Marine	Marine
Cone material	$MgSiO_2$	$CaCO_3$	$CaCO_3$	$CaCO_3$
Serpentinization	No	Yes	Yes	Yes

[1]Price et al. (2017). [2]Postec et al. (2015). [3]Quéméneur et al. (2014). [4]Kelley et al. (2005). [5]Lecoeuvre et al. (2021).

Our subsampling of the chimney samples (**Supplementary Figures 1**, **2**) have allowed for us to distinguish oxic, low oxygen, and anoxic habitats within the chimneys. The inferred metabolisms suggest that O_2 and perhaps SO_4^{2-} are important electron acceptors, along with NO_3^{2-}, whereas H_2 and H_2S may be the most important electron donors. It appears that sulfur metabolisms may play a crucial role. With the observation that O_2 and SO_4^{2-} may be entrained deeper within the system, H_2S observed in the vent fluids may be produced by SO_4 (or thiosulfate) reduction with H_2. Support for this observation comes from Rucker et al. (2022), who conducted thermodynamic calculations of Gibbs free energy to evaluate the highest energy yielding reactions as a proxy for microbial metabolism. The most energetically favorable reactions in all mixing schemes for Strýtan includes CO_2 or O_2 reduction with H_2, or O_2 reduction with H_2S oxidation. Numerous NO_3^- reduction reactions are also favorable, and NO_3^- reduction

with H_2S oxidation is among the "top five most" energetically yielding reactions.

As noted above, the only previous microbiological study conducted at SHF was published in 2001 and used cultivation-dependent and clone library methodologies (Marteinsson et al., 2001b). Of the ~100 bacteria described in Marteinsson et al. (2001b), accession numbers were only available for eight of them. To compare the taxonomy of those eight sequences from 2001 to our current dataset, we performed a BLASTn search of the sequences against the current (Nov. 2021) NCBI SRA database (**Supplementary Table 4**). Most notable is the presence of *Thermocrinis albus* (referred to as Aquificales in Marteinsson et al., 2001b), which dominated clone-libraries in the 2001 study and accounted for 19 and 34% of the amplicon libraries from Big Strýtan chimney and Arnarnesstrýtan vent fluids, respectively, in the present study (**Supplementary Table 3**, **4**). We similarly detected members of the Actinobacteriota, Nitrospirota, Caulobacteraceae, and Burkholderiales at SHF (Marteinsson et al., 2001b).

It should be noted that 16S rRNA derived discussion of metabolic capacity may not accurately represent what is happening in the natural environment. Future study of metagenomic and metranscriptomic data from this site will help clarify the metabolic strategies employed at SHF and the current work is a first insight.

Comparison of Strýtan Hydrothermal Field to other alkaline hydrothermal vent sites

To put the unique nature of Strýtan Hydrothermal Field into context, we compared the microbial composition reported here to the two most similar ecosystem classes–alkaline submarine hydrothermal vents and alkaline terrestrial hot springs. Aside from SHF, the only other studied alkaline submarine hydrothermal vents are hosted in ultramafic rocks, rather than basalt, and are fueled by serpentinization, which creates high pH and millimolar concentrations of hydrogen and methane (**Table 4**). Prony hydrothermal field (PHF), located in New Caledonia is a shallow vent (16–47 m) where freshwater fluids influenced by serpentinization mix with seawater (**Table 4**; Quéméneur et al., 2014; Postec et al., 2015). The Lost City and Old City hydrothermal fields, also fueled by serpentinization, are much deeper (700–900 m and 3,100 m, respectively) and the source water for the vents is marine, rather than freshwater (**Table 4**; Kelley et al., 2005; Lecoeuvre et al., 2021). While elevated compared to seawater, the H_2 and CH_4 concentrations at SHF are in the micromolar range and therefore not as elevated as is found at serpentinite-hosted sites (**Table 4**). Therefore, high pH is the strongest geochemical

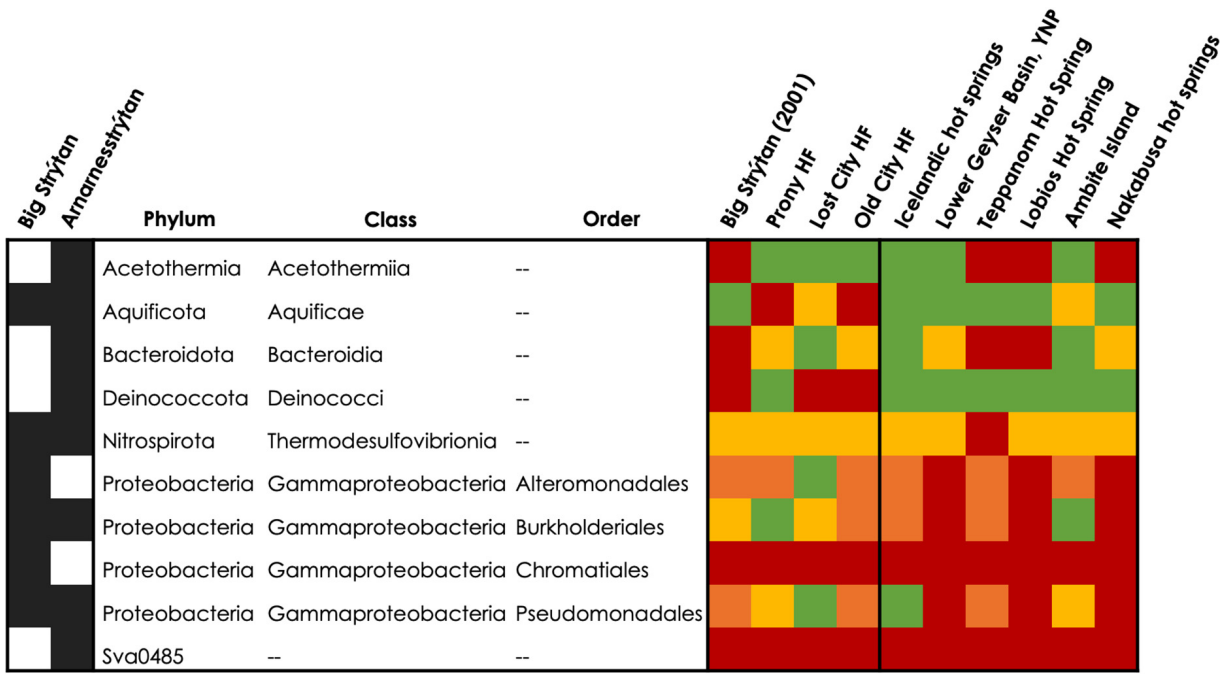

FIGURE 5
Detection of abundant taxa from SHF at other alkaline submarine hydrothermal vents and hot springs. Abundant ASVs (>5%) are listed at the class level, or order level for Proteobacteria. In the heatmap, the colors represent: red = not present, orange = phylum present (or class for Proteobacteria), yellow = class present (or order for Proteobacteria), and green = detected at a lower taxonomic level or the same level as in the current study. Additional details about these abundant ASV's can be found in **Tables 2**, **3** and **Supplementary Table 3**.

similarity between SHF and serpentinite-hosted hydrothermal vents.

Similarities between phylum through genus for the single observed Archeon and class through genus for Bacteria were included with the lowest common taxonomic level reported in **Supplementary Table 3**, with the closest matches highlighted in bright colors and higher (more distant) matches in faint colors. Commonalities between PHF and SHF include Acetothermia, *Thermus*, and Rhodocyclaceae (Gammaproteobacteria), as well as an unclassified bacterium, with 99% sequence similarity. Lost City and Old City hydrothermal fields shared Nitrosopumilaceae, Acetothermia, Thermodesulfovibrionia, Thiomicrospiraceaea, and various families belonging to the Bacteroidota and Gammaproteobacteria within SHF (**Figure 5** and **Supplementary Table 3**). Notably, *Flavobacterium* and *Thermocrinis* abundant in SHF were absent in other alkaline submarine systems.

Our BLASTn results of abundant (>5%) ASVs indicate that the inhabitants of SHF are actually more similar to terrestrial hot spring samples than to marine sites (**Tables 2**, **3**). Therefore, we additionally compared our diversity data to alkaline terrestrial hot springs (**Table 5** and **Figure 5** and **Supplementary Table 3**), such as Lower Geyser Basin, Yellowstone National Park, United States, Teppanom Hot Spring in Thailand, Lobios Hot Spring, Spain, Ambitle Island in Papua New Guinea, Nakabusa Hot Springs, Japan, and geothermal springs from southern Iceland. Notably, SHF has a higher pH than these sites (with the exception of other Icelandic sites) and a potentially high energy mixing zone where geothermal waters come into contact with oxygenated seawater (**Table 5**).

Thermocrinis and *Thermus* are two hallmark genera of terrestrial hot spring systems and were detected in most of the hot spring sites compared here (**Figure 5** and **Supplementary Table 3**; Reysenbach et al., 1994; Blank et al., 2002; Nakagawa and Fukui, 2002, 2003; Purcell et al., 2007; Boomer et al., 2009; Meyer-Dombard et al., 2011; Meyer-Dombard and Amend, 2014; López-López et al., 2015; Nishihara et al., 2018; Martinez et al., 2019). However the exact species detected at SHF, *Thermocrinis albus* and *Thermus islandicus*, were only previously found in other hot springs in Iceland (**Figure 5** and **Supplementary Table 3**; Marteinsson et al., 2001a; Tobler and Benning, 2011). Additional taxa that were found in terrestrial hot springs and SHF include the Nitrosopumilus, Acetothermia, Thermodesulfovibrionia, and Desulfobacteriota. Abundant taxa that are unique to SHF, compared to alkaline submarine and terrestrial geothermal systems, include Thermoanaerobaculaceae, Hydrogenispora, *Hydrogenophaga*, Sutterellaceae, Ca. *Alysiosphaera*, Ca. *Thiobios*, SAR324, and Sva0485 (**Figure 5** and **Supplementary Table 3**).

TABLE 5 Comparison geochemistry of SHF and terrestrial hot spring sites.

	Geographic location	pH	Temp °(C)
Strýtan HF[1,2]	Iceland	10.2	70
Icelandic hot springs[3]	Iceland	9–10	70–90
Lower geyser basin[4,5,6,7]	Yellowstone NP, United States	8–9.5	70–90
Teppanom hot spring[8]	Thailand	9	89
Lobios hot spring[9]	Spain	8.2	76
Ambitle Island[10]	Papua New Guinea	8.5	93.5
Nakabusa hot springs[11,12]	Japan	8.9	72–80

[1]This Study. [2]Price et al. (2017). [3]Tobler and Benning (2011). [4]Reysenbach et al. (1994). [5]Blank et al. (2002). [6]Boomer et al. (2009). [7]Meyer-Dombard et al. (2011). [8]Purcell et al. (2007). [9]López-López et al. (2015). [10]Meyer-Dombard and Amend (2014). [11]Nakagawa and Fukui (2003). [12]Nishihara et al. (2018).

Conclusion

Strýtan Hydrothermal Field is a unique site, both geochemically and microbiologically. Close relatives to sequences found here have been described in submarine hydrothermal vents, terrestrial hot springs, Antarctica, the deep subsurface, and geothermal ground waters, suggesting it represents an amalgamation of various different environments and therefore a unique habitat. Community members from the vent fluids are mostly aerobic heterotrophic bacteria; however, within the chimneys we see taxa putatively capable of acetogenesis, sulfur-cycling, and hydrogen metabolism. Previous studies have hypothesized that alkaline vents, such as the ones described here could be a potential site for the origin of life on Earth (Russell, 2009; Russell et al., 2010). Additionally, the steep sodium gradient at SHF, which is not present at the other vents, could make it an even more likely analog for the cradle of life (Martin and Russell, 2007; Lane and Martin, 2012; Price et al., 2017). While the presence of O_2 in seawater at SHF and other alkaline vents—and therefore a bioenergetically favorable oxygen gradient with reduced hydrothermal fluids—makes these sites inexact analogs for the early Earth, which was anoxic at the time of the origin of life (e.g., Farquhar et al., 2000; Johnson et al., 2014), this may actually position these systems as optimal analogs for habitable environments on other planets. In particular, both Mars (due to photochemistry and hydrogen escape) and Europa (due to radiolysis of surface ice followed by mixing with the subsurface ocean) possess now, and likely have for much of their history, O_2 at concentrations that may be sufficient to support aerobic metabolisms (Hand et al., 2007; Lanza et al., 2016; Stamenković et al., 2018; Ward et al., 2019). Future metagenome-, metatranscriptome-, and culture-based work at SHF may therefore serve as an excellent natural laboratory to investigate the possibility of the origin and survival of life elsewhere in the solar system. Here we demonstrate that SHF is not only geochemically distinctive compared to other submarine hydrothermal vents, but also microbiologically unique. Future studies of the system may

further help us to decipher the possible roles of both freshwater and marine alkaline hydrothermal systems in the origin of life.

Data availability statement

The data presented in this study are deposited in the NCBI SRA repository, accession number PRJNA861241.

Author contributions

KT, LW, WB, SM, RP, and DG contributed to the conception and design of the study. KT, LW, RP, DG, and SM participated in the sample collection and processing. KT, LW, ZK, AS, HP, RP, and WB contributed to the data analysis, curation, methodology, visualization, and validation. KT wrote the original draft. SM organized the field expedition and acquired the funding. All authors contributed to the interpretation, contributed to the review, editing, and approval of the final submitted version.

Funding

This research was supported in part by the ELSI Origins Network (EON), which was supported by a grant from the John Templeton Foundation and also partially supported by the NASA Astrobiology Institute Rock-Powered Life team and NASA Habitable Worlds program grant 80NSSC20K0228. SM acknowledges support from JSPS KAKENHI Grant No. JP20H00195 and RP received partial funding for this work from the Hanse-Wissenschaftskolleg Institute for Advanced Study, Delmenhorst, Germany.

Acknowledgments

Erlendur Bogason was instrumental in the work and we are grateful to the Strýtan Divecenter in Hjalkeyri, Iceland. Additionally, we thank Ryuhei Nakamura and Masahiro Yamamoto for their contributions during the field sampling expedition and Jake Lowe for his comments on the manuscript draft. We are grateful to the Icelandic National Energy Authority and Environment Agency for issuing permits for this work. We especially acknowledge members of the University of Akureyri for a warm welcome and laboratory support Profs. Hreiðar Þór Valtýsson, Jóhann Örlygsson, Ásta Margrét Ásmundsdóttir, and Rannveig Björnsdóttir.

Conflict of interest

The authors declare that the research was conducted in the absence of any commercial or financial relationships that could be construed as a potential conflict of interest.

Publisher's note

All claims expressed in this article are solely those of the authors and do not necessarily represent those of their affiliated organizations, or those of the publisher, the editors and the reviewers. Any product that may be evaluated in this article, or claim that may be made by its manufacturer, is not guaranteed or endorsed by the publisher.

Author disclaimer

The opinions expressed in this publication are those of the author(s) and do not necessarily reflect the views of EON or the John Templeton Foundation.

Supplementary material

The Supplementary Material for this article can be found online at: https://www.frontiersin.org/articles/10.3389/fmicb.2022.960335/full#supplementary-material

References

Adam, P. S., Borrel, G., and Gribaldo, S. (2018). Evolutionary history of carbon monoxide dehydrogenase/acetyl-CoA synthase, one of the oldest enzymatic complexes. *Proc. Natl. Acad. Sci. U.S.A.* 115, E1166–E1173. doi: 10.1073/pnas.1716667115

Akagawa-Matsushita, M., Matsuo, M., Koga, Y., and Yamasato, K. (1992). *Alteromonas atlantica* sp. nov. and *Alteromonas carrageenovora* sp. nov., bacteria that decompose algal polysaccharides. *Int. J. Syst. Evol. Microbiol.* 42, 621–627. doi: 10.1099/00207713-42-4-621

Altschul, S. F., Gish, W., Miller, W., Myers, E. W., and Lipman, D. J. (1990). Basic local alignment search tool. *J. Mol. Biol.* 215, 403–410. doi: 10.1016/S0022-2836(05)80360-2

Anda, D., Büki, G., Krett, G., Makk, J., Márialigeti, K., Erõss, A., et al. (2014). Diversity and morphological structure of bacterial communities inhabiting the Diana-Hygieia Thermal Spring (Budapest, Hungary). *Acta Microbiol. Immunol. Hung.* 61, 329–346. doi: 10.1556/amicr.61.2014.3.7

Arshad, A., Dalcin Martins, P., Frank, J., Jetten, M. S. M., Op den Camp, H. J. M., and Welte, C. U. (2017). Mimicking microbial interactions under nitrate-reducing conditions in an anoxic bioreactor: enrichment of novel Nitrospirae bacteria distantly related to *Thermodesulfovibrio*. *Environ. Microbiol.* 19, 4965–4977. doi: 10.1111/1462-2920.13977

Aszalós, J. M., Szabó, A., Megyes, M., Anda, D., Nagy, B., and Borsodi, A. K. (2020). Bacterial diversity of a high-altitude permafrost thaw pond located on

ojos del salado (dry andes, altiplano-atacama region). *Astrobiology* 20, 754–765. doi: 10.1089/ast.2018.2012

Berg, I. A. (2011). Ecological aspects of the distribution of different autotrophic CO2 fixation pathways. *Appl. Environ. Microbiol.* 77, 1925–1936. doi: 10.1128/AEM.02473-10

Bjornsdottir, S. H., Petursdottir, S. K., Hreggvidsson, G. O., Skirnisdottir, S., Hjorleifsdottir, S., Arnfinnsson, J., et al. (2009). *Thermus islandicus* sp. nov., a mixotrophic sulfur-oxidizing bacterium isolated from the *Torfajokull geothermal* area. *Int. J. Syst. Evol. Microbiol.* 59, 2962–2966. doi: 10.1099/ijs.0.007013-0

Blank, C. E., Cady, S. L., and Pace, N. R. (2002). Microbial composition of near-boiling silica-depositing thermal springs throughout Yellowstone National Park. *Appl. Environ. Microbiol.* 68, 5123–5135. doi: 10.1128/AEM.68.10.5123-5135.2002

Boomer, S. M., Noll, K. L., Geesey, G. G., and Dutton, B. E. (2009). Formation of multilayered photosynthetic biofilms in an alkaline thermal spring in Yellowstone National Park, Wyoming. *Appl. Environ. Microbiol.* 75, 2464–2475. doi: 10.1128/AEM.01802-08

Bozal, N., Montes, M. J., Tudela, E., and Guinea, J. (2003). Characterization of several *Psychrobacter* strains isolated from Antarctic environments and description of *Psychrobacter luti* sp. nov. and *Psychrobacter fozii* sp. nov. *Int. J. Syst. Evol. Microbiol.* 53, 1093–1100. doi: 10.1099/ijs.0.02457-0

Branscomb, E., Biancalani, T., Goldenfeld, N., and Russell, M. (2017). Escapement mechanisms and the conversion of disequilibria; the engines of creation. *Phys. Rep.* 677, 1–60. doi: 10.1016/j.physrep.2017.02.001

Brazelton, W. J., McGonigle, J. M., Motamedi, S., Pendleton, H. L., Twing, K. I., Miller, B. C., et al. (2022). Metabolic strategies shared by basement residents of the Lost City hydrothermal field. *Appl. Environ. Microbiol.* [Epub ahead of print]. doi: 10.1101/2022.01.25.477282

Callahan, B. J., McMurdie, P. J., Rosen, M. J., Han, A. W., Johnson, A. J. A., and Holmes, S. P. (2016). DADA2: high-resolution sample inference from Illumina amplicon data. *Nat. Methods* 13, 581–583. doi: 10.1038/nmeth.3869

Chaudhary, D. K., Kim, D.-U., Kim, D., and Kim, J. (2019). *Flavobacterium petrolei* sp. nov., a novel psychrophilic, diesel-degrading bacterium isolated from oil-contaminated Arctic soil. *Sci. Rep.* 9:4134. doi: 10.1038/s41598-019-40667-7

Chen, P., Zhou, H., Huang, Y., Xie, Z., Zhang, M., Wei, Y., et al. (2021). Revealing the full biosphere structure and versatile metabolic functions in the deepest ocean sediment of the Challenger Deep. *Genome Biol.* 22:207. doi: 10.1186/s13059-021-02408-w

Chivian, D., Brodie, E. L., Alm, E. J., Culley, D. E., Dehal, P. S., DeSantis, T. Z., et al. (2008). Environmental genomics reveals a single-species ecosystem deep within Earth. *Science* 322, 275–278. doi: 10.1126/science.1155495

Corman, J. R., Poret-Peterson, A. T., Uchitel, A., and Elser, J. J. (2016). Interaction between lithification and resource availability in the microbialites of Río Mesquites, Cuatro Ciénegas, México. *Geobiology* 14, 176–189. doi: 10.1111/gbi.12168

Couradeau, E., Roush, D., Guida, B. S., and Garcia-Pichel, F. (2017). Diversity and mineral substrate preference in endolithic microbial communities from marine intertidal outcrops (Isla de Mona, Puerto Rico). *Biogeosciences* 14, 311–324. doi: 10.5194/bg-14-311-2017

Eder, W., and Huber, R. (2002). New isolates and physiological properties of the Aquificales and description of *Thermocrinis albus* sp. nov. *Extremophiles* 6, 309–318. doi: 10.1007/s00792-001-0259-y

Espín, Y., Aranzulla, G., Álvarez-Ortí, M., and Gómez-Alday, J. J. (2020). Microbial community and atrazine-degrading genetic potential in deep zones of a hypersaline lake-aquifer system. *Appl. Sci.* 10:7111. doi: 10.3390/app10207111

Farquhar, J., Bao, H., and Thiemens, M. (2000). Atmospheric influence of Earth's earliest sulfur cycle. *Science* 289, 756–758. doi: 10.1126/science.289.5480.756

García-Davis, S., Reyes, C. P., Lagunes, I., Padrón, J. M., Fraile-Nuez, E., Fernández, J. J., et al. (2021). Bioprospecting antiproliferative marine microbiota from submarine Volcano Tagoro. *Front. Mar. Sci.* 8:687701. doi: 10.3389/fmars.2021.687701

Geptner, A., Kristmannsdóttir, H., Kristjansson, J., and Marteinsson, V. (2002). Biogenic saponite from an active submarine hot spring, Iceland. *Clays Clay Miner.* 50, 174–185. doi: 10.1346/000986002760832775

Hand, K. P., Carlson, R. W., and Chyba, C. F. (2007). Energy, chemical disequilibrium, and geological constraints on Europa. *Astrobiology* 7, 1006–1022. doi: 10.1089/ast.2007.0156

Hudson, R., de Graaf, R., Strandoo Rodin, M., Ohno, A., Lane, N., McGlynn, S. E., et al. (2020). CO2 reduction driven by a pH gradient. *Proc. Natl. Acad. Sci. U.S.A.* 117, 22873–22879. doi: 10.1073/pnas.2002659117

Hügler, M., Huber, H., Molyneaux, S. J., Vetriani, C., and Sievert, S. M. (2007). Autotrophic CO2 fixation via the reductive tricarboxylic acid cycle in different lineages within the phylum Aquificae: evidence for two ways of citrate cleavage. *Environ. Microbiol.* 9, 81–92. doi: 10.1111/j.1462-2920.2006.01118.x

Johnson, J. E., Gerpheide, A., Lamb, M. P., and Fischer, W. W. (2014). O2 constraints from Paleoproterozoic detrital pyrite and uraninite. *GSA Bull.* 126, 813–830. doi: 10.1130/B30949.1

Karnachuk, O. V., Frank, Y. A., Lukina, A. P., Kadnikov, V. V., Beletsky, A. V., Mardanov, A. V., et al. (2019). Domestication of previously uncultivated *Candidatus Desulforudis audaxviator* from a deep aquifer in Siberia sheds light on its physiology and evolution. *ISME J.* 13, 1947–1959. doi: 10.1038/s41396-019-0402-3

Kelley, D. S., Karson, J. A., Früh-Green, G. L., Yoerger, D. R., Shank, T. M., Butterfield, D. A., et al. (2005). A serpentinite-hosted ecosystem: the Lost City hydrothermal field. *Science* 307, 1428–1434. doi: 10.1126/science.1102556

Kozich, J. J., Westcott, S. L., Baxter, N. T., Highlander, S. K., and Schloss, P. D. (2013). Development of a dual-index sequencing strategy and curation pipeline for analyzing amplicon sequence data on the MiSeq illumina sequencing platform. *Appl. Environ. Microbiol.* 79, 5112–5120. doi: 10.1128/AEM.01043-13

Lane, N., and Martin, W. F. (2012). The origin of membrane bioenergetics. *Cell* 151, 1406–1416. doi: 10.1016/j.cell.2012.11.050

Lang, S. Q., and Brazelton, W. J. (2020). Habitability of the marine serpentinite subsurface: a case study of the Lost City hydrothermal field. *Philos. Trans. R. Soc. Math. Phys. Eng. Sci.* 378:20180429. doi: 10.1098/rsta.2018.0429

Lanza, N. L., Wiens, R. C., Arvidson, R. E., Clark, B. C., Fischer, W. W., Gellert, R., et al. (2016). Oxidation of manganese in an ancient aquifer, Kimberley formation, Gale crater, Mars. *Geophys. Res. Lett.* 43, 7398–7407. doi: 10.1002/2016GL069109

Lecoeuvre, A., Ménez, B., Cannat, M., Chavagnac, V., and Gérard, E. (2021). Microbial ecology of the newly discovered serpentinite-hosted Old City hydrothermal field (southwest Indian ridge). *ISME J.* 15, 818–832. doi: 10.1038/s41396-020-00816-7

López, G., Diaz-Cárdenas, C., Shapiro, N., Woyke, T., Kyrpides, N. C., David Alzate, J., et al. (2017). Draft genome sequence of *Pseudomonas extremaustralis* strain USBA-GBX 515 isolated from Superparamo soil samples in Colombian Andes. *Stand. Genomic Sci.* 12:78. doi: 10.1186/s40793-017-0292-9

López, N. I., Pettinari, M. J., Stackebrandt, E., Tribelli, P. M., Põtter, M., Steinbüchel, A., et al. (2009). *Pseudomonas extremaustralis* sp. nov., a Poly(3-hydroxybutyrate) producer isolated from an antarctic environment. *Curr. Microbiol.* 59, 514–519. doi: 10.1007/s00284-009-9469-9

López-López, O., Knapik, K., Cerdán, M.-E., and González-Siso, M.-I. (2015). Metagenomics of an alkaline hot spring in galicia (Spain): microbial diversity analysis and screening for novel lipolytic enzymes. *Front. Microbiol.* 6:1291. doi: 10.3389/fmicb.2015.01291

Marteinsson, V. T., Kristjánsson, J. K., Kristmannsdóttir, H., Dahlkvist, M., Sæmundsson, K., Hannington, M., et al. (2001b). Discovery and description of giant submarine smectite cones on the Seafloor in Eyjafjordur, Northern Iceland, and a novel thermal microbial habitat. *Appl. Environ. Microbiol.* 67, 827–833. doi: 10.1128/AEM.67.2.827-833.2001

Marteinsson, V. T., Hauksdóttir, S., Hobel, C. F. V., Kristmannsdóttir, H., Hreggvidsson, G. O., and Kristjánsson, J. K. (2001a). Phylogenetic diversity analysis of subterranean hot springs in Iceland. *Appl. Environ. Microbiol.* 67, 4242–4248. doi: 10.1128/AEM.67.9.4242-4248.2001

Martin, M. (2011). Cutadapt removes adapter sequences from high-throughput sequencing reads. *EMBnet J.* 17, 10–12. doi: 10.14806/ej.17.1.200

Martin, W., and Russell, M. J. (2007). On the origin of biochemistry at an alkaline hydrothermal vent. *Philos. Trans. R. Soc. B Biol. Sci.* 362, 1887–1926. doi: 10.1098/rstb.2006.1881

Martinez, J. N., Nishihara, A., Lichtenberg, M., Trampe, E., Kawai, S., Tank, M., et al. (2019). Vertical distribution and diversity of phototrophic bacteria within a hot spring microbial mat (Nakabusa Hot Springs, Japan). *Microb. Environ.* 34, 374–387. doi: 10.1264/jsme2.ME19047

McCollom, T. M., and Seewald, J. S. (2007). Abiotic synthesis of organic compounds in deep-sea hydrothermal environments. *Chem. Rev.* 107, 382–401. doi: 10.1021/cr0503660

McMurdie, P. J., and Holmes, S. (2013). phyloseq: an R package for reproducible interactive analysis and graphics of microbiome census data. *PLoS One* 8:e61217. doi: 10.1371/journal.pone.0061217

Meyer-Dombard, D. R., and Amend, J. P. (2014). Geochemistry and microbial ecology in alkaline hot springs of Ambitle Island, Papua New Guinea. *Extremophiles* 18, 763–778. doi: 10.1007/s00792-014-0657-6

Meyer-Dombard, D. R., Swingley, W., Raymond, J., Havig, J., Shock, E. L., and Summons, R. E. (2011). Hydrothermal ecotones and streamer biofilm

communities in the Lower Geyser Basin, Yellowstone National Park. *Environ. Microbiol.* 13, 2216–2231. doi: 10.1111/j.1462-2920.2011.02476.x

Monnin, C., Chavagnac, V., Boulart, C., Ménez, B., Gérard, M., Gérard, E., et al. (2014). The low temperature hyperalkaline hydrothermal system of the Prony bay (New Caledonia). *Astrobiol. Exobiol.* 11, 6221–6267. doi: 10.5194/bgd-11-6221-2014

Morotomi, M. (2014). "The Family Sutterellaceae," in *The Prokaryotes: Alphaproteobacteria and Betaproteobacteria*, eds E. Rosenberg, E. F. DeLong, S. Lory, E. Stackebrandt, and F. Thompson (Berlin: Springer), 1005–1012.

Nakagawa, T., and Fukui, M. (2003). Molecular characterization of community structures and sulfur metabolism within microbial streamers in Japanese Hot Springs. *Appl. Environ. Microbiol.* 69, 7044–7057. doi: 10.1128/AEM.69.12.7044-7057.2003

Nakagawa, T., and Fukui, M. (2002). Phylogenetic characterization of microbial mats and streamers from a Japanese alkaline hot spring with a thermal gradient. *J. Gen. Appl. Microbiol.* 48, 211–222.

Nishihara, A., Thiel, V., Matsuura, K., McGlynn, S. E., and Haruta, S. (2018). Phylogenetic diversity of nitrogenase reductase genes and possible nitrogen-fixing bacteria in thermophilic chemosynthetic microbial communities in nakabusa hot springs. *Microb. Environ.* 33, 357–365. doi: 10.1264/jsme2.ME18030

Onstott, T. C., McGown, D. J., Bakermans, C., Ruskeeniemi, T., Ahonen, L., Telling, J., et al. (2009). Microbial communities in subpermafrost saline fracture water at the Lupin Au Mine, Nunavut, Canada. *Microb. Ecol.* 58, 786–807. doi: 10.1007/s00248-009-9553-5

Orlygsson, J., and Kristjansson, J. K. (2014). "The Family Hydrogenophilaceae," in *The Prokaryotes: Alphaproteobacteria and Betaproteobacteria*, eds E. Rosenberg, E. F. DeLong, S. Lory, E. Stackebrandt, and F. Thompson (Berlin: Springer), 859–868.

Païssé, S., Goñi-Urriza, M., Coulon, F., and Duran, R. (2010). How a bacterial community originating from a contaminated coastal sediment responds to an oil input. *Microb. Ecol.* 60, 394–405. doi: 10.1007/s00248-010-9721-7

Pinet, P. R. (2019). *Invitation to Oceanography*. Burlington, MA: Jones & Bartlett Learning.

Postec, A., Quéméneur, M., Bes, M., Mei, N., Benaïssa, F., Payri, C., et al. (2015). Microbial diversity in a submarine carbonate edifice from the serpentinizing hydrothermal system of the Prony Bay (New Caledonia) over a 6-year period. *Front. Microbiol.* 6:857. doi: 10.3389/fmicb.2015.00857

Price, R., Boyd, E. S., Hoehler, T. M., Wehrmann, L. M., Bogason, E., Valtɾsson, H. Þ, et al. (2017). Alkaline vents and steep Na+ gradients from ridge-flank basalts—Implications for the origin and evolution of life. *Geology* 45, 1135–1138. doi: 10.1130/G39474.1

Proskurowski, G., Lilley, M. D., Seewald, J. S., Früh-Green, G. L., Olson, E. J., Lupton, J. E., et al. (2008). Abiogenic hydrocarbon production at lost city hydrothermal field. *Science* 319, 604–607. doi: 10.1126/science.1151194

Pruesse, E., Peplies, J., and Glöckner, F. O. (2012). SINA: accurate high-throughput multiple sequence alignment of ribosomal RNA genes. *Bioinformatics* 28, 1823–1829. doi: 10.1093/bioinformatics/bts252

Purcell, D., Sompong, U., Yim, L. C., Barraclough, T. G., Peerapornpisal, Y., and Pointing, S. B. (2007). The effects of temperature, pH and sulphide on the community structure of hyperthermophilic streamers in hot springs of northern Thailand. *FEMS Microbiol. Ecol.* 60, 456–466. doi: 10.1111/j.1574-6941.2007.00302.x

Quéméneur, M., Bes, M., Postec, A., Mei, N., Hamelin, J., Monnin, C., et al. (2014). Spatial distribution of microbial communities in the shallow submarine alkaline hydrothermal field of the Prony Bay, New Caledonia. *Environ. Microbiol. Rep.* 6, 665–674. doi: 10.1111/1758-2229.12184

Reysenbach, A. L., Wickham, G. S., and Pace, N. R. (1994). Phylogenetic analysis of the hyperthermophilic pink filament community in Octopus Spring, Yellowstone National Park. *Appl. Environ. Microbiol.* 60, 2113–2119. doi: 10.1128/aem.60.6.2113-2119.1994

Rinke, C., Schmitz-Esser, S., Loy, A., Horn, M., Wagner, M., and Bright, M. (2009). High genetic similarity between two geographically distinct strains of the sulfur-oxidizing symbiont "*Candidatus Thiobios* zoothamnicoli.". *FEMS Microbiol. Ecol.* 67, 229–241. doi: 10.1111/j.1574-6941.2008.00628.x

Rohland, N., and Reich, D. (2012). Cost-effective, high-throughput DNA sequencing libraries for multiplexed target capture. *Genome Res.* 22, 939–946. doi: 10.1101/gr.128124.111

Rucker, H. R., Ely, T. D., LaRowe, D. E., Giovannelli, D., and Price, R. E. (2022). Quantifying the bioavailable energy in an ancient hydrothermal vent on Mars and a modern Earth-based analogue. *bioRxiv* [Preprint]. bioRxiv: 2022.09.09.507253.

Russell, M. (2009). The alkaline solution to the emergence of life: energy, entropy and early evolution. *Acta Biotheor.* 57, 389–394. doi: 10.1007/s10441-007-9026-5

Russell, M. J., Hall, A. J., and Martin, W. (2010). Serpentinization as a source of energy at the origin of life. *Geobiology* 8, 355–371. doi: 10.1111/j.1472-4669.2010.00249.x

Sekiguchi, Y., Muramatsu, M., Imachi, H., Narihiro, T., Ohashi, A., Harada, H., et al. (2008). *Thermodesulfovibrio aggregans* sp. nov. and *Thermodesulfovibrio thiophilus* sp. nov., anaerobic, thermophilic, sulfate-reducing bacteria isolated from thermophilic methanogenic sludge, and emended description of the genus *Thermodesulfovibrio*. *Int. J. Syst. Evol. Microbiol.* 58, 2541–2548. doi: 10.1099/ijs.0.2008/000893-0

Sheik, C. S., Reese, B. K., Twing, K. I., Sylvan, J. B., Grim, S. L., Schrenk, M. O., et al. (2018). Identification and removal of contaminant sequences from ribosomal gene databases: Lessons from the census of deep life. *Front. Microbiol.* 9:840. doi: 10.3389/fmicb.2018.00840

Shiraishi, F., Matsumura, Y., Chihara, R., Okumura, T., Itai, T., Kashiwabara, T., et al. (2019). Depositional processes of microbially colonized manganese crusts, Sambe hot spring, Japan. *Geochim. Cosmochim. Acta* 258, 1–18. doi: 10.1016/j.gca.2019.05.023

Stamenković, V., Ward, L. M., Mischna, M., and Fischer, W. W. (2018). O2 solubility in Martian near-surface environments and implications for aerobic life. *Nat. Geosci.* 11, 905–909. doi: 10.1038/s41561-018-0243-0

Tobler, D. J., and Benning, L. G. (2011). Bacterial diversity in five Icelandic geothermal waters: temperature and sinter growth rate effects. *Extremophiles* 15:473. doi: 10.1007/s00792-011-0378-z

Umezawa, K., Kojima, H., Kato, Y., and Fukui, M. (2021). Dissulfurispira thermophila gen. nov., sp. nov., a thermophilic chemolithoautotroph growing by sulfur disproportionation, and proposal of novel taxa in the phylum Nitrospirota to reclassify the genus *Thermodesulfovibrio*. *Syst. Appl. Microbiol.* 44:126184. doi: 10.1016/j.syapm.2021.126184

Van Trappen, S., Vandecandelaere, I., Mergaert, J., and Swings, J. (2004). *Flavobacterium degerlachei* sp. nov., *Flavobacterium frigoris* sp. nov. and *Flavobacterium micromati* sp. nov., novel psychrophilic bacteria isolated from microbial mats in Antarctic lakes. *Int. J. Syst. Evol. Microbiol.* 54, 85–92. doi: 10.1099/ijs.0.02857-0

Van Trappen, S., Vandecandelaere, I., Mergaert, J., and Swings, J. (2005). *Flavobacterium fryxellicola* sp. nov. and *Flavobacterium psychrolimnae* sp. nov., novel psychrophilic bacteria isolated from microbial mats in Antarctic lakes. *Int. J. Syst. Evol. Microbiol.* 55, 769–772. doi: 10.1099/ijs.0.03056-0

Wang, X., and Pecoraro, L. (2021). Diversity and co-occurrence patterns of fungal and bacterial communities from alkaline sediments and water of julong high-altitude hot springs at Tianchi Volcano, Northeast China. *Biology* 10:894. doi: 10.3390/biology10090894

Ward, L. M., and Shih, P. M. (2019). The evolution and productivity of carbon fixation pathways in response to changes in oxygen concentration over geological time. *Free Radic. Biol. Med.* 140, 188–199. doi: 10.1016/j.freeradbiomed.2019.01.049

Ward, L. M., Stamenković, V., Hand, K., and Fischer, W. W. (2019). Follow the oxygen: comparative histories of planetary oxygenation and opportunities for aerobic life. *Astrobiology* 19, 811–824. doi: 10.1089/ast.2017.1779

Willems, A., Busse, J., Goor, M., Pot, B., Falsen, E., Jantzen, E., et al. (1989). Hydrogenophaga, a new genus of hydrogen-oxidizing bacteria that includes *Hydrogenophaga flava* comb. nov. (Formerly *Pseudomonas flava*), *Hydrogenophaga palleronii* (Formerly *Pseudomonas palleronii*), *Hydrogenophaga pseudoflava* (Formerly *Pseudomonas pseudoflava* and "*Pseudomonas carboxy* do flava"), and *Hydrogenophaga taeniospiralis* (Formerly *Pseudomonas taeniospiralis*). *Int. J. Syst. Evol. Microbiol.* 39, 319–333. doi: 10.1099/00207713-39-3-319

Wirth, R., Sikorski, J., Brambilla, E., Misra, M., Lapidus, A., Copeland, A., et al. (2010). Complete genome sequence of *Thermocrinis albus* type strain (HI 11/12T). *Stand. Genom. Sci.* 2, 194–202. doi: 10.4056/sigs.761490

Youssef, N. H., Farag, I. F., Rudy, S., Mulliner, A., Walker, K., Caldwell, F., et al. (2019). The Wood–Ljungdahl pathway as a key component of metabolic versatility in candidate phylum Bipolaricaulota (Acetothermia, OP1). *Environ. Microbiol. Rep.* 11, 538–547. doi: 10.1111/1758-2229.12753

Zeglin, L. H., Wang, B., Waythomas, C., Rainey, F., and Talbot, S. L. (2016). Organic matter quantity and source affects microbial community structure and function following volcanic eruption on Kasatochi Island, Alaska. *Environ. Microbiol.* 18, 146–158. doi: 10.1111/1462-2920.12924

frontiers | Frontiers in Microbiology

TYPE Original Research
PUBLISHED 21 December 2022
DOI 10.3389/fmicb.2022.1043414

OPEN ACCESS

EDITED BY
Brett J. Baker,
The University of Texas at Austin,
United States

REVIEWED BY
Xiyang Dong,
Third Institute of Oceanography of the Ministry of Natural Resources, China
Daniel Colman,
Montana State University, United States

*CORRESPONDENCE
Cassandre Sara Lazar
✉ lazar.cassandre@uqam.ca

SPECIALTY SECTION
This article was submitted to Extreme Microbiology, a section of the journal Frontiers in Microbiology

RECEIVED 13 September 2022
ACCEPTED 01 December 2022
PUBLISHED 21 December 2022

CITATION
Lazar CS, Schmidt F, Elvert M, Heuer VB, Hinrichs K-U and Teske AP (2022) Microbial diversity gradients in the geothermal mud volcano underlying the hypersaline Urania Basin.
Front. Microbiol. 13:1043414.
doi: 10.3389/fmicb.2022.1043414

Microbial diversity gradients in the geothermal mud volcano underlying the hypersaline Urania Basin

Cassandre Sara Lazar[1]*, Frauke Schmidt[2], Marcus Elvert[2], Verena B. Heuer[2], Kai-Uwe Hinrichs[2] and Andreas P. Teske[3]

[1]Department of Biological Sciences, Université du Québec à Montréal, Montréal, QC, Canada, [2]Organic Geochemistry Group, Department of Geosciences, MARUM Center for Marine Environmental Sciences, University of Bremen, Bremen, Germany, [3]Department of Earth, Marine and Environmental Sciences, University of North Carolina at Chapel Hill, Chapel Hill, NC, United States

Mud volcanoes transport deep fluidized sediment and their microbial communities and thus provide a window into the deep biosphere. However, mud volcanoes are commonly sampled at the surface and not probed at greater depths, with the consequence that their internal geochemistry and microbiology remain hidden from view. Urania Basin, a hypersaline seafloor basin in the Mediterranean, harbors a mud volcano that erupts fluidized mud into the brine. The vertical mud pipe was amenable to shipboard Niskin bottle and multicorer sampling and provided an opportunity to investigate the downward sequence of bacterial and archaeal communities of the Urania Basin brine, fluid mud layers and consolidated subsurface sediments using 16S rRNA gene sequencing. These microbial communities show characteristic, habitat-related trends as they change throughout the sample series, from extremely halophilic bacteria (KB1) and archaea (*Halodesulfoarchaeum* spp.) in the brine, toward moderately halophilic and thermophilic endospore-forming bacteria and uncultured archaeal lineages in the mud fluid, and finally ending in aromatics-oxidizing bacteria, uncultured spore formers, and heterotrophic subsurface archaea (Thermoplasmatales, Bathyarchaeota, and Lokiarcheota) in the deep subsurface sediment at the bottom of the mud volcano. Since these bacterial and archaeal lineages are mostly anaerobic heterotrophic fermenters, the microbial ecosystem in the brine and fluidized mud functions as a layered fermenter for the degradation of sedimentary biomass and hydrocarbons. By spreading spore-forming, thermophilic Firmicutes during eruptions, the Urania Basin mud volcano likely functions as a source of endospores that occur widely in cold seafloor sediments.

KEYWORDS

archaea, bacteria, hypersaline basin, cold seep, marine subsurface sediments, Urania Basin

1 Introduction

The Urania Basin is situated southwest off the coast of Crete, in the inner plateau of the Mediterranean Ridge characterized by the presence of Messinian salt evaporites within the sediments, hundreds of meters below the seafloor (Westbrook and Reston, 2002). With a chloride content of 120 g/L, i.e., more than five times of that in Mediterranean seawater, Urania Basin brine is the least saline of the Mediterranean DHABs (deep hypersaline anoxic basin); yet Urania Basin brine contains exceptionally high levels of methane (up to 5.56 mM) and sulfide (up to 16 mM) (Borin et al., 2009), making Urania Basin one of the most sulfidic marine water bodies on Earth (Karisiddaiah, 2000; Charlou et al., 2003). Despite these extreme conditions, active microbial communities are present (van der Wielen et al., 2005) and contribute to biogeochemical cycling of carbon and sulfur in the deep anoxic hypersaline brine of the Urania Basin.

A unique feature of the Urania Basin is the presence of an active mud volcano in the southwestern part of the horseshoe-shaped basin, found by a CTD survey (conductivity, temperature, depth) during the R/V Urania expedition that discovered the basin in 1993. Elevated temperatures of up to 55°C coincide with active mud volcanism underneath the brine layer (Corselli et al., 1996; Fusi et al., 1996). A direct association between brines and active mud volcanism has been previously documented by exotic deposits sampled in the outer rim of the basin (Hübner et al., 2003) and by the presence of sediments containing Plio-Pleistocene microfossils at the bottom of the basin (Aloisi et al., 2006). The fluidized mud volcano sediment, consisting of micrometer-sized particles, nannofossils, carbonate and gypsum grains, constitutes a convectively mixed suspended seafloor that extends vertically over 110 m before transitioning into solidified subsurface sediment (Aiello et al., 2020).

The Urania Basin mud volcano provides a valuable model system to test the working hypothesis that mud volcanoes bring deep subsurface microorganisms to the surface and distribute them across the deep-sea floor. As conduits of fluid migration from the deep subsurface to the seafloor, mud volcanoes provide windows into the deep subseafloor biosphere (Hoshino et al., 2017) that is otherwise only accessible by deep drilling. Since the chemistry of the discharging fluidized muds varies within and between sites, different combinations of brine, methane, gaseous and liquid hydrocarbons, sulfides, nutrients and low-molecular weight organic acids shape the resident microbial communities and their activities, as shown in numerous individual studies (Joye et al., 2009; Pachiadaki et al., 2010, 2011; Lazar et al., 2011a,b, 2012; Pachiadaki and Kormas, 2013). Mud volcanoes are pulsating with fluidized mud that frequently overflows their surrounding seafloor basins (McDonald et al., 2000; Hübner et al., 2003; Teske and Joye, 2020) and by the same token deposit fluid mud-hosted bacteria and archaea. Mud volcano and cold seep geofluids have been proposed as the carrier medium for seeding surficial seafloor sediments with endospore-forming thermophilic Firmicutes that could not grow under cold *in situ* conditions (Hubert et al., 2009; Rattray et al., 2022).

To explore the spatially shifting microbial community in the Urania Basin brine/mud volcano system, we analyzed bacterial and archaeal 16S rRNA gene amplicons along a vertical profile from consolidated subseafloor sediments at the underlying seabed at the bottom of the mud volcano (the "pit"), through fluidized mud volcano sediment layers that extend from the subsurface seabed to the bottom of the brine lake, to the overlying brine lake. This approach was supported by analysis of gaseous hydrocarbons and hydrocarbon lipid biomarkers from selected sediment samples. A previous 16S rRNA gene sequencing survey of deep mud fluid sediment has uncovered diverse bacterial and archaeal populations (Yakimov et al., 2007) but did not produce a microbial profile through all three layers (subsurface sediment, fluid mud layers, brine fluid). The geochemical and microbiological changes observed along this depth profile indicate that each sediment and brine layer has selected for its unique microbial community.

2 Materials and methods

2.1 Sediment sampling

Brine, mud fluids and subseafloor sediments were sampled in the Urania Basin during cruise M84/1 (DARCSEAS) of R/V Meteor in February 2011. Two CTD casts GeoB15101-1 and GeoB15101-6 (35°13.86′N, 21°28.30′E) deployed twenty-four Niskin bottles each at increasing water depths, and samples were used for stable ion measurements (Aiello et al., 2020) and DNA extractions, respectively. Based on stable ion concentrations and CTD pressure readings, the seawater-brine interface was located between 3,461 and 3,463 m water depth (mwd), and the brine/fluid mud interface between 3,607 and 3,610 m water depth (Aiello et al., 2020). Within the fluid mud layers, sampling depths were conservatively based on CTD cable length since the high density of the mud interfered with reliable pressure measurements by the CTD sensors as soon as the CTD entered the fluid mud layer. For GeoB15101-1, bottles 1 (70 m water depth, mwd) to 8 (3,461 mwd) sampled the overlying seawater, whereas bottles 9 (3,463 mwd) to 24 (3,598 mwd) sampled the hypersaline brine lake. For cast GeoB15101-6 (used in this study), bottle 1 sampled overlying seawater (3,000 mwd), and bottles 2 (3,560 mwd) to 7 (3,605 mwd) sampled the hypersaline brine. The underlying mud fluid layers were sampled in 10-m intervals by bottles 8 (3,610 m cable length) to 20 (3,730 m cable length). The deepest mud fluid sample, no. 21, was collected at a cable length of 3,736 m when the sediment became sufficiently consolidated to prevent further sinking of the CTD. Subsamples taken from the 24 Niskin bottles of the CTD cast GeoB15101-6—sampled progressively from the seawater, through the Urania brine lake, down to the seafloor—clearly demonstrated the fluid mud layer starting with bottle 8, and

continuing downcore toward gradually darker mud (**Figure 1**). The bottom of the fluidized mud layer (sample 21, 3,736 m cable length) was 110 m below the expected seafloor depth, where brine transitions into mud, based on echo-sounder data (Zabel, 2012).

The subsequently deployed gravity core GeoB15101-7 (35°13.87′N, 21°28.30′E) recovered 4.5 m of the consolidated sediments below the mud fluid layers, and depths for these sediment samples are given in cm from the top of the core. Subsamples of each Niskin bottle of cast GeoB15101-6 as well as selected gravity core sections of cast GeoB15101-7 were immediately stored at −20°C for subsequent molecular analyses, including hydrocarbon lipid biomarkers. Concentration measurements of methane and ethane were carried out onboard the ship, whereas investigation of the gaseous hydrocarbon's stable carbon isotopes was performed in the home lab.

2.2 Hydrocarbon measurements

Concentrations of dissolved methane and ethane were determined according to previously reported protocols (Pimmel and Claypool, 2001; D'Hondt et al., 2003), using two to three mL of brine, mud fluid and subseafloor sediment samples (see **Supplementary Methods** for details). Isotope values of methane and ethane are reported in the delta notation ($\delta^{13}C$) relative to the Vienna Pee Dee Belemnite (VPDB) standard using a calibrated in-house CO_2 reference gas standard. For hydrocarbon lipid biomarker analysis of two gravity core sediments samples from 10 to 30 and 260–280 cm core depth, 50 g of freeze-dried sample material was extracted using a modified Bligh and Dyer protocol (Sturt et al., 2004). Hydrocarbons were identified *via* their known mass spectra and concentrations were calculated from their peak area in the FID chromatogram relative to the injection standard (see **Supplementary Methods** for details).

2.3 DNA extraction, PCR amplification and 16S rRNA gene library construction

Samples chosen for molecular analyses included Niskin bottles 5 (3,590 mwd, hypersaline brine), 8 (3,610 m, top of the mud fluid layer), 14 (3,670 m, middle of the mud fluid layer) and 21 (3,736 m, bottom of the mud fluid layer) from the GeoB15101-6 CTD cast (**Figure 1**), and depth sections 10–30 and 260–280 cmbsf of the GeoB15101-7 gravity core. DNA was extracted using a bead beating soil extraction kit on 10 g of wet sediment for the mud fluid and gravity core samples (UltraClean® Mega Soil DNA Isolation Kit, MO BIO, CA now QIAGEN), and using 50 mL of filtered brine (PowerSoil® DNA Isolation Kit, Mo BIO, CA now QIAGEN). The extracted DNA was then purified using the Wizard DNA Clean-Up System (Promega, Wisconsin, USA).

Archaeal 16S rRNA genes were amplified using the primers A24F (5′-CGGTTGATCCTGCCGGA-3′) and A1492R (5′-GGCTACCTTGTTACGACTT-3′) (Casamayor et al., 2000) and the Flexi GoTaq DNA polymerase (Promega, WI). A total of 35 PCR cycles (1 min denaturation at 94°C, 1′30 min annealing at 50°C, and 2 min elongation at 72°C) were run in a BIO-RAD iCycler (Hercules, CA). A nested PCR using the primer set A24F (5′-CGGTTGATCCTGCCGGA-3′; Casamayor et al., 2000) and Arch915R (5′-GTGCTCCCCCGCCAATTCCT-3′, Stahl and Amann, 1991) was necessary in order to obtain sufficient amounts of archaeal 16S rRNA gene amplicons for cloning, using the following conditions: 1 min denaturation at 94°C, 1′30 min annealing at 58°C, and 2 min elongation at 72°C, repeated for 35 cycles.

Bacterial 16S rRNA genes were amplified using the B8F-B1492R primer set (5′-AGRGTTTGATCCTGGCTCAG-3 and 5′-CGGCTACCTTGTTACGACTT-3; Teske et al., 2002) using the following PCR conditions: 1 min denaturation at 94°C, 1′30 min annealing at 50°C, and 2 min elongation at 72°C, repeated for 26 cycles to limit contamination since the extracted DNA concentrations were extremely low. A nested PCR using the primer combination B27F (5′-AGA GTTTGATCCTGGCTCAG-3′) and U1406R (5′-GACGGGC GGTGTGTRCA-3′; Heuer et al., 1997) was necessary to obtain sufficient amplicon material for cloning, using the following conditions: 1 min denaturation at 94°C, 1′30 min annealing at 50°C, and 2 min elongation at 72°C, repeated for 30 cycles. PCR products were purified using the QIAquick Gel Extraction Kit (QIAGEN, CA, USA) prior to cloning, and were then cloned using the TOPO XL cloning kit (Invitrogen, CA). After inserting the PCR amplified genes into the provided plasmid, the plasmid DNA was incorporated into *Escherichia coli* TOPO10 One Shot cells. Transformed cells were grown overnight, and colonies were collected for Sanger sequencing.

2.4 DNA sequencing and phylogenetic analysis

The microbial census of the Urania Basin mud layers is deliberately based on nearly full-length 16S rRNA gene clone libraries for Bacteria (1,379 bp in *E. coli* standard notation) and widely used large fragments for archaea (890 bp for the Archaea), in order not to compromise the phylogenetic placement and taxonomic identification of potentially novel microbial populations in this unusual extreme habitat, and to provide a well-curated reference dataset for 16S-rRNA based comparison that is not limited by sequence length. Furthermore, given the nature of the extremely hypersaline samples, DNA analyses *via* high-throughput sequencing revealed themselves to be ineffective by only yielding a dozen reads.

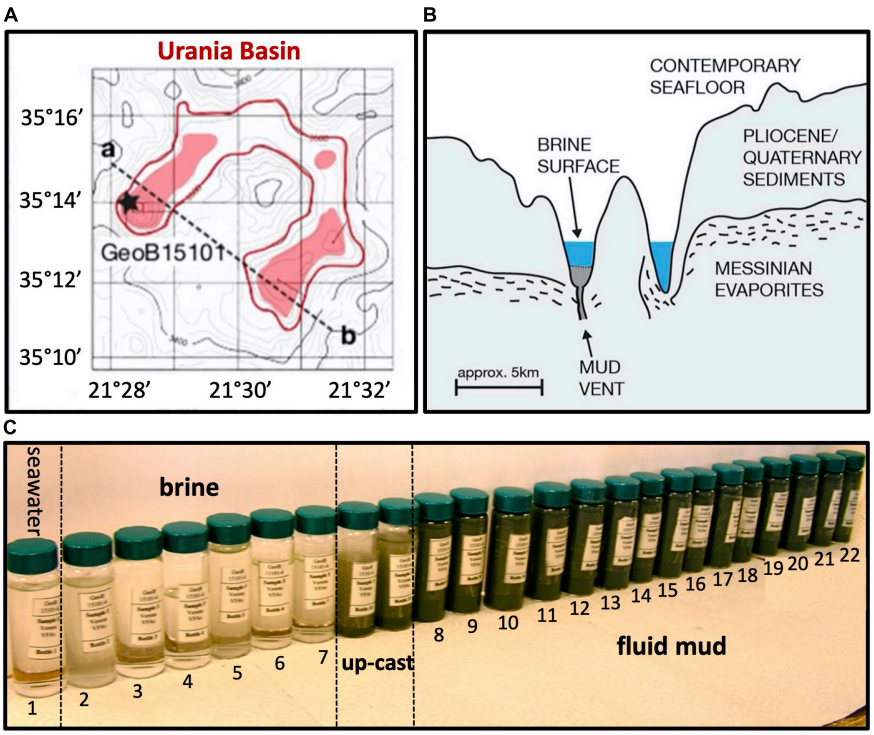

FIGURE 1
(A) Lower left, bathymetry of Urania Basin with bottom brines highlighted in red, and profile line drawn from the mud volcano in the northwestern end toward the southeastern end of Urania Basin. **(B)** Geologic sketch of Urania Basin, following the profile line between points a and b. **(C)** Sample vials with Niskin bottle samples from seawater, brine, and fluidized mud. The samples between brine and mud layer represent perturbed samples from the CTD upcast (GeoB15101-6, Zabel, 2012) at 3,605 and 3,610 m depth. All figure panels modified from Aiello et al. (2020).

Sequences were obtained by Genewiz (South Plainfield, NJ) on an ABI Prism 3730xl sequencer using the M13R primer. Chimeras were identified with Mothur's chimera slayer feature (Schloss et al., 2009), complemented by Blast analysis of sequence segments, and removed from phylogeny inferences. For initial phylogenetic analyses, the 16S rRNA gene sequences were edited in the BioEdit v7.0.5 program (Hall, 1999) and aligned by using the SINA webaligner (Pruesse et al., 2012).[1] The alignment was then manually checked using ARB (Ludwig et al., 2004) and initial phylogenetic trees were calculated using the neighbor-joining method in ARB. Robustness of the inferred topology was tested by bootstrap resampling with 1,000 replicates. Final phylogeny figures were constructed with sequences selected from cultured bacteria and archaea and complemented by environmental sequences (limited to *ca*. 50–80 sequences for readability), and manually aligned for secondary rRNA structure to ensure consistent comparisons of homologous nucleotide positions across variable and hypervariable regions (Schloss, 2013); subsequently, tree topology was checked by 1,000 bootstrap replicates (Swofford, 2000). Whenever possible, pure-culture isolates with close sequence similarity to Urania Basin clones (for genus level > 95%, Schloss and Handelsman, 2005) were preferred for phylogenetic comparisons, to limit the inherent uncertainties of sequence-based physiological inferences (see Langille et al., 2013 for discussion). For uncultured lineages, Urania Basin sequences were identified as specifically as possible by comparisons to published subgroup analyses and phylogenies, with metagenomes when possible. The sequence data reported here were submitted to the GenBank nucleotide sequence database under the accession numbers OP352539-OP352606, OP352609-OP352677, OP352609-OP352677, OP352680-OP352749, OP352780-OP352844, OP389299-OP389989, and OP856603-OP856629.

3 Results

3.1 Depth stratification and biogeochemistry

During CTD deployment, a prominent halocline was detected at about 3,465 mwd, and corresponded to a salinity

1 http://www.arb-silva.de/aligner

increase from ~39 to ~152 PSU (practical salinity unit), a 2.5°C increase in temperature (14–16.5°C) and the complete depletion of free oxygen; this transition marks the seawater-brine interface (Zabel, 2012). Once the CTD cast went through the brine layer and reached the depth of the seafloor, identified by onboard echo sounder at approximately 3,600 m, the cable tension did not drop, and the deployment was continued below that depth. About 160 m within the brine, at 3,625 mwd, a second density boundary was detected below which the CTD malfunctioned, and from then on depth was measured in cable length. The deployment continued until 3,735 m cable length, when a relatively fast decrease of the cable tension indicated a third boundary as the CTD rosette reached sufficiently consolidated sediments that stopped further sinking. This depth was 110 m below the expected seafloor depth based on echo sounder data (Zabel, 2012).

Overlying the subseafloor sediments and fluidized muds of the Urania Basin like a lid, a massive brine layer extends between 3,463 and 3,610 mwd. The samples recovered in Niskin bottles returned clear brine fluids from the 3,465 m to 3,610 mwd interval (**Figure 1**). The redox potential in the brine lake was extremely negative at 3,560 mwd, i.e., –427 mV, consistent with previous results showing that oxygen was completely depleted in the reducing brine lake environment (Borin et al., 2009). The brine contained chloride and sodium at constant concentrations of 2,823 and 2,450 mM, respectively (Aiello et al., 2020), *ca.* 4.5 times higher than in the underlying fluid mud and subseafloor sediments (**Figure 2**).

For over 110 vertical meters below the brine layer, the Niskin bottles collected fluid mud (**Figure 1**) with much higher density (>1.6 g/cm^3) than the brine (1.13 g/cm^3), comparable to the bulk-saturated density of similar pelagic sediments (Fusi et al., 1996). The water content in the fluid mud ranges between ~61 and 68%, which is above the Attemberg's liquid limit measured for similar sediments recovered during ODP Leg 160 at the Olimpi Mud Volcano field (Kopf et al., 1998). The flat pore water profiles of Na^+ and Cl^- across the fluid mud layer suggest some internal mixing

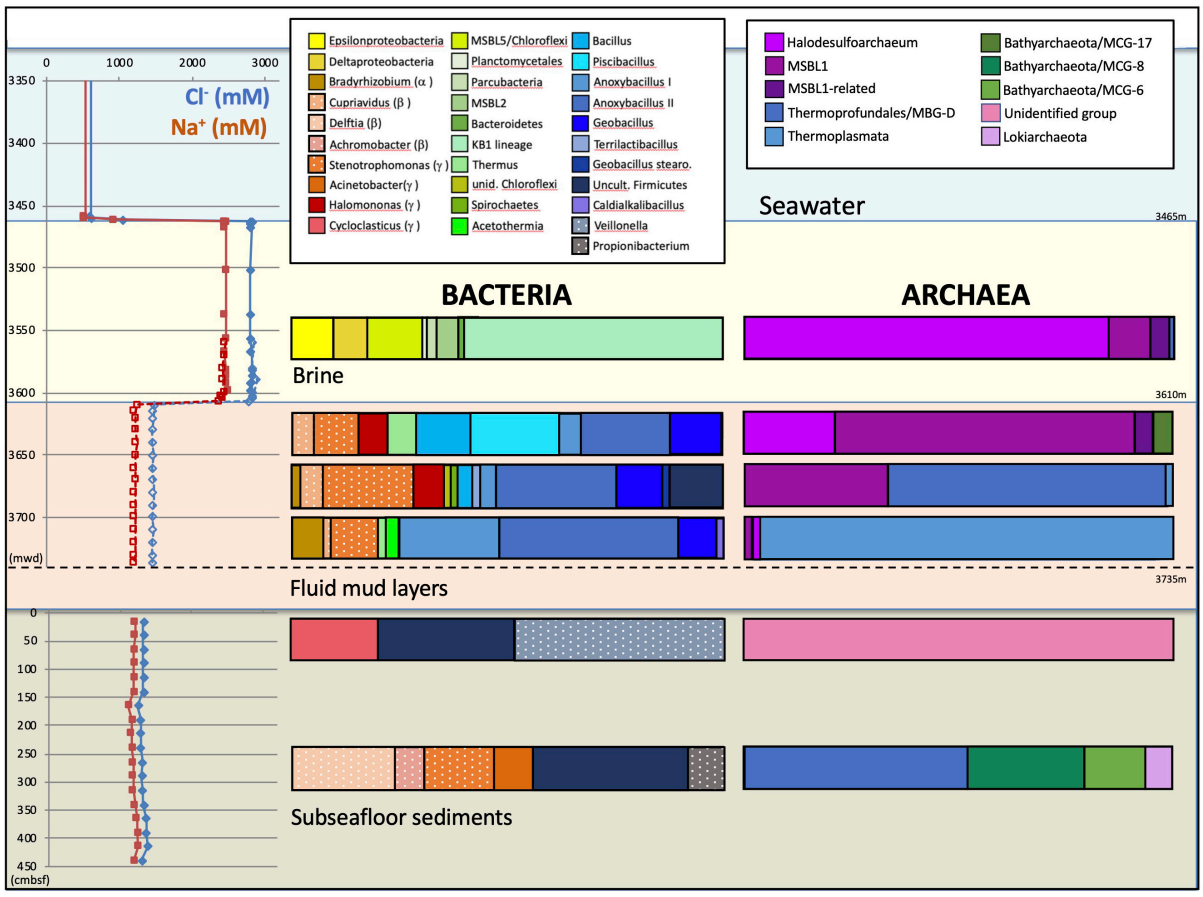

FIGURE 2
Depth profiles of water and sediment porewater geochemistry and phylogenetic affiliations of the archaeal and bacterial 16S rRNA gene sequences for the three Urania Basin habitats: subseafloor sediments, mud fluid layers and brine lake. For the subseafloor sediments, depth is given in cm below the top of the gravity core. Depth is given as CTD depth for the brine fluid, and as cable length for the fluid mud layer. Sodium and chloride concentration profiles are derived from Aiello et al. (2020). Presumable contaminants are shown with a white dot pattern.

to obscure internal biogeochemical stratification (**Figure 2**). Internal mixing is also supported by consistent total sulfur concentrations, dominated by sulfate, near 95 and 53 mM for brine and fluid mud, respectively (Aiello et al., 2020). Above-seawater salinities suggest that the fluid mud was mixed with pre-existing brine fluids. In lakes, temperature and salt differences between two bodies of water/sediment can lead to double-diffusive convection cells, which can highly enhance vertical transport of heat and salt (Boehrer, 2012). Consistent with the maximum depth reached by CTD rosette deployment in the fluid mud layers, the Gravity corer (GeoB15101-7) encountered a resistant sediment layer at about 3,735 m cable length. The Gravity corer returned 4.5 m of sediment, soupy and homogeneous within the upper 80 cm but increasingly firm below; the sediment at the very bottom of the core was consolidated.

3.2 Gases and hydrocarbon lipid biomarkers

Previously measured temperatures of 45°C in the bottom of the southwestern part of the basin (Corselli et al., 1996) are a strong indicator of a deep subsurface reservoir fueling fluids and mud to the Urania Basin seafloor. Since high pressure and temperature transform buried organic matter to hydrocarbons, the consolidated subseafloor sediment samples obtained by gravity coring were examined for methane and ethane, as well as hydrocarbon lipid biomarkers. The concentrations of methane and ethane are consistently high, 0.14–0.79 mM and 0.03–0.13 mM in the brine, respectively, and 0.4–3.3 mM and 0.07–0.60 mM, respectively, in the consolidated subseafloor sediments (**Supplementary Table 1**). The $\delta^{13}C$ values of methane and ethane in the fluid mud layers are rather invariable (approximately –30.7 and –30.2‰, respectively) and nearly identical to $\delta^{13}C$ values in the subseafloor sediment (approximately –30.3 and ∼ –29.1‰, respectively). Both are indicating a deep thermogenic source, which is corroborated by exceptionally low C_1/C_2 ratios of ∼5 in the fluid mud and in the sediments (**Supplementary Table 1**).

Polycyclic aromatic molecules in subseafloor sediments (**Supplementary Table 2**) included compounds typically found in petroleum such as naphthalene, fluorine, phenanthrene or pyrene but also high amounts of benzidine. The portion of polyaromatic hydrocarbons was high compared to the relative sum of identified hydrocarbons, including odd n-alkanes in the range from C_{21} to C_{33} as well as terpenoids such as squalene, Hop-17,21-ene and lycopane, i.e., 82.6% in the deep subseafloor sample (260–280 cm core depth) and 86.7% in the shallow sample (10–30 cm core depth). The extremely high proportion of thermally altered hydrocarbons detected in the subseafloor sediments of the Urania Basin is consistent with the hypothesis of a deep, hot reservoir that charges deep sediments and fluidized mud with gas of thermocatalytic or hydrothermal origin (Karisiddaiah, 2000; Hübner et al., 2003).

3.3 Microbial community of the Urania Basin brine

The bacterial and archaeal community of Urania basin, as evaluated by 16S rRNA gene sequencing (**Table 1** and **Supplementary Table 3**), underwent pronounced compositional changes between brine, fluid mud and bottom sediment samples (**Figure 2**). Since these samples differ mainly by salinity, and less by biomarker content (only the bottom sediment) or by gas concentration and isotopic signature, microbial community differences are likely to be connected to salinity; extreme halophiles would be expected in the brine layer and might diminish in the fluid muds below.

Indeed, the uncultured halophilic Kebrit deep group 1 (KB-1) dominated the bacterial 16S rRNA data set from the brine sample (**Figure 3** and **Table 1**). This bacterial lineage was first detected in brine sediments from the Kebrit Deep, Red Sea (Eder et al., 1999), and has so far been exclusively found in saline and hypersaline habitats, anoxic brines and sediments (Eder et al., 2001, 2002; Antunes et al., 2011; Ferrer et al., 2012). Yakimov et al. (2013) suggested that KB-1 could carry out reductive cleavage of glycine betaine and consequently produce acetate and methylamines, which could be used by halophilic methylotrophic H_2-producing methanogens, such as the putatively methanogenic uncultured MSBL-1 group (Nigro et al., 2016). KB-1 also shares the carbon monoxide dehydrogenase (subunit CooS) and the Acetyl-CoA synthase (subunit AcsB) of the CO_2-fixing acetyl-CoA pathway with *Candidatus* Acetothermum autotrophicum, a member of its sister lineage Acetothermia (Nigro et al., 2016), suggesting shared physiological flexibility with both autotrophic and acetogenic potential (Youssef et al., 2019). Six sequences were affiliated with sulfate-reducing bacteria (**Figure 4**). Three of these sequences were affiliated with the *Desulfobacterium anilini* group within the *Desulfobacteraceae*, a cluster of obligately aromatics-degrading sulfate-reducing bacteria that oxidize and remineralize substituted aromatics and polyaromatic substrates (Teske, 2019). Two sequences were related to the haloalkaliphilic genus *Desulfonatronobacter* (Sorokin et al., 2012), and one clone belonged to the family *Desulfobulbaceae*, a diverse group of incompletely oxidizing sulfate-reducing or elemental sulfur-disproportionating bacteria (Kuever et al., 2005). Generally, sulfate-reducing bacteria have access to high sulfate concentrations in the brine and fluid mud layers (Aiello et al., 2020). Eight sequences were affiliated with ε-Proteobacteria, chemolithoautotrophs that probably use the reverse TCA cycle to fix carbon, and usually thrive in sulfidic interface environments, for example the redoxcline of sulfidic waters (Schmidtova et al., 2009). Four sequences

TABLE 1 Summary of Urania Basin 16S rRNA gene sequences and their phylogenetic affiliations based on Genbank searches for Bacteria and Archaea.

Sample	Total clones	Proteobacteria	Other bacteria	Grampositives	Archaea
Brine layer/Sample 5	82 bact. clones 93 arch. clones	4 *Desulfatiglandales* (δ) 1 *D. natronobacter* (δ) 1 *Desulfococcus* sp. (δ) 1 *Desulfobulbales* (δ) 2 *Sulfurimonas* sp. (ε) 2 *Sulfurovum* sp. (ε) 4 *Arcobacter* sp. (ε)	10 MSBL5 1 Planctomycetales 2 Parcubacteria 3 MSBL2 1 MSBL2-related 1 Bacteroidetes 2 KB1 (type 1) 47 KB1 (type 2)		79 *Halodesulfoarchaeum* sp. 9 MSBL1 4 MSBL1 sister lineage 1 Thermoprofundales/MBGD
Upper fluid mud layer/Sample 8	59 bact. clones 90 arch. clones	6 *Stenotrophomonas* sp. (γ)* 3 *Cupriavidus* sp. (β)* 4 *Halomonas* sp. (γ)	4 *Thermus* sp.	7 *Bacillus* sp. 12 *Piscibacillus* sp. 3 *Anoxybacillus* sp. (near *A. flavithermus*) 12 *Anoxybacillus* sp. (near *A. geothermalis*) 7 *Geobacillus* sp. (*near G. pallidus*)	63 MBSL1 4 MSBL1 sister lineage 19 *Halodesulfoarchaeum* sp. 4 Bathyarchaeota/ MCG-17
Central fluid mud layer/Sample 14	57 bact. clones 95 arch. clones	1 *Bradyrhizobium* (α) 12 *Stenotrophomonas* sp.(γ)* 3 *Cupriavidus* sp. (β)* 4 *Halomonas* sp. (γ)	1 Chloroflexi 1 Spirochete	2 *Bacillus* sp. 1 *Terrilactibacillus* sp. 2 *Anoxybacillus* sp. (near *A. flavithermus)* 16 *Anoxybacillus* sp. (near *A. geothermalis*) 6 *Geobacillus* sp. (*near G. pallidus*) 1 *Geobacillus* sp. (near *G. stearothermophilus*) 7 uncult. Firmicutes	32 MSBL1 62 Thermoprofundales/MBGD 1 Marine Thermoplasmata
Lower fluid mud layer/Sample 21	56 bact. clones 93 arch. clones	4 *Bradyrhizobium* sp. (α) 6 *Stenotrophomonas* sp. (γ)* 1 *Cupriavidus* sp. (β)*	2 Acetothermia 1 *Thermus* sp.	12 *Anoxybacillus* sp. (near *A. flavithermus*) 24 *Anoxybacillus* sp. (near *A. geothermalis*) 5 *Geobacillus* sp. (near *G. pallidus*) 1 *Caldialkalibacillus* sp.	2 MSBL1 1 *Halodesulfoarchaeum* sp. 90 Marine Thermoplasmata
Sediment core 10–30 cm	80 bact. clones 85 arch. clones	16 *Cycloclasticus* sp. (γ)		25 uncultured Firmicutes 39 *Veillonellaceae* sp.*	85 Urania Basin Euryarchaeotal Group (UBEG)
Sediment core 260–280 cm	75 bact. clones 73 arch. clones	12 *Stenotrophomonas* sp. (γ)* 18 *Delftia* sp. (β)* 7 *Acinetobacter* sp. (γ) 5 *Achromobacter* sp. (β)*		27 uncultured Firmicutes 6 *Propionibacterium* sp.*	38 Thermoprofundales/MBGD 20 Bathyarchaeota/MCG-8 10 Bathyarchaeota/ MCG-6 5 Lokiarchaeota

Sequence similarities in % to Genbank matches are listed in **Supplementary Table 3**. Asterisks identify likely contaminants.

were affiliated to the genus *Arcobacter*, efficient CO_2 fixers in hypoxic sulfide-rich habitats that oxidize sulfide to produce elemental sulfur while surviving under severe electron acceptor limitation (Wirsen et al., 2002). The remaining sequences were affiliated with the sulfide-oxidizing, nitrate-, or sulfur-reducing genera *Sulfurimonas* and *Sulfurovum* (Campbell et al., 2006). Sequences affiliated with uncultured, presumably halophilic bacterial lineages from seafloor brine lakes (Bannock Brine Basin) were recovered in the Urania brine, and include the MSBL5 lineage within the Chloroflexi, and the MSBL2 lineage that is currently not closely affiliated with other bacteria (Daffonchio et al., 2006). Other bacterial community members were represented by small numbers of clones of most likely heterotrophic and/or fermentative groups among the Planctomycetes, Parcubacteria (Castelle et al., 2017), and Bacteroidetes (**Figure 3** and **Table 1**).

The archaeal sequences in the brine were dominated by anaerobic halophiles (**Figure 5** and **Table 1**). Archaeal 16S rRNA gene sequences in the Urania Basin brine were closely related to *Halodesulfoarchaeum formicicum*, a lithoheterotroph that oxidizes formate or H_2 with elemental sulfur, thiosulfate or DMSO as the electron acceptor, and to *Haloanaeroarchaeum*

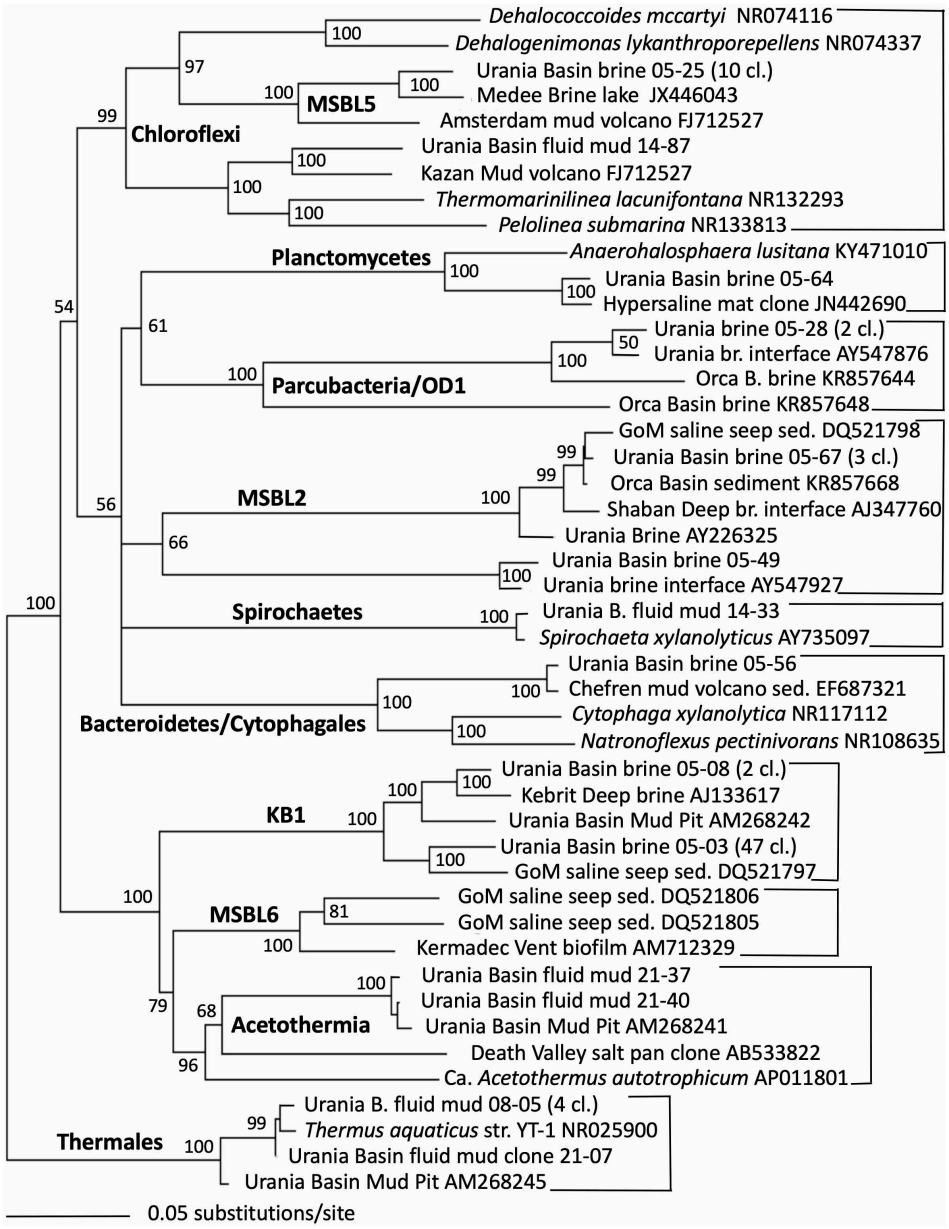

FIGURE 3
Phylogeny of general bacteria-affiliated 16S rRNA genes based on distance minimum evolution analysis and 1,000 neighbor-joining bootstrap iterations using PAUP (Swofford, 2000).

sulfureducans, which oxidizes acetate by sulfur respiration (Sorokin et al., 2018). The Urania Basin haloarchaeal counterparts to these cultured strict anaerobes are frequently recovered from the highly reducing and sulfide-rich Urania Basin brine. Other members of the archaeal brine community include members of the uncultured, presumably methanogenic MSBL1 lineage (Daffonchio et al., 2006) that grow potentially in syntrophy with KB1 bacteria (Yakimov et al., 2013), four clones of a MSBL1-related sister lineage, and a single clone of the heterotrophic Thermoprofundales (Zhou et al., 2019).

3.4 Microbial community of the Urania Basin fluid mud layers

The taxonomic affiliation of bacterial sequences in the fluid mud layers changed considerably from those in the brine layer, to such a degree that the clone libraries showed no overlap at all (**Figure 2** and **Table 1**). Instead of being affiliated with diverse sulfur-cycling delta- and epsilonproteobacteria and phylum-level halophilic lineages, most bacterial sequences of the three fluid mud layers comprised sequences specifically

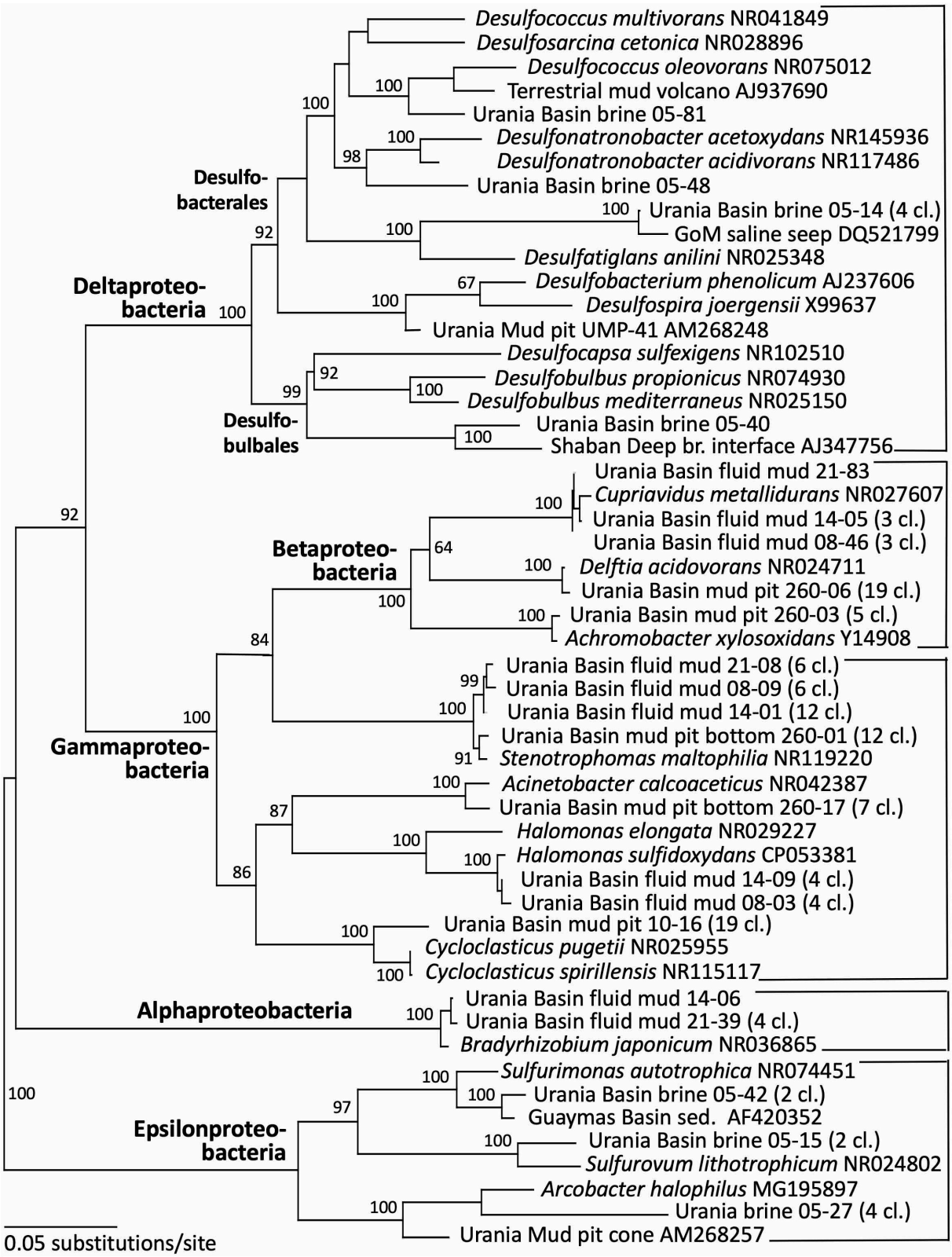

FIGURE 4
Phylogeny of the Proteobacteria-affiliated 16S rRNA genes based on distance minimum evolution analysis and 1,000 neighbor-joining bootstrap iterations using PAUP (Swofford, 2000).

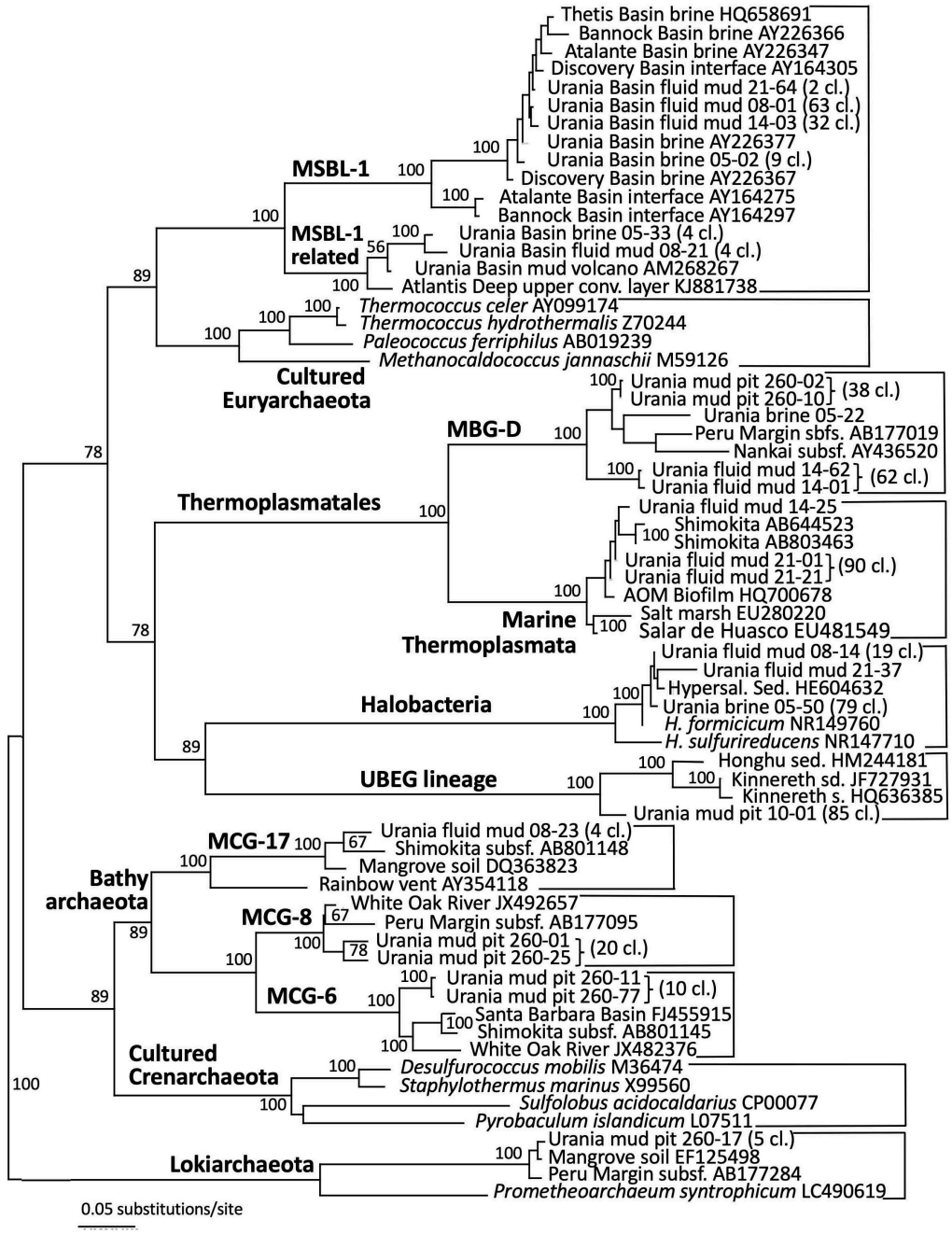

FIGURE 5
Phylogeny of the Archaea-affiliated 16S rRNA genes based on distance minimum evolution analysis and 1,000 neighbor-joining bootstrap iterations using PAUP (Swofford, 2000).

affiliated with genera of the family *Bacillaceae* within the Firmicutes (**Figure 6**). The upper fluid mud layer yielded a higher proportion of sequences affiliated with moderately halophilic and alkaliphilic *Bacillaceae* related to the genus *Piscibacillus* (Amoozegar et al., 2009), and—a little more distant but within the same monophyletic cluster—halophilic *Bacillaceae* of the genera *Terrilactibacillus*, *Halobacillus,* and *Pontibacillus* cultured from Urania Basin sediment (Sass et al., 2008). The halophile-related clones co-occur in the upper fluid mud layer with clones related to moderately thermophilic genera *Anoxybacillus* and *Geobacillus*, facultatively anaerobic chemoorganotrophs with a fermentative metabolism (Pikuta et al., 2000; Nazina et al., 2001). In the central and lower fluid mud layer, the halophile-related clones are no

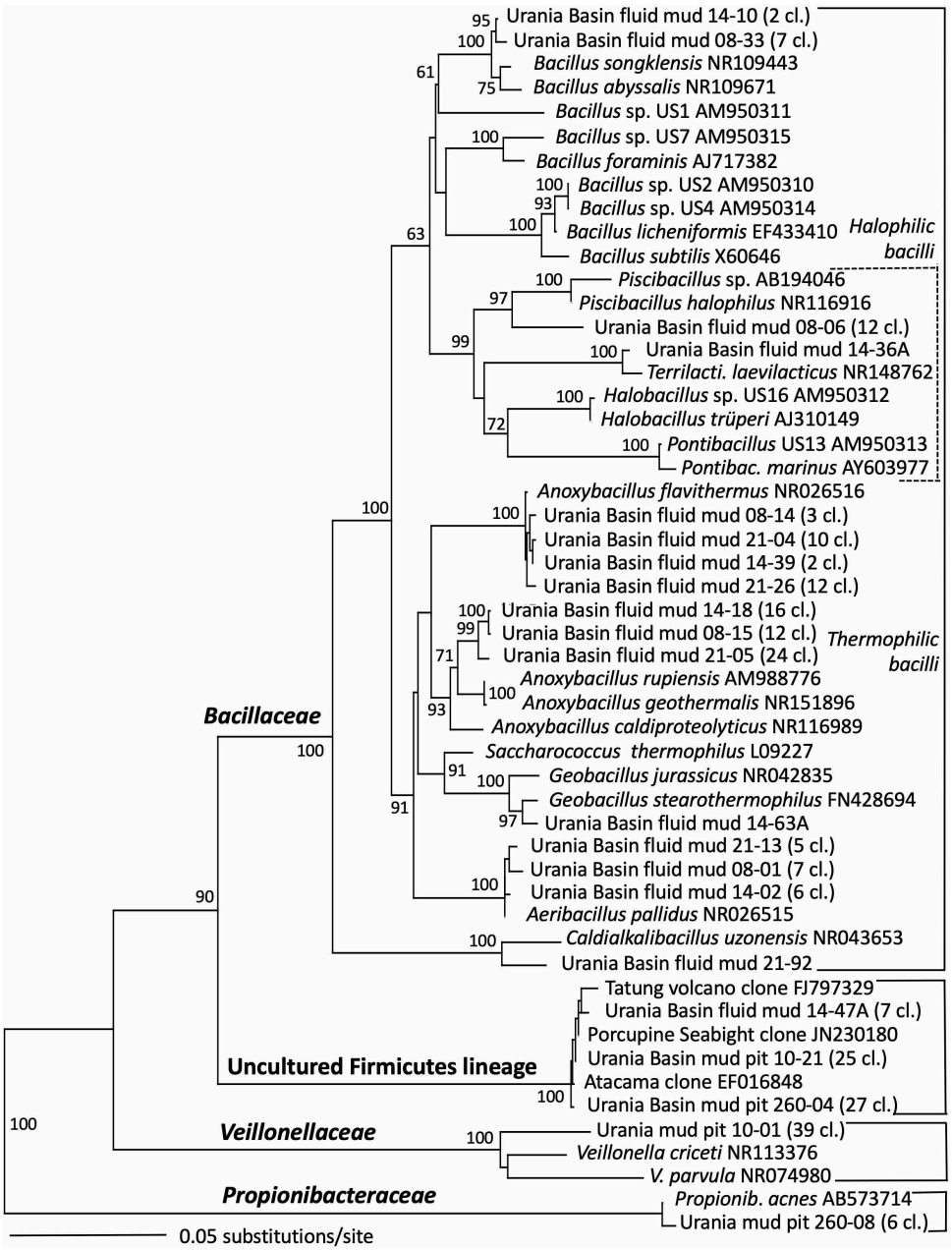

FIGURE 6
Phylogeny of the Firmicutes-affiliated 16S rRNA genes based on distance minimum evolution analysis and 1,000 neighbor-joining bootstrap iterations using PAUP (Swofford, 2000).

longer recovered, and the thermophilic lineages, especially *Anoxybacillus*, predominate. The *Anoxybacillus*-affiliated clones fall into two distinct clusters, one very similar to *Anoxybacillus flavithermus* (Pikuta et al., 2000), whereas the second and more frequently recovered cluster represents a sister lineage to the thermophilic, alkalitolerant, facultatively or strictly anaerobic species *A. rupiensis* and *A. geothermalis* (Filippidou et al., 2016). In contrast to the apparent halophile-thermophile transition, all fluid mud layers yielded almost equal numbers of clones affiliated with the thermophilic, alkalitolerant, but aerobic species *Geobacillus pallidus*, recently renamed *Aeribacillus pallidus* (Miñana-Galbis et al., 2010). We speculate that these populations represent a terrestrial import that remains detectable due to endospore formation.

Other *Bacillaceae*-affiliated lineages were recovered less frequently, or in only a single layer. Clones related to the marine species *Bacillus songklensis* (Kang et al., 2013) and *Bacillus abyssalis* (You et al., 2013) of the thermophilic,

endospore-forming genus *Bacillus* were recovered from the upper and middle fluid mud horizon. A sequence each from the middle and bottom layer of the mud fluid were affiliated with the thermophilic, heterotrophic, alkalitolerant, and hydrocarbon-degrading species *Geobacillus stearothermophilus* (Nazina et al., 2001) and *Caldalkalibacillus uzonensis* (Zhao et al., 2008), respectively. Further, the central mud layer yielded clones of an uncultured Firmicutes lineage that has consistently close Genbank matches in diverse marine and terrestrial sediment and subsurface environments, and thus appears to represent an evolutionary lineage with a preference for these habitats (**Figure 6** and **Table 1**).

Gamma-, Beta- and Alphaproteobacterial clones formed the second major bacterial group detected in the fluid mud layers, affiliated with the genera *Delftia*, *Cupriavidus*, *Stenotrophomonas*, *Halomonas* and *Bradyrhizobium* (**Figure 4** and **Table 1**). Of these, the genus *Halomonas* (Vreeland et al., 1980) consisting of halotolerant or halophilic, aerobic or facultatively anaerobic isolates from diverse saline environments, occurs specifically in marine environments (Wang and Shao, 2021, and refs. therein). The *Halomonas* clones are closely related to *Halomonas sulfidoxydans*, a highly sulfide-tolerant marine sediment species that oxidizes sulfide aerobically or with nitrate or N_2O as electron acceptor (Wang and Shao, 2021). *Rhizobium* strains were among the most consistently isolated bacteria from subsurface Mediterranean sapropels (Suess et al., 2004, 2006). In contrast, the hydrocarbon-degrading freshwater and soil bacterium and opportunistic pathogen *Delftia* (Wen et al., 1999; Højgaard et al., 2022), the heavy metal-resistant soil bacterium *Cupriavidus* (Vandamme and Coenye, 2004) and the plant-and human-associated bacterium *Stenotrophomonas* (Ryan et al., 2009) lack marine or subsurface associations. We caution that these sequences were most likely introduced as contaminants during handling of samples, reagents or PCRs, and we are reporting them to provide reference sequences for critical evaluations of microbial community surveys in extreme habitats (**Table 1**).

The upper and lower mud fluid samples yielded sequences related to *Thermus aquaticus,* a heterotrophic, thermophilic bacterium from thermal springs in Yellowstone National Park that uses several sugars and organic acids as carbon sources (Brock and Freeze, 1969). The genus contains aerobic as well as facultatively anaerobic strains, for example a facultatively anaerobic *Thermus* sp. isolated from South African Gold mines oxidizes organic compounds such as lactate with Fe (III) and/or Mn (IV) as electron acceptors (Kieft et al., 1999). Sequences affiliated with *Thermus* sp. were reported independently at 3,727 m depth in the deep fluid mud of the Urania Basin mud volcano (Yakimov et al., 2007), indicating that this thermophile is indeed a member of this microbial ecosystem.

The archaeal profile of the mud layers shows a transition from predominantly *Halodesulfoarchaeum*- and MSBL-1-affiliated clones in the top layer toward uncultured Thermoplasmatales lineages, specifically the Thermoprofundales [formerly Marine Benthic Group D (MBG-D)] in the middle layer and a previously undescribed Thermoplasmata lineage in the bottom layer (**Figure 4** and **Table 1**). Extensive Genbank searches and comparisons with published phylogenies specified the phylogenetic position of the Urania Basin clones within the globally distributed and highly diverse Thermoplasmatales. The clones from the middle mud layer were affiliated with the marine sediment subclusters 6, 7, and 8 of the Thermoprofundales (Zhou et al., 2019), indicating tolerance to marine salinity at a minimum. MBG-D sequences have previously been found in abundance in hypersaline, sulfidic methane seep sediments in the Gulf of Mexico (Lloyd et al., 2006), and MBG-D was the major archaeal group in highly sulfidic anoxic sediments of the Salton Sea (Swan et al., 2010). The marine Thermoplasmata clones of the lower mud layer represented a sister lineage of the uncultured DHVE-9/20c-4 clade (Durbin and Teske, 2012) that was originally found at hydrothermal vents (Pagé et al., 2004). Genomic reconstruction has predicted that marine subsurface Thermoplasmatales are involved in detrital matter degradation, as well as acetogenesis (Lloyd et al., 2013; Lazar et al., 2017). The Urania Basin phylotypes were only distantly related to cultured sulfur-and iron-reducing Thermoplasmatales, for example the genera *Thermoplasma*, *Picrophilus*, or *Aciduliprofundum*.

Detection of MSBL1 archaea-related sequences is consistent with previous observations of this group in Urania Basin mud fluids (Yakimov et al., 2007) and the brine lake of the Urania Basin (van der Wielen et al., 2005). The MSBL1 archaea have been detected in many hypersaline environments, such as an endoevaporitic microbial mat (Sørensen et al., 2005), the Bannock, Urania and Thetis brine lakes (Daffonchio et al., 2006; Borin et al., 2009; La Cono et al., 2011), or Tunisian multipond solar salterns (Baati et al., 2008).

3.5 Microbial community of the Urania Basin subseafloor sediments

Sequences from the subseafloor sediments (the "mud pit") differed considerably from those in the overlying fluid mud layers and brine (**Figure 2**). The uncultured subsurface Firmicutes lineage-affiliated clones that were previously identified in the middle fluid mud layer occurred in larger proportions in both subseafloor sediment samples (**Figure 6** and **Table 1**). The upper gravity core sediments (10–30 cm) yielded sequences affiliated with the fermentative, anaerobic genus *Veillonella*, a widely occurring inhabitant of animal and human intestinal and oral mucosa and an unlikely community member of Urania Basin (van den Bogert et al., 2013). The lower core section (260–280 cmbsf) yielded sequences closely related to the fermentative Actinobacterium *Propionibacterium acnes*, reclassified as *Cutibacterium acnes*, a common epibiont

on human skin (Scholz and Kilian, 2016). Due to their likely human origin, we regard the *Veillonella* and *Cutibacterium* sequences as contaminants.

Gammaproteobacterial sequences recovered from the upper gravity core sediments (10–30 cmbsf) were affiliated with the genus *Cycloclasticus*, which utilizes various aromatic hydrocarbons such as naphthalene, phenanthrene, biphenyltoluene, xylene or pyrene as the sole carbon and energy source (Wang et al., 2008; Lai et al., 2012). Cultured representatives of the genus *Cycloclasticus* are strictly aerobic, but their counterparts in anaerobic Urania Basin sediments might represent a related but distinct anaerobic group, compatible with the sequence divergence (*ca.* 4%) between the cultured strains the Urania Basin clones (**Figure 4**). Clones from the deeper core section (260–280 cmbsf) were affiliated with the gammaproteobacterial genus *Acinetobacter*, capable of hydrocarbon degradation in hydrocarbon-polluted soils or in oilfield production liquids (Chaîneau et al., 1995; Gong et al., 2012). Sequences of the gamma- and betaproteobacterial genera *Stenotrophomonas* (associated with human clinical samples; Ryan et al., 2009), *Delftia* (an opportunistic emergent pathogen; Højgaard et al., 2022) and *Achromobacter* (described from human sample material; Yabuuchi and Yano, 1981), were found in the deep gravity core sample (260–280 cmbsf) and represent likely contaminants from human contact and handling in the lab.

Archaeal sequence datasets from the upper layers of the gravity core (10–30 cmbsf) were exclusively composed of an uncultured Euryarchaeotal Group (**Figure 5**). This lineage is not phylogenetically close to any known cultured or uncultured archaeal lineage, and the closest uncultured clones were retrieved from lake sediments or Arctic thermal springs. Extensive chimera checks of whole and partial sequences did not uncover any evidence for a mosaic sequence; all sections of the 16S rRNA gene remained ≈15% different from other sequences in Genbank. We called this group Urania Basin Euryarchaeota Group (UBEG).

The deeper gravity core sample (260–280 cmbsf) was dominated by the same uncultured Thermoprofundales lineage as in the middle fluid mud layer, and by heterotrophic, anaerobic and presently uncultured Bathyarchaeota of the MCG-6 and MCG-8 subgroups (Kubo et al., 2012). These Bathyarchaeota were distinct from the subgroup MCG-17 clones that were recovered in the upper fluid mud layer (**Figure 5**). Of these subgroups, MCG-6 has a wide environmental distribution in soil, hot springs, estuarine and marine sediments, whereas MCG-8 and MCG-17 are specifically associated with estuarine and marine sediments (Xiang et al., 2016). Finally, sequences affiliated with the Lokiarchaeota (Spang et al., 2015) were found in smaller numbers. Mixed archaeal communities of Thermoplasmatales, Bathyarchaeota and Lokiarchaeota are characteristic for marine sediments, and were already found in the first major sequencing survey of marine deep-sea sediments (Vetriani et al., 1999).

4 Discussion

The bacterial and archaeal communities of the Urania Basin brine fluids, fluid mud layers and deep sediments show characteristic, habitat-related trends as they change throughout the sample series, after discounting contaminant sequences affiliated to bacteria associated with medical, human, or animal samples (*Achromobacter*, *Delfia*, *Propionibacterium, Stenotrophomonas*, *Veillonellaceae*) or terrestrial soil (*Cupriavidus*). Sequences affiliated with sulfur-cycling Epsilon- and Deltaproteobacteria, extremely halophilic KB1 bacteria, and extremely halophilic *Halodesulfoarchaeum* spp. in the brine are replaced by sequences affiliated with diverse Firmicutes, and by halophilic archaea (putatively methanogenic MSBL-1) and Thermoplasmatales in the fluid mud layers. Toward deeper fluid mud layers the Firmicutes change from halophilic (*Piscibacillus*) to thermophilic (*Anoxybacillus*) lineages, and the Archaea change from extreme halophiles (*Halodesulfoarchaeum* and MSBL1) toward subsurface sediment lineages (Thermoprofundales and Thermoplasmata). Finally, the deep subsurface sediment below the mud volcano retains sequences related to uncultured Firmicutes, hydrocarbon-degrading Gammaproteobacteria (*Cycloclasticus* spp., *Acinetobacter* spp.), and marine subsurface archaea of the Bathyarchaeota, Thermoprofundales, and Lokiarchaeota, plus an unidentified archaeal group that appears only in the upper gravity core sample. Nearly all bacterial and archaeal clones are affiliated to heterotrophic groups, indicating that this downward microbial succession (brine—fluid mud—subsurface sediment) degrades organic substrates and hydrocarbons that are available in the brine, fluid mud layers, and subsurface sediment.

The mud volcano fluids and subsurface sediment microbial communities resemble each other in the presence of gram-positive, sometimes thermophilic, and presumably spore-forming genera and families within the phylum Firmicutes. Thus, the Urania Basin sediment microbiota provide an illustrative example for a "firmicute hotspot," the previously postulated point sources that distribute endospore-forming, moderately thermophilic Firmicutes across cold marine sediments world-wide (Hubert et al., 2009; Müller et al., 2014; Gittins et al., 2022). These spore-forming bacteria require a certain minimum temperature but cannot grow in deep-sea surficial sediments that are permanently cold. Possible sources include hydrothermal vents, mud volcanoes, and terrestrial sedimentation. Hydrothermal vents have generally very low proportions of gram-positive bacteria, which require lab enrichment for detection (Castro et al., 2021). Terrestrial imports appear likely in some coastal locations (Lee et al., 2005). However, mud volcanoes are the most promising source of

these widespread seafloor thermophiles (Rattray et al., 2022). The Urania Basin Mud volcano, prone to occasional eruptions (Hübner et al., 2003) adds to the database of sources for widely spread gram-positive bacteria in the deep-sea. We speculate further that the carbon and energy source for at least some of these Firmicutes might be petroleum-derived hydrocarbons of deep subsurface origin, since polyaromatic compounds and long-chain alkanes are abundant in the fluidized mud and subseafloor sediment of Urania Basin.

The high contribution of gram-positive Firmicutes in this study stands in contrast to the near-absence of gram-positive bacteria (a single Actinomycete clone) in a previous survey of the Urania mud volcano (Yakimov et al., 2007). These differences might reflect different nucleic acid extraction protocols and PCR targets: chemical extraction of RNA *via* QIAGEN RNA/DNA mini extraction kit followed by reverse transcription to cDNA (Yakimov et al., 2007) vs. bead-beating cell breakage before kit-based DNA extraction and column purification in this study. The mechanical force of bead-beating has very likely increased the recovery of DNA from spore-forming gram-positive bacteria. When bead-beating techniques are used for cell disruption and DNA extraction, gram-positive spore-forming bacteria are recovered from diverse marine sediments (for example, Teske et al., 2002). We note that any DNA-based study might include dead or dormant cells. We also note that the previous study did not involve a nested PCR approach (Yakimov et al., 2007), and thus avoided a likely source of contaminating sequences.

Active sulfur and methane cycling characterize the brine/seawater transition of Urania Basin, where seawater sulfate and subsurface methane overlap (Borin et al., 2009). At present, our data do not rule out active sulfur and methane cycling in the deep brine and the mud volcano fluid. Although the PCR data of this study indicate that sequences affiliated with microbial taxa involved in sulfur cycling appear to be limited to the brine layer, sequences related to sulfur-oxidizing Epsilon- and sulfate-reducing Deltaproteobacteria have been recovered as dominant and active groups by rRNA transcript sequencing from deep fluid mud of Urania Basin (Yakimov et al., 2007). The mud volcano sediments and the overlying brine contain millimolar amounts of methane and sulfate (Borin et al., 2009; Zabel, 2012) and would in principle allow sulfate-dependent methane oxidation to take place. Although anaerobic sulfate-dependent methane-oxidizing archaea (ANME) were not found in this survey, they were detected as a single clone in the deep mud volcano fluid (Yakimov et al., 2007). Few studies have reported on ANME archaea in hypersaline environments. ANME-1 archaea were detected in a moderately briny, sulfidic methane seep in the Gulf of Mexico (Lloyd et al., 2006), and (in low numbers) in the bottom sediments of Orca Basin in the Gulf of Mexico (Nigro et al., 2020). ANME1 and ANME2 archaea were found in the Red Sea seafloor brine lakes (Atlantis II and Discovery Deep), predominantly in a sediment sample with high total sulfur content (Siam et al., 2012). A consensus reading of the available data indicates that small populations of ANME archaea exist in hypersaline basins and in the Urania Basin mud volcano, but these hard-to-find sequences are not comparable to the global microbial community signature of marine methane seeps, methane/sulfate interfaces or methane-rich subsurface sediments that are dominated by ANME archaea and deltaproteobacterial sulfate reducers (Ruff et al., 2015). Accordingly, we do not observe any evidence of decreasing concentrations of ^{13}C-isotope enrichments in the methane pool.

Overall, this study highlights the diversity of bacteria and archaea thriving in the extremely harsh conditions of the Urania Basin brine lake and mud volcano. Further activity measurement or culture-based experiments could help understand which microbial metabolisms play a role in the Urania Basin, or how the microbes work together to survive in such an environment.

Data availability statement

The datasets presented in this study can be found in online repositories. The names of the repository/repositories and accession number(s) can be found in the article/ **Supplementary material**.

Author contributions

CL collected Urania Basin samples, extracted DNA, performed PCR amplification, cloned the PCR amplicons, and submitted them for sequencing, performed the first set of phylogenetic analyses, and wrote the first version of this manuscript. FS, ME, and VH performed and tabulated geochemical analyses of Urania Basin samples, including the methane and ethane analyses. K-UH obtained funding for the DARC LIFE project and for the Expedition to Urania Basin and developed the scientific rationale for sampling site selection. AT advised CL on the sequencing project, prepared the phylogenetic trees in this manuscript, and wrote the second version of the manuscript. All authors revised and finalized the manuscript.

Funding

This study was funded by the European Research Council under the European Union's Seventh Framework Programme-Ideas Specific Programme; by (ERC Grant agreement no. 247153) (Advanced Grant DARCLIFE; principal investigator, K-UH). Current subsurface research in the Teske Lab was supported by the NSF-BIO 2048489 and by NASA Exobiology award A22-0244-001 (UNC subcontract).

Acknowledgments

We would like to thank the chief scientist Matthias Zabel, officers and crew of R/V *Meteor* cruise M84-1 (DARCSEAS I), as well as the shipboard scientific community for their help at sea.

Conflict of interest

The authors declare that the research was conducted in the absence of any commercial or financial relationships that could be construed as a potential conflict of interest.

Publisher's note

All claims expressed in this article are solely those of the authors and do not necessarily represent those of their affiliated organizations, or those of the publisher, the editors and the reviewers. Any product that may be evaluated in this article, or claim that may be made by its manufacturer, is not guaranteed or endorsed by the publisher.

Supplementary material

The Supplementary Material for this article can be found online at: https://www.frontiersin.org/articles/10.3389/fmicb.2022.1043414/full#supplementary-material

SUPPLEMENTARY TABLE 1
Concentration and ^{13}C stable isotope values of methane and ethane in Urania Basin brine, fluid mud, and subsurface sediment samples.

SUPPLEMENTARY TABLE 2
Concentrations of hydrocarbons in the subseafloor of the Urania Basin. PAH/HC, portion of polyaromatic hydrocarbons relative to sum of all identified hydrocarbons; Thermal HC/HC, portion of thermally altered hydrocarbons relative to sum of all identified hydrocarbons.

SUPPLEMENTARY TABLE 3
Similarities of Urania Basin phylotypes and related sequences of pure cultures and environmental phylotypes. Genbank numbers for bacteria and archaea are: OP389385-OP389468 and OP389469-OP389561 in sample 5; OP352680-OP352749 and OP389299-OP389384 in sample 8; OP352780-OP389844 and OP389717-OP389809 in sample 14; OP389562-OP389631 and OP389897-OP389989 in sample 21; OP352539-OP352606, OP389632-OP389716, and OP856603-OP856618 in sample GC-10-30; OP352609-OP352677, OP389811-OP389896, and OP856619-OP856629 for sample GC-260-280.

SUPPLEMENTARY DATA SHEET 1
Supplementary methods.

References

Aiello, I. W., Beaufort, L., Goldhammer, T., Heuer, V. B., Hinrichs, K.-U., and Zabel, M. (2020). Anatomy of a 'suspended' seafloor in the dense brine waters of the deep hypersaline Urania basin. *Deep Sea Res. II* 171:104626. doi: 10.1016/j.dsr2.2019.07.014

Aloisi, G., Cita, M. B., and Castradori, D. (2006). Sediment injection in the pit of the Urania anoxic brine lake (Eastern Mediterranean). *Rend. Lincei Sci. Fis.* 17, 243–262. doi: 10.1007/BF02904765

Amoozegar, M. A., Sánchez-Porro, C., Rohban, R., Hajighasemi, M., and Ventosa, A. (2009). *Piscibacillus halophilus* sp. nov., a moderately halophilic bacterium from a hypersaline Iranian lake. *Int. J. Syst. Evol. Microbiol.* 59, 3095–3099. doi: 10.1099/ijs.0.012013-0

Antunes, A., Ngugi, D. K., and Stingl, U. (2011). Microbiology of the Red Sea (and other) deep-sea anoxic brine lakes. *Environ. Microbiol. Rep.* 3, 416–433. doi: 10.1111/j.1758-2229.2011.00264.x

Baati, H., Guermazi, S., Amdouni, R., Gharsalla, N., Sghir, A., and Ammar, E. (2008). Prokaryotic diversity of a Tunisian multipond solar saltern. *Extremophiles* 12, 505–518. doi: 10.1007/s00792-008-0154-x

Boehrer, B. (2012). "Double-diffusive convection in lakes," in *Encyclopedia of lakes and reservoirs. Encyclopedia of earth sciences series*, eds L. Bengtsson, R. W. Herschy, and R. W. Fairbridge (Dordrecht, NL: Springer).

Borin, S., Brusetti, L. F., Mapelli, G., D'Auria, T., Brusa, M., Marzorati, A., et al. (2009). Sulfur cycling and methanogenesis primarily drive microbial colonization of the highly sulfidic Urania deep hypersaline basin. *Proc. Natl. Acad. Sci. U.S.A.* 106, 9151–9156. doi: 10.1073/pnas.0811984106

Brock, T. D., and Freeze, H. (1969). *Thermus aquaticus* gen. n. and sp. n., a nonsporulating extreme Thermophile. *J. Bacteriol.* 98, 289–297. doi: 10.1128/jb.98.1.289-297.1969

Campbell, B. J., Engel, A. S., Porter, M. L., and Takai, K. (2006). The versatile epsilon-proteobacteria: Key players in sulphidic habitats. *Nat. Rev. Microbiol.* 6, 458–468. doi: 10.1038/nrmicro1414

Casamayor, E. O., Schäfer, H., Baneras, L., Salio, C. P., and Muyzer, G. (2000). Identification of and spatio-temporal differences between microbial assemblages from two neighboring sulfurous lakes: Comparison by microscopy and denaturing gradient gel electrophoresis. *Appl. Environ. Microbiol.* 66, 499–508. doi: 10.1128/AEM.66.2.499-508.2000

Castelle, C. J., Brown, C. T., Thomas, B. C., Williams, K. H., and Banfield, J. F. (2017). Unusual respiratory capacity and nitrogen metabolism in a *Parcubacterium* (OD1) of the candidate phyla radiation. *Sci. Rep.* 7:40101. doi: 10.1038/srep40101

Castro, S. P., Borton, M. A., Regan, K., Hrabe de Angelis, I., Wrighton, K. C., Teske, A. P., et al. (2021). Degradation of biological macromolecules supports uncultured microbial populations in Guaymas Basin hydrothermal sediments. *ISME J.* 15, 3480–3497. doi: 10.1038/s41396-021-01026-5

Chaîneau, C.-H., Morel, J.-L., and Oudot, J. (1995). Microbial degradation in soil microcosms of fuel oil hydrocarbons from drilling cuttings. *Environ. Sci. Technol.* 29, 1615–1621. doi: 10.1021/es00006a027

Charlou, J. L., Donval, J. P., Zitter, T., Roy, N., Jean-Baptiste, P., Foucher, J. P., et al. (2003). Evidence of methane venting and geochemistry of brines on mud volcanoes of the Eastern Mediterranean Sea. *Deep Sea Res.* 50, 941–958. doi: 10.1016/S0967-0637(03)00093-1

Corselli, C., Basso, D., de Lange, G., and Thomson, J. (1996). Mediterranean ridge accretionary complex yields rich surprises. *EOS* 77, 227–227. doi: 10.1029/96EO00159

D'Hondt, S. L., Jørgensen, B. B., and Miller, D. J. (2003). *Proc. ODP, Init. Repts., 201*. College Station, TX: Ocean Drilling Program.

Daffonchio, D., Borin, S., Brusa, T., Brusetti, L., van der Wielen, P. W., Bolhuis, H., et al. (2006). Stratified prokaryote network in the oxic–anoxic transition of a deep-sea halocline. *Nature* 440, 203–207. doi: 10.1038/nature04418

Durbin, A. M., and Teske, A. (2012). Archaea in organic-lean and organic-rich marine subsurface sediments: An environmental gradient reflected in distinct phylogenetic lineages. *Front. Microbiol.* 3:168. doi: 10.3389/fmicb.2012.00168

Eder, W., Jahnke, L. L., and Huber, R. (2001). Microbial diversity of the brine-seawater interface of the Kebrit deep, Red Sea, studied via 16S rRNA gene sequences and cultivation methods. *Appl. Environ. Microbiol.* 67, 3077–3085. doi: 10.1128/AEM.67.7.3077-3085.2001

Eder, W., Ludwig, W., and Huber, R. (1999). Novel 16S rRNA gene sequences retrieved from highly saline brine sediments of Kebrit deep, Red Sea. *Arch. Microbiol.* 172, 213–218. doi: 10.1007/s002030050762

Eder, W., Schmidt, M., Koch, M., Garbe-Schönberg, D., and Huber, R. (2002). Prokaryotic phylogenetic diversity and corresponding geochemical data of the brine–seawater interface of the Shaban deep, Red Sea. *Environ. Microbiol.* 4, 758–763. doi: 10.1046/j.1462-2920.2002.00351.x

Ferrer, M., Werner, J., Chernikova, T. N., Bargiela, R., Fernández, L., La Cono, V., et al. (2012). Unveiling microbial life in the new deep-sea hypersaline Lake Thetis. Part II: A metagenomic study. *Environ. Microbiol.* 14, 268–281. doi: 10.1111/j.1462-2920.2011.02634.x

Filippidou, S., Jaussi, M., Junier, T., Wunderlin, T., Jeanneret, N., Plamieri, F., et al. (2016). *Anoxybacillus geothermalis* sp. nov., a facultatively anaerobic, endospore-forming bacterium isolated from mineral deposits in a geothermal station. *Int. J. Syst. Evol. Microbiol.* 66, 2944–2951. doi: 10.1099/ijsem.0.001125

Fusi, N., Aloisi de Larderel, G., Borello, A., Amelio, O., Castradori, D., Negri, A., et al. (1996). Marine geology of the MEDRIFF corridor, Mediterranean Ridge. *Isl. Arc* 5, 420–439. doi: 10.1111/j.1440-1738.1996.tb00163.x

Gittins, D. A., Desiage, P.-A., Morrison, N., Rattray, J. E., Bhatnagar, S., Chakraborty, A., et al. (2022). Geological processes mediate a microbial dispersal loop in the deep biosphere. *Sci. Adv.* 8:eabn3485. doi: 10.1126/sciadv.abn3485

Gong, X. C., Liu, Z. S., Guo, P., Chi, C. Q., Chen, J., Wang, X. B., et al. (2012). Bacteria in crude oil survived autoclaving and stimulated differentially by exogenous bacteria. *PLoS One* 7:e40842. doi: 10.1371/journal.pone.0040842

Hall, T. A. (1999). BioEdit: A user-friendly biological sequence alignment editor and analysis program for Windows 95/98/NT. *Nucl. Acids Symp. Ser.* 41, 95–98.

Heuer, H., Krsek, M., Baker, P., Smalla, K., and Wellington, E. M. (1997). Analysis of actinomycetes communities by specific amplification of genes encoding 16S rRNA and gel-electroophoretic separation in denaturating gradients. *Appl. Environ. Microbiol.* 63, 3233–3241. doi: 10.1128/aem.63.8.3233-3241.1997

Højgaard, S. M. M., Rezahosseini, O., Knudsen, J. D., Fuglebjerg, N. J. U. M., Skov, M., Nielsen, S. D., et al. (2022). Characteristics and outcomes of patients with *Delftia acidovorans* infections: A retrospective cohort study. *Microbiol. Spectr.* 10:e0032622. doi: 10.1128/spectrum.00326-22

Hoshino, T., Toki, T., Ijiri, A., Morono, Y., Machiyama, H., Ashi, J., et al. (2017). Atribacteria from the subseafloor sedimentary biosphere disperse to the hydrosphere through submarine mud volcanoes. *Front. Microbiol.* 8:1135. doi: 10.3389/fmicb.2017.01135

Hubert, C., Loy, A., Nickel, M., Arnosti, C., Baranyi, C., Brüchert, V., et al. (2009). A constant flux of diverse thermophilic bacteria into the cold arctic seabed. *Science* 325, 1541–1544. doi: 10.1126/science.1174012

Hübner, A., De Lange, G. J., Dittmer, J., and Halbach, P. (2003). Geochemistry of an exotic sediment layer above sapropel S-1: Mud expulsion from the Urania Basin, Eastern Mediterranean? *Mar. Geol.* 197, 49–61. doi: 10.1016/S0025-3227(03)00085-9

Joye, S. B., Samarkin, V. A., Orcutt, B. N., MacDonald, I. R., Hinrichs, K.-U., Elvert, M., et al. (2009). Metabolic variability in seafloor brines revealed by carbon and sulphur dynamics. *Nat. Geosci.* 2, 349–354. doi: 10.1038/ngeo475

Kang, H., Weerawongwiwat, V., Kim, J.-H., Sukhoom, A., and Kim, W. (2013). *Bacillus songklensis* sp. nov., isolated from soil. *Int. J. Syst. Evol. Microbiol.* 63, 4189–4195. doi: 10.1099/ijs.0.050682-0

Karisiddaiah, S. M. (2000). Diverse methane concentrations in anoxic brines and underlying sediments, eastern Mediterranean Sea. *Deep Sea Res. I* 47, 1999–2008. doi: 10.1016/S0967-0637(00)00010-8

Kieft, T. L., Fredrickson, J. K., Onstott, T. C., Gorby, Y. A., Kostandarithes, H. M., Bailey, T. J., et al. (1999). Dissimilatory reduction of Fe(III) and other electron acceptors by a *Thermus* isolate. *Appl. Environ. Microbiol.* 65, 1214–1221. doi: 10.1128/AEM.65.3.1214-1221.1999

Kopf, A., Robertson, A. H. F., Clennell, M. B., and Flecker, R. (1998). Mechanism of mud extrusion on the Mediterranean Ridge accretionary complex. *Geo Mar. Lett.* 18, 97–114. doi: 10.1007/s003670050058

Kubo, K., Lloyd, K. G., Biddle, J. F., Amann, R., Teske, A., and Knittel, K. (2012). Archaea of the miscellaneous crenarchaeotal group (MCG) are abundant, diverse and widespread in marine sediments. *ISME J.* 6, 1949–1965. doi: 10.1038/ismej.2012.37

Kuever, J., Rainey, F. A., and Widdel, F. (2005). "Order III. Desulfobacterales ord. nov.: Family II. Desulfobulbaceae ord. nov. fam. nov," in *Bergey's manual of systematic bacteriology*, eds G. Garrity, D. Brenner, N. Krieg, et al. (Berlin: Springer), 988–998.

La Cono, V., Smedile, F., Bortoluzzi, G., Arcadi, E., Maimone, G., Messina, E., et al. (2011). Unveiling microbial life in new deep-sea hypersaline Lake Thetis. Part I: Prokaryotes and environmental settings. *Environ. Microbiol.* 13, 2250–2268. doi: 10.1111/j.1462-2920.2011.02478.x

Lai, Q., Li, W., Wang, B., Yu, Z., and Shao, Z. (2012). Complete genome sequence of the pyrene-degrading bacterium *Cycloclasticus* sp. strain P1. *J. Bacteriol.* 194:6677. doi: 10.1128/JB.01837-12

Langille, M., Zaneveld, J., Caporaso, J., MacDonald, D., Knights, D., Reyes, J. A., et al. (2013). Predictive functional profiling of microbial communities using 16S rRNA marker gene sequences. *Nat. Biotechnol.* 31, 814–821. doi: 10.1038/nbt.2676

Lazar, C. S., Baker, B. J., Seitz, K., Hinrichs, K.-U., and Teske, A. (2017). Genomic reconstruction of multiple lineages of uncultured benthic archaea suggests distinct biogeochemical roles and ecological niches. *ISME J.* 11, 1118–1129. doi: 10.1038/ismej.2016.189

Lazar, C. S., L'Haridon, S., Pignet, P., and Toffin, L. (2011a). Archaeal populations in hypersaline sediments underlying orange microbial mats in the Napoli mud volcano. *Appl. Environ. Microbiol.* 77, 3120–3131. doi: 10.1128/AEM.01296-10

Lazar, C. S., Parkes, R. J., Cragg, B. A., L'Haridon, S., and Toffin, L. (2011b). Methanogenic diversity and activity un hypersaline sediments of the centre of the Napoli mud volcano, Eastern Mediterranean Sea. *Environ. Microbiol.* 13, 2078–2091. doi: 10.1111/j.1462-2920.2011.02425.x

Lazar, C. S., Parkes, R. J., Cragg, B. A., L'Haridon, S., and Toffin, L. (2012). Methanogenic activity and diversity in the centre of the Amsterdam mud volcano, Eastern Mediterranean Sea. *FEMS Microbiol. Ecol.* 81, 1–12. doi: 10.1111/j.1574-6941.2012.01375.x

Lee, Y.-J., Wagner, I. D., Brice, M. E., Kevbrin, V. V., Mills, G. L., Romanek, C. S., et al. (2005). Thermosediminibacter oceani gen. nov., sp. nov., and Thermosediminibacter litoperuensis sp. nov., new anaerobic thermophilic bacteria isolated from Peru Margin. *Extremophiles* 9, 375–383. doi: 10.1007/s00792-005-0453-4

Lloyd, K. G., Lapham, L., and Teske, A. (2006). An anaerobic methane-oxidizing community of ANME-1 archaea in hypersaline Gulf of Mexico sediments. *Appl. Environ. Microbiol.* 72, 7218–7230. doi: 10.1128/AEM.00886-06

Lloyd, K. G., Schreiber, L., Petersen, D. G., Kjeldsen, K. U., Lever, M. A., Steen, A. D., et al. (2013). Predominant archaea in marine sediments degrade detrital proteins. *Nature* 496, 215–218. doi: 10.1038/nature12033

Ludwig, W., Strunk, O., Westram, R., Richter, L., Meier, H., Buchner, A., et al. (2004). ARB: A software environment for sequence data. *Nucleic Acids Res.* 32, 1363–1371. doi: 10.1093/nar/gkh293

McDonald, I. R., Buthman, D. B., Sager, W. W., Peccini, M. B., and Guinasso, N. L. (2000). Pulsed oil discharge from a mud volcano. *Geology* 28, 907–910. doi: 10.1130/0091-7613(2000)28<907:PODFAM>2.0.CO;2

Miñana-Galbis, D., Pinzón, D. L., Lorén, J. G., Manresa, Á, and Oliart-Ros, R. M. (2010). Reclassification of *Geobacillus pallidus* (Scholz et al. 1988) Banat et al. 2004 as *Aeribacillus pallidus* gen. nov., comb. nov. *Int. J. Syst. Evol. Microbiol.* 60, 1600–1604. doi: 10.1099/ijs.0.003699-0

Müller, A. L., de Rezende, J. R., Hubert, C. R. J., Kjeldsen, K. U., Lagkouvardos, I., Berry, D., et al. (2014). Endospores of thermophilic bacteria as tracers of microbial dispersal by ocean currents. *ISME J.* 8, 1153–1165. doi: 10.1038/ismej.2013.225

Nazina, T. N., Tourova, T. P., Poltaraus, A. B., Novikova, E. V., Grigoryan, A. A., Ivanova, A. E., et al. (2001). Taxonomic study of aerobic thermophilic bacilli: Descriptions of *Geobacillus subterraneus* gen. nov., sp. nov. and *Geobacillus uzenensis* sp. nov. from petroleum reservoirs and transfer of *Bacillus stearothermophilus*, *Bacillus thermocatenulatus*, *Bacillus thermoleovorans*, *Bacillus kaustophilus*, *Bacillus thermodenitrificans* to *Geobacillus* as the new combinations *G. stearothermophilus*. *Int. J. Syst. Evol. Microbiol.* 51, 433–446. doi: 10.1099/00207713-51-2-433

Nigro, L. M., Elling, F. J., Hinrinchs, K.-U., Joye, S. B., and Teske, A. (2020). Microbial ecology and biogeochemistry of hypersaline sediments in Orca Basin. *PLoS One* 15:e0231676. doi: 10.1371/journal.pone.0231676

Nigro, L. M., Hyde, A. S., MacGregor, B. J., and Teske, A. (2016). Phylogeography, salinity adaptations and metabolic potential of the candidate division KB1 bacteria based on a partial single cell genome. *Front. Microbiol.* 7:1266. doi: 10.3389/fmicb.2016.01266

Pachiadaki, M. G., and Kormas, K. A. (2013). Interconnectivity versus isolation of prokaryotic communities in European deep-sea mud volcanoes. *Biogeosciences* 10, 2821–2831. doi: 10.5194/bg-10-2821-2013

Pachiadaki, M. G., Kallionaki, A., Shlmann, D., De Lange, A., and Kormas, K. J. (2011). Diversity and spatial distribution of prokaryotic communities along a sediment vertical profile of a deep-sea mud volcano. *Microb. Ecol.* 62, 655–668. doi: 10.1007/s00248-011-9855-2

Pachiadaki, M. G., Lykousis, V., Stefanou, E. G., and Kormas, K. A. (2010). Prokarotic community structure and diversity in the sediments of an active submarine mud volcano (Kazan mud volcano, East Mediterranean Sea). *FEMS Microbiol. Ecol.* 72, 429–444. doi: 10.1111/j.1574-6941.2010.00857.x

Pagé, A., Juniper, S. K., Olagnon, M., Alain, K., Desrosiers, G., Quérellou, J., et al. (2004). Microbial diversity associated with a *Paralvinella sulfincola* tube and the adjacent substratum on an active deep-sea vent chimney. *Geobiology* 2, 225–238. doi: 10.1111/j.1472-4677.2004.00034.x

Pikuta, E., Lysenko, A., Chuvilskaya, N., Mendrock, U., Hippe, H., Suzina, N., et al. (2000). *Anoxybacillus pushchinensis* gen. nov., sp. nov., a novel anaerobic, alkaliphilic, moderately thermophilic bacterium from manure, and description of *Anoxybacillus flavithermus* comb. nov. *Int. J. Syst. Evol. Microbiol.* 50, 2109–2117. doi: 10.1099/00207713-50-6-2109

Pimmel, A., and Claypool, G. (2001). *Introduction to shipboard organic geochemistry on the JOIDES resolution.* ODP Technical Note, 30. College Station TX: Ocean Drilling Program. doi: 10.2973/odp.tn.30.2001

Pruesse, E., Peplies, J., and Glöckner, F. O. (2012). SINA: Accurate high-throughput multiple sequence alignment of ribosomal RNA genes. *Bioinformatics* 28, 1823–1829. doi: 10.1093/bioinformatics/bts252

Rattray, J. E., Chakraborty, A., Elizondo, G., Ellefson, E., Bernard, B., Brooks, J., et al. (2022). Endospores associated with deep seabed geofluid features in the eastern Gulf of Mexico. *Geobiology* 20, 823–836. doi: 10.1111/gbi.12517

Ruff, E., Biddle, J. F., Teske, A., Knittel, K., Boetius, A., and Ramette, A. (2015). Global dispersion and local diversification of the methane seep microbiome. *Proc. Natl. Acad. Sci. U.S.A.* 112, 4015–4020. doi: 10.1073/pnas.1421865112

Ryan, R. P., Monchy, S., Cardinale, M., Taghavi, S., Crossman, L., Avison, M. B., et al. (2009). The versatility and adaptation of bacteria from the genus *Stenotrophomonas*. *Nat. Rev. Microbiol.* 7, 514–525. doi: 10.1038/nrmicro2163

Sass, A., McKew, B. A., Sass, H., Fichtel, J., Timmis, K. N., and McGenity, T. J. (2008). Diversity of *Bacillus*-like organisms from deep-sea hypersaline anoxic sediments. *Saline Syst.* 4:8. doi: 10.1186/1746-1448-4-8

Schloss, P. D. (2013). Secondary structure improves OTU assignments of 16S rRNA gene sequences. *ISME J.* 7, 457–460. doi: 10.1038/ismej.2012.102

Schloss, P. D., and Handelsman, J. (2005). Introducing DOTUR, a computer program for defining operational taxonomic units and estimating species richness. *Appl. Environ. Microbiol.* 71, 1501–1506. doi: 10.1128/AEM.71.3.1501-1506.2005

Schloss, P. D., Westcott, S. L., Ryabin, T., Hall, J. R., Hartmann, M., Hollister, E. B., et al. (2009). Introducing mothur: Open-source, platform-independent, community-supported software for describing and comparing microbial communities. *Appl. Environ. Microbiol.* 75, 7537–7541. doi: 10.1128/AEM.01541-09

Schmidtova, J., Hallam, S. J., and Baldwin, S. A. (2009). Phylogenetic diversity of transition and anoxic zone bacterial communities within a near-shore anoxic basin: Nitinat lake. *Environ. Microbiol.* 11, 3233–3251. doi: 10.1111/j.1462-2920.2009.02044.x

Scholz, C. F. P., and Kilian, M. (2016). The natural history of cutaneous *Propionibacteria*, and reclassification of selected species within the genus *Propionibacterium* to the proposed novel genera *Acidipropionibacterium* gen. nov., *Cutibacterium* gen. nov., and *Pseudopropioninbacterium* gen. nov. *Int. J. Syst. Evol. Microbiol.* 66, 4422–4432. doi: 10.1099/ijsem.0.001367

Siam, R., Mustafa, G. A., Sharaf, H., Moustafa, A., Ramadan, A. R., Antunes, A., et al. (2012). Unique prokaryotic consortia in geochemically distinct sediments from Red Sea Atlantis II and discovery deep brine pools. *PLoS One* 7:e42872. doi: 10.1371/journal.pone.0042872

Sørensen, K. B., Canfield, D. E., Teske, A. P., and Oren, A. (2005). Community composition of a hypersaline endoevaporitic microbial mat. *Appl. Environ. Microbiol.* 71, 7352–7365. doi: 10.1128/AEM.71.11.7352-7365.2005

Sorokin, D. Y., Messina, E., La Cono, V., Ferrer, M., Ciordia, S., Mena, M. C., et al. (2018). Sulfur respiration in a group of facultatively anaerobic Natronoarchaea ubiquitous in hypersaline soda lakes. *Front. Microbiol.* 9:02359. doi: 10.3389/fmicb.2018.02359

Sorokin, D. Y., Tourova, T. P., Panteleeva, A. N., and Muyzer, G. (2012). *Desulfonatronobacter acidivorans* gen. nov., sp. nov. and *Desulfobulbus alkaliphilus* sp. nov., haloalkaliphilic heterotrophic sulfate-reducing bacteria from soda lakes. *Int. J. Syst. Evol. Microbiol.* 62, 2107–2113. doi: 10.1099/ijs.0.029777-0

Spang, A., Saw, J. H., Jørgensen, S. L., Zaremba-Niedzwiedzka, K., Martijn, J., Lind, A. E., et al. (2015). Complex archaea that bridge the gap between prokaryotes and eukaryotes. *Nature* 521, 173–179. doi: 10.1038/nature14447

Stahl, D. A., and Amann, R. (1991). "Development and application of nucleic acid probes in bacterial systematics," in *Sequencing and hybridization techniques in bacterial systematics*, eds E. Stackebrandt and M. Goodfellow (New York, NY: John Wiley & Sons), 205–248.

Sturt, H. F., Summons, R. E., Smith, K., Elvert, M., and Hinrichs, K. U. (2004). Intact polar membrane lipids in prokaryotes and sediments deciphered by high-performance liquid chromatography/ electrospray ionization multistage mass spectrometry–new biomarkers for biogeochemistry and microbial ecology. *Rapid Commun. Mass Spectrom.* 18, 617–628. doi: 10.1002/rcm.1378

Suess, J., Engelen, B., Cypionka, H., and Sass, H. (2004). Quantitative analysis of bacterial communities from Mediterranean sapropels based on cultivation-dependent methods. *FEMS Microbiol. Ecol.* 51, 109–121. doi: 10.1016/j.femsec.2004.07.010

Suess, J., Schubert, K., Sass, H., Cypionka, H., Overmann, J., and Engelen, B. (2006). Widespread distribution and high abundance of *Rhizobium radiobacter* within Mediterranean subsurface sediments. *Environ. Microbiol.* 8, 1753–1763. doi: 10.1111/j.1462-2920.2006.01058.x

Swan, B. K., Ehrhardt, C. J., Reifel, K. M., Moreno, L. I., and Valentine, D. L. (2010). Archaeal and bacterial communities respond differently to environmental gradients in anoxic sediments of a California hypersaline lake, the Salton Sea. *Appl. Environ. Microbiol.* 76, 757–768. doi: 10.1128/AEM.02409-09

Swofford, D. L. (2000). *PAUP*. Phylogenetic analysis using parsimony (and other methods)*, 4th Edn. Sunderland, MA: Sinauer Associates.

Teske, A. (2019). "Hydrocarbon-degrading anaerobic microbial communities in natural oil seeps," in *Microbial communities utilizing hydrocarbons and lipids: Members, metagenomics and ecophysiology*, ed. T. J. McGenity (Cham: Springer). doi: 10.1007/978-3-030-14785-3_3

Teske, A., and Joye, S. B. (2020). "The gulf of mexico: An introductory survey of a seep-dominated seafloor landscape," in *Marine hydrocarbon seeps–microbiology and biogeochemistry of a global marine habitat*, eds A. Teske and V. Carvalho (Berlin: Springer), 69–100. doi: 10.1007/978-3-030-34827-4_4

Teske, A., Hinrichs, K. U., Edgcomb, V., de Vera Gomez, A., Kysela, D., Sylva, S. P., et al. (2002). Microbial diversity in hydrothermal sediments in the Guaymas Basin: Evidence for anaerobic methanotrophic communities. *Appl. Environ. Microbiol.* 68, 1994–2007. doi: 10.1128/AEM.68.4.1994-2007.2002

van den Bogert, B., Erkus, O., Boekhorst, J., de Goffau, M., Smid, E. J., Zoetendal, E. G., et al. (2013). Diversity of human small intestinal *Streptococcus* and *Veillonella* populations. *FEMS Microbiol. Ecol.* 85, 376–388. doi: 10.1111/1574-6941.12127

van der Wielen, P. W. J. J., Bolhuis, H., Borin, S., Daffonchio, D., Corselli, C., Giuliano, L., et al. (2005). The enigma of prokaryotic life in deep hypersaline anoxic basins. *Science* 307, 121–123. doi: 10.1126/science.1103569

Vandamme, P., and Coenye, T. (2004). Taxonomy of the genus *Cupriavidus*: A tale of lost and found. *Int. J. Syst. Evol. Microbiol.* 54, 2285–2289. doi: 10.1099/ijs.0.63247-0

Vetriani, C., Jannasch, H. W., MacGregor, B. J., Stahl, D. A., and Reysenbach, A. L. (1999). Population structure and phylogenetic characterization of marine benthic archaea in deep-sea sediments. *Appl. Environ. Microbiol.* 65, 4375–4384. doi: 10.1128/AEM.65.10.4375-4384.1999

Vreeland, R. H., Litchfield, C. D., Martin, E. L., and Elliot, E. (1980). *Halomonas elongata*, a new genus and species of extremely salt-tolerant bacteria. *Int. J. Syst. Bacteriol.* 30, 485–495. doi: 10.1007/s11274-012-1020-7

Wang, B., Lai, Q., Cui, Z., Tan, T., and Shao, Z. (2008). A pyrene-degrading consortium from deep-sea sediment of the West Pacific and its key member *Cycloclasticus* sp. P1. *Environ. Microbiol.* 10, 1948–1963. doi: 10.1111/j.1462-2920.2008.01611.x

Wang, L., and Shao, Z. (2021). Aerobic denitrification and heterotrophic sulfur oxidation in the genus *Halomonas* revealed by six novel species characterizations and genome-based analysis. *Front. Microbiol.* 12:652766. doi: 10.3389/fmicb.2021.652766

Wen, A., Fegan, M., Hayward, C., Chakraborty, S., and Sly, L. I. (1999). Phylogenetic relationships among members of the Comamonadaceae and description of *Delftia acidovorans* (den Dooren de Jong 1926 and Tamaoka et al. 1987) gen. nov., comb. nov. *Int. J. Syst. Microbiol.* 49, 567–576. doi: 10.1099/00207713-49-2-567

Westbrook, G. K., and Reston, T. J. (2002). The accretionary complex of the Mediterranean Ridge: Tectonics, fluid flow and the formation of brine lakes. *Mar. Geol.* 186, 1–8. doi: 10.1016/S0025-3227(02)00169-X

Wirsen, C. O., Sievert, S. M., Cavanaugh, C. M., Molyneaux, S. J., Ahmad, A., Taylor, L. T., et al. (2002). Characterization of an autotrophic sulfide-oxidizing marine *Arcobacter* sp. that produces filamentous sulfur. *Appl. Environ. Microbiol.* 68, 316–325. doi: 10.1128/AEM.68.1.316-325.2002

Xiang, X., Wang, R., Wang, H., Ging, L., Man, B., and Xu, Y. (2016). Distribution of Bathyarchaeota communities across different terrestrial settings and their potential ecological functions. *Sci. Rep.* 7:45028. doi: 10.1038/srep45028

Yabuuchi, E., and Yano, I. (1981). *Achromobacter* gen. nov. and *Achromobacter xylosoxidans* (ex Yabuuchi and Ohyama 1971) nom. rev. *Int. J. Syst. Bacteriol.* 31, 477–478. doi: 10.1099/00207713-31-4-477

Yakimov, M. M., Giuliano, L., Cappello, S., Denaro, R., and Golyshin, P. N. (2007). Microbial community of a hydrothermal mud vent underneath the deep-sea anoxic brine lake Urania (Eastern Mediterranean). *Orig. Life Evol. Biosph.* 37, 177–188. doi: 10.1007/s11084-006-9021-x

Yakimov, M. M., La Cono, V., Slepak, V. Z., La Spada, G., Arcadi, E., Messina, E., et al. (2013). Microbial life in the lake Medeé, the largest deep-sea salt-saturated formation. *Sci. Rep.* 3:3554. doi: 10.1038/srep03554

You, Z.-Q., Li, J., Qin, S., Tian, X.-P., Wang, F.-Z., Zhang, S., et al. (2013). *Bacillus abyssalis* sp. nov., isolated from a sediment of the South China Sea. *Antonie Van Leeuwenhoek* 103, 963–969. doi: 10.1007/s10482-013-9875-7

Youssef, N. H., Farag, I. F., Rudy, S., Mulliner, A., Walker, K., Caldwell, F., et al. (2019). The wood-Ljungdahl pathway as a key component of metabolic versatility in Candidate phylum Bipolaricaulota (Acetothermia, OP1). *Environ. Microbiol. Rep.* 11, 538–547. doi: 10.1111/1758-2229.12753

Zabel, M. (2012). RV METEOR, cruise report M84/L1. Biogeochemistry and methane hydrates of the black sea, oceanography of the Mediterranean, shelf sedimentation and cold water carbonates. *DFG Senatskommission Ozeanogr.* 39, 1–38.

Zhao, W., Zhang, C. L., Romanek, C. S., and Wiegel, J. (2008). Description of *Caldalkalibacillus uzonensis* sp. nov. and emended description of the genus *Caldalkalibacillus*. *Int. J. Syst. Evol. Microbiol.* 58, 1106–1108. doi: 10.1099/ijs.0.65363-0

Zhou, Z., Liu, Y., Lloyd, K. G., Pan, J., Yang, Y., Gu, J.-D., et al. (2019). Genomic and transcriptomic insights into the ecology and metabolism of benthic archaeal cosmopolitan, Thermoprofundales (MBG-D archaea). *ISME J.* 13, 885–901. doi: 10.1038/s41396-018-0321-8

frontiers | Frontiers in Microbiology

TYPE Original Research
PUBLISHED 06 January 2023
DOI 10.3389/fmicb.2022.1060168

OPEN ACCESS

EDITED BY
S. Emil Ruff,
Marine Biological Laboratory (MBL),
United States

REVIEWED BY
Stefan M. Sievert,
Woods Hole Oceanographic Institution,
United States
Andreas Teske,
University of North Carolina at Chapel Hill,
United States

*CORRESPONDENCE
Sven Le Moine Bauer
✉sven.bauer@uib.no

SPECIALTY SECTION
This article was submitted to Extreme Microbiology, a section of the journal Frontiers in Microbiology

RECEIVED 02 October 2022
ACCEPTED 01 December 2022
PUBLISHED 06 January 2023

CITATION
Le Moine Bauer S, Lu G-S, Goulaouic S, Puzenat V, Schouw A, Barreyre T, Pawlowsky-Glahn V, Egozcue JJ, Martelat J-E, Escartin J, Amend JP, Nomikou P, Vlasopoulos O, Polymenakou P and Jørgensen SL (2023) Structure and metabolic potential of the prokaryotic communities from the hydrothermal system of Paleochori Bay, Milos, Greece. *Front. Microbiol.* 13:1060168. doi: 10.3389/fmicb.2022.1060168

Structure and metabolic potential of the prokaryotic communities from the hydrothermal system of Paleochori Bay, Milos, Greece

Sven Le Moine Bauer[1]*, Guang-Sin Lu[2,3], Steven Goulaouic[1], Valentine Puzenat[4], Anders Schouw[5], Thibaut Barreyre[1], Vera Pawlowsky-Glahn[6], Juan José Egozcue[7], Jean-Emmanuel Martelat[8], Javier Escartin[9], Jan P. Amend[10], Paraskevi Nomikou[11], Othonas Vlasopoulos[11], Paraskevi Polymenakou[12] and Steffen Leth Jørgensen[1]

[1]Center for Deep Sea Research, Department of Earth Science, University of Bergen, Bergen, Norway, [2]Cooperative Institute for Climate, Ocean and Ecosystem Studies, University of Washington, Seattle, WA, United States, [3]NOAA Pacific Marine Environmental Laboratory, Seattle, WA, United States, [4]Institut de Physique du Globe de Paris, CNRS, Université Paris Cité, Paris, France, [5]Center for Deep Sea Research, Department of Biology, University of Bergen, Bergen, Norway, [6]Department of Computer Science, Applied Mathematics and Statistics, University of Girona, Girona, Spain, [7]Department of Civil and Environmental Engineering, University Politécnica de Cataluña, Barcelona, Spain, [8]Université de Lyon, UCBL, ENSL, CNRS, Laboratoire de Géologie LGL-TPE, Villeurbanne, France, [9]Laboratoire de Géologie (CNRS UMR8538), Ecole Normale Supérieure de Paris, PSL University, Paris, France, [10]Departments of Earth Sciences and Biological Sciences, University of Southern California, Los Angeles, CA, United States, [11]Faculty of Geology and Geoenvironment, National and Kapodistrian University of Athens, Athens, Greece, [12]Institute of Marine Biology Biotechnology and Aquaculture, Hellenic Center for Marine Research, Heraklion, Greece

Introduction: Shallow hydrothermal systems share many characteristics with their deep-sea counterparts, but their accessibility facilitates their study. One of the most studied shallow hydrothermal vent fields lies at Paleochori Bay off the coast of Milos in the Aegean Sea (Greece). It has been studied through extensive mapping and its physical and chemical processes have been characterized over the past decades. However, a thorough description of the microbial communities inhabiting the bay is still missing.

Methods: We present the first in-depth characterization of the prokaryotic communities of Paleochori Bay by sampling eight different seafloor types that are distributed along the entire gradient of hydrothermal influence. We used deep sequencing of the 16S rRNA marker gene and complemented the analysis with qPCR quantification of the 16S rRNA gene and several functional genes to gain insights into the metabolic potential of the communities.

Results: We found that the microbiome of the bay is strongly influenced by the hydrothermal venting, with a succession of various groups dominating the sediments from the coldest to the warmest zones. Prokaryotic diversity and abundance decrease with increasing temperature, and thermophilic archaea overtake the community.

Discussion: Relevant geochemical cycles of the Bay are discussed. This study expands our limited understanding of subsurface microbial communities in acidic shallow-sea hydrothermal systems and the contribution of their microbial activity to biogeochemical cycling.

KEYWORDS

Milos, shallow hydrothermal vent field, microbial community, functional genes, 16S rRNA sequencing, thermal gradient

Introduction

Marine hydrothermalism is a phenomenon where seawater percolates though the crust or the sediments, becomes heated by volcanic or tectonic activity, and returns to the seafloor in the form of focused or diffuse hydrothermal venting. During its journey through the subsurface, the seawater reacts with the substrate, resulting in hydrothermal fluids that are often enriched in metals and reduced compounds while being depleted in oxidized compounds (Alt, 1995). At venting sites, the physical and chemical gradients generated by the mixing of the fluids and the seawater allows for the growth of unique microbial communities (Orcutt et al., 2011; Price and Giovannelli, 2017). While such hydrothermal vents can be found at all depths, a separation is made around 200 m depth to differentiate deep and dark hydrothermal systems on one hand and shallow and photic hydrothermal systems on the other hand (Tarasov et al., 2005; Price and Giovannelli, 2017).

As of 2020, around 70 shallow systems are reported in the InterRidge 3.4 database (Beaulieu and Szafranski, 2020). While they occur in a variety of tectonically active settings, they are mostly associated with submarine volcanism, island and intra-oceanic arcs, ridge environments, intraplate oceanic volcanism, continental margins, and rift basins (Tarasov et al., 2005) and can be found all around the world (see for a review Price and Giovannelli, 2017). Despite similarities with their deep-sea counterparts, shallow systems present also significant particularities, such as the presence of light allowing photosynthesis, and the common presence of a gas phase due to a lower hydrostatic pressure than in the deep sea. They are furthermore exposed to stronger time-dependent external forcing such as tidal influence, wind- and wave-driven circulation, and coastal processes such as land-derived nutrient loading (Chen et al., 2005; Yücel et al., 2013; Price et al., 2015; Price and Giovannelli, 2017).

Milos Island and its surroundings, situated on the Hellenic Volcanic Arc in the South Aegan Sea, is one of the most studied shallow hydrothermal vent system (Figure 1A). This arc was formed by the convergence of the African plate beneath the Aegean micro-plate and has been volcanically active since the Pliocene (Varnavas and Cronan, 2005; Jolivet et al., 2013). The subduction results in magmas of intermediate to felsic composition, influenced by andesitic to dacitic volcanic rocks and low-grade (greenschist facies) metamorphic rocks that compose the host rock at Milos (see Fytikas et al., 1986, and references within). Overlying the igneous and metamorphic rocks are carbonate-rich sediments with elevated concentrations of lead and zinc (Karageorgis et al., 1998). Although the last volcanic eruption at Milos was ~90 ka ago, remnant heat from the quiescent magma system still drives hydrothermal circulation on land and offshore, making it one of the largest shallow-sea hydrothermal systems described to date, covering ~35 km^2 (Dando et al., 1995a). The most intense submarine venting identified to date occurs at Paleochori Bay (Figure 1A), off the south-eastern coastline at water depths from 3 m to at least 300 m (Dando et al., 2000). The venting fluids are chemically reduced, rich in sulfide and mercury, and acidic (pH ~ 4.4), with temperatures up to 122°C (Dando et al., 1995a, 2000; Valsami-Jones et al., 2005; Price R.E. et al., 2013; Roberts et al., 2021). Furthermore, the fluids from Milos have to date the highest arsenic concentrations of any submarine vent analyzed, with concentrations approximately 3,000 times higher than seawater values (Price et al., 2015). The gas phase is mainly composed of CO_2 (commonly exceeding 90%), with lower amounts of H_2, H_2S and CH_4 (Dando et al., 1995a). Low salinity fluids can also be found with different metal enrichments, resulting from the reliquefaction of the gas phase (Valsami-Jones et al., 2005). The hydrothermal discharge mixes with oxic, slightly alkaline seawater to produce white, yellow, orange, and brown manganese, iron, arsenic and sulfur mineral precipitates (Wenzhöfer et al., 2000; Kotopoulou et al., 2022) that are easily visible using satellite, drone, or underwater vehicle imagery (Khimasia et al., 2020; Martelat et al., 2020; Puzenat et al., 2021). This hydrothermalised seafloor provides surfaces and sources of nutrients and energy for microbial communities at or near the seafloor (Dando et al., 1998; Price R.E. et al., 2013; Gilhooly et al., 2014; Godelitsas et al., 2015).

Microbes in a system like Milos play several ecological roles, by fixing CO_2 through chemo- and photolithoautotrophy, remineralizing organic matter, and mediating several metal cycles. Dando et al. (1995b) and Sievert et al. (1999) were the first to study

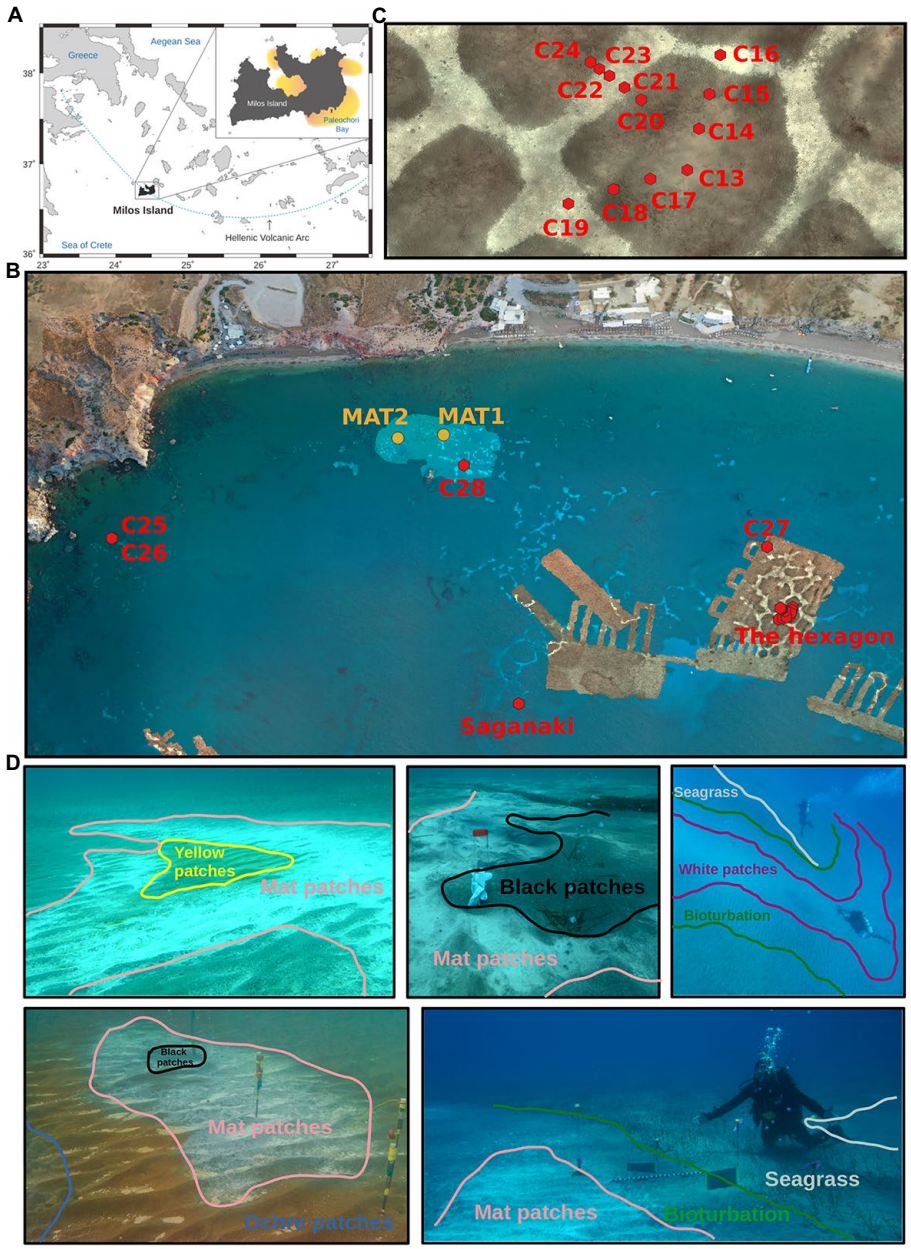

FIGURE 1
Map and photographies of the sampling locations. **(A)** Localization of Milos and Paleochori Bay. **(B)** Localization of the cores taken in Paleochori Bay. **(C)** Zoom into the location of "The hexagon." **(D)** Photographies of the various types of seafloor investigated here. The lower right picture represents the Saganaki vent field. The colors used are consistent throughout the figures, with light blue/grey for seagrass patches, green for bioturbation, blue for ochre patches, dark pink for white patches, salmon for mat patches, black for black patches, and yellow for yellow patches. See Puzenat et al. (2021) for details on the publicly available AUV and drone background photomosaics in **(B,C)** (Martelat et al., 2019; Puzenat et al., 2019a,b).

the microbiology of the hydrothermal field of Paleochori Bay on Milos, followed by Brinkhoff et al. (1999) which focused on sulfur oxidizers. Since, several new microbial species have been isolated from the bay (Jochimsen et al., 1997; Arab et al., 2000; Sievert and Kuever, 2000; Schlesner et al., 2001), while other studies have looked at the microbial communities in general using most probable numbers, denaturing gradient gel electrophoresis, fluorescence *in situ* hybridization, lipid analysis and 16S rRNA gene clone libraries (Sievert et al., 1999; Giovannelli et al., 2013; Price R. et al., 2013; Sollich et al., 2017). There are to date only two studies on Paleochori Bay that involve deep-sequencing technology of the 16S rRNA marker gene, both focusing on a single vent (Bühring and Sievert, 2017; Sievert et al., 2022). A detailed structural analysis of the communities throughout

Paleochori Bay and their links to patterns of fluid discharge is therefore still missing. Similarly, little is known about prokaryotic abundances, as the quantification of microbial communities both in Paleochori Bay and in the neighboring Spathi Bay has only been done on a limited number of samples (Sievert et al., 1999; Giovannelli et al., 2013; Callac et al., 2017; Fru et al., 2018).

In this study, we report the first in-depth characterization of the prokaryotic communities of Paleochori Bay using deep sequencing of the 16S rRNA marker gene as well as quantitative polymerase chain reaction (qPCR) quantification of the 16S rRNA gene and several functional genes. The study uses samples collected during 2 field expeditions in 2014 and 2019, summing to a total of 84 samples over 20 sediment cores, 2 microbial mats, and seawater. Our results provide a high-resolution description of the microbial communities inhabiting a wide range of habitats along hydrothermal gradients in the bay. Furthermore, we also discuss *in situ* interactions between the biosphere and the geochemical environment in the bay and review previous publications on the topic.

Materials and methods

In this study, data collected during two different field campaigns are presented, called thereafter Saganaki and CarDHynAl datasets. The two datasets were produced using protocols with slight differences which are highlighted below. Both datasets describe microbial community composition using deep sequencing of the 16S rRNA marker gene, while qPCR analysis was performed only on the CarDHynAl dataset. A graphical summary of the Material and methods can be found in Supplementary material 1.

Sampling

Saganaki dataset

Saganaki is a single vent site located ~300 m offshore in Paleochori Bay (36.671490053°N, 24.516882251°E) at a water depth of 12 m (Figure 1B). It is characterized by temperatures up to 76.2°C in the shallow subsurface (~10 cmbsf), weak to moderate gas venting, and the colonization of the sediment surface by a white ~1 cm thick microbial mat. Areas of flourishing seagrass surround the area of active venting, separated from the white mats by a transition zone (~1 m wide) of sediment where the burrowing activity of the mud shrimp *Calianassa truncata* is visible. In May 2014, scuba divers measured *in situ* temperatures and collected sediment cores and water samples. Sediments were cored with polycarbonate tubes and sealed underwater with rubber caps. Four sediment cores were collected along a 2 m transect, starting from the center of a white mat, through a transition zone, and ending in a seagrass-covered region (Figure 1D). A background area, devoid of seagrass and visually unaffected by venting, was also sampled. Sediment cores were immediately subsampled onshore by collecting 2 cm-thick slices in sterile falcon tubes. Subsamples were then stored and shipped on dry ice and then kept frozen at −80°C until processing. A seawater sample was also taken at less than 1 m depth in the vicinity of Saganaki. All cores and samples are listed in Supplementary material 2.

CarDHynAl dataset

In September 2019, a field campaign was organized for the CarDHynAl project to map and characterize temperature outflows (Puzenat et al., 2021) and microbial communities in Paleochori Bay. The sediments were sampled throughout Palaeochori Bay, from 3 to 10 m depth, and from a variety of visually different seafloor types such as background sand, bioturbation sand, ochre sand, white precipitates, zones covered with microbial mats, yellow sand, and black sand (Figure 1D). A hydrothermal hexagonal seafloor pattern in the south-east of the bay (36.672334236°N, 24.519504665°E; Figures 1B,C) was used to sample a high-resolution sediment transect across a zone of diffuse hydrothermal outflow. Sediment cores were taken using plexiglass tubes of 3.6 cm in diameter. Upon recovery of the cores, the sediment was immediately pushed out of the tubes and subsampled by using tip-sectioned syringes. Subsamples were stored at −20°C within the hour of sampling until further processing. Furthermore, 2 mat samples were collected using syringes (Figure 1B). All samples are listed in Supplementary material 2. Eleven fluid samples were also sampled around 5 cm below seafloor using a syringe connected to a short tubing (see list in Supplementary material 3). Temperatures were measured using a thermal blanket and multiple thermal probes as described in Puzenat et al. (2021).

Fluid analyses

Within an hour after sampling, the fluids from the CarDHynAl dataset were split into two aliquots of 10 ml. Few grains of zinc acetate were added to the aliquot for anion analysis, and 0.3 ml of concentrated nitric acid was added to the aliquot for cation analysis. Samples were then kept at room temperature until analysis. Major anions were measured using Ion Chromatography (IC, Metrohm CompactIC), and major cations were measured using Inductively coupled plasma optical emission spectrometry (ICP-OES, Thermo Scientific iCAP 7,600).

DNA extraction and sequencing

Saganaki dataset

Around 0.5 g of sand/sediment samples were homogenized using a sterile mortar and pestle, and bulk environmental DNA was extracted from both sediments and fluids according to the method of Mills et al. (2012). Negative controls were routinely used to confirm the absence of contamination during the process. Extracted DNA samples were then sent to Molecular Research DNA (Shallowater, TX, United States) for sequencing of the 16S rRNA

gene using an Illumina Miseq platform with universal 515f and 806r primers (Caporaso et al., 2011). The list of all primers and PCR programs used in this study can be found in Supplementary material 4.

CarDHynAl dataset

DNA was extracted from ~0.5 g of sediment/mat using the Dneasy® PowerLyzer® Power Soil Kit (Qiagen) following the manufacturer's instructions and a FastPrep 24 Tissue Homogenizer (MP Biomedical). Negative controls were routinely run to assess contamination throughout the protocol. In order to produce amplicon libraries for sequencing, a 2-step amplification approach was used as described in Berry et al. (2011). First, triplicate PCRs were run on each sample using the HotStarTaq kit (Qiagen) and the 519F and 805R primers (see Supplementary material 4). After pooling of the triplicates and cleaning of the amplicons using AMPure XP beads (Beckman Coulter, Inc.), a second PCR was run to attach tags and sequencing adaptors to the PCR products. The final products were cleaned again using AMPure XP beads, and pooled equimolarly prior to sequencing on an Ion Torrent 7467 PGM machine at the University of Bergen.

Sequence processing

After retrieval of the sequences, they were processed using an adaptation of the «alternative VSEARCH pipeline» (Rognes, 2021). In short, the two datasets were first separately trimmed of their primers using Cutadapt 3.2 (Martin, 2011), truncated at 220 bp and quality filtered at a max expected error of 1 for the Saganaki dataset and 2 for the CarDHynAl dataset using VSEARCH v.2.19.0 (Rognes et al., 2016). The reason for the difference is that Illumina produces higher quality sequences, allowing for a stricter cleaning process. Both datasets where then concatenated and processed in VSEARCH as follow: Dereplication and removal of singletons, clustering of OTUs at 97% similarity, *denovo* and reference-based chimera removal (using SILVA138.1 (Quast et al., 2013)), and finally mapping of the pre-dereplication sequences to the OTUs. The OTUs were further curated using LULU v.0.1.0 (Frøslev et al., 2017), prior to be given taxonomic assignments using the CREST4 LCA classifier (Lanzén et al., 2012) and the SILVA138.1 database. Finally, the remaining OTUs were run through a thorough decontamination process: Removal of OTUs with no domain assignments, contamination removal using the frequency approach in the *decontam* package (Davis et al., 2018), contamination removal using a list of known contaminants (Eisenhofer et al., 2019), and removal of low-abundance OTUs (Bokulich et al., 2013). The script used to process the sequences is available from https://github.com/MeinzBeur/LeMoineBauer-2022-Milos.

qPCR

Quantitative PCR was used on the DNA extracted from the samples of the CarDHynAl dataset in order to quantify a selection of genes involved in various metabolic pathways. Several genes were successfully quantified: *aprA*, *dsrA* and *soxB* (sulfur cycle), *arrA* and *aoxB* (arsenic cycle), *nirK* and *nirS* (nitrogen cycle), and *mcrA* (CO2/methane cycle). For these genes, the standard curve allows to quantify down to ~10^3 copies per gram of sediments. As well, two primer sets targeting separately the archaeal and bacterial 16S rRNA genes were used to quantify prokaryotic abundances. However, primer sets targeting the archaeal *amoA*, bacterial *amoA*, and *hzo* (nitrogen cycle) did not show any product during preliminary PCR screening on a selection of samples. They were therefore not used for qPCR and the genes were considered to be not present in the dataset. Furthermore, primer sets targeting *arsC, arxA* and *arsB* (arsenic cycle) and *psbA* (algal photosynthesis) did not produce any amplicon during preliminary PCR testing on a selection of samples either. However, due to the lack of a positive control, we cannot rule out the possibility of unsuccessful PCR protocol optimization for these genes. Finally, qPCR assays of the *nifH* gene (nitrogen fixation) and *pmoA* (methane/CO2 cycle) showed abnormal amplification pattern (likely due to low amplification efficiency) and were therefore not further used. The genes were however present in our samples. All qPCRs were run on a StepOne™ Real-Time PCR System (ThermoFisher Scientific) using the Quantitect SYBR green PCR kit (Qiagen). Gene copy numbers are given as copies per gram sediment but are not scaled for the number of copies per cell, and therefore do not represent true cell abundance. Total 16S rRNA copy numbers (or prokaryotic 16S rRNA numbers) were calculated as the sum of bacterial and archaeal 16S rRNA gene copies. A summary of all successfully and failed primer sets used, along with primer sequences, thermocycler programs and comments can be found in Supplementary material 4.

Statistical analysis

The different cores were positioned and assigned to seafloor types by carefully comparing *in situ* observations and published photomosaics (Martelat et al., 2019; Puzenat et al., 2019a,b). All statistical analyses were made in R v.4.1.2 (R Core Team, 2021), with the recurrent use of the phyloseq package (McMurdie and Holmes, 2013) and the ggplot2 package (Wickham et al., 2022). The alpha diversity was assessed using the Shannon diversity index, as it is robust to differences in sequencing depth. The index was computed at the OTU level. Barplots of the compositions are shown at the family, phylum, and domain level. For the rest of the study, the analyses were made at the family taxonomic level, as this showed to be a good balance between keeping relevant taxonomic information and decreasing the noise created by having more and rarer taxa in the dataset. We followed the principle of Compositional Data Analysis (Aitchison, 1986; Pawlowsky-Glahn et al., 2015; Gloor et al., 2017). After clustering at the family level, 63% of our OTU table were zeros, and we therefore decided to add 1 as a pseudo count to all counts of the table as this zero-imputation method has been shown to be more efficient than other methods for very sparse data (i.e., with high proportion of zeros; Lubbe et al., 2021). The OTU table

was then clr-transformed, centered, and subjected to principal component analysis based on singular value decomposition. The scores of the form biplot were then extracted and plotted in R using a modified version of geom_link2 (Pedersen, 2021). In order to describe the different seafloor types, we computed balances using the selbal R-functions (Rivera-Pinto et al., 2018) as such approach has been suggested to be more suitable for compositional data than simple differential abundance analysis (Quinn et al., 2021). In our study, the algorithm identifies two groups of microbial taxa of which the ratio will statistically differ between samples belonging to different seafloors (For more explanation, see Supplementary Data 8). The script used to process the sequences is available from https://github.com/MeinzBeur/LeMoineBauer-2022-Milos.

Results and discussion

Seafloor types of Paleochori Bay

The seafloor of Paleochori Bay exhibits a wide range of distinct visual diversity (Figure 1D). These differences can easily be linked to the influence of the hydrothermal activity, and each seafloor type can be constrained by its temperature range (Puzenat et al., 2021). As temperature is known to be a major structuring variable of microbial communities in hydrothermal systems (Lagostina et al., 2021), we decided to classify our samples according to the seafloor type they were taken from. This resulted in 8 different seafloor types, described here and shown in Figure 1D. (i) Background sediments are gray/beige and appear unimpacted by hydrothermal activity, with temperatures in cores at Saganaki and in the CarDHynAl dataset similar to that in local seasonal seawater (19°C and 23–25°C, respectively). (ii) Seagrass patches are covered by the sparse growth of *Cymodocea nodossa*. Despite being only 2 meters away from a venting place, the seagrass core at Saganaki shows temperatures close to the background seafloor, only rising from 19 to 21°C in the upper 20 cm of the sediments. Pore water chemistry from Saganaki's seagrass and background cores show strong similarities, except for slightly higher dissolved iron, As(III), dissolved organic carbon and total dissolved nitrogen in seagrass patches (data not shown). (iii) The bioturbation seafloor has the same color as the background seafloor but is easily identified by the burrowing activity of the mud shrimp *Calianassa truncata*. The zone is typically present as a band of up to a couple of meters width that surrounds the white hydrothermal patches but can also be found in bigger patches disconnected from visible hydrothermal activity (Puzenat et al., 2021). At Saganaki, the increase in temperature from 23.1 to 34.2°C in the upper 20 cm is in agreement with the measurements from Puzenat et al. (between 21.7 and 41.4°C at 35 cm depth). The temperatures at the seafloor interface are close to seawater temperatures. (iv) Ochre patches are characterized by the brown color of the sand, due to the precipitation of iron and manganese oxides (Wenzhöfer et al., 2000), and can be found surrounding warmer seafloor areas (e.g., white and mat patches, described below), or in broad and isolated patches. Temperatures at 35 cm depth vary between 42.0 and 54.7°C (Puzenat et al., 2021). (v) White patches can be recognized by the presence of a superficial white dust precipitate, and were mainly observed in the eastern zone of Paleochori Bay, near the hexagon. This seafloor type is under stronger hydrothermal influence than the previous types described, and the fluids sampled in this seafloor show notably a higher silicon content than the Background ones (Supplementary Data 3). Nevertheless, we did not observe intense venting zones or thick microbial mats on the seafloor. It is however likely that a gradual transition can be observed from white patches to mat patches (see below). Puzenat et al. measured temperatures at 35 cm depth between 52.8 and 73°C with an average of 66.8°C (Puzenat et al., 2021). (vi) Mat patches exhibit dark gray/black sand and are characterized by white fluffy microbial mats of up to a couple of centimeters that accumulate in the ripple marks. It appears in the vicinity of strongly degassing black patches or very hot yellow patches. It is therefore subject to intense hydrothermal venting, as shown by the fluid chemistry (Supplementary material 3). Temperatures for this environment are very heterogeneous (Puzenat et al., 2021), but measurements for our two cores show temperatures of 54.3 and 57.6°C at 10 cm and rising to 59.8 and 71.3°C by 20 cm, respectively. (vii) Black patches are found in association with intense degassing sites, where no bacterial mat grows anymore. The temperatures are between 30 and 40°C near the surface and reach 90°C at 10 cm depth. The chemical analysis of the fluid however shows very little difference compared to seawater, except for the increase in silicon concentrations (Supplementary Data 3). This suggests limited hydrothermal fluid flow at this degassing location, and/or that there is a strong recharge of seawater at that location, as suggested previously (Wenzhöfer et al., 2000; Yücel et al., 2013). (viii) Yellow patches are recognizable by their yellow/orange sand and are also subject to very high hydrothermal impact, exhibiting similar temperature as the black patches (around 90°C at 10 cm depth). However, the degassing is much weaker and the pore fluid chemistry showed very strong hydrothermal influence (Supplementary Data 3). Notably, we measured an arsenic concentration of 84.3 µM.

Microbial community structure of the different seafloor types

A compositional data principal component analysis [CoDa-PCA; (Aitchison, 1983; Pawlowsky-Glahn et al., 2015)] of all 81 seafloor samples provided a visual assessment of microbial community structures from OTUs to phylum level. The general clustering pattern remained consistent at each taxonomic level (Supplementary material 5), but here we present only the family level analyses, apart from the Shannon diversity index which was computed using OTUs. The family level was chosen for the following reasons: (1) We wanted to decrease the noise that would be present in OTU level analyses, (2) it separates the abundant families *Arcobacteraceae*, *Sulfurimonadaceae* and *Sulfurovaceae*

which have a distinct distribution pattern and would be clustered together at a higher taxonomic level, (3) it allows to reduce the dissimilarity observed between the CarDHynAl and Saganaki datasets that could arise from differences in sample preparation and primer sets used, and (4) it decreases the occurrences of zero counts in the dataset that need to be accounted for in the compositional analysis.

On the resulting ordination, PC1 explains 30% of the variance, PC2 explains 14% and PC3 explains 9%. PC1 is segregating the samples along the first part of the temperature gradient, with the cold background and seagrass samples on the left side, and then in order bioturbation, ochre patches, and white patches when moving along PC1 (Figure 2A). On the warmer end of PC1, PC2 then separates the remaining cores, with the mat patches first and finally the yellow and black patches in the upper right corner. The correlation between PC1 and temperature is also visible within each core, with the shallower and colder end of each core being almost systematically aiming to the left side of PC1. This pattern is lost in the background and seagrass seafloors where there is almost no temperature gradient throughout the cores. The CoDa-PCA analysis also shows that the samples from the Saganaki dataset tend to separate from the samples of the CarDHynAl dataset along PC3 (Supplementary material 5), as well as PC2 for the Bioturbation and Mat patches (Figure 2A). While the use of different primer sets (see Supplementary material 6 for the *in silico* primer analysis) are likely influencing the separation, real biological heterogeneity within each seafloor type is also possible. Despite these differences, the Saganaki dataset shows the same correlation between PC1 and temperature, strengthening our observation of temperature and hydrothermal activity being the main structuring factor (in agreement with Dando et al., 1995b; Sievert et al., 1999; Sollich et al., 2017). This hydrothermal impact on microbial communities is also observable on the diversity, as shown by the decrease of the Shannon diversity index along the temperature gradient (Figure 2C; Sievert et al., 1999). Furthermore, absolute 16S rRNA concentrations decrease from around 10^8 to 10^4 copies per gram sediments when getting closer to the vents (Figure 2D). Our estimates are however around an order of magnitude lower than in previous studies that used direct cell counts (Sievert et al., 1999 and Giovannelli et al., 2013), likely due to the different methods used (Lloyd et al., 2013). Finally, the archaeal fraction of the community composition increases with temperature (Supplementary Data 7; Sievert et al., 2000a), which is also observed in other hydrothermal systems (Lagostina et al., 2021). The hydrothermal impact is also highlighted by fluid/seawater mixing models at Milos, which suggest that microbial metabolic strategies often shift with mixing ratio, and therefore temperature (Lu et al., 2020).

The following sections describe the prokaryotic communities inhabiting each type of seafloor. However, the ordination and the diversity analysis highlighted a strong similarity between the communities inhabiting the seagrass and background seafloors, the bioturbation and ochre patch seafloors, and the black and yellow patch seafloors (Figures 2A,C). Therefore, these seafloor types will be described together from now on. This also allows us to use the selbal R-functions on all groups, while the low number of samples for some seafloor types would have otherwise prevented it.

Background and seagrass patches

The background seafloor possesses the second highest absolute prokaryote abundance of our dataset after the bioturbation samples (Figure 2D), with 16S rRNA copy numbers ranging from 1.66e+7 to 1.03e+8 copy.g^{-1} sediment. Deeper samples tend to have lower absolute abundances than the shallow ones, which is mainly linked to the decrease in Bacteria (Figure 3). Based on these qPCR measurements, Archaea copies account for 1.0 to 22.1% of the total prokaryote gene copies and are less influenced by depth than Bacteria (Figure 3). No quantitative data are available for the seagrass seafloor type but considering the similarity with the background seafloor type one might expect similarly high 16S rRNA copy numbers.

The background and seagrass cores are the most diverse of our samples (Figure 2C). Their prokaryotic community composition at the phylum taxonomic level is shown in Figure 4 and at the family level in Supplementary Material 7. The composition of the seagrass core is very similar to the background core from the Saganaki dataset (Figure 4). Background and seagrass samples can be segregated from the others using the balance of *Desulfatiglandaceae* and *Unclassified_Woesearchaeales* against *Desulfosarcinaceae*, with balance values between −2.54 and −1.60 (median −1.97) for the background and seagrass samples, and between −1.58 and 4.96 (median 0.00) for the others (Figure 5A; Supplementary Material 8).

Bioturbation and ochre patches

The bioturbation zone has the highest prokaryote abundance of our dataset (Figure 2D), with 16S rRNA copy numbers ranging from 1.22e+6 to 1.95e+8 copy.g^{-1} sediment. The deeper samples exhibit the lower counts, with a decrease of around 2 orders of magnitude in the top 15 cm (Figure 3). Based on these qPCR measurements, Archaea copies represent between 1.8 and 20.3% of the total prokaryote gene copies. The core from the ochre patch shows little variation in prokaryote copy numbers, with a total of 1.6e+7 to 2.48e+7 16S rRNA copy.g^{-1} sediment. Neither Bacteria nor Archaea copy numbers decrease in the top 15 cm, and therefore the relative abundance of Archaea remains between 6.0 and 7.7% (Figure 3). The low Archaea content in the bioturbation and ochre patches is similar to the background and seagrass seafloor type, suggesting a rather low hydrothermal impact on these zones.

The CoDa-PCA analysis shows that the bioturbation and ochre patches act as a transition zone, with the deepest samples clustering with the warmer seafloors, while the shallower samples are similar to the background and seagrass samples (Figure 2A). This is also observed in the spatial distribution of these patches, which are often surrounding warmer white and mat patches. The bioturbation and ochre patches cores are less diverse than the background and seagrass samples (Figure 2C). Their prokaryotic community composition at the phylum taxonomic level is shown

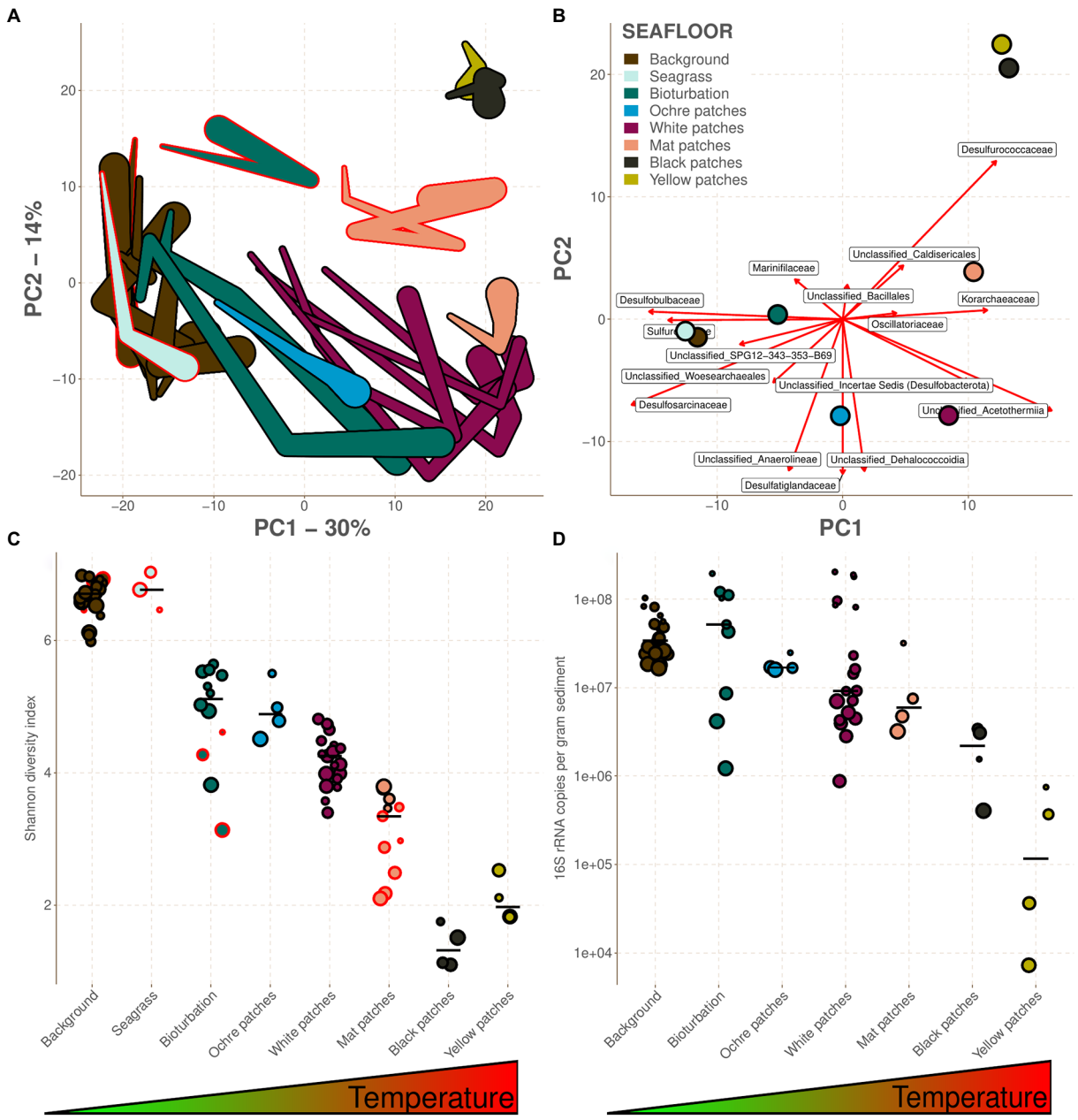

FIGURE 2
Heterogeneity between the different seafloor types. The color legend as given in B is true for the whole figure. Samples from the Saganaki dataset have a red border, while the ones from the CarDHynAl dataset have a black border. **(A)** Form CoDa-biplot, representing 44% of the variance. It approximately reflects the Aitchison distances between the 16S rRNA composition of the sample at the family taxonomic level. Each linked samples represent a core, with the width of the link being proportional to depth of the sample. **(B)** Covariance CoDa-biplot where the center of each seafloor type is shown, as well as the taxa involved in the balances described in the text. **(C)** Shannon diversity index of each sample grouped per seafloor type. **(D)** Absolute prokaryotic abundance as copies of 16S rRNA per gram of sediment quantified by qPCR. For **(C,D)**, the seafloor types are ordered by increasing temperature/hydrothermal influence, and the bars represent the median.

in Figure 4 and at the family level in Supplementary material 7. The high heterogeneity of the community within and between each bioturbation and ochre patch core (Figure 2A), as well as its similarity with the center of the dataset (centers plotted close to the origin of PC1 and PC2 on Figure 2B) makes it more difficult to characterizes this seafloor types using selbal. The resulting balance opposes *Unclassified_SPG12-343-353-B69* to *Desulfobulbaceae, Unclassified_Anaerolineae* and *Marinifilaceae*, with balance values between −3.17 and −1.60 (median −2.06) for the bioturbation and ochre patch samples, while all other samples have values between −1.75 and 2.10 (median −0.42; Figure 5B; Supplementary material 8). Major compositional differences can be seen between the bioturbation cores from the Saganaki and the CarDHynAl datasets. We suggest that the Saganaki core exhibits

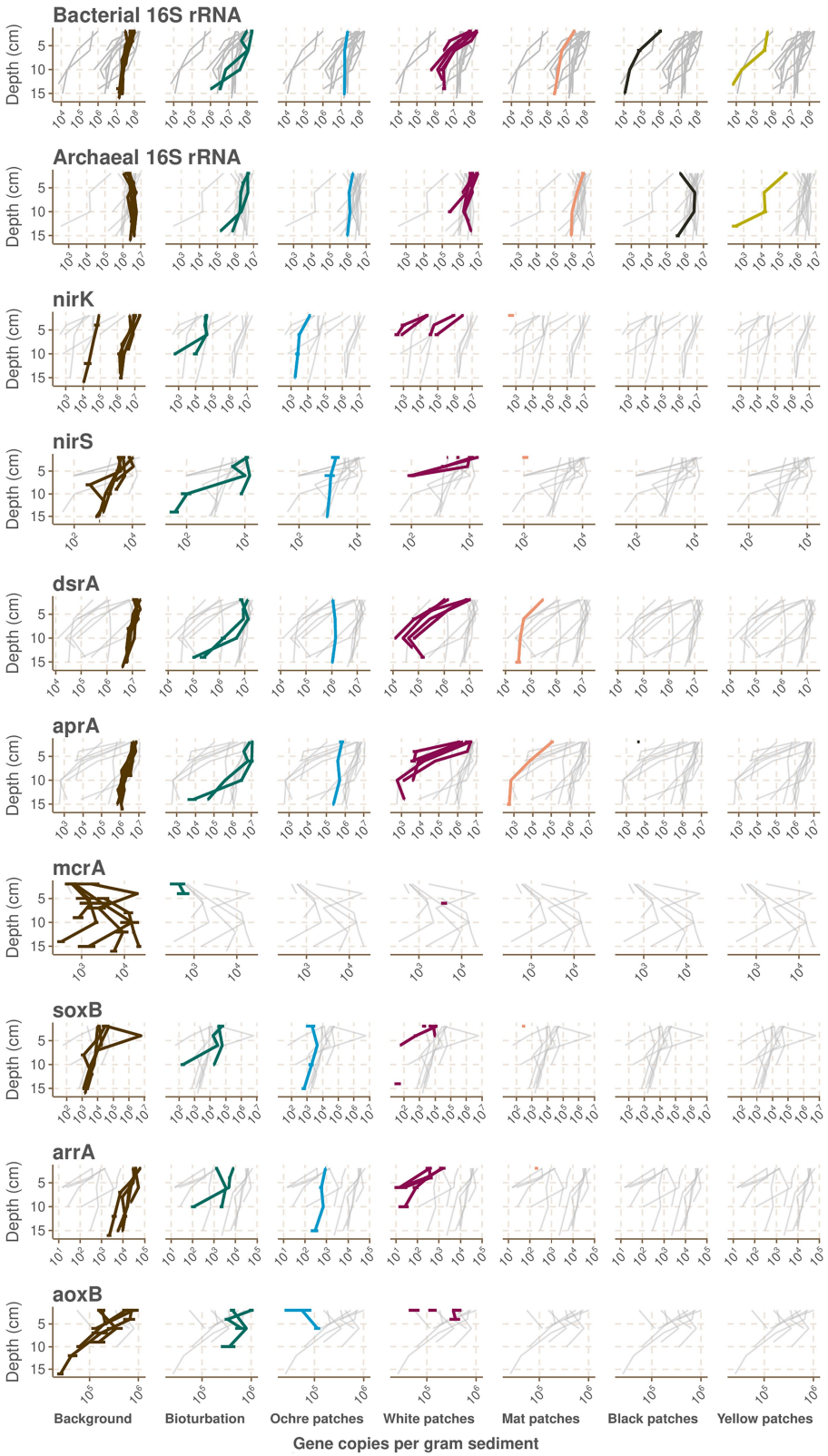

FIGURE 3
Absolute abundances per gram of sediments of various genes in the samples from the CarDHynAl dataset measured by qPCR. Samples are plotted according to their depth and their seafloor type. For each plot, the gray background lines represent the values for this gene in the other seafloor types. Horizontal error lines represent the standard deviation of qPCR triplicates.

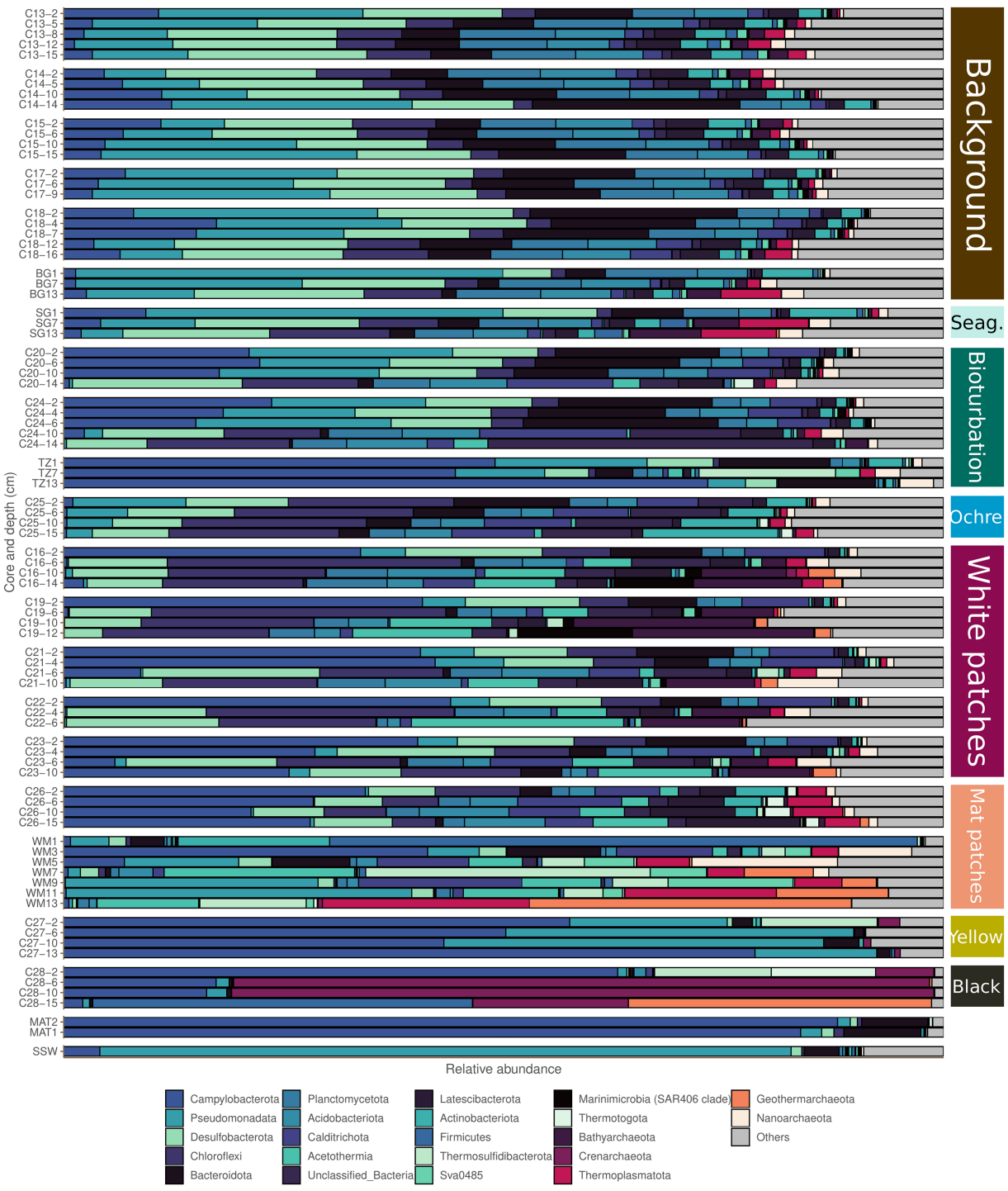

FIGURE 4
Microbial community compositions of the different seafloor types based on 16S rRNA analysis. The barplots show phyla that represent at least 10% of the community in at least one sample from the dataset. The color code to the right for the seafloor types is as in Figure 2.

warmer temperatures, as supported by the presence of taxa mainly found in cores from warmer seafloor types (Figure 4 and Supplementary material 7), its lower diversity compared to the CarDHynal core, and the geographical location of the Saganaki bioturbation zone that surrounds a mat patch, which is warmer than the white patch the CarDHynAl bioturbation zone surrounds. The composition of the ochre patch is similar to a subcomposition of the bioturbation patch, where *Sulfurovaceae* has been removed. The presence of iron oxidizing *Zetaproteobacteria* in ochre patches at the nearby Spathi Bay has

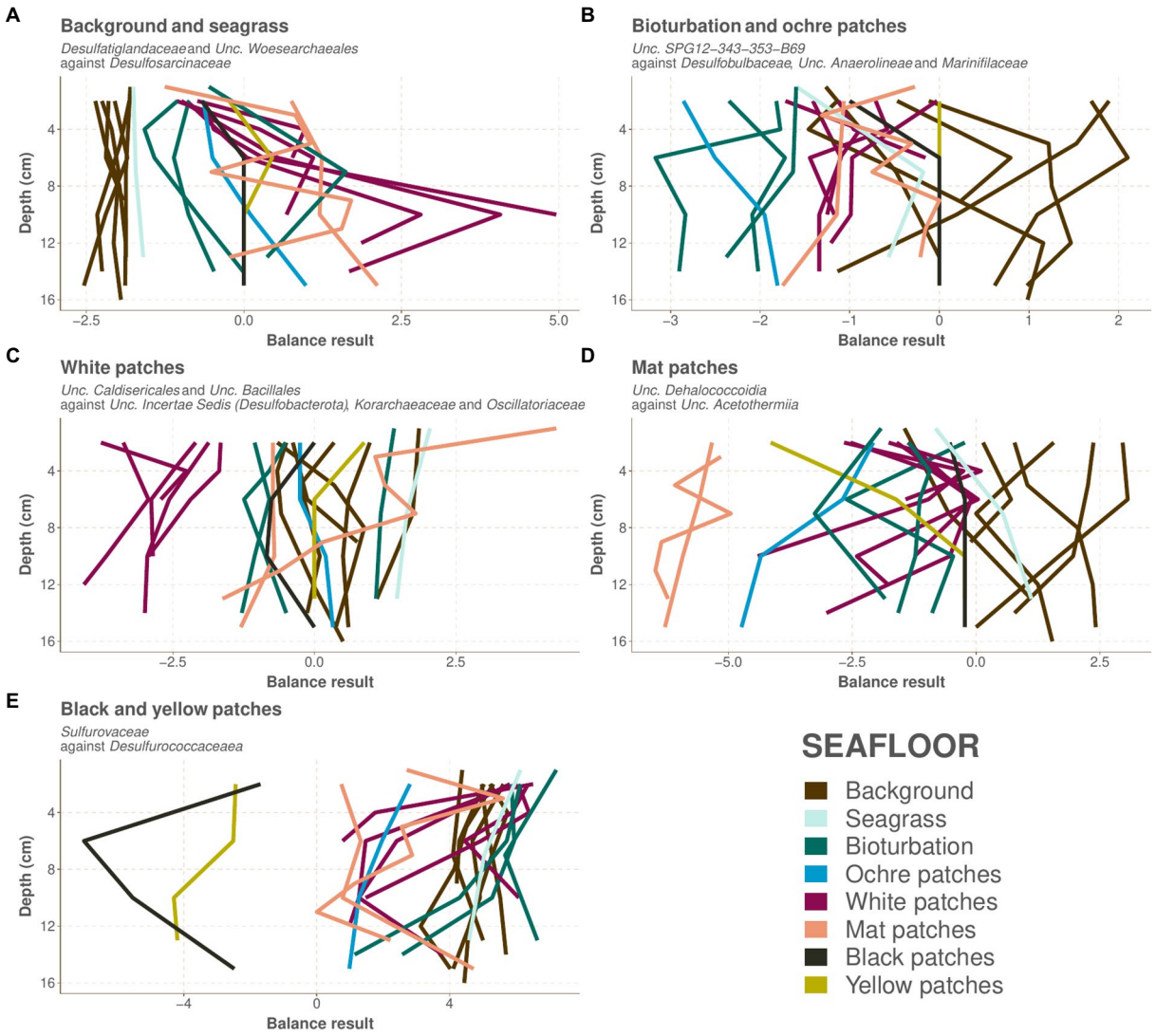

FIGURE 5
Values for the balances selected by the selbal algorithm for the separation of each group of seafloors. The values are plotted against depth, and each path represents one core, colored as in Figure 2. The color code for the seafloor types is as in Figure 1. **(A)** Background and seagrass, **(B)** bioturbation and ochre patches, **(C)** white patches, **(D)** mat patches, **(E)** black and yellow patches.

been shown through qPCR (Callac et al., 2017), but our sequencing data do not support this in our ochre core, with only few *Zetaproteobacteria* sequences detected in the surface of the core (data not shown).

White patches

In the cores from the white patches, the 16S rRNA gene copy numbers range from 8.74e+5 to 2.03e+8 copy.g^{-1} sediment, with a strong decrease with depth (Figure 2D). The decrease is particularly visible for Bacteria, and therefore the relative abundance of Archaea increases with depth, with values between 2.6 and 55.9% of the total prokaryote copies according to qPCR data (Figure 3).

The white patches show a further decrease in diversity compared to previously described seafloor types. Their prokaryotic community composition at the phylum taxonomic level is shown in Figure 4 and at the family level in Supplementary material 7. The balance *Unclassified_Caldisericales* and *Unclassified_Bacillales* against *Unclassified_Incertae Sedis (Desulfobacterota)*, *Korarchaeaceae* and *Oscillatoriaceae* segregates the white patch samples from the rest, with values from −4.07 to −1.66 (median −2.85) for the white patches and from −1.62 to 4.27 (median 0.00) for the others (Figure 5C; Supplementary material 8). Puzenat et al. (2021) reports some very strong gradients of temperature within the white patches, which is also reflected in the change of composition along the cores. For example, the logratio of *Sulfurovaceae* over *Unclassified_Bathyarchaeota* systematically decreases with depth in each core, turning negative around 4–6 cm depth.

Mat patches

The cores from the mat patch show lower absolute 16S rRNA abundance than cores from colder seafloor types, with values going from 3.2e+6 to 4.1e+7 copy.g^{-1} sediments (Figure 2D). Both Bacteria and Archaea copy numbers decrease with depth, and the relative abundance of Archaea goes from 6.4 to 25.6% of the total prokaryote copies according to qPCR data.

Mat patches samples have a lower diversity than the colder seafloors. Their prokaryotic community composition at the phylum taxonomic level is shown in Figure 4 and at the family level in Supplementary material 7. The CoDa-PCA analysis (Figure 2A) and the barplots reveal that the 2 cores exhibit different compositions. For the selbal analysis, we removed the sample WM1 (1 cm deep in the Saganaki core), due to the complete lack of similarity with the rest of the core (We suggest that the surface community of the sediments may be influenced by the surroundings; see discussion in the "Sulfur cycling" section). The selbal analysis selected the balance *Unclassified_Dehalococcoidia* against *Unclassified_Acetothermiia* to segregate this seafloor type from the others, with balance values between −6.48 and −4.95 (median −6.00) for the mat patch samples and between −4.74 and 3.06 (median −0.36) for the others (Figure 5D; Supplementary material 8). We observe some differences between the Saganaki core and the CarDHynAl core, with for example a much stronger decrease in the logratio of *Arcobacteraceae* over *Unclassified_Geothermarchaeota* in the Saganaki core, along with a lower diversity (Figure 2C). This could be linked to different core temperatures, as well as the different types of fluids at the sampling location: The Saganaki core shows the presence of low salinity fluids in the deep section while the CarDHynAl core had high salinity fluids (Supplementary Data 3). Based on clone libraries, differences in bacterial and archaeal community composition between high and low salinity cores has already been shown (Price R. et al., 2013). It is difficult to compare the results we obtain with the ones from Price et al., but taken together these observations suggest some heterogeneity in the mat patches that cannot be constrained by only a few cores.

Black and yellow patches

These seafloor types have the lowest absolute 16S rRNA abundance of the dataset, with values ranging from 4.0e+5 to 3.4e+6 copy.g^{-1} sediment for the black patch and from 7.2e+3 to 7.5e+5 copy.g^{-1} sediment for the yellow patch (Figure 2D). While both Archaea and Bacteria copies decrease with depth in the yellow patch, Archaea remains stable in the top 15 cm of the black patch (Figure 3). According to qPCR data, Archaea 16S rRNA copies account for 34.1 to 99.1% of the total in black patches, and 3.7 to 42.9% in yellow patches.

Black and yellow patches are the seafloor types with the lowest diversity within our dataset. Their prokaryotic community composition at the phylum taxonomic level is shown in Figure 4 and at the family level in Supplementary material 7. The CoDa-PCA analysis (Figure 2A) clusters both seafloor types together, but the barplots reveal that the 2 cores exhibit different compositions. Notably, the logratio of *Sulfurimonadaceae* over *Desulfurococcaceae* is positive in the yellow patch, while it is negative in the black patch. The selbal algorithm selected the balance *Sulfurovaceae* against *Desulfurococcaceae* to discriminate these two seafloor types from the others, with balance values between −7.01 and −1.69 (median −3.35) for the samples from the black and yellow patches and between 0.00 and 7.21 (median 4.58) for the others (Figure 5E; Supplementary material 8). The fact that *Desulfurococcaceae* are almost only detected in these seafloor types plays an important role in the balance. *Stetteria hydrogenophila*, a member of this family, has been previously isolated at Milos in sediments of 107°C (Jochimsen et al., 1997).

Microbial mats

Two different types of microbial mats were sampled in this study, with MAT1 growing on a rock in a flow of hydrothermal fluids, while MAT2 was a 2 cm thick mat lying on top of the Mat patches (as already described in Dando et al., 1995b). The microbial mats are entirely devoid of Archaea (only 0.1% of the community in the mat sample attached to the rock). Both samples present the same community pattern, with a composition dominated by *Campylobacterota* (around 80% of the community), as well as some *Bacteroidetes* (Figure 4). This composition is similar to mats observed in deep sea hydrothermal systems, such as at Loki's Castle Vent Field (Stokke et al., 2015). Both samples contain the families *Sulfurimonadaceae* and *Arcobacteraceae*, but *Sulfurovaceae* is only present in the mat sample from the rock. The genus *Arcobacter* has already been found in the mats previously (Sievert et al., 1999), and has been suggested to possibly play a key role in their formation (Sievert et al., 2007). However, the composition described here is in contradiction to earlier descriptions who showed the dominance of *Achromatium volutans* in the mats, a genus not detected in our study (Dando et al., 1995b; Fitzsimons et al., 1997). Similarly, Fitzsimons et al. (1997) reported the presence of *Thiobacillus* sp. in the mat, which we did not detect. Diatoms have also been reported in the mats, but we did not investigate these here (Sievert et al., 1999).

Seawater

The seawater sample of the Saganaki dataset is completely different from any other sample taken in this study (Figure 4). The taxa with highest relative abundance belong to Clade I of SAR11 and the AEGEAN-169 marine group (both *Alphaproteobacteria*), the SAR86 clade and the *Halieaceae* (both *Gammaproteobacteria*) and the *Puniceicoccaceae* (*Verrucomicrobiota*).

Microbial metabolic capabilities in Paleochori sediments

In addition to our extensive sequencing data of the prokaryotic communities, we have also quantified several functional genes using qPCR on the CarDHynAl dataset. In the following section, we discuss these results in light of previous studies on bioenergetic

landscapes (Lu et al., 2020), most probable numbers of various functional groups (Sievert et al., 1999), and reaction rates (Dando et al., 1995b; Bayraktarov et al., 2013; Gilhooly et al., 2014; Houghton et al., 2019) to investigate some metabolic capabilities of the communities. It is however important to note that the detection of functional genes in the DNA extraction of a sample merely suggests the potential for the community to perform the metabolic pathway but does not imply its use. We divide the discussion into the following geochemical processes relevant to this ecosystem: Organic carbon remineralization, nitrogen cycling, sulfur cycling, iron cycling, methanogenesis, and arsenic cycling.

Organic carbon remineralization

In sediments, microbes typically use organic matter (OM) deposited from the seawater as an electron donor. The process oxidizes the organic matter through the reduction of various electron acceptors, which will be used in sequence according to the amount of energy released: Oxygen first, then nitrate, manganese, iron, sulfate, and carbon dioxide. The more organic matter present in the sediments, the faster these electron acceptors will be depleted, and the penetration of oxygen in sediments is therefore closely linked to organic matter content (Middelburg, 2019). In hydrothermal settings, the pattern is however more complex as rising fluids are also a source of electron donors, allowing the growth of autotrophic species that will in turn be a new source of OM for remineralization. At Milos, oxygen has been shown to penetrate the sediments with only a few centimeters at the venting sites and a few millimeters to no penetration at all when leaving the vents (Sievert et al., 1999; Wenzhöfer et al., 2000; Yücel et al., 2013). The deeper penetration at vents is however suggested to be due to short-scaled seawater recharge patterns rather than lower OM content. Indeed, Dando et al. (1995b) showed that there is more total organic carbon (TOC) at the vents compared to background sediments, which they suggest reflects an increase in microbial biomass at the venting sites. However, Giovannelli et al. (2013) rather show a decrease in microbial biomass and abundance when leaving the vents, and therefore hypothesize that the higher TOC at vents is due to a decrease in remineralization. This effect is likely enhanced by the inhibition of sulfate reduction under the acidic conditions created by the hydrothermal fluids (Bayraktarov et al., 2013). Our qPCR results of bacterial and archaeal 16S rRNA genes confirm the previous observations that microbial abundance decreases with increasing temperature (Figures 2D, 3). Organic matter remineralization is nevertheless likely a important process in Paleochori Bay, as suggested by the regular detection of putative heterotrophs such as *Acidimicrobiia*, *Anaerolineae*, *Bacteroidia*, *Fusobacteriia*, *Thermodesulfobacteria* and *Thermotogae* (this study; Sievert et al., 2000a,b, 2022; Giovannelli et al., 2013; Price R. et al., 2013; Price R.E. et al., 2013).

Nitrogen cycling

The *nirK* gene, involved in heterotrophic and autotrophic denitrification, has highest absolute abundance (around 10e+7 copies per gram sediment) in the shallowest samples of the background cores, and shows decreasing trends with depth and increasing temperature (Figure 3). There is however some variance, with for example the background core C18 that exhibits concentrations 2 orders of magnitude lower than the other background cores, suggesting some heterogeneity even within the background seafloor. As well, the white patches have higher concentrations of *nirK* than the colder bioturbation and ochre patch seafloor types close to the surface, however *nirK* falls below detection limit at sediment depth below 6 cm in the white patches. *NirK* is then only detected at 2 cm depth in the mat patches and is absent in the very hot black and yellow patches. However, the *nirK* gene has been shown to divide into two phylogenetically distinct clades, and our primers amplify only a clade composed of *Alphaproteobacteria* plus few *Gamma-* and *Betaproteobacteria* (Helen et al., 2016). Most *nirK* gene diversity is found in the other clade, which include members of *Bacteroidetes*, *Chloroflexi*, *Nitrospirae*, *Firmicutes*, *Actinobacteria*, *Planctomycetes*, and several archaeal lineages. This can potentially explain why we do not detect the *nirK* gene in warmer seafloor. Our quantification of the *nirS* gene shows a similar pattern, but once more our primer set has been shown to omit numerous taxa, including members of the *Campylobacterota* which are dominant in the hydrothermally influenced sediments and known to reduce nitrate and nitrite (Murdock and Juniper, 2017). Nitrate/nitrite reduction is likely still happening at higher temperatures, as supported by models showing that the energy released by sulfide oxidation coupled to nitrite reduction could support much of the chemolithotrophic primary production at the venting site (Lu et al., 2020). Such chemolithotrophic nitrate-reducing sulfur-oxidizing bacteria have been isolated from Milos in the past, but they are mesophilic and therefore unlikely to grow directly at the venting site (Kuever et al., 2002). The identification of potential denitrifier in our dataset using the 16S rRNA sequences is difficult, as the process is potentially performed by a wide phylogenetic range of microbes (Helen et al., 2016). Nevertheless, most *Campylobacterota* can use nitrate as a terminal elecron acceptor, and we also detect the presence in the bioturbation and ochre patch seafloors of the *Calditrichaceae* family which are moderately thermophilic and some members are known to grow by respiring nitrate (Bonch-Osmolovskaya and Kublanov, 2021).

We do not detect in our 16S rRNA dataset any *Nitrosopumilaceae*, a family known for the potential of its members to oxidize ammonia aerobically (Qin et al., 2017). Consistently, no bacterial or archaeal *amoA* gene was detected in the CarDHynAl dataset. However, we detect high relative abundances of *Geothermarchaeaceae* in the mat patch core from the Saganaki dataset. While very little is known about this family, they also belong to the *Thaumarchaeota/Nitrososphaeraeota* phylum. This, along with the observation that ammonia oxidation is exergonic under these conditions (Lu et al., 2020), could suggest that *Geothermarchaeaceae* might be involved in this process.

Sulfur cycling

Sulfur cycling in marine sedimentary environments is a complex network of connected biotic and abiotic reactions driven largely by the marine sulfate reservoir as the ultimate sulfur source. These processes transform sulfur species between the oxidized (sulfate) and reduced (sulfide) end members, along with numerous intermediate valence compounds (reviewed in Jørgensen et al., 2019). *DsrA* and *aprA*, involved in sulfate reduction, display a similar distribution pattern as *nirK*, with around 10e+7 copies per gram sediment in the shallowest background cores, and a decrease with increasing depth and temperature (Figure 3). Most of the previous studies at Milos on sulfate reduction have shown a similar trend. Notably, the same *dsrA* qPCR trend was found in the neighboring Spathi Bay, albeit with much higher gene copy concentration compared to this study (Callac et al., 2017). Sulfate reduction rates were found to peak in the upper 2 cm, although with no relation to the distance from the vent (Dando et al., 1995b), while other isotopic studies found an increase of sulfate reduction when leaving the vents (Bayraktarov et al., 2013; Houghton et al., 2019). Only one study reported that no obvious isotopic signature for biotic sulfur cycling could be found (Gilhooly et al., 2014), but they suggest that this could be linked to a lack of available TOC for remineralization in their samples, highlighting once more the spatial heterogeneity within each type of seafloor at Paleochori Bay. Most probable number studies found an increase of sulfate reducing bacteria away from the vent (Sievert et al., 1999). However, we find members of the *Desulfobacterota* phylum, of which many members can reduce sulfate using *dsrAB* (Waite et al., 2020), throughout our dataset. While lower pH has been shown to inhibit sulfate reduction at Milos, some sulfate reducers can also adapt to life at low pH (Bayraktarov et al., 2013). In support, the thermophilic sulfate-reducing bacterium *Desulfacinum hydrothermale* was isolated from pH 5 sediments (Sievert and Kuever, 2000). However, in our study, the family *Syntrophobacteraceae*, to which *D. hydrothermale* belongs, is mainly detected in seafloors with colder temperatures and pH close to neutral. In our core from the black patch, we find the genus *Staphylothermus*, a sulfur reducing hyperthermophilic Archaeon belonging to the family *Desulfurococcaceae* also isolated from Milos (Supplementary Data 7; Arab et al., 2000; Hao and Ma, 2003).

In areas of hydrothermal activity, the advective influx of reduced sulfur species can also fuel the growth of sulfur oxidizing organisms (Sievert et al., 2008, 2022). At Milos, the fluids contain abundant H_2S (Fitzsimons et al., 1997), and the sulfidic zone has been shown to reach or nearly reach the seafloor, except directly at the vent where seawater microcirculation allows for oxygen to penetrate a few centimeters (Wenzhöfer et al., 2000; Yücel et al., 2013). As a result, many studies at Milos have reported the presence of bacteria able to oxidize sulfide (SOB). The most striking feature is the presence of cotton-like white microbial mats whether lying on the mat patches or attached to rocks where fluids come out (Dando et al., 1995b). We find that these mats consist to around 80% of *Arcobacteraceae*, *Sulfurimonadaceae*, and *Sulfurovaceae,* which contain the well-known marine SOB genera *Arcobacter*, *Sulfurimonas*, and *Sulfurovum*, respectively (Wirsen et al., 2002; Inagaki et al., 2003, 2004; Sievert et al., 2007). In the sediments, the energy densities of sulfide oxidation are very variable, suggesting highly localized processes, but with higher potential for autotrophy in the more hydrothermally influenced areas where sulfide oxidation coupled to the reduction of oxygen, nitrate, and/or nitrite could support much of the chemolithotrophic primary production (Lu et al., 2020; Sievert et al., 2022). As well, sulfur isotopic analyses suggest that H_2S is oxidized by microbes close to the venting zone (Houghton et al., 2019). However, our qPCR analysis of the *soxB* gene shows that the gene is most abundant in the background samples, decreasing with depth and increasing temperature to finally be only present in the shallowest sample of the mat patch seafloor type (Figure 3). The presence of SOB in the background and bioturbation seafloor types was already shown using most probable number dilution series (Brinkhoff et al., 1999; Sievert et al., 1999), and isotopic studies then suggested that they could recycle the sulfide produced by sulfate reducer (Houghton et al., 2019). The rapidly changing geochemical conditions at Milos, for example due to waves and storms, could shift the direction of the reaction, explaining why we observe both sulfate reducers and sulfide oxidizers in the same samples (Figure 4; Supplementary material 7). The absence of *soxB* genes in our warmer cores is likely the result of primer specificity. Indeed, we measure very low gene abundance of *soxB* in our samples (around 10e+4 in the background and the seagrass seafloors) in comparison to the high abundance of bacterial 16S rRNA copies (around 10e+7 in the same seafloors), and *in silico* analysis shows that our *soxB* primers do not target *Campylobacterota* (Supplementary Data 6). Our sequencing data show a change in the family distribution within the *Campylobacterota* phylum: While *Sulfurovaceae* dominate in the background, seagrass and white patches, they are then replaced by *Arcobacteraceae* and *Sulfurimonadaceae* in the mat, yellow and black patches (Supplementary material 7). The bioturbation seafloor type shows all three families, and our ochre patch core seems mostly devoid of *Campylobacterota*, despite the *soxB* gene being detected there. Recently, the *Sulfurovaceae* family was similarly not detected in an *in-situ* carbon fixation experiment in the mat patches (Sievert et al., 2022). However, community compositions of 0–1 cmbsf hydrothermal and background sediment where *Sulfurovaceae* is a major part of the composition in both types of sediments have been described (Giovannelli et al., 2013). They report that *Epsilonproteobacteria* (now *Campylobacterota*) represent 60% of each prokaryotic community, which is much more than what we measured. However, superficial sediment communities are likely impacted by microbial mats and seawater communities, and are therefore highly dissimilar to deeper samples as seen in some of our cores (data not shown). The genus *Thiomiscrospira,* and the strain *Thiomicrospira* sp. Milos-T1 isolated at Milos, has been suggested to be a major actor of sulfur oxidation in Paleochori Bay (Brinkhoff et al., 1999), but these results were not supported in a recent study (Sievert et al., 2022),

and in our dataset the family *Thiomicrospiraceae* is mainly present only in the yellow patch composition. Similarly, the family of the sulfur oxidizing bacteria *Halothiobacillus kellyi* isolated at Milos (Sievert et al., 2000b) represents at best 0.9% of any sample.

Finally, the family *Desulfocapsaceae* and the genus *Desulfocapsa* known for sulfur disproportionation (Finster et al., 1998) are detected in the background cores (Supplementary material 7). This reaction had been shown to be exergonic in most niches around hydrothermal systems (Alain et al., 2022), but we cannot confirm its use at Milos with our dataset.

Iron cycling

We did not directly investigate the presence of genes involved in iron reduction in our study. Nevertheless, dissimilatory iron reducing bacteria have been found at Milos in the colder seafloor types, seemingly correlated to Fe(III) concentrations (Sievert et al., 1999). It is however difficult to identify which organisms are responsible for iron reduction. The iron reducer *Deferrisoma palaeochoriense* has been isolated from Paleochori Bay (Pérez-Rodríguez et al., 2016), but we find *Deferrisomataceae*, its family, to represent a maximum of 0.3% of the community of any sample in our dataset. Similarly, the *Deferribacteraceae* (Huber and Stetter, 2015), the *sva1033* family of the *Desulfobacterota* (supposed to perform dissimilatory iron reduction (Wunder et al., 2021)), and the *Archaeoglobaceae* (to which *Geoglobus* belongs (Kashefi et al., 2002; Slobodkina et al., 2009)) represent at best 0.2% of the community in any sample. Among the taxa with higher relative abundance, the order *Actinomarinales,* representing up to 14.6% of the community in the ochre patches, have been shown to have a gene cluster related to the acquisition of Fe(III) (López-Pérez et al., 2020).

Methanogenesis

McrA in our study is detected only in the background and in 3 single samples in the bioturbation and white patch seafloors. In the background cores, the gene abundance peaks between 5 and 10 cm. This would suggest that methanogenesis would only occur at a specific horizon. While Callac et al. also found the highest *mcrA* copies in their background reference sediments, they also detect the gene in the brown and white sediments and do not have an abundance peak at a few centimeters depth (Callac et al., 2017). Based on the data available, the relevance of methanogenesis at Milos remains elusive.

Arsenic cycle

Arsenic is a compound that is ubiquitous in the marine biosphere, where it is poisonous to most organisms due to its chemical similarity with phosphate (Bidlack, 2002). However, some prokaryotes have developed strategies to detoxify from arsenic, and sometimes even use it as an energy source (Páez-Espino et al., 2009; Tsai et al., 2009). In Paleochori Bay, the hydrothermal venting discharges high concentrations of arsenic, with concentrations of up to 78 μM previously measured in low salinity fluids (Price R.E. et al., 2013). At the yellow patch location of our C27 core, we measured concentrations of arsenic of 84 μM in high salinity fluids (Supplementary material 3), and observed under scanning electron microscopy the precipitation of arsenic oxides and orpiment (As_2S_3) coating the sand grains as described previously (Supplementary material 3; Price R.E. et al., 2013; Godelitsas et al., 2015). We investigated the adaptation of prokaryotes to arsenic by quantifying the *arrA* (Arsenate respiratory reductase) and *aoxB* (Arsenite oxidase) genes involved in energy production. We also tried to amplify *arxA,* also involved in energy production, and *arsB* and *C,* involved in detoxification, but with no avail. Both *arrA* and *aoxB* showed similar abundance pattern, with highest concentrations found in the shallow background sediments, and a decrease with increasing depth and temperature (Figure 3). The *arrA* gene is not detected beyond the shallowest sample in the mat patch seafloor, while the *aoxB* gene is not present beyond the white patches. We do not detect these genes in the core from the yellow patch, where high concentrations of arsenic are measured. While seemingly counter-intuitive, similar results were found in the nearby Spathi Bay, where higher concentrations of *aoxB*, *arrA*, *arsB*, *acr3-1* and *acr3-2* were found away from the venting zone (Fru et al., 2018). The authors suggest that in the vicinity of the vents, the acidic fluids and high sulfur concentrations effectively trap arsenic into orpiment by precipitation. The lack of such arsenic sink further away correlates with the increase of arsenic-related genes. Also, arsenic-resistance genes are much more abundant than arsenic-metabolism genes, suggesting the ability of the community to rapidly adapt to arsenic surges in the system (Fru et al., 2018). Similar to our qPCR analysis, our 16S rRNA sequencing data does not show any clear response of the community composition to the high arsenic concentrations in the yellow patch. This observation matches the results from Callac et al., who did not find arsenic to be a major selector for carbon fixation genes in the nearby Spathi Bay (Callac et al., 2017). Price et al. found some *aioA* (other name of *aox*) sequences in the mat patches, but the clones, belonging to *Alphaproteobacteria* and *Betaproteobacteria,* showed little overlap with their 16S rRNA data (Price R. et al., 2013), suggesting that these are not major parts of the community composition. This is consistent with the models showing that reactions using As(V) as an electron acceptor can provide only very little energy at Milos (Lu et al., 2020). However, we found that As(III) is present in low concentrations in the shallows to middle depths in the bioturbation core from Saganaki (data not shown). In this core we also find the presence of the *Sulfurospirillaceae* family, to which the Fe(III) and As(V) respiring bacterium *Sulfospirillium barnesii* belongs (Stolz et al., 1999), and the presence of arsenic could therefore be linked to the desorption of arsenic upon the dissolution of solid iron phases (Herbel and Fendorf, 2006).

Conclusion and future perspectives

The present study has provided a significant upgrade in our understanding of the prokaryotic communities in the Paleochori Bay of Milos. For the first time we present a thorough description

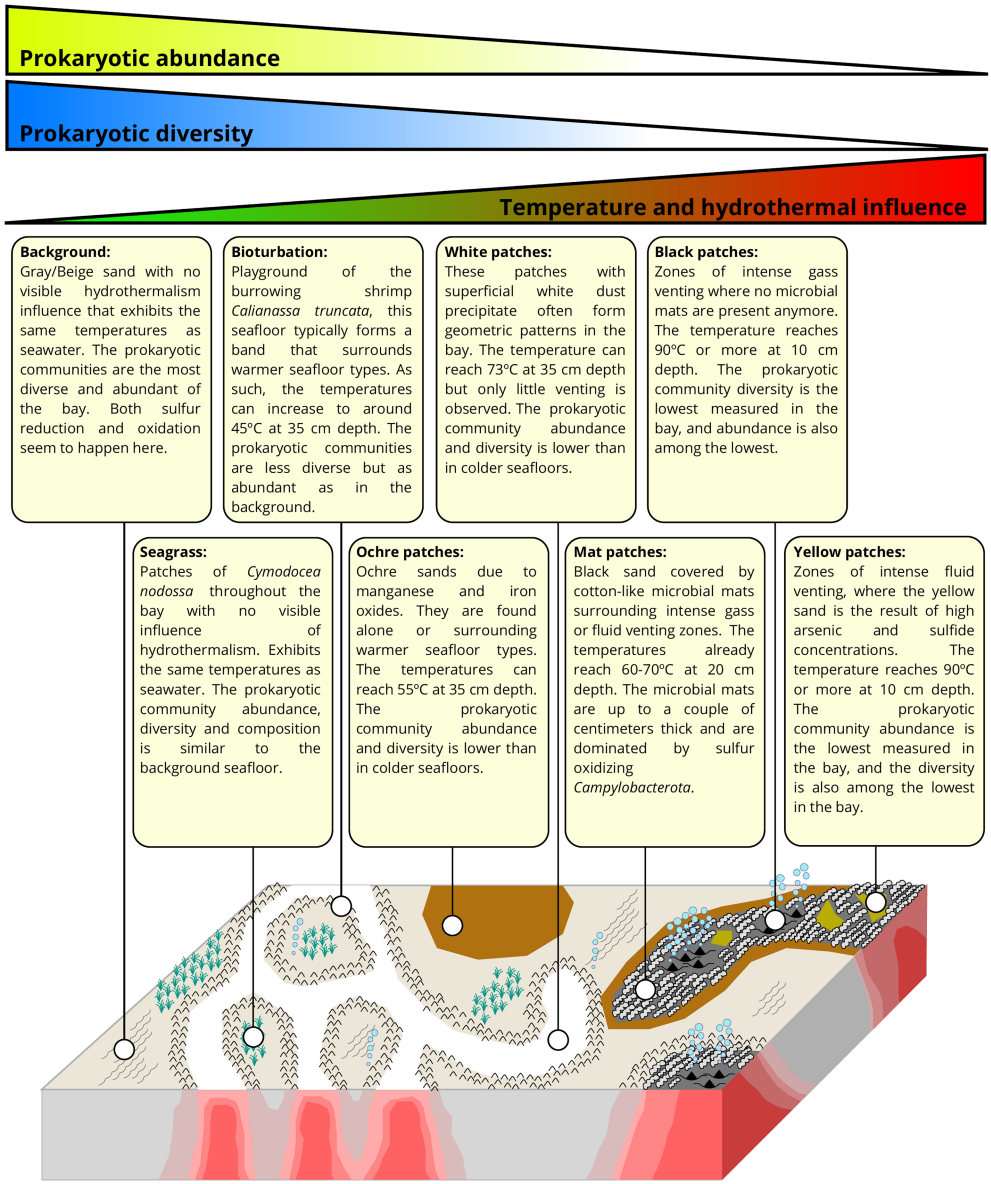

FIGURE 6
Description of the various seafloors observed in Paleochori Bay, along with the general trends of abundance, diversity, and composition of the prokaryotic communities (modified from the hydrothermal distribution model for Milos in Puzenat et al. (2021)).

of the visual diversity of seafloor types present in the bay and the prokaryotic communities inhabiting them (Figure 6). Our results show the strong impact of hydrothermal activity on community composition, abundance, diversity, and metabolic potential. It should however be noted that we observe some heterogeneity within seafloor types, and hence our samples are unlikely to cover the entire span of microbial diversity inhabiting the bay.

Furthermore, several aspects of the ecosystem are still poorly investigated, and we find the following potential research subjects very relevant to further increase our understanding of the microbial communities inhabiting Paleochori Bay. (i) The physical, chemical, and microbiological heterogeneity of some seafloor types are not well constrained. Notably we present only one core taken from the ochre patches while they represent a massive surface area. As well, the difference between low-salinity and high-salinity communities in the mat patches needs further investigation. (ii) A major difference between deep and shallow hydrothermal systems is the possibility for phototrophic organisms to play a role in the food chain. During our sequence decontamination protocol, we removed in some samples up to 8% of reads assigned to chloroplasts. This mainly happened in the colder seafloor types, suggesting higher importance of phototrophy there. However, the importance of phototrophy in the ecosystem is yet to be investigated. (iii) While we have presented here a substantial dataset of 16S rRNA gene sequences, the general understanding of the microbial communities would highly benefit from transcriptomic studies. This could for

example help understanding why sulfur reducers and oxidizers are present in the same samples, and also constrain the temporal impact of tides on the communities. (iv) Sulfur oxidizing microbial mats are common in hydrothermal systems. However, due to its temporal instability, the mats at Paleochori Bay are ideal to investigate their development and growth, allowing for *in situ* experiments on mat growth that would be otherwise difficult in the deep sea. (v) Viruses are known to be key player in marine ecosystems (Suttle, 2007; Rohwer et al., 2009; Sime-Ngando, 2014), and are likely to play a strong ecological and evolutionary role in deep hydrothermal systems (Ortmann and Suttle, 2005; Castelán-Sánchez et al., 2019). In shallow systems, Manini et al. (2008) described a rather low viral abundance, but there is to our knowledge no other investigation of the viral community in shallow hydrothermal systems. Milos, with its high temporal variability, would be an ideal place to study and monitor the virus-host dynamics at play. (vi) Milos is a major natural discharge of arsenic and therefore an ideal place to investigate how organisms cope with this highly poisonous compound. Godelitsas et al. (2015) and our study identified potentially biogenic arsenic-sulfide filaments and spirals (Supplementary Data 3), which have previously been suggested to result from the mineralization of hyphae (Dekov et al., 2013). Further investigations on arsenotrophy and arsenic detoxification based on cultures or molecular approaches could potentially help developing new arsenic bioremediation approaches.

Data availability statement

The data presented in the study are deposited in the European Nucleotide Archive database, project accession number PRJEB56441.

Author contributions

SL, VP, AS, TB, J-EM, JEs, JA, PP, and OV participated in the sampling campaign at Milos. SL, G-SL, and SG did the laboratory work. SL, VP-G, and JEg analyzed the data. SL, G-SL VP-G, JEg, JA, and SJ actively participated in the writing of the article. All coauthors read and approved the manuscript.

Funding

Funding for the Saganaki dataset and JPA and G-SL was provided by NSF grants OIA-0939564 to the Center for Dark Energy Biosphere Investigations (C-DEBI). The CarDHynAl project was partially funded by INSU-CNRS Tellus and Syster Projects to JEs (2016) and J-EM (2018), and with partial support by RAMONES, funded by the European Union's Horizon 2020 Research and Innovation Program, under grant agreement number 101017808 (to JEs and PN). The laboratory work was supported by the Trond Mohn Foundation and the University of Bergen through the Centre for Deep Sea research (grant TMS2020TMT13). VP-G and JEg are supported by the Spanish Ministry of Science and Innovation and the European Regional Development Fund [grant numbers PID2021-125380OB-I00 and PID2021-123833OB-I00 (MCIN/AEI/FEDER)].

Conflict of interest

The authors declare that the research was conducted in the absence of any commercial or financial relationships that could be construed as a potential conflict of interest.

Publisher's note

All claims expressed in this article are solely those of the authors and do not necessarily represent those of their affiliated organizations, or those of the publisher, the editors and the reviewers. Any product that may be evaluated in this article, or claim that may be made by its manufacturer, is not guaranteed or endorsed by the publisher.

Supplementary material

The Supplementary material for this article can be found online at: https://www.frontiersin.org/articles/10.3389/fmicb.2022.1060168/full#supplementary-material

References

Aitchison, J. (1983). Principal component analysis of compositional data. *Biometrika* 70, 57–65. doi: 10.2307/2335943

Aitchison, J. (1986). The Statistical Analysis of Compositional Data. Available at: https://link.springer.com/book/9780412280603 (Accessed October 1, 2022).

Alain, K., Aronson, H. S., Allioux, M., Yvenou, S., and Amend, J. P. (2022). Sulfur disproportionation is exergonic in the vicinity of marine hydrothermal vents. *Environ. Microbiol.* 24, 2210–2219. doi: 10.1111/1462-2920.15975

Alt, J. C. (1995). "Subseafloor processes in Mid-Ocean ridge Hydrothennal systems" in *Seafloor Hydrothermal Systems: Physical, Chemical, Biological, and Geological Interactions* (USA: AmericanJohn Wiley & Sons, Ltd), 85–114.

Arab, H., Völker, H., and Thomm, M. (2000). *Thermococcus aegaeicus* sp. nov. and *Staphylothermus hellenicus* sp. nov., two novel hyperthermophilic archaea isolated from geothermally heated vents off Palaeochori Bay, Milos, Greece. *Int. J. Syst. Evol. Microbiol.* 50, 2101–2108. doi: 10.1099/00207713-50-6-2101

Bayraktarov, E., Price, R., Ferdelman, T., and Finster, K. (2013). The pH and pCO2 dependence of sulfate reduction in shallow-sea hydrothermal CO2 – venting sediments (Milos Island, Greece). *Front. Microbiol.* 4:111. doi: 10.3389/fmicb.2013.00111

Beaulieu, S. E., and Szafranski, K. (2020). Inter Ridge Global Database of Active Submarine Hydrothermal Vent Fields, Version 3.4. Available at: https://vents-data.interridge.org/terms_of_use (Accessed January 06, 2022).

Berry, D., Mahfoudh, K. B., Wagner, M., and Loy, A. (2011). Barcoded primers used in multiplex amplicon pyrosequencing bias amplification. *Appl. Environ. Microbiol.* 77, 7846–7849. doi: 10.1128/AEM.05220-11

Bidlack, W. R. (2002). Casarett & Doull's toxicology: the basic science of poisons, 6th ed. *J. Am. Coll. Nutr.* 21, 289–290. doi: 10.1080/07315724.2002.10719223

Bokulich, N. A., Subramanian, S., Faith, J. J., Gevers, D., Gordon, J. I., Knight, R., et al. (2013). Quality-filtering vastly improves diversity estimates from Illumina amplicon sequencing. *Nat. Methods* 10, 57–59. doi: 10.1038/nmeth.2276

Bonch-Osmolovskaya, E. A., and Kublanov, I. V. (2021). "Calditrichaceae," in *Bergey's Manual of Systematics of Archaea and Bacteria*. (USA: John Wiley & Sons, Ltd), 1–3.

Brinkhoff, T., Sievert, S. M., Kuever, J., and Muyzer, G. (1999). Distribution and diversity of sulfur-oxidizing *Thiomicrospira* spp. at a shallow-water hydrothermal vent in the Aegean Sea (Milos, Greece). *Appl. Environ. Microbiol.* 65, 3843–3849. doi: 10.1128/AEM.65.9.3843-3849.1999

Bühring, S. I., and Sievert, S. M. (2017). *4. The Shallow Submarine Hot Vent System Off Milos (Greece) – A Natural Laboratory for the Study of Hydrothermal Geomicrobiology*. Germany: De Gruyter, 85–106.

Callac, N., Posth, N. R., Rattray, J. E., Yamoah, K. K. Y., Wiech, A., Ivarsson, M., et al. (2017). Modes of carbon fixation in an arsenic and CO2-rich shallow hydrothermal ecosystem. *Sci. Rep.* 7:14708. doi: 10.1038/s41598-017-13910-2

Caporaso, J. G., Lauber, C. L., Walters, W. A., Berg-Lyons, D., Lozupone, C. A., Turnbaugh, P. J., et al. (2011). Global patterns of 16S rRNA diversity at a depth of millions of sequences per sample. *PNAS* 108, 4516–4522. doi: 10.1073/pnas.1000080107

Castelán-Sánchez, H. G., Lopéz-Rosas, I., García-Suastegui, W. A., Peralta, R., Dobson, A. D. W., Batista-García, R. A., et al. (2019). Extremophile deep-sea viral communities from hydrothermal vents: structural and functional analysis. *Mar. Genomics* 46, 16–28. doi: 10.1016/j.margen.2019.03.001

Chen, C.-T. A., Zeng, Z., Kuo, F.-W., Yang, T. F., Wang, B.-J., and Tu, Y.-Y. (2005). Tide-influenced acidic hydrothermal system offshore NE Taiwan. *Chem. Geol.* 224, 69–81. doi: 10.1016/j.chemgeo.2005.07.022

Dando, P. R., Aliani, S., Arab, H., Bianchi, C. N., Brehmer, M., Cocito, S., et al. (2000). Hydrothermal studies in the Aegean Sea. *Phys. Chem. Earth* 25, 1–8. doi: 10.1016/S1464-1909(99)00112-4

Dando, P. R., Hughes, J. A., Leahy, Y., Niven, S. J., Taylor, L. J., and Smith, C. (1995a). Gas venting rates from submarine hydrothermal areas around the island of Milos, Hellenic volcanic arc. *Cont. Shelf Res.* 15, 913–929. doi: 10.1016/0278-4343(95)80002-U

Dando, P. R., Hughes, J. A., and Thiermann, F. (1995b). Preliminary observations on biological communities at shallow hydrothermal vents in the Aegean Sea. *Geol. Soc. Lond. Spec. Publ.* 87, 303–317. doi: 10.1144/GSL.SP.1995.087.01.23

Dando, P., Thomm, M., Arab, H., Brehmer, M., Hooper, L. R. E., Jochimsen, B., et al. (1998). Microbiology of Shallow Hydrothermal Sites off Palaeochori Bay, Milos (Hellenic Volcanic Arc). Undefined. Available at: https://www.semanticscholar.org/paper/Microbiology-of-shallow-hydrothermal-sites-off-Bay%2C-Dando-Thomm/63459813952a7504bad15b0743c601464c2233a3 (Accessed January 05, 2022).

Davis, N. M., Proctor, D. M., Holmes, S. P., Relman, D. A., and Callahan, B. J. (2018). Simple statistical identification and removal of contaminant sequences in marker-gene and metagenomics data. *Microbiome* 6:226. doi: 10.1186/s40168-018-0605-2

Dekov, V. M., Bindi, L., Burgaud, G., Petersen, S., Asael, D., Rédou, V., et al. (2013). Inorganic and biogenic as-sulfide precipitation at seafloor hydrothermal fields. *Mar. Geol.* 342, 28–38. doi: 10.1016/j.margeo.2013.06.006

Eisenhofer, R., Minich, J. J., Marotz, C., Cooper, A., Knight, R., and Weyrich, L. S. (2019). Contamination in low microbial biomass microbiome studies: issues and recommendations. *Trends Microbiol.* 27, 105–117. doi: 10.1016/j.tim.2018.11.003

Finster, K., Liesack, W., and Thamdrup, B. (1998). Elemental sulfur and thiosulfate disproportionation by *Desulfocapsa sulfoexigens* sp. nov., a new anaerobic bacterium isolated from marine surface sediment. *Appl. Environ. Microbiol.* 64, 119–125. doi: 10.1128/AEM.64.1.119-125.1998

Fitzsimons, M. F., Dando, P. R., Hughes, J. A., Thiermann, F., Akoumianaki, I., and Pratt, S. M. (1997). Submarine hydrothermal brine seeps off Milos, Greece. Observations and geochemistry. *Mar. Chem.* 57, 325–340. doi: 10.1016/S0304-4203(97)00021-2

Frøslev, T. G., Kjøller, R., Bruun, H. H., Ejrnæs, R., Brunbjerg, A. K., Pietroni, C., et al. (2017). Algorithm for post-clustering curation of DNA amplicon data yields reliable biodiversity estimates. *Nat. Commun.* 8:1188. doi: 10.1038/s41467-017-01312-x

Fru, E. C., Callac, N., Posth, N. R., Argyraki, A., Ling, Y.-C., Ivarsson, M., et al. (2018). Arsenic and high affinity phosphate uptake gene distribution in shallow submarine hydrothermal sediments. *Biogeochemistry* 141, 41–62. doi: 10.1007/s10533-018-0500-8

Fytikas, M., Innocenti, F., Kolios, N., Manetti, P., Mazzuoli, R., Poli, G., et al. (1986). Volcanology and petrology of volcanic products from the island of Milos and neighbouring islets. *J. Volcanol. Geotherm. Res.* 28, 297–317. doi: 10.1016/0377-0273(86)90028-4

Gilhooly, W. P., Fike, D. A., Druschel, G. K., Kafantaris, F.-C. A., Price, R. E., and Amend, J. P. (2014). Sulfur and oxygen isotope insights into sulfur cycling in shallow-sea hydrothermal vents, Milos, Greece. *Geochem. Trans.* 15:12. doi: 10.1186/s12932-014-0012-y

Giovannelli, D., d'Errico, G., Manini, E., Yakimov, M., and Vetriani, C. (2013). Diversity and phylogenetic analyses of bacteria from a shallow-water hydrothermal vent in Milos island (Greece). *Front. Microbiol.* 4:184. doi: 10.3389/fmicb.2013.00184

Gloor, G. B., Macklaim, J. M., Pawlowsky-Glahn, V., and Egozcue, J. J. (2017). Microbiome datasets are compositional: and this is not optional. *Front. Microbiol.* 8:2224. doi: 10.3389/fmicb.2017.02224

Godelitsas, A., Price, R. E., Pichler, T., Amend, J., Gamaletsos, P., and Göttlicher, J. (2015). Amorphous as-sulfide precipitates from the shallow-water hydrothermal vents off Milos Island (Greece). *Mar. Chem.* 177, 687–696. doi: 10.1016/j.marchem.2015.09.004

Hao, X., and Ma, K. (2003). Minimal sulfur requirement for growth and sulfur-dependent metabolism of the hyperthermophilic archaeon *Staphylothermus marinus*. *Archaea* 1, 191–197. doi: 10.1155/2003/626017

Helen, D., Kim, H., Tytgat, B., and Anne, W. (2016). Highly diverse nirK genes comprise two major clades that harbour ammonium-producing denitrifiers. *BMC Genomics* 17:155. doi: 10.1186/s12864-016-2465-0

Herbel, M., and Fendorf, S. (2006). Biogeochemical processes controlling the speciation and transport of arsenic within iron coated sands. *Chem. Geol.* 228, 16–32. doi: 10.1016/j.chemgeo.2005.11.016

Houghton, J. L., Gilhooly, W. P., Kafantaris, F.-C. A., Druschel, G. K., Lu, G.-S., Amend, J. P., et al. (2019). Spatially and temporally variable sulfur cycling in shallow-sea hydrothermal vents, Milos, Greece. *Mar. Chem.* 208, 83–94. doi: 10.1016/j.marchem.2018.11.002

Huber, H., and Stetter, K. O. (2015). "*Deferribacteraceae fam*. Nov" in *Bergey's Manual of Systematics of Archaea and Bacteria* (USA: John Wiley & Sons, Ltd), 1.

Inagaki, F., Takai, K., Kobayashi, H., Nealson, K. H., and Horikoshi, K. (2003). *Sulfurimonas autotrophica* gen. Nov., sp. nov., a novel sulfur-oxidizing ε-proteobacterium isolated from hydrothermal sediments in the mid-Okinawa trough. *Int. J. Syst. Evol. Microbiol.* 53, 1801–1805. doi: 10.1099/ijs.0.02682-0

Inagaki, F., Takai, K., Nealson, K. H., and Horikoshi, K. (2004). *Sulfurovum lithotrophicum* gen. Nov., sp. nov., a novel sulfur-oxidizing chemolithoautotroph within the ε-Proteobacteria isolated from Okinawa trough hydrothermal sediments. *Int. J. Syst. Evol. Microbiol.* 54, 1477–1482. doi: 10.1099/ijs.0.03042-0

Jochimsen, B., Peinemann-Simon, S., Völker, H., Stüben, D., Botz, R., Stoffers, P., et al. (1997). *Stetteria hydrogenophila*, gen. Nov. and sp. nov., a novel mixotrophic sulfur-dependent crenarchaeote isolated from Milos, Greece. *Extremophiles* 1, 67–73. doi: 10.1007/s007920050016

Jolivet, L., Faccenna, C., Huet, B., Labrousse, L., Le Pourhiet, L., Lacombe, O., et al. (2013). Aegean tectonics: strain localisation, slab tearing and trench retreat. *Tectonophysics* 597-598, 1–33. doi: 10.1016/j.tecto.2012.06.011

Jørgensen, B. B., Findlay, A. J., and Pellerin, A. (2019). The biogeochemical sulfur cycle of marine sediments. *Front. Microbiol.* 10:849. doi: 10.3389/fmicb.2019.00849

Karageorgis, A., Anagnostou, C., Sioulas, A., Chronis, G., and Papathanassiou, E. (1998). Sediment geochemistry and mineralogy in Milos bay, SW Kyklades, Aegean Sea, Greece. *J. Mar. Syst.* 16, 269–281. doi: 10.1016/S0924-7963(97)00020-1

Kashefi, K., Tor, J. M., Holmes, D. E., Gaw Van Praagh, C. V., Reysenbach, A.-L., and Lovley, D. R. (2002). Geoglobus ahangari gen. Nov., sp. nov., a novel hyperthermophilic archaeon capable of oxidizing organic acids and growing autotrophically on hydrogen with Fe(III) serving as the sole electron acceptor. *Int. J. Syst. Evol. Microbiol.* 52, 719–728. doi: 10.1099/00207713-52-3-719

Khimasia, A., Rovere, A., and Pichler, T. (2020). Hydrothermal areas, microbial mats and sea grass in Paleochori Bay, Milos, Greece. *J. Maps* 16, 348–356. doi: 10.1080/17445647.2020.1748131

Kotopoulou, E., Godelitsas, A., Göttlicher, J., Steininger, R., Price, R., Fike, D. A., et al. (2022). Metastable iron (mono) sulfides in the Shallow-Sea hydrothermal sediments of Milos, Greece. *ACS Earth Space Chem.* 6, 920–931. doi: 10.1021/acsearthspacechem.1c00305

Kuever, J., Sievert, S., Stevens, H., Brinkhoff, T., and Muijzer, G. (2002). Microorganisms of the oxidative and reductive part of the Sulphur cycle at a shallow-water hydrothermal vent in the aegean sea (Milos, Greece) (niet eerder opgenomen). *Cah. Biol. Mar.* 43, 413–416.

Lagostina, L., Frandsen, S., Mac Gregor, B. J., Glombitza, C., Deng, L., Fiskal, A., et al. (2021). Interactions between temperature and energy supply drive microbial communities in hydrothermal sediment. *Commun Biol* 4, 1006–1014. doi: 10.1038/s42003-021-02507-1

Lanzén, A., Jørgensen, S. L., Huson, D. H., Gorfer, M., Grindhaug, S. H., Jonassen, I., et al. (2012). CREST–classification resources for environmental sequence tags. *PLoS One* 7:e49334. doi: 10.1371/journal.pone.0049334

Lloyd, K. G., May, M. K., Kevorkian, R. T., and Steen, A. D. (2013). Meta-analysis of quantification methods shows that archaea and bacteria have similar abundances

in the subseafloor. *Appl. Environ. Microbiol.* 79, 7790–7799. doi: 10.1128/AEM.02090-13

López-Pérez, M., Haro-Moreno, J. M., Iranzo, J., and Rodriguez-Valera, F. (2020). Genomes of the "Candidatus Actinomarinales" order: highly streamlined marine epipelagic Actinobacteria. *mSystems* 5, 5, e01041–e01020. doi: 10.1128/mSystems.01041-20

Lu, G.-S., LaRowe, D. E., Fike, D. A., Druschel, G. K., Iii, W. P. G., Price, R. E., et al. (2020). Bioenergetic characterization of a shallow-sea hydrothermal vent system: Milos Island, Greece. *PLoS One* 15:e0234175. doi: 10.1371/journal.pone.0234175

Lubbe, S., Filzmoser, P., and Templ, M. (2021). Comparison of zero replacement strategies for compositional data with large numbers of zeros. *Chemom. Intell. Lab. Syst.* 210:104248. doi: 10.1016/j.chemolab.2021.104248

Manini, E., Luna, G. M., Corinaldesi, C., Zeppilli, D., Bortoluzzi, G., Caramanna, G., et al. (2008). Prokaryote diversity and virus abundance in shallow hydrothermal vents of the Mediterranean Sea (Panarea Island) and the Pacific Ocean (North Sulawesi-Indonesia). *Microb. Ecol.* 55, 626–639. doi: 10.1007/s00248-007-9306-2

Martelat, J.-E., Escartín, J., and Barreyre, T. (2020). Terrestrial shallow water hydrothermal outflow characterized from out of space. *Mar. Geol.* 422:106119. doi: 10.1016/j.margeo.2020.106119

Martelat, J.-E., Puzenat, V., Escartin, J., and Grandjean, P. (2019). *Milos Shallow Water Hydrothermal System: Drone Seafloor Photomosaics (July/September 2019 Fieldwork)*. France: SEANOE.

Martin, M. (2011). Cutadapt removes adapter sequences from high-throughput sequencing reads. *EMBnet.journal* 17, 10–12. doi: 10.14806/ej.17.1.200

McMurdie, P. J., and Holmes, S. (2013). Phyloseq: an R package for reproducible interactive analysis and graphics of microbiome census data. *PLoS One* 8:e61217. doi: 10.1371/journal.pone.0061217

Middelburg, J. J. (2019). "Carbon processing at the seafloor" in *Marine Carbon Biogeochemistry: A Primer for Earth System Scientists. Springer Briefs in Earth System Sciences*. ed. J. J. Middelburg (Cham: Springer International Publishing), 57–75.

Mills, H., Kiel Reese, B., and St Peter, C. (2012). Characterization of microbial population shifts during sample storage. *Front. Microbiol.* 3:49. doi: 10.3389/fmicb.2012.00049

Murdock, S. A., and Juniper, S. K. (2017). Capturing compositional variation in denitrifying communities: a multiple-primer approach that includes *Epsilonproteobacteria*. *Appl. Environ. Microbiol.* 83, e02753–e02716. doi: 10.1128/AEM.02753-16

Orcutt, B. N., Sylvan, J. B., Knab, N. J., and Edwards, K. J. (2011). Microbial ecology of the Dark Ocean above, at, and below the seafloor. *Microbiol. Mol. Biol. Rev.* 75, 361–422. doi: 10.1128/MMBR.00039-10

Ortmann, A. C., and Suttle, C. A. (2005). High abundances of viruses in a deep-sea hydrothermal vent system indicates viral mediated microbial mortality. *Deep-Sea Res. I Oceanogr. Res. Pap.* 52, 1515–1527. doi: 10.1016/j.dsr.2005.04.002

Páez-Espino, D., Tamames, J., de Lorenzo, V., and Cánovas, D. (2009). Microbial responses to environmental arsenic. *Biometals* 22, 117–130. doi: 10.1007/s10534-008-9195-y

Pawlowsky-Glahn, V., Egozcue, J. J., and Tolosana-Delgado, R. (2015). *Modeling and Analysis of Compositional Data*. USA: Wiley.

Pedersen, T. L. (2021). Ggforce: Accelerating "ggplot 2". R package version 0.3.3. Available at: https://CRAN.R-project.org/package=ggforce (Accessed August 08, 2022).

Pérez-Rodríguez, I., Rawls, M., Coykendall, D. K., and Foustoukos, D. I. Y. (2016). (2016). *Deferrisoma palaeochoriense* sp. nov., a thermophilic, iron (III)-reducing bacterium from a shallow-water hydrothermal vent in the Mediterranean Sea. *Int. J. Syst. Evol. Microbiol.* 66, 830–836. doi: 10.1099/ijsem.0.000798

Price, R. E., and Giovannelli, D. (2017). "A review of the geochemistry and microbiology of marine shallow-water hydrothermal vents" in *Reference Module in Earth Systems and Environmental Sciences* (Netherland: Elsevier)

Price, R. E., LaRowe, D. E., Italiano, F., Savov, I., Pichler, T., and Amend, J. P. (2015). Subsurface hydrothermal processes and the bioenergetics of chemolithoautotrophy at the shallow-sea vents off Panarea Island (Italy). *Chem. Geol.* 407-408, 21–45. doi: 10.1016/j.chemgeo.2015.04.011

Price, R., Lesniewski, R., Nitzsche, K., Meyerdierks, A., Saltikov, C., Pichler, T., et al. (2013). Archaeal and bacterial diversity in an arsenic-rich shallow-sea hydrothermal system undergoing phase separation. *Front. Microbiol.* 4:158. doi: 10.3389/fmicb.2013.00158

Price, R. E., Savov, I., Planer-Friedrich, B., Bühring, S. I., Amend, J., and Pichler, T. (2013). Processes influencing extreme as enrichment in shallow-sea hydrothermal fluids of Milos Island, Greece. *Chem. Geol.* 348, 15–26. doi: 10.1016/j.chemgeo.2012.06.007

Puzenat, V., Escartin, J., and Martelat, J.-E. (2019a). *Milos Shallow Water Hydrothermal System: Shapefiles for AUV and Drone Photomosaic Interpretations and Instrument Locations*. France: SEANOE.

Puzenat, V., Escartín, J., Martelat, J.-E., Barreyre, T., Le Moine Bauer, S., Nomikou, P., et al. (2021). Shallow-water hydrothermalism at Milos (Greece): nature, distribution, heat fluxes and impact on ecosystems. *Mar. Geol.* 438:106521. doi: 10.1016/j.margeo.2021.106521

Puzenat, V., Gracias, N., Martelat, J.-E., Escartin, J., and Garcia, R. (2019b). *Milos Shallow Water Hydrothermal System: AUV Seafloor Photomosaics (July 2019 Fieldwork)*. France: SEANOE.

Qin, W., Heal, K. R., Ramdasi, R., Kobelt, J. N., Martens-Habbena, W., Bertagnolli, A. D., et al. (2017). *Nitrosopumilus maritimus* gen. Nov., sp. nov., *Nitrosopumilus cobalaminigenes* sp. nov., *Nitrosopumilus oxyclinae* sp. nov., and *Nitrosopumilus ureiphilus* sp. nov., four marine ammonia-oxidizing archaea of the phylum Thaumarchaeota. *Int. J. Syst. Evol. Microbiol.* 67, 5067–5079. doi: 10.1099/ijsem.0.002416

Quast, C., Pruesse, E., Yilmaz, P., Gerken, J., Schweer, T., Yarza, P., et al. (2013). The SILVA ribosomal RNA gene database project: improved data processing and web-based tools. *Nucleic Acids Res.* 41, D590–D596. doi: 10.1093/nar/gks1219

Quinn, T. P., Gordon-Rodriguez, E., and Erb, I. (2021). A critique of differential abundance analysis, and advocacy for an alternative. *Arxiv Preprint*. doi: 10.48550/arXiv.2104.07266

R Core Team (2021). *R: A Language and Environment for Statistical Computing*. R Foundation for Statistical Computing, Vienna, Austria.

Rivera-Pinto, J., Egozcue, J. J., Pawlowsky-Glahn, V., Paredes, R., Noguera-Julian, M., and Calle, M. L. (2018). Balances: a new perspective for microbiome. *Analysis* 3:e00053-18. doi: 10.1128/mSystems.00053-18

Roberts, H., Price, R., Brombach, C.-C., and Pichler, T. (2021). Mercury in the hydrothermal fluids and gases in Paleochori Bay, Milos, Greece. *Marine Chem.* 233:103984. doi: 10.1016/j.marchem.2021.103984

Rognes, T. (2021). Alternative VSEARCH Pipeline Torognes/Vsearch Wiki Git Hub. Available at: https://github.com/torognes/vsearch/wiki/Alternative-VSEARCH-pipeline (Accessed January 08, 2022).

Rognes, T., Flouri, T., Nichols, B., Quince, C., and Mahé, F. (2016). VSEARCH: a versatile open source tool for metagenomics. *PeerJ* 4:e2584. doi: 10.7717/peerj.2584

Rohwer, F., Prangishvili, D., and Lindell, D. (2009). Roles of viruses in the environment. *Environ. Microbiol.* 11, 2771–2774. doi: 10.1111/j.1462-2920.2009.02101.x

Schlesner, H., Lawson, P. A., Collins, M. D., Weiss, N., Wehmeyer, U., Völker, H., et al. (2001). *Filobacillus milensis* gen. Nov., sp. nov., a new halophilic spore-forming bacterium with Orn-D-Glu-type peptidoglycan. *Int. J. Syst. Evol. Microbiol.* 51, 425–431. doi: 10.1099/00207713-51-2-425

Sievert, S. M., Brinkhoff, T., Muyzer, G., Ziebis, W., and Kuever, J. (1999). Spatial heterogeneity of bacterial populations along an environmental gradient at a shallow submarine hydrothermal vent near Milos Island (Greece). *Appl. Environ. Microbiol.* 65, 3834–3842. doi: 10.1128/AEM.65.9.3834-3842.1999

Sievert, S. M., Bühring, S. I., Gulmann, L. K., Hinrichs, K.-U., Pop Ristova, P., and Gomez-Saez, G. V. (2022). Fluid flow stimulates chemoautotrophy in hydrothermally influenced coastal sediments. *Commun Earth Environ* 3, 1–10. doi: 10.1038/s43247-022-00426-5

Sievert, S. M., Heidorn, T., and Kuever, J. (2000b). *Halothiobacillus kellyi* sp. nov., a mesophilic, obligately chemolithoautotrophic, sulfur-oxidizing bacterium isolated from a shallow-water hydrothermal vent in the Aegean Sea, and emended description of the genus *Halothiobacillus*. *Int. J. Syst. Evol. Microbiol.* 50, 1229–1237. doi: 10.1099/00207713-50-3-1229

Sievert, S. M., Hügler, M., Taylor, C. D., and Wirsen, C. O. (2008). "Sulfur oxidation at Deep-Sea hydrothermal vents" in *Microbial Sulfur Metabolism*. eds. C. Dahl and C. G. Friedrich (Berlin, Heidelberg: Springer), 238–258.

Sievert, S. M., and Kuever, J. (2000). *Desulfacinum hydrothermale* sp. nov., a thermophilic, sulfate-reducing bacterium from geothermally heated sediments near Milos Island (Greece). *Int. J. Syst. Evol. Microbiol.* 50, 1239–1246. doi: 10.1099/00207713-50-3-1239

Sievert, S. M., Wieringa, E. B. A., Wirsen, C. O., and Taylor, C. D. (2007). Growth and mechanism of filamentous-sulfur formation by Candidatus Arcobacter sulfidicus in opposing oxygen-sulfide gradients. *Environ. Microbiol.* 9, 271–276. doi: 10.1111/j.1462-2920.2006.01156.x

Sievert, S. M., Ziebis, W., Kuever, J., and Sahm, K. (2000a). Relative abundance of archaea and bacteria along a thermal gradient of a shallow-water hydrothermal vent quantified by rRNA slot-blot hybridization. *Microbiology* 146, 1287–1293. doi: 10.1099/00221287-146-6-1287

Sime-Ngando, T. (2014). Environmental bacteriophages: viruses of microbes in aquatic ecosystems. *Front. Microbiol.* 5:355. doi: 10.3389/fmicb.2014.00355

Slobodkina, G. B., Kolganova, T. V., Querellou, J., Bonch-Osmolovskaya, E. A., and Slobodkin, A. I. Y. (2009). *Geoglobus acetivorans* sp. nov., an iron (III)-reducing archaeon from a deep-sea hydrothermal vent. *Int. J. Syst. Evol. Microbiol.* 59, 2880–2883. doi: 10.1099/ijs.0.011080-0

Sollich, M., Yoshinaga, M. Y., Häusler, S., Price, R. E., Hinrichs, K.-U., and Bühring, S. I. (2017). Heat stress dictates microbial lipid composition along a thermal gradient in marine sediments. *Front. Microbiol.* 8:1550. doi: 10.3389/fmicb.2017.01550

Stokke, R., Dahle, H., Roalkvam, I., Wissuwa, J., Daae, F. L., Tooming-Klunderud, A., et al. (2015). Functional interactions among filamentous *Epsilonproteobacteria* and *Bacteroidetes* in a deep-sea hydrothermal vent biofilm. *Environ. Microbiol.* 17, 4063–4077. doi: 10.1111/1462-2920.12970

Stolz, J. F., Ellis, D. J., Blum, J. S., Ahmann, D., Lovley, D. R., and Oremland, R. S. (1999). *Sulfurospirillum barnesii* sp. nov. and *Sulfurospirillum arsenophilum* sp. nov., new members of the *Sulfurospirillum* clade of the epsilon proteobacteria. *Int. J. Syst. Bacteriol.* 49, 1177–1180. doi: 10.1099/00207713-49-3-1177

Suttle, C. A. (2007). Marine viruses — major players in the global ecosystem. *Nat. Rev. Microbiol.* 5, 801–812. doi: 10.1038/nrmicro1750

Tarasov, V. G., Gebruk, A. V., Mironov, A. N., and Moskalev, L. I. (2005). Deep-sea and shallow-water hydrothermal vent communities: two different phenomena? *Chem. Geol.* 224, 5–39. doi: 10.1016/j.chemgeo.2005.07.021

Tsai, S.-L., Singh, S., and Chen, W. (2009). Arsenic metabolism by microbes in nature and the impact on arsenic remediation. *Curr. Opin. Biotechnol.* 20, 659–667. doi: 10.1016/j.copbio.2009.09.013

Valsami-Jones, E., Baltatzis, E., Bailey, E. H., Boyce, A. J., Alexander, J. L., Magganas, A., et al. (2005). The geochemistry of fluids from an active shallow submarine hydrothermal system: Milos island, Hellenic volcanic arc. *J. Volcanol. Geotherm. Res.* 148, 130–151. doi: 10.1016/j.jvolgeores.2005.03.018

Varnavas, S. P., and Cronan, D. S. (2005). Submarine hydrothermal activity off Santorini and Milos in the central Hellenic volcanic arc: a synthesis. *Chem. Geol.* 224, 40–54. doi: 10.1016/j.chemgeo.2005.07.013

Waite, D. W., Chuvochina, M., Pelikan, C., Parks, D. H., Yilmaz, P., Wagner, M., et al. (2020). Proposal to reclassify the proteobacterial classes *Deltaproteobacteria* and *Oligoflexia*, and the phylum *Thermodesulfobacteria* into four phyla reflecting major functional capabilities. *Int. J. Syst. Evol. Microbiol.* 70, 5972–6016. doi: 10.1099/ijsem.0.004213

Wenzhöfer, F., Holby, O., Glud, R. N., Nielsen, H. K., and Gundersen, J. K. (2000). In situ microsensor studies of a shallow water hydrothermal vent at Milos, Greece. *Mar. Chem.* 69, 43–54. doi: 10.1016/S0304-4203(99)00091-2

Wickham, H., Chang, W., Henry, L., Pedersen, T. L., Takahashi, K., Wilke, C., et al. (2022). Ggplot 2: Create Elegant Data Visualisations Using the Gra the Grammar of Graphics. Available at: https://CRAN.R-project.org/package=ggplot2 (Accessed August 08, 2022).

Wirsen, C. O., Sievert, S. M., Cavanaugh, C. M., Molyneaux, S. J., Ahmad, A., Taylor, L. T., et al. (2002). Characterization of an autotrophic sulfide-oxidizing marine Arcobacter sp. that produces filamentous sulfur. *Appl. Environ. Microbiol.* 68, 316–325. doi: 10.1128/AEM.68.1.316-325.2002

Wunder, L. C., Aromokeye, D. A., Yin, X., Richter-Heitmann, T., Willis-Poratti, G., Schnakenberg, A., et al. (2021). Iron and sulfate reduction structure microbial communities in (sub-)Antarctic sediments. *ISME J.* 15, 3587–3604. doi: 10.1038/s41396-021-01014-9

Yücel, M., Sievert, S. M., Vetriani, C., Foustoukos, D. I., Giovannelli, D., and Le Bris, N. (2013). Eco-geochemical dynamics of a shallow-water hydrothermal vent system at Milos Island, Aegean Sea (eastern Mediterranean). *Chem. Geol.* 356, 11–20. doi: 10.1016/j.chemgeo.2013.07.020

frontiers | Frontiers in Microbiology

TYPE Original Research
PUBLISHED 22 February 2023
DOI 10.3389/fmicb.2023.1063139

OPEN ACCESS

EDITED BY
Brett J. Baker,
The University of Texas at Austin, United States

REVIEWED BY
Paul Evans,
The University of Queensland, Australia
Hiroyuki Imachi,
Japan Agency for Marine-Earth Science and Technology (JAMSTEC), Japan

*CORRESPONDENCE
William D. Orsi
✉ w.orsi@lrz.uni-muenchen.de

SPECIALTY SECTION
This article was submitted to Extreme Microbiology, a section of the journal Frontiers in Microbiology

RECEIVED 06 October 2022
ACCEPTED 17 January 2023
PUBLISHED 22 February 2023

CITATION
Coskun ÖK, Gomez-Saez GV, Beren M, Ozcan D, Hosgormez H, Einsiedl F and Orsi WD (2023) Carbon metabolism and biogeography of candidate phylum "*Candidatus* Bipolaricaulota" in geothermal environments of Biga Peninsula, Turkey. *Front. Microbiol.* 14:1063139. doi: 10.3389/fmicb.2023.1063139

Carbon metabolism and biogeography of candidate phylum "*Candidatus* Bipolaricaulota" in geothermal environments of Biga Peninsula, Turkey

Ömer K. Coskun[1], Gonzalo V. Gomez-Saez[1,2], Murat Beren[3], Dogacan Ozcan[3], Hakan Hosgormez[3], Florian Einsiedl[4] and William D. Orsi[1,2]*

[1]Department of Earth and Environmental Sciences, Paleontology and Geobiology, Ludwig-Maximilians-Universität München, Munich, Germany, [2]GeoBio-Center[LMU], Ludwig-Maximilians-Universität München, Munich, Germany, [3]Department of Geological Engineering, Istanbul University-Cerrahpasa, Istanbul, Türkiye, [4]Chair of Hydrogeology, TUM School of Engineering and Design, Technical University of Munich, Munich, Germany

Terrestrial hydrothermal springs and aquifers are excellent sites to study microbial biogeography because of their high physicochemical heterogeneity across relatively limited geographic regions. In this study, we performed 16S rRNA gene sequencing and metagenomic analyses of the microbial diversity of 11 different geothermal aquifers and springs across the tectonically active Biga Peninsula (Turkey). Across geothermal settings ranging in temperature from 43 to 79°C, one of the most highly represented groups in both 16S rRNA gene and metagenomic datasets was affiliated with the uncultivated phylum "*Candidatus* Bipolaricaulota" (former "*Ca.* Acetothermia" and OP1 division). The highest relative abundance of "*Ca.* Bipolaricaulota" was observed in a 68°C geothermal brine sediment, where it dominated the microbial community, representing 91% of all detectable 16S rRNA genes. Correlation analysis of "*Ca.* Bipolaricaulota" operational taxonomic units (OTUs) with physicochemical parameters indicated that salinity was the strongest environmental factor measured associated with the distribution of this novel group in geothermal fluids. Correspondingly, analysis of 23 metagenome-assembled genomes (MAGs) revealed two distinct groups of "*Ca.* Bipolaricaulota" MAGs based on the differences in carbon metabolism: one group encoding the bacterial Wood-Ljungdahl pathway (WLP) for H_2 dependent CO_2 fixation is selected for at lower salinities, and a second heterotrophic clade that lacks the WLP that was selected for under hypersaline conditions in the geothermal brine sediment. In conclusion, our results highlight that the biogeography of "*Ca.* Bipolaricaulota" taxa is strongly correlated with salinity in hydrothermal ecosystems, which coincides with key differences in carbon acquisition strategies. The exceptionally high relative abundance of apparently heterotrophic representatives of this novel candidate Phylum in geothermal brine sediment observed here may help to guide future enrichment experiments to obtain representatives in pure culture.

KEYWORDS

"*Candidatus* Bipolaricaulota", deep biosphere, hydrothermal, carbon fixation, pangenomics, phylogenomics

Introduction

All of the Earth's ecosystems are built on the fixation of carbon dioxide into organic carbon by metabolic carbon fixation pathways. Out of seven carbon fixation pathways known to date (Fuchs, 2011, Sánchez-Andrea et al., 2020), the Wood-Ljungdahl pathway (WLP) is found in a wide range of anaerobic bacterial and archaeal lineages. This pathway has been proposed as one of the ancient metabolic carbon fixation pathways where the last common ancestor of all organisms (LUCA) might have been used to fix carbon in anaerobic hydrothermal settings in the early Earth (Fuchs, 2011).

"*Candidatus* Bipolaricaulota" (Hao et al., 2018), formerly known as OP1 (Hugenholtz et al., 1998) and "*Candidatus* Acetothermum autotrophicum" (Takami et al., 2012), are deeply branching in the bacteria domain with members capable of fixing carbon autotrophically *via* an ancient WLP pathway (Takami et al., 2012). The phylogenetic analysis of the carbon monoxide dehydrogenase enzyme of "*Ca.* Bipolaricaulota," a key feature of the CO_2 fixation in the WLP, placed this as one of the most ancient carbon-fixing organisms that have been detected to date (Takami et al., 2012). A recent metagenomic study investigating "*Ca.* Bipolaricaulota" in a serpentinization-driven ecosystem also concluded that this phylum is among the earliest evolving bacterial lineages (Colman et al., 2022). These suggested that members of the "*Ca.* Bipolaricaulota" retain ancestral traits of the WLP that evolved on the early Earth, and the WLP is a metabolism that has been predicted for the LUCA (Martin et al., 2008; Fuchs, 2011). "*Ca.* Bipolaricaulota" have been found in hot springs (Hugenholtz et al., 1998; Tobler and Benning, 2011), deep-sea hydrothermal environments (Teske et al., 2002; Stott et al., 2008), subsurface thermophilic mat communities (Takami et al., 2012), oil fields (Hu et al., 2016), the sediment of hypersaline lagoons (Fernandez et al., 2016), serpentinized subsurface fluids (Colman et al., 2022), and anaerobic bioreactors (Hao et al., 2018). Based on its phylogenomic divergence, it has been proposed as a novel candidate phylum (Hao et al., 2018).

Recently, a complete metagenome-assembled genome (MAG) of the phylum "*Ca.* Bipolaricaulis" anaerobic sp. Ran-1 was obtained from an anaerobic sludge digestor, and this MAG showed a potential chemoheterotrophic mode of lifestyle where members of this bacterium derive energy primarily *via* heterotrophic fermentation (Hao et al., 2018). Moreover, the first photographs of these cells revealed an unusual morphology that exhibited bipolar prosthecae (Hao et al., 2018). The WLP was reported to be ubiquitous in the candidate phylum (by analyzing 14 MAGs), and used in four different catabolic capabilities, namely, (1) homoacetogenic fermentation, (2) autotrophy, (3) syntrophic oxidation of acetate, and (4) respiratory capacity while using oxygen or nitrate as a terminal electron acceptor (Youssef et al., 2019). As such, metabolically versatile memberes of the candidate phylum Bipolaricaulota (Acetothermia, OP1) likely uses the WLP in homoacetogenic fermentation (Youssef et al., 2019).

During 2019–2021, we performed a survey of microbial diversity in geothermal environments on the Biga Peninsula, Turkey, a geothermal field spanning more than 9,000 km^2. We examined the genomic potential within microbial communities from 11 different geothermal environments in the Biga Peninsula and around the vicinity of Edremit from diverse geothermal conditions including brine pools and subsurface (60–1,350 m below surface) hydrothermal aquifers. This survey revealed several environments where "*Ca.* Bipolaricaulota" reached notably high levels of relative abundance in the microbial communities (>90%). We proceeded to investigate how the diverse geothermal and physicochemical conditions of the Biga Peninsula influence the distribution of "*Ca.* Bipolaricaulota". By using shotgun metagenomic techniques and bioinformatic tools, four MAGs associated with "*Ca.* Bipolaricaulota" were assembled and their carbon metabolism and biogeographic distribution across the geothermal environments was assessed. Our analyses show how the carbon metabolism of this novel phylum is distributed across key geothermal environments.

Materials and methods

Field sampling

Sediment and fluid samples were collected in the summertime between 2019 and 2021 from geothermal springs and boreholes in the Biga Peninsula and in the vicinity of Edremit Town (Balikesir, Turkey) (**Figure 1** and **Supplementary Table 1**). Hydrothermal sediments (Tuzla, Hidirlar, Büyükılıca, and Nebiler) were collected directly from the hot spring ponds using falcon tubes or with a shovel. Hot spring fluids (10–20 L) were collected from geothermal pools directly from the spring and immediately filtered (0.2 μm; Millipore Express, Merck, Darmstadt, Germany) from three sites, namely, Tuzla, Hidirlar, and Nebiler, using a peristaltic pump (Masterflex E/S 07571-05, Cole Parmer, USA). Several geothermal fluids were sampled from existing boreholes where deeply sourced hydrothermal aquifer water is constantly pumped to the surface. These fluids were collected either from a water collector (Güre 250 m-deep borehole) or directly from the pipe opening (Güre 1,390 m-deep borehole, Bardakcilar boreholes, Can, and Entur). Additional information on the fluid chemistry boreholes is found in **Supplementary Table 1**.

Physicochemical analyses

Electrical conductivity (Ec) (WTW, Cond 3110 Set 1, Weilheim, Germany), temperature, salinity (WTW, Cond 3110 Set 1, Weilheim, Germany), pH (WTW, pH 3110 Set 2, Weilheim, Germany), dissolved oxygen (WTW Oxi 3310, Weilheim, Germany), and total dissolved solids (TDS) were measured in the field using handheld probes. Fluids were filtered through 0.2-μm hydrophilic polyethersulfone (PES) filters (Millipore Express, Merck, Darmstadt, Germany) placed within in-line filter holders. Filters were stored in 15 mL sterile falcon tubes and immediately placed on dry ice, shipped back to Germany, and stored at −80°C until DNA extractions at the University of Munich (LMU Munich). Geochemical analysis of the fluids was performed as described previously (Einsiedl et al., 2020; **Supplementary Table 1**). Briefly, samples for laboratory-based measurements of major anion and cation concentrations and water isotopes (δ^2H and $\delta^{18}O$) were collected in 1.5 mL tubes after filtering with 0.2 μm PES filters (Millipore Express, Merck, Darmstadt, Germany). All samples were stored on dry ice. Laboratory measurements were done in the hydrogeology department of the Technical University of Munich (TUM) and the General Directorate of Mineral

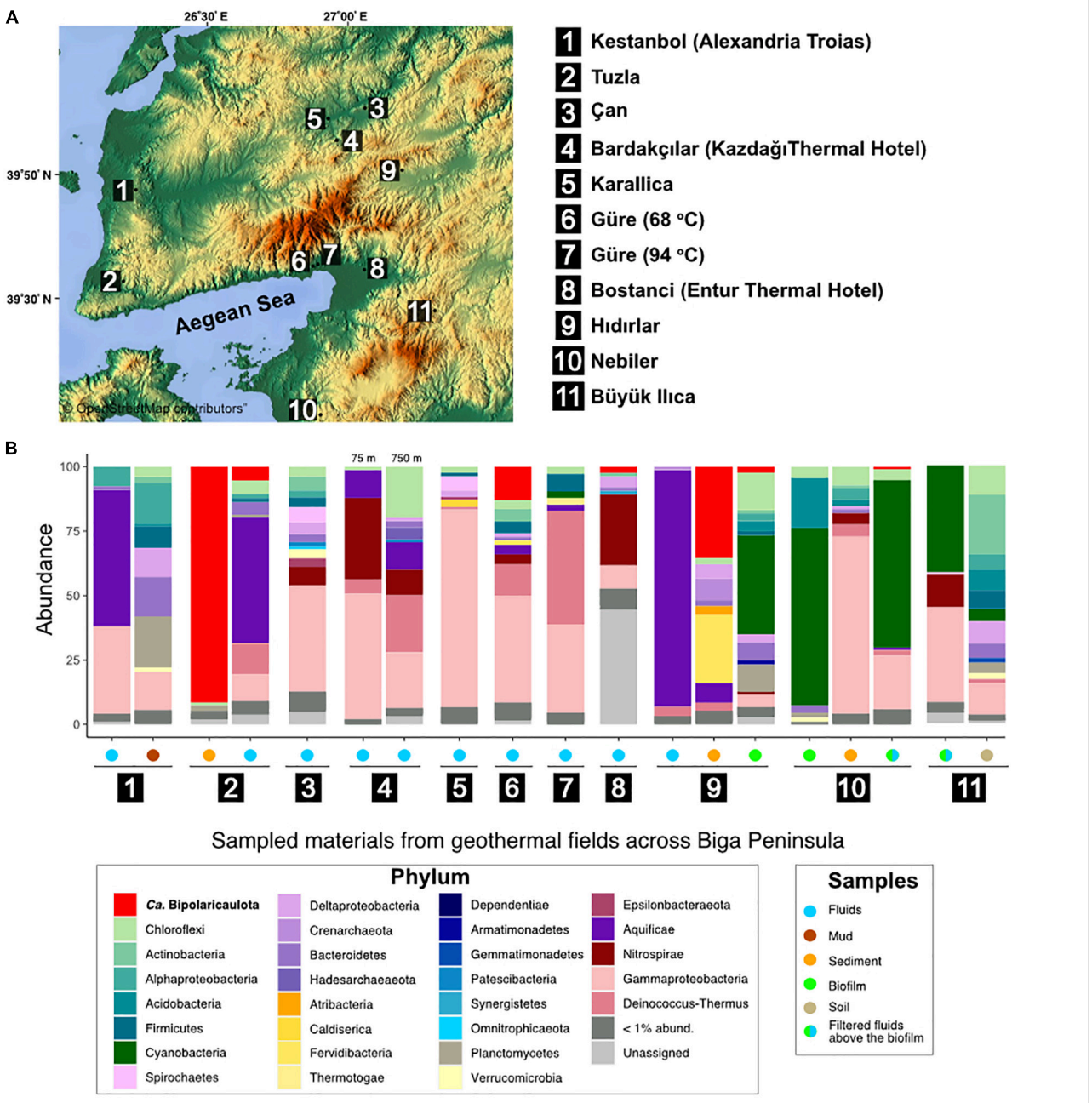

FIGURE 1
Study sites and microbial community structure. **(A)** Map showing the location of the 11 geothermal sampling sites in Biga Peninsula, Turkey. The legend shows the names of the samples corresponding to the numbers on the map. **(B)** Microbial community structure of collected samples (filtered fluids, sediments, mud, and biofilm samples) from the studied geothermal represented as relative abundance of 16S rRNA gene sequences (y axis). These bars are only displayed for those samples where a phylum/class reached relative abundance in the 16S rRNA gene dataset >1% in any of the samples. Legends show corresponding groups (left) and type of samples (right). The map used in this figure was created by Maps-For-Free which is credited in the image (https://maps-for-free.com/#close).

Research and Exploration of Turkey (MTA) (**Supplementary Table 1**).

DNA extraction

DNA was extracted as described previously for filters (Orsi et al., 2015) and sediments (Coskun et al., 2018). DNA from the sediments was performed exactly as described previously (Coskun et al., 2018). For the filters, some modifications to the original DNA extraction protocol (Orsi et al., 2015) were made. For the filters, the silica bead contents from four 2 mL Lysing Matrix E tubes (MP Biomedicals, Solon, OH, USA) was poured into a 15-ml falcon tube containing the filter 4 ml of a sterile-filtered sucrose ethylenediaminetetraacetic lysis buffer (0.75 M sucrose, 0.05 M Tris-Base, 0.02 M ethylenediaminetetraacetic, 0.4 M NaCl, 4 ml 10% sodium dodecyl sulfate, and pH 9.0) was added to the tubes and then bead beating was performed for 40 s using a Fast-Prep 5G homogenizer (MP Biomedicals, OH, USA) at a speed of 6 m/s. Samples were subsequently heated for 2 min at 99°C. After heating, 25 ml of

20 mg/ml proteinase K was added, and tubes were incubated at 55°C overnight with constant gentle rolling in a Bambino oven. DNA was extracted and purified from the lysate using the DNeasy Blood and Tissue Kit (Qiagen). Extracted DNA was quantified fluorometrically using a Qubit 3.0 Fluorometer (Invitrogen, Eugene, OR, USA).

PCR of 16S rRNA genes and bioinformatic analysis

Universal primers targeting the V4 hypervariable region of 16S ribosomal RNA (rRNA) genes were used to PCR amplify the gene fragments from DNA extracts from the environmental samples. We used a version of the 515F primer with a single-base change (in bold) to increase the coverage of certain taxonomic groups including the archaea (515F-Y, 5′-GTG**Y**CAGCMGCCGCGGTAA; Parada et al., 2016). PCR reactions were carried out as described previously (Coskun et al., 2019). The 16S rRNA genes were subjected to dual-indexed barcoded sequencing of 16S rRNA gene amplicons on the Illumina MiniSeq as described previously (Pichler et al., 2018).

The MiniSeq reads (Pichler et al., 2018) were quality trimmed and assembled using USEARCH version 11.0.667 with the default parameters (Edgar, 2010). Reads were then *de novo* clustered at 97% identity using UPARSE; operational taxonomic units (OTUs) represented by a single sequence were discarded (Edgar, 2013). Taxonomic assignments were generated by QIIME 1.9.1 (Caporaso et al., 2010) using the implemented BLAST method against the SILVA rRNA gene database release 132 (Quast et al., 2013). The genera *Pseudomonas*, *Ralstonia*, *Variovorax,* or *Streptococcus* were also removed as these are common contaminants of molecular reagent kits (Salter et al., 2014) and we typically find these genera in DNA extraction blanks from our lab (Coskun et al., 2018; Pichler et al., 2018). Statistical analyses and plots were performed using R. Studio version 3.3.0 (RStudio Team, 2015). The 16S rRNA gene sequence data is stored in the NCBI Short Read Archive under BioProject ID PRJNA888248.

Metagenomic analysis

Samples selected for metagenomic shotgun sequencing (see **Supplementary Figure 1**) were prepared into metagenomic libraries using the Nextera XT DNA Library Prep Kit (Illumina) by following the manufacturer instructions with some modifications. The starting concentration of genomic DNA could not be set to 0.2 ng as suggested by the manufacturer due to low DNA content in some samples. Instead, the PCR program in the amplification step of the tagmented DNA was modified from 12 to 15 cycles to increase the resulting DNA yield from <1 nM concentration to the values between 5 and 10 nM as previously done (Coskun et al., 2021). Quality control and quantification of the metagenomic libraries were done on an Agilent 2100 Bioanalyzer System using high-sensitivity DNA reagents and DNA chips (Agilent Genomics). Metagenomic libraries were diluted to 1 nM and pooled together to be sequenced on the Illumina MiniSeq platform. SqueezeMeta (Tamames and Puente-Sánchez, 2018) and the Anvi'o snakemake workflow (Köster and Rahmann, 2012; Eren et al., 2015) were used for downstream analysis in co-assembly mode with default settings. In short, the SqueezeMeta workflow deployed Trimmomatic for adapter removing, trimming, and quality filtering by setting the parameters: leading = 8, trailing = 8, sliding window = 10:15, and minimum length = 30 (Bolger et al., 2014). Contigs were assembled using a Megahit assembler with a minimum length of 200 nucleotides (Li et al., 2015). Open reading frames (genes and rRNAs; ORFs) were called using Prodigal (Hyatt et al., 2010); rRNAs genes were determined by Barrnap[1]. The Diamond software (Buchfink et al., 2015) was used to search for gene homologies in the databases GenBank nr for taxonomic assignment, eggNOG v4.5 (Huerta-Cepas et al., 2016), and KEGG (Kanehisa, 2000). The cutoff values for assigning hits to specific taxa were performed at an e value of $1 \times e^{-3}$ and a minimum amino acid similarity of 40 for taxa and 30 for functional assignment, which was the default settings of SqueezeMeta. Bowtie2 (Langmead and Salzberg, 2012) was used to map the read onto contigs and genes. Anvi'o snakemake workflow (anvi'o v7) was used to bin and refine the MAGs. MaxBin (Wu et al., 2016), CONCOCT (Alneberg et al., 2014), and Metabat2 (Kang et al., 2019) were used for the binning, and the DAS Tool (Sieber et al., 2018) was used to choose the best bin for each population. The completeness and contamination of the bins were checked in anvi'o v7 based on the "Bacteria_71" single-copy gene database embedded in anvi'o v7. The metagenomic sequence data is stored at https://doi.org/10.6084/m9.figshare.21286227.v1 and entered in the NCBI Short Read Archive under BioProject ID PRJNA888248.

For the pangenomic analysis, the MAGs to compare against our study were downloaded from public databases deposited as a part of research efforts (Takami et al., 2012; Jungbluth et al., 2017; Parks et al., 2017; Hao et al., 2018; Kadnikov et al., 2019; Smith et al., 2019; Youssef et al., 2019; Liu et al., 2020; Reysenbach et al., 2020; Zhou et al., 2020; Bhattarai et al., 2021; Schneider et al., 2021; Wang et al., 2021; Brazelton et al., 2022; Speth et al., 2022). **Supplementary Table 2** provides information on the 23 origins of all the genomes examined in this study.

Phylogenomics of "*Ca.* Bipolaricaulota"

A total of 69 different sets of ribosomal genes (in total) were determined by anvi'o (Eren et al., 2015) using the "Bacteria_71" ribosomal protein dataset in anvio's "anvi-get-sequences-for-hmm-hits" command (Eren et al., 2015). These ribosomal proteins were aligned using muscle (Edgar, 2004), and the phylogenetic tree was constructed using FastTree Version 2.1.10 (Price et al., 2010) using BLOSUM45, which is embedded in anvi'o (Eren et al., 2015).

Statistical analysis

For the statistical assessment of the influence of the environmental parameters on "*Ca.* Bipolaricaulota" and the rest of the identified phyla in the fluids, we applied a redundancy analysis (RDA) (**Figure 2**). RDA is a multiple linear regression between the explanatory variables (environmental parameters) and the response

1 github.com/tseemann/barrnap

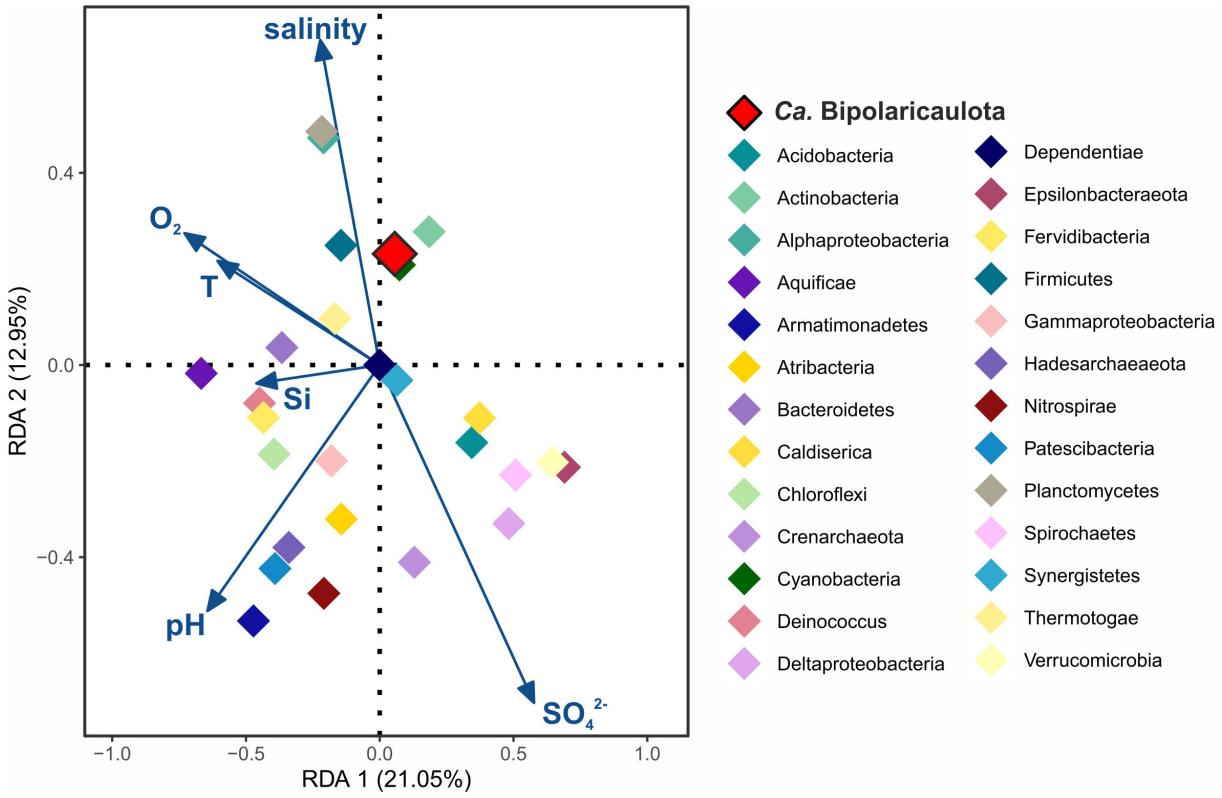

FIGURE 2
Redundancy analysis (RDA) ordination plot for Biga Peninsula Phylum operational taxonomic units (OTUs) distribution constrained by six environmental variables. Environmental parameters (blue arrows) included: oxygen concentration (O_2), temperature (T), pH, salinity, silica (Si), and sulfate (SO_4^{2-}) concentration. Color codes of the different phylum are the same as in **Figure 1**, being "*Ca.* Bipolaricaulota" highlighted in red.

variables (OTUs abundance per different phylum), followed by a principal component analysis (PCA). Sediment, biofilm, mud, and soil samples were discarded from the analysis as physicochemical parameters were only measured from the fluids. Previous to the RDA plot, Pearson correlations ($r > 0.8$, $P < 0.05$) were applied to all physicochemical parameters (**Supplementary Table 1**) and only those parameters that did not correlate among themselves (O_2, T, pH, salinity, [Si] and [SO_4^{2-}]) were included in the further regression. A total of 177 OTUs grouped into 27 different phyla were included in the RDA plot, including those OTUs representing >1% of the relative abundance in any sampling site (**Figure 2** and **Supplementary Table 1**). Statistical analyses were performed using the R software package using the *corrplot* package (Wei et al., 2013) and the *vegan* package (Oksanen et al., 2013), and plots were displayed using the *ggplot2* package (Wickham, 2016).

Results

Fluid geochemistry and the origin of thermal waters in Biga Peninsula

The origin of the different geothermal fluids sampled from different sites in the Biga Peninsula (**Figure 1A**) was assessed using stable isotopic composition, δ^2H and $\delta^{18}O$, of the geothermal fluids (**Figure 3**). The results showed that the isotopic composition of most samples fell between the global meteoric water line (GMWL; Craig, 1961) and East Mediterranean meteoric water line (EMMWL; Gat and Carmi, 1970). The exceptions to this trend were geothermal fluids sampled from Kestanbol, Tuzla, and Can (**Figure 3**), as their δ^2H vs. $\delta^{18}O$ values did not plot between the EMMWL and GMWL (**Figure 3**). The geothermal fluids sampled from Tuzla and Kestanbol were likely affected by higher salinities, as they had higher conductivity values and were enriched with high NaCl concentrations, whereas the other sites were dominated by $NaSO_4$-enriched waters (**Supplementary Table 1**). The Ec value of the Kestanbol geothermal field was between the definition of high saline waters (~15,000 to ~55,000 µS/cm according to USGS standards), which equals a salinity of 20 g/kg. On the contrary, the measured conductivity of the geothermal fluid at Tuzla (80,000 µS/cm) showed that the sampled fluids were brine, as this Ec value corresponds to a salinity of 55 g/kg, which is much higher than the Mediterranean seawater (38 g/kg) (Nessim et al., 2015).

16S rRNA gene profile of hydrothermal ecosystems in the studied area

Across 11 geothermal sites from the Biga Peninsula and the vicinity of Edremit 29 phyla were detected with relative abundance higher than 1% in the 16S rRNA gene datasets (**Figure 1B**). The overall microbial community from the studied geothermal sites, which display a broad spectrum of different geochemical conditions (**Supplementary Table 1**), was dominated

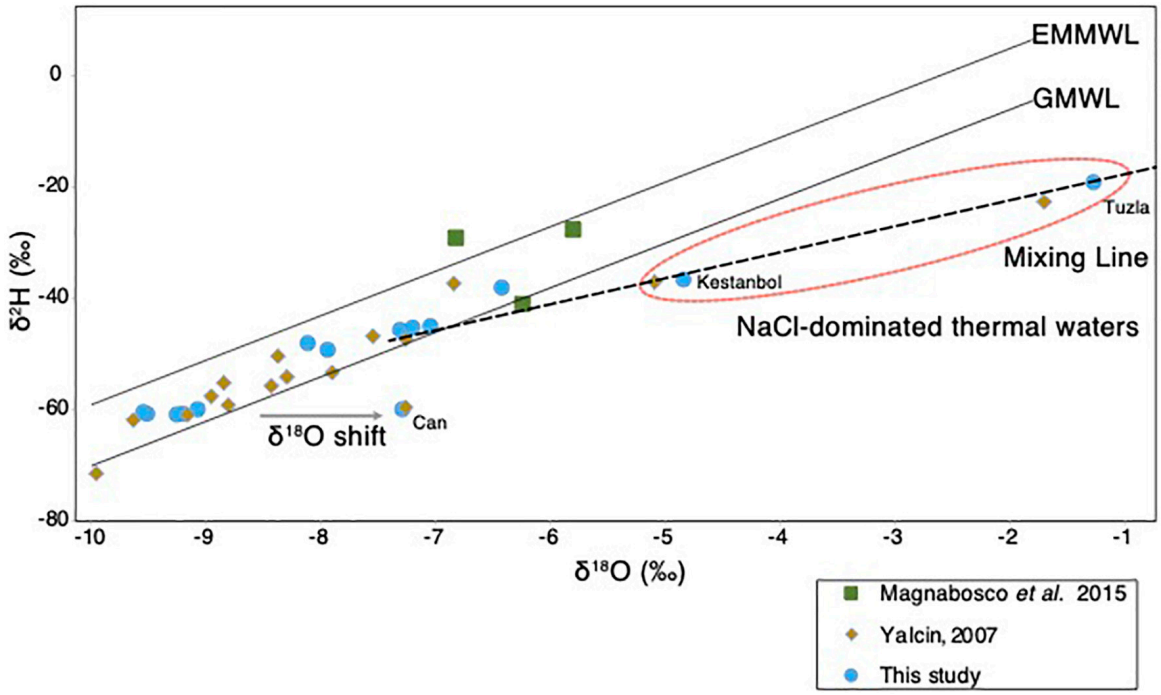

FIGURE 3
Isotopic composition of the geothermal waters. The δ^2H (‰) and $\delta^{18}O$ (‰) plot of thermal waters obtained in the study (blue), and other studies (Yalcin, 2007; Magnabosco et al., 2016). The GMWL and EMMWL stand for Global Meteoric Water Line (Craig, 1961) and East Mediterranean Water Line (Gat and Carmi, 1970). The hypersaline brine waters at the Tuzla site (**Figure 1**) that do not fall on the EMMWL or GMWL are highlighted in red circle.

by OTUs affiliated with known thermophilic groups within the Gammaproteobacteria, Deinococcus-Thermus, Chloroflexi, Aquificae, "*Ca.* Bipolaricaulota", Planctomycetes, Cyanobacteria, and Acidobacteria (**Figure 1B**).

OTUs affiliated with Gammaproteobacteria (particularly uncultured members of the family Hydrogenophilaceae) were found to be relatively dominant in filtered hydrothermal fluids from Can (40.9%), Güre (41.1%), Karailica (76%), Bardakcilar (21.6 and 48.7% in 750 and 75 m-deep boreholes, respectively), Kestanbol (34%), and a sediment sample from Nebiler (68.7%). OTUs affiliated with the Aquificae dominated the microbial community in the filtered fluids from Hidirlar (91.8%; mainly *Hydrogenobacter* sp.), Kestanbol (52.8%, *Hydrogenivirga* sp.), and Tuzla (48.5%, *Hydrogenivirga* sp.), and were well represented in Bardakcilar geothermal fluids from 75 and 750 m-deep boreholes with 10% relative abundance. Bacterial OTUs affiliated with the Deinococcus-Thermus phylum were also relatively abundant in the filtered fluids from the deepest sampled well from this study (1,390 m with a temperature of 94°C) in Güre town (43.9%), 750-m-deep borehole in Bardakcilar geothermal field (22.2%), and were relatively abundant in the fluids of Tuzla village (11.8%) and Güre 260 m-deep borehole (12.1%). On the contrary, biofilms and filters taken above the biofilms from hot springs of Buyukilica, Hidirlar, and Nebiler geothermal fields were predominated by OTUs associated with Cyanobacteria with relative abundances ranging from 38.4 to 68.9%.

The relative abundance of the total 16S rRNA gene sequence reads assigned to "*Ca.* Bipolaricaulota" varied substantially between the different sites sampled and ranged from <1 to 91.5% in terms of their fractional abundance of total 16S rRNA gene sequences (**Figure 1**). The highest abundance of "*Ca.* Bipolaricaulota" (5 abundant OTUs; 91.5% of the total reads) was found in the sediments of a 68.1°C brine pool (Tuzla) (**Figure 1**). Moreover, the "*Ca.* Bipolaricaulota" in sediment samples from the 78°C Hidirlar geothermal field had a 35.5% relative abundance. OTUs affiliated with "*Ca.* Bipolaricaulota" were also detected in all of the sampled subsurface geothermal wells, extending down to a depth of 1,300 m below the Earth's surface at the Güre borehole (**Figure 1**) and were relatively abundant specifically in a 260 m-deep borehole in the Güre region with 12.9% relative abundance.

"*Ca.* Bipolaricaulota" distribution in geothermal environments correlated with physicochemical parameters

RDA analysis showed that the major microbial groups detected at the Biga Peninsula were differently affected by the environmental conditions of the fluids, as they were clustered in different ordination spaces that positively or negatively related to different geochemical parameters (salinity, pH, O_2, Si, SO_4^{2-}, and temperature) in the RDA (**Figure 2**). The first RDA axis explained 21.05% of the OTUs variability and the second RDA axis explained 12.95%. The distribution of "*Ca.* Bipolaricaulota" OTUs in the various geothermal environments sampled (**Figure 1**) was positively related to salinity and negatively related to pH and sulfate concentration (**Figure 2**). Out of all five key physicochemical parameters tested (salinity, pH, O_2, Si, SO_4^{2-}, and temperature), salinity had the strongest relationship with the biogeographic distribution of "*Ca.* Bipolaricaulota" taxa (**Figure 2**).

Microbial composition within metagenomes and metagenome-assembled genomes

In line with the 16S rRNA gene-based microbial community structure (**Figure 1**), taxonomical annotations of open reading frames (ORFs) from the samples showed that microbial communities were dominated by the Aquificae, Proteobacteria, Nitrospirae, Deinococcus-Thermus, Bacteroidetes, and Crenarchaeota at different proportions (**Supplementary Figure 1**). On the contrary, the differences in relative abundances of microbial communities between 16S rRNA profiles and ORFs showed unexpected discrepancies, especially in the samples where members of "*Ca.* Bipolaricaulota" were detected (**Figure 1** and **Supplementary Figure 1**). For example, sediment samples from Tuzla brine exhibited a 4% relative abundance of ORFs annotated as "*Ca.* Bipolaricaulota" (**Supplementary Figure 1**), whereas the 16S rRNA gene sequences from this sample was dominated by this candidate phylum (**Figure 1**). It should be noted that based on the 60% similarity threshold of ORFs in Squeezemeta (Tamames and Puente-Sánchez, 2018), some ORFs could not be taxonomically assigned whose relative abundances reached around 50% in Tuzla brine (**Supplementary Figure 1**). 137 MAGs were assembled from the samples taken from the Biga Peninsula and the vicinity of Edremit town (**Supplementary Tables 3**, **4**), which were used to investigate the metabolic potential of "*Ca.* Bipolaricaulota" in more detail.

MAGs affiliated with "*Ca.* Bipolaricaulota"

Out of a total of 137 MAGs, four of them were taxonomically assigned to "*Ca.* Bipolaricaulota", with completeness ranging from 91.5 to 83% (0% redundancy) and redundancy varying from 0 to 4% based on the presence of single copy genes (see the Section "Materials and methods") (**Supplementary Table 2**). Read mapping against these MAGs revealed that they had a relatively high abundance in the metagenomes, reaching up to 10% of binned total reads in the Tuzla geothermal brine sample (**Figure 4**). This high relative abundance of the "*Ca.* Bipolaricaulota" TUZ33 MAG in the Tuzla brine sediments coincided with a high relative abundance of "*Ca.* Bipolaricaulota" 16S rRNA gene OTUs in this same sample that reached >90% relative abundance (**Figure 1**). In contrast, the other three "*Ca.* Bipolaricaulota" MAGs (CK84, CK101, and HID15) were largely restricted to geothermal fluids with much lower salinities (measured as Ec) (**Figure 4** and **Supplementary Table 4**). Of these MAGs, the HID15 had the highest relative abundance at the Hidirlar geothermal sediments, whereas MAGs CK84 and CK101 had their highest relative abundances in the subsurface borehole Entur (300 m) (**Figure 4** and **Supplementary Table 4**).

A phylogenomic analysis of a concatenated single-copy gene alignment revealed the phylogenetic relation of the MAGs sampled in our study to existing MAGs from other studies (**Figure 4**). Two MAGs (CK101 and CK84) from the less-saline Turkish geothermal sites had the closest phylogenetic affiliation to the deeply branching *Candidatus* 'Acetothermum autotrophicum' (Takami et al., 2012). MAG HID15 with the highest relative abundance in the geothermal sediments from the Hidirlar site (**Figure 1**) was affiliated with Order Bipolaricaulales and branched basal to a larger clade, including the Ran_1 MAG that was recovered from anaerobic sludge (Hao et al., 2018). The fourth MAG (TUZ33) that was highly abundant in the geothermal brine pool from Tuzla (**Figure 1**) branched basal to the *Candidatus* 'Acetothermum autotrophicum' clade and was clustered within Order RBG-16-55-9 (**Figure 4**).

WLP and energy metabolism of "*Ca.* Bipolaricaulota" genomes

We compared the "*Ca.* Bipolaricaulota" MAGs reconstructed from the Turkish geothermal sites (**Figure 5** and **Supplementary Figure 2**) to most of the publicly available mid/high-quality "*Ca.* Bipolaricaulota" MAGs using pangenomic analysis in order to better understand the carbon metabolism of this phylum (**Supplementary Tables 2**, **5**). The pangenome analysis uncovered that pairwise average nucleotide identities were spanning from nearly 65 to 99.9% in the "*Ca.* Bipolaricaulota" phylum (**Figure 5** and **Supplementary Table 2**). The MAG from the Turkish geothermal fluids with the highest average nucleotide identity to the deeply branching *Candidatus* 'Acetothermum autotrophicum' (Takami et al., 2012) was found to be CK101 (**Figure 5**). The pangenomic analysis shows that the core genome within "*Ca.* Bipolaricaulota" is relatively small compared to the flexible genome content of the individual MAGs (**Supplementary Figure 2**). The majority of the "*Ca.* Bipolaricaulota" pangenome is dominated by singleton genes (those genes detected in only one MAG and not any other MAGs) (**Supplementary Figure 2**). Pathways for fermentation were prevalent in the "*Ca.* Bipolaricaulota" MAGs (**Supplementary Figure 2**).

The pangenomic analysis identified two groups of "*Ca.* Bipolaricaulota" MAGs: one that contained the WLP pathway for H_2-dependent CO_2 fixation (Schuchmann and Müller, 2016) and another group of "*Ca.* Bipolaricaulota" MAGs that did not contain this pathway (**Figure 5**; **Supplementary Figure 2** and **Supplementary Table 5**). The concatenated single-copy gene alignment revealed that the presence or absence of the WLP was restricted to particular clades and branches, and did not correlate with a monophyletic pattern (**Figure 5**). From our Turkish geothermal sites, three of the MAGs (CK84, CK101, and HID15) contained the WLP pathway (**Figure 5** and **Supplementary Figure 2**), whereas the fourth MAG (TUZ33) did not encode it (**Figure 5** and **Supplementary Figure 2**). Pyruvate:ferredoxin oxidoreductases were found in 17 MAGs, 12 of which had complete/incomplete genes encoding WLP components (CK101, CK84, jdFR48, jdFR52, Olivine4, UBA3560, UBA3574, *Candidatus* 'Acetothermum autotrophicum', GSL_GSL3510, SZUA1496, UMWA_0174, and HID15) (**Supplementary Table 5**). A total of 12 MAGs encoded membrane-bound hydrogenases (alpha, beta, and mbhJ were observed) [EC:1.12.7.2]. In addition, 10 WLP-encoding MAGs had subunits of heterodisulfide reductase, which is involved in electron bifurcation (Buckel and Thauer, 2018; **Supplementary Table 5**). Moreover, all MAGs had the capacity for multiple fermentation pathways (**Supplementary Figure 2**).

Discussion

Despite featuring more than 2,000 geothermal sources within 460 geothermal fields (Mertoglu et al., 2020), the geothermal

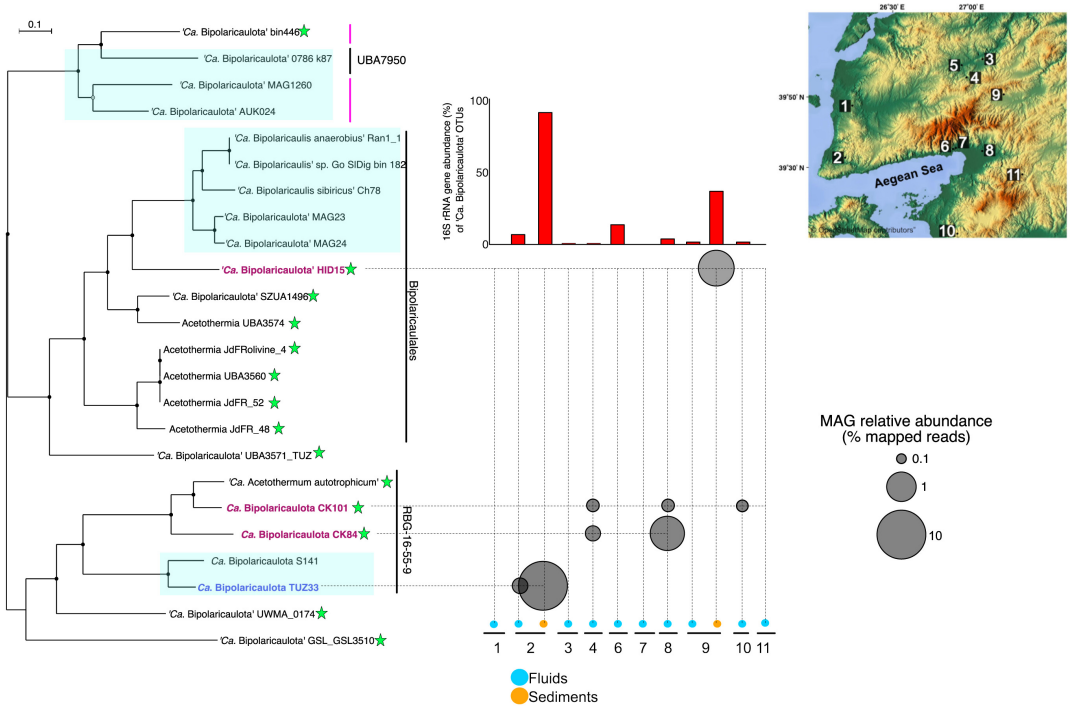

FIGURE 4
The phylogenetic tree is an analysis of concatenated 69 ribosomal proteins extracted from 23 metagenome assembled genomes affiliated to '*Ca.* Bipolaricaulota'. Black circles at nodes represent bootstrap support of 90%, gray circles represent bootstrap support from 70 to 90%, and white circles represent bootstrap support from 70 to 50%. Blue boxes represent the MAGs with no Wood-Ljungdahl pathway (WLP) encoded. The green stars show the MAGs containing the WLP. Bold and colored fonts represent the MAGs assembled from the geothermal sites in this study (dark blue and red). The bubble plot shows the relative abundance of the "*Ca.* Bipolaricaulota" MAGs assembled in this study corresponding to their position in the phylogenetic tree. The histograms above the bubble plot show the relative abundance of '*Ca.* Bipolaricaulota' from 16S rRNA gene datasets for each sampling location. The map represents the sampling locations, which are also shown in **Figure 1** and **Supplementary Figure 1**.

environments of Turkey are historically undersampled for microbial communities. There are few studies from geothermal springs and aquifers in Turkey that have mainly applied cultivation-based techniques that have isolated thermophilic organisms (Belduz et al., 2003; Çelikoğlu and Cankılıç, 2016; Guven et al., 2018). However, how the microbial diversity and metabolism relates to the diverse physicochemical conditions of the numerous geothermal environments is still poorly understood.

The origin of the thermal waters in the Biga Peninsula

The origin of geothermal waters in the Biga Peninsula was determined using the stable isotopic composition, δ^2H and $\delta^{18}O$, of the fluids (**Figure 3**). The results showed that the isotopic composition of most samples, together with deep water from a South African gold mine (Magnabosco et al., 2016), fell between the global meteoric water line (GMWL; Craig, 1961) and the East Mediterranean meteoric water line (EMMWL; Gat and Carmi, 1970), suggesting that the subsurface hydrothermal water had been replenished by modern meteoric water (**Figure 3**). An exception to this trend was found in the samples from Tuzla, Kestanbol, and Can, which had higher salinities and did not plot on the EMMWL and GMWL (**Figure 3**). These results were also in line with the findings published by Yalcin (2007). Samples taken from Kestanbol and Tuzla contained high amounts of sodium and chloride, hence they have been classified as NaCl-dominated waters (Yalcin, 2007). The stable isotopic composition of the thermal waters in these areas, δ^2H and $\delta^{18}O$, fell onto a mixing line between meteoric waters and deep-seated hot brine waters whose origin is not known, which is consistent with the previous study (Yalcin, 2007). It has been proposed that the origin of water could be the fossil water trapped in Miocene sediments (Balderer, 1997), whereas another study stressed that hypersalinity in these waters could result from the dissolution of salt deposits (Vengosh et al., 2002). In our study, we identified a $\delta^{18}O$-shift in Can thermal water, most likely explained by CO_2 input from a geological source, which was also suggested by a previous study that investigated thermal waters in the Biga Peninsula (Yalcin, 2007).

Carbon metabolism of "*Ca.* Bipolaricaulota"

Our pangenome analysis indicates that the WLP is restricted to a subset of clades within the '*Ca.* Bipolaricaulota' (**Figures 4**, **5**). The WLP can function in reductive (CO_2-reduction to acetyl-CoA) and oxidative (acetate utilization) directions depending on the metabolic demands of a microorganism. The reductive WLP is used in the reductive direction for energy conversion and autotrophic carbon fixation in acetogens and methanogens (Ragsdale and Pierce, 2008). The WLP may be involved in homoacetogenic fermentation during the anaerobic oxidation of sugars and amino acids (Schuchmann and Müller, 2016), coupled with autotrophy to fix CO_2 into biomass

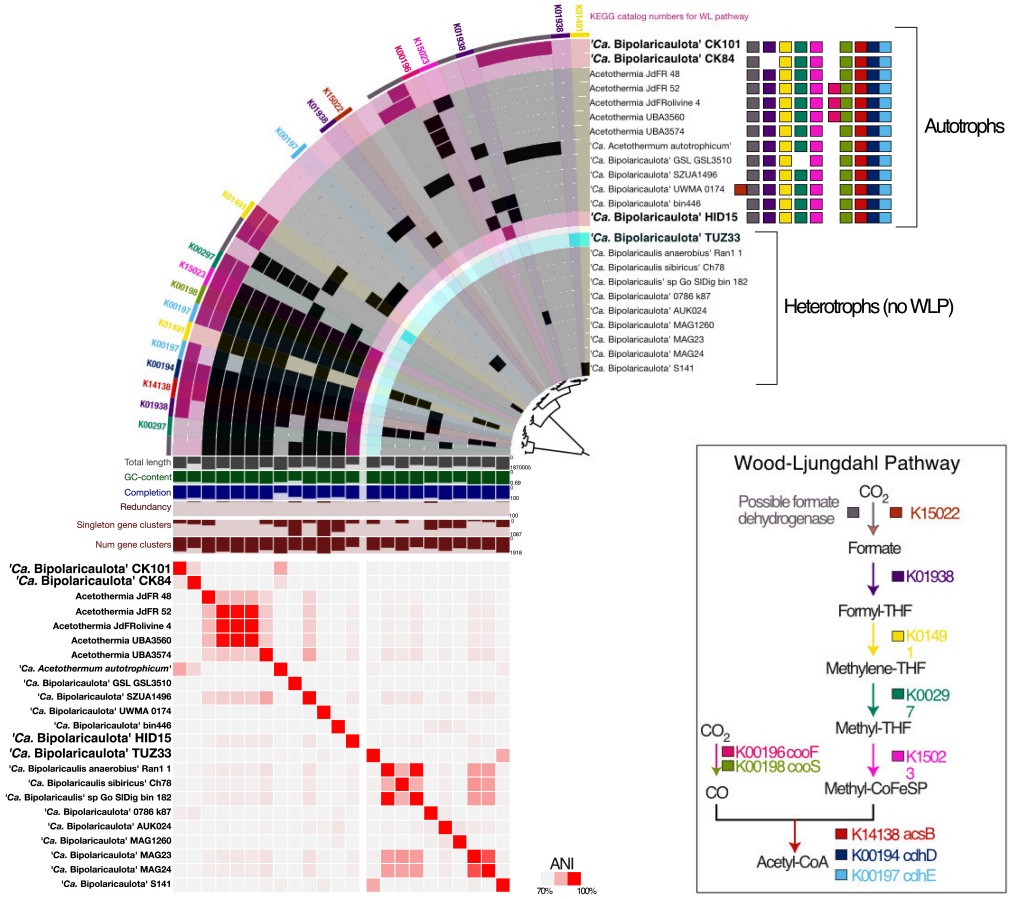

FIGURE 5
Comparative genomic analysis of gene clusters encoding Wood-Ljungdahl pathway (WLP) **(top row)**, and those lacking the WLP **(bottom row)**. The metagenome-assembled genomes (MAGs) recovered in this study are shown with bold letters and bigger font size; the MAGs taken from the public databases are displayed in black with relatively smaller font size. The heatmap shows average nucleotide identity between MAGs across the entire core genome. Values were calculated in the anvio v7 using pyANI (Pritchard et al., 2016). The colored squares represent the enzymes catalyzing the WLP.

(Fuchs, 2011). However, it is possible that the WLP is reversible and in the reverse direction, it would potentially function as oxidation of acetate, producing CO_2 and H_2 as end products (Müller et al., 2013). In oxidative WLP, acetate is oxidized to form CO_2 and H_2, which is performed by syntrophic acetate-oxidizing bacteria (SAO) when growing with hydrogenotrophic methanogens. Thus, the WLP provides exceptional metabolic flexibility to the organisms if they can use it in both directions.

H_2 production during fermentation of organic matter by "*Ca.* Bipolaricaulota" was indicated for a strain inhabiting anaerobic sludge, where it might support syntrophic interactions with H_2 utilizing methanogenic archaea and/or sulfate-reducing bacteria (Hao et al., 2018).

The WLP leads from two molecules of CO_2 that are reduced *via* H_2 making acetyl-CoA, which can contribute to biomass synthesis, ATP production via substrate-level-phosphorylation, and also provides reducing power to drive a proton motive force at the membrane for ATP synthesis (Schuchmann and Müller, 2016). It is a key metabolism for many homoacetogenic bacteria and helps to increase the efficiency of ATP production via fermentation under energy-limited conditions, such as those in anoxic environments lacking high-energy terminal electron acceptors with extremely low redox potential (Schuchmann and Müller, 2016). In our pangenome analysis of the WLP in "*Ca.* Bipolaricaulota", we identified many key WLP genes, including *acsB* (K14138), *cdhD* (K00194), and *cdhE* (K00197). However, some necessary genes for the WLP were missing in most MAGs (**Figure 5**; **Supplementary Figure 2** and **Supplementary Table 5**), whereas the complete WLP was detected in the "*Ca.* Bipolaricaulota" MAGs JdFR 48, JdFR 52, and *Acetothermium autotrophicum*. This is in accordance with prior results (Youssef et al., 2019). Our phylogenomic analysis shows that the WLP is specific to particular sub-groups of "*Ca.* Bipolaricaulota" but is not phylum-wide distributed. The WLP containing MAGs in several geothermal environments of the Biga Peninsula can apparently fix carbon dioxide (CK101, CK84, and HID15) (**Figure 5**), but also have the genomic capacity for fermentation (**Supplementary Figure 2**). Therefore, their energy metabolism bears a resemblance to homoacetogens that use the WLP to harness CO_2 as an electron sink to improve ATP production efficiencies under energy-limited conditions (Schuchmann and Müller, 2016).

Salinity controls the distribution of "*Ca.* Bipolaricaulota" in geothermal fluids

The highest abundance of "*Ca.* Bipolaricaulota" was found in the sediments of a geothermal brine pool at the Tuzla site,

and our statistical analysis shows that OTUs affiliated with "*Ca.* Bipolaricaulota" correlated most strongly with salinity compared to five other key physicochemical parameters such as temperature, O_2, pH, Si, and SO_4^{2-} (**Figure 2**). This indicates that salinity is a key driver of the biogeographic distribution for some members of this particular clade. Notably, the "*Ca.* Bipolaricaulota" MAGs that were dominant in this brine setting are lacking the WLP, indicating that they are heterotrophs (**Figure 5**). In line with our analysis, it has been reported that the Tuzla sample contains nearly twice the amount of salt concentration compared to the same concentrations in seawater as sodium and chloride concentrations, which reach 17 and 68 mg/L, respectively (Baba et al., 2009). These findings are consistent with other studies that found an affinity of this group for brine environments such as in Orca Basin (Nigro et al., 2016), Hephaestus and Kryos basins (Fisher et al., 2021), hypersaline stratified layers of Ursu Lake (Baricz et al., 2021), saline pan sediments in the Kalahari Desert of southern Africa (Genderjahn et al., 2018), anoxic hypersaline layers of Witpan in South Africa, and in surface sediments of salty Siberian soda lakes (Vavourakis et al., 2018). Our findings show that (a) the WLP encoding (carbon-fixing) "*Ca.* Bipolaricaulota" MAGs are enriched at lower salinities (**Figures 1**, **4**, **5**) and (b) they were still detected in the brine at a relatively low abundance, suggesting that they are halotolerant.

Energy metabolism and survival under extreme conditions

Many of the WLP-encoding MAGs in the pangenome analysis encode fermentation pathways that are known to produce formate, H_2, and acetate (**Supplementary Figure 2**). These MAGs also encode the pyruvate: ferredoxin oxidoreductase complex (porABCD) that produces acetyl-CoA from pyruvate, thereby generating reduced ferredoxin. The encoded Acetyl-CoA synthases (acs) can then produce ATP (for energy) and acetate (as a fermentation product) during fermentation (**Supplementary Table 5**). The potentially produced formate and H_2 from fermentation processes (**Supplementary Figure 2**), could be utilized by syntrophic partners (Hao et al., 2018). Also, in line with a recent metagenomic study conducted in Samail Ophiolite in Oman, the fermentation capability of "*Ca.* Bipolaricaulota" MAGs has been shown, especially in MAGs associated with Order RBG-16-55-9, where they dominate alkaline fluids (Colman et al., 2022). The combined potential for fermentation in the MAGs, which also encode the WLP, highlights the genomic capacity of some "*Ca.* Bipolaricaulota" to survive *via* mixotrophy (combining H_2-dependent CO_2 fixation *via* the WLP with heterotrophy). The mixotrophic "*Ca.* Bipolaricaulota" might exhibit a homoacetogenic fermentation metabolism, which is a common feature of many anaerobic heterotrophic bacteria living close to the energy limit of life (Schuchmann and Müller, 2016). Specifically, CO_2 acts as an electron sink (*via* the WLP) during the oxidation of organic matter during fermentation in order to provide a reducing potential to drive a proton motive force at the membrane (Schuchmann and Müller, 2016). The encoded heterodisulfide reductases in the MAGs suggest the potential for electron bifurcation to play a role in linking the fermentation and WLP processes (Schuchmann and Müller, 2016).

The extreme energy limitation of the deep subsurface environments sampled here (up to 1,300 m below the surface) presents a challenge for microbial life to survive. It is proposed that a prosthecate provides a competitive advantage for "*Ca.* Bipolaricaulota" to survive under nutrient-limited conditions by increasing the surface area for nutrient uptake (Hao et al., 2018). This would be important for energy-limited environments such as the deep subsurface. However, the Ran1 MAG from which the prosthecates were observed (Hao et al., 2018) shares less than 70% average nucleotide identity with the MAGs recovered from the Turkish geothermal settings here (**Figure 5** and **Supplementary Table 2**) and is part of a more derived clade within the Bipolaricaulales Order that does not encode WLP (**Figure 4**). This level of ANI difference likely corresponds to different microbial genera (Konstantinidis and Tiedje, 2005) and indicates the in-group diversity of the proposed novel phylum "*Ca.* Bipolaricaulota" (Hao et al., 2018; Youssef et al., 2019) is relatively large. Moreover, the flexible genomes of the Ran1 MAG and the MAGs from the geothermal aquifers of Turkey show minimal overlap (**Figure 5**). The large genetic difference and the large differences in flexible genome content raise the possibility that "*Ca.* Bipolaricaulota" in the Turkish geothermal settings has a different phenotype that may not have prosthecate, but additional microscopy is needed to confirm this. Future studies combining metagenomics with microscopy, cultivation, and phylogenomics will help to reveal how phenotypic traits correlate with life histories in the novel candidate phylum "*Ca.* Bipolaricaulota".

Data availability statement

The data presented in this study are deposited in https://doi.org/10.6084/m9.figshare.21286227.v1 and in the NCBI Short Read Archive repository, accession number PRJNA888248.

Author contributions

ÖKC, MB, DO, and HH performed sampling. ÖKC and FE performed lab work. ÖKC, GVG-S, WDO, and FE performed data analysis. ÖKC and WDO designed the study. OKC, GVG-S, and WDO wrote the manuscript. All authors contributed to the article and approved the submitted version.

Funding

This study was supported by the Deutsche Forschungsgemeinschaft (DFG, German Research Foundation)—Project-ID 364653263—TRR 235 to WDO, under Germany's Excellence Strategy—EXC 2077-390741603, and by the DFG —Project-ID GO 3267/2-1—to GVG-S.

Acknowledgments

We are grateful for the support of the management and the staff of Kazdagi Thermal Resort & Spa. We also thank Mustafa Coskun and Halil Gültekin who participated as part of the field campaign in 2019 and 2020.

Conflict of interest

The authors declare that the research was conducted in the absence of any commercial or financial relationships that could be construed as a potential conflict of interest.

Publisher's note

All claims expressed in this article are solely those of the authors and do not necessarily represent those of their affiliated organizations, or those of the publisher, the editors and the reviewers. Any product that may be evaluated in this article, or claim that may be made by its manufacturer, is not guaranteed or endorsed by the publisher.

Supplementary material

The Supplementary Material for this article can be found online at: https://www.frontiersin.org/articles/10.3389/fmicb.2023.1063139/full#supplementary-material

References

Alneberg, J., Bjarnason, B., de Bruijn, I., Schirmer, M., Quick, J., Ijaz, U., et al. (2014). Binning metagenomic contigs by coverage and composition. *Nat. Methods* 11, 1144–1146. doi: 10.1038/nmeth.3103

Baba, A., Yuce, G., Deniz, O., and Ugurluoglu, D. (2009). Hydrochemical and isotopic composition of tuzla geothermal field (Canakkale-Turkey) and its environmental impacts. *Environ. Forensics* 10, 144–161. doi: 10.1080/15275920902873418

Balderer, W. (1997). "Mechanisms and processes of groundwater circulation in tectonically active areas," in *Active tectonics of northwestern anatolia-the marmara poly-project*, eds C. Shindler and M. Pfister (Zürich: Hochschulverlag AG an der ETH Zurich-Swiss), 375–416.

Baricz, A., Chiriac, C., Andrei, A., Bulzu, P., Levei, E., Cadar, O., et al. (2021). Spatio-temporal insights into microbiology of the freshwater-to-hypersaline, oxic-hypoxic-euxinic waters of Ursu Lake. *Environ. Microbiol.* 23, 3523–3540. doi: 10.1111/1462-2920.14909

Belduz, A., Dulger, S., and Demirbag, Z. (2003). Anoxybacillus gonensis sp. nov., a moderately thermophilic, xylose-utilizing, endospore-forming bacterium. *Int. J. Syst. Evol. Microbiol.* 53, 1315–1320. doi: 10.1099/ijs.0.02473-0

Bhattarai, B., Bhattacharjee, A., Coutinho, F., and Goel, R. (2021). Viruses and their interactions with bacteria and archaea of hypersaline great Salt Lake. *Front. Microbiol.* 12:701414. doi: 10.3389/fmicb.2021.701414

Bolger, A., Lohse, M., and Usadel, B. (2014). Trimmomatic: a flexible trimmer for Illumina sequence data. *Bioinformatics* 30, 2114–2120. doi: 10.1093/bioinformatics/btu170

Brazelton, W., McGonigle, J., Motamedi, S., Pendleton, H., Twing, K., Miller, B., et al. (2022). Metabolic strategies shared by basement residents of the Lost City hydrothermal field. *Appl. Environ. Microbiol.* 88, e0092922. doi: 10.1128/aem.00929-22

Buchfink, B., Xie, C., and Huson, D. (2015). Fast and sensitive protein alignment using DIAMOND. *Nat. Methods.* 12, 59–60. doi: 10.1038/nmeth.3176

Buckel, W., and Thauer, R. (2018). Flavin-based electron bifurcation, ferredoxin, flavodoxin, and anaerobic respiration with protons (Ech) or NAD+ (Rnf) as electron acceptors: a historical review. *Front. Microbiol.* 9:401. doi: 10.3389/fmicb.2018.00401

Caporaso, J., Kuczynski, J., Stombaugh, J., Bittinger, K., Bushman, F., Costello, E., et al. (2010). QIIME allows analysis of high-throughput community sequencing data. *Nat. Methods* 7, 335–336. doi: 10.1038/nmeth.f.303

Çelikoğlu, E., and Cankılıç, M. (2016). Prokaryotic diversity of hot springs in Balikesİr and Kütahya, Turkey. *Appl. Ecol. Environ. Res.* 14, 429–440. doi: 10.15666/aeer/1404_429440

Colman, D., Kraus, E., Thieringer, P., Rempfert, K., Templeton, A., Spear, J., et al. (2022). Deep-branching acetogens in serpentinized subsurface fluids of Oman. *Proc. Natl. Acad. Sci. U.S.A.* 119:e2206845119. doi: 10.1073/pnas.2206845119

Coskun, ÖK., Özen, V., Wankel, S., and Orsi, W. (2019). Quantifying population-specific growth in benthic bacterial communities under low oxygen using H218O. *ISME J.* 13, 1546–1559. doi: 10.1038/s41396-019-0373-4

Coskun, ÖK., Pichler, M., Vargas, S., Gilder, S., and Orsi, W. (2018). Linking uncultivated microbial populations and benthic carbon turnover by using quantitative stable isotope probing. *Appl. Environ. Microbiol.* 84, e01083–e01018. doi: 10.1128/AEM.01083-18

Coskun, ÖK., Vuillemin, A., Schubotz, F., Klein, F., Sichel, S., Eisenreich, W., et al. (2021). Quantifying the effects of hydrogen on carbon assimilation in a seafloor microbial community associated with ultramafic rocks. *ISME J.* 16, 257–271. doi: 10.1038/s41396-021-01066-x

Craig, H. (1961). Isotopic variations in meteoric waters. *Science* 133, 1702–1703. doi: 10.1126/science.133.3465.1702

Edgar, R. (2004). MUSCLE: multiple sequence alignment with high accuracy and high throughput. *Nucleic Acids Res.* 32, 1792–1797. doi: 10.1093/nar/gkh340

Edgar, R. (2010). Search and clustering orders of magnitude faster than BLAST. *Bioinformatics.* 26, 2460–2461. doi: 10.1093/bioinformatics/btq461

Edgar, R. (2013). UPARSE: highly accurate OTU sequences from microbial amplicon reads. *Nat. Methods* 10, 996–998. doi: 10.1038/nmeth.2604

Einsiedl, F., Wunderlich, A., Sebilo, M., Coskun, ÖK., Orsi, W., and Mayer, B. (2020). Biogeochemical evidence of anaerobic methane oxidation and anaerobic ammonium oxidation in a stratified lake using stable isotopes. *Biogeosciences* 17, 5149–5161. doi: 10.5194/bg-17-5149-2020

Eren, A., Esen, ÖC., Quince, C., Vineis, J., Morrison, H., Sogin, M., et al. (2015). Anvi'o: an advanced analysis and visualization platform for 'omics data. *PeerJ.* 3:e1319. doi: 10.7717/peerj.1319

Fernandez, A., Rasuk, M., Visscher, P., Contreras, M., Novoa, F., Poire, D., et al. (2016). Microbial diversity in sediment ecosystems (Evaporites domes, microbial mats, and crusts) of hypersaline laguna tebenquiche, Salar de Atacama, Chile. *Front. Microbiol.* 7:1284. doi: 10.3389/fmicb.2016.01284

Fisher, L., Pontefract, A., Som, S., Carr, C., Klempay, B., Schmidt, B., et al. (2021). Current state of athalassohaline deep-sea hypersaline anoxic basin research-recommendations for future work and relevance to astrobiology. *Environ. Microbiol.* 23, 3360–3369. doi: 10.1111/1462-2920.15414

Fuchs, G. (2011). Alternative pathways of carbon dioxide fixation: insights into the early evolution of life? *Annu. Rev. Microbiol.* 65, 631–658. doi: 10.1146/annurev-micro-090110-102801

Gat, J., and Carmi, I. (1970). Evolution of the isotopic composition of atmospheric waters in the Mediterranean Sea area. *J. Geophys. Res.* 75, 3039–3048. doi: 10.1029/JC075i015p03039

Genderjahn, S., Alawi, M., Mangelsdorf, K., Horn, F., and Wagner, D. (2018). Desiccation- and saline-tolerant bacteria and archaea in kalahari pan sediments. *Front. Microbiol.* 9:2082. doi: 10.3389/fmicb.2018.02082

Guven, K., Matpan Bekler, F., and Gul Guven, R. (2018). "Thermophilic and Halophilic microorganisms isolated from extreme environments of Turkey, with potential biotechnological applications," in *Extremophiles in eurasian ecosystems: ecology, diversity, and applications*, eds D. Egamberdieva, N. Birkeland, H. Panosyan, and W. Li (Singapore: Springer Singapore), 219–264. doi: 10.1007/978-981-13-0329-6_8

Hao, L., McIlroy, S., Kirkegaard, R., Karst, S., Fernando, W., Aslan, H., et al. (2018). Novel prosthecate bacteria from the candidate phylum Acetothermia. *ISME J.* 12, 2225–2237. doi: 10.1038/s41396-018-0187-9

Hu, P., Tom, L., Singh, A., Thomas, B., Baker, B., Piceno, Y., et al. (2016). Genome-Resolved Metagenomic Analysis Reveals Roles for Candidate Phyla and Other Microbial Community Members in Biogeochemical Transformations in Oil Reservoirs. *MBio.* 7, e01669–15. doi: 10.1128/mBio.01669-15

Huerta-Cepas, J., Szklarczyk, D., Forslund, K., Cook, H., Heller, D., Walter, M., et al. (2016). eggNOG 4.5: a hierarchical orthology framework with improved functional annotations for eukaryotic, prokaryotic and viral sequences. *Nucleic Acids Res.* 44, D286–D293. doi: 10.1093/nar/gkv1248

Hugenholtz, P., Pitulle, C., Hershberger, K., and Pace, N. (1998). Novel division level bacterial diversity in a Yellowstone hot spring. *J. Bacteriol.* 180, 366–376. doi: 10.1128/JB.180.2.366-376.1998

Hyatt, D., Chen, G., Locascio, P., Land, M., Larimer, F., and Hauser, L. (2010). Prodigal: prokaryotic gene recognition and translation initiation site identification. *BMC Bioinform.* 11:119. doi: 10.1186/1471-2105-11-119

Jungbluth, S., Amend, J., and Rappé, M. (2017). Metagenome sequencing and 98 microbial genomes from Juan de Fuca Ridge flank subsurface fluids. *Sci. Data.* 4:170037. doi: 10.1038/sdata.2017.37

Kadnikov, V., Mardanov, A., Beletsky, A., Frank, Y., Karnachuk, O., and Ravin, N. (2019). Complete genome sequence of an uncultured bacterium of the candidate phylum bipolaricaulota. *Microbiology* 88, 461–468. doi: 10.1134/S0026261719040064

Kanehisa, M. (2000). KEGG: kyoto encyclopedia of genes and genomes. *Nucleic Acids Res.* 28, 27–30. doi: 10.1093/nar/28.1.27

Kang, D., Li, F., Kirton, E., Thomas, A., Egan, R., An, H., et al. (2019). MetaBAT 2: an adaptive binning algorithm for robust and efficient genome reconstruction from metagenome assemblies. *PeerJ.* 7:e7359. doi: 10.7717/peerj.7359

Konstantinidis, K., and Tiedje, J. (2005). Genomic insights that advance the species definition for prokaryotes. *Proc. Natl. Acad. Sci. U.S.A.* 102, 2567–2572. doi: 10.1073/pnas.0409727102

Köster, J., and Rahmann, S. (2012). Snakemake–a scalable bioinformatics workflow engine. *Bioinformatics* 28, 2520–2522. doi: 10.1093/bioinformatics/bts480

Langmead, B., and Salzberg, S. (2012). Fast gapped-read alignment with Bowtie 2. *Nat. Methods.* 9, 357–359. doi: 10.1038/nmeth.1923

Li, D., Liu, C., Luo, R., Sadakane, K., and Lam, T. (2015). MEGAHIT: an ultra-fast single-node solution for large and complex metagenomics assembly via succinct de Bruijn graph. *Bioinformatics* 31, 1674–1676. doi: 10.1093/bioinformatics/btv033

Liu, Y., Chen, J., Liu, Z., Shou, L., Lin, D., Zhou, L., et al. (2020). Anaerobic degradation of paraffins by thermophilic actinobacteria under methanogenic conditions. *Environ Sci Technol.* 54, 10610–10620. doi: 10.1021/acs.est.0c02071

Magnabosco, C., Ryan, K., Lau, M., Kuloyo, O., Sherwood Lollar, B., Kieft, T., et al. (2016). A metagenomic window into carbon metabolism at 3 km depth in Precambrian continental crust. *ISME J.* 10, 730–741.

Martin, W., Baross, J., Kelley, D., and Russell, M. (2008). Hydrothermal vents and the origin of life. *Nat. Rev. Microbiol.* 6, 805–814.

Mertoglu, O., Simsek, S., and Basarir, N. (2020). "Geothermal energy use: projections and country update for Turkey," in *Proceedings of the world geothermal congress*, (Reykjavik).

Müller, B., Sun, L., and Schnürer, A. (2013). First insights into the syntrophic acetate-oxidizing bacteria–a genetic study. *Microbiologyopen* 2, 35–53. doi: 10.1002/mbo3.50

Nessim, R., Tadros, H., Abou Taleb, A., and Moawad, M. (2015). Chemistry of the Egyptian Mediterranean coastal waters. *Egypt. J. Aquat. Res.* 41, 1–10. doi: 10.1016/j.ejar.2015.01.004

Nigro, L., Hyde, A., MacGregor, B., and Teske, A. (2016). Phylogeography, salinity adaptations and metabolic potential of the candidate division KB1 bacteria based on a partial single cell genome. *Front. Microbiol.* 7:1266. doi: 10.3389/fmicb.2016.01266

Oksanen, J., Blanchet, F., Kindt, R., Legendre, P., Minchin, P., O'Hara, R., et al. (2013). *Vegan: community ecology package. R package version. 2.0-10.*

Orsi, W., Smith, J., Wilcox, H., Swalwell, J., Carini, P., Worden, A., et al. (2015). Ecophysiology of uncultivated marine euryarchaea is linked to particulate organic matter. *ISME J.* 9, 1747–1763. doi: 10.1038/ismej.2014.260

Parada, A., Needham, D., and Fuhrman, J. (2016). Every base matters: assessing small subunit rRNA primers for marine microbiomes with mock communities, time series and global field samples. *Environ. Microbiol.* 18, 1403–1414. doi: 10.1111/1462-2920.13023

Parks, D., Rinke, C., Chuvochina, M., Chaumeil, P., Woodcroft, B., Evans, P., et al. (2017). Recovery of nearly 8,000 metagenome-assembled genomes substantially expands the tree of life. *Nat. Microbiol.* 2, 1533–1542. doi: 10.1038/s41564-017-0012-7

Pichler, M., Coskun, ÖK., Ortega-Arbulú, A., Conci, N., Wörheide, G., Vargas, S., et al. (2018). A 16S rRNA gene sequencing and analysis protocol for the Illumina MiniSeq platform. *Microbiologyopen.* 7:e00611. doi: 10.1002/mbo3.611

Price, M., Dehal, P., and Arkin, A. (2010). FastTree 2–approximately maximum-likelihood trees for large alignments. *PLoS One* 5:e9490. doi: 10.1371/journal.pone.0009490

Pritchard, L., Glover, R., Humphris, S., Elphinsonte, J., and Toth, I. (2016). Geomics and taxonomy in diagnostics for food security: Soft-rotting enterobacterial plant pathogens. *Anal. Methods* 8, 12–24.

Quast, C., Pruesse, E., Yilmaz, P., Gerken, J., Schweer, T., Yarza, P., et al. (2013). The SILVA ribosomal RNA gene database project: improved data processing and web-based tools. *Nucleic Acids Res.* 41, D590–D596. doi: 10.1093/nar/gks1219

Ragsdale, S., and Pierce, E. (2008). Acetogenesis and the Wood-Ljungdahl pathway of CO(2) fixation. *Biochim. Biophys. Acta.* 1784, 1873–1898.

Reysenbach, A., St John, E., Meneghin, J., Flores, G., Podar, M., Dombrowski, N., et al. (2020). Complex subsurface hydrothermal fluid mixing at a submarine arc volcano supports distinct and highly diverse microbial communities. *Proc. Natl. Acad. Sci. U.S.A.* 117, 32627–32638.

RStudio Team. (2015). *RStudio: integrated development for R.* Boston, MA: RStudio, Inc.

Salter, S., Cox, M., Turek, E., Calus, S., Cookson, W., Moffatt, M., et al. (2014). Reagent and laboratory contamination can critically impact sequence-based microbiome analyses. *BMC Biol.* 12:87. doi: 10.1186/s12915-014-0087-z

Sánchez-Andrea, I., Guedes, I., Hornung, B., Boeren, S., Lawson, C., Sousa, D., et al. (2020). The reductive glycine pathway allows autotrophic growth of Desulfovibrio desulfuricans. *Nat. Commun.* 11:5090.

Schneider, D., Zühlke, D., Poehlein, A., Riedel, K., and Daniel, R. (2021). Metagenome-assembled genome sequences from different wastewater treatment stages in Germany. *Microbiol. Resour. Announc.* 10:e0050421.

Schuchmann, K., and Müller, V. (2016). Energetics and application of heterotrophy in acetogenic bacteria. *Appl. Environ. Microbiol.* 82, 4056–4069.

Sieber, C., Probst, A., Sharrar, A., Thomas, B., Hess, M., Tringe, S., et al. (2018). Recovery of genomes from metagenomes via a dereplication, aggregation and scoring strategy. *Nat. Microbiol.* 2018, 836–843.

Smith, A., Kieft, B., Mueller, R., Fisk, M., Mason, O., Popa, R., et al. (2019). Carbon fixation and energy metabolisms of a subseafloor olivine biofilm. *ISME J.* 13, 1737–1749.

Speth, D., Yu, F., Connon, S., Lim, S., Magyar, J., Peña-Salinas, M., et al. (2022). Microbial communities of Auka hydrothermal sediments shed light on vent biogeography and the evolutionary history of thermophily. *ISME J.* 16, 1750–1764.

Stott, M., Saito, J., Crowe, M., Dunfield, P., Hou, S., Nakasone, E., et al. (2008). Culture-independent characterization of a novel microbial community at a hydrothermal vent at Brothers volcano, Kermadec arc, New Zealand. *J. Geophys. Res.* 113:B08S06. doi: 10.1029/2007JB005477

Takami, H., Noguchi, H., Takaki, Y., Uchiyama, I., Toyoda, A., Nishi, S., et al. (2012). A deeply branching thermophilic bacterium with an ancient acetyl-CoA pathway dominates a subsurface ecosystem. *PLoS One* 7:e30559.

Tamames, J., and Puente-Sánchez, F. (2018). SqueezeMeta, a highly portable, fully automatic metagenomic analysis pipeline. *Front. Microbiol.* 9:3349.

Teske, A., Hinrichs, K., Edgcomb, V., de Vera Gomez, A., Kysela, D., Sylva, S., et al. (2002). Microbial diversity of hydrothermal sediments in the Guaymas Basin: evidence for anaerobic methanotrophic communities. *Appl. Environ. Microbiol.* 68, 1994–2007.

Tobler, D., and Benning, L. (2011). Bacterial diversity in five Icelandic geothermal waters: temperature and sinter growth rate effects. *Extremophiles* 15, 473–485.

Vavourakis, C., Andrei, A., Mehrshad, M., Ghai, R., Sorokin, D., and Muyzer, G. (2018). A metagenomics roadmap to the uncultured genome diversity in hypersaline soda lake sediments. *Microbiome* 6:168. doi: 10.1186/s40168-018-0548-7

Vengosh, A., Helvacı, C., and Karamanderesi, İH. (2002). Geochemical constraints for the origin of thermal waters from western Turkey. *Appl. Geochem.* 17, 163–183.

Wang, W., Tao, J., Yu, K., He, C., Wang, J., Li, P., et al. (2021). Vertical stratification of dissolved organic matter linked to distinct microbial communities in subtropic estuarine sediments. *Front Microbiol.* 12:697860.

Wei, T., Simko, V., Levy, M., Xie, Y., Jin, Y., and Zemla, J. (2013). *corrplot: Visualization of a correlation matrix. R package version 073.230.*

Wickham, H. (2016). *ggplot2: Elegant graphics for data analysis*. Cham: Springer International Publishing, 3–10.

Wu, Y., Simmons, B., and Singer, S. (2016). MaxBin 2.0: an automated binning algorithm to recover genomes from multiple metagenomic datasets. *Bioinformatics* 32, 605–607.

Yalcin, T. (2007). Geochemical characterization of the Biga Peninsula thermal waters (NW Turkey). *Aquat. Geochem.* 13, 75–93.

Youssef, N., Farag, I., Rudy, S., Mulliner, A., Walker, K., Caldwell, F., et al. (2019). The Wood-Ljungdahl pathway as a key component of metabolic versatility in candidate phylum Bipolaricaulota (Acetothermia, OP1). *Environ. Microbiol. Rep.* 11, 538–547.

Zhou, Z., Liu, Y., Pan, J., Cron, B., Toner, B., Anantharaman, K., et al. (2020). Gammaproteobacteria mediating utilization of methyl-, sulfur- and petroleum organic compounds in deep ocean hydrothermal plumes. *ISME J.* 14, 3136–3148.

frontiers | Frontiers in Microbiology

TYPE Original Research
PUBLISHED 11 August 2023
DOI 10.3389/fmicb.2023.1134114

OPEN ACCESS

EDITED BY
Brett J. Baker,
The University of Texas at Austin, United States

REVIEWED BY
Florence Schubotz,
University of Bremen, Germany
Craig Everroad,
National Aeronautics and Space Administration, United States

*CORRESPONDENCE
Donato Giovannelli
✉ donato.giovannelli@unina.it

†These authors share first authorship

‡PRESENT ADDRESS
Alessandra Ferrillo,
Norwegian University of Life Sciences, Aas, Norway

RECEIVED 29 December 2022
ACCEPTED 25 July 2023
PUBLISHED 11 August 2023

CITATION
Barosa B, Ferrillo A, Selci M, Giardina M, Bastianoni A, Correggia M, di Iorio L, Bernardi G, Cascone M, Capuozzo R, Intoccia M, Price R, Vetriani C, Cordone A and Giovannelli D (2023) Mapping the microbial diversity associated with different geochemical regimes in the shallow-water hydrothermal vents of the Aeolian archipelago, Italy. *Front. Microbiol.* 14:1134114. doi: 10.3389/fmicb.2023.1134114

Mapping the microbial diversity associated with different geochemical regimes in the shallow-water hydrothermal vents of the Aeolian archipelago, Italy

Bernardo Barosa[1†], Alessandra Ferrillo[1†‡], Matteo Selci[1], Marco Giardina[1], Alessia Bastianoni[1], Monica Correggia[1], Luciano di Iorio[1], Giulia Bernardi[2], Martina Cascone[1], Rosaria Capuozzo[1], Michele Intoccia[1], Roy Price[3], Costantino Vetriani[4,5], Angelina Cordone[1] and Donato Giovannelli[1,5,6,7,8]*

[1]Department of Biology, University of Naples "Federico II", Naples, Italy, [2]Blue Marine Foundation, London, United Kingdom, [3]School of Marine and Atmospheric Sciences, Stony Brook, NY, United States, [4]Department of Biochemistry and Microbiology, Rutgers University, New Brunswick, NJ, United States, [5]Department of Marine and Coastal Science, Rutgers University, New Brunswick, NJ, United States, [6]Istituto per le Risorse Biologiche e Biotecnologiche Marine, Consiglio Nazionale Delle Ricerche, CNR-IRBIM, Ancona, Italy, [7]Earth-Life Science Institute, Tokyo Institute of Technology, Ookayama, Tokyo, Japan, [8]Marine Chemistry and Geochemistry Department–Woods Hole Oceanographic Institution, Woods Hole, MA, United States

Shallow-water hydrothermal vents are unique marine environments ubiquitous along the coast of volcanically active regions of the planet. In contrast to their deep-sea counterparts, primary production at shallow-water vents relies on both photoautotrophy and chemoautotrophy. Such processes are supported by a range of geochemical regimes driven by different geological settings. The Aeolian archipelago, located in the southern Tyrrhenian sea, is characterized by intense hydrothermal activity and harbors some of the best sampled shallow-water vents of the Mediterranean Sea. Despite this, the correlation between microbial diversity, geochemical regimes and geological settings of the different volcanic islands of the archipelago is largely unknown. Here, we report the microbial diversity associated with six distinct shallow-water hydrothermal vents of the Aeolian Islands using a combination of 16S rRNA amplicon sequencing along with physicochemical and geochemical measurements. Samples were collected from biofilms, fluids and sediments from shallow vents on the islands of Lipari, Panarea, Salina, and Vulcano. Two new shallow vent locations are described here for the first time. Our results show the presence of diverse microbial communities consistent in their composition with the local geochemical regimes. The shallow water vents of the Aeolian Islands harbor highly diverse microbial community and should be included in future conservation efforts.

KEYWORDS

shallow-water vents, Aeolian archipelago, 16S rRNA amplicon sequencing, microbial diversity, marine protected areas, hydrothermal vents

1. Introduction

The vast and diverse metabolic repertoire of microorganisms enables their ubiquitous distribution on our planet, making them key mediators of biogeochemical cycles on a planetary scale (Falkowski et al., 2008). Notwithstanding their ubiquity, their distribution and the environmental factors shaping it, are not fully resolved. However, significant correlations between microbial community composition and environmental geochemistry have been established in diverse environments (Jorgensen et al., 2012; Alsop et al., 2014; Liu et al., 2014; Yamamoto et al., 2019). Geothermal environments are ideal systems to study the complex relationships between community composition and geochemistry due to the wide geochemical gradients present across proximal geographic distances, and relatively constrained microbial communities (Power et al., 2018). Additionally, geothermal ecosystems harbor diverse communities of extremophiles that are an untapped source of potential biotechnological compounds (Sayed et al., 2020). Hence, there is an increasing necessity to characterize in detail the microbial diversity in these ecosystems and to prioritize their conservation.

Marine hydrothermal vents are dynamic systems where water is discharged through the Earth's crust in areas where there is enough heat to drive fluid circulation, e.g., plate boundaries and mid-ocean ridges (Price and Giovannelli, 2017; Brovarone et al., 2020). The interaction between the seawater with the hot, deep-subsurface lithologies, promotes the leaching of inorganic reduced species, such as volatiles and metals (McDermott et al., 2018). Upon arrival at the surface, the mixing of the reduced hydrothermal fluids (enriched in electron donors) with the oxidized sea water (enriched in electron acceptors), creates a thermodynamic disequilibrium that fuels diverse microbial consortia and sustains complex food webs (Dahle et al., 2015; Price et al., 2015; Reed et al., 2015). In contrast with their deep-sea counterparts, shallow-water hydrothermal vents (SWHV) are closer to the surface, thus they are strongly influenced by solar energy. In these shallow systems, the primary production is reliant upon a mixture of phototrophy and chemolithotrophy, making them high-energy environments (Tarasov et al., 2005; Gomez-Saez et al., 2017). Additionally, the shallower depths and the resultant decrease in pressure allow for the presence of a generally abundant free gas phase (Bastianoni et al., 2022). The proximity to landmasses promotes the input of terrigenous organic carbon to the system, while tidal waves and tides make SWHV transient ecosystems subject to strong dynamic forcing (Giovannelli et al., 2013; Yücel et al., 2013; Price and Giovannelli, 2017).

The shallow-water hydrothermal vents of the Aeolian archipelago are some of the most studied marine shallow vents in the world. The archipelago, located north of Sicily, is composed of seven volcanic islands (Stromboli, Vulcano, Panarea, Salina, Lipari, Alicudi, and Filicudi) and several sea-mounts. The archipelago lies between the Tyrrhenian sea back-arc basin and the Calabrian fore-arc. While most of its volcanic activity developed during the Quaternary period, it continues to the present day on some of the islands (Vulcano and Stromboli) in the form of volcanic eruptions and secondary geothermal manifestations (Gamberi et al., 1997). The geomorphism of the region is very dynamic, marked by the presence of rock types belonging mainly to the calc-alkaline, shoshonitic, and potassium associations (De Astis et al., 2000; Peccerillo and Turco, 2004). The islands of Lipari, Salina, and Vulcano, are aligned on an NNW–SSE striking fault, while a NNE–SSW to NE–SW striking fault affects the islands of Stromboli and Panarea (De Astis et al., 2003; Favallim et al., 2005). Most of the described marine geothermal activity is present along the coast of the islands of Vulcano and Panarea, where the majority of microbiological studies on the shallow-water vents have been focused so far. Despite this, additional sites of geothermal activities have been described on the other islands (Cardellini et al., 2003; Inguaggiato et al., 2012, 2013).

Previous studies have mapped the thermodynamic chemical reaction landscape of SWHVs of Vulcano and Panarea islands, showing that a wide range of exergonic chemical reactions are capable of sustaining diverse metabolic strategies (Amend et al., 2003; Rogers and Amend, 2005, 2006; Rogers et al., 2007; Price et al., 2015). Accordingly, through metagenomics analysis, amplicon sequencing, and DGGE analysis, previous studies reported complex and diverse microbial communities inhabiting these ecosystems (Gugliandolo and Italiano, 1999; Simmons and Norris, 2002; Rogers and Amend, 2005, 2006; Rusch et al., 2005; Lentini et al., 2007, 2014; Manini et al., 2008; White et al., 2008; Maugeri et al., 2009, 2010, 2013; Gugliandolo et al., 2012, 2015; Placido et al., 2015; Antranikian et al., 2017; Fagorzi et al., 2019; Gugliandolo and Maugeri, 2019; Sciutteri et al., 2022). These communities were found to be enriched in sulfur-oxidizing chemolithoautotrophic bacteria at higher temperatures and at lower temperatures by heterotrophic and photoautotrophic-based life-styles. Furthermore, thermophilic microorganisms have been isolated from several vents (Hafenbradl et al., 1996; Deckert et al., 1998; Lentini et al., 2007; Gugliandolo et al., 2012). However, only a few studies tried to couple in more detail both the geochemistry of the shallow vents and the microbial communities inhabiting them. In addition, these studies were conducted exclusively on the SWHV of Vulcano and Panarea, with the exception of one study, based on culture-dependent approaches that included communities from Lipari and Stromboli (Gugliandolo and Italiano, 1999). Currently, there is a lack of a more comprehensive survey of the microbial communities associated with the diversity of shallow-water hydrothermal vent ecosystems of the Aeolian archipelago.

To address this, and to understand how geochemically different shallow-water hydrothermal vents shape the microbial community composition, we used a combination of 16S rRNA gene amplicon sequencing and geochemical approaches to survey six shallow-water hydrothermal vents located in four different islands of the Archipelago, including two new locations that have never been characterized in the literature before. Our results show that shallow-water hydrothermal vents of the Aeolian islands are ecosystems that support diverse and complex microbial communities, providing important ecological roles to the surrounding marine environment. For this reason, they should be included in current and future conservation efforts.

2. Materials and methods

2.1. Sampling and site description

The samples were retrieved on the AEO19 expedition to the islands of the Aeolian archipelago: Vulcano, Panarea, Salina, and Lipari in the summer of 2019. Six different locations were sampled:

Vulcano - Levante Bay (LB), Vulcano - Levante Port (PL); Panarea - Bottaro (BO), Panarea - Baia Calcara (BC), Salina - Pollara (PO), and Lipari - Pietra del bagno (PB) (Figure 1), representing different shallow-water geothermal environments. All the samples were retrieved by SCUBA divers, using sterile falcon tubes and syringes. To accomplish a broader characterization of the different sites, different types of samples were collected: sediments, hydrothermal fluids, and biofilms. In the sites Levante Bay, Pollara, Baia Calcara, and Pietra del Bagno, abundant white microbial mats were observed near the venting sites. The shallow vents across the sampled locations were sulfide-rich, with the exception of the Pietra del Bagno site, where the presence of conspicuous orange precipitates suggests the presence of iron-rich hydrothermal fluids. Intense degassing was observed in the Bottaro venting site. All samples were stored either at +4°C or −20°C in accordance to the specific protocols for later processing in the lab. Subsamples used for molecular analysis and organic matter determination were stored frozen at −20°C, while samples for the determination of the major ions were filtered through a 0.22 µm filter and stored at +4°C. Temperature was measured *in situ* using a waterproof thermocouple, while pH, oxidation–reduction potential, conductivity, and dissolved oxygen were measured using a multi-parameter sensor probe (Hanna- multiparameter, model HI98194) on the boat immediately after the dive, with a fluid sample collected with syringes at the seafloor.

2.2. Sedimentary organic matter

The determination of the concentration of pigments (chlorophyll-*a* and phaeopigments) was carried out according to Lorenzen and Downs (1986). Briefly, the samples were supplemented with 90% of acetone and further incubated in the dark, at 4°C, for 12 h. After incubation, in order to remove the sediments, the samples were centrifuged and the concentration of chlorophyll-*a* and phaeopigments was estimated using a spectrofluorometer (at wavelengths of 430 nm and 630 nm), before and after being supplemented with 200 µL of 0.1 N HCl, respectively. Pigment concentrations were normalized to sediment dry weight (Manini et al., 2003).

Total protein concentrations were determined according to Hartree (1972), and further modified for analysis of sediment samples from Fabiano et al. (1995). The total carbohydrate concentrations were determined according to Gerchakov and Hatcher (1972), and expressed as glucose equivalents. Total lipids were extracted from the sediments by a direct elution with chloroform and methyl alcohol (1:1 v/v), and further determined according to Bligh and Dyer (1959). The readings were performed spectrophotometrically. The concentrations of carbohydrates, proteins and lipids were converted to carbon equivalents using the conversion factors, 0.40, 0.49 and 0.75 µg C × µg^{-1}, respectively, and further normalized to sediment dry weight (Fabiano et al., 1995). The biopolymeric carbon (BPC), calculated through the sum of the concentration of carbohydrates,

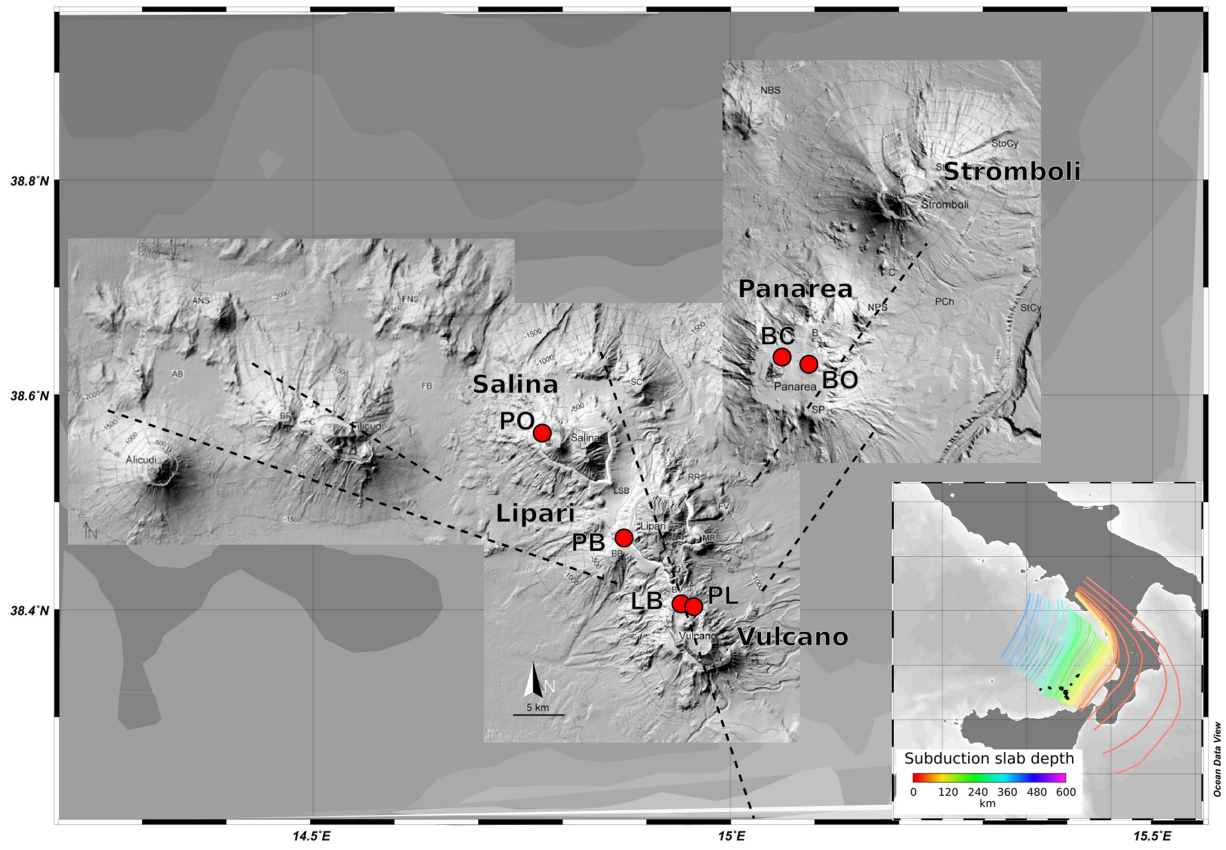

FIGURE 1
Map of the volcanic Aeolian island archipelago, located north of Sicily. Sample sites are shown in red. Major fault systems are illustrated here, as well as the gradient of the different slab depths (100–250 Km).

proteins and lipids, represents the fraction of the total organic carbon potentially available to heterotrophs and benthic consumers in the environment. All measurements are reported as an average of three replicates.

2.3. Geochemical analysis

The concentrations of major cations (sodium-Na^+, potassium-K^+, magnesium-Mg^{2+} and calcium-Ca^+) and anions (chlorine-Cl^-, sulfate-SO_4^{2-} and bromide-Br^-) of the hydrothermal fluids were measured using ion chromatography (ECO, IC Metrohm) equipped with conductivity detectors in two independent measurements. Calibration curves for the ion species of interest were run in the range of 0.1 and 10 ppm with $R \geq 0.999$. In order to reduce the amount of Cl^- and Na^+ entering the system, before the analysis, all samples were filtered (0.22 μm) and diluted to guarantee a conductivity of 600 μS/cm. All dilutions were made using 18.2 MΩ/cm type I water, which was also used as a blank for blank subtractions. Anions were run using a 3.2 mM Na_2CO_3 + 1 mM $NaHCO_3$ mobile phase on a Metrosep A Supp 5 column equipped with a 0.15 M ortho-Phosphoric acid suppressor. The flow of the anionic eluent was 0.7 mL min-1 for 30 min, effective for good resolution of all anions in the standard solution. Cations were run using a 2.5 mM HNO_3 + 0.5 mM $(COOH)_2 \times 2H_2O$ mobile phase on a Metrosep C4 column. The flow of the cationic eluent was 0.9 mL min-1 with a total separation of 35 min, effective for good resolution of all cations in the standard solution. Data acquisition and analysis were carried out through MagIC Net 3.3 software. Additionally, calibration curves were carried out using certified CPA chem external standards for each of the anions and cations analyzed. Detection limits for each of the ions analyzed correspond to 95% confidence levels, and were as follows: Mg^{2+} (0.08 mM), Na^+ (0.3 mM), Ca^{2+} (0.3 mM), K^+ (0.7 mM), SO_4^{2-} (0.03 mM), Br^- (0.02 mM), Cl^- (0.1 mM).

2.4. DNA extraction and amplicon sequencing

DNA extraction was performed using the DNeasy PowerSoil Kit (QIAGEN), following the manufacturer's instructions, with small modifications. The modifications of the protocol included a further elution step to better recover the DNA from the column. For samples where the PowerSoil kit protocol resulted in low quantity of DNA, a modified phenol-chloroform extraction method was employed (Cordone et al., 2005, 2011; Zanfardino et al., 2016), specifically adapted for the conditions found in shallow-water hydrothermal vents, such as the higher presence of clays and anions (Giovannelli et al., 2013, 2016). Briefly, 0.8 g of sediment was suspended in 850 μL of extraction buffer (100 mM Na_2HPO_4 pH 8, 100 mM tris–HCL pH 8, 100 mM EDTA pH 8, 1.5 M NaCl, 1% CTAB) and further supplemented with 100 μL of Lysozyme (100 mg/mL), followed by two incubation periods at 37°C for 30 min, the latter after the addition of 5 μL of Proteinase K (1 mg/mL). Subsequently, 50 μL of 20% SDS was added to the samples and incubated 1 h at 65°C, with regular mixing. The sediments were removed through consecutive centrifugations (2 × 14,000 g) after the addition of a solution of phenol:chloroform:isoamyl alcohol (25:24:1/24:1). The supernatant was collected and supplemented with Na-acetate (0.1 vol) and isopropanol 100%, and incubated at room temperature for 12 h. The precipitated DNA was then washed with 70% ice-cold ethanol, and re-suspended in 50 μL of Tris–HCL. DNA was visualized with agarose gel electrophoresis and quantified spectrophotometrically and spectrofluorimetrically (NanoDrop and Qubit). Obtained DNA was sequenced at the Integrated Microbiome Resource (IMR)[1] using primers targeting the V4-V5 of the 16S rRNA (515FB = GTGYCAGCM GCCGCGGTAA 926R = CCGYCAATTYMTTTRAGTTT515FB), using Illumina MiSeq technology.

2.5. Bioinformatic and statistical analysis

The raw sequence data was processed using the DADA2 package (Callahan et al., 2017). The analysis of the quality profile was carried out after removing primers and adapters. Sequences with an average call quality for each base between 20 and 40, were retained for downstream analysis. DADA2, through estimation of the error profile for each possible transition, identifies amplicon sequencing variants (ASVs). Taxonomy was assigned to the ASVs by matching with the SILVA Database, release 138.1[2] (Quast et al., 2013). Taxonomic assignments, together with the variant abundance table, were used to calculate diversity indices and investigate microbial diversity with the Phyloseq package (McMurdie and Holmes, 2013), as previously reported (Cordone et al., 2022). Briefly, the ASVs count table and the assigned taxonomy were combined into a *phyloseq* object. Mitochondria, Chloroplast, and Eukaryotic sequences were removed. Then, groups related to human pathogens and common DNA extraction contaminants (Sheik et al., 2018) were removed. The remaining reads represented 96.97% of the original reads, with 149,351 reads assigned to 2,145 ASVs preserved for downstream analysis. Diversity analyzes were carried out using the Phyloseq package (McMurdie and Holmes, 2013) with the relative abundance values set to 100%. Top abundance ASVs and genera were further defined as having accumulative abundances above 0.1%. Additionally, the alpha diversity was investigated using Shannon diversity index. The beta diversity was investigated using the UniFrac diversity index (Unweighted and Weighted) as implemented in the vegan package (Oksanen et al., 2018). Subsequently, the resultant similarity matrix was plotted using non-metric multidimensional scaling techniques. The resulting ordination was used to investigate the correlation between the environmental and geochemical variables using environmental fitting (*envfit* and *ordisurf* functions in vegan). All statistical investigations, data processing and plotting were carried out in the R statistical software version 4.1.2 (R Core Team, 2021), using the vegan (Oksanen et al., 2018), ggplot2 (Wickham, 2011), and the packages supra-referred. All the sequences analyzed in this study are available through the European Nucleotide Archive (ENA) under project accession PRJEB54611 under the ENA Umbrella project CoEvolve PRJEB55081. A complete R script containing all the steps to reproduce our analysis is available at https://github.com/giovannellilab/Barosa_et_al_Aeolian_shallow_vent_diversity with

1 https://imr.bio
2 www.arb-silva.de

DOI: https://doi.org/10.5281/zenodo.7480614 together with all the environmental and geochemical data.

3. Results

3.1. Physico-chemical parameters and sedimentary organic matter content

The physico-chemical parameters of the hydrothermal sites sampled in the present study are presented in Table 1. Overall, the physico-chemical parameters measured varied between the sites. The shallow-water vent sediment temperatures at the sampled venting orifice ranged from 28°C in Pollara to 90°C in Baia Calcara. The salinity ranged from 33.0 psu in Levante Bay to 41.5 psu in Pietra del Bagno. Dissolved oxygen (DO) values ranged from 11% in Levante Bay to 57.3% in Pietra del Bagno. Additionally, the oxidation–reduction potential of the different sites was negative for Levante Bay, Bottaro, and Levante Port, while Baia Calcara, Bottaro, and Pietra del Bagno had positive reduction potentials. The pH was slightly acidic for every sample, with the exception of Bottaro, which had circumneutral pH (8).

The sampled sediments showed a wide range of sedimentary organic matter content, with concentrations of biopolymeric organic carbon (BPC) ranging from 99.44 μg C g^{-1} (± 2.22) in Pollara to 3499.0 μg C g^{-1} (± 2740.5) in Bottaro. The higher values of BPC in Bottaro, as well as the high variability between the measured replicates, was hypothesized to be related to the presence of a biofilm ingrained in the coarse sediment. Total protein and carbohydrates ranged from 492.88 μg C g^{-1} (± 39.5) and 39.23 μg C g^{-1} (± 4.64) in Levante Bay to 6547.72 μg C g^{-1} (± 599.9) and 1756.92 μg C g^{-1} (± 279.88) in Bottaro, respectively. Total lipids ranged from 10.17 μgC g^{-1} (± 3.02) in Pollara to 222.48 μg C g-1 (± 65.91) in Levante Port. Protein to carbohydrate ratios ranged from 1.1 in Pietra del Bagno to 15.2 in Baia Calcara. Chlorophyll-*a* concentration values ranged from 0.01 μg g^{-1} (± 0.003) in Levante Bay to 6.9 μg g^{-1} (± 0.126) in Levante Port. The highest chlorophyll-*a* concentrations were measured at the moderate temperature sites, Bottaro and Levante Port, while the lowest values were measured at the high temperature sites, Levante Bay and Baia Calcara (Figure 2).

3.2. Geochemical analysis

The concentration of the major elements in the hydrothermal fluids were measured in the forms of major anions and cations (Figure 3; Table 2). Chloride concentrations ranged from 535.9 (% RDS 0.38) to 701.9 mM (% RDS 0.38), compared to 618.0 mM in seawater. Bottaro, Pollara and Pietra del Bagno have the highest Cl^- values. Sulfate concentrations ranged from 22.71 mM (% RDS 0.69) in Baia Calcara to 27.89 mM (% RDS 0.69) in Pietra del Bagno. Sulfate was depleted in the hydrothermal fluids of all the samples compared to seawater concentrations (32.9 mM). Additionally, Br^- concentrations ranged from 0.74 mM (% RDS 0.59) in Levante Bay to 0.91 mM (% RDS 0.59) in Bottaro, compared to sea water concentrations (0.94 mM). As for the major cations, Mg^{2+} concentrations ranged from 49.04 mM (% RDS 3.8) in Levante Bay to 62.36 mM (% RDS 3.8) in Bottaro, compared to seawater concentrations of 58.3 mM. Bottaro and Pollara were the only sites where fluids were enriched in Mg^{2+}, relative to seawater. The concentrations of K^+, Ca^{2+} and Na^+ ranged from 11.18 mM (% RDS 11.75) in Pollara to 13.23 mM (% RDS 11.75) in Levante Bay, from 8.55 mM (% RDS 10.37) in Pietra del Bagno to 17.87 mM (% RDS 10.37) in Bottaro, and from 445.9 mM (% RDS 7.4) in Levante Port to 551.6 mM (% RDS 7.4) in Bottaro, compared to the seawater concentrations of 11.0 mM, 11.1 mM and 547.0 mM, respectively. Additionally, we combined our data from previous publish data on the geochemistry of the fluids sampled from the shallow water hydrothermal vents of Vulcano, Panarea, and Stromboli (Italiano and Nuccio, 1991; Sedwick and Stüben, 1996; Gugliandolo et al., 2006; Rogers et al., 2007; Sieland, 2009; Tassi et al., 2009; Inguaggiato et al., 2013; Price et al., 2015; Kürzinger, 2019). Fluid data from the present study falls within a mixing trend resembling Type 3 fluids previously described by Price et al., 2015.

3.3. Microbial diversity

The bacterial diversity of the shallow-water hydrothermal vents of the Aeolian archipelago was investigated using the V4-V5 variable region of the 16S rRNA gene. After guaranteeing high-quality data (quality check and data filtering steps), a total of 149,351 reads were obtained, and 2,145 ASVs identified. Regarding the alpha diversity of the different sample types, the biofilm samples had lower alpha diversity measure (3) in comparison with the fluid and sediment samples (4.3 and 4.2, respectively). In terms of variability, the fluid samples showed less sample variability (the difference between the lowest diversity value points to the highest) in relation to the biofilm and sediment samples, which could be related to the differences in the matrix of the different sample types (Figure 4A). For instance, deep

TABLE 1 Location (GPS coordinates), depth, and the physico-chemical parameters measured on the venting fluids at the different sampled locations.

Station	Island	Latitude (°N)	Longitude (°E)	Depth (m)	Temperature (°C)	Salinity (PSU)	DO (%)	ORP (mV)	pH
LB	Vulcano	38.416729	14.959821	0.2	83.9	33.0	11	−295	5.8
PL	Vulcano	38.4161941	14.9611976	6.1	52	37.7	24.4	−202	5.22
BC	Panarea	38.64557	15.076182	15	90	37.5	43	150	5.26
BO	Panarea	38.6388904	15.1104468	6.5	46	40.94	15	−260	5.4
PO	Salina	38.574516	14.799716	10	28	39.0	48	121	5.6
PB	Lipari	38.47514	14.898117	12	45	41.5*	57.3	77	8.08

ORP - Oxido-reduction potential; DO - Dissolved oxygen; *Value of salinity for Pietra del Bagno calculated from Cl– concentrations using the formula: Salinity (ppt) = 0.00180665 × Cl– (mg/L).

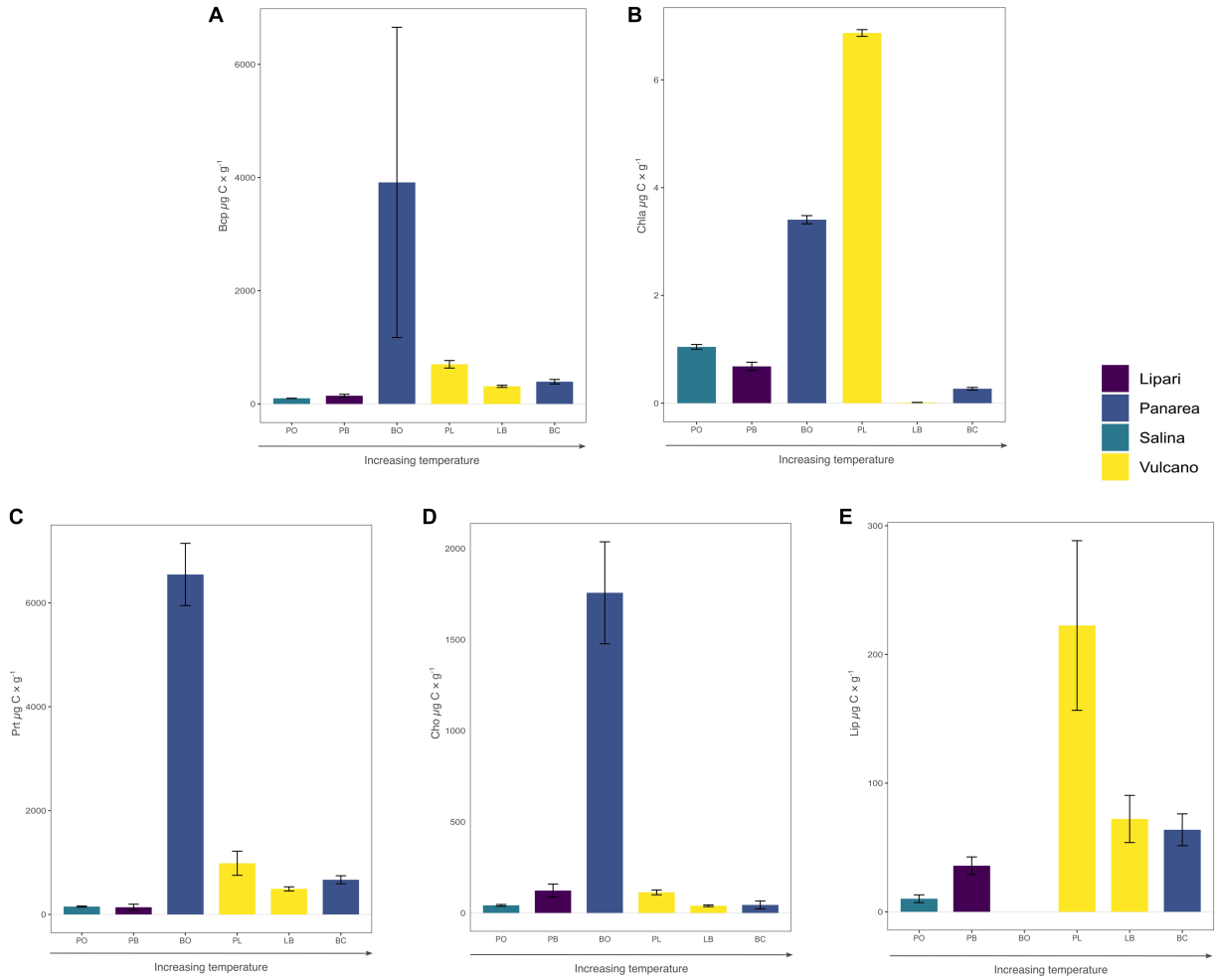

FIGURE 2
Content and quality of the organic matter measured in the sampled sediments. **(A)** Biopolymeric organic carbon (BCP); **(B)** Chlorophyll-a pigments content; **(C)** Proteins; **(D)** Carbohydrates; **(E)** Lipids. All sites are organized by increasing temperatures and are expressed in µg g^{-1} of dry sediment. Error bars represent standard deviation ($n = 3$).

geothermal fluids impose a stronger bottleneck in terms of possible redox couples and ecological niches to the microbial communities, compared to the sediment samples. Additionally, the temperature was found to be a major driver of diversity between samples (Pearson correlation test, $R^2 = 0.41$), where higher temperature sites showed a decrease in alpha diversity (Figure 4B).

The high-temperature sites, Baia Calcara and Levante Bay, characterized by temperatures above 80°C, were dominated by members belonging to Campylobacterota (formerly Epsilonproteobacteria), Proteobacteria, Aquificota, Bacteroidota, Chloroflexi and Acidobacteriota phylum (Figure 5). Among Campylobacterota, the order Campylobacterales was present in high abundances in all the high-temperature sites. Within Campylobacteriales, the genus *Nitratifactor* was only present at higher abundances (44%) in the biofilm sample of Baia Calcara, followed by *Sulfurimonas* (average abundance of 6.08% between the biofilm and sediment samples of Baia Calcara), *Campylobacter* (average abundance of 9% between the fluid and sediment sample of Levante Bay), and *Sulfurovum* genera (6.55% in the fluid sample of Levante Bay). The phylum Proteobacteria was composed entirely by class Gammaproteobacteria in the Baia Calcara site (average abundance of 12% between sediments and biofilm samples), and by Gammaproteobacteria and Alphaproteobacteria in the Levante Bay site (average abundance of 15% in both sample types and 8.5% in the fluid samples, respectively). Within Gammaproteobacteria, the orders Chromatiales and Thiomicrospirales were present in the highest abundances (average abundance of 24.6% at Levante Bay between the fluid and sediment samples, and 13.3% between the sediments and biofilm samples of Baia Calcara and the fluid samples of Levante Bay, respectively), with ASVs classified only to the genus *Candidatus thiobios* and *Thiomicrorhabdus*. The order Nitrococcales was present in lower abundances (average abundance of 6.1% between both sampling sites and all sample types, with the exception of the sediments of Levante Bay), and composed by the genus *Sulfurivirga*. Among Alphaproteobacteria, all ASVs were classified into the order Rhodobacterales in both the fluid and sediment samples of Levante Bay (average abundance of 8.5%), however, it was not possible to resolve them down to the genus level. The phylum Aquificota was composed entirely of members belonging to the order Hydrogenothermales, and the genus *Hydrogenothermus*, and only

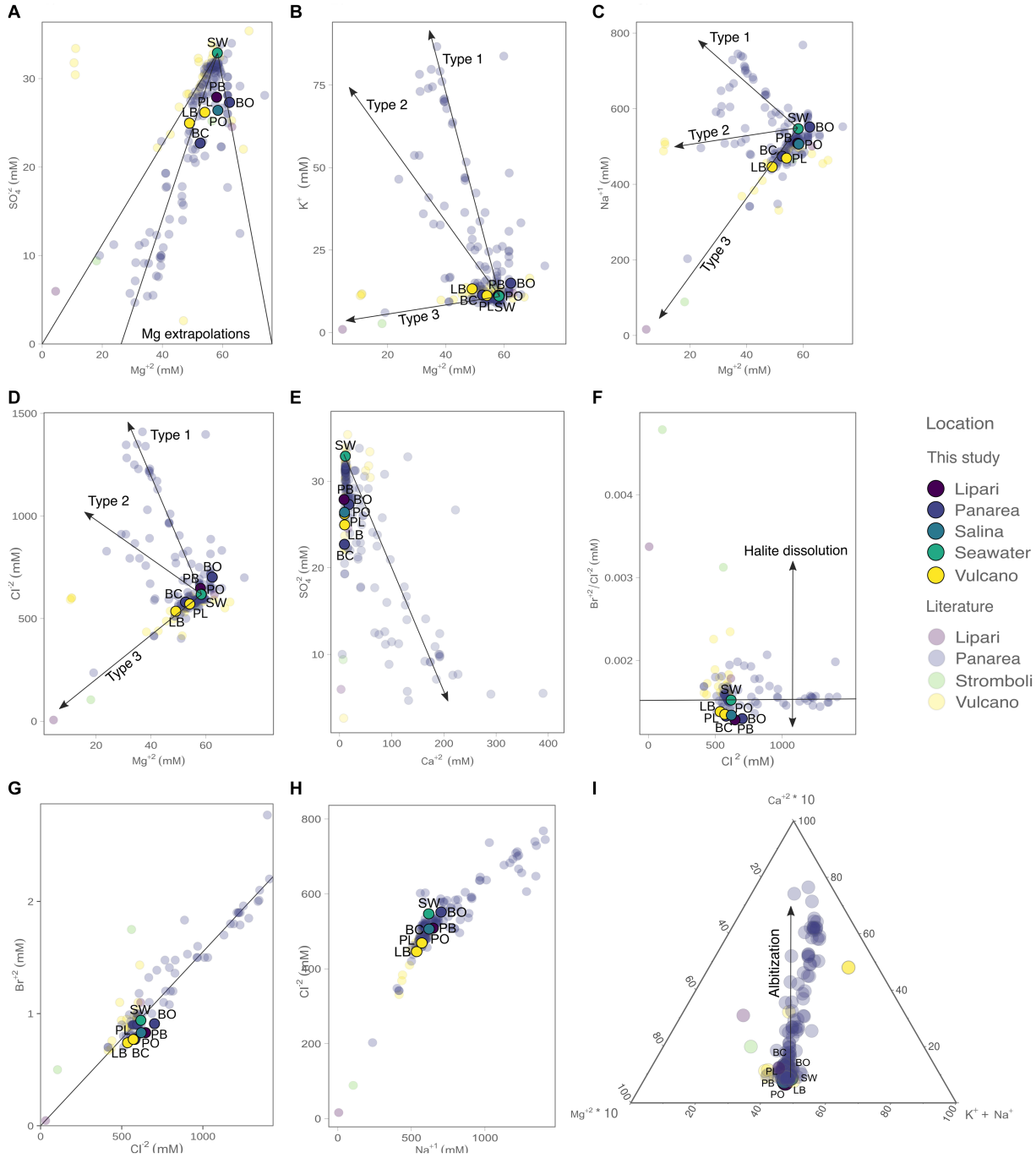

FIGURE 3
Concentrations of the major anions and cations measured in the present study (bold colors), as well as from previous reports from the Literature (opaque colors): **(A)** SO_4^{2-} vs. Mg^{2+}, with the three visible Mg^{2+} end-member extrapolations; **(B)** K^+ vs. Mg^{2+} with the three fluid mixing trends observed; **(C)** Na^+ vs. Mg^{2+}; **(D)** Cl^- vs. Mg^{2+}; **(E)** SO_4^{2-} vs. Ca^{2+} (vector illustrating end-member extrapolation); **(F)** Br^-/Cl^- ratio vs. Cl^-, where it is possible to infer the presence of halite in solution; **(G)** Br^- vs. Cl^- and extrapolations to zero; **(H)** Cl^- vs. Na^+; **(I)** ternary plot with the influence of albitization on the hydrothermal fluids. The literature data was retrieved from Italiano and Nuccio (1991), Sedwick and Stüben (1996), Gugliandolo et al. (2006), Rogers et al. (2007), Sieland (2009), Tassi et al. (2009), Inguaggiato et al. (2013), Price et al. (2015), and Kürzinger (2019).

observed at the sediment samples of Baia Calcara (25.09%). Within Bacteroidota, only the order Flavobacteriales was identified in both the sediment and fluid samples at the Levante Bay site (average abundance of 9.3%), however, no ASVs were classified to the genus level. Acidobacteriota and Chloroflexi, albeit present in lower abundances (5.14% in sediment samples of Baia Calcara and 5.51% in fluid samples of Levante Bay, respectively), had as most abundant, members belonging to the order Thermoanaerobaculares, genus *subgroup* 23, and to the class *Anaerolineae*, respectively (Table 3).

Moderate-temperature sites, such as Bottaro, Pietra del Bagno, and Levante Port, characterized by temperatures ranging from 40°C to 53°C, presented a higher diversity of bacterial phyla. These sites

TABLE 2 Concentrations of the major anions and cations (mM) of the hydrothermal fluids from the Aeolian Shallow-water vents.

Station	Island	Mg^{2+}	Na^{+}	Ca^{2+}	K^{+}	SO_4^{2-}	Br^{-}	Cl^{-}
LB	Vulcano	49.04	445.9	9.65	13.23	24.96	0.74	535.9
PL	Vulcano	54.13	469.1	9.47	11.19	26.19	0.77	571.2
BC	Panarea	52.6	474.1	9.25	11.37	22.71	0.77	580.6
BO	Panarea	62.36	551.6	17.87	14.96	27.31	0.91	701.9
PO	Salina	58.46	506.3	9.41	11.18	26.41	0.83	620.2
PB	Lipari	58.06	508.6	8.55	11.32	27.89	0.83	647.4
Sea Water	–	58.3	547.0	11.1	11.0	32.9	0.94	618.0

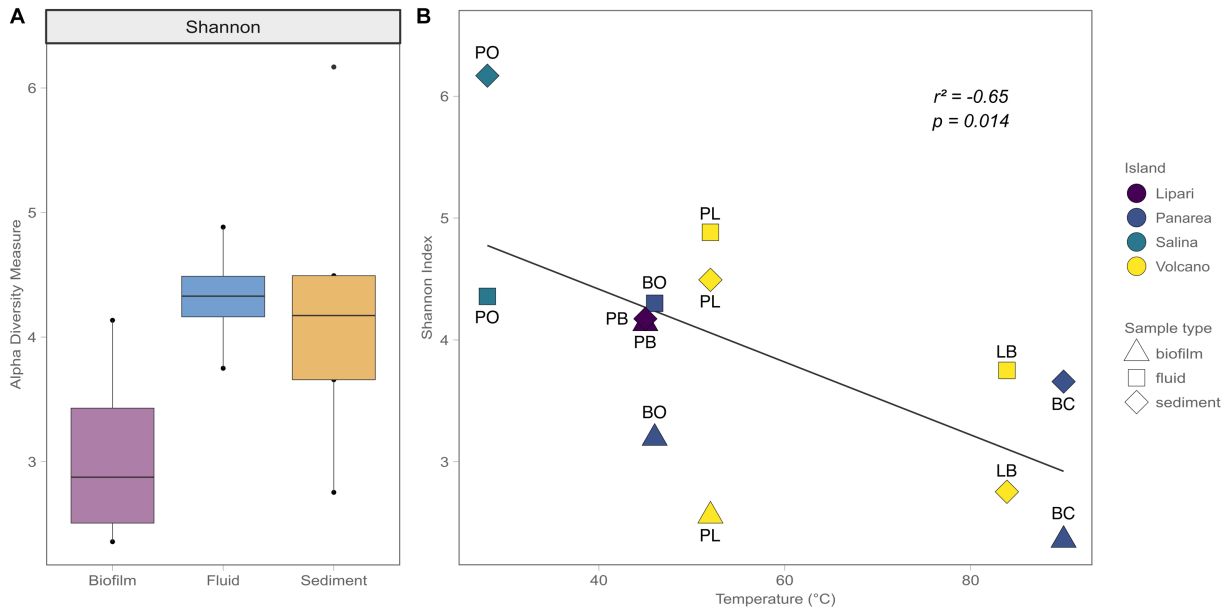

FIGURE 4
Shannon Alpha diversity indexes. **(A)** Alpha diversity measures in relation to the different sample types (Biofilm, Fluid, Sediment). **(B)** Alpha diversity measures in relation to the temperature, with the different Islands sampled, as well the different sample types.

were dominated by members belonging to Campylobacterota, Proteobacteria, Bacteroidota, Calditrichota, Chloroflexi, Cyanobacteria, as well as the Archaeal phylum Crenarchaeota and Altiarchaeota at low abundances. Among Campylobacteriota, the order Campylobacterales was only identified at the sediments and biofilm samples of the Levante Port site, with the highest abundant ASVs belonging to the family *Arcobacteraceae* (37.92% at the sediment samples), without classification to the genus level. Additionally, it was also possible to classify Campylobacterales into the genera *Thiovulum* and *Sulfurimonas* in the biofilm samples (23.40 and 19.40%, respectively), and *Sulfurovum* in the sediment samples (6.51%). Within Proteobacteria, the order Rhodobacterales (21.96% in biofilm sample at Bottaro and 5.70% in biofilm sample of Pietra del Bagno) was the most abundant group, however, it was not possible to classify them down to the genus level. Additionally, the family *Mariprofundaceae* and the assigned genus *Mariprofundus*, was the second most abundant genus within Proteobacteria (15.03%) and only present at the sediment samples of Pietra del Bagno. While in lower abundances, it was possible to identify the family *Thioprofundae*, composed by the genus *Thioprofundum* (7.47% in the sediment samples of Levante Port), and the family *Colwelliaceae*, where all the ASVs were assigned to the genus *Colwellia* (11.54% in biofilm sample of Pietra del Bagno). Moreover, it was also possible to identify the family *Thioglobaceae*, with the ASVs assigned to the clade SUP05 cluster (8.03% in the biofilm samples of Pietra del Bagno). Within the Bacteroidota, the order Flavobactereales constituted most of the ASVs (26.17% in the biofilm sample of Bottaro); however, classification could not be resolved to the genus level. Lower abundance ASVs belonging to Bacteroidota were also assigned to the order Ignobacteriales and the clade LheB3-7 (11.52% in sediment samples of Levante Port). The phyla Aquificota, similarly to the high-temperature sites, was composed entirely of ASVs belonging to the genus *Hydrogenothermus*, and only present at the fluid sample of Bottaro (16.57%). Among Calditrichota, the genus *Caldithrix* represented all the ASVs (17.32% in the sediment sample of Pietra del Bagno and 8.06% in the fluid sample of Bottaro). Additionally, the phototrophic bacterial phyla Cyanobacteria, was composed by the genus *Synechococcus* of the order Synechococcales in only the fluid samples (6.03 and 5.55% in Levante Port and Bottaro, respectively). The Archaeal phyla were detected in low abundances. Archaeal ASVs

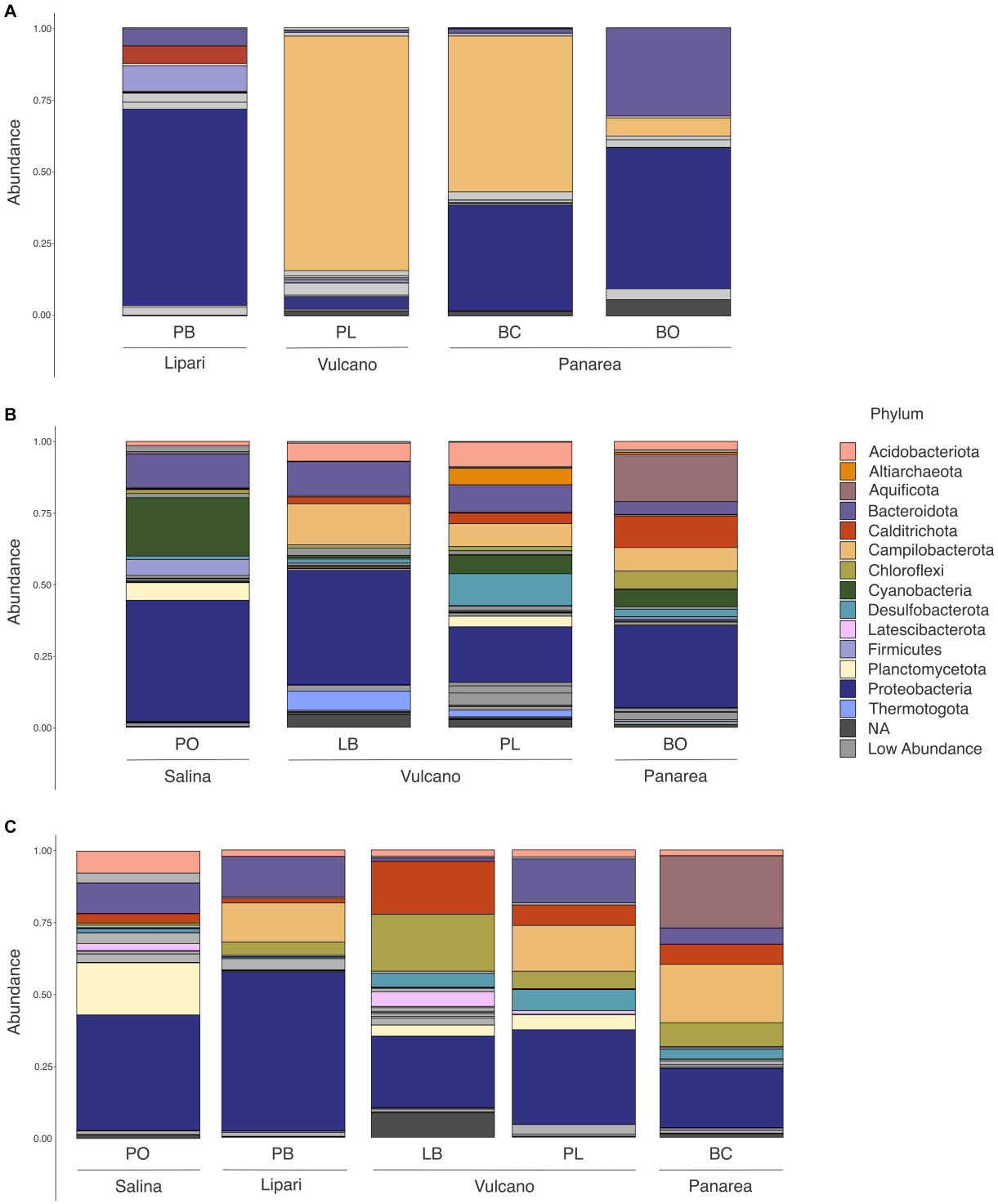

FIGURE 5
Phylum level abundance and distribution of the 16S rRNA diversity in all of the sample sites and sample types at the different islands of the Aeolian Archipelago. For simplicity, only abundances above 5% at each site are illustrated. **(A)** Biofilm samples; **(B)** Fluid samples; **(C)** Sediment samples.

were classified into the genera *Candidatus_Nitrosopumilus* and *Candidatus_Altiarchaeum* (6.06% in the biofilm sample of Pietra del Bagno and 5.76% in the fluid sample of Levante Port, respectively). Interestingly, some lower abundance ASVs could not be classified up to the phylum level (8.59% in the sediment sample of Pietra del Bagno and 5.67% in the biofilm sample of Bottaro, respectively).

The lowest temperature site, Pollara, at the island of Salina, marked by temperatures of 28°C, was dominated by Cyanobacteria, Proteobacteria, Bacteroidota, and Firmicutes. The majority of the ASVs at lower temperatures were assigned to the phylum Cyanobacteria and the species *Synechococcus* sp. CC9902 (20.15% in the fluid sample). The order Alteromonadales with the genus

TABLE 3 Taxonomic affiliation of the most abundant ASVs through SILVA database (to the lowest possible taxonomic resolution) and Ezbiocloud closest relative.

Sample type	SILVA classification	Ez-biocloud classification	Similarity (%)	Acc. no.
Biofilm	*Nitratifractor*	JQ611125_s	97.32	JQ611125
Biofilm	*Thiomicrorhabdus*	*Galenea microaerophila*	99.73	JQ080912
Biofilm	*Sulfurimonas*	JN873929_s	98.39	JN873929
Biofilm	*Sulfurivirga*	*Sulfurivirga caldicuralii*	99.73	jgi.1107633
Biofilm	Bacteria	JF320743_s	95.99	JF320743
Biofilm	*Rhodobacteraceae*	*Actibacterium pelagium*	*100*	NSBU01000007
Biofilm	*Arcobacteraceae*	AY922188_s	100	AY922188
Biofilm	*Flavobacteriaceae*	*Urechidicola croceu*	95.38	KX066850
Biofilm	*Colwellia*	*Colwellia rossensis*	100	U14581
Biofilm	SUP05_cluster	Maorithyas hadalis gill symbiont I	99.2	AB042413
Biofilm	*Nitrincolaceae*	AM402959_s	99.2	AM402959
Biofilm	Candidatus Nitrosopumilus	*Nitrosopumilus cobalaminigenes*	98.67	KX950757
Biofilm	*Sulfitobacter*	EU795102_s	100	EU795102
Biofilm	*Thiovulum*	DQ295692_s	92.25	DQ295692
Sediments	*Hydrogenothermus*	*Hydrogenothermus marinus*	99.2	AJ292525
Sediments	*Thiomicrorhabdus*	*Galenea microaerophila*	99.73	JQ080912
Sediments	*Sulfurivirga*	*Sulfurivirga caldicuralii*	99.73	jgi.1107633
Sediments	*Sulfurimonas*	JN873929_s	98.39	JN873929
Sediments	*Anaerolineae*	JF320743_s	96.52	JF320743
Sediments	Candidatus_Thiobios	AY310506_s	98.13	AY310506
Sediments	*Campylobacter*	JQ287068_s	98.12	JQ287068
Sediments	*Flavobacteriaceae*	*Urechidicola croceus*	95.38	KX066850
Sediments	*Rhodobacteraceae*	*Actibacterium pelagium*	100	NSBU01000007
Sediments	*Anaerolineaceae*	FJ905697_s	94.39	FJ905697
Sediments	*Mariprofundus*	*Mariprofundus aestuarium*	99.73	CP018799
Sediments	*Calditrix*	*Calditrix abyssi*	98.94	CM001402
Sediments	Bacteria	JF320743_s	95.99	JF320743
Sediments	*Calditrix*	DQ925879_s	94.69	DQ925879
Sediments	*Woeseia*	JF344416_s	99.2	JF344416
Sediments	*Rhodothermaceae*	EU925913_s	99.19	EU925913
Sediments	*Rhodobacteraceae*	*Actibacterium pelagium*	100	NSBU01000007
Fluids	*Hydrogenothermus*	*Hydrogenothermus marinus*	99.2	AJ292525
Fluids	*Calditrix*	*Calditrix abyssi* DSM 13497(T)	98.94	CM001402
Fluids	*Synechococcus* CC9902	*Synechococcus sp.* CC9902	99.47	CP000097
Fluids	*Rhodobacteraceae*	*Actibacterium pelagium* JN33(T)	100	NSBU01000007
Fluids	Candidatus_Thiobios	AY310506_s	98.13	AY310506
Fluids	*Flavobacteriaceae*	*Urechidicola croceus* LPB0138(T)	95.38	KX066850
Fluids	*Sulfurovum*	HM591450_s	97.32	HM591450
Fluids	*Campylobacter*	JQ287068_s	98.12	JQ287068
Fluids	*Sulfurivirga*	*Sulfurivirga caldicuralii*	99.73	jgi.1107633
Fluids	*Thiomicrorhabdus*	*Galenea microaerophila*	99.73	JQ080912
Fluids	Subgroup_23	EU542513_s	98.39	EU542513
Fluids	Candidatus_Altiarchaeum	*Altarchaeum hamiconexum*	96.55	JAACVF010000098
Fluids	*Pseudoalteromonas*	*Pseudoalteromonas shioyasakiensis*	100	AB720724
Fluids	NS5_marine_group	PAC001209_s	100	PAC001209
Fluids	*Anoxybacillus*	*Anoxybacillus rupiensis*	100	AJ879076

Pseudoalteromonas (7.53% in the fluid sample), and the order Steroidobacterales, with the genus *Woesia* (9.15% in the sediment sample) were the most abundant within Proteobacteria. The phyla Bacteroidetes was composed of the orders Flavobacteriales and Rhodothermales (5.83% in the fluid sample and 5.06% in the sediment sample, respectively).

To understand the role of the environmental parameters and the geochemistry in the structuring of the microbial communities inhabiting the SWHV of the Aeolian islands, we investigated the beta-diversity using both quantitative and qualitative approaches, more specifically, using weighted and unweighted UNIFRAC dissimilarity indexes, respectively, followed by environmental fitting. The unweighted UniFrac nMDS analysis shows a statistically significant separation between the communities of the islands of Lipari and Salina, and Vulcano and Panarea (ADONIS, $p = 0.0016$, $n = 6$). Additionally, the same separation was found between the composition of the communities of the biofilm samples, compared to the other sample types analyzed in the present study (ADONIS, $p = 0.0075$, $n = 6$). Through linear vector fitting versus the nMDS ordination, we observe which are the main parameters that better explain the microbial diversity of our samples (Figure 6). The group of Vulcano and Panarea can be explained by the temperature, and the group of Salina and Lipari, by the major cations and anions, Mg^{2+}, Na^{+}, and Br^{-}. Using the weighted UniFrac, which weights the abundance of the taxa present, we found the same statistically significant separations between the same island groups (ADONIS, $p = 0.0075$, $n = 6$), and between biofilms and the other sample types analyzed in the present study (ADONIS, $p = 0.0475$, $n = 6$). However, we found differences regarding the main parameters explaining the abundance of microbial communities with vector fitting. For instance, here the biofilm samples of Levante Port and Baia Calcara were mainly explained by temperature and longitude. Additionally, the microbial diversity of Bottaro and Levante Port, in contrast with the unweighted version, are also explained by the major anions and cations, with the addition of Cl^{-}.

4. Discussion

Shallow-water hydrothermal vents are marine environments associated with volcanic activity and tectonically active margins. Due to their unique characteristics, such as the presence of light, proximity to landmasses, and dynamic geochemistry, they harbor a highly diverse microbial consortia (Tarasov et al., 2005; Price and Giovannelli, 2017). The Aeolian archipelago is one of the most studied shallow-water hydrothermal systems in the world (Gugliandolo and Italiano, 1999; Simmons and Norris, 2002; Rogers and Amend, 2005; Rusch et al., 2005; Lentini et al., 2007, 2014; Manini et al., 2008; Maugeri et al., 2009, 2010, 2013; Gugliandolo et al., 2015; Gugliandolo and Maugeri, 2019). However, the role of the diverse geochemical environments found in the different islands in controlling the microbial community structure, is still poorly understood, and usually investigated in a handful of sites. To address this, we surveyed 6 different shallow water vents located in four different islands, combining 16S rRNA amplicon sequencing with geochemical and physico-chemical data. To the best of our knowledge, two of the investigated shallow vents (Pietra del Bagno and Pollara) were never reported before in the literature.

4.1. Geochemistry of the Aeolian shallow-water hydrothermal vents

Hydrothermal systems are characterized by the convective circulation of water that percolates into the crust, gets heated, and then is discharged at the sea floor. During this journey, the fluids are chemically and physically transformed by subsurface processes, such as temperature-dependent water-rock reactions, leaching of transition metals and volatiles from the host lithologies, and phase-separation events (Fournier, 2007; German and Seyfried, 2014). These processes, although occurring in a dynamic continuum, are generally separated into three distinct areas: the recharge zone, the reaction zone, and the upflow zone. Due to the inherent characteristics of the locations within the subsurface where they take place, these areas are marked by the occurrence of different processes. The recharge zone is characterized by the fixation of alkali metals, boron, and the fixation of Mg^{2+} associated with the mineralization of smectite and chlorite. Deep in the system (reaction zone), anorthite is transformed to albite (albitization), resulting in the exchange of Na^{+} and Si^{4+} for Ca^{+} into the fluids, as well as metal mobilization. Additionally, the high temperatures and pressures present at depth allow phase separation events, separating the low weight ions (migrate to the vapor phase) from the heavier weight ions (remain in the fluids). Cl^{-}, by remaining in the fluid phase, modifies the salinity content of the hydrothermal fluids. In the upflow zone, further low-temperature water-rock reactions can occur, such as the precipitation of anhydrite and other minerals (Berndt et al., 1988; Tivey, 2007; Alt, 2013; German and Seyfried, 2014). During ascent, the fluids can either be channeled, feeding directly from deep subsurface reservoirs, or diffuse, with significant mixing of end member fluids with seawater prior to discharge. All together these processes entail different ratios of mixing with seawater, contributing to additional alterations to the fluids before they are discharged at the seafloor where they are collected (Price and Giovannelli, 2017). By analyzing the enrichment and depletion of major ions and cations in vent fluids, we can have a deeper understanding of the main processes occurring in the subsurface. These geochemical processes define the geochemical space available for microbial communities to thrive in these ecosystems, and are fundamental in investigating the microbial diversity of shallow-water hydrothermal vents (Price et al., 2015; Price and Giovannelli, 2017).

In the present study, we leverage the information available in the already published literature on the geochemistry of hydrothermal fluids of the shallow vents of Vulcano, Panarea, and Stromboli (Figure 3) combined with new data. Furthermore, we add for the first time geochemical data for the shallow vents of Lipari and Salina (Pietra del Bagno and Pollara, respectively). It is important to note that subsurface processes at shallow-water hydrothermal vents hosted in volcanic arc settings have not been characterized to the same level of detail as Mid-Ocean Ridge hosted deep-sea systems. For this reason, our study relies on previous characterization of Panarea fluids by Price et al. (2015) and conceptually extended to the other shallow vents investigated. By combining published and new geochemical data we identified three mixing trends (Type 1, Type 2, and Type 3) already described for Panarea by Price et al. (2015).

The observed different trends reveal that these hydrothermal fluids evolved differently, and therefore were subjected to different subsurface processes within the Panarea hydrothermal system. Data

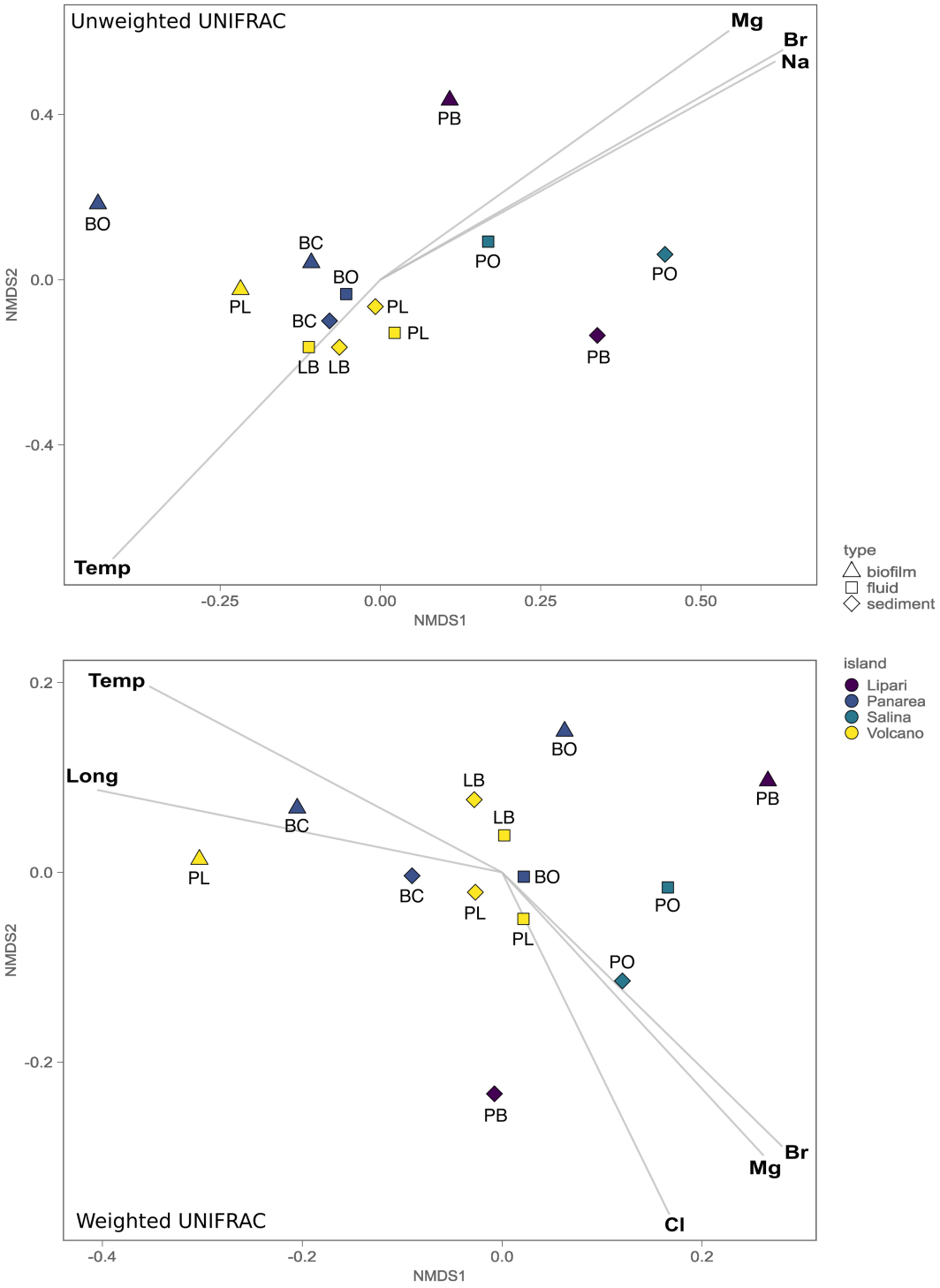

FIGURE 6
Non-metric multidimensional scaling (nMDS, stress 0.075) plot of the 16S gene amplicon microbial diversity based both the weighted and unweighted UniFrac measures, overlaid with environmental vector fitting, illustrating vectors with significant p values ($p < 0.01$).

from Vulcano, Lipari, and Salina shallow vents shows that fluids from diverse islands fall within the Type 3 trend (Figure 3). These fluids do not show enrichments of major anions and cations, but instead, show depletions of the major species. The evolution of Type 3 fluids results in acidic fluids, with concentrations of major ions similar to sea-water concentrations, whereas type 1 and type 2 fluids are the result of deep recirculating brine and focused upflow of shallower brines, respectively. This suggests that the difference between these fluid types is directly related to subsurface processes, such as phase-separation deep in the system, the scrubbing of exsoluted gasses that percolate up the crust, as well as the mixing of the diffuse flow fluids with sea-water (Price et al., 2015). Based on our data, it appears that the evolution of

Type 3 fluids might be a common process in the shallow water vents of the Aeolian Archipelago. Additionally, and as evident in Price et al. (2015), most of the fluids, including the ones in the present study, do not extrapolate to zero in both SO_4^{2-} and Mg^{2+}. This can be related to seawater mixing as the fluids approach the surface, due to their diffuse nature. However, in the Bottaro site, the fluids are enriched in Mg^{2+}. It was hypothesized that Mg^{2+} enrichments in Panarea could be related to the leaching of host rocks due to acidification, by means of argillic alteration (Reeves et al., 2011). Since volcanic arc hydrothermal systems are not exposed to the same pressures compared to their deep-sea counterparts (Price and Giovannelli, 2017), the presence of free gas phases may also be contributing to the depletion of Na^+ and Cl^- observed relative to sea water (Figure 3), altering the salinities of the fluids as they percolate through the hydrothermal system. All the fluid samples collected in our study had Br^-/Cl^- ratios lower than seawater, suggesting the presence of dissolved halite in solution. Albitization, which occurs deep in the system and results in the release of Ca^+ in exchange for Na^+ (Alt, 2013), does not seem to be a major process affecting the evolution of our fluid samples, compared to other fluids recovered from Panarea and Vulcano (Figure 3).

While the geochemical composition of the fluids is an important parameter in controlling the diversity of microbial communities, the availability of organic carbon for heterotrophic consumption is fundamental in driving community composition. In hydrothermal systems organic carbon can either be delivered through the subsurface fluids as dissolved organic carbon produced or recycled at depth (Fullerton et al., 2021), or from the water column, either as sinking organic matter particles, lateral advections of surface primary productivity, and terrigenous run offs (Gomez-Saez et al., 2015; Price and Giovannelli, 2017; LaRowe et al., 2020). Additionally, it could be directly produced *in situ* by a diverse community of phototrophic and chemolithotrophic microorganisms (Price and Giovannelli, 2017). The organic carbon delivered to the system is accumulated in the sediments, and analyzing the sedimentary organic matter content can provide an estimate of the organic load on the vent system. In our data the sedimentary organic matter, measured as biopolymeric organic carbon (BPC) was highly variable between the different sites, and did not show linear relationships with temperature, in contrast to what has been observed in a previous study on a shallow-water hydrothermal vent system (Giovannelli et al., 2013; Figure 2A). The lowest amounts of BPC was measured in the site with the lowest temperatures (Pollara, 28°C and Pietra del Bagno, 45°C), and could be related to a to hydrodynamic processes, perturbing the system in these specific locations (Bao et al., 2018), as well as to the fact that these sites are further away from the coast, and thus representing lower amounts of terrigenous inputs to the system. The high concentrations found in Bottaro are instead related to the thick microbial biofilms attached to the sand and gravel. The concentration of chlorophyll-*a* (chl-*a*) pigments was lower at the higher temperatures sites (>80°C; Figure 2B) in line with previous observations (Giovannelli et al., 2013). The presence of Chl-*a* in the sediments can be either related to input of fresh organic carbon from the water column or to the presence of phototrophs in the sediments and biofilms of the vent. The presence of known phototrophs in the sediment and biofilm samples (see below) suggests that the high chlorophyll concentrations found in the same sites are the results of *in situ* production, possibly taking advantage of the nutrients and CO_2 released by the shallow vents. Additionally, the chl-*a* values were higher at the Levante Port and Bottaro sites, which had similar depths (average 6.4 meters), suggesting that beside temperature, the depth of the shallow vent could play a role in controlling the presence and abundance of photosynthetic organisms.

4.2. Microbial diversity

Previous studies conducted at shallow-water hydrothermal vents have demonstrated that a highly diverse microbial consortia inhabit these ecosystems (Hoaki et al., 1995; Sievert et al., 2000; Manini et al., 2008; Maugeri et al., 2009, 2010; Zhang et al., 2012; Price et al., 2013; Kerfahi et al., 2014; Lentini et al., 2014; Dávila-Ramos et al., 2015; Gugliandolo et al., 2015; Gomez-Saez et al., 2017). In the present study, we found that the microbial communities of the Aeolian Islands shallow-water vents are dominated by members belonging to diverse phyla, such as Proteobacteria, Campylobacteriota, Bacteroidota, Cyanobacteria, Chloroflexi, among others present at lower abundances. The major lineages found here have been reported in other shallow-water vents (Maugeri et al., 2010; Zhang et al., 2012; Kerfahi et al., 2014; Lentini et al., 2014; Dávila-Ramos et al., 2015; Gugliandolo et al., 2015; Gomez-Saez et al., 2017; Price and Giovannelli, 2017), illustrating their important ecological role in the functioning of the shallow-water vent ecosystem.

Our data shows that temperature is a major driver explaining the microbial diversity (alpha-diversity, Pearson correlation test, $R^2 = 0.41$, $p < 0.05$). High-temperature sites (>80°C) were characterized by lower diversity in comparison to lower and moderate temperatures sites (28°C to 50°C; Figure 4B). Temperature has been shown to be one of the major factors controlling microbial diversity in a number of diverse geothermal ecosystems, including shallow-water vent environments (Giovannelli et al., 2013; Gugliandolo et al., 2015), deep-sea hydrothermal vents (Dick et al., 2013; Ding et al., 2017), and hot springs (Chan et al., 2017; Fullerton et al., 2021).

High-temperature locations, such as Baia Calcara and Levante Bay sites in the islands of Vulcano and Panarea, respectively, were characterized by temperatures above 80°C. The microbial communities inhabiting these high-temperature shallow vents were dominated by groups related to known chemolithoautotrophic, thermophilic bacteria, harnessing energy through the oxidation of reduced sulfur species and hydrogen. These types of metabolic strategies have been widely reported in shallow-water, deep-sea hydrothermal vents, as well as hot-springs (Tarasov et al., 2005; Yamamoto and Takai, 2011; Inskeep et al., 2013; Price and Giovannelli, 2017). The Baia Calcara and Levante Bay sites had as most abundant, ASVs related to the genera *Nitratifactor*, *Thiomicroarhdbus*, *Hydrogenothermus*, *Candidatus_thiobios,* and the family *Rhodobactereceae*. The biofilm community at the Baia Calcara site was mostly composed of members belonging to *Nitratifactor* and *Thiomicroarhdbus*. *Nitratifactor* has been previously described in shallow and deep-sea hydrothermal systems (Zhang et al., 2012; Zeng et al., 2021). The closest sequence to our ASVs was recovered from a shallow-water hydrothermal system in Kueishan Island, Taiwan (unpublished data). Interestingly, this group was not present in the sediment samples of the same site. Additionally, the genus *Thiomicroarhdbus* was also present in high abundances in the biofilm samples, and in lower abundance also in the sediment sample. It was possible to assign this ASVs to the species *Galenea microaerophila*

(99.73% similarity) (Giovannelli et al., 2012). Initially described from a shallow-water vent from Paleochori Bay, on the island of Milos, *Galenea microaerophila* grows chemolithoautotrophically, through the oxidation of thiosulfate as electron donor, and oxygen (5%) as electron acceptor (Giovannelli et al., 2012). The sediment sample at Baia Calcara was mostly composed by the genus *Hydrogenothermus*, of the phylum Aquificota. This ancestral and deep-branching bacterial phylum is highly prevalent in geothermal environments (Hedlund et al., 2015; Giovannelli et al., 2017), and it is capable of fixing CO_2 into biomass using energy derived from H_2S and H_2 with either elemental sulfur, nitrate or oxygen (at low partial pressures) as electron acceptor. The dominant ASV in our dataset was related to the species *Hydrogenothermus marinus* (99.2% similarity), a hydrogen-oxidizing, chemolithoautotrophic, thermophilic bacterium (Stöhr et al., 2001) originally isolated from sediment samples from Vulcano island.

At the fluid and sediment samples at Levante Bay, the other high temperature site, the family *Rhodobactereceae* and the genus *Candidatus* thiobios were present in highest abundances. The family Rhodobactereceae is widespread in marine environments, and are capable of growing through the utilization of multiple organic, as well as inorganic compounds, contributing to their vast ecological diversity (Pohlner et al., 2019). In our study, it could also be identified in moderate to lower temperature sites. The ASVs classified as *Rhodobactereceae* were further related to the species *Actibacterium pelagium* (100% similarity), which have been isolated from the seawater of the Mediterranean Sea, Pacific and Atlantic Oceans, growing heterotrophically on a variety of organic carbon sources (Guo et al., 2017). Even though members belonging to *Rhodobactereceae* have been previously identified in other hydrothermal systems (Forget et al., 2010; Zhang et al., 2012; Pohlner et al., 2019), to our knowledge, this is the first time this species has been reported in a hydrothermal vent environment. The genus *Candidatus* thiobios is associated with ectosymbiotic bacteria growing on the marie ciliate *Zoothamnium niveum*, commonly found in sulfide-rich habits, including hydrothermal vents (Rinke et al., 2006; Bright et al., 2014). The presence of high abundance of this genus could be related to the presence of the *Zoothamnium niveum* inhabiting this specific site.

Both sites (Baia Calcara and Levante Bay), included lower abundances of sequences assigned to the genus *Sulfurimonas*, *Sulfurivirga*, *Sulforovum*, and *Campylobacter*, all belonging to the Campylobacterota phylum (formerly known as Epsilonproteobacteria). Members of the *Sulfurimonas* genus are widespread in sulfidic environments and are capable of using multiple reduced sulfur species as electron donors, such as thiosulfate, hydrogen sulfide, and elemental sulfur (Han and Perner, 2015). The genus *Sulfurivirga* could be assigned to the species *Sulfurivirga caldiculari* (99.73% similarity), a thiosulfate-oxidizing, thermophilic, chemolithoautotrophic bacterium, described in a shallow-water vent system in Japan (Takai et al., 2006). Similarly, *Sulfurovum* is also associated with thiosulfate oxidation and chemolithoautotrophy (Inagaki et al., 2004). *Campylobacter*, within Campylobacteriota, is ubiquitous in hydrothermal environments, including shallow-water hydrothermal vents (Rinke et al., 2006; Anderson et al., 2011; Giovannelli and Vetriani, 2017; Wang et al., 2017). These genera have been associated with high-temperature high sulfidic locations in other shallow-water, as well as deep-sea hydrothermal systems (Forget et al., 2010; Zhang et al., 2012; Giovannelli et al., 2013; Gugliandolo et al., 2015; Gomez-Saez et al., 2017; Price and Giovannelli, 2017). Members of the Campylobacterota are present in most sites presenting higher temperatures (Levante Bay, Levante Port, Bottaro, Baia Calcara and Pietra del Bagno) and dominate the biofilm communities of Levante Port and Baia Calcara. Hydrothermal vents are often enriched in reduced sulfur species (German and Seyfried, 2014; Price and Giovannelli, 2017). The presence of sulfur-related metabolisms, coupled to inorganic carbon fixation, highlights the importance of these types of metabolic strategies for the function of hydrothermal systems, as well as the importance of these ecosystems to mediate the biogeochemical cycles of sulfur and carbon. Additionally, these high temperature locations had the highest protein/carbohydrate ratios (15.2 in Baia Calcara and 12.6 in Levante Port), suggesting high *in situ* productivity. Since at these locations, recovered ASVs are related to known chemolithoautotrophic groups, indicates that they are major contributors to primary productivity in high temperature shallow water hydrothermal vents. Similarly, Gomez-Saez et al. (2017), reported that chemoautotrophy constitutes an important contribution to fresh organic matter production, accounting for up to 65% of autotrophic carbon fixation in the shallow-water hydrothermal vents of Dominica.

At moderate to low temperatures an increase in phototrophic microbial lineages was observed, also reflected in the quantities of BPC and Chlorophyll-*a*. The prevalent photosynthetic group observed in this study was assigned to the genus *Synechococcus* and to the species *Synechococcus* sp. CC9902 (99.47% similarity), belonging to the phylum Cyanobacteria. The presence of phototrophs in shallow-water hydrothermal systems is well documented, as well as a key feature of these systems (Tarasov et al., 1990, 1999, 2005; Sievert et al., 2000; Zhang et al., 2012; Maugeri et al., 2013; Price et al., 2013; Lentini et al., 2014; Dávila-Ramos et al., 2015; Gugliandolo et al., 2015; Gomez-Saez et al., 2017; Price and Giovannelli, 2017). Here, *Synechococcus* sp. CC9902 was present in lower abundances at moderate temperatures in Bottaro and Levante Port, and high abundances in Pollara, the lowest temperature site. *Synechococcus* sp. CC9902 is widespread in the oceans and is described as having increased plasticity to diverse saline concentrations and light intensities (Ludwig and Bryant, 2012; Kim et al., 2018). Furthermore, the presence of this taxon has already been described in shallow-water hydrothermal vent environments (Maugeri et al., 2013). However, in other shallow-water vents systems, the specific lineages within Cyanobacteria differ. This suggests that in shallow-water hydrothermal vents the photoautotrophic niche space can be occupied by diverse lineages of phototrophic taxa. Notwithstanding, it is important to note that, even though the presence of Cyanobacteria in shallow water hydrothermal vents is well documented, the possibility of mixing with background seawater cannot be discarded. For instance, it has been shown that fluid mixing with seawater could be the result of the convective cells in porous media (Yücel et al., 2013).

The shallow water vent Pietra del Bagno, Lipari, due to the presence of orange precipitates surrounding the venting site, was deemed to be iron-rich. The sediment community was mainly composed by the family *Anaerolineares* of the phylum Chloroflexi, and the genus *Mariprofundus* belonging to Proteobacteria. Members belonging to Chloroflexi are ecologically and physiologically diverse, allowing them to colonize a wide variety of environments (Ward et al., 2018; Vuillemin et al., 2020). Despite being originally associated with anoxygenic phototrophy, they are also known to employ other metabolic strategies (McIlroy et al., 2017). The family *Anaerolineares*

is associated with hydrocarbon oxidation and is known to have important roles in the functioning of anaerobic digestion systems (McIlroy et al., 2017). Nonetheless, they have been reported in deep-sea and shallow-water hydrothermal vents (Rajasabapathy et al., 2018; McGonigle et al., 2020; Wang et al., 2020). The closest relative to our sequences was reported from Fe-rich hydrothermal sediments of two submarine volcanoes of the Tonga volcanic arc (Forget et al., 2010). Interestingly, this bacterial family has also been observed to be present in high abundances in Fe-enriched locations (Hoshino et al., 2016; Ward et al., 2017). Other members of Chloroflexi, such as *Ardenticatena maritima*, grow by dissimilatory iron-reduction (Kawaichi et al., 2013). Thus, it is possible that *Anaerolineares* can couple the oxidation of organic matter to iron-reduction, making them major players in the biomineralization of organic matter in shallow-water vent environments.

The genus *Mariprofundus* of Zetaproteobacteria are well-known iron(II)-oxidizers that couple the iron (II) oxidation to the reduction of oxygen or nitrate (Chiu et al., 2017; McAllister et al., 2019). Members belonging to the phyla Zetaproteobacteria are widespread in hydrothermal Fe-rich environments (Emerson and Moyer, 2002; Emerson et al., 2010; Forget et al., 2010; Gomez-Saez et al., 2017; McAllister et al., 2019). Within *Mariprofundus*, it was possible to assign to the species *Mariprofundus aestuarium* (99.73% similarity), previously isolated from redox-stratified water columns, and capable of growing through the oxidation of iron (II) (Chiu et al., 2017). Additionally, albeit in lower abundances, it was possible to identify the genus *Caldithrix*. More specifically, we could assign our sequences to the species *Caldithrix abyssi* (98.94% similarity). This species is a known chemolithoautotroph, capable of growing anaerobically through the reduction of nitrate, using hydrogen as an electron donor (Miroshnichenko et al., 2003). Our geochemical analysis did not identify nitrate in the fluids at this site (data not shown); however, it was recently found that an environmentally assembled genome (MAG) of this species codes for a homolog of an extracellular respiratory system found in *Geobacter*, associated with iron reduction (Fortney et al., 2018). Given that this terminal electron acceptor was not tested in the original isolate (Miroshnichenko et al., 2003), the coupling of hydrogen oxidation to iron reduction could potentially suggest a metabolic strategy employed by *Caldithrix*. Notably, previous studies conducted at Fe-rich shallow-water vents have reported similar communities to the ones observed at this site (Handley et al., 2010; Meyer-Dombard et al., 2013; Gomez-Saez et al., 2017). Thus, these lineages can be considered to be important in driving the iron cycling in the shallow-water vent ecosystem, making important contributions to the biogeochemical cycles of iron. Interestingly, it was not possible to identify iron oxidizers in the biofilm community in high abundance at the same site. Conversely, the genus *Collwelia* was present in high abundances, followed by the clade SUP05. Members belonging to *Collwelia* are psychrophilic, heterotrophic bacteria, ubiquitous in cold marine environments (Techtmann et al., 2016), including sea ice (Zhang et al., 2008), polar sediments (Wang et al., 2015), and deep-sea trenches (Nogi et al., 2004). Specifically, we identified the species *Colwellia rossensis* (100% similarity), isolated from coastal Antarctic sea ice (Bowman et al., 1998). Colwellia species have been isolated from marine environments, and are characteristically psychrophiles (Bowman et al., 1998). The presence of ASVs related to this species at higher temperatures suggests a bigger temperature gradient to which this group is adapted to. The clade SUP05 is composed of known sulfur-oxidizing bacteria, also described as having a heterotrophic-based metabolism (Spietz et al., 2019; Morris and Spietz, 2022). At this location, the protein to carbohydrate ratios is 1.13. As reported by Pusceddu et al. (2003), since proteins are readily mobilized, as compared to carbohydrates, low ratios suggest the presence of aged organic matter (not freshly produced), and probably indicates external input as a potential source of organic matter to the biofilm communities.

Additionally, in moderate temperatures sites, it was possible to identify in higher abundance the families *Flavobactereceae* and *Arcobactereceae*, in the biofilms of Bottaro and Levante Port, and the genus *IheB3-7* at the sediment sample of Levante Port. The family *Flavobacteriaceae* of the Phylum Bacteroidetes, ubiquitous in marine environments, are known to degrade complex hydrocarbons, with large numbers of glycosyl hydrolases and peptidases encoded in the genomes of this bacterial group (Gavriilidou et al., 2020). Moreover, the family *Arcobactereceae*, also widely distributed in marine environments (Venâncio et al., 2022), has been reported in shallow vent hydrothermal environments (Maugeri et al., 2009; Gugliandolo et al., 2015; Gomez-Saez et al., 2017).

At the lowest temperature site (Pollara), Cyanobacteria was the most abundant group, and with lower abundances, the genera *Pseudoalteromonas*, *Woesia*, NS5 marine group, and *Anoxybacillus*. These microbial groups are associated with heterotrophic metabolisms, and given the protein/carbohydrate ratios at this location of 3.64, as well as Chla-a concentration of 1.0 $\mu g\, g^{-1}$, suggests that these groups rely on the export of organic carbon from the water column into the vent system, coupled with the usage of aged organic matter derived from external input, and *in situ* production from phototrophic organisms. *Pseudoalteromonas*, *Woesia*, and NS5 marine group are widely distributed in marine environments (Holmström and Kjelleberg, 1999; Du et al., 2016; Priest et al., 2022). Additionally, *Anoxybacillus* was also reported in deep-sea hydrothermal vent sediments (Cheng et al., 2021). Here, it was possible to assign *Anoxybacillus* to the species *Anoxybacillus rapiensis* (100% similarity), a thermophilic, anaerobic, heterotrophic bacterium, isolated from diverse hot springs in Bulgaria (Derekova et al., 2007).

While temperature is one of the key variables controlling the microbial diversity in our dataset, other environmental parameters contribute significantly in shaping microbial communities of the different sample types collected (fluids, sediments and biofilms) across the geochemically diverse vents sampled. This has been recently demonstrated in hot springs (Fullerton et al., 2021), where a combination of the geological settings, the aqueous geochemistry and trace element availability provided strong explanatory power of the beta diversity turnover among the sampled springs. In this work unweighted and weighted UniFrac based multivariate analysis (Figure 6) revealed the presence of three statistically significant groups. The first was composed of the biofilm samples, where no significant correlations with the measured parameters were found to significantly explain the diversity. The biofilm composition and architecture are found to be influenced by both deterministic, as well as stochastic effects. For instance, previous studies have shown that biofilm thickness drives the biofilm community and diversity (Suarez et al., 2019), combined with the age of the biofilm and other environmental variables. The second major group, encompassing the samples of fluids and sediments from the islands Vulcano and Panarea, could be explained by the temperature. As discussed above, these

locations were marked by moderate to high temperatures, with ASVs associated with microbial lineages related to the oxidation of hydrogen or reduced sulfur species. In hydrothermal systems fluid ascent is facilitated by the permeability of lithospheric fault systems, allowing a more focused channeling of the fluids to the surface (Pearce et al., 2019). Moreover, hydrothermal systems further away from fault systems are likely to show weak thermal anomalies (Taillefer et al., 2018). Consistent with this, the site with the lowest temperature, Pollara in Salina, is the sampling site further away from known fault systems in the area. Interestingly, we found that temperature and Mg^{2+} follow opposite correlation patterns. Magnesium is depleted in end-member hydrothermal fluids, resulting from water-rock reactions during the circulation of the fluids in the hydrothermal system (Alt, 2013). The presence of higher quantities of Mg^{2+} in low temperature sites, can entail less degree of water-reactions, which could be a function of the weak thermal anomalies found in the island of Salina and Lipari. Consistent with this, these islands present less geothermal activity compared to the other island samples in this study.

In the third group, encompassing the sites from the islands of Salina and Lipari, the microbial diversity was explained by the major anions and cations Mg^{2+}, Br^{-}, and Na^{+}. Despite the geochemical analysis encompassing our samples in combination with the literature available placed our samples within Type 3 fluids, small variations of the major anions and cations show statistically significant correlation with the microbial distribution in both these islands. Diverse subsurface processes could result in similar concentrations of the major anions and cations, but result in a differential enrichment of minor elements, such as trace elements (Rollinson and Pease, 2021). Recent studies have shown that trace elements play key roles in shaping microbial niche occupation, as well as have been used to improve the cultivation of extremophilic organisms from natural hot springs (Meyer-Dombard et al., 2012; Shafiee et al., 2021).

Similarly to the unweighted UniFrac, with the weighted version, which weights the abundance of the taxa present, we found the same statistically significant separation between the communities of Vulcano/Panarea and Salina/Lipari, as well as the biofilm samples and the other samples types. However, conversely to the unweighted UniFrac, we found the temperature to be correlated with the abundance of taxa of Baia Calcara and Levante Port biofilm communities. These were dominated by thermophilic communities belonging to *Nitratifractor* and *Thiomicrorhabdus*. Therefore, both these parameters can act as strong selective pressures, driving not the structuring of the biofilm communities of Baia Calcara and Levante Port, but selecting for thermophilic, chemolithoautotrophic groups. The correlation with longitude could be related with the location of the islands within the Aeolian volcanic arc. It has been previously demonstrated that the magmatic composition of the Aeolian arc exhibits within-islands variations (Peccerillo et al., 2013). These differences could entail differential inputs of magmatic volatiles into the hydrothermal fluids, which in turn could be influencing the microbial communities inhabiting the shallow-water hydrothermal vents. It was also possible to find the major elements correlating with the abundance of the communities of the islands of Lipara and Salina, and with weighted UniFrac, the communities of Vulcano and Salina.

In the Aeolian Archipelago it is possible to find a highly diverse set of marine habitats. These habitats, in turn, harbor an abundant number of species, some of which with endangered status (Álvarez et al., 2019). For this reason, over the years, there have been increasing efforts to enhance the conservation measures on the Aeolian Islands, through the practices of sustainable fishing, tourism, and community education (Álvarez et al., 2019). The presence of high hydrothermal activity should further augment the need for conservation practices in these islands, for different reasons. One is that the microbial communities inhabiting these vents play important ecological roles for the entire shallow marine ecosystem (Tarasov et al., 2005; Price and Giovannelli, 2017), potentially sustaining primary productivity in surrounding ecosystems (Price and Giovannelli, 2017). Given their key roles as primary producers, these microbial communities sustain complex food webs on the surrounding islands. Secondly, extreme environments are often looked upon for the isolation of microorganisms that produce industrially and medically relevant metabolites, such as novel enzymes and antibiotics (Littlechild, 2015; Sayed et al., 2020; Petrillo et al., 2021). For instance, novel enzyme-producing Bacillus have been isolated from the Island of Panarea, whereas novel hydrolases have been identified on environmental DNA libraries from the sediments of the shallow-vents of the island of Vulcano (Lentini et al., 2007; Gugliandolo et al., 2012; Placido et al., 2015). Thirdly, in recent years there have been efforts to apply conservation status to deep-sea hydrothermal vents (Van Dover, 2012; Van Dover et al., 2018). We argue that shallow-water hydrothermal vents play an equally important role in the functioning of marine ecosystems, and should be explicitly acknowledged in marine spatial planning and conservation efforts, not only because of their uniqueness, but because they represent an accessible window for us to appreciate the intricate relationships between the geosphere and biosphere.

5. Conclusion

In conclusion, our study shows that the Aeolian archipelago shallow water hydrothermal vents harbors a highly diverse microbial consortia. In line with previous studies conducted in these unique ecosystems, we found the presence of ASVs related to organisms employing diverse metabolic strategies, ranging from chemolithoautotrophy, heterotrophy and phototrophy. Furthermore, we found those same groups to be correlated strongly with temperature, where we could observe a transition from higher temperatures (mainly ASVs related to chemolithoautotrophic groups) to moderate and lower temperatures (mainly ASVs related to phototrophic and heterotrophic groups). This transition is commonly observed in geothermal environments, and can be considered as a definite characteristic of these systems. Furthermore, through the analysis of BPC, we found that different types of organic matter are available to the resident communities, from terrigenous input exported to the system, as well as *in situ* production by chemolithoautotrophic and phototrophic groups. This supports the literature on how shallow water hydrothermal vents are considered high energy environments. Through beta diversity analysis, we found the presence of three significant groups, composed of the biofilm samples, and the sediment and fluid samples of the islands of Vulcano and Panarea, and Lipari and Salina. The group of Vulcano and Panarea was correlated with temperature, as these locations were marked by moderate to high temperatures, and they were dominated by ASVs related to chemolithoautotrophic groups. As for the group of Lipari and Salina, the distribution of the microbial communities was

correlated with major ions. This suggests that subsurface water rock reactions have an influence on the concentration of the major ions, which in turn, can influence the microbial communities inhabiting these shallow water hydrothermal vents. Additionally, we found that the longitude, together with the temperature, was a significant vector in the weighted UNIFRAC. This correlation could be due to the location of the islands within the Aeolian volcanic arc and the different geothermal activity within each island.

Additionally, our compilation of fluid data from previous studies showed the same trend noted by Price et al. (2015), wherein in these hydrothermal systems, one can find 3 types of fluid evolution, showing differential enrichments and depletions of the major anions and cations, and therefore hinting at different subsurface processes taking place in the different islands. Given that the Aeolian archipelago shallow water hydrothermal vents, and the microbial communities inhabiting them, have important ecological roles for the surrounding marine environment, we think it is important their inclusion into present and future conservation efforts. Finally, shallow-water vents and the volcanic arc lithologies at which they occur are still understudied, compared to the basaltic, mid-ocean ridge lithologies from their deep-sea counter-parts. Our study is the first stage of a deeper characterization of the Aeolian archipelago shallow-water systems, and future studies will shed light on the ecological role of the communities in these systems, as well as on the local biogeochemical cycles.

Data availability statement

The datasets presented in this study can be found in online repositories. The names of the repository/repositories and accession number(s) can be found below: https://www.ebi.ac.uk/ena, PRJEB54611, https://zenodo.org/record/7480614.

Author contributions

BB carried out data analysis, geochemical experiments and wrote the first draft of the manuscript. BB, AF, MS, MG, AB, MCO, and LD produced the geochemical and microbiological data. MS and AF carried out Dada2 and Phyloseq and statistical analysis. AF, AC, MC, GB, RP, MI, CV, and DG planned the expedition and collected the samples. RP, CV, AC, and DG supervised the study. All authors contributed equally to the final version of the manuscript.

Funding

This work is partially funded by the European Research Council (ERC) under the European Union's Horizon 2020 research and innovation program (grant agreement No. 948972) to DG. Partial funding was from the NASA Habitable Worlds program under grant 80NSSC20K0228 to REP.

Acknowledgments

The authors wish to thank the Blue Marine Foundation (https://www.bluemarinefoundation.com/) for support in organizing the sampling expedition and for the use of the zodiac. They also thank the Salina diving center for providing the diving logistics necessary to carry out the sampling and Luca Magni for assistance with the dives and location access.

Conflict of interest

The authors declare that the research was conducted in the absence of any commercial or financial relationships that could be construed as a potential conflict of interest.

Publisher's note

References

Alsop, E. B., Boyd, E. S., and Raymond, J. (2014). Merging metagenomics and geochemistry reveals environmental controls on biological diversity and evolution. *BMC Ecol.* 14:16. doi: 10.1186/1472-6785-14-16

Alt, J. C. (2013). "Subseafloor processes in Mid-Ocean ridge Hydrothennal systems" in *Geophysical monograph series*. eds. S. E. Humphris, R. A. Zierenberg, L. S. Mullineaux and R. E. Thomson (Washington, DC: American Geophysical Union), 85–114.

Álvarez, H., Perry, A. L., García, S., Blanco, J., and Aguilar, R. (2019). Towards the creation of a marine protected area in the Aeolian Islands. *MarXiv* 2019:b9dqc. doi: 10.31230/osf.io/b9dqc

Amend, J. P., Rogers, K. L., Shock, E. L., Gurrieri, S., and Inguaggiato, S. (2003). Energetics of chemolithoautotrophy in the hydrothermal system of Vulcano Island, southern Italy. *Geobiology* 1, 37–58. doi: 10.1046/j.1472-4669.2003.00006.x

Anderson, I., Sikorski, J., Zeytun, A., Nolan, M., Lapidus, A., Lucas, S., et al. (2011). Complete genome sequence of *Nitratifractor salsuginis* type strain (E9I37-1T). *Stand. Genomic Sci.* 4, 322–330. doi: 10.4056/sigs.1844518

Antranikian, G., Suleiman, M., Schäfers, C., Adams, M. W. W., Bartolucci, S., Blamey, J. M., et al. (2017). Diversity of bacteria and archaea from two shallow marine hydrothermal vents from Vulcano Island. *Extremophiles* 21, 733–742. doi: 10.1007/s00792-017-0938-y

Bao, R., van der Voort, T. S., Zhao, M., Guo, X., Montluçon, D. B., McIntyre, C., et al. (2018). Influence of hydrodynamic processes on the fate of sedimentary organic matter on continental margins. *Glob. Biogeochem. Cycles* 32, 1420–1432. doi: 10.1029/2018GB005921

Bastianoni, A., Cascone, M., De Moor, J. M., Barry, P. H., Price, R., Cordone, A., et al. (2022). *The missing carbon budget puzzle piece: Shallow-water hydrothermal vents contribution to global CO_2 fluxes.*

Berndt, M. E., Seewald, J. S., and Seyfried, W. E. (1988). Hydrothermal alteration processes at Mid Ocean ridges:Constrains from diabase alteration experiments, hot-spring fluids and composition of the oceanic crust. *Can. Mineral.* 26, 787–804.

Bligh, E. G., and Dyer, W. J. (1959). A rapid method of Total lipid extraction and purification. *Can. J. Biochem. Physiol.* 37, 911–917. doi: 10.1139/o59-099

Bowman, J. P., Lewis, T. E., Staley, J. T., and McMeekin, T. A. (1998). *Colwellia demingiae* sp. nov., *Colwellia hornerae* sp. nov., *Colwellia rossensis* sp. nov. and *Colwellia psychrotropica* sp. nov.: psychrophilic Antarctic species with the ability to synthesize

docosahexaenoic acid (22: 63). *Int. J. Syst. Bacteriol.* 48, 1171–1180. doi: 10.1099/00207713-48-4-1171

Bright, M., Espada-Hinojosa, S., Lagkouvardos, I., and Volland, J.-M. (2014). The giant ciliate *Zoothamnium niveum* and its thiotrophic epibiont *Candidatus* Thiobios zoothamnicoli: a model system to study interspecies cooperation. *Front. Microbiol.* 5:145. doi: 10.3389/fmicb.2014.00145

Brovarone, A. V., Butch, C. J., Ciappa, A., Cleaves, H. J., Elmaleh, A., Faccenda, M., et al. (2020). Let there be water: how hydration/dehydration reactions accompany key earth and life processes#. *Am. Mineral.* 105, 1152–1160. doi: 10.2138/am-2020-7380

Callahan, B. J., McMurdie, P. J., and Holmes, S. P. (2017). Exact sequence variants should replace operational taxonomic units in marker-gene data analysis. *ISME J.* 11, 2639–2643. doi: 10.1038/ismej.2017.119

Cardellini, C., Chiodini, G., and Frondini, F. (2003). Application of stochastic simulation to CO_2 flux from soil: mapping and quantification of gas release: simulation of soil CO_2 flux. *J. Geophys. Res. Solid Earth* 108:2165. doi: 10.1029/2002JB002165

Chan, C. S., Chan, K.-G., Ee, R., Hong, K.-W., Urbieta, M. S., Donati, E. R., et al. (2017). Effects of physiochemical factors on prokaryotic biodiversity in Malaysian Circumneutral Hot Springs. *Front. Microbiol.* 8:1252. doi: 10.3389/fmicb.2017.01252

Cheng, J.-H., Wang, Y., Zhang, X.-Y., Sun, M.-L., Zhang, X., Song, X.-Y., et al. (2021). Characterization and diversity analysis of the extracellular proteases of thermophilic *Anoxybacillus caldiproteolyticus* 1A02591 from Deep-Sea hydrothermal vent sediment. *Front. Microbiol.* 12:643508. doi: 10.3389/fmicb.2021.643508

Chiu, B. K., Kato, S., McAllister, S. M., Field, E. K., and Chan, C. S. (2017). Novel pelagic Iron-oxidizing Zetaproteobacteria from the Chesapeake Bay Oxic–anoxic transition zone. *Front. Microbiol.* 8:1280. doi: 10.3389/fmicb.2017.01280

Cordone, A., D'Errico, G., Magliulo, M., Bolinesi, F., Selci, M., Basili, M., et al. (2022). Bacterioplankton diversity and distribution in relation to phytoplankton community structure in the Ross Sea surface waters. *Front. Microbiol.* 13:722900. doi: 10.3389/fmicb.2022.722900

Cordone, A., Lucchini, S., Felice, M., and Ricca, E. (2011). Direct and indirect control of Lrp on LEE pathogenicity genes of *Citrobacter rodentium*. *FEMS Microbiol. Lett.* 325, 64–70. doi: 10.1111/j.1574-6968.2011.02411.x

Cordone, A., Mauriello, E. M. F., Pickard, D. J., Dougan, G., De Felice, M., and Ricca, E. (2005). The lrp gene and its role in type I fimbriation in *Citrobacter rodentium*. *J. Bacteriol.* 187, 7009–7017. doi: 10.1128/JB.187.20.7009-7017.2005

Dahle, H., Økland, I., Thorseth, I. H., Pederesen, R. B., and Steen, I. H. (2015). Energy landscapes shape microbial communities in hydrothermal systems on the Arctic Mid-Ocean ridge. *ISME J.* 9, 1593–1606. doi: 10.1038/ismej.2014.247

Dávila-Ramos, S., Estradas-Romero, A., Prol-Ledesma, R. M., and Juárez-López, K. (2015). Bacterial populations (first record) at two shallow hydrothermal vents of the Mexican Pacific West coast. *Geomicrobiol J.* 32, 657–665. doi: 10.1080/01490451.2014.980526

De Astis, G., Peccerillo, A., Kempton, P. D., La Volpe, L., and Wu, T. W. (2000). Transition from calc-alkaline to potassium-rich magmatism in subduction environments: geochemical and Sr, Nd, Pb isotopic constraints from the island of Vulcano (Aeolian arc). *Contrib. Mineral. Petrol.* 139, 684–703. doi: 10.1007/s004100000172

De Astis, G., Ventura, G., and Vilardo, G. (2003). Geodynamic significance of the Aeolian volcanism (Southern Tyrrhenian Sea, Italy) in light of structural, seismological, and geochemical data: geodynamics of the Aeolian volcanism. *Tectonics* 22:1040. doi: 10.1029/2003TC001506

Deckert, G., Warren, P. V., Gaasterland, T., Young, W. G., Lenox, A. L., Graham, D. E., et al. (1998). The complete genome of the hyperthermophilic bacterium *Aquifex aeolicus*. *Nature* 392, 353–358. doi: 10.1038/32831

Derekova, A., Sjøholm, C., Mandeva, R., and Kambourova, M. (2007). *Anoxybacillus rupiensis* sp. Nov., a novel thermophilic bacterium isolated from Rupi basin (Bulgaria). *Extremophiles* 11, 577–583. doi: 10.1007/s00792-007-0071-4

Dick, G. J., Anantharaman, K., Baker, B. J., Li, M., Reed, D. C., and Sheik, C. S. (2013). The microbiology of deep-sea hydrothermal vent plumes: ecological and biogeographic linkages to seafloor and water column habitats. *Front. Microbiol.* 4:124. doi: 10.3389/fmicb.2013.00124

Ding, J., Zhang, Y., Wang, H., Jian, H., Leng, H., and Xiao, X. (2017). Microbial community structure of deep-sea hydrothermal vents on the ultraslow spreading southwest Indian ridge. *Front. Microbiol.* 8:1012. doi: 10.3389/fmicb.2017.01012

Du, Z.-J., Wang, Z.-J., Zhao, J.-X., and Chen, G.-J. (2016). *Woeseia oceani* gen. Nov., sp. nov., a chemoheterotrophic member of the order Chromatiales, and proposal of Woeseiaceae fam. Nov. *Int. J. Syst. Evol. Microbiol.* 66, 107–112. doi: 10.1099/ijsem.0.000683

Emerson, D., Fleming, E. J., and McBeth, J. M. (2010). Iron-oxidizing Bacteria: an environmental and genomic perspective. *Annu. Rev. Microbiol.* 64, 561–583. doi: 10.1146/annurev.micro.112408.134208

Emerson, D., and Moyer, C. L. (2002). Neutrophilic Fe-oxidizing Bacteria are abundant at the Loihi seamount hydrothermal vents and play a major role in Fe oxide deposition. *Appl. Environ. Microbiol.* 68, 3085–3093. doi: 10.1128/AEM.68.6.3085-3093.2002

Fabiano, M., Danovaro, R., and Fraschetti, S. (1995). A three-year time series of elemental and biochemical composition of organic matter in subtidal sandy sediments of the Ligurian Sea (northwestern Mediterranean). *Cont. Shelf Res.* 15, 1453–1469. doi: 10.1016/0278-4343(94)00088-5

Fagorzi, C., Del Duca, S., Venturi, S., Chiellini, C., Bacci, G., Fani, R., et al. (2019). Bacterial communities from extreme environments: Vulcano Island. *Diversity* 11:140. doi: 10.3390/d11080140

Falkowski, P. G., Fenchel, T., and Delong, E. F. (2008). The microbial engines that drive Earth's biogeochemical cycles. *Science* 320, 1034–1039. doi: 10.1126/science.1153213

Favallim, M., Karátson, D., Mazzuoli, R., Pareschi, M. T., and Ventura, G. (2005). Volcanic geomorphology and tectonics of the Aeolian archipelago (southern Italy) based on integrated DEM data. *Bull. Volcanol.* 68, 157–170. doi: 10.1007/s00445-005-0429-3

Forget, N. L., Murdock, S. A., and Juniper, S. K. (2010). Bacterial diversity in Fe-rich hydrothermal sediments at two South Tonga arc submarine volcanoes: bacterial diversity in Fe oxide samples. *Geobiology* 8, 417–432. doi: 10.1111/j.1472-4669.2010.00247.x

Fortney, N. W., He, S., Converse, B. J., Boyd, E. S., and Roden, E. E. (2018). Investigating the composition and metabolic potential of microbial communities in chocolate pots Hot Springs. *Front. Microbiol.* 9:2075. doi: 10.3389/fmicb.2018.02075

Fournier, R. O. (2007). "Hydrothermal systems and volcano geochemistry" in *Volcano deformation*. ed. D. Dzurisin (Berlin, Heidelberg: Springer Berlin Heidelberg), 323–341.

Fullerton, K. M., Schrenk, M. O., Yücel, M., Manini, E., Basili, M., Rogers, T. J., et al. (2021). Effect of tectonic processes on biosphere–geosphere feedbacks across a convergent margin. *Nat. Geosci.* 14, 301–306. doi: 10.1038/s41561-021-00725-0

Gamberi, F., Marani, M., and Savelli, C. (1997). Tectonic, volcanic and hydrothermal features of a submarine portion of the Aeolian arc (Tyrrhenian Sea). *Mar. Geol.* 140, 167–181. doi: 10.1016/S0025-3227(97)00020-0

Gavriilidou, A., Gutleben, J., Versluis, D., Forgiarini, F., van Passel, M. W. J., Ingham, C. J., et al. (2020). Comparative genomic analysis of Flavobacteriaceae: insights into carbohydrate metabolism, gliding motility and secondary metabolite biosynthesis. *BMC Genomics* 21:569. doi: 10.1186/s12864-020-06971-7

Gerchakov, S. M., and Hatcher, P. G. (1972). Improved technique for analysis of carbohydrates in sediments. 1. *Limnol. Oceanogr.* 17, 938–943. doi: 10.4319/lo.1972.17.6.0938

German, C. R., and Seyfried, W. E. (2014). "Hydrothermal processes" in *Treatise on geochemistry*. ed. K. K. Turekian (Amsterdam, Netherlands: Elsevier), 191–233.

Giovannelli, D., d'Errico, G., Fiorentino, F., Fattorini, D., Regoli, F., Angeletti, L., et al. (2016). Diversity and distribution of prokaryotes within a shallow-water pockmark Field. *Front. Microbiol.* 7:941. doi: 10.3389/fmicb.2016.00941

Giovannelli, D., d'Errico, G., Manini, E., Yakimov, M., and Vetriani, C. (2013). Diversity and phylogenetic analyses of bacteria from a shallow-water hydrothermal vent in Milos island (Greece). *Front. Microbiol.* 4:184. doi: 10.3389/fmicb.2013.00184

Giovannelli, D., Grosche, A., Starovoytov, V., Yakimov, M., Manini, E., and Vetriani, C. (2012). *Galenea microaerophila* gen. Nov., sp. nov., a mesophilic, microaerophilic, chemosynthetic, thiosulfate-oxidizing bacterium isolated from a shallow-water hydrothermal vent. *Int. J. Syst. Evol. Microbiol.* 62, 3060–3066. doi: 10.1099/ijs.0.040808-0

Giovannelli, D., Sievert, S. M., Hügler, M., Markert, S., Becher, D., Schweder, T., et al. (2017). Insight into the evolution of microbial metabolism from the deep-branching bacterium, *Thermovibrio ammonificans*. *Elife* 6:e18990. doi: 10.7554/eLife.18990

Giovannelli, D., and Vetriani, C. (2017). From extreme environments to human pathogens: an evolutionary journey. *Biochemist* 39, 4–9. doi: 10.1042/BIO03906004

Gomez-Saez, G. V., Pop Ristova, P., Sievert, S. M., Elvert, M., Hinrichs, K.-U., and Bühring, S. I. (2017). Relative importance of chemoautotrophy for primary production in a light exposed marine shallow hydrothermal system. *Front. Microbiol.* 8:702. doi: 10.3389/fmicb.2017.00702

Gomez-Saez, G. V., Riedel, T., Niggemann, J., Pichler, T., Dittmar, T., and Bühring, S. I. (2015). Interaction between iron and dissolved organic matter in a marine shallow hydrothermal system off Dominica Island (Lesser Antilles). *Mar. Chem.* 177, 677–686. doi: 10.1016/j.marchem.2015.10.003

Gugliandolo, C., and Italiano, F. (1999). Submarine hydrothermal vents of the Aeolian Islands: relationship between microbial communities and thermal fluids. *Geomicrobiol J.* 16, 105–117. doi: 10.1080/014904599270794

Gugliandolo, C., Italiano, F., and Maugeri, T. L. (2006). *The submarine hydrothermal system of Panarea (southern Italy): Biogeochemical processes at the thermal fluids-sea bottom interface*.

Gugliandolo, C., Lentini, V., Bunk, B., Overmann, J., Italiano, F., and Maugeri, T. L. (2015). Changes in prokaryotic community composition accompanying a pronounced temperature shift of a shallow marine thermal brine pool (Panarea Island, Italy). *Extremophiles* 19, 547–559. doi: 10.1007/s00792-015-0737-2

Gugliandolo, C., Lentini, V., Spanò, A., and Maugeri, T. L. (2012). New bacilli from shallow hydrothermal vents of Panarea Island (Italy) and their biotechnological potential: Bacilli from shallow vents of Panarea Island (Italy). *J. Appl. Microbiol.* 112, 1102–1112. doi: 10.1111/j.1365-2672.2012.05272.x

Gugliandolo, C., and Maugeri, T. L. (2019). Phylogenetic diversity of Archaea in shallow hydrothermal vents of Eolian Islands, Italy. *Diversity* 11:156. doi: 10.3390/d11090156

Guo, L.-L., Wu, Y.-H., Xu, X.-W., Huang, C.-J., Xu, Y.-Y., Cheng, H., et al. (2017). *Actibacterium pelagium* sp. nov., a novel alphaproteobacterium, and emended

description of the genus *Actibacterium*. *Int. J. Syst. Evol. Microbiol.* 67, 5080–5086. doi: 10.1099/ijsem.0.002417

Hafenbradl, D., Keller, M., Dirmeier, R., Rachel, R., Roßnagel, P., Burggraf, S., et al. (1996). *Ferroglobus placidus* gen. Nov., sp. nov., a novel hyperthermophilic archaeum that oxidizes Fe^{2+} at neutral pH under anoxic conditions. *Arch. Microbiol.* 166, 308–314. doi: 10.1007/s002030050388

Han, Y., and Perner, M. (2015). The globally widespread genus Sulfurimonas: versatile energy metabolisms and adaptations to redox clines. *Front. Microbiol.* 6:989. doi: 10.3389/fmicb.2015.00989

Handley, K. M., Boothman, C., Mills, R. A., Pancost, R. D., and Lloyd, J. R. (2010). Functional diversity of bacteria in a ferruginous hydrothermal sediment. *ISME J.* 4, 1193–1205. doi: 10.1038/ismej.2010.38

Hartree, E. F. (1972). Determination of protein: a modification of the Lowry method that gives a linear photometric response. *Anal. Biochem.* 48, 422–427. doi: 10.1016/0003-2697(72)90094-2

Hedlund, B. P., Reysenbach, A.-L., Huang, L., Ong, J. C., Liu, Z., Dodsworth, J. A., et al. (2015). Isolation of diverse members of the Aquificales from geothermal springs in Tengchong, China. *Front. Microbiol.* 6:157. doi: 10.3389/fmicb.2015.00157

Hoaki, T., Nishijima, M., Miyashita, H., and Maruyama, T. (1995). Dense Community of Hyperthermophilic Sulfur-Dependent Heterotrophs in a geothermally heated shallow submarine biotope near Kodakara-Jima Island, Kagoshima, Japan. *Appl. Environ. Microbiol.* 61, 1931–1937. doi: 10.1128/aem.61.5.1931-1937.1995

Holmström, C., and Kjelleberg, S. (1999). Marine *Pseudoalteromonas* species are associated with higher organisms and produce biologically active extracellular agents. *FEMS Microbiol. Ecol.* 30, 285–293. doi: 10.1016/S0168-6496(99)00063-X

Hoshino, T., Kuratomi, T., Morono, Y., Hori, T., Oiwane, H., Kiyokawa, S., et al. (2016). Ecophysiology of Zetaproteobacteria associated with shallow hydrothermal Iron-Oxyhydroxide deposits in Nagahama Bay of Satsuma Iwo-Jima, Japan. *Front. Microbiol.* 6:1554. doi: 10.3389/fmicb.2015.01554

Inagaki, F., Takai, K., Nealson, K. H., and Horikoshi, K. (2004). *Sulfurovum lithotrophicum* gen. Nov., sp. nov., a novel sulfur-oxidizing chemolithoautotroph within the ε-Proteobacteria isolated from Okinawa trough hydrothermal sediments. *Int. J. Syst. Evol. Microbiol.* 54, 1477–1482. doi: 10.1099/ijs.0.03042-0

Inguaggiato, S., Calderone, L., Inguaggiato, C., Mazot, A., Morici, S., and Vita, F. (2012). Long-time variation of soil CO_2 fluxes at the summit crater of Vulcano (Italy). *Bull. Volcanol.* 74, 1859–1863. doi: 10.1007/s00445-012-0637-6

Inguaggiato, S., Jácome Paz, M. P., Mazot, A., Delgado Granados, H., Inguaggiato, C., and Vita, F. (2013). CO_2 output discharged from Stromboli Island (Italy). *Chem. Geol.* 339, 52–60. doi: 10.1016/j.chemgeo.2012.10.008

Inskeep, W. J., Jay, Z. G., Tringe, S. J., Herrgård, M. B., and Rusch, D.YNP Metagenome Project Steering Committee and Working Group Members (2013). The YNP metagenome project: environmental parameters responsible for microbial distribution in the Yellowstone geothermal ecosystem. *Front. Microbiol.* 4:67. doi: 10.3389/fmicb.2013.00067

Italiano, F., and Nuccio, P. M. (1991). Geochemical investigations of submarine volcanic exhalations to the east of Panarea, Aeolian Islands, Italy. *Clin. Lab. Stand. Inst.* 46, 125–141. doi: 10.1016/0377-0273(91)90079-F

Jorgensen, S. L., Hannisdal, B., Lanzen, A., Baumberger, T., Flesland, K., Fonseca, R., et al. (2012). Correlating microbial community profiles with geochemical data in highly stratified sediments from the Arctic Mid-Ocean ridge. *Proc. Natl. Acad. Sci.* 109, E2846–E2855. doi: 10.1073/pnas.1207574109

Kawaichi, S., Ito, N., Kamikawa, R., Sugawara, T., Yoshida, T., and Sako, Y. (2013). *Ardenticatena maritima* gen. Nov., sp. nov., a ferric iron- and nitrate-reducing bacterium of the phylum 'Chloroflexi' isolated from an iron-rich coastal hydrothermal field, and description of *Ardenticatenia classis* nov. *Int. J. Syst. Evol. Microbiol.* 63, 2992–3002. doi: 10.1099/ijs.0.046532-0

Kerfahi, D., Hall-Spencer, J. M., Tripathi, B. M., Milazzo, M., Lee, J., and Adams, J. M. (2014). Shallow water marine sediment bacterial community shifts along a natural CO_2 gradient in the Mediterranean Sea off Vulcano, Italy. *Microb. Ecol.* 67, 819–828. doi: 10.1007/s00248-014-0368-7

Kim, Y., Jeon, J., Kwak, M. S., Kim, G. H., Koh, I., and Rho, M. (2018). Photosynthetic functions of *Synechococcus* in the ocean microbiomes of diverse salinity and seasons. *PLoS One* 13:e0190266. doi: 10.1371/journal.pone.0190266

Kürzinger, V.. (2019). *Determination and differentiation of the hydrothermal precipitates of Panarea, Italy*. Freiberg Online Geoscience, p. 54.

LaRowe, D. E., Arndt, S., Bradley, J. A., Estes, E. R., Hoarfrost, A., Lang, S. Q., et al. (2020). The fate of organic carbon in marine sediments–new insights from recent data and analysis. *Earth-Sci. Rev.* 204:103146. doi: 10.1016/j.earscirev.2020.103146

Lentini, V., Gugliandolo, C., Bunk, B., Overmann, J., and Maugeri, T. L. (2014). Diversity of prokaryotic Community at a Shallow Marine Hydrothermal Site Elucidated by Illumina sequencing technology. *Curr. Microbiol.* 69, 457–466. doi: 10.1007/s00284-014-0609-5

Lentini, V., Gugliandolo, C., and Maugeri, T. L. (2007). Identification of enzyme-producing thermophilic bacilli isolated from marine vents of Aeolian Islands (Italy). *Ann. Microbiol.* 57, 355–361. doi: 10.1007/BF03175073

Littlechild, J. A. (2015). Enzymes from extreme environments and their industrial applications. *Front. Bioeng. Biotechnol.* 3:161. doi: 10.3389/fbioe.2015.00161

Liu, J., Hua, Z.-S., Chen, L.-X., Kuang, J.-L., Li, S.-J., Shu, W.-S., et al. (2014). Correlating microbial diversity patterns with geochemistry in an extreme and heterogeneous environment of mine tailings. *Appl. Environ. Microbiol.* 80, 3677–3686. doi: 10.1128/AEM.00294-14

Lorenzen, C. J., and Downs, J. N. (1986). The specific absorption coefficients of chlorophyllide and pheophorbide in 90% acetone, and comments on the fluorometric determination of chlorophyll and pheopigments1. *Limnol. Oceanogr.* 31, 449–452. doi: 10.4319/lo.1986.31.2.0449

Ludwig, M., and Bryant, D. A. (2012). *Synechococcus* sp. strain PCC 7002 transcriptome: acclimation to temperature, salinity, oxidative stress, and Mixotrophic growth conditions. *Front. Microbiol.* 3:354. doi: 10.3389/fmicb.2012.00354

Manini, E., Fiordelmondo, C., Gambi, C., Pusceddu, A., and Danovaro, R. (2003). Benthic microbial loop functioning in coastal lagoons: a comparative approach. *Oceanol. Acta* 26, 27–38. doi: 10.1016/S0399-1784(02)01227-6

Manini, E., Luna, G. M., Corinaldesi, C., Zeppilli, D., Bortoluzzi, G., Caramanna, G., et al. (2008). Prokaryote diversity and virus abundance in shallow hydrothermal vents of the Mediterranean Sea (Panarea Island) and the Pacific Ocean (North Sulawesi-Indonesia). *Microb. Ecol.* 55, 626–639. doi: 10.1007/s00248-007-9306-2

Maugeri, T. L., Lentini, V., Gugliandolo, C., Cousin, S., and Stackebrandt, E. (2010). Microbial diversity at a hot, Shallow-Sea hydrothermal vent in the southern Tyrrhenian Sea (Italy). *Geomicrobiol J.* 27, 380–390. doi: 10.1080/01490450903451518

Maugeri, T. L., Lentini, V., Gugliandolo, C., Italiano, F., Cousin, S., and Stackebrandt, E. (2009). Bacterial and archaeal populations at two shallow hydrothermal vents off Panarea Island (Eolian Islands, Italy). *Extremophiles* 13, 199–212. doi: 10.1007/s00792-008-0210-6

Maugeri, T. L., Lentini, V., Spanò, A., and Gugliandolo, C. (2013). Abundance and diversity of Picocyanobacteria in shallow hydrothermal vents of Panarea Island (Italy). *Geomicrobiol J.* 30, 93–99. doi: 10.1080/01490451.2011.653088

McAllister, S. M., Moore, R. M., Gartman, A., Luther, G. W., Emerson, D., and Chan, C. S. (2019). The Fe(II)-oxidizing Zetaproteobacteria: historical, ecological and genomic perspectives. *FEMS Microbiol. Ecol.* 95:fiz015. doi: 10.1093/femsec/fiz015

McDermott, J. M., Sylva, S. P., Ono, S., German, C. R., and Seewald, J. S. (2018). Geochemistry of fluids from Earth's deepest ridge-crest hot-springs: Piccard hydrothermal field, mid-Cayman rise. *Geochim. Cosmochim. Acta* 228, 95–118. doi: 10.1016/j.gca.2018.01.021

McGonigle, J. M., Lang, S. Q., and Brazelton, W. J. (2020). Genomic evidence for Formate metabolism by Chloroflexi as the key to unlocking deep carbon in lost City microbial ecosystems. *Appl. Environ. Microbiol.* 86, e02583–e02519. doi: 10.1128/AEM.02583-19

McIlroy, S. J., Kirkegaard, R. H., Dueholm, M. S., Fernando, E., Karst, S. M., Albertsen, M., et al. (2017). Culture-independent analyses reveal novel Anaerolineaceae as abundant primary fermenters in anaerobic digesters treating waste activated sludge. *Front. Microbiol.* 8:1134. doi: 10.3389/fmicb.2017.01134

McMurdie, P. J., and Holmes, S. (2013). Phyloseq: an R package for reproducible interactive analysis and graphics of microbiome census data. *PLoS One* 8:e61217. doi: 10.1371/journal.pone.0061217

Meyer-Dombard, D. R., Amend, J. P., and Osburn, M. R. (2013). Microbial diversity and potential for arsenic and iron biogeochemical cycling at an arsenic rich, shallow-sea hydrothermal vent (Tutum Bay, Papua New Guinea). *Chem. Geol.* 348, 37–47. doi: 10.1016/j.chemgeo.2012.02.024

Meyer-Dombard, D. R., Shock, E. L., and Amend, J. P. (2012). Effects of trace element concentrations on culturing thermophiles. *Extremophiles* 16, 317–331. doi: 10.1007/s00792-012-0432-5

Miroshnichenko, M. L., Kostrikina, N. A., Chernyh, N. A., Pimenov, N. V., Tourova, T. P., Antipov, A. N., et al. (2003). *Caldithrix abyssi* gen. Nov., sp. nov., a nitrate-reducing, thermophilic, anaerobic bacterium isolated from a mid-Atlantic ridge hydrothermal vent, represents a novel bacterial lineage. *Int. J. Syst. Evol. Microbiol.* 53, 323–329. doi: 10.1099/ijs.0.02390-0

Morris, R. M., and Spietz, R. L. (2022). The physiology and biogeochemistry of SUP05. *Annu. Rev. Mar. Sci.* 14, 261–275. doi: 10.1146/annurev-marine-010419-010814

Nogi, Y., Hosoya, S., Kato, C., and Horikoshi, K. (2004). *Colwellia piezophila* sp. nov., a novel piezophilic species from deep-sea sediments of the Japan trench. *Int. J. Syst. Evol. Microbiol.* 54, 1627–1631. doi: 10.1099/ijs.0.03049-0

Oksanen, J., Blanchet, F. G., Friendly, M., Kindt, R., Legendre, P., McGlinn, D., et al. (2018). *Vegan: Community ecology package*. Available at: https://CRAN.R-project.org/package=vegan (Accessed January 23, 2019).

Pearce, R. K., Sánchez de la Muela, A., Moorkamp, M., Hammond, J. O. S., Mitchell, T. M., Cembrano, J., et al. (2019). Interaction between hydrothermal fluids and fault systems in the in the southern Andes revealed by magnetotelluric and seismic data. *Geophysics* 2019:1143. doi: 10.1002/essoar.10501143.1

Peccerillo, A., De Astis, G., Faraone, D., Forni, F., and Frezzotti, M. L. (2013). Compositional variations of magmas in the Aeolian arc: implications for petrogenesis and geodynamics. *Geol. Soc. Lond. Mem.* 37, 491–510. doi: 10.1144/M37.15

Peccerillo, A., and Turco, E. (2004). Petrological and geochemical variations of Plio-quaternary volcanism in the Tyrrhenian Sea area: regional distribution of magma types,

petrogenesis and geodynamic implications. *Per. Mineral* 73, 231–251. doi: 10.1016/S1871-644X(06)80016-1

Petrillo, C., Castaldi, S., Lanzilli, M., Selci, M., Cordone, A., Giovannelli, D., et al. (2021). Genomic and physiological characterization of Bacilli isolated from salt-pans with plant growth promoting features. *Front. Microbiol.* 12:2517. doi: 10.3389/fmicb.2021.715678

Placido, A., Hai, T., Ferrer, M., Chernikova, T. N., Distaso, M., Armstrong, D., et al. (2015). Diversity of hydrolases from hydrothermal vent sediments of the Levante Bay, Vulcano Island (Aeolian archipelago) identified by activity-based metagenomics and biochemical characterization of new esterases and an arabinopyranosidase. *Appl. Microbiol. Biotechnol.* 99, 10031–10046. doi: 10.1007/s00253-015-6873-x

Pohlner, M., Dlugosch, L., Wemheuer, B., Mills, H., Engelen, B., and Reese, B. K. (2019). The majority of active Rhodobacteraceae in marine sediments belong to uncultured genera: a molecular approach to link their distribution to environmental conditions. *Front. Microbiol.* 10:659. doi: 10.3389/fmicb.2019.00659

Power, J. F., Carere, C. R., Lee, C. K., Wakerley, G. L. J., Evans, D. W., Button, M., et al. (2018). Microbial biogeography of 925 geothermal springs in New Zealand. *Nat. Commun.* 9:2876. doi: 10.1038/s41467-018-05020-y

Price, R. E., and Giovannelli, D. (2017). "A review of the geochemistry and microbiology of marine shallow-water hydrothermal vents" in *Reference module in earth systems and environmental sciences* ed. S. A. Elias (Amsterdam, Netherlands: Elsevier).

Price, R. E., LaRowe, D. E., Italiano, F., Savov, I., Pichler, T., and Amend, J. P. (2015). Subsurface hydrothermal processes and the bioenergetics of chemolithoautotrophy at the shallow-sea vents off Panarea Island (Italy). *Chem. Geol.* 407–408, 21–45. doi: 10.1016/j.chemgeo.2015.04.011

Price, R. E., Lesniewski, R., Nitzsche, K. S., Meyerdierks, A., Saltikov, C., Pichler, T., et al. (2013). Archaeal and bacterial diversity in an arsenic-rich shallow-sea hydrothermal system undergoing phase separation. *Front. Microbiol.* 4:158. doi: 10.3389/fmicb.2013.00158

Priest, T., Heins, A., Harder, J., Amann, R., and Fuchs, B. M. (2022). Niche partitioning of the ubiquitous and ecologically relevant NS5 marine group. *ISME J.* 16, 1570–1582. doi: 10.1038/s41396-022-01209-8

Pusceddu, A., Dell'Anno, A., Danovaro, R., Manini, E., Sara, G., and Fabiano, M. (2003). Enzymatically hydrolyzable protein and carbohydrate sedimentary pools as indicators of the trophic state of detritus sink systems: a case study in a Mediterranean coastal lagoon. *Estuaries* 26, 641–650. doi: 10.1007/BF02711976

Quast, C., Pruesse, E., Yilmaz, P., Gerken, J., Schweer, T., Yarza, P., et al. (2013). The SILVA ribosomal RNA gene database project: improved data processing and web-based tools. *Nucleic Acids Res.* 41, D590–D596. doi: 10.1093/nar/gks1219

R Core Team. (2021). *R: A language and environment for statistical computing, 2015*. Vienna, Austria: R Core Team.

Rajasabapathy, R., Mohandass, C., Bettencourt, R., Colaço, A., Goulart, J., and Meena, R. M. (2018). Bacterial diversity at a shallow-water hydrothermal vent (Espalamaca) in Azores Island. *Curr. Sci.* 115:2110. doi: 10.18520/cs/v115/i11/2110-2121

Reed, D. C., Breier, J. A., Jiang, H., Anantharaman, K., Klausmeier, C. A., Toner, B. M., et al. (2015). Predicting the response of the deep-ocean microbiome to geochemical perturbations by hydrothermal vents. *ISME J.* 9, 1857–1869. doi: 10.1038/ismej.2015.4

Reeves, E. P., Seewald, J. S., Saccocia, P., Bach, W., Craddock, P. R., Shanks, W. C., et al. (2011). Geochemistry of hydrothermal fluids from the PACMANUS, northeast Pual and Vienna woods hydrothermal fields, Manus Basin. *Papua New Guinea. Geochim. Cosmochim. Acta* 75, 1088–1123. doi: 10.1016/j.gca.2010.11.008

Rinke, C., Schmitz-Esser, S., Stoecker, K., Nussbaumer, A. D., Molnár, D. A., Vanura, K., et al. (2006). "*Candidatus* Thiobios zoothamnicoli," an Ectosymbiotic bacterium covering the Giant marine ciliate *Zoothamnium niveum*. *Appl. Environ. Microbiol.* 72, 2014–2021. doi: 10.1128/AEM.72.3.2014-2021.2006

Rogers, K. L., and Amend, J. P. (2005). Archaeal diversity and geochemical energy yields in a geothermal well on Vulcano Island, Italy. *Geobiology* 3, 319–332. doi: 10.1111/j.1472-4669.2006.00064.x

Rogers, K. L., and Amend, J. P. (2006). Energetics of potential heterotrophic metabolisms in the marine hydrothermal system of Vulcano Island, Italy. *Geochim. Cosmochim. Acta* 70, 6180–6200. doi: 10.1016/j.gca.2006.08.046

Rogers, K. L., Amend, J. P., and Gurrieri, S. (2007). Temporal changes in fluid chemistry and energy profiles in the Vulcano Island hydrothermal system. *Astrobiology* 7, 905–932. doi: 10.1089/ast.2007.0128

Rollinson, H., and Pease, V. (2021). *Using geochemical data to understand geological processes*. Cambridge, UK: Cambridge University Press.

Rusch, A., Walpersdorf, E., deBeer, D., Gurrieri, S., and Amend, J. P. (2005). Microbial communities near the oxic/anoxic interface in the hydrothermal system of Vulcano Island, Italy. *Chem. Geol.* 224, 169–182. doi: 10.1016/j.chemgeo.2005.07.026

Sayed, A. M., Hassan, M. H. A., Alhadrami, H. A., Hassan, H. M., Goodfellow, M., and Rateb, M. E. (2020). Extreme environments: microbiology leading to specialized metabolites. *J. Appl. Microbiol.* 128, 630–657. doi: 10.1111/jam.14386

Sciutteri, V., Smedile, F., Vizzini, S., Mazzola, A., and Vetriani, C. (2022). Microbial biofilms along a geochemical gradient at the shallow-water hydrothermal system of Vulcano Island, Mediterranean Sea. *Front. Virol.* 13:840205. doi: 10.3389/fmicb.2022.840205

Sedwick, P., and Stüben, D. (1996). Chemistry of shallow submarine warm springs in an arc-volcanic setting: Vulcano Island, Aeolian archipelago, Italy. *Mar. Chem.* 53, 147–161. doi: 10.1016/0304-4203(96)00020-5

Shafiee, R. T., Diver, P. J., Snow, J. T., Zhang, Q., and Rickaby, R. E. M. (2021). Marine ammonia-oxidising archaea and bacteria occupy distinct iron and copper niches. *ISME Commun.* 1:1. doi: 10.1038/s43705-021-00001-7

Sheik, C. S., Reese, B. K., Twing, K. I., Sylvan, J. B., Grim, S. L., Schrenk, M. O., et al. (2018). Identification and removal of contaminant sequences from ribosomal gene databases: lessons from the census of deep life. *Front. Microbiol.* 9:840. doi: 10.3389/fmicb.2018.00840

Sieland, R. (2009). Chemical and isotopic investigations of submarine fluid discharges from Panarea, Aeolian Islands, Italy. *Freiberg Online Geol.*:21:887. doi: 10.23689/fidgeo-887

Sievert, S. M., Kuever, J., and Muyzer, G. (2000). Identification of 16S ribosomal DNA-defined bacterial populations at a shallow submarine hydrothermal vent near Milos Island (Greece). *Appl. Environ. Microbiol.* 66, 3102–3109. doi: 10.1128/AEM.66.7.3102-3109.2000

Simmons, S., and Norris, P. (2002). Acidophiles of saline water at thermal vents of Vulcano, Italy. *Extremophiles* 6, 201–207. doi: 10.1007/s007920100242

Spietz, R. L., Lundeen, R. A., Zhao, X., Nicastro, D., Ingalls, A. E., and Morris, R. M. (2019). Heterotrophic carbon metabolism and energy acquisition in *Candidatus Thioglobus singularis* strain PS1, a member of the SUP05 clade of marine Gammaproteobacteria. *Environ. Microbiol.* 21, 2391–2401. doi: 10.1111/1462-2920.14623

Stöhr, R., Waberski, A., Völker, H., Tindall, B. J., and Thomm, M. (2001). *Hydrogenothermus marinus* gen. Nov., sp. nov., a novel thermophilic hydrogen-oxidizing bacterium, recognition of *Calderobacterium hydrogenophilum* as a member of the genus *Hydrogenobacter* and proposal of the reclassification of *Hydrogenobacter acidophilus* as *Hydrogenobaculum acidophilum* gen. Nov., comb. nov., in the phylum '*Hydrogenobacter*/Aquifex. *Int. J. Syst. Evol. Microbiol.* 51, 1853–1862. doi: 10.1099/00207713-51-5-1853

Suarez, C., Piculell, M., Modin, O., Langenheder, S., Persson, F., and Hermansson, M. (2019). Thickness determines microbial community structure and function in nitrifying biofilms via deterministic assembly. *Sci. Rep.* 9:5110. doi: 10.1038/s41598-019-41542-1

Taillefer, A., Guillou-Frottier, L., Soliva, R., Magri, F., Lopez, S., Courrioux, G., et al. (2018). Topographic and faults control of hydrothermal circulation along dormant faults in an Orogen. *Geochem. Geophys. Geosystems* 19, 4972–4995. doi: 10.1029/2018GC007965

Takai, K., Miyazaki, M., Nunoura, T., Hirayama, H., Oida, H., Furushima, Y., et al. (2006). *Sulfurivirga caldicuralii* gen. Nov., sp. nov., a novel microaerobic, thermophilic, thiosulfate-oxidizing chemolithoautotroph, isolated from a shallow marine hydrothermal system occurring in a coral reef. *Jpn. Int. J. Syst. Evol. Microbiol.* 56, 1921–1929. doi: 10.1099/ijs.0.64297-0

Tarasov, V. G., Gebruk, A. V., Mironov, A. N., and Moskalev, L. I. (2005). Deep-sea and shallow-water hydrothermal vent communities: two different phenomena? *Chem. Geol.* 224, 5–39. doi: 10.1016/j.chemgeo.2005.07.021

Tarasov, V. G., Gebruk, A. V., Shulkin, V. M., Kamenev, G. M., Fadeev, V. I., Kosmynin, V. N., et al. (1999). Effect of shallow-water hydrothermal venting on the biota of Matupi harbour (Rabaul caldera, New Britain Island, Papua New Guinea). *Cont. Shelf Res.* 19, 79–116. doi: 10.1016/S0278-4343(98)00073-9

Tarasov, V. G., Propp, M. V., Propp, L. N., Zhirmunsky, A. V., Namsakakv, B. B., Gorlenko, V. M., et al. (1990). Shallow-water Gasohydrothermal vents of Ushishir volcano and the ecosystem of Kraternaya bight (the Kurile Islands). *Mar. Ecol.* 11, 1–23. doi: 10.1111/j.1439-0485.1990.tb00225.x

Tassi, F., Capaccioni, B., Caramanna, G., Cinti, D., Montegrossi, G., Pizzino, L., et al. (2009). Low-pH waters discharging from submarine vents at Panarea Island (Aeolian Islands, southern Italy) after the 2002 gas blast: origin of hydrothermal fluids and implications for volcanic surveillance. *Appl. Geochem.* 24, 246–254. doi: 10.1016/j.apgeochem.2008.11.015

Techtmann, S. M., Fitzgerald, K. S., Stelling, S. C., Joyner, D. C., Uttukar, S. M., Harris, A. P., et al. (2016). *Colwellia psychrerythraea* strains from distant Deep Sea basins show adaptation to local conditions. *Front. Environ. Sci.* 4:3. doi: 10.3389/fenvs.2016.00033

Tivey, M. K. (2007). Generation of seafloor hydrothermal vent fluids and associated mineral deposits. *Oceanography* 20, 50–65. doi: 10.5670/oceanog.2007.80

Van Dover, C. (2012). Hydrothermal vent ecosystems and conservation. *Oceanography* 25, 313–316. doi: 10.5670/oceanog.2012.36

Van Dover, C. L., Arnaud-Haond, S., Gianni, M., Helmreich, S., Huber, J. A., Jaeckel, A. L., et al. (2018). Scientific rationale and international obligations for protection of active hydrothermal vent ecosystems from deep-sea mining. *Mar. Policy* 90, 20–28. doi: 10.1016/j.marpol.2018.01.020

Venâncio, I., Luís, Â., Domingues, F., Oleastro, M., Pereira, L., and Ferreira, S. (2022). The prevalence of Arcobacteraceae in aquatic environments: a systematic review and Meta-analysis. *Pathogens* 11:244. doi: 10.3390/pathogens11020244

Vuillemin, A., Kerrigan, Z., D'Hondt, S., and Orsi, W. D. (2020). Exploring the abundance, metabolic potential and gene expression of subseafloor Chloroflexi in million-year-old oxic and anoxic abyssal clay. *FEMS Microbiol. Ecol.* 96:fiaa223. doi: 10.1093/femsec/fiaa223

Wang, L., Cheung, M. K., Liu, R., Wong, C. K., Kwan, H. S., and Hwang, J.-S. (2017). Diversity of Total bacterial communities and chemoautotrophic populations in sulfur-rich sediments of shallow-water hydrothermal vents off Kueishan Island, Taiwan. *Microb. Ecol.* 73, 571–582. doi: 10.1007/s00248-016-0898-2

Wang, W., Li, Z., Zeng, L., Dong, C., and Shao, Z. (2020). The oxidation of hydrocarbons by diverse heterotrophic and mixotrophic bacteria that inhabit deep-sea hydrothermal ecosystems. *ISME J.* 14, 1994–2006. doi: 10.1038/s41396-020-0662-y

Wang, F.-Q., Lin, X.-Z., Chen, G.-J., and Du, Z.-J. (2015). *Colwellia arctica* sp. nov., isolated from Arctic marine sediment. *Antonie Van Leeuwenhoek* 107, 723–729. doi: 10.1007/s10482-014-0366-2

Ward, L. M., Hemp, J., Shih, P. M., McGlynn, S. E., and Fischer, W. W. (2018). Evolution of Phototrophy in the Chloroflexi phylum driven by horizontal gene transfer. *Front. Microbiol.* 9:260. doi: 10.3389/fmicb.2018.00260

Ward, L. M., Idei, A., Terajima, S., Kakegawa, T., Fischer, W. W., and McGlynn, S. E. (2017). Microbial diversity and iron oxidation at Okuoku-hachikurou Onsen, a Japanese hot spring analog of Precambrian iron formations. *Geobiology* 15, 817–835. doi: 10.1111/gbi.12266

White, J. R., Escobar-Paramo, P., Mongodin, E. F., Nelson, K. E., and DiRuggiero, J. (2008). Extensive genome rearrangements and multiple horizontal gene transfers in a population of *Pyrococcus* Isolates from Vulcano Island, Italy. *Appl. Environ. Microbiol.* 74, 6447–6451. doi: 10.1128/AEM.01024-08

Wickham, H. (2011). ggplot2. *Wiley Interdiscip. Rev. Comput. Stat.* 3, 180–185. doi: 10.1002/wics.147

Yamamoto, K., Hackley, K. C., Kelly, W. R., Panno, S. V., Sekiguchi, Y., Sanford, R. A., et al. (2019). Diversity and geochemical community assembly processes of the living rare biosphere in a sand-and-gravel aquifer ecosystem in the Midwestern United States. *Sci. Rep.* 9:13484. doi: 10.1038/s41598-019-49996-z

Yamamoto, M., and Takai, K. (2011). Sulfur metabolisms in epsilon- and gamma-Proteobacteria in Deep-Sea hydrothermal fields. *Front. Microbiol.* 2:192. doi: 10.3389/fmicb.2011.00192

Yücel, M., Sievert, S. M., Vetriani, C., Foustoukos, D. I., Giovannelli, D., and Le Bris, N. (2013). Eco-geochemical dynamics of a shallow-water hydrothermal vent system at Milos Island, Aegean Sea (eastern Mediterranean). *Chem. Geol.* 356, 11–20. doi: 10.1016/j.chemgeo.2013.07.020

Zanfardino, A., Migliardi, A., D'Alonzo, D., Lombardi, A., Varcamonti, M., and Cordone, A. (2016). Inactivation of MSMEG_0412 gene drastically affects surface related properties of *Mycobacterium smegmatis*. *BMC Microbiol.* 16:267. doi: 10.1186/s12866-016-0888-z

Zeng, X., Alain, K., and Shao, Z. (2021). Microorganisms from deep-sea hydrothermal vents. *Mar. Life Sci. Technol.* 3, 204–230. doi: 10.1007/s42995-020-00086-4

Zhang, D.-C., Yu, Y., Xin, Y.-H., Liu, H.-C., Zhou, P.-J., and Zhou, Y.-G. (2008). *Colwellia polaris* sp. nov., a psychrotolerant bacterium isolated from Arctic Sea ice. *Int. J. Syst. Evol. Microbiol.* 58, 1931–1934. doi: 10.1099/ijs.0.65596-0

Zhang, Y., Zhao, Z., Chen, C.-T. A., Tang, K., Su, J., and Jiao, N. (2012). Sulfur metabolizing microbes dominate microbial communities in andesite-hosted Shallow-Sea hydrothermal systems. *PLoS One* 7:e44593. doi: 10.1371/journal.pone.0044593

Frontiers in Microbiology

Explores the habitable world and the potential of microbial life

The largest and most cited microbiology journal which advances our understanding of the role microbes play in addressing global challenges such as healthcare, food security, and climate change.

Discover the latest Research Topics

See more →

Frontiers

Avenue du Tribunal-Fédéral 34
1005 Lausanne, Switzerland
frontiersin.org

Contact us

+41 (0)21 510 17 00
frontiersin.org/about/contact